Studies on the use of anhydrides in novel catalytic asymmetric transformations

Trinity College Dublin

A thesis submitted to the University of Dublin for the degree of

Doctor of Philosophy

by

Francesco Manoni

Under the supervision of

Prof. Stephen Connon

December 2013

Declaration

I declare that this thesis has not been submitted as an exercise for a degree at this or any other university and it is entirely my own work. Due acknowledgements and references are given to the work of others.

I agree to deposit this thesis in the University's open access institutional repository or allow the library to do so on my behalf, subject to Irish Copyright Legislation and Trinity College Library conditions of use and acknowledgement.

r and S. J. Connon, *Angew. Chem. Int. Ed.*, 2010,

an and S. J. Connon, *New J. Chem.*, 2011, **35**, 551

e, S. Tallon and S. J. Connon, *Org. Lett.*, 2012, **14**, 1850.

F. Manoni, C. Cornaggia, J. Murray, S. Tallon and S. J. Connon, *Chem. Commun.*, 2012, **48**, 6502.

F. Manoni and S. J. Connon, *Angew. Chem. Int. Ed.*, 2014, accepted for publication.

Table of contents

Acknowledgments

Firstly I would like to thank my parents and my family for the encouragement and support they gave me during this new chapter of my life. It would not have been easy without you. Thank you all.

I am deeply thankful to my supervisor Prof. Stephen Connon for the opportunity to undertake a research project under his guidance and for the constant motivation and precious support he gave me throughout all these years.

My biggest 'thank you' goes to my 'strabiliant' girlfriend Miriam, who had the patience to tolerate me during one of the most stressful times of my life and was so lovely to proof read the entire thesis without complaints. You are the only one who could put up with me, you are unique, and I am the luckiest person in the world to have you. Words cannot express my gratitude. Thank you <u>so much</u>, Mim.

I also wish to thank all the members of both the Connon and the Southern group for having made these years less stressful and more enjoyable with all the jokes and funny moments we had together. Thank you Lauren, Seán, Linda, Claire-Louise, Sivaji, Simon, Cormac, Carole, Alessandro, Sarah, Ollie, Anna, Aldo, Esther, Zaida, Michelle, Franciane and Nagaraju.

A special thank goes to the 'Little Italy' part of the group: Emiliano and Claudio. We have done and said pretty much everything in that lab, to the constant surprise of the people around. We laughed a lot and I am extremely thankful to both of you for the moments we spent together.

Finally I would like to thank all the staff in the Chemistry department for their help along the way. Special thanks to Dr. John O'Brien, Dr. Manuel Ruether, Dr. Martin Feeney, Dr. Thomas McCabe and Dr. Gary Hessman.

Abstract

In this thesis the possibility of using bifunctional cinchona alkaloid-derived organocatalysts to promote the enantioselective cycloaddition reaction of enolisable anhydrides to various electrophiles to form annulated structures with high stereocontrol has been demonstrated.

The reaction between homophthalic anhydrides and aldehydes under mild conditions allowed the enantioselective synthesis of dihydroisocoumarins, a natural class of compounds possessing a variety of biological effects, in high yields, diastereoselectivity and enantioselectivity.

The methodology was later expanded to include the use of aryl succinic anhydrides which produced paraconic acid derivatives (abundant in nature and possessing biological activity), in high yields and with excellent stereocontrol.

The expansion of the substrate scope with regard to the electrophilic species was later investigated. It was found that the catalytic asymmetric reaction between homophthalic anhydrides and trisubstituted nitroalkenes can be used to form two new carbon-carbon bonds and produce structures bearing three stereocentres (one of which is quaternary) in high yield and stereoselectivity.

The evaluation of alkyliden-2-oxindoles as substrates in the reaction with enolisable anhydrides was also studied. The results obtained proved the feasibility of the process allowing the synthesis, in high yields and with excellent stereocontrol, of spirooxindoles bringing about enantioselective Tamura reactions for the first time. Both aromatic- and glutaconic-derived anhydrides have been found to be capable of producing highly functionalised structures when reacted with one of two different alkiliden-2-oxindoles. It was also found that a decarboxylative process takes place in the reactions involving glutaconic-derived anhydrides, furnishing cyclohexenone products bearing two stereocentres. Furthermore, it was demonstrated that when the reaction involving homophthalic anhydrides is performed at low temperatures, the selective formation of an alternative diastereomer in high yield and stereocontrol could be achieved.

The first thiolate-catalysed crossed- aldehyde-ketone Tishchenko reaction has also been reported in this thesis. It has been demonstrated that the use of bromomagnesium

thiolate can efficiently promote the Tishchenko reaction between a number of aldehydes and trifluoromethyl ketones in high yields.

The reaction was later investigated under the influence of microwave radiation in order to increase the rate of the process that required extensive reaction times at high temperatures in certain cases. The process proved extremely efficient, promoting the reaction in very short time, however it resulted in lower yields compared to the thermal variant.

Abbreviations

(q)	Quaternary
abs. config.	Absolute configuration
Ac	Acetyl
AcOH	Acetic acid
AD	Asymmetric dihydroxylation
APCI	Atmospheric-pressure chemical ionization
app. d	Apparent doublet
app. s	Apparent singlet
app. t	Apparent triplet
Ar	Aryl
B	Base
b.p.	Boiling point
Bn	Benzyl
Boc	*tert*-Butoxycarbonyl
bs	Broad singlet
c-	*cyclo-*
cat.	Catalyst
CI	Chemical ionisation
CIP	Cahn–Ingold–Prelog
COD	1,5-Cyclooctadiene
conc.	Concentrated
conv.	Conversion
CSP	Chiral stationary phase
Cys	Cysteine
d	Days
d	Doublet
DABCO	1,4-diazabicyclo[2.2.2]octane
DBU	1,8-Diazabicyclo[5.4.0]undec-7-ene
dd	Doublet of doublets
ddd	Doublet of doublet of doublets
DIAD	Diisopropyl azodicarboxylate
DIP	Direct insertion probe
DIPAMP	Ethane-1,2-diylbis[(2-methoxyphenyl)phenylphosphane]
DIPEA	*N,N*-Diisopropylethylamine
DMAP	4-(Dimethylamino)pyridine
DMC	2-Chloro-1,3-dimethylimidazolinium chloride
DMF	Dimethylformamide
DMSO	Dimethyl sulfoxide
DPPA	Diphenylphosphoryl azide

dr	Diastereomeric ratio
E	Electrophile
EDG	Electron donating group
ee	Enantiomeric excess
EI	Electron ionisation
equiv.	Equivalent
ESI	Electrospray ionization
Et	Ethyl
EtOAc	Ethyl acetate
EtOH	Ethanol
EWG	Electron withdrawing group
FDA	Food and Drug Administration
G3PDHase	Glyceraldehyde-3-phosphate dehydrogenase
h	Hours
His	Histidine
HMPA	Hexamethyl phosphoramide
HNEt$_2$	Diethyl amine
HOMO	Highest occupied molecular orbital
HPLC	High Performance Liquid Chromatography
HRMS	High-resolution mass spectrometry
i-	*iso-*
IPA	*iso*-Propyl alcohol
i-Pr	Isopropyl
i-Pr$_2$NEt	*N,N'*-Diisopropylethylamine (Hünig's base)
i-PrOH	2-propanol
IR	Infrared
IUPAC	International Union of Pure and Applied Chemistry
KHMDS	Potassium bis(trimethylsilyl)amide
LA	Lewis acid
LDA	Lithium diisopropylamide
L-DOPA	L-3,4-DIHYDROXYPHENYLALANINE
LiHMDS	Lithium bis(trimethylsilyl)amide
lit.	Literature
LUMO	Lowest unoccupied molecular orbital
m	Multiplet
m-	*meta-*
m.p.	Melting point
m/z	Mass/Charge
Me	Methyl
MeOH	Methanol
min	Minutes

mol. sieves	Molecular sieves
MTBE	Methyl-*tert*-butyl ether
MW	Microwave
n-	*normal*-
NAD$^+$/NADH	Nicotinamide adenine dinucleotide
NaHMDS	Sodium bis(trimethylsilyl)amide
NEt$_3$	Triethylamine
NMR	Nuclear magnetic resonance
NOE	Nuclear Overhauser Effect
Nu	Nucleophile
o-	*ortho*-
OAc	Acetate
p-	*para*-
Ph	Phenyl
Pr	Propyl
prod.	Product
p-TSA	*p*-Toluenesulfonic acid
q	Quartet
quant.	Quantitative
R$_f$	Retardation factor
rt	Room temperature
s	Singlet
SIPr	1,3-bis(2,6-diisopropylphenyl)imidazolin-2-ylidene
sub.	Substrate
t	Triplet
t-	*tert*-
t-Bu	*tert*-Butyl
t-BuOH	*tert*-Butyl alcohol
temp.	Temperature
tert-	*tertiary*-
TFA	Trifluoroacetic acid
TFAA	Trifluoroacetic anhydride
THF	Tetrahydrofuran
TLC	Thin layer chromatography
TMS	Trimethylsilyl
TMSCHN$_2$	Trimethylsilyl diazomethane
TMSCN	Trimethylsilyl cyanide
UV	Ultraviolet
v/*v*	Volume/Volume
w/*v*	Weight/Volume

1. Introduction

1.1   Asymmetric synthesis: a general introduction

Asymmetric synthesis, also referred as stereoselective synthesis, is defined by IUPAC as: 'A chemical reaction (or reaction sequence) in which one or more new elements of chirality are formed in a substrate molecule and which produces the stereoisomeric (enantiomeric or diastereomeric) products in unequal amounts.'[1]

During the last few decades, the ability to synthesise one enantiomer/diastereomer exclusively has played a crucial role in the pharmaceutical industry.[2,3]

In nature, a wide number of molecules with biological activity contain stereocentres. For example, biological molecules such as proteins, enzymes, receptors, carbohydrates and many others are composed of building blocks produced entirely as a single enantiomer, such as amino acids and sugars. Often, the interaction of different enantiomers of the same molecule with the same receptors will lead to completely different results.[4] Isolation of D-asparagine for the first time, in 1886, by the Italian chemist Arnaldo Piutti, is an example. The scientist found a remarkable difference in the taste of the two enantiomers: L-asparagine was flavourless, while D-asparagine was extremely sweet.[5]

As a result of the thalidomide scandal in early 1960s, the Food and Drug Administration (FDA) announced a new policy statement for the development of new stereoisomeric drugs in 1992.[6] From then on, all chiral drug candidates must be synthesised and evaluated as a single enantiomer before approval is given. This highlighted the importance of stereoselective synthesis as a method to 'control' chirality in organic synthesis.[6]

During a reaction process in an achiral environment, the transition states that lead to the two enantiomers of a product possess identical energies, and so lead to a 50:50 mixture of both (also called a racemic mixture). If the energies of the respective transition states leading to the enantiomers can be modified in such a way that one is lower than the other, the preferential formation of one enantiomer over the other one results, leading to an enantioenriched mixture. A common way to do so is to introduce a chiral feature in

either the substrate, reagent, catalyst or environment. This is known as asymmetric induction[1] and is a key element in asymmetric synthesis.

The main strategies for the synthesis of enantiopure molecules are:

- The resolution of a racemic mixture
- Ex-chiral pool synthesis
- The use of a chiral auxiliary
- Asymmetric catalysis
  - Transition metal catalysis
  - Biocatalysis
  - Organocatalysis

The resolution of a racemic mixture is probably the oldest method used by chemists to obtain enantiopure compounds from a mixture containing an equal amount of both enantiomers. It was discovered in 1848 by the French chemist and microbiologist Louis Pasteur, who resolved a mixture of 'left-handed' and 'right-handed' tartaric acid salts by manual separation of the crystals, leading to the discovery of chirality.[7] Currently, this type of resolution is usually achieved by the conversion of a racemic mixture into a mixture of diastereomers by reaction with an enantiopure chiral resolving agent. This will lead to a mixture of compounds with completely different physical properties that will allow for their separation, usually by crystallisation.[8] This technique, however effective, presents a number of drawbacks. Two extra steps are required (formation and cleavage of the pair) and generally a 50% maximum yield of one enantiomer can be obtained.

Ex-chiral pool synthesis is a synthetic strategy based on the use of natural, readily available enantiopure molecules, such as sugars or amino acids, as starting materials.[9] The chiral information introduced will (generally) be preserved along the synthetic steps and will be used (if necessary) to control the stereochemical outcome of subsequent transformations. It is particularly suited to those substrates that are structurally similar to the chiral starting material employed.[10,11]

Chiral auxiliaries, introduced by E. J. Corey in 1975 with enantiopure 8-phenylmenthol,[12] have played a central role in asymmetric synthesis for many years.[13,14]

They are enantiopure molecules that do not directly participate in the reaction. Generally they are temporarily bonded to the substrate prior to the asymmetric step(s) of the synthesis in order to achieve asymmetric induction (*i.e.* diastereocontrol), and then removed afterwards. The auxiliaries must be inexpensive as they are used in stoichiometric amounts, and are preferably available as both enantiomers. They should also be easily introduced/removed (in high yields) in order to minimise waste.

Asymmetric catalysis normally refers to a process in which an achiral molecule is converted to a chiral one in the presence of a chiral catalyst.[15–17] The low catalyst loading required (typically 0.1-10 mol%) and the possibility to obtain a 100% yield of a single enantiomer made this technique one of the most popular and widely used in recent years, particularly in industry.[18] Typical catalysts are composed of chiral complexes between metals and chiral ligands. The breakthrough in this field occurred in 1968 with a discovery by William Knowles and his colleagues at Monsanto Company. Following Wilkinson's work on catalytic hydrogenation with triphenylphosphine complexes of rhodium chloride,[19] Knowles and co-workers decided to replace the achiral ligand originally used with an enantiopure chiral one (DIPAMP, **4**, Scheme 1.1). In doing so, they were able to catalyse the enantioselective addition of hydrogen to just one face of the prochiral olefinic substrate **1**, generating **2** bearing the new stereocentre in high enantioselectivity.[20] Later on, this process was commercialised to produce the anti-Parkinson drug L-DOPA (**3**, Scheme 1.1).
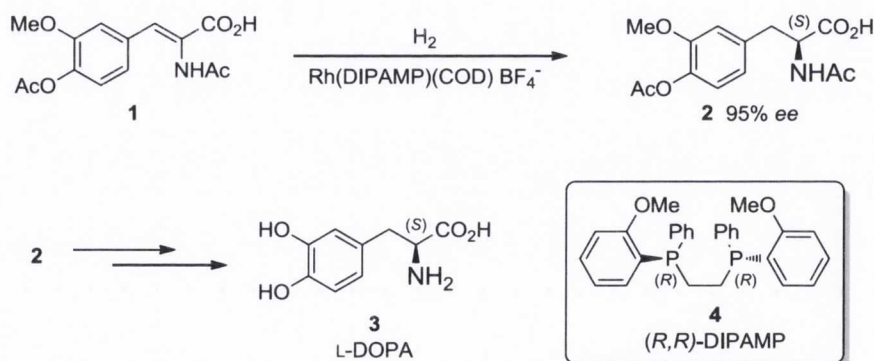
Scheme 1.1   Enantioselective synthesis of L-DOPA.

In recognition for his contribution to chemistry, Knowles was awarded the Nobel Prize, sharing it with Ryoji Noyori, also for his work on asymmetric catalytic hydrogenation, and with K. Barry Sharpless for his work on catalytic asymmetric oxidation.

Biocatalysis is the branch of asymmetric catalysis that applies the use of enzymes and microbes in synthetic chemistry.[21] Enzymes are among the most efficient molecules capable of catalysing reactions, and they are responsible for almost all metabolic reactions in living organisms. The interest in using such molecules in asymmetric catalysis arose from their extremely high chemo-, regio- and enantioselectivity in many chemical transformations. Such high selectivity made them a valid alternative to conventional chemical catalysts, especially in industry.[22,23] Furthermore, with just a few by-products, enzymes proved to be extremely environmentally friendly. However, their use is not without drawbacks, such as limited substrate scope, availability in only one enantiomeric form, they perform best in water (and not organic solvents) and they sometimes suffer from inhibition by the product.[24]

Asymmetric organocatalysis is the newest subdomain within the enormous field of enantioselective catalysis. It is based on the use of small organic molecules as catalysts in the absence of metal ions.[25] Although it has been known for more than a century that small organic molecules can promote reactions,[26] this new area of catalysis has been deeply studied only over the last decade.[27–29] The organic molecules most often utilised derive from a wide variety of naturally occurring substances that are generally air/moisture stable, non-toxic and are often available as both enantiomers. As a result, this technique is often inexpensive and easy to use, as the execution of a reaction does not normally require special conditions such as inert atmosphere or use of ultra-dry solvents/reagents.

The first significant work in organocatalysis arguably dates back to the early 1970s when Eder, Sauer and Wiechert,[30] and Hajos and Parrish[31] separately reported that a catalytic amount of proline (**6**) promoted the intramolecular aldol cyclisation of triketones (*i.e.* **5**) to furnish **7** in high yields and with excellent enantioselectivity (Scheme 1.2). Utilising this novel reaction it was then possible to generate important chiral intermediates for the total synthesis of subunits (*e.g.* **8**, Scheme 1.2) of steroids such as cortisone (**9**) with high optical purity, without resorting to resolution of a racemic mixture.[32,33]
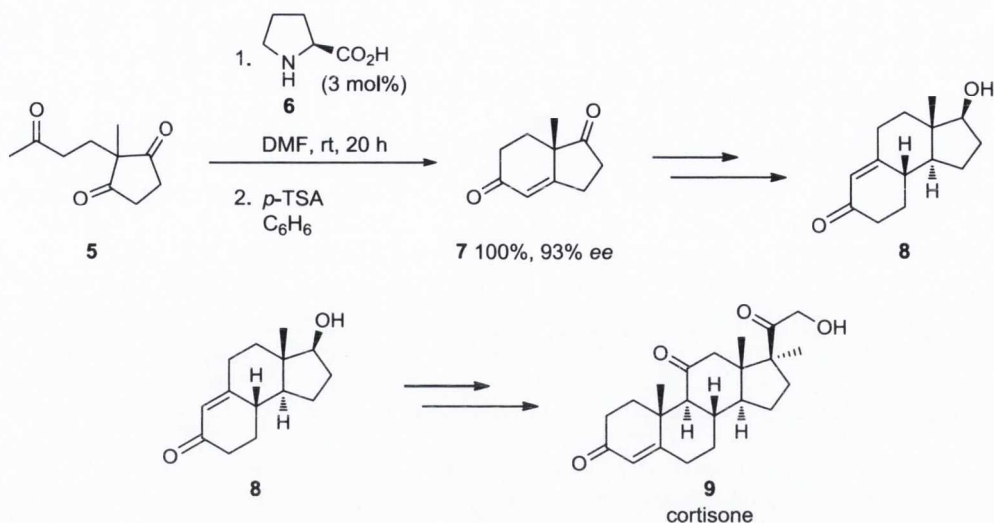
Scheme 1.2   The Hajos-Parrish-Eder-Sauer-Wiechert reaction and subsequent elaboration to cortisone.

In the late 1990s, Yang,[34] Shi,[35] Denmark,[36] Miller,[37] Jacobsen,[38] Corey,[39] and their co-workers (among other research groups) reported the use of small organic molecules as enantioselective catalysts in organic synthesis. In 2000, two publications defined the beginning of organocatalysis as an independent field of research in asymmetric catalysis.[40,41] The authors reported the possibility of employing simple, chiral, cyclic secondary amines as catalysts for the asymmetric functionalisation of carbonyl compounds, introducing two of the main modes of activation in organocatalysis.[29]

1.1.1   Organocatalysis: principal modes of action

The first of the studies introduced above was carried out by List and co-workers.[40] They reported the first example of a direct intermolecular asymmetric aldol reaction between an excess of acetone (**10**) with aldehydes such as **11**, catalysed by a non-metallic molecule (*e.g.* (*S*)-proline, **6**) to furnish **12** (Scheme 1.3); extending the scope of the reaction reported by Hajos and Parrish in 1974.[31]
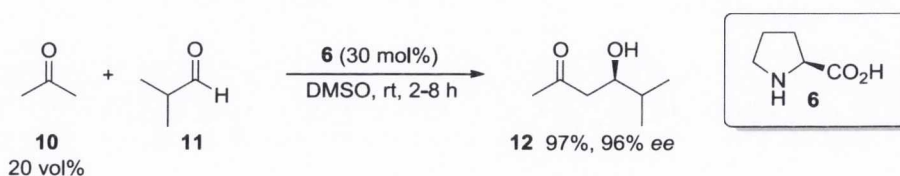
Scheme 1.3   Proline-catalysed intermolecular asymmetric aldol reaction.

The authors proposed that the reaction occurs *via* an enamine intermediate, in the same way that enzymes, such as class I aldolases operate.[42,43] They defined this new catalytic species as a "micro-aldolase", highlighting the capability of proline to use both amino acid functionalities in order to facilitate every step of the catalytic cycle. Initial activation of the carbonyl moieties **10** by the acid functionality of the (*S*)-proline (**6**, Scheme 1.4) facilitates the nucleophilic attack on the ketone by the amino group, generating the hemiaminal **13**. Loss of a molecule of water to form the iminium species **14** and subsequent deprotonation by the carboxylate of (*S*)-proline leads to the formation of **15**, which forms a new carbon-carbon bond with a molecule of aldehyde to generate **18** *via* the highly organised pre-transition state **17**. A subsequent hydrolysis step generates the aldol reaction product **12** and regenerates the catalyst (*i.e.* **6**).
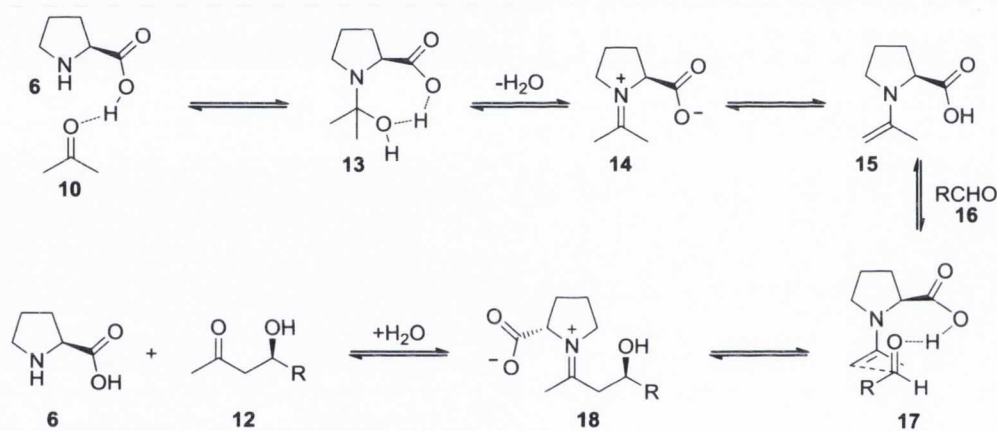
Scheme 1.4 Proposed mechanism for the proline-catalysed intermolecular asymmetric aldol reaction.

Soon after this, MacMillan and co-workers described the first enantioselective organocatalytic Diels-Alder reaction between dienes such as **19** and α,β-unsaturated aldehydes (*i.e.* **20**) to give **22**.[41] The authors described the use of synthetic enantiopure amines, such as the imidazolidinone **21** (Scheme 1.5), as catalysts for the activation of **20** by condensation to form an iminium ion intermediate (**23a**, Scheme 1.5).

They postulated that the reversible formation of the iminium ions could emulate the mechanism of activation of carbonyl compounds by Lewis acids. The key step in the explanation of the observed enantioselectivity is the preferential adoption of the (*E*)-conformation **23a** over the disfavoured (*Z*)-conformation **23b** by the activated iminium intermediate. Computational studies have shown that in order to avoid steric interaction

between the geminal dimethyl group on the catalyst and the double bond of the substrate, the formation of the (*E*)-isomer is favoured.[41]
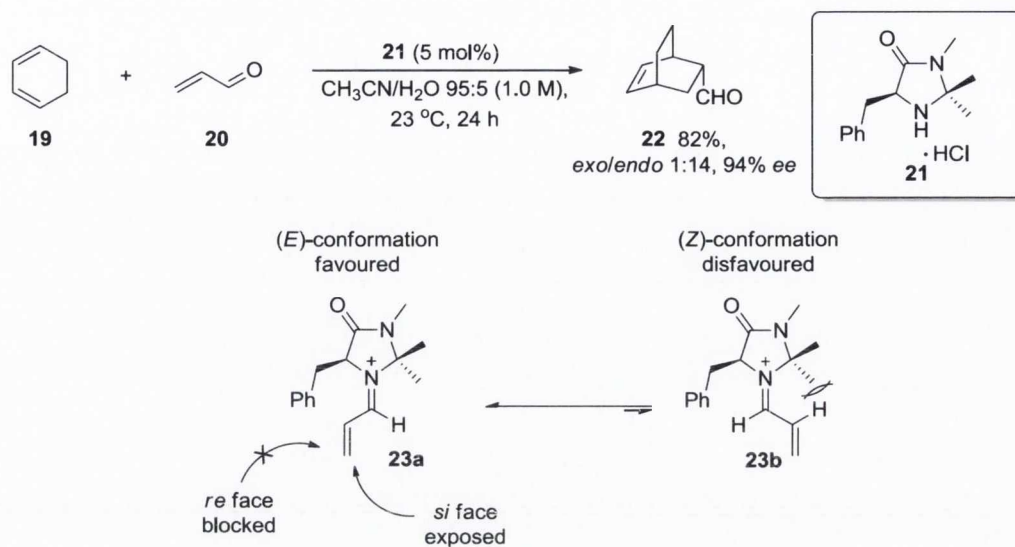
Scheme 1.5   Asymmetric organocatalysed Diels-Alder reaction.

Furthermore, the catalyst's benzyl group proved to be an extremely efficient shield for the *re* face of the (*E*)-iminium ion **23a**, leaving only the *si* face exposed to reaction (Scheme 1.5).[29,44,45]

As previously mentioned, the two studies reported above represent two of most common activation modes in organocatalysis (*i.e.* enamine catalysis and iminium catalysis) which constitute the asymmetric aminocatalysis. A common feature in this type of asymmetric catalysis is the formation of the iminium ion that lowers the energy of the lowest unoccupied molecular orbital (LUMO) of the system (Scheme 1.6).[44,46] As a consequence, for isolated π systems such as **24**, the formation of the iminium ion increases the acidity of the α proton in the substrate (*e.g.* **25**), leading to fast deprotonation with consequent formation of the enamine **26** (Scheme 1.6). This reactive intermediate species, considered an enolate equivalent, possesses increased energy of the highest occupied molecular orbital (HOMO), thus allowing the substrate to readily react with electrophiles *via* nucleophilic addition (*e.g.* the proline-catalysed intermolecular asymmetric aldol reaction).[40] In the case of conjugated π systems, such as **27**, the iminium ion formed (*i.e.* **28**) becomes more activated toward nucleophiles as a consequence of the lowering of the LUMO energy (Scheme 1.6), hence facilitating

reactions such as the transformation depicted in Scheme 1.5 (*e.g.* asymmetric organocatalysed Diels-Alder reaction).[41]
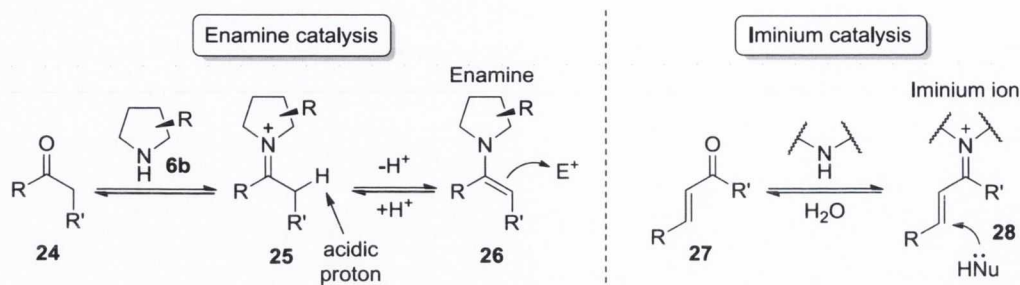
Scheme 1.6   Aminocatalysis activation modes.

Another common activation mode employed in organocatalysis is based on the use of non-covalent interactions between small (synthetic) molecules, capable of acting as hydrogen bond (H-bond) donors, and substrates. These molecules, through general acid catalysis, are able to stabilise the developing negative charge in the transition state of a reaction, thus enhancing the reactivity of the electrophile towards nucleophilic attack, in the same way as Lewis acids.[47] While the use of Lewis acid metal-based catalysts has been proved to offer a high degree of tunability,[48,49] a number of drawbacks associated with the employment of such catalytic species highlighted the possibility of using small molecules capable of acting as H-bond donors.[47]

1.2   Hydrogen bond donating molecules: historical perspective

In nature, enzymes frequently resort to H-bonding interactions in order to promote a number of chemical transformations (*e.g.* amide hydrolysis catalysed by serine proteases).[50]

In the same way, during the early 1980s, a number of studies reported enhanced stereoselectivity and substrate activation in reactions catalysed by small molecules capable of H-bonding.[51–53] Concurrently, pioneering investigations conducted by Hine *et al.* using phenols and phenol derivatives (*e.g.* **30**) as catalysts for the addition of diethylamine to phenyl glycidyl ether (**29**), revealed the superior catalytic activity of 1,8-biphenylenediol (**30**) compared to that of phenol itself in the formation of **31** (Scheme 1.7).[54,55]
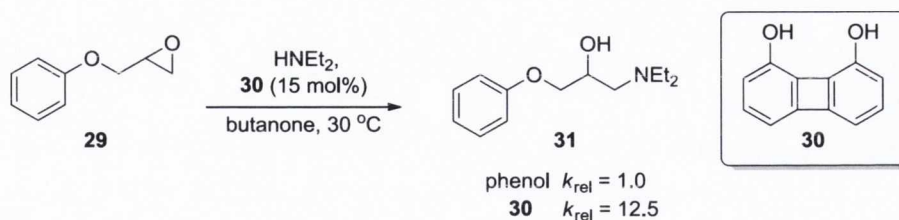
Scheme 1.7   Biphenylenediol-catalysed epoxide-opening reaction.

These results have been rationalised by Hine and co-workers, who proposed a double H-bond donation from the catalyst **30** to the substrate electrophile **29**. This theory was strengthened by earlier studies conducted by the same team on the X-ray analysis of crystalline 1:1 adducts of 1,8-biphenylenediol (**30**) and Lewis bases. These demonstrated that 1,8-biphenylenediol (**30**) was capable of forming two strong H-bonding interactions with the same oxygen atom of molecules such as 1,2,6-trimethyl-4-pyridone, hexamethyl phosphoramide (HMPA) and 2,6-dimethyl-γ-pyrone.[56]

Later, rate acceleration of Diels-Alder reactions promoted by a substituted biphenylenediol was rationalised by Kelly *et al.*, who proposed the catalyst double H-bond donation as explanation for the results obtained.[57] This was later found to also be in agreement with computational studies performed by Jorgensen and co-workers[58,59] which aimed to rationalise the observed acceleration of Diels-Alder reactions and Claisen rearrangements when the reactions were performed in water.

It was now clear that the use of species capable of the simultaneous donation of two H-bonds was a valid strategy for electrophile activation in synthetic chemistry.[50]

Between the end of 1980s and the beginning of 1990s, Etter and co-workers reported that *N,N'*-diarylureas with electron-withdrawing substituent (*i.e.* –NO$_2$) in the *meta* position readily co-crystallised with a wide number of Lewis base molecules, such as nitroaromatic compounds, ethers, ketones and sulfoxides due to their higher H-bond donating capacity.[60,61] This work, along with the previously mentioned examples, constitute the basis for what will become one of the most important types of electrophile activation in organocatalysis.

1.2.1   Organocatalysts containing (thio)urea moieties

The first example reported in the literature of general acid-catalysed reactions involving the use of urea derivatives as catalysts, was disclosed by Curran and co-workers.[62,63]

They found that catalytic amounts of diarylurea **33** were able to promote the allylation of cyclic α-sulfinyl radicals with improved yield and diastereoselectivity relative to the uncatalysed process.[62] Later, the same group demonstrated that the same catalyst (*i.e.* **33**) could be efficiently used in the Claisen rearrangement of **32** to **37**, leading to rate accelerations up to 22-fold when used in stoichiometric amounts (Scheme 1.8).[63] In order to improve both the solubility in organic solvents and compatibility with radical processes, the catalyst used in these reactions (*i.e.* **33**) was obtained upon modifications of the original structure reported by Etter: a trifluoromethyl group and an octyl ester were introduced at both phenyl rings, replacing the original *m*-nitro groups. A thiourea variant **34** (Scheme 1.8) of the catalyst was also examined for the first time as a H-bond donor; however, the temperature required for the Claisen rearrangement reaction to proceed at a convenient rate complicated the direct comparison between the performances of the two catalysts due to the gradual decomposition of **34** under these conditions.[63]

mol% 33	k_{rel}
0	1.0
10	2.7
40	5.0
100	22.4

33 X = O, R = H
34 X = S, R = H
35 X = O, R = Me
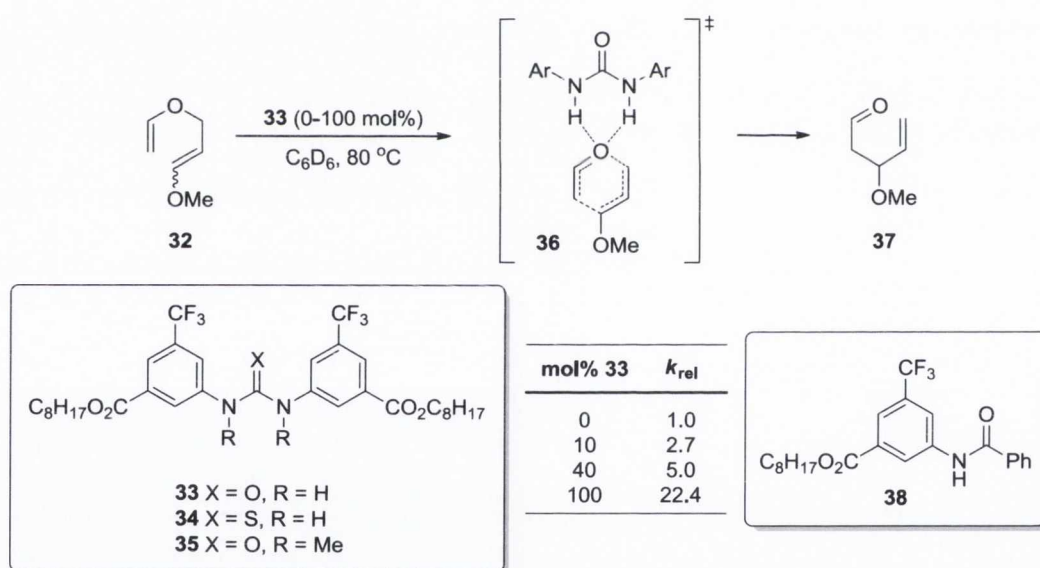
Scheme 1.8   Claisen rearrangement promoted by (thio)urea derivatives.

The results obtained were explained by the model of double H-bonding catalysis proposed by Hine *et al.* just a few years before. Evidence for the proposed transition state **36** was also obtained from the failure of both dialkylurea **35** and benzanilide **38** to promote the reaction when used as catalysts (Scheme 1.8).[63]

Inspired by these results, Schreiner and co-workers reported a series of computational studies demonstrating the structural similarities of a H-bonded complex of *N*-acyloxazolidinone **39** with the *N,N'*-disubstituted electron-poor thiourea **41** and the corresponding Lewis acid (AlCl₃) complex.[64] These studies were then confirmed by the observation of a rate acceleration of the Diels-Alder reaction between cyclopentadiene (**40**) and the α,β-unsaturated compound **39** in the presence of either the thiourea derivative **41** or the even more acidic **42**, to give products **43a** and **43b** (Scheme 1.9).[64]

cat.	conditions	% yield	*dr* (**43a** : **43b**)
-	benzene, 130 °C	55	36 : 64
AlCl₃	CHCl₃, -78 °C	95	92 : 8
41	CHCl₃, rt	74	77 : 23
42	CHCl₃, rt	78	81 : 19

41 R¹ = CF₃, R² = H
42 R¹ = R² = CF₃
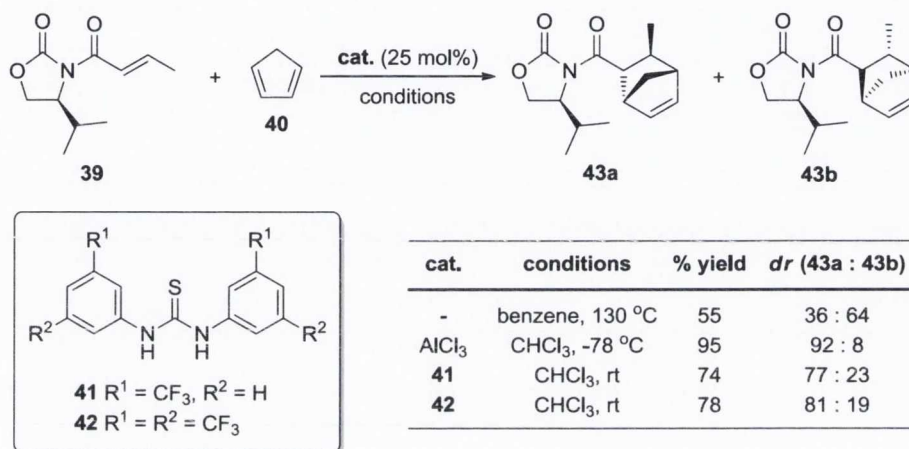
Scheme 1.9   Diels-Alder reaction catalysed by diarylthioureas.

One year later, the same group, evaluating the catalytic effect of a small library of symmetrical *N,N'*-disubstituted thioureas in the [4+2] cycloaddition reaction between cyclopentadiene (**40**) and a series of α,β-unsaturated ketones/aldehydes, such as **44**, to obtain product **46**, clarified why the structure of the catalyst **42** proved to be superior in terms of rate acceleration compared to the others tested (Scheme 1.10).[65] The result was rationalised by a combination of two major factors. Firstly, the increased acidity of the N-H protons in **42** compared to **41**, caused by the presence of an extra trifluoromethyl group on each aromatic ring, will augment the H-bond donating ability of the catalyst. Secondly, the presence of a structure-rigidifying H-bonding interaction (*i.e.* **A**, Scheme 1.10) between the Lewis basic sulfur atom of the thiourea and the polarised (by the adjacent electron-withdrawing group) *ortho*-protons of the substituted anilines. This computationally determined interaction would also facilitate the catalysis, reducing the entropy loss arising upon binding of the substrate to the catalyst **42**.[65]

11
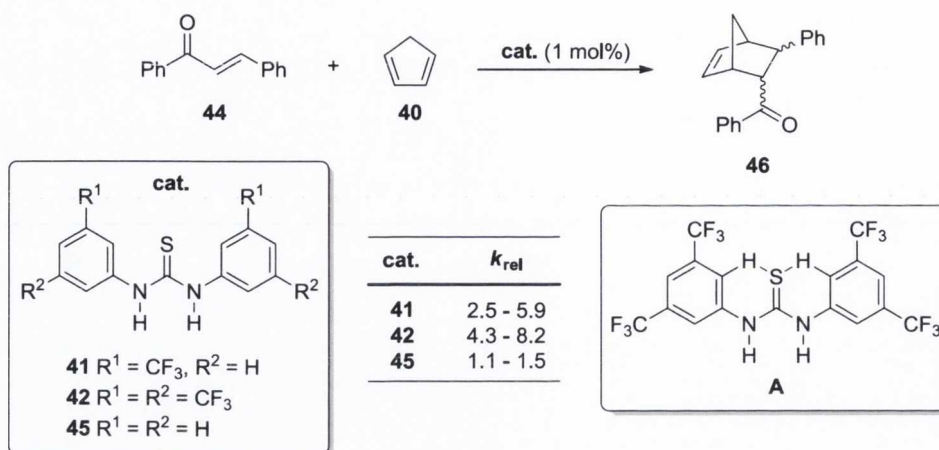
Scheme 1.10 Diarylthiourea substituent effect in the catalysed [4+2] cycloaddition reaction.

In the following years many other research groups around the world moved their attention towards this new and promising area of catalysis, expanding the scope of this type of activation to a greater number of chemical transformations. A few selected examples from the remarkable number of publications available in literature are presented below.

In 2003, Takemoto *et al.* reported the promotion of the nucleophilic addition of cyanide (TMSCN) and ketene silyl acetals to nitrones by a variety of diaryl(thio)ureas.[66] High yields and significant rate accelerations were observed. These were explained in terms of interactions between nitrones and thioureas according to the model proposed by Schreiner and co-workers. This was supported by NMR spectroscopic experimental data.[66]

In 2004, Connon *et al.* described a DABCO-promoted Baylis-Hillman reaction between methyl acrylate (**47**) and aromatic aldehydes such as **48** to produce **50**, that was accelerated by catalytic amounts of acidic diaryl(thio)ureas (Scheme 1.11).[67] Appreciable increase in the reaction rate, compared to the uncatalysed process, was observed when using the diarylurea **49** as catalyst (Scheme 1.11). The mechanism proposed involved binding and stabilisation of the Zwitterionic ammonium enolate intermediate **51** (Scheme 1.11) to the catalyst with concomitant acceleration of its addition to the aldehyde (the rate-determining step of the reaction).
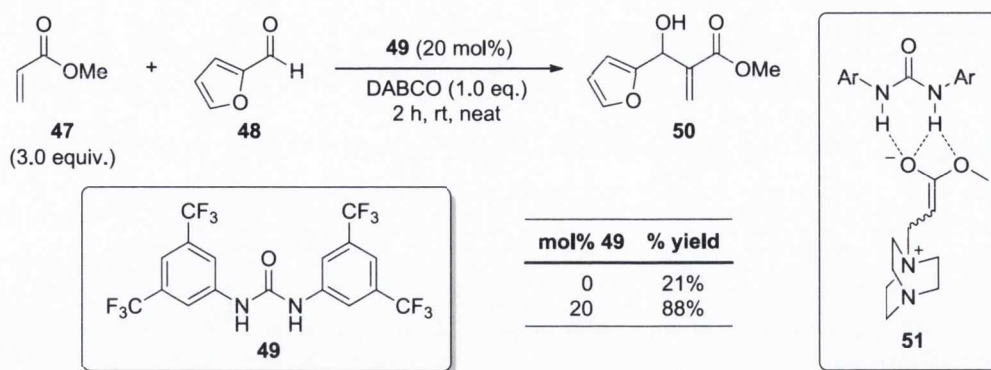
Scheme 1.11 Baylis-Hillman reaction catalysed by the *N,N*-diarylurea **49**.

During the same year, a study conducted by Ricci and co-workers demonstrated the use of diaryl(thio)ureas as catalysts for the acceleration of the Friedel-Crafts alkylation of aromatic and heteroaromatic *N*-containing derivatives with nitroalkenes.[68] The group hypothesised an electrophilicity-enhancing interaction between the nitroolefins and the urea catalysts as an explanation of the results obtained.

Three years later, in 2007, Schreiner *et al.* developed a procedure for the reduction of a variety of aldimines using diarylthiourea **42** as a hydrogen-bonding catalyst in presence of the Hantzsch ester as a formal source of hydrogen.[69] Under the optimised conditions at 1 mol% catalyst loading, the activation of the substrate by the thiourea derivative catalyst **42** allowed the reaction to proceed in 15 hours at room temperature with high product yields.

In 2008, Connon and co-workers reported that catalytic amounts of electron-deficient diarylurea **49** can be used as a H-bonding catalyst in order to promote the sulfonium ylide-mediated epoxidation reaction (Corey-Chaykovsky reaction) of a broad range of aldehydes for the first time (Scheme 1.12).[70]
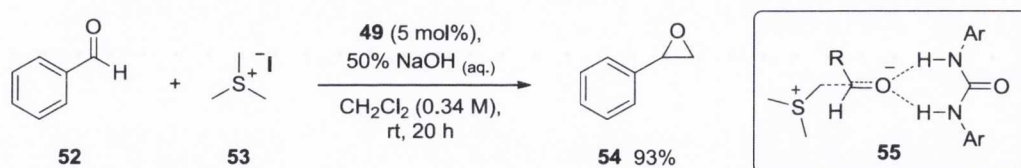
Scheme 1.12 *N,N*-Diarylurea-catalysed Corey-Chaykovsky reaction.

The reaction between benzaldehyde (**52**) and **53** for example, promoted by catalyst **49** under the conditions depicted in Scheme 1.12, furnished product **54** in high yield. The

role of the catalyst, as explained, was to stabilise the developing negative charge on the oxygen heteroatom (**55**, Scheme 1.12) during the rate-determining step (*i.e.* addition of the ylide to the aldehyde).

In 2011, Connon *et al.* also described the first transthioesterification reaction catalysed by urea-derivative H-bond donors between bulky chiral thioesters and unhindered achiral thiols.[71] The combined use of the urea catalyst with a co-catalyst base (DIPEA) allowed this process to take place efficiently at room temperature.

1.2.2 Chiral (thio)urea moieties as organocatalysts

In 1998, Jacobsen and co-workers, while studying and evaluating new ligands for the metal ion-promoted asymmetric hydrocyanation of imines (Strecker reaction), found that the reaction carried out in presence of one specific ligand but in absence of the metal (*i.e.* the control reaction) unexpectedly furnished better results, providing enhanced enantioselectivity.[38] The group then, while embarking upon a series of combinatorial experiments aimed at optimising the catalyst structure in order to obtain the highest level of stereocontrol, identified the thiourea derivative **59** as the most efficient catalyst (Scheme 1.13). The catalyst was then evaluated under optimised conditions in the Strecker reaction involving aromatic and aliphatic imine derivatives such as **56** and **57** respectively, using HCN (**58**). The results proved the ability of **59** as powerful asymmetric catalyst, furnishing the Strecker adduct products **60** and **61** in good yield and high enantioselectivity (Scheme 1.13).
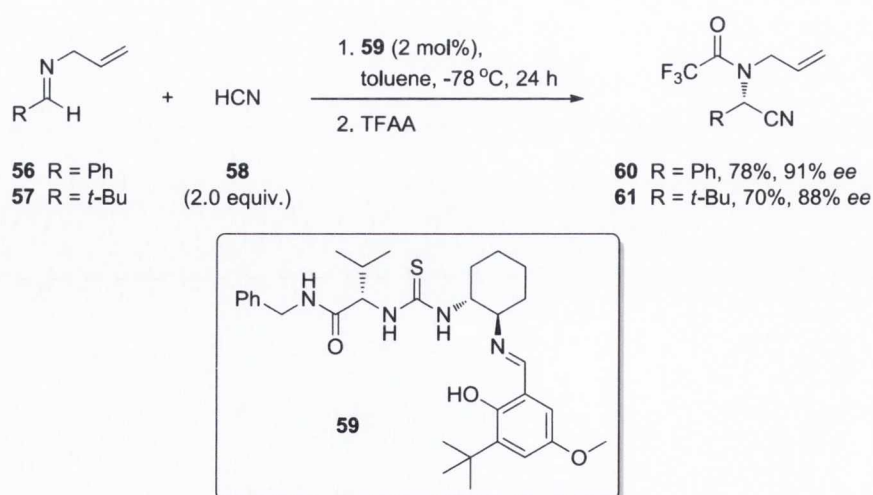
Scheme 1.13 Asymmetric Strecker reaction with chiral thiourea derivative catalyst **59**.

It was demonstrated by computational and mechanistic studies that, in order to reduce the steric hindrance with the bulky imine substituents, the catalyst favourably binds the (Z)-isomer of the imine by donating two hydrogen bonds to the imine lone pair.[72] Further optimisations carried out by the same group resulted in the development of better-performing catalysts with concomitant expansion of the scope of the reaction to a wider variety of imine derivatives.[73] Among these, the catalytic enantioselective Strecker reaction involving ketoimines allowed the synthesis of enantiopure quaternary amino acids for the first time using such a process.[74]

In the following years, the same group expanded the scope of this new type of chiral (thio)urea organocatalysts, efficiently applying them to other stereoselective chemical transformations such as Mannich reactions,[75] hydrophosphonylation reactions,[76] Pictet-Spengler reactions[77] and nitro-Mannich reactions.[78]

1.3   Chiral bifunctional organocatalysts containing (thio)urea moieties

Soon after the discovery of the potential of the chiral (thio)ureas as catalysts, the concept of introducing a second functionality (*i.e.* a Lewis base) into the structure of the catalyst began to be investigated. This allowed the extension of the applicability of such catalysts to the reactions that require simultaneous activation of both electrophile and nucleophile; in a fashion that better mimics the mode of action of enzymes.

The first example of bifunctional organocatalysis promoted by (thio)urea derivatives was introduced in 2003 by Takemoto and co-workers. They reported that a catalytic amount of **64** was able to promote the Michael reaction of malonates (*e.g.* **62**) to nitroolefins (*e.g.* **63**) with high enantioselective formation of **65** under the optimised conditions (Scheme 1.14).[79] They demonstrated that in order to obtain high yields and selectivity, both the thiourea moiety and the tertiary amino group have to be present on the same chiral scaffold. During further optimisation aimed at expanding the scope of both nucleophilic and electrophilic reaction components, they proposed a pre-transition state assembly to rationalised the observed stereocontrol.[80]
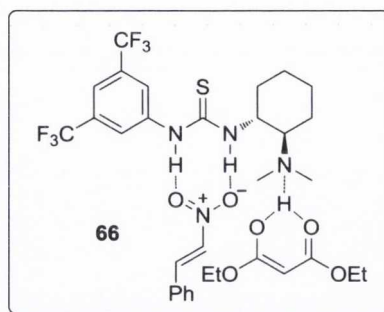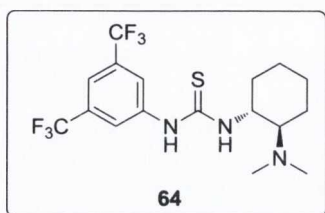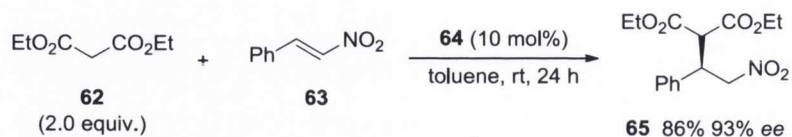
Scheme 1.14 The first bifunctional thiourea-based organocatalyst used in a Michael reaction.

They postulated that the H-bond donation from the (thio)urea to the nitroalkene and the deprotonation of the malonate (in the transition state) by the tertiary amine, simultaneously exploited by the catalyst, would be able to control the approach of the pronucleophile to just one face of the thiourea-activated nitroolefin (**66**, Scheme 1.14).[80]

The group then expanded the applicability of catalyst **64** to other substrates, reporting the results of studies in which the molecule was able to promote the addition of malonitrile to α,β-unsaturated imides[81] and the nitro-Mannich reaction (aza-Henry) of imines.[82,83]
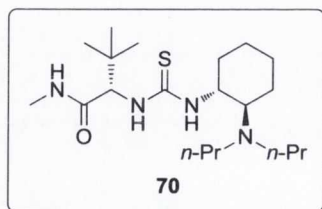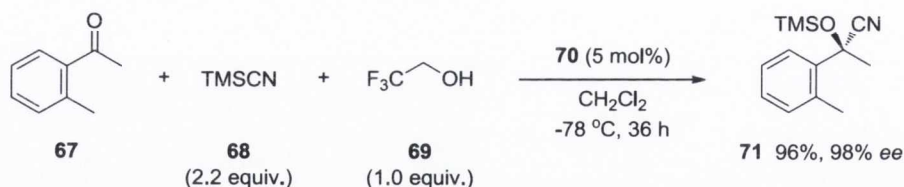
Scheme 1.15 Cyanosilylation of ketones catalysed by thiourea derivative **70**.

Jacobsen and co-workers also directed their attention towards bifunctional catalysis modifying their catalysts (*e.g.* **59**, Scheme 1.13) by removal of the Schiff-base and

incorporation of a tertiary amine. They reported that low loadings of catalyst **70** efficiently promoted the enantioselective cyanosilylation of ketones such as **67** using trimethylsilyl cyanide (**68**) and a stoichiometric amount of 2,2,2-trifluoroethanol (**69**) as additive for the *in situ* generation of HCN, furnishing products such as **71** in high yield and enantioselectivity (Scheme 1.15).[84]

1.4   Cinchona alkaloids as bifunctional organocatalysts: an invaluable structural template

After the discovery of the antimalarial property of the bark of several species of a western South American tree (the cinchona trees) at the beginning of the seventeenth century, cinchona alkaloids were introduced to the European market and the active compounds (*e.g.* quinine (**72**)) were isolated.[85] The major constituents of the extract of the bark are quinine (**72**), cinchonidine (**73**) and their *pseudo*enantiomers quinidine (**74**) and cinchonine (**75**) and together they constitute the 'starting point' for any cinchona alkaloid-based organocatalyst (Figure 1.1).[86] The simultaneous presence of an electrophile-activating H-bond donating hydroxy function and a bulky basic quinuclidine positioned in close proximity on a reasonably rigid chiral structure, combined with the readily accomplished tunability of the C-9 hydrogen bond donating substituent, together with the low cost and availability of both *pseudo*enantiomers, made these bifunctional molecules and their derivatives very successful in asymmetric organocatalysis.[87]

| 72 | 73 | 74 | 75 |
| quinine | cinchonidine | quinidine | cinchonine |
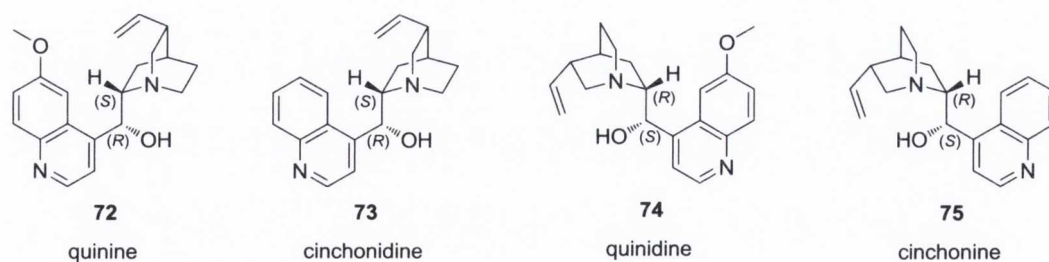
Figure 1.1   Selected cinchona alkaloids.

One of the first important uses of these alkaloids in organic chemistry dates to 1853, when Pasteur used them as resolving agents for the separation of a racemic mixture of tartaric acid.[88] Their first use as asymmetric catalysts was for the rate acceleration of the addition of HCN (**58**) to benzaldehyde (**52**), described in 1912 by Breding and Fiske (Scheme 1.16).[89]
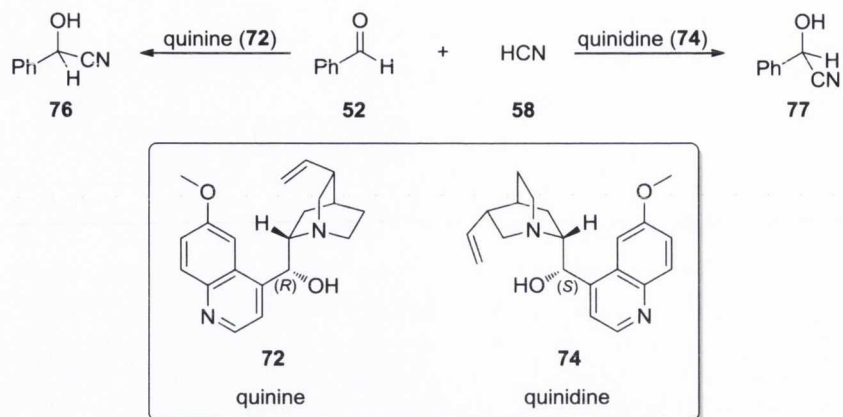
Scheme 1.16 The cinchona alkaloid-catalysed addition of HCN (**58**) to benzaldehyde (**52**).

Although this work reported low product enantiomeric excess (as optical rotation), it demonstrated the possibility of obtaining enantioenriched products (such as **76** and **77**) of opposing chirality if the reaction was performed using either quinine (**72**) or its *pseudo*enantiomer quinidine (**74**).

It was not until the early 1980s that the potential of cinchona alkaloids in asymmetric catalysis began to be realised. Based on seminal studies by Pracejus,[90] Wynberg and co-workers reported the use of cinchona alkaloids (*e.g.* **73**) and other natural and modified alkaloids in the enantioselective addition of aromatic thiols such as **79**, to cyclic α,β-unsaturated ketones such as **78**, furnishing the thioether product **80** (Scheme 1.17).[51] The authors attributed the selectivity obtained to the bifunctional mode of action of cinchona alkaloids. The hydroxy group was posited to act as a H-bond donor for the activation of the electrophile (*i.e.* **78**) while the tertiary amine acts as a chiral base to deprotonate the thiol **79** in the transition state.
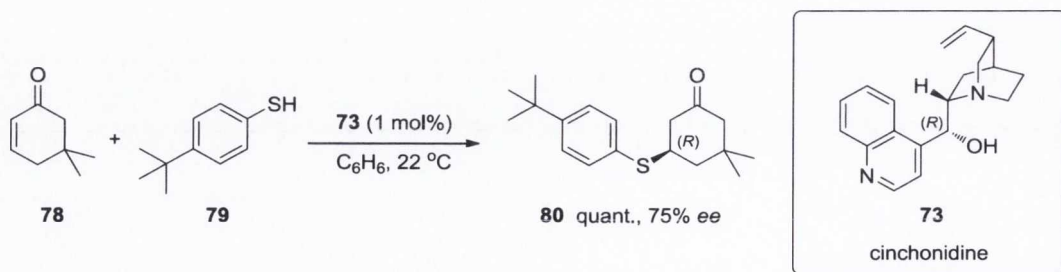
Scheme 1.17 Enantioselective addition of thiols to cyclic enones catalysed by cinchona alkaloids.

From this point on, the use of cinchona alkaloids as bifunctional asymmetric catalysts in organocatalysis began to slowly expand but the popularity of these molecules and their derivatives grew exponentially from the late 1990s.[85–87,91,92] An ever increasing number of research groups around the globe turned their attention to this growing research field, developing new catalysts to expand the reaction scope and nowadays cinchona alkaloids and their derivatives are considered to be "privileged chiral catalysts" in organocatalysis as they already were in metal-catalysed processes.[93] An important example of the use of cinchona alkaloids as metal ligands is the osmium-catalysed asymmetric dihydroxylation (AD) developed by Sharpless and co-workers for which the author was awarded a share of the Nobel Prize in chemistry in 2001.[94]

1.4.1 Cinchona alkaloid organocatalyst functionalisation: common structural modifications

As previously mentioned, many structural modifications of the most common cinchona alkaloids have been investigated over the years in order to achieve better performance in a wider number of reactions.

The core of these catalysts can be easily modified by chemical transformations to adapt their electronic and structural characteristics to tailor the anticipated requirements associated with catalysis of specific reactions.

quinine numbering

common structural
modification positions
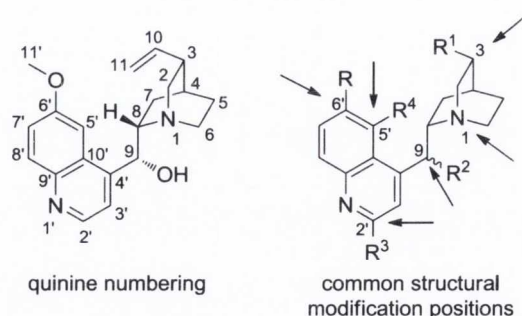
Figure 1.2   Quinine numbering and the positions most frequently modified.

As shown in Figure 1.2, there are six positions on the structure (*i.e.* N-1, C-3, C-9, C-2', C-5' and C-6') that have been commonly modified. With the molecules generated from these modifications it is now possible to catalyse a diverse array of organic transformation classes in a highly stereoselective manner.

19

1.4.1.1 Modification at C-9

The most commonly modified position of cinchona alkaloids is certainly the C-9 position. The naturally present chiral secondary alcohol can be easily substituted or derivatised, with either retention or inversion of the configuration, in order to either achieve control over the H-bond donating characteristics (introduction of (thio)ureas, amides, *etc.*) or to bring about a completely different catalyst mode of action (*e.g.* aminocatalysis by substitution with the free amino group), to that possible using the parent alkaloid.

1.4.1.1.1 Introduction of (thio)urea moieties

After the pivotal work of Takemoto on bifunctional chiral thiourea derivatives as organocatalysts[79,80,82] and during a time when the use of cinchona alkaloids in asymmetric organocatalysis was growing fastest,[86] four different authors intent on developing more powerful H-bond donating cinchona alkaloid derivatives, independently began to evaluate the use of C-9 (thio)urea substituted structures.

Chen and co-workers were the first to evaluate thiourea organocatalysts derived from cinchonidine (**73**, Figure 1.1) and cinchonine (**75**, Figure 1.1) in the enantioselective Michael addition of thiols to α,β-unsaturated imides.[95] Although the reactions proceeded in high yields, the product enantiomeric excess obtained were extremely poor (<20% *ee*).
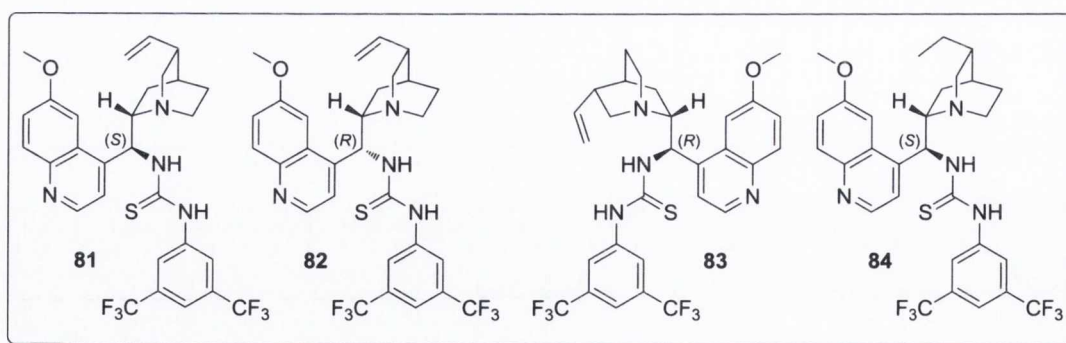
Figure 1.3   Thiourea-substituted cinchona alkaloid organocatalysts for the Michael reaction.

Soon afterwards, Soòs *et al.* reported the use of four thiourea-substituted cinchona alkaloid catalysts (Figure 1.3) in the Michael-type addition of nitromethane (**85**) to (*E*)-chalcone (**44**, Scheme 1.18).[96]

Catalysts **81** and **82** were obtained from quinine (**72**, Figure 1.1) with C-9 inversion and retention of configuration respectively, and catalyst **83** from quinidine (**74**, Figure 1.1) with C-9 inversion of configuration. The results obtained were quite unexpected: catalyst **82** completely failed to promote the reaction while **81** and **83** furnished product **86** in moderate to good yields and high enantioselectivity.

cat.	yield (%)	ee (%)	abs. config.
81	71	95	(*R*)
82	0	-	-
83	59	86	(*S*)
84	93	96	(*R*)
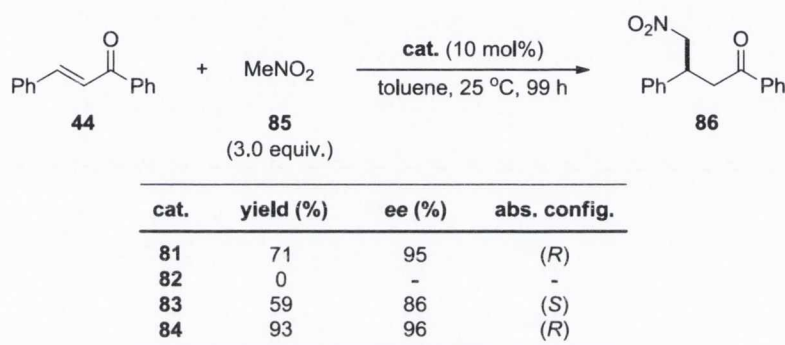
Scheme 1.18 Enantioselective addition of nitromethane (**85**) to (*E*)-chalcone (**44**) catalysed by thiourea-substituted cinchona alkaloids.

These results demonstrate the importance of possessing the correct relative orientation of the catalytic active groups for effective bifunctional catalysis to occur: the thiourea-substituted cinchona alkaloid organocatalyst bearing the 'natural' stereochemistry (*i.e.* **82**) proved to be inactive. A further improvement of the reaction in terms of both enantioselectivity and yield was obtained when the reaction was performed in presence of catalyst **84**, synthesised from dihydroquinine with inversion of configuration.

Shortly after Soòs' report,[96] Connon and co-workers published a series of studies which examined the effect that substitution of the C-9 hydroxy group by an aryl(thio)urea, with both retention and inversion of configuration, would have on catalyst performance. They synthesised a small library of (thio)urea-substituted catalysts derived from dihydroquinidine (**89**) and dihydroquinine (**90**) and evaluated them in the asymmetric addition of dimethylmalonate (**87**) to nitrostyrene (**63**, Scheme 1.19).[97]
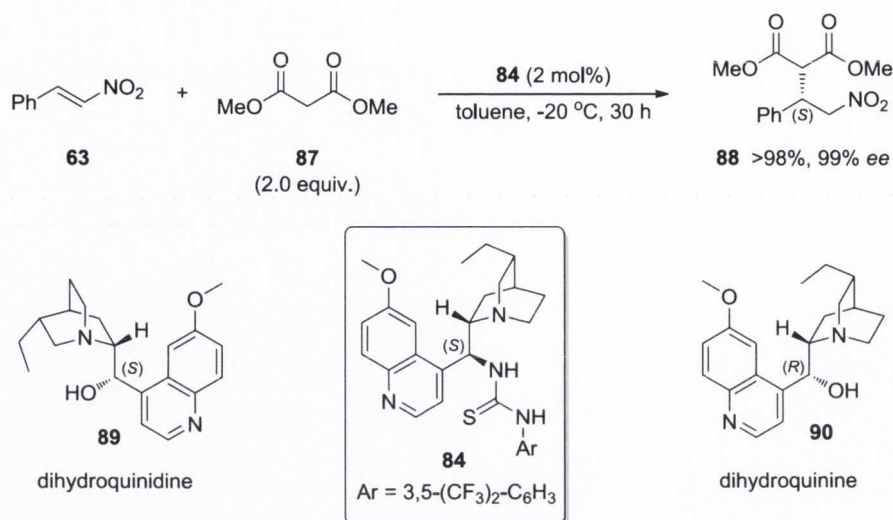
Scheme 1.19 Michael addition catalysed by thiourea cinchona alkaloid derivative.

The most successful catalyst proved to be **84**, the use of which allowed the generation of product **88** in high yields and enantioselectivity under the optimised conditions. From the results obtained, they rationalised that modifications such as substitution of the C-9 hydroxy group with a (thio)urea moiety and the C-9 stereochemistry inversion are both required in order to achieve high stereocontrol and reaction rate, with superior activity exhibited by the thiourea species.[97] This demonstrated again the strong relationship between the relative stereochemistry of catalysts at C-8/C-9 and their activity as bifunctional organocatalysts, as already reported by Soòs[96] and previously discussed here.

Concurrently, Dixon *et al.* reported the evaluation of a family of C-9 substituted cinchona alkaloid organocatalysts derived, with inversion of configuration relative to the natural alkaloid, from cinchonine (**75**, Figure 1.1), in the Michael addition of **87** to **63** (Scheme 1.20).[98] This work corroborated the results reported by Connon[97] and Soòs[96] regarding the requirement for the correct arrangement of the two chiral catalyst functionalities in order to achieve high yields and enantioselectivity. The superior activity of catalysts capable of double H-bonding compared to single H-bond donors was also highlighted when (sulfon)amide-substituted cinchona alkaloid catalysts (*i.e.* **93**, **94** and **95**, Scheme 1.20) were evaluated in the reaction.[98] Under the optimised conditions, catalyst **91** promoted the addition of **87** to **63**, giving **92** in high yield and enantioselectivity (Scheme 1.20).
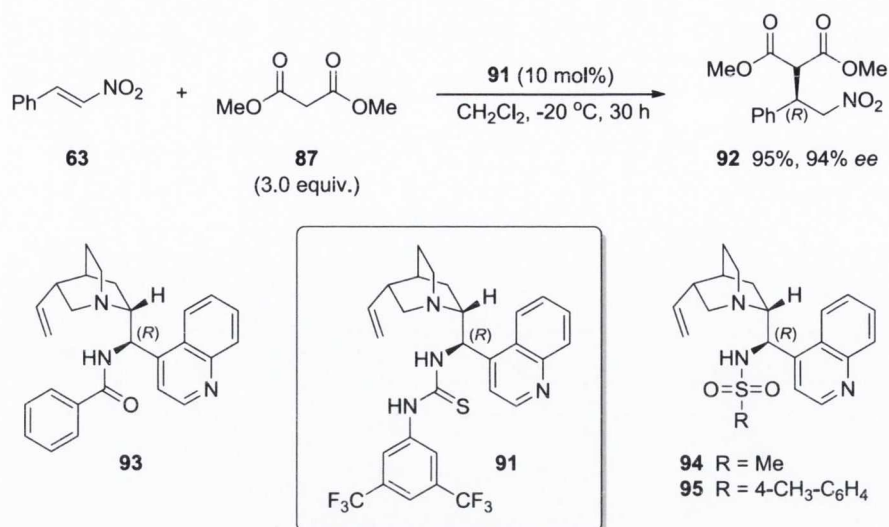
Scheme 1.20 Cinchonine thiourea derivatives as an enantioselective organocatalyst for the Michael reaction.

1.4.1.1.2 Introduction of squaramide moieties

Within the pool of H-bond donating asymmetric catalysts[92] the leading role has been played, for many years, by chiral structures based on (thio)urea derivatives.[47] Although other H-bond donors have appeared in the literature over the years, the ability of (thio)urea derivatives to form two H-bonds with a substrate and direct it to a particular and well-defined geometry, forms the basis for their incredible success.

Recently, Rawal and co-workers, while exploring new motifs for H-bond donation, developed a new class of catalyst capable of such activation based on squaramides.[99]

These unusual molecules proved to be highly active as H-bond donors as a result of their particular structure which confers to these molecules a behaviour very similar to (thio)urea moieties and yet exhibits significant physical differences that make them distinct (Figure 1.4).[100]

Derived from squaric acid (**96**), secondary squaramides (**97**, **I**, Figure 1.4) exhibit duality in H-bonding as they possess the ability of both anion and cationic recognition (a property much more limited in (thio)ureas), allowing the interaction with donors, acceptors and mixed donors-acceptors species, forming up to four H-bonds (**II**, Figure 1.4).[100,101] Considered as vinylogous amides, squaramides are structurally more rigid than their (thio)urea counterparts, as the lone pair of both nitrogen atoms can be

delocalised through the ring system, restricting the two C-N bond rotations and imparting a planar structure to the molecule (**III**, Figure 1.4).[100,101]
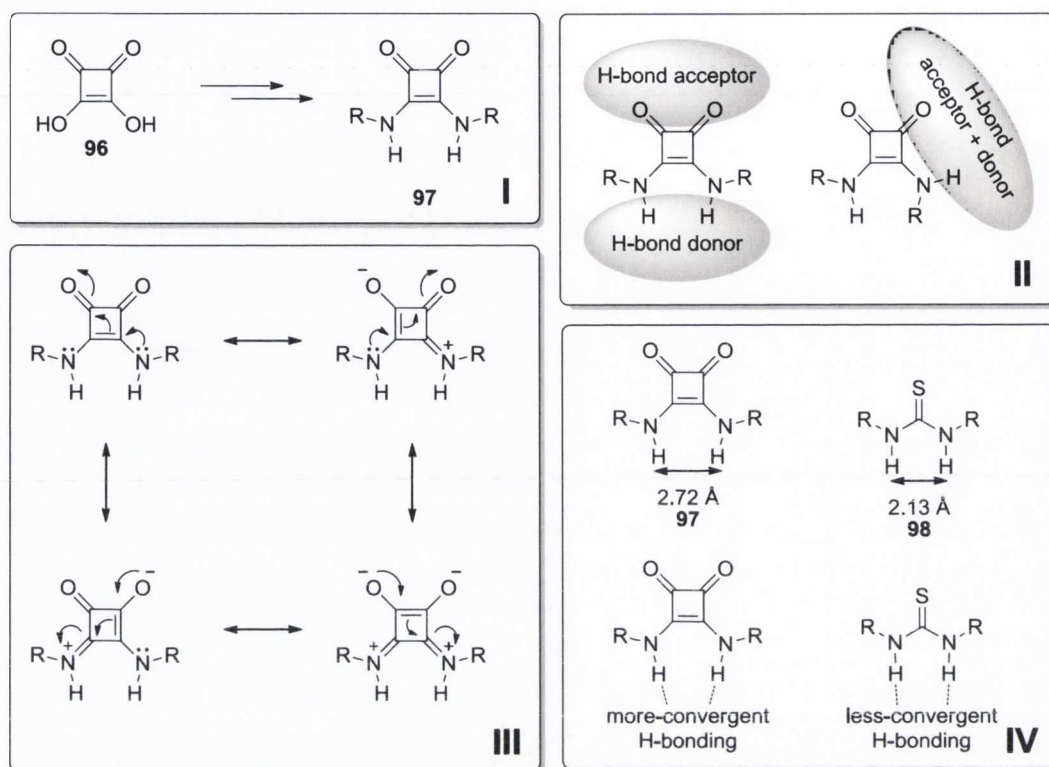
Figure 1.4   The physical and structural properties of the squaramides.

Higher aromaticity (according to the Hückel rule ($4n + 2$; $n = 0$)) obtained upon H-bond formation, is the basis of the superior H-bond donating ability of squaramides compared to (thio)urea.[100,101] It is also presumed that the greater distance between the two acidic hydrogen atoms[99] (*i.e.* **97** = 2.72 Å, **98** = 2.13 Å) and their more convergent orientation imposed by the ring structure could also be responsible for the different binding proprieties and thus influence transition states in asymmetric catalysis, in a different way to thiourea analogues (**IV**, Figure 1.4).[100]

For these reasons, Rawal and co-workers decided to develop a squaramide C-9 substituted cinchona alkaloid organocatalyst and evaluate it in the addition of 1,3-dicarbonyl compounds (*e.g.* **99**) to nitroolefins (*e.g.* **63**, Scheme 1.21).[99] Catalyst **100** proved to be extremely efficient at promoting the addition of **99** to **63** at low loading, furnishing the adduct product **101** in high yield and enantioselectivity.
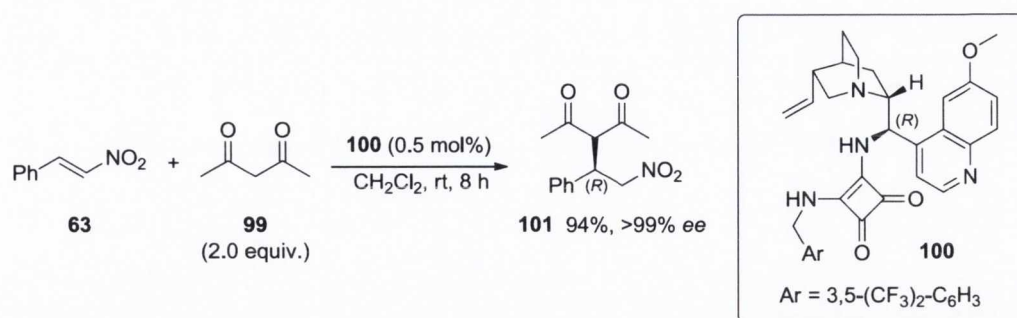
Scheme 1.21 A squaramide-based cinchona alkaloid organocatalyst for a Michael-type reaction.

As a result of Rawal's influential study[99] the use of squaramide-substituted cinchona alkaloids and, in general, squaramide-based H-bonding catalysts began to expand and currently several other applications of this new type of hydrogen-bonding group have been reported.[100]

1.4.1.1.3 Other C-9 substitutions

The cinchona alkaloid C-9 substitutions described in the previous section are not the only strategies studied and reported in the literature. Other structures have been designed and proved to be extremely efficient in catalysing many chemical transformations. Some examples include ester groups,[102] sulfonamides[103] and aryl groups.[104,105]

Another very commonly employed modification is the substitution of the C-9 hydroxy group with a free amino group. The structures generated by this transformation belong to the group used in asymmetric aminocatalysis[106,107] based on either 'enamine' catalysis or 'iminium' catalysis for the activation of nucleophile or electrophiles, respectively. This was briefly discussed in Section 1.1.1 and will not be discussed further here, as they are outside the scope of this thesis.

1.4.1.2 Modification at C-6'

In 1999, Hatakeyama and co-workers published a series of studies which aimed to improve catalysis of the Baylis-Hillman reaction by using demethylated cinchona alkaloids as promoters.[108] The most successful catalyst reported was the conformationally rigid, cyclic ether quinidine-derived cyclic ether **102** (Figure 1.5). The stereoselectivity observed was attributed to the resulting augmentation of

nucleophilicity of the amine due to the reduced steric hindrance around the nitrogen, in conjunction with the H-bond donating potential associated with by the C-6' demethylated phenolic hydroxy group.[108]

In 2004 Deng *et al.* described the use of demethylated cinchona alkaloids such as **103** (Figure 1.5) as efficient catalysts for the enantioselective Michael-type reaction between malonates and nitroolefins in high yield and enantioselectivity.[109] They claimed that both hydroxy groups were participating in the stabilisation and organisation of the transition state, in combination with the basic quinuclidine ring.

In 2006 Hiemstra *et al.*, developed a new cinchona-based organocatalyst that was capable of H-bond donation for the addition of nitromethane to carbonyl compounds (the Henry reaction). Inspired by the earlier study reported by Soòs,[96] they described the synthesis of a 6'-thiourea-substituted, C-9-oxy-benzylated cinchona alkaloid derivative **104** (Figure 1.5) as an efficient promoter of the reaction in high yield and enantioselectivity.[110] They proposed a plausible mechanism in which the activation of the aldehyde by double H-bonding to the thiourea moiety and the activating effect of the basic nitrogen atom of the quinuclidine ring on nitromethane, constitute the basis for such high stereocontrol.
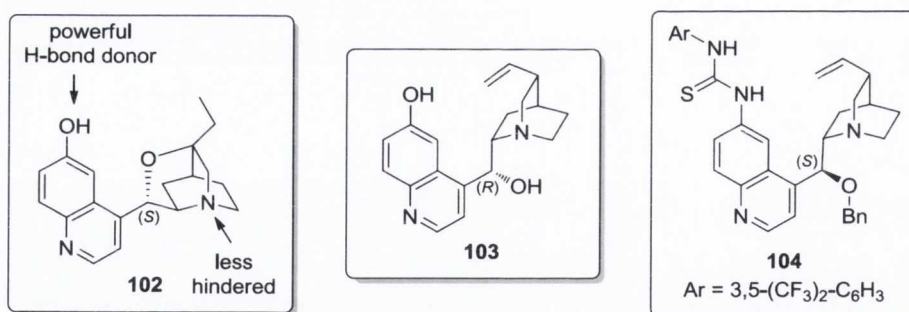
Figure 1.5   Selected C-6' modified cinchona alkaloids: representative examples.

Other more recent reports of the use of C-6' substituted cinchona alkaloid derivatives have emerged. For example, the enantioselective aza Morita-Baylis-Hillman reaction,[111] annulation reaction[112] and asymmetric conjugate addition of thiols[113] have been shown to be susceptible to asymmetric catalysis by these bifunctional molecules.

1.4.1.3 Modification at C-2'

The modification of the cinchona alkaloid core structure at the C-2' position was first introduced in 2006 by Gaunt and co-workers in order to fine tune the catalysts' behaviour. Studying the use of quinine and quinidine derivatives such as **105** (Figure 1.6) in the catalytic enantioselective intramolecular cyclopropanation reaction of halogenated ketones *via* quinuclidine-ammonium ylide intermediates **106**[114] (Figure 1.6), they noticed that the reactions carried out with **105** were furnishing products with high yields but poor enantiomeric excesses. They attributed this to the catalyst- and starting material-consuming formation of the unreactive ammonium ylide intermediate **107** (Figure 1.6) by reaction of the quinoline nitrogen with the α-haloketone. They therefore introduced a methyl substituent at the C-2' position to sterically hinder the quinoline nitrogen atom in order to retard the formation of **108**. Utilising catalyst **109** (Figure 1.6), the reactions proceeded smoothly, furnishing the desired products in higher yields and excellent enantioselectivity.
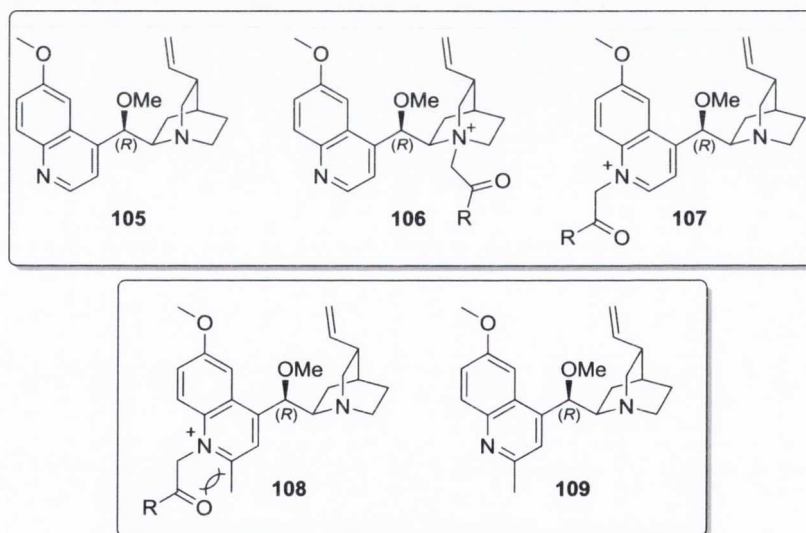
Figure 1.6   A C-2' modification to improve catalysis of a intramolecular cyclopropanation reaction.

Another example in the literature of bifunctional catalysts which uses C-2' modifications of the structural core of cinchona alkaloids was published by Deng *et al.* in 2012.[115] Studying the asymmetric isomerisation of imines catalysed by cinchona alkaloid derivatives to furnish trifluoromethyl amines, the group, in order to improve the catalytic activity and enantioselectivity, developed a series of cinchona alkaloid

derivatives and evaluated them as promoters of the isomerisation reaction of the aromatic trifluoromethyl imines. Catalyst **111**, which contains a chlorine atom as substituent at C-2' position, proved to be the most efficacious in the promotion of the reaction of aromatic and aliphatic imines such as **110** and **115**, furnishing the desired products **113** and **116** in high yield and enantioselectivity (Scheme 1.22). These molecules, after acid hydrolysis, furnished the relative chiral amines **114** and **117** respectively in high *ee*.
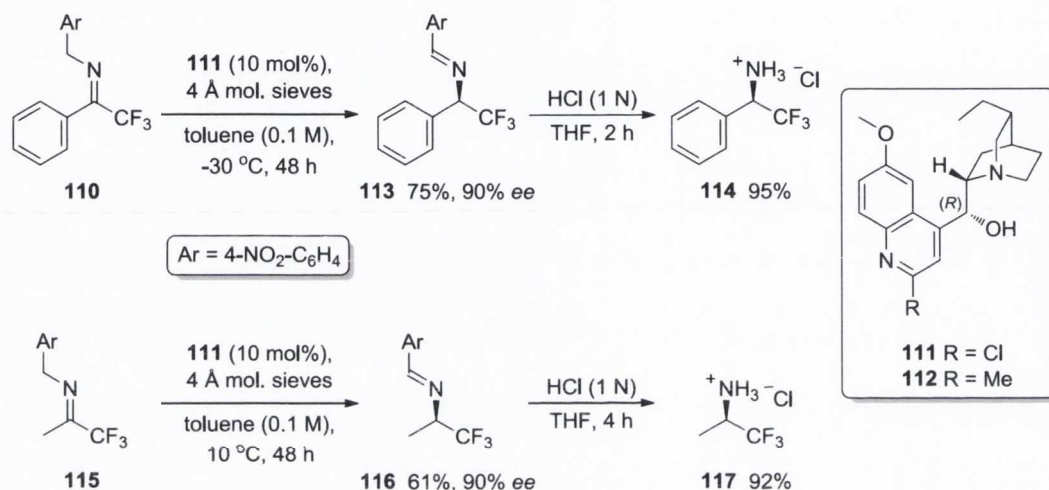
Scheme 1.22 Asymmetric isomerisation of imines catalysed by C-2' substituted cinchona alkaloid organocatalysts.

The authors stated that the presence of the C-9 hydroxy group in the structure was crucial for high activity and stereocontrol. They also reported that the electronic nature of the substituent at C-2' has a fundamental influence on the enantioselectivity of the process, as the C-2' methylated variant **112** catalysed the reaction with lower stereocontrol than **111**.[115]

Other examples of C-2' substituted cinchona alkaloid derivatives are available in the literature; however, they are confined either to different areas of asymmetric catalysis (*e.g.* aminocatalysis),[116] or different areas of chemistry such as organometallic chemistry where they are used as ligands.[117]

1.4.1.4 Modification at C-5'

In 2011 Connon *et al.* reported a study in which new cinchona alkaloid-based bifunctional organocatalysts with modified distances between the two catalytic

functionalities were prepared. Based on the seminal studies of Jørgensen[118] and Deng,[119] they decided to explore the effect that different substituents on C-9 and C-5' positions would have on the performance of a small library of catalysts in the enantioselective addition of nitromethane (**85**) to trifluoromethylketones (the Henry reaction) (Scheme 1.23).[120] Catalyst **120** proved to be optimal for the promotion of the addition of **85** to both aromatic and aliphatic trifluoromethylketones **118** and **119**, giving the products **121** and **122** in good yield and high enantioselectivity (Scheme 1.23).
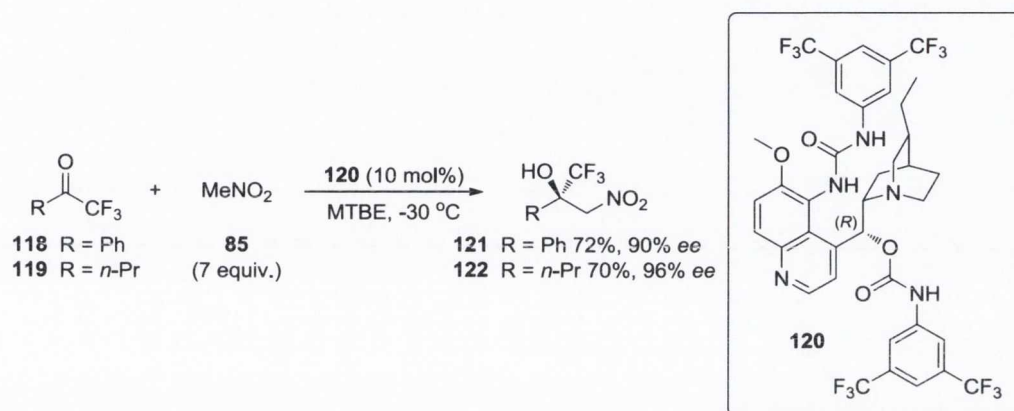
Scheme 1.23   C-5' substituted cinchona alkaloid-derived organocatalyst in the Henry reaction.

One year later, the same group, studying the relationship between the acidity of thiols in organocatalysed conjugated addition reactions and the enantioselectivity observed, developed a new C-5' substituted cinchona alkaloid catalyst **123** (Figure 1.7) with an alternative C-9 substituent to the one previously reported **120** (Scheme 1.23).
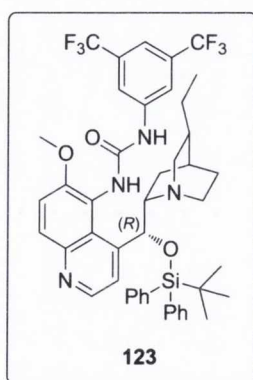
Figure 1.7   C-9 variant of catalyst **120** for the enantioselective addition of thiols to nitroalkenes.

Catalyst **123** promoted the enantioselective addition of various thiols to aromatic nitroalkenes in good yield and excellent enantioselectivity.[121]

1.4.1.5 Other modifications

The modifications of cinchona alkaloids reported above constitute the most common and widely used in asymmetric bifunctional catalysis. However, there are two more fundamental types of derivatives that are widely used in asymmetric catalysis which, for their peculiarity, belong to their own specific field.

The first of these relies on the immobilisation of the catalyst on a heterogeneous support in order to simplify the recovery of the catalyst at the end of the reaction. The immobilisation of cinchona alkaloid organocatalysts is usually achieved by chemical transformation of the terminal olefinic double bond on the quinuclidine ring.[122] The two supports commonly used are polymers[123] and magnetic nanoparticles[124] and these form part of the vast domain of solid-supported catalysis.[125]

The second is based on the derivatisation of cinchona alkaloid organocatalysts into chiral non-racemic salts, usually by alkylation of the nucleophilic nitrogen atom of the quinuclidine ring. The catalysts obtained can then be used in asymmetric phase transfer catalysis as a practical strategy for asymmetric organic synthesis.[126,127]

1.5 Formal cycloaddition reactions involving cyclic anhydrides: an historical overview

Anhydrides are of enormous synthetic significance as they (in general terms) occupy territory conveniently positioned between the highly reactive acyl halides and the more stable but considerably less reactive carboxylic acid ester electrophiles, and as such they have been used as electrophilic acyl transfer agents[128] for over a century.[129] While their chemistry is almost completely dominated by their electrophilicity, a relatively small number of cases involving the participation of enolisable anhydrides as nucleophiles in aldol-like coupling processes have been reported.[130]

The first example of an anhydride acting as a nucleophile was reported in 1868 by Perkin. He found that high temperature treatment of a mixture of aliphatic enolisable anhydrides **125** and salicylaldehyde (**124**) in presence of a weak carboxylate base such as sodium acetate, led to the formation of coumarins **126** (Scheme 1.24).[131,132]
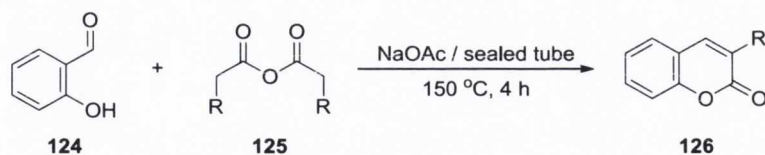
Scheme 1.24 Synthesis of coumarins by Perkin reaction between salicylic aldehyde (**124**) and enolisable aliphatic anhydrides.

He later expanded his original work, evaluating the reaction of other aromatic aldehydes **127** with several aliphatic enolisable anhydrides **125**. In all cases the product formed was an α,β-unsaturated acid such as **128** (Scheme 1.25).[133]
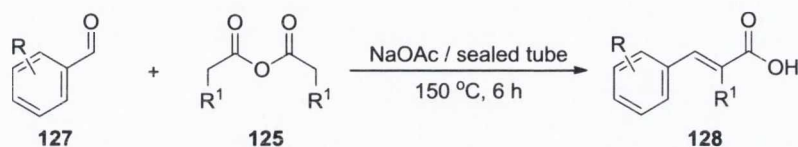
Scheme 1.25 Perkin reaction between aromatic aldehydes and enolisable aliphatic anhydrides.

In the same report he also described the use of cyclic enolisable anhydrides, such as succinic anhydride (**129**) in the reaction with benzaldehyde (**52**) in presence of sodium succinate (**130**) that, upon decarboxylation of the intermediate, gave the product **131** (Scheme 1.26).[133]
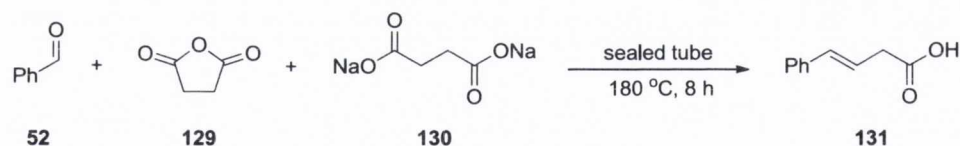
Scheme 1.26 Perkin reaction between benzaldehyde (**52**) and succinic anhydride (**129**).

Many years passed before Fittig and co-workers clarified the mechanism of action of the process. They repeated the reactions first discovered by Perkin but at lower temperatures (*i.e.* 100 °C) and concluded that, the reaction, similar to an aldol reaction, is an addition process of the anhydride to the aldehyde involving the formation of a β-hydroxy intermediate **132** followed by dehydration, leading to product **133** (Scheme 1.27).[134]

132 **133**
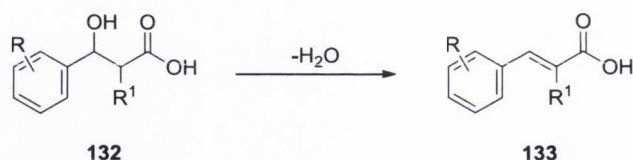
Scheme 1.27 Addition intermediate dehydration proposed by Fittig.

Further proof of the involvement of a β-hydroxy intermediate came also from the reaction between succinic anhydride (**129**) and benzaldehyde (**52**). Fittig stated that when the reaction is conducted at 100 °C the product formed is a substituted γ-butyrolactone called γ-phenylparaconic acid (**135**), formed by lactonisation of the intermediate hydroxy acid **134**. This molecule, if heated at temperatures above 150 °C, decarboxylates to furnish the product **131**; which was also observed by Perkin in his original study (Scheme 1.28).[134,135]

52 **129** **134** **135** **131**
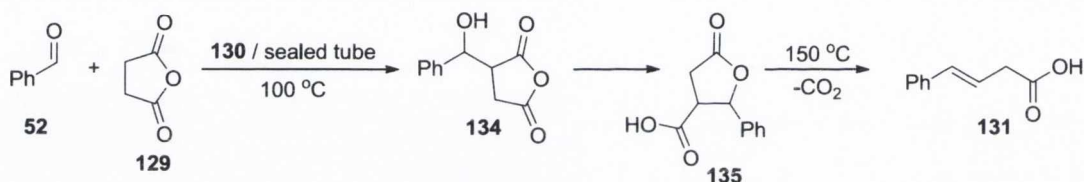
Scheme 1.28 Anhydride addition to benzaldehyde (**52**) followed by lactonisation proposed by Fittig.

Müller later described the condensation of the sodium enolate of homophthalic anhydride (**136**) with benzaldehyde (**52**) to form a dihydroisocoumarin derivative by a cycloaddition process between the two species that, similar to the cycloaddition of succinic anhydride to benzaldehyde, produced a lactone.[136]

In 1958 Pinder and co-workers, inspired by Müller's work, repeated the reaction using piperonaldehyde (**137**) to obtain the cycloaddition product **138**, confirming the reactivity observed in Müller's original study (Scheme 1.29).[137]

136 **137** **138**
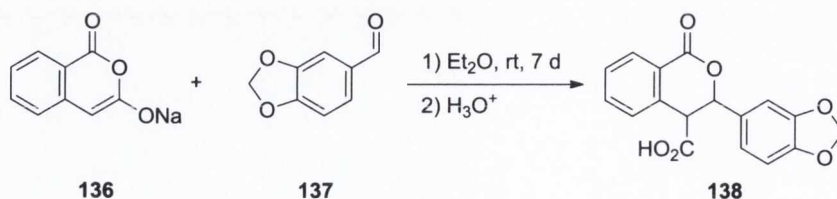
Scheme 1.29 Dihydroisocoumarin synthesis by condensation of homophthalic anhydride enolate (**136**) and aldehydes.

A decade later in 1969, while developing a new synthetic process for the synthesis of analogues of the alkaloid nicotine (**141**), Castagnoli *et al.* reported the first cycloaddition reaction between cyclic anhydrides and imines.[138] The reaction between succinic anhydride (**129**) and *N*-benzylidenemethanamine (**139**) under thermal conditions furnished the cycloadduct product **140** in good yield as mixture of diastereomers that ^{1}H NMR spectroscopic analysis demonstrated to be the *trans*-**140** (major) and *cis*-**140** (minor) isomers (Scheme 1.30).
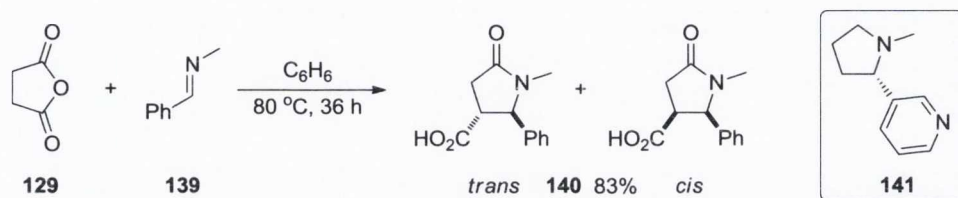
Scheme 1.30 Thermal cycloaddition of succinic anhydride (**129**) to imines.

They later expanded the scope of this reaction, extending it to glutaric anhydride (**143**).[139,140] The group, while studying the synthesis of nitrogen analogues of tetrahydrocannabinols, demonstrated that the *trans*-stereochemistry of the oxacycle in the unnatural tetrahydrocannabinols was a fundamental factor in order to obtain a potent physiological response.[139]
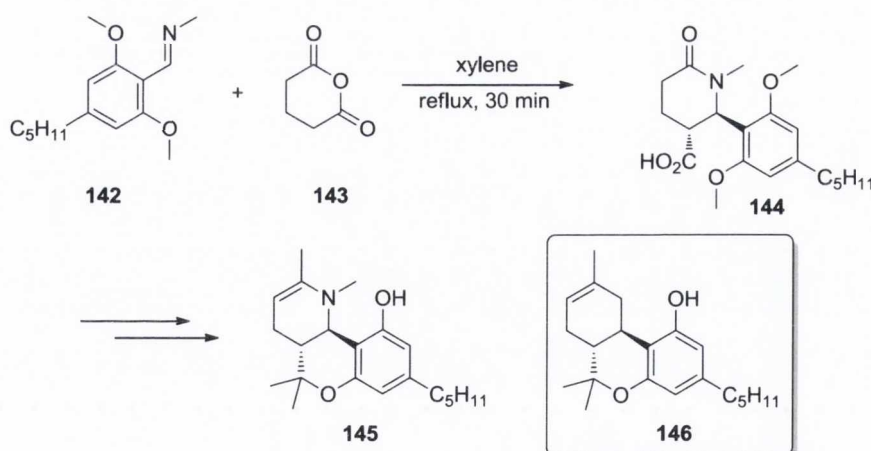
Scheme 1.31 Glutaric anhydride (**143**) cycloaddition to imines in natural product analogue synthesis.

They therefore applied the cycloaddition protocol discovered years before to glutaric anhydride as a strategy for the synthesis of the natural product analogue.[139,140] Following that procedure, the reaction between glutaric anhydride (**143**) and the imine

142 furnished the *trans*-cycloadduct **144** which, after purification by fractional crystallisation, was employed in the synthesis of **145**, an analogue of the natural product $\Delta^{1(6)}$-*trans*-tetrahydrocannabinol ($\Delta^{1(6)}$-THC, **146**, Scheme 1.31)[140] one of the two psychoactive constituents of *Cannabis Sativa*.[141]

A short time after, two reports, by Haimova *et al.*[142] and by Cushman and co-workers,[143] independently (and almost simultaneously), described the use of homophthalic anhydride (**147**) and derivatives in the cycloaddition reaction with imines such as **148** as an efficient method for the synthesis of substituted dihydroisoquinolonic acids (*e.g.* **149**) as mixture of *cis* and *trans* diastereomers (Scheme 1.32). The reaction proved to be wide in scope, as different homophthalic anhydrides and several imines were compatible, giving good yields and in some cases good diastereoselectivity.[143] However, some stereochemical differences between the two studies were revealed and years later explained by Cushman to be a consequence of epimerisation occurring during work-up.[144]
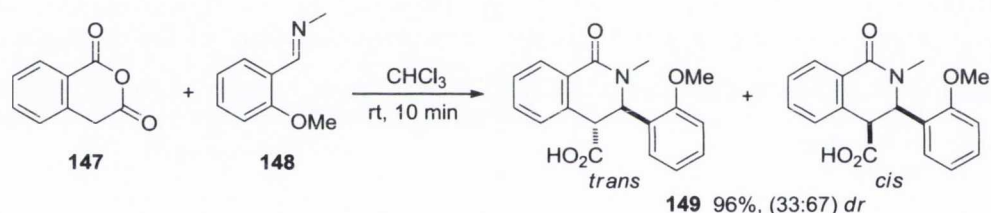
Scheme 1.32 Cycloaddition of homophthalic anhydride (**147**) to imines.

The cycloaddition reaction involving homophthalic anhydride was later expanded by Tamura *et al.* to different types of electrophiles and was used as a simple route to condensed phenolic compounds.[145] In 1981 the group described the regiospecific Diels-Alder reaction between **147** and carbon-carbon multiple bonds (*e.g.* **150**) under thermal conditions to furnish aromatic naphthol derivatives such as **151** (Scheme 1.33).
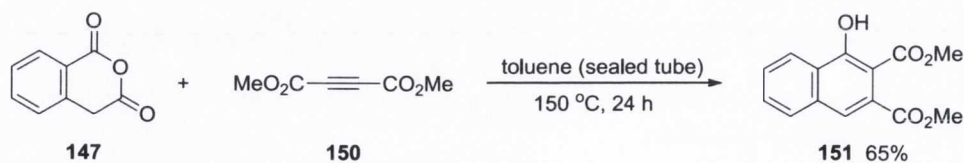
Scheme 1.33 Cycloaddition of homophthalic anhydride (**147**) to carbon-carbon multiple bonds.

They also proposed a series of plausible mechanisms (described in Section 1.5.3) in order to explain the formation of the products[146] suggesting that the anhydride was acting as a diene while the unsaturated alkenes / alkynes were acting as dienophiles.[145,146]

1.5.1   Cycloaddition reactions of anhydrides with imines

The cycloaddition reaction between imines and cyclic anhydrides has been widely used in synthetic chemistry.[130] However, since the first synthetic report by Castagnoli and co-workers in 1969,[138] the stereochemical outcome of the reaction could never be controlled. Castagnoli *et al.* did however report work in 1971 which aimed to clarify the mechanism of this reaction. They conducted a series of experiments on the thermal reaction between a series of aromatic imines and succinic anhydride.[147] They demonstrated that electron-donating *para*-substituents on the benzaldehyde-derived Schiff base increased the reactivity of the imines, furnishing higher yields of *cis/trans* diastereomers mixtures, with the *trans*-isomer as the major product.[147] This was in contrast to the Perkin-type mechanism (*i.e.* nucleophilic attack of the anhydride enol tautomer on the electrophile), which at the time was considered to be the likely reaction pathway, because a decrease in the reactivity of the imines was expected as a result of their reduced electrophilicity when substituted with electron-donating moieties. For this reason a different mechanism, based on the initial iminolysis of the anhydride by nucleophilic attack of the nitrogen atom of the imines on the electrophilic anhydrides was proposed, however this was not extensively studied.[147] The stereochemical outcomes of the reaction were also analysed, however only the ratio between the *cis* and the *trans* products formed in the reaction was reported. Although this work only partially addressed the stereochemical outcomes of the reaction, it formed the basis for the development of a new mechanism which was revealed by Cushman and co-workers in 1987.[144]

The group conducted a series of studies on the cycloaddition reaction between homophthalic anhydride and a series of *para*-substituted imines; examining the electronic and steric effects that different substituents either on the nitrogen atoms or in *para* position of the Schiff base would have on the ratio between the *cis* and *trans* products formed in the reactions. They proposed three plausible mechanisms as a

rationalisation for the stereochemical outcome of the reaction and, from the data gathered from these experiments, they were able to identify the correct one.[144]

The first of these (Scheme 1.34)[144] involved a Diels-Alder reaction between the dienol tautomer **152** of **147** and the imine **153** (acting as a dienophile), in the same manner as reported in Tamura's studies involving carbon-carbon multiple bonds as dienophiles (discussed in detail in Section 1.5.3)[145]
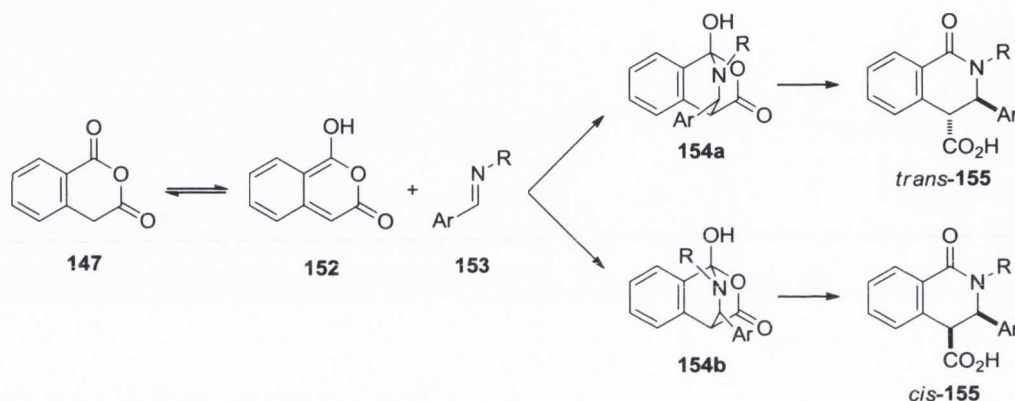
Scheme 1.34 Proposed Diels-Alder mechanism for the cycloaddition of imines and anhydrides.

This pathway was mainly excluded because imines, generally considered (at the time) to be weak dienophiles in the Diels-Alder reaction, were found to react at room temperature considerably faster than the species reported by Tamura which required several hours at high temperature (or promotion by a strong base) in order to furnish satisfactory yields. The authors also suggested that, from the likely intermediates **154a** and **154b** proposed for the Diels-Alder pathway (Scheme 1.34), bulky substituents on the nitrogen atom of the Schiff base **153** should lead to the formation of the *trans* product primarily, as **154a** would be favoured over **154b**. The results proved the opposite was true as the imines with bulky substituent on the nitrogen atom predominantly produced the *cis* product.[144]

The second possibility for the reaction mechanism was a step-wise pathway based on the nucleophilic attack of the enol **156** on the imine **153** electrophilic carbon (a Perkin-type reaction), followed by the formation of lactam **158** upon reaction between the amine and the anhydride functionalities *via* the tetrahedral intermediate **157** (Scheme 1.35).[144]
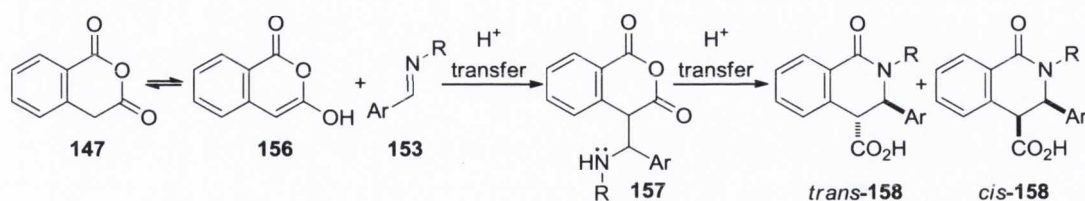
Scheme 1.35 Perkin's type proposed mechanism for the annulation reaction between anhydrides and imines.

This mechanism was also proved unlikely as, in a competition experiment carried out in presence of both imine **153** and benzaldehyde (**52**), the reaction with homophthalic anhydride (**147**), according to Perkin's mechanism, should have formed lactone **159** predominantly as the more electrophilic aldehyde should react faster with the anhydride than the imine which would generate the lactam **158**. The results of their experiment however proved that this was not the case as the reaction produced the lactam **158** almost exclusively (Scheme 1.36).[144]
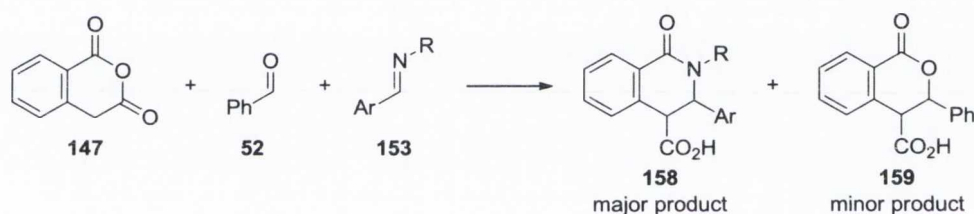
Scheme 1.36 Electrophile competition in the cycloaddition reaction of anhydrides.

The third mechanism postulated was found to provide the most accurate explanation of the reactivity and stereochemical outcome of the reaction. It consists of the iminolysis of the anhydride **147** by nucleophilic attack by the nitrogen of the imine **153**.[144] This generates the Zwitterionic intermediate **160** which, upon enolisation to **161**, intramolecularly attacks the iminium ion, forming the lactam product **158** (Scheme 1.37). Following this pathway, imines with *E* geometry should generate exclusively *cis* products while Schiff bases with *Z* geometry should lead only to the *trans* products. However, experiments proved that mixtures of *cis/trans* diastereomers are generally produced. As an explanation, the authors proposed two different rate-limiting steps for the formation of the two diastereomers. For the *cis*-isomer of **158** they assumed that the slow step would be the iminolysis of the anhydride **147** by the nucleophilic attack by the nitrogen atom of the Schiff base **153**; while in the formation the *trans*-diastereomer of **158** the rate-limiting step could be the *E-Z* isomerisation of the imine **153**.
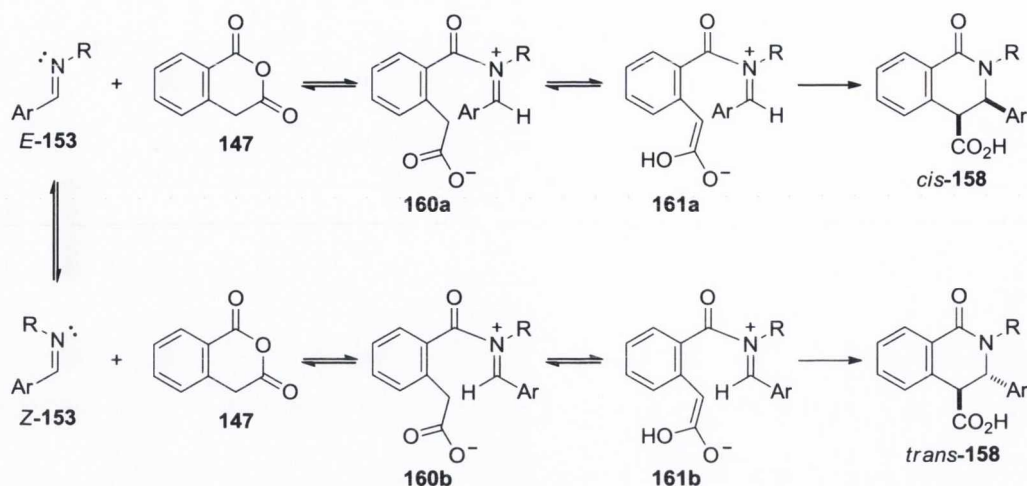
Scheme 1.37 Iminolysis as mechanism of the cycloaddition of anhydride to imines.

Following this theory, it is clear that any substituent on the imine **153** that would favour its isomerisation to the Z-isomer would also be responsible for an augment in yield of the *trans*-diastereomer as product and, conversely, any substituent that would disfavour the isomerisation would be accountable for the more stereoselective formation of the *cis*-isomer. Comparison between imines **162a**, **162b** and **162c** (Scheme 1.38), all bearing the small methyl group as substituent on the nitrogen atom, highlights the electronic effect of the substituent on the aromatic ring.[144]

162	R^1	R^2	163 *dr (trans:cis)*
a	Me	NO$_2$	97:3
b	Me	H	83:17
c	Me	N(CH$_3$)$_2$	20:80
d	*t*-Bu	H	0:100
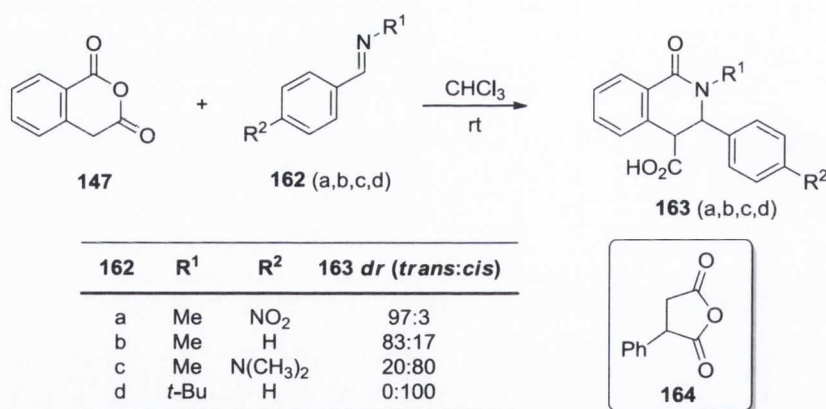
Scheme 1.38 Effect of the substituents of the imines on the stereochemical outcome of the cycloaddition reaction with anhydride.

Electron-withdrawing substituents such as that on imine **162a**, lower the barrier to the isomerisation to the Z-isomer, leading to *trans*-**163a** as the major product, while electron-donating substitution, as in the imine **162c**, inhibits the isomerisation and leads to a majority of *cis*-**163c**. It has also been shown that bulky substituents on the nitrogen

atom of the Schiff base tend to shift the isomerisation equilibrium to the *E*-isomer in order to avoid steric clash with the aromatic ring, thus resulting in more selective production of the *cis*-product.[144] Comparing imine **162d** to **162b** (Scheme 1.38) gives a clear example of this effect, where isomerisation of the double bond is completely inhibited or is too slow to take place, thus leading only to the *cis*-isomer of product **163d**. To provide further proof this postulated mechanism, the reaction was extended to the use of phenylsuccinic anhydride (**164**, Scheme 1.38). The same types of substituent effects described in the use of **147** were observed using **164**, albeit to a lesser extent. However, the low reactivity of **164** compared to **147**, resulted in the need for higher temperatures in order to allow the reaction to proceed in moderate yields. Shaw and co-workers later demonstrated that the difference in the rate of the reaction between the two anhydrides depends on the formation of the enolate Zwitterionic-type intermediate (*e.g.* **161**, Scheme 1.37).[148] Anhydrides such as **147** are capable of stabilising the negative charge of **161**, delocalising it along the aromatic ring and therefore favouring the formation of **158**. Phenylsuccinic anhydride (**164**) also possesses this ability, but the stabilisation effect is weaker, thus resulting in a slower reaction rate and subsequently the need for higher temperatures that would inevitably affect the stereochemical outcome of the reaction. Shaw proved that either introduction of an electron-withdrawing substituent (*e.g.* –NO$_2$)[148] at the appropriate position on the aromatic ring of the phenylsuccinic anhydride (**164**), or the exchange of the phenyl unite for a better anion-stabilising species (*e.g.* –SR),[149,150] facilitated the formation of the enolate intermediate thus allowing the reaction to proceed at room temperature, furnishing the lactam product in high yield and diastereoselectivity.[148–150]

1.5.2   Cycloaddition reactions of anhydrides with aldehydes

The cycloaddition reaction involving anhydrides and aldehydes has generally received considerably less attention than the imine variant. The reaction is generally limited to homophthalic anhydrides and aromatic aldehydes and requires stoichiometric (or more) amounts of either a base[151–154] or a Lewis acid[155] in order to proceed.

The mechanism of the reaction involving the aldehydes is different to that of imines, and is depicted in Scheme 1.39. The oxygen atom of aldehydes is not nucleophilic enough to attack the anhydride according the mechanism proposed for the imines, and thus it has been proposed that the reaction begins with enolisation of the anhydride **147**,

promoted by either a base or a Lewis acid moiety.[130] The reactive enol(ate) species **156** and **156a** formed, are now sufficiently nucleophilic to attack the electrophilic aldehydes **52** and **52a**, generating the tetrahedral alkoxides **165a** and **165b** which then lactonise in an intermolecular process to form the dihydroisocoumarin product **159** as mixture of the *cis/trans* diastereomers, with the *trans* generally preferred (Scheme 1.39).[130]
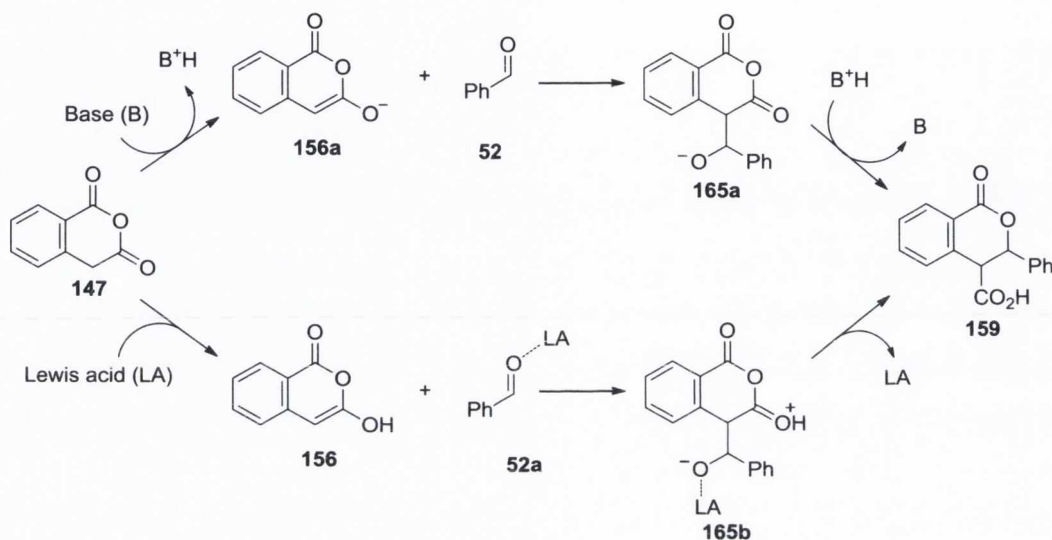
Scheme 1.39 Proposed mechanism of addition of homophthalic anhydride (**147**) to aldehydes catalysed by base and Lewis acid.

Not long after Pinder's report in 1958[137] (see Section 1.5), a number of other studies on the base-promoted cycloaddition reaction appeared in the literature.[151,156] However, these publications described the use of this strategy only for synthetic purposes without addressing either any stereochemical issues associated with the reaction or examination of its mechanism.
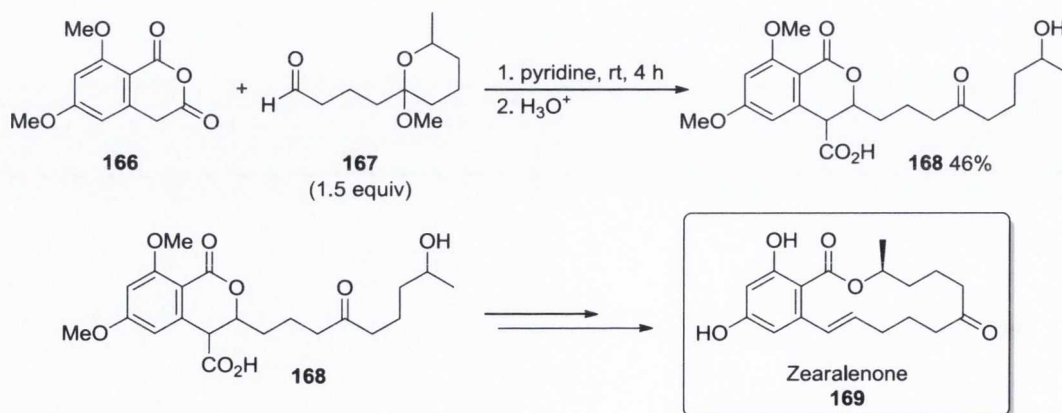
Scheme 1.40 Cycloaddition reaction in the synthesis of natural product **169** precursor.

For example, the synthesis of **168**, precursor of the natural product Zearalenone (**169**), was achieved by Girotra *et al.* by reacting anhydride **166** with aldehyde **167** in pyridine at room temperature for 4 h (Scheme 1.40).[156] A small library of cycloadduct products as *cis/trans* mixtures, synthesised by the sodium carbonate (Na_2CO_3)-promoted reaction between homophthalic anhydrides and aromatic aldehydes, was reported by Nakajima *et al.* as part of work which aimed to synthesise antifungal molecules.[151]

In 1991 Kita and co-workers experimented for the first time with the use of strong bases in the cycloaddition of **147** to aldehydes.[152] Based on previous studies concerning the strong base-promoted cycloaddition of carbon-carbon multiple bond compounds to **147**,[157] (Tamura's reaction) they embarked on a series of experiments aimed at evaluating the temperature effect on the reaction between **147** and **52** when promoted by different bases (Scheme 1.41).

base	conditions	% yield (170)	% yield (171)
Na_2CO_3	benzene, rt, 24 h	35	43
NaH	THF, 0 °C to rt, 24 h	83	-
NaH	THF, 50 °C, 33 h	5	82
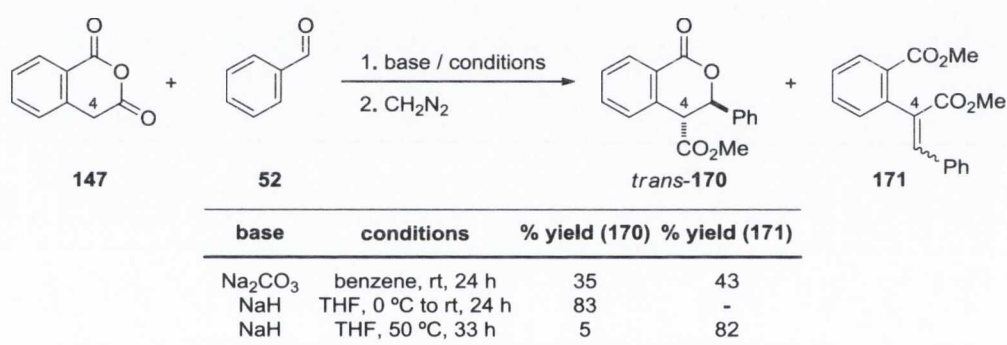
Scheme 1.41 Effect of temperature on the base-promoted cycloaddition of homophthalic anhydride (**147**) to benzaldehyde (**52**).

The use of Na_2CO_3, as previously documented by Nakajima,[151] furnished the cycloadduct product, which was isolated as methyl ester **170** after reaction with diazomethane. However, Kita also reported isolation of the C-4 methylene condensed product **171** not described in Nakajima's work. They then directed their attention to the use of a strong base such as sodium hydride as a reaction promoter. The results outlined in Scheme 1.41 demonstrated that the cycloadduct **170** was the product predominantly formed at low temperature while the methylene C-4 condensed **171** was the product predominantly formed at higher temperature. The group then synthesised a homophthalic anhydride derivative that contained both the anhydride and aldehyde functionalities **172** and evaluated it in the intramolecular cycloaddition reaction with various types of bases at different temperatures to furnish **173** (Scheme 1.42).[152]

41
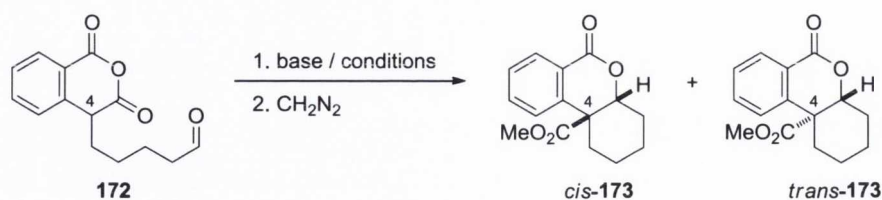
base	conditions	% yield (*cis*-173)	% yield (*trans*-173)
NaH	THF, 0 °C - rt, 10 min	32	26
LDA	THF, -78 °C, 1 h; rt, 30 min	26	27
Na$_2$CO$_3$	benzene, rt, 65 h	14	15
-	o-dichlorobenzene, 200 °C, sealed tube, 24 h	14	7

Scheme 1.42 Base and temperature effect on anhydride-aldehyde intramolecular cycloaddition.

In this case, due to the absence of the acidic proton in the C-4 position of the structures generated, the reaction formed the annulated product exclusively as a mixture of *cis/trans* diastereomers in low to moderate yields. However, no data concerning the 'real' diastereoselectivity of the reaction was reported as no spectroscopic analysis of the crude mixture was made. The two diastereomers were quantified after their isolation upon crystallisation and their yields subsequently calculated.

Gesquiere and his co-workers later described the cycloaddition reaction between aldehydes/ketones and homophthalic anhydrides promoted by the Lewis acid boron trifluoride–diethyl ether complex (**176**, Scheme 1.43).[155] This molecule plays a dual role in the reaction as it both coordinates to the aldehydes to enhance their electrophilicity, and binds the anhydride, promoting the formation of the enolates.[130] This strategy proved to be extremely efficient, as the reaction of anhydrides **147** and **174** with benzaldehyde (**52**), promoted by an excess of **176**, proceeded smoothly and produced the annulated products **159** and **177** in high yields. The reaction involving ketones however proved to be more challenging; most likely due to the lower reactivity of these functional groups. For example the reaction between ketone **175** and **147** furnished the product **178** in only 22% yield. In this work, as already reported by Kita,[152] no stereochemical analysis of the crude mixture was carried out and the ratio between the two stereoisomers was determined by quantification upon crystallisation when possible. The Lewis acid used (*i.e.* **176**) also proved to be, in comparison to the basic moieties previously reported, a better promoter for the reaction as no formation of the C-4 methylene condensed product (a Perkin-type product) was reported.

42

prod.	time (h)	% yield	% yield (*trans*)	% yield (*cis*)
159	5	81	38	43
177	14	90	90	0
178	14	22	-	-
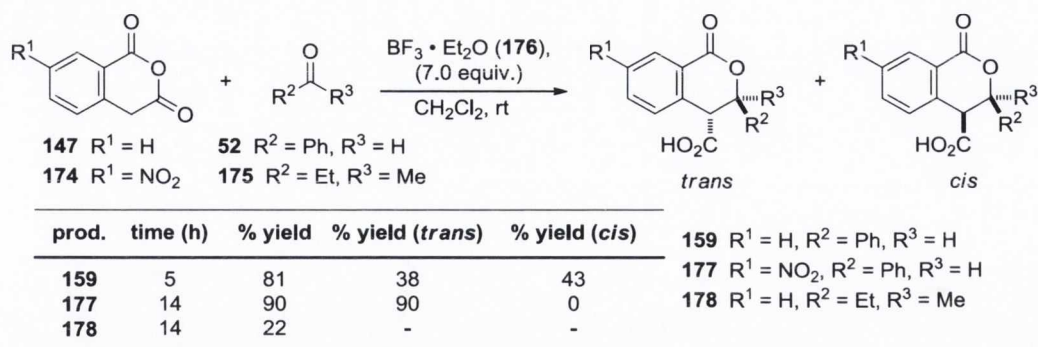
Scheme 1.43 Lewis acid-induced cycloaddition of homophthalic anhydrides to aldehydes and ketones.

Although Kita[152] and Gesquiere[155] were among the first to study the stereochemical outcome of the reaction, it was not until 2004 that a series of more complete and in-depth studies addressing this aspect of the process was reported in the literature. Palamareva and co-workers[153] studied the cycloaddition of homophthalic anhydride (**147**) with a range of aromatic aldehydes catalysed by a stoichiometric amount of 4-dimethylaminopyridine (DMAP, **180**) under mild conditions, measuring the diastereoselectivity obtained by ^{1}H NMR spectroscopic analysis of the crude mixture after the work up. The reactions generally proceeded to completion affording the mixture of diastereomers as the main product, with preferential formation of the *trans* isomer, with no side Perkin's product formation. For example, using benzaldehyde (**52**) as the electrophile, product **159** was formed in 100% yield and 70:30 diastereomeric ratio (Scheme 1.44). When the reaction was performed using relatively electron-rich aldehydes such as furfural (**48**), or aldehyde **179**, along with the diastereomeric mixtures (*i.e.* **181a:181b** and **182a:182b**), the reaction also furnished alkene products **181c** and **182c** in up to 30% yield. This example however, is case-limited, as use of the other electron-donating aldehydes evaluated in the reaction gave significantly lower amounts of Perkin-type side products (<10%).

prod.	time (h)	% yield	% ratio (a:b:c)
159	2	100	70:30:0
181	2.5	98	80:16:4
182	1.5	100	62:8:30
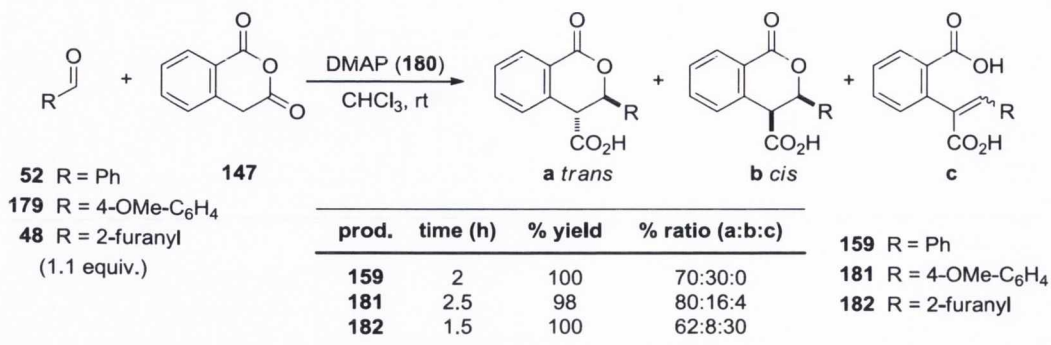
Scheme 1.44 DMAP-catalysed cycloaddition between homophthalic anhydride (**147**) and aldehydes.

1.5.2.1 The scope of the reaction: the anhydride component

The use of different cyclic anhydrides in the reaction involving aldehydes has been much more limited and has received less attention than the imine variant. This is mainly due to the different mechanisms through which the two reactions proceed. As previously described, the imine mechanism is based on the nucleophilic attack of the nitrogen atom of the Schiff base on the electrophilic anhydride; while formation of anhydride enol(ate) and its consequent nucleophilic attack on the electrophilic carbonyl compounds is the characteristic pathway adopted by reactions involving aldehydes. For this reason, it is clear that formation of the enol(ate) of the cyclic anhydride is fundamental in order to promote the reaction. For aromatic anhydrides such as homophthalic anhydride (**147**) this can be easily achieved, as the negative charge formed can be stabilised by conjugation with the fused aromatic ring. However, for simpler structures such as succinic anhydride (**129**), the lack of this stabilisation effect prevents the reaction from proceeding if not performed at high temperatures or with the use of strong base and Lewis acids.

In 1983, Lawlor *et al.* embarked on a series of studies involving the optimisation of the reaction between succinic anhydride (**129**) and aromatic aldehydes.[158] In order to improve the results of the thermal version of the process reported years before by Fittig and co-workers,[135] Lawlor developed a new synthetic protocol based on the concomitant use of a Lewis acid (*i.e.* ZnCl₂) and triethylamine. Using this methodology **129** was reacted with a series of aromatic aldehydes/ketones such as **183** and **184** to furnish (*via* intermediates **185** and **186**) products **187** and **188**, derivatives of the

abundant natural structural core, paraconic acid[159] (*i.e.* **189**, Scheme 1.45).[158] However no details regarding the stereochemical outcome were reported.
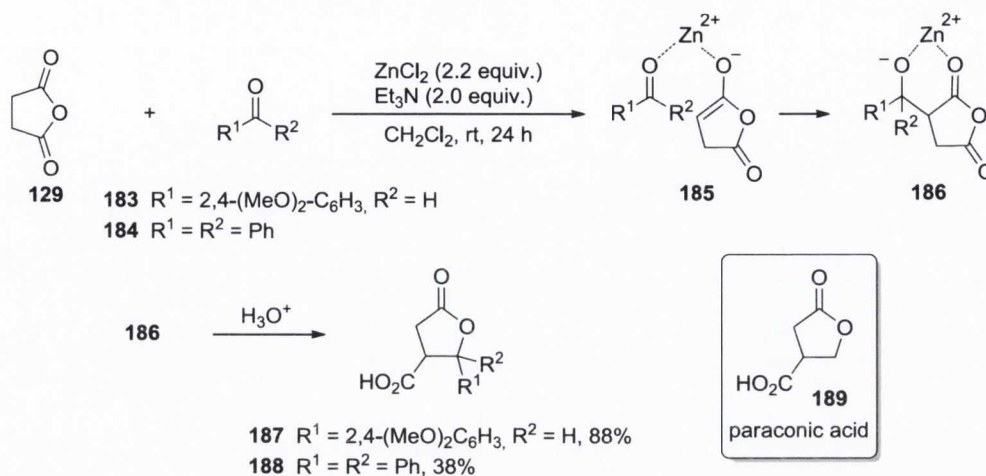
Scheme 1.45 Lewis acid/base-catalysed cycloaddition reaction of succinic anhydride (**129**) to aldehydes and ketones.

Almost a decade later, this procedure was applied to the synthesis of other natural products bearing the same core structure.[160] In this work, the authors reported that the reaction between succinic anhydride (**129**) and piperonal (**137**) under the same conditions described by Lawlor, furnished (in 75% yield) a *cis/trans* diastereomeric mixture of the acid product in 33:67 ratio, subsequently separated by fractional crystallisation.[160] In a very recent report the use of the same protocol is described in the synthesis of D_1 dopamine agonists, reacting succinic anhydride with a substituted benzaldehyde.[161] However, this work reports the use of this procedure as synthetic protocol exclusively and no description of the stereochemistry of the products formed is addressed.

The reaction can also be promoted by the use of weak bases such as sodium acetate under thermal conditions.[162–164] However, low yields and no stereochemical outcomes are reported in these studies.

The use of substituted succinic anhydrides such as **190** in the base-mediated cycloaddition reaction to aldehyde **191** is also reported (Scheme 1.46).[165–167]
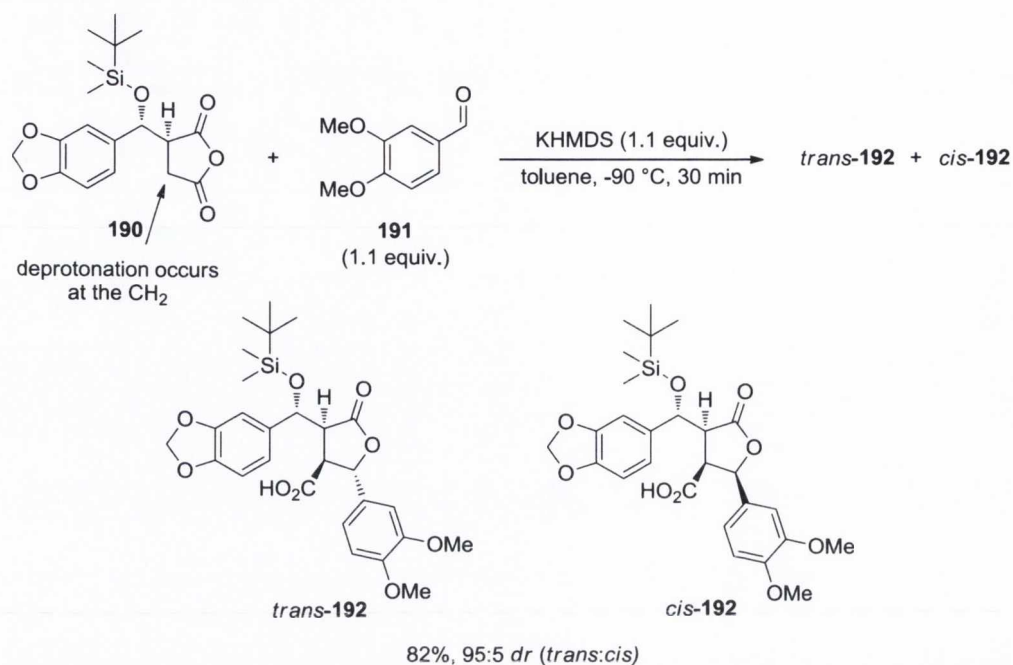
Scheme 1.46 Use of the substituted succinic anhydride **190** in the cycloaddition reaction to aldehyde **191**.

However, these substitutions were not made in order to favour the enolate formation by stabilising the negative charge formed, but rather from synthetic necessity. Indeed, the formation of the enolates, promoted by the use of strong hindered bases such as lithium alkoxides[168] and Na-, K- or LiHMDS,[165–167] took place by deprotonation of the methylene CH_2 carbon instead of the substituted CH carbon furnishing the paraconic acid derivatives such as **192** in good yields and high diastereoselectivity.

1.5.3 Cycloaddition reactions of anhydrides with other electrophiles

The reactions between cyclic aromatic anhydrides and electrophiles other than aldehydes and imines, have been widely studied and used over the years.[130]

The reaction was firstly reported by Tamura *et al.* as an extension of the previously known cycloaddition of imines and aldehydes to homophthalic anhydride (**147**).[145] They demonstrated that when **147** is heated at reflux in toluene in presence of unsaturated carbon-carbon multiple bonds moieties such as **193** and **195**, the condensed phenolic systems **194** and **196** are regioselectively produced, albeit in low to moderate yield (Scheme 1.47).[145]
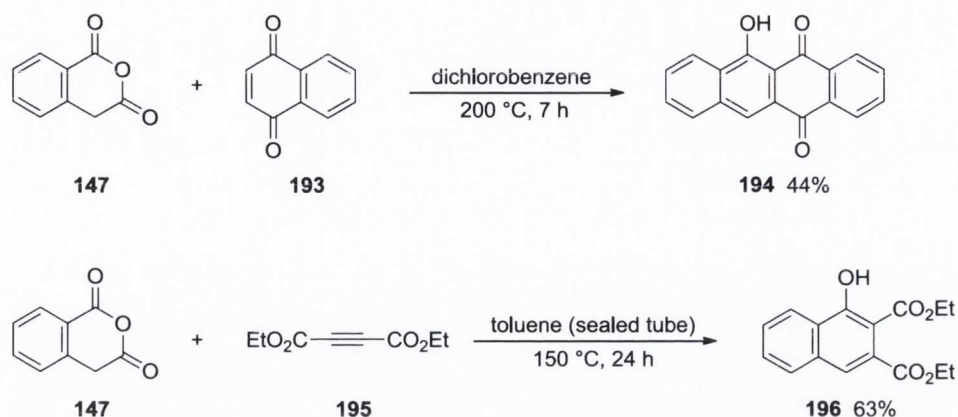
Scheme 1.47 Cycloaddition reaction between homophthalic anhydride (**147**) and carbon-carbon multiple bonds species.

Two plausible mechanisms were also reported in order to explain the reaction pathway and its regioselectively[145] and two years later a third possible explanation was described in conjunction with the previous two in a new report by the same group.[146]

The first proposed mechanism consisted of the thermal concerted [4+2] cycloaddition of the diene intermediate **197**, formed by decarboxylation of **147**, to the generic dienophile **199**, to form the adduct **200a** that, upon tautomerisation to **200b** and subsequent formal loss of molecular hydrogen, generates the aromatic product **201** (Scheme 1.48).[146]
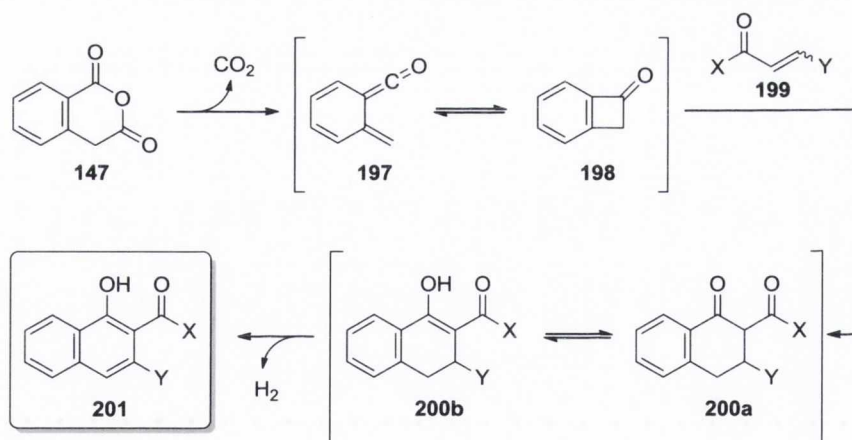
Scheme 1.48 Proposed [4+2] cycloaddition mechanism for the cycloaddition reaction between homophthalic anhydride (**147**) and dienophiles.

This mechanism has been ruled out based on the fact that formation of the intermediate **198** has never been observed in the reaction. In addition **147** has been recovered from the process unchanged, although generation of **197** from **147** has been documented to occur at higher temperature.[169] Further evidence to disprove this mechanism came from

the difference in yield of **201** when formed by reaction between **147** and **199** in one case, and **198** and **199** in the other case under identical conditions.[146]

The second possible proposed pathway was based on the stepwise Michael addition of the homophthalic anhydride-derived enol **156** to the dienophile **199**, to produce **202**, followed by an intermolecular cyclisation which leads to the cycloadduct **203**. This, after decarboxylation to **200c**, tautomerisation to **200b** and subsequent formal loss of molecular hydrogen, generates the product **201** (Scheme 1.49).[146]
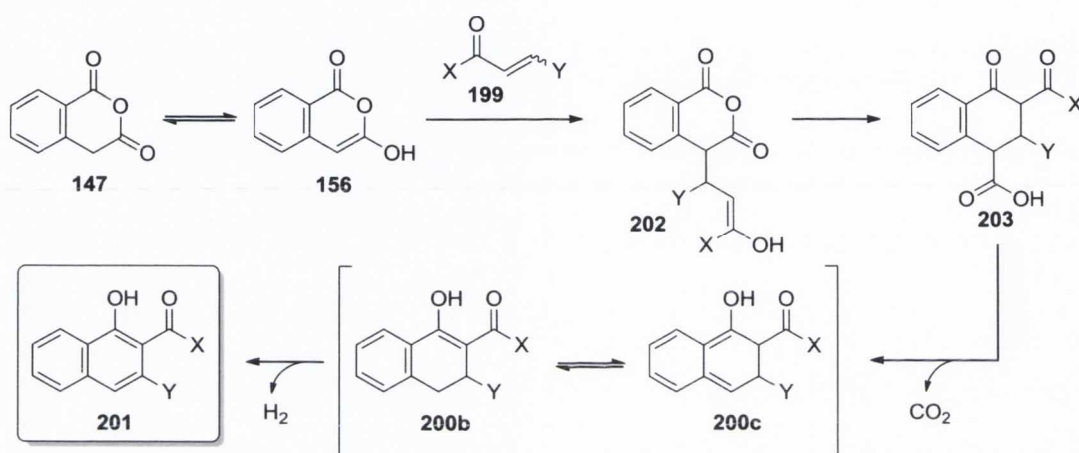
Scheme 1.49 The proposed Michael addition mechanism for the cycloaddition reaction between homophthalic anhydride (**147**) and dienophiles.

This mechanism, known for example in the reaction between phthalide anions and various dienophiles,[170] has also been discarded; as reaction of the lithium enolate **204** of the homophthalic anhydride (**147**) with several known Michael acceptors of general structure as **205** (where R is a leaving group), failed to form product **206**.[157]
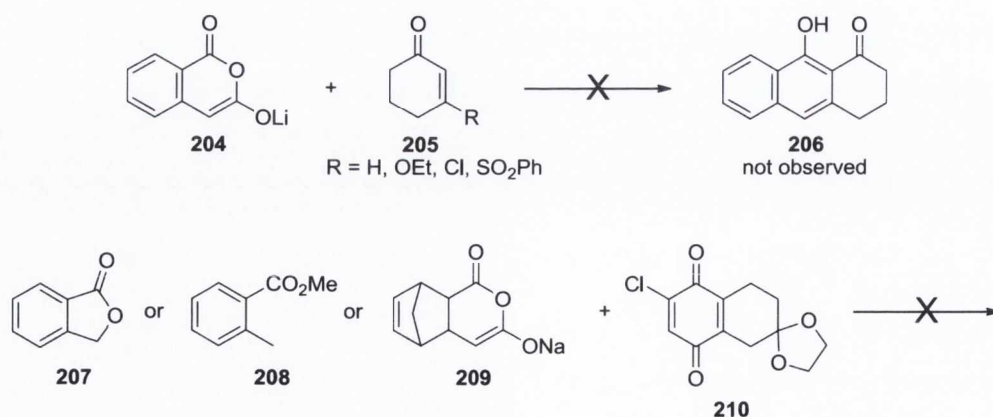
Scheme 1.50 Disproof of proposed Michael reaction mechanism.

In the same manner, no reaction products (above trace levels) were observed when lithium salts of known donors for the Michael reaction (*i.e.* **207** and **208**) were evaluated in the addition reaction to **210**. Furthermore, when the anhydride-derived sodium enolate **209** was evaluated in the addition reaction to compound **210**, no formation of the expected annulated product was observed even under forcing conditions (Scheme 1.50).[157]

A third mechanism was postulated in order to explain the previous results. This pathway is based on the Diels-Alder reaction between the conjugated dienol tautomer **152** of **147** and the electrophile **199** to furnish, after decarboxylation to **200c** and tautomerisation to **200b**, the product **201** (Scheme 1.51).[146]
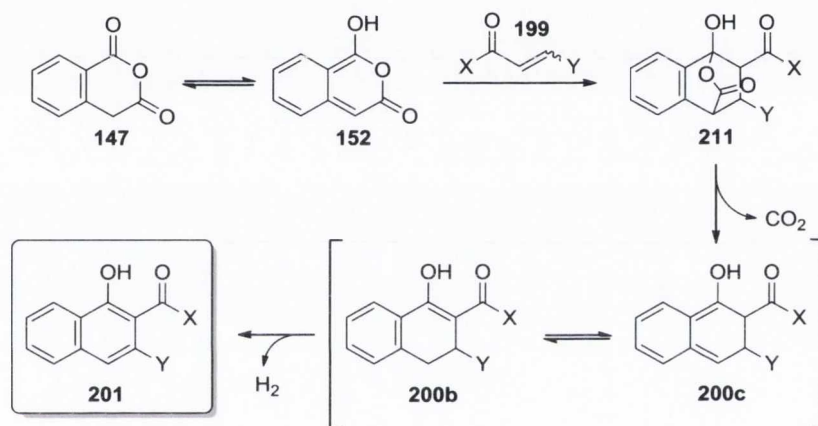
Scheme 1.51 Diels-Alder reaction as proposed mechanism for the cycloaddition of homophthalic anhydride (**147**) to dienophiles.

In this reaction, homophthalic anhydride acts as the diene through its tautomeric dienol **152** while the role of dienophile is played by the electrophile **199**.

The anhydride enolate **209** failed to react in the transformation depicted in Scheme 1.50 due to its inability to generate the dienol tautomer, thus precluding the Diels-Alder reaction with the dienophile **210**.[157] Similarly, the formation of the naphthol derivative **206** from the reaction between **204** and **205** failed as cyclic enones are known to be extremely poor dienophiles in the Diels-Alder[171] if not activated by either Lewis acidic moieties[172] or by ring strain.[173] Although evidence collected by the Tamura *et al.* strongly support the Diels-Alder concerted mechanism that is currently considered the most probable pathway for the reaction, the stepwise Michael process cannot be fully discarded.

The regioselectivity of the reaction was demonstrated by reacting homophthalic anhydrides (such **147** and **212**) with asymmetrically substituted unsaturated species such as **213** or **217**.[146] Under the reported conditions, **214**, **215** and **218** were found to be the only products obtained, with no formation of their regioisomers **216** and **219** (Scheme 1.52).

147 R = H   **213**

212 R = OMe

214 R = H, 41%   **216**

215 R = OMe, 25%   not observed

147   **217**   **218** 19%   **219**

not observed
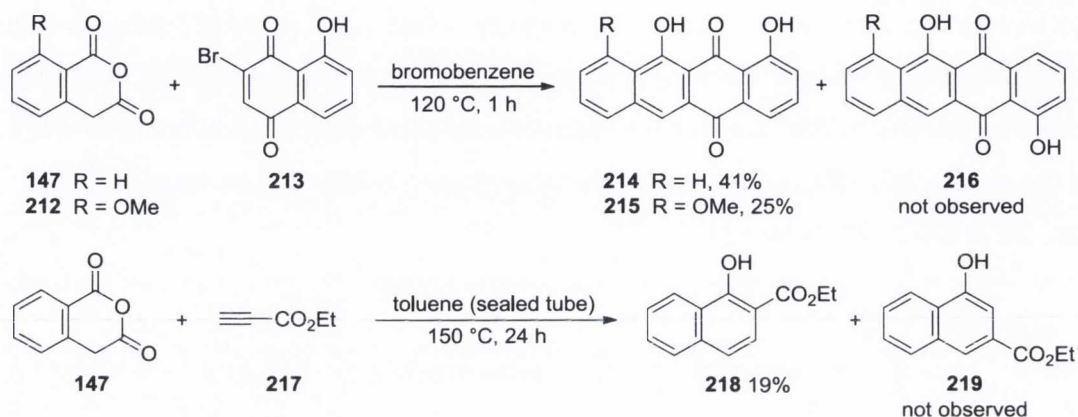
Scheme 1.52   Regioselectivity in the cycloaddition reaction with asymmetric carbon-carbon multiple bonds.

Regiocontrol in the concerted process (*i.e.* Diels-Alder reaction) presumably arises from the exclusive attack by the carbon of the diene **152** (Figure 1.8) possessing the largest HOMO coefficient, on the unsubstituted alkene carbon of **213** (or alkyne in the case of **217**) which possess the largest LUMO coefficient (Figure 1.8).[174,175]

152   EtO$_2$C—≡—H **217**   **213a**

Largest HOMO coefficient   Largest LUMO coefficient
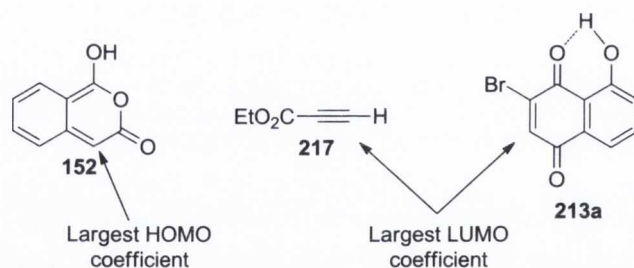
Figure 1.8   Rationale for the regioselectivity in the formal cycloaddition of homophthalic anhydride to dienophiles.

In the case of a stepwise pathway (*i.e.* Michael addition), this can be rationalised by considering that formation of the first carbon-carbon bond (*i.e.* nucleophilic attack of the enolate) would preferentially occur at the carbon atoms indicated in Figure 1.8, because the negative charge formed can be subsequently stabilised by the resulting formation of enolate products. In the case involving **213**, enhancement of the

electrophilicity of the carbon indicated and further negative charge stabilisation can be achieved by H-bond formation as shown in **213a** (Figure 1.8).

A base-promoted variant of the reaction was later developed by the same group in order to improve the conditions for the formation of cycloaddition products that generally required high temperatures for several hours and furnished products in moderate yields.[157] Using two separate methods based on the use of a strong base such as lithium diisopropylamide (LDA) or sodium hydride (NaH), the reactions could be executed under milder conditions to furnish products in good to high yields. Comparisons between the thermal and base-induced version of some sample reactions are shown in Scheme 1.53.

prod.	conditions	% yield
220	thermal	42
	A	68
151	thermal	65
	B	94
222	thermal	0
	B	46
224	B	83

Conditions:
A: LDA/THF, -78 °C, 30 min, to rt
B: NaH/THF 0 °C, 20 min, to 20 °C, 20 min
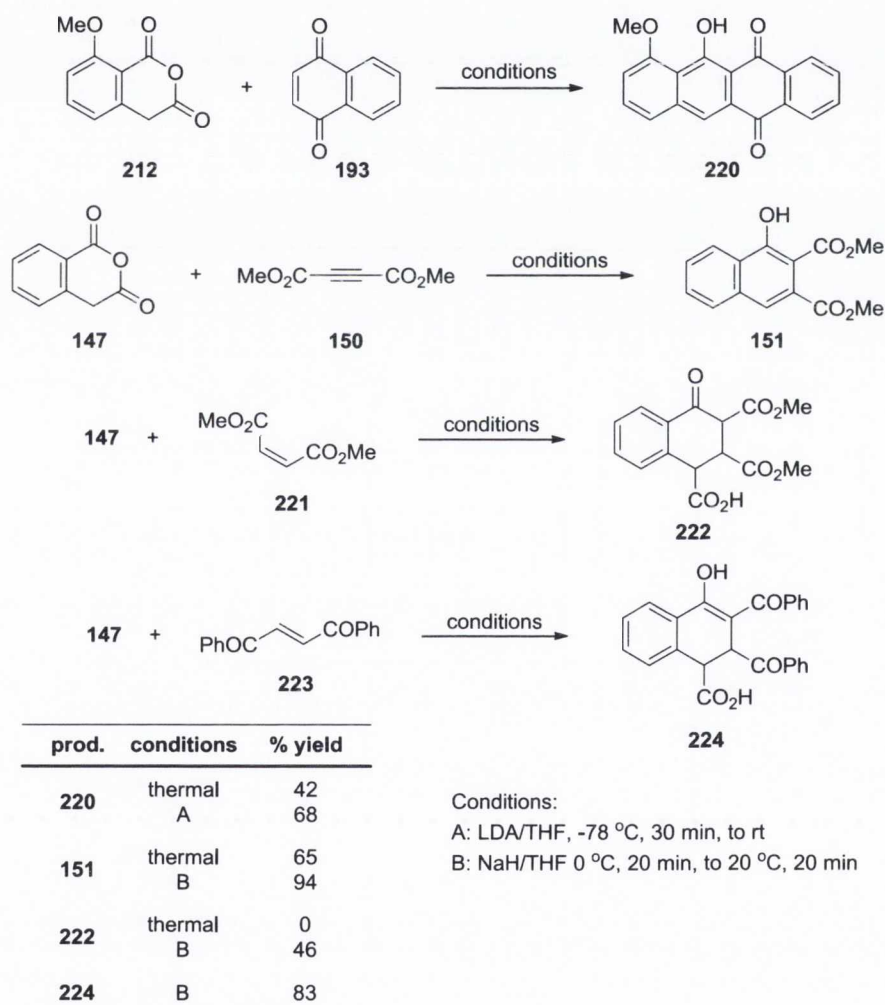
Scheme 1.53 Comparison between thermal and base-induced cycloaddition reactions of homophthalic anhydrides to dienophiles.

Some substrates, such as **221** and **223**, are reported to form cycloadduct products only in the base-promoted variant of the reaction, producing structures such **222** and **224** as a result of the reaction process proceeding without the decarboxylation step. Although this result is of interest as the reaction leads to structures bearing up to three stereocentres, neither an explanation of such reactivity nor stereochemical rationale were provided.[157]

This new protocol involving milder reaction conditions was then applied as an efficient strategy in the synthesis of natural products with pharmacological activity, such as antibiotics[176] and antracyclinone precursors such as daunomycinone (**227**), a primary metabolite of the chemotherapeutic drug daunomycin (**228**).[177] For example the thermal regioselective cycloaddition reaction of the conjugated acid of **225** to the unsaturated compound **210** to form **226**, had been already reported by the same group.[178] However, in order to improve the yield of the reaction (which was generally low), the lithium enolate **225** was successfully employed as the diene component, furnishing a good product yield (Scheme 1.54).[177]
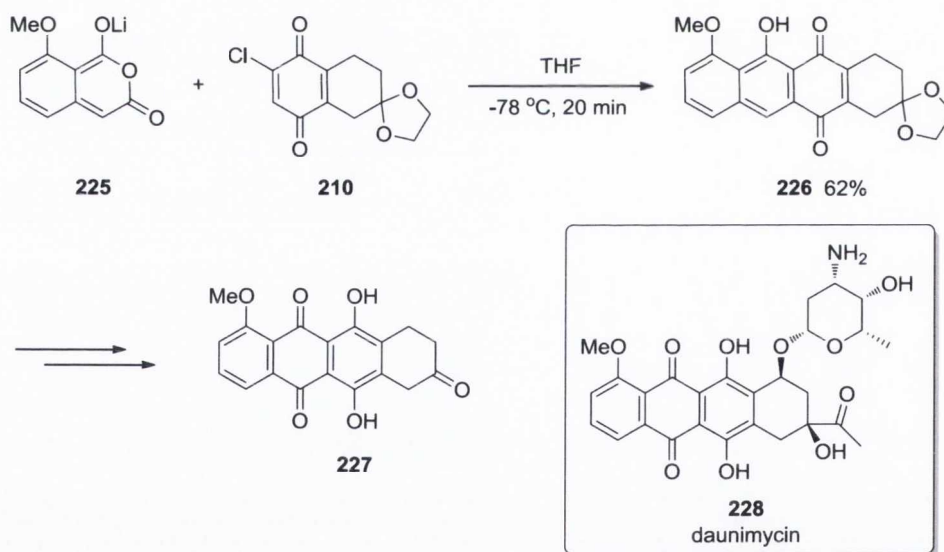
Scheme 1.54 Daunomycinone synthesis by cycloaddition of anhydride enolate (**225**) to unsaturated compound (**210**).

Another important example of the application in the total synthesis of natural products was reported by Danishefsky and co-workers. They applied the strong base-promoted cycloaddition reaction of homophthalic anhydride to dienophiles as an elegant strategy in the total synthesis of Lactonamycin, a powerful antibiotic and antitumor molecule.[179]

Cycloaddition reactions with other types of electrophile have also been reported. For example α,β-unsaturated aldimines (1-aza-1,3-butadienes) have been shown to react with homophthalic anhydride.[180,181] However the reaction led to a mixture of products generated by different competitive addition mechanisms between the two species (*i.e.* Michael addition, iminolysis at C-1 and iminolysis at C-3) that, in general, could not be controlled by modification of the conditions.

Another report described the reaction between homophthalic anhydride and substituted (bromomethyl)-benzonitrile to produce isoquinolinone derivatives by a stepwise process promoted by bases such as triethylamine.[182]

1.5.4   The use of homophthalic anhydride analogues: heteroaromatic anhydrides

The use of heteroaromatic anhydride analogues of **147** as dienes in the base-promoted cycloaddition reaction to dienophiles has also been studied. Anhydrides derived from indole (*i.e.* **229**), benzofuran (*i.e.* **230**) and thiophene (*i.e.* **231**, Figure 1.9) have been reported to react with different types of dienophiles, producing polycyclic hydroxylated compounds in low to good yields.[183,184] Furthermore, aliphatic anhydrides such as **232**, and **233**, which are capable of tautomerisation to the dienol form, have been proven to be suitable substrates in the synthesis of precursors of the natural product daunomycin (**228**).[185,186]
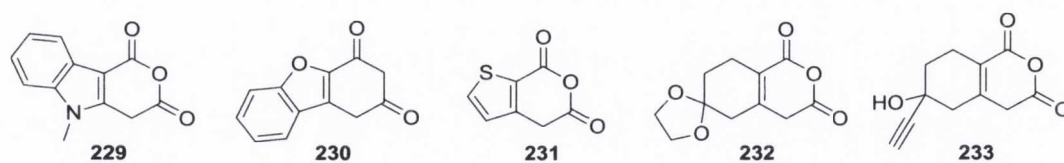
Figure 1.9   Heteroaromatic anhydrides as dienes for the formal cycloaddition to dienophiles.

At the beginning of 1990s, an intramolecular variant of the reaction was also developed, demonstrating the general applicability of this process. C-4 Substituted homophthalic anhydrides bearing an alkyl chain with a triple bond, such as **234**, and their heteroaromatic analogues such as **236**, undergo intramolecular strong base-promoted cycloaddition at room temperature. The reaction, which favours the formation of 6-membered rings over 5-memebered structures proceeds quickly, furnishing products **235** and **237** in moderate yields (Scheme 1.55).[187,188]
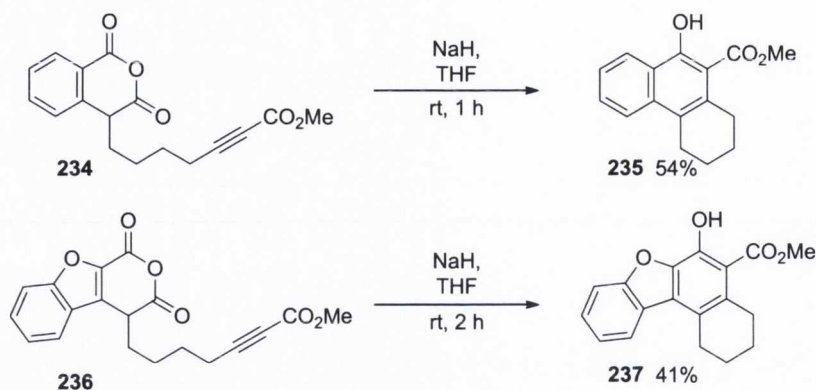
Scheme 1.55 Intramolecular cycloaddition between substituted aromatic anhydrides and carbon-carbon triple bond species.

1.5.4.1 Glutaconic anhydrides and 2-pyrone derivatives

Glutaconic anhydride (**244**, Scheme 1.56) derivatives have also featured as dienes in the cycloaddition reaction to dienophiles.[189,190] The β-methyl derivative **238** however, failed to produce the desired product **241** under thermal conditions when reacted with quinones such as **240** (Scheme 1.56). To circumvent this problem, the molecule was trapped in the dienolic form by methylation of the enol **239** through reaction with diazomethane, forming **242**. This readily reacts with **240** under thermal conditions, furnishing **243** in good yield (Scheme 1.56).[189] This new strategy was then applied to the synthesis of natural products.[190]
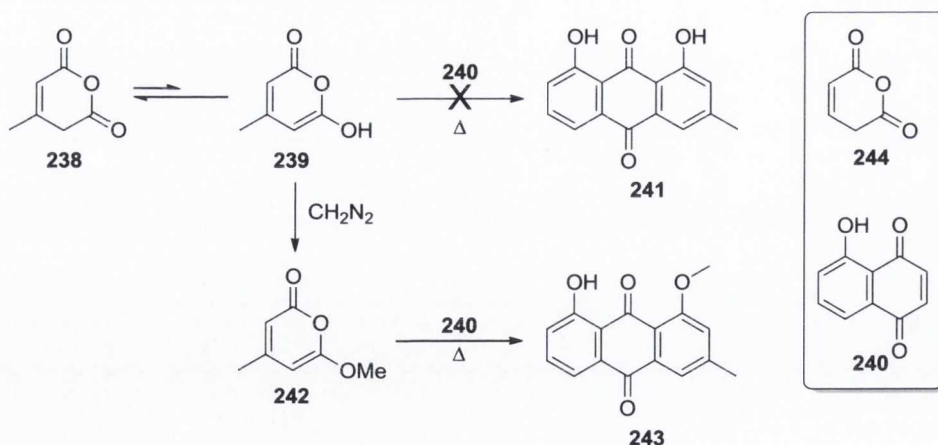
Scheme 1.56 Glutaconic anhydride derivatives as diene for the Diels-Alder reaction with dienophiles.

The Diels-Alder reaction of 2-pyrone (**249**, Scheme 1.57) and its derivatives with various dienophiles is a very similar process to those presented above. Although these

substrates have been well-studied and used as dienes for the synthesis of multifunctional (chiral) compounds,[191] their low reactivity as dienes hindered their use in asymmetric variant of this reaction. Quite recently, a bifunctional organocatalytic asymmetric version of the process, promoted by cinchona alkaloid organocatalysts was reported.[192,193] Diels-Alder reactions catalysed by **247** between 3-hydroxy-2-pyrone (**245**) and α,β-unsaturated ketones, such as **246**, bearing electron-withdrawing substituents on the double bond, produced **248** in good yield and high enantioselectivity with high preference for the *exo*-adduct (Scheme 1.57).[192]
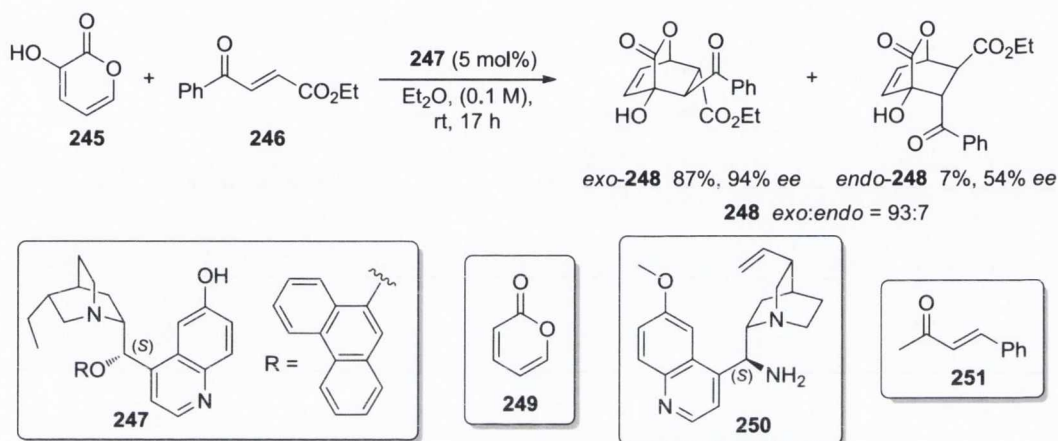
Scheme 1.57 Enantioselective organocatalysed Diels-Alder reaction between 3-
             hydroxy- 2-pyrone (**245**) and unsaturated ketones.

However, catalyst **247** proved to be an ineffective chiral promoter for simpler α,β-unsaturated ketones such as **251**, furnishing high product yields but with no stereocontrol. For this reason Deng *et al.* later reported the use of C-9 NH₂-substituted quinine **250**, in combination with catalytic amounts of trifluoroacetic acid (TFA), as an efficient catalyst for the reaction between **245** and **251**, furnishing products in high yields and enantioselectivity.[193]

1.6 The Tishchenko reaction: a brief overview

The Tishchenko reaction is the catalytic disproportionation of two aldehyde molecules **16** to give an ester product **252** (Scheme 1.58). This reaction has been widely studied as it allows chemists to synthesise esters and lactones in a non-conventional way and, over the last century, several different applications of this alternative protocol have been reported.[194,195]
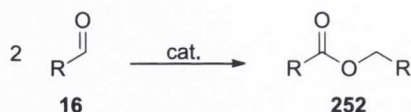
Scheme 1.58 The Tishchenko reaction.

The reaction was discovered by Claisen in 1887, when he found that treatment of benzaldehyde with different types of sodium alkoxides gave benzyl benzoate in good yields.[196] His method, however, was limited to non-enolisable aldehydes, as the strong basicity of the alkoxides used could also catalyse aldol reactions for all aldehydes bearing an acidic α proton. Later, in 1906, a Russian chemist named W. E. Tischtschenko reported that aluminium and magnesium alkoxides could promote the same reaction also for enolisable aldehydes, giving the desired products in good yields with no aldol by-product formation.[197,198] The superior behaviour of these catalysts has been attributed to the stronger Lewis acidity of the aluminium ion (Al^{3+}) which, with the empty p-orbital, coordinates to the carbonyl oxygen atom of the aldehyde.[194,195] Furthermore, the concomitant lower basicity of aluminium alkoxides, compared to the sodium alkoxides reported by Claisen years before, suppressed the aldol pathway, thereby promoting the Tishchenko reaction exclusively.[194,195] The scope expansion of the reaction provided by the use of aluminium alkoxides enhanced the applicability of the process, and for this reason the reaction was named after Tischtschenko: the Tishchenko reaction (anglicised).[194,195]

Since the discovery of this reaction, a wide number of both homogenous and heterogeneous catalysts have been reported as extremely active promoters for the Tishchenko reaction, which has been used in several applications and industrial processes (*e.g.* the preparation of ethyl acetate from acetaldehyde).[199–202] These reactions, which simply consist of the coupling of an aldehyde either to itself or to a

different carbonyl moiety (aldehyde, ketone), all rely on a hydride-shift between the two moieties in order to generate the products.[194,195] For this reason, selectivity issues in the formation of a sole product in high yields, especially in the reaction involving two different aldehydes, have been raised. Indeed, controlling which molecule acts as a hydride donor and which one acts as acceptor is the key factor limiting the synthetic utility of this process.

1.6.1 Proposed mechanisms

Over the years, a number of different mechanisms have been proposed for the Tishchenko reaction promoted by aluminium alkoxides. Among these, the two most commonly accepted were presented by Lin *et al.* in 1952,[203] and by Ogata and co-workers in 1969.[204]

Lin postulated a stepwise esterification process in which the aluminium alkoxide acts exclusively as a Lewis acid moiety (Scheme 1.59). A similar mechanism had however already been presented by Luder and co-workers almost ten years before but was interpreted as a special case of Cannizaro reaction.[205] The reaction begins with the aluminium coordination to the carbonyl oxygen of one molecule of aldehyde **16** *via* the empty p-orbital of the metal atom of the catalyst **253**, generating the alkoxide **254**. This is then attacked by the oxygen atom of a second molecule of aldehyde **16** to give the adduct **255** which, after 1,3-hydride shift, leads to product **252** and regeneration of catalyst **253** (Scheme 1.59).
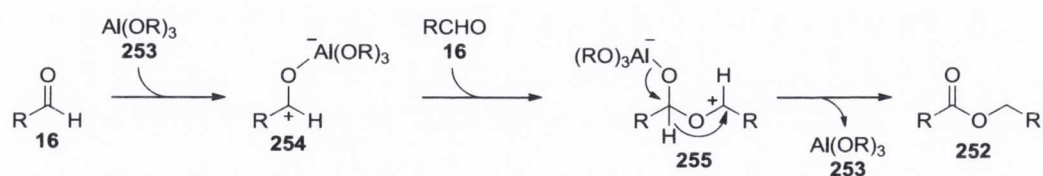
Scheme 1.59 Mechanism for the Tishchenko reaction proposed by Lin.

Ogata's mechanism consists of a very similar pathway but the active catalyst (*i.e.* **260**, Scheme 1.60) is generated at the beginning of the reaction in an alkoxide transfer step.[206] In the same way as outlined above, the process starts with the coordination of the aldehyde **16** to the Lewis acidic metal ion **256**, forming **257**, but, instead of a direct 1,3-hydride shift, an alkoxide transfer from the aluminium chelating agent to the aldehyde is proposed to take place, leading to the adduct **258**. The mechanism now

continues with a second aldehyde species that coordinates to the aluminium Lewis acid generating **259**, which, after an intramolecular hydride transfer, furnishes the mixed ester **261** and catalyst **260**, which continues to propagate the reaction as the actual catalytic species, forming the desired product **252** (Scheme 1.60).[204]
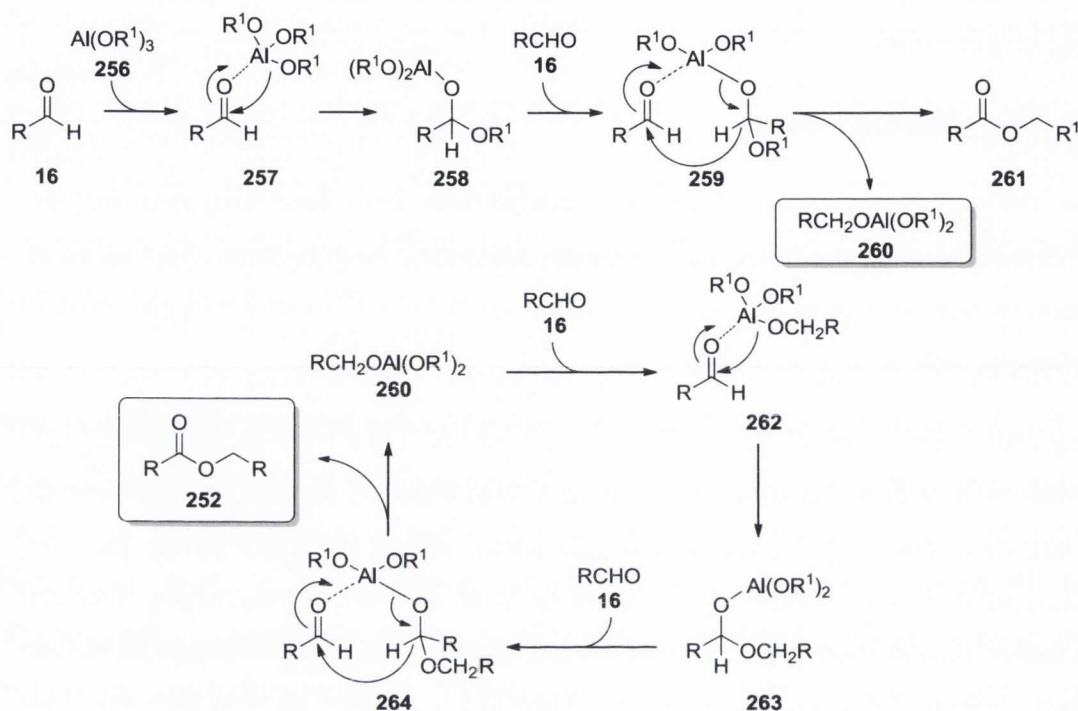
Scheme 1.60 Ogata's mechanism for the Tishchenko reaction catalysed by aluminium alkoxides.

This proposed mechanism was verified by experimental evidence of the formation of the mixed ester **261**, which is related to the amount of catalyst used and is no longer considered a side reaction but the main pathway at low conversion.[194] It has also been demonstrated that the transfer of a benzyloxide from the aluminium to the aldehyde (from **262** to **263**, Scheme 1.60) is much faster than the transfer of bulkier substituents such as *t*-butoxide or *i*-propoxide (from **257** to **258**, Scheme 1.60)[204] commonly used in this class of aluminium catalysts. This is reflected in the rate-determining step of the reaction which in the case of bulky substituents is considered to be the alkoxide transfer, while for the less bulky benzyloxide is considered to be the hydride transfer in **264**. In the early stages of the reaction this leads to the formation of the mixed ester **261** (in an amount proportional to the quantity of catalyst used) and of catalyst **260**. This active species then coordinates to a molecule of aldehyde forming **262** that quickly and

selectively transfers the benzyloxide to the aldehyde, producing **263** that, after coordination of a second molecule of aldehyde to **264** and hydride transfer, gives the desired product **252** and regenerates the catalyst **260** (Scheme 1.60).[204]

1.6.2 Catalysts for the Tishchenko reaction

Over the years many different catalyst structures have been proposed as active promoters for the Tishchenko reaction.[194,195] Even for the most complex catalytic structures evaluated in these reactions, the mechanism of action can generally be inferred to happen through one of the previously mentioned pathways, allowing their division into groups according to the type of core metal used (Figure 1.10).
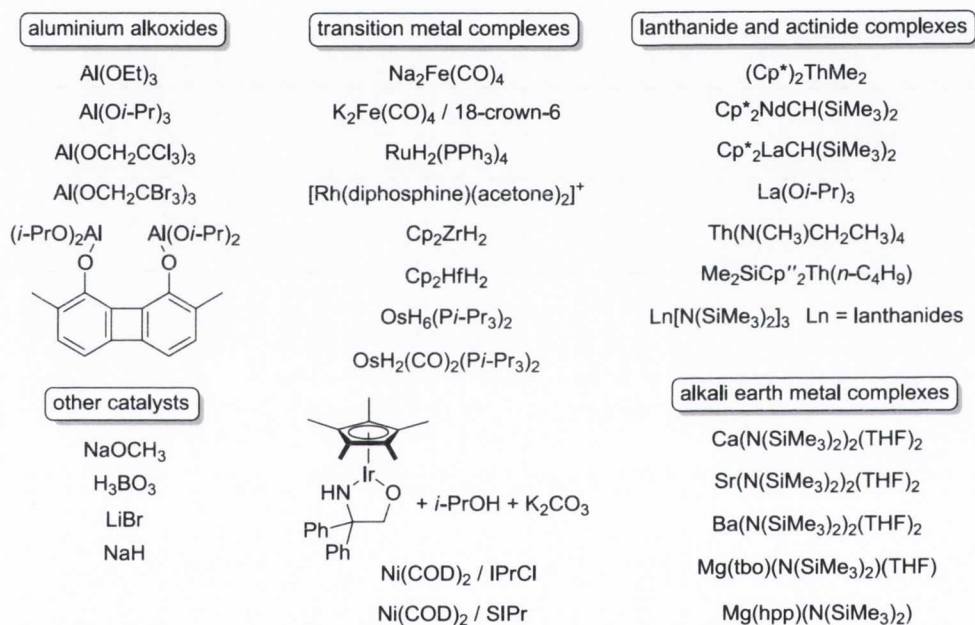
Figure 1.10 Catalyst families for the Tishchenko reaction.

The most commonly studied and used, as a result of the seminal discovery made by Tischtschenko, is the family of aluminium alkoxides.[203–212] Among them, those made by Maruoka *et al.* proved to be particularly interesting, as faster reactions were achieved due to the effect of the double coordination to the aldehyde exploited by the use of their bidentate *bis*-aluminium alkoxide catalysts.[210,211]

Another important family of catalysts is defined by structures containing a transition metal at the active site such as: iron,[213,214] ruthenium,[215,216] rhodium,[217] zirconium,[218] hafnium,[218] osmium,[219] iridium[220] and nickel.[221,222] In 1978 and later in 1982 Yamamoto

et al., evaluating hydridoruthenium complexes as promoters for the transition metal-catalysed Tishchenko reaction, proposed a slightly different mechanism.[215,216] This was based on a series of oxidative additions, reductive eliminations, insertions and β-eliminations typical of transition metal complexes. However, no strong experimental evidence was collected in order to prove their hypothesis or indeed, to rule out Ogata's pathway.

Stapp and co-workers in 1973 proved that catalytic amounts of boric acid catalyse the disproportionation of several different aldehydes, but high reaction temperatures were generally required to obtain good yields, and in some cases aldol condensate was the predominant product.[223]

Other families of catalysts which efficiently promote the reaction have been developed and reported in the literature. Among these, the use of lanthanide and actinide complexes;[224–228] alkali metal salts such as lithium bromide[229] or sodium hydride;[230,231] and the use of alkali earth metals such as calcium, strontium, barium[232] and magnesium complexes[233] can be mentioned.

1.6.3 Intermolecular crossed-Tishchenko reaction

Although the study and development of efficient catalysts for the dimerisation of both aliphatic and aromatic aldehydes has been intensively investigated (*vide supra*), the major problem relating to the selectivity of the process in the reaction involving two different carbonyl species (that theoretically will lead to four different products) has not been resolved until very recently.

1.6.3.1 Reaction between two different aldehydes

In the early studies, the selective formation of a single mixed ester product was attempted using two aldehydes with different steric/electronic characteristics.[203,204] Aliphatic aldehydes were found to be better hydride donors compared to their aromatic counterparts.[203,204] For this reason, reactions were generally performed using an excess of the less reactive moiety in order to facilitate the 'reduction' of the more reactive species. However, this strategy failed, as the difference in reactivity was not enough to guarantee selectivity to the process and mixtures of the four possible products were generally obtained.[203,204]

More recently, other catalytic systems based on actinide complexes[227,228] and heterogeneous-based catalysts[234–236] have been developed in order to improve the selectivity in the product formation; however, results were not encouraging as high selectivity was never achieved. Improved results were obtained in 1993 by Ishii and co-workers in the crossed reaction of butyraldehyde with two equivalents of benzaldehyde, catalysed by zirconium complexes.[218] Under these conditions the group was able to obtain 71% selectivity in the formation of the product (benzyl butyrate) in which the aliphatic aldehyde was oxidised while the aromatic reduced, but only in moderate yields.

Very recently Ogoshi *et al.*, inspired by their previous results in the Tishchenko reaction of aldehydes catalysed by nickel(0)-*N*-heterocyclic carbene complexes,[221] reported the application of a similar catalyst involving the use of **266** as the carbene in the crossed-reaction of two different aldehydes.[222]
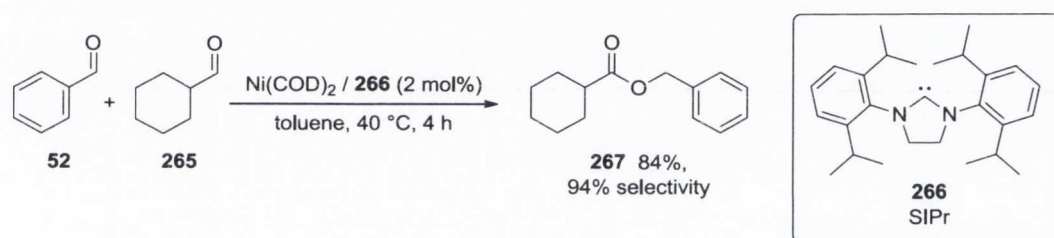
Scheme 1.61 Nickel-catalysed crossed-Tishchenko reaction.

They found that under optimised conditions an equimolar amount of aliphatic (*e.g.* **265**) and aromatic aldehyde (*e.g.* **52**) can be converted to the respective mixed ester product **267**, formed by oxidation of the aliphatic aldehyde and reduction of the aromatic aldehyde, in 94% selectivity and 84% yield. They also proposed a new reaction mechanism for this Ni(0)-mediated process, basing it on experimental evidence.[222]

1.6.3.2 Reaction between aldehyde and ketone

The intermolecular Tishchenko reaction involving two different carbonyl moieties, such as an aldehyde and a ketone, has been less thoroughly investigated. Only two reports addressing the reaction have been published in literature. The first, reported by Urry *et al.* in 1967, described the synthesis in good yields of mixed esters **270** from the reactions of both aliphatic and aromatic aldehydes (*e.g.* **52**) with chloroperfluoro and perfluoro ketones (*e.g.* **268**) promoted by benzoyl peroxide (**269**, Scheme 1.62).[237]

However, the process has not been referred to as a Tishchenko reaction, as the reaction has been deemed to take place *via* a free-radical chain addition.
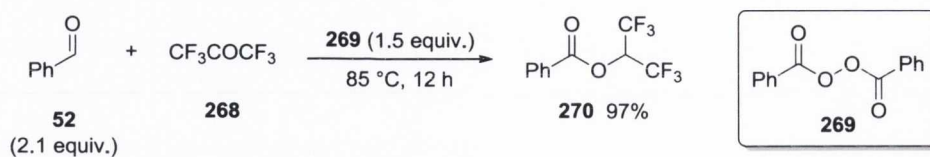
Scheme 1.62 Intermolecular "Tishchenko" reaction between benzaldehyde (**52**) and perfluoro ketone **268** catalysed by benzoyl peroxide (**269**).

The second and more recent report has been published by Scheidt and co-workers and is based on the reaction between aromatic aldehydes such as **52** and α-ketoesters (*e.g.* **270**), catalysed by *N*-heterocyclic carbenes (*e.g.* **271**) and diazabicyclo[5.4.0]undec-7-ene (DBU) to furnish products such as **272** in good yields (Scheme 1.63).[238]
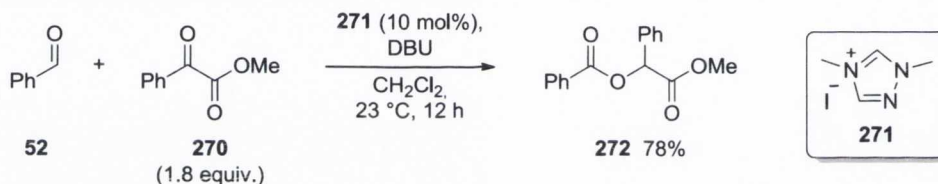
Scheme 1.63 Intermolecular Tishchenko reaction between benzaldehyde (**52**) and α-ketoester **270** catalysed by *N*-heterocyclic carbene **271** and DBU.

The reaction proved to be wide in scope, as several activated ketones were successfully employed, furnishing products in good yields. The authors explained the reaction pathway as a variation of the benzoin condensation mechanism, stressing that the two key steps of the reaction, the hydride transfer and the acylation, take place in different points of the catalytic cycle.[238] This was also proven by conducting the reaction in different solvents. Reactions performed in the aprotic dichloromethane produced exclusively the desired mixed ester products in good yields, while the use of a protic solvent such as methanol led to the formation of the alcohols formed by hydride transfer to the ketones with no mixed ester formation.[238]

1.6.4 Intramolecular Tishchenko reaction

The formation of lactones is an important step in the synthesis of many natural products.[239–241] The Tishchenko reaction has been successfully applied to lactone

synthesis: an intramolecular reaction between two carbonyl functionalities can be used to catalytically produce cyclic esters.

In 1991 Uenishi and co-workers demonstrated that 5-oxo-4-silyloxyhexanals such as **273** can be converted to δ-lactones (*e.g.* **274**) by a Tishchenko reaction promoted by stoichiometric amounts of trivalent samarium reagents such as $(t\text{-BuO})SmI_2$ or an aged SmI_2 solution (presumably containing Sm^{3+} ion) in good yields (Scheme 1.64).[242]
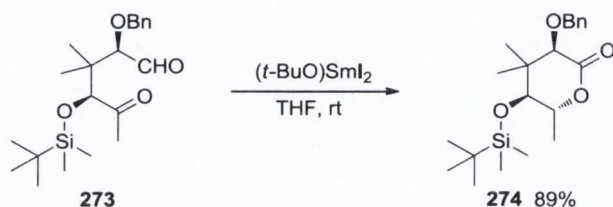
Scheme 1.64   Intramolecular Tishchenko reaction of 5-oxo-4-silyloxyhexanals to furnish δ-lactones.

They noticed that reactions with only divalent samarium (SmI_2) present, was furnishing the pinacol product exclusively, while small additions of methanol to the reaction, also containing SmI_2, produced a mixture of pinacol adduct and the desired lactones. They stated that the *in situ* generation of the trivalent samarium species $MeOSmI_2$ from SmI_2 was responsible for the catalysis.[242] The use of a bulkier alcohol such as *t*-butanol resulted in the production of the lactone only, with *trans* stereochemistry between the ketoaldehyde terminal methyl and the silyloxy groups exclusively (Scheme 1.64).[242]

Similar results were achieved years later by Fang *et al.*, who reported that 5-trimethylsilyl-5-oxopentanal can be converted to the relative δ-trimethylsilyl-δ-lactone by the intramolecular Tishchenko reaction promoted by stoichiometric amounts of SmI_2 and methanol.[243] The mechanism proposed consisted of the Lewis acid (SmI_2)-promoted addition of methanol to the aldehyde, followed by an intramolecular hydride shift to the ketone group with generation of the δ-hydroxyester intermediate which after cyclisation to δ-lactone, regenerates the catalyst.

Recently, other reports addressing the intramolecular Tishchenko reaction for the formation of lactones and phthalides appeared in the literature. The catalytic systems developed were based on metal (*i.e.* rhodium[244,245] and ruthenium[246]) complexes or on the employment of nucleophiles[247] or photochemical conditions.[247] They proved to be

extremely efficient in promoting the reaction, furnishing products in good to high yield and, in the cases where asymmetric products were formed, high stereocontrol was achieved.

1.6.4.1 The stereoselective intramolecular thiol/SmI$_2$-catalysed aldehyde-ketone Tishchenko reaction

Inspired by the results obtained three years before,[243] Fang *et al.* reported a catalytic version of the reaction using a combination of SmI$_2$ and 2-propanethiol (*i*-PrSH) as co-catalysts in low to moderate loading.[248] Under the optimised conditions the reaction proved to be extremely efficient and wide in scope, as several ketoaldehydes such as **275** and **276** were transformed into the respective lactones **277** and **278** in short reaction times, with high yields and with no formation of side aldol or pinacol products (Scheme 1.65). The reactions involving substrates bearing chiral centres such as **279** and **281** exhibited excellent stereocontrol as high diastereoselectivity in the formation of **280** and **282** respectively has been obtained, especially when the reactions were performed at low temperature (Scheme 1.65).[248]
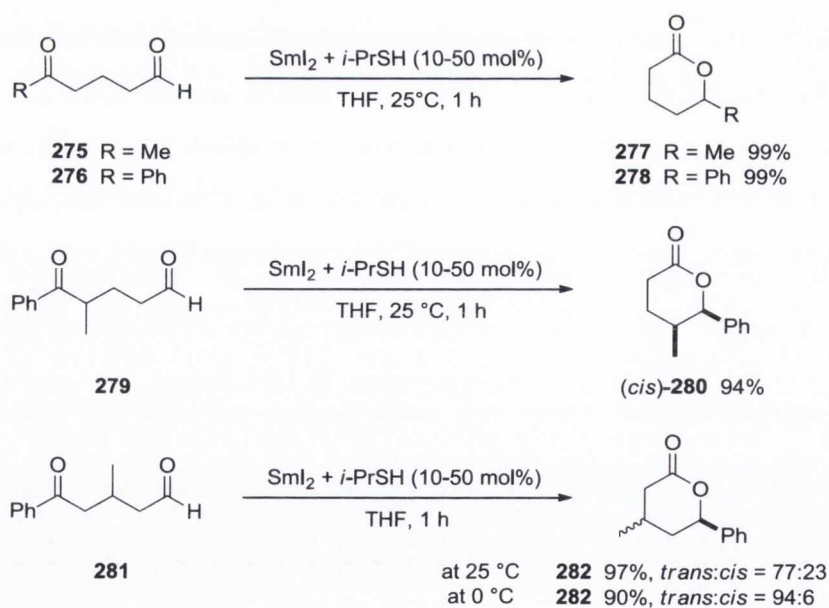
Scheme 1.65   SmI$_2$/*i*-PrSH catalysed Tishchenko reaction.

The catalytic cycle is depicted in Scheme 1.66. It begins with the addition of the catalytic species **284** to the aldehyde **283** activated by the Lewis acid to give the hemithioacetal intermediate **285**. This can then undergo an intramolecular hydride shift

to give the thioester **286**, which then lactonises in an irreversible process, leading to the lactone product **287** and regeneration of the catalyst **284**. The choice of using thiols has been rationalised by considering the higher nucleophilicity of mercaptans compared to the alcohols previously used. Moreover, the thioester **286** formed during the catalytic cycle is more electrophilic than the corresponding ester, facilitating the lactonisation step.[248]
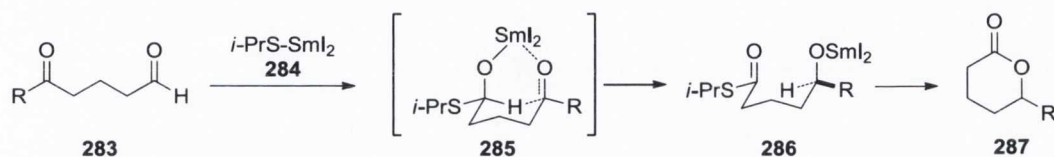
Scheme 1.66   Proposed catalytic cycle for the intramolecular thiol-SmI₂ catalysed aldehyde-ketone Tishchenko reaction.

The stereochemical outcome of the reaction has been explained by considering the geometry of the transition state **289** (Scheme 1.67). When the ketoaldehyde chain presents substituents, such as in case of substrate **288**, two six-membered transition states (*i.e.* **289a** and **289b**) for the hydride transfer step are possible.[248] However, equatorial disposition of the substituents such as in **289a** is energetically favoured compared to the axial one in **289b**. This will lead to the formation, after the lactonisation step, exclusively of the *cis* product **290** for 4,5-disubstituted lactones (*e.g.* **280**, Scheme 1.65) and predominantly of the *trans* product (**291**) for 3,5-disubstituted lactones (*e.g.* **282**, Scheme 1.65).
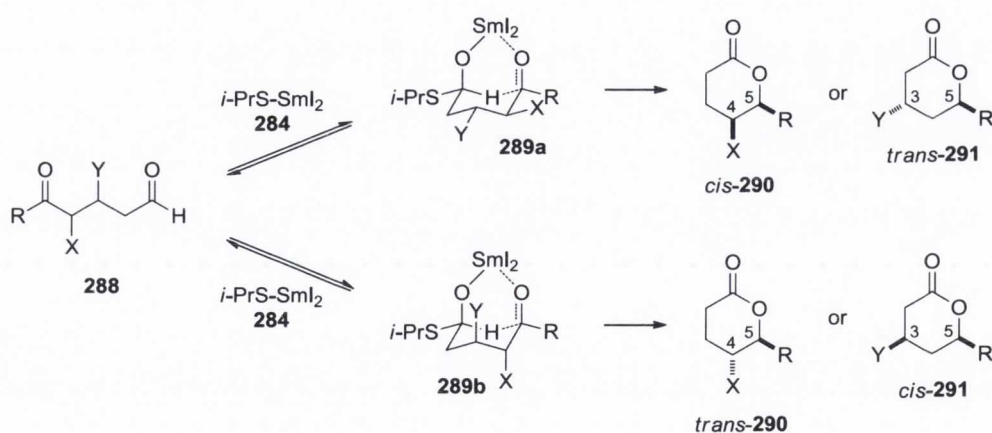
Scheme 1.67 Rationale of the stereochemical outcome for the reaction.

Fang and co-workers also developed an asymmetric version of the reaction employing the use of several chiral enantiopure thiols.[249] Under the optimised conditions 5-

oxoalkanales were converted to δ-lactones in good yield but only moderate enantioselectivity. Of the wide number evaluated, the best thiol catalyst proved to be **293**. This molecule, derived from (1*R*,2*S*)-(-)-norephedrine, mediated the conversion of ketoaldehydes such as **276** and **292** to their respective δ-lactones **278** and **294**.[249]

276 R = Ph
292 R = *n*-undecyl

(*S*)-**278** R = Ph 83%, 49% *ee*
(*R*)-**294** R = *n*-undecyl 75%, 74% *ee*

293
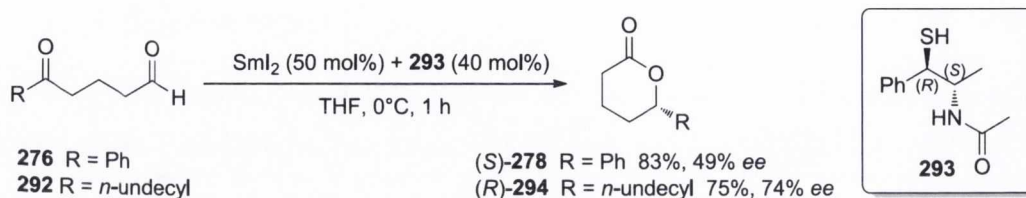
Scheme 1.68 Enantioselective intramolecular thiol/SmI$_2$-catalysed aldehyde-ketone crossed-Tishchenko reaction.

1.7 Objectives of this thesis

- Development of the first asymmetric cycloaddition reaction between homophthalic anhydrides and aldehydes promoted by cinchona alkaloid-derived organocatalysts for the synthesis of dihydroisocoumarin-derived products.

- Expansion of the scope to the use of aryl-substituted succinic anhydrides in the reaction with aldehydes for the synthesis of paraconic acid-derived structures bearing a quaternary stereocentre.

- Evaluation of Michael acceptors such as trisubstituted nitroalkenes in the cycloaddition reaction with homophthalic anhydrides for the formation of structures bearing three stereocentres, one of which is quaternary.

- Expansion of the scope to the use of alkylidene-2-oxindoles in the reaction with several aromatic and glutaconic-derived anhydrides for the synthesis of highly functionalised products bearing three stereocentres, one of which is a quaternary spiro-carbon.

- Development of the first thiolate-catalysed Tishchenko reaction between aldehydes and trifluoromethyl ketones, and its improvement under microwave irradiation.

Results and discussion

As described in Section 1.5, the formal cycloaddition of (enolisable) anhydrides to different types of electrophiles has been widely studied over the years, and in a number of cases it has been applied to the synthesis of natural compounds.[130] Although the processes are often diastereoselective, no study is currently known in the literature in which the enantioselectivity of this powerful strategy, which can form up to two carbon-carbon bonds and three stereogenic centres in one single step, has been controlled. The development of a process capable of furnishing high levels of enantiocontrol would be highly desirable.

For this reason we embarked upon the development of an asymmetric catalytic variant of these reactions using cinchona alkaloid organocatalysts as promoters of the processes. During this study, the author of this thesis was cooperating with fellow researchers and, unless specified, all results reported in the following sections derive from work carried by the author alone.

2. The asymmetric organocatalytic formal cycloaddition of homophthalic anhydrides to aldehydes

As discussed in Section 1.5.2, the cycloaddition reaction between aldehydes such as **52** and homophthalic anhydride (**147**) can be promoted by stoichiometric (or greater) amounts of either base[151–154] or Lewis acid,[155] furnishing annulated products such as **159** containing the bicyclic dihydroisocoumarins structural unit **295** (Scheme 2.1).
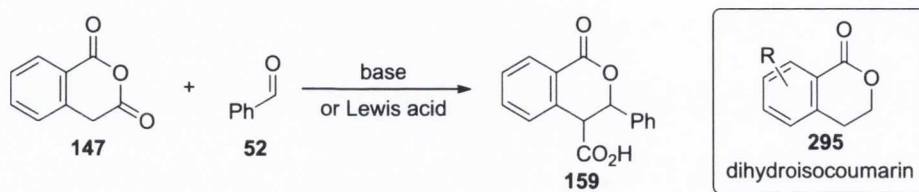
Scheme 2.1   Formal cycloaddition of homophthalic anhydride (**147**) to benzaldehyde (**52**).

Despite both the synthetic potential of these densely functionalised products, and the wide range of chiral natural products (and derivatives) which contain the dihydroisocoumarin core structure **295** (which possess a remarkable range of cytotoxic/antiproliferative,[250–252] phytotoxic,[253] antimicrobial,[254,255] antifungal,[256] antiulcer/antiinflammatory,[257,258] antimalarial,[259] antioxidant[260] and antiallergic[261] properties), no catalytic asymmetric variants of this reactions have been reported.

We reasoned that this absence is related to the difficulty in persuading electrophilic species such as homophthalic anhydrides to attack an aldehyde as a nucleophile, without either reacting with itself (an anhydride is usually regarded as a more reactive electrophile than an aldehyde) or the catalyst in a deleterious fashion.

Our group (among others)[262–271] has recently been engaged in the use of cinchona alkaloid-derived bifunctional organocatalysts to promote the asymmetric addition of alcohol[272] and thiol[103,273] nucleophiles to cyclic anhydrides and related electrophiles.[104] These catalysts rely on the confluence of relatively weak synergistic catalyst-substrate interactions (mostly the donation of hydrogen bonds to the anhydride electrophile and general-base catalysis of the nucleophilic addition of the pronucleophile). Since these catalysts are compatible with cyclic anhydride substrates (hitherto only when the anhydrides are being employed as electrophiles), and have been known (in isolated

cases) to activate aldehyde/ketone electrophiles,[110,120,121] we proposed that in the absence of a powerful pronucleophile these bifunctional catalysts could be employed to bring about the activation of an enolisable anhydride as a nucleophile through catalysis of the equilibrium between it and its enol form (with concomitant suppression of the anhydride's propensity to act as an electrophile), while simultaneously activating the aldehyde through hydrogen bond donation/general acid catalysis (Figure 2.1) in a controlled chiral environment.

H-bond donating
activate the aldehyde electrophile
(general acid catalysis)

quinuclidine ring
deprotonates the anhydride
nucleophile (enol)
(general base catalysis)
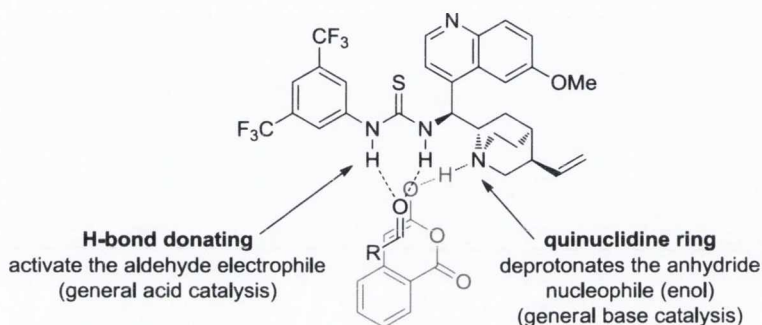
Figure 2.1   Proposed bifunctional asymmetric organocatalytic strategy for the formal cycloaddition between anhydrides and aldehydes.

2.1   Preliminary experiments

To test our hypothesis we chose to evaluate, in preliminary studies, the reaction between benzaldehyde (**52**) and homophthalic anhydride (**147**, Table 2.1). The latter was synthesised by reaction of readily available homophthalic acid (**296**) with acetic anhydride (Scheme 2.2).
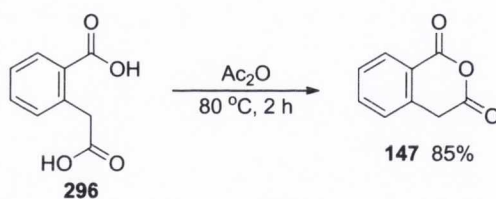
Scheme 2.2   Synthesis of homophthalic anhydride (**147**).

Using THF as solvent, **147** and **52** were reacted together in either the absence or the presence of catalytic amounts of catalyst at room temperature under the conditions shown in Table 2.1 to furnish **159** as a mixture of diastereomeric (*trans* and *cis*) products. The choice of this solvent was based on previous observations made in our group. It is believed that for bifunctionally-catalysed reactions that form acids from

anhydrides, the pK_a of the acid products can be increased (compared to other solvents) by the use of ethereal solvents, thus preventing product inhibition of catalysis *via* protonation of the catalyst's quinuclidine moiety.

Table 2.1   Preliminary experiments on the cycloaddition between homophthalic anhydride (**147**) and benzaldehyde (**52**).
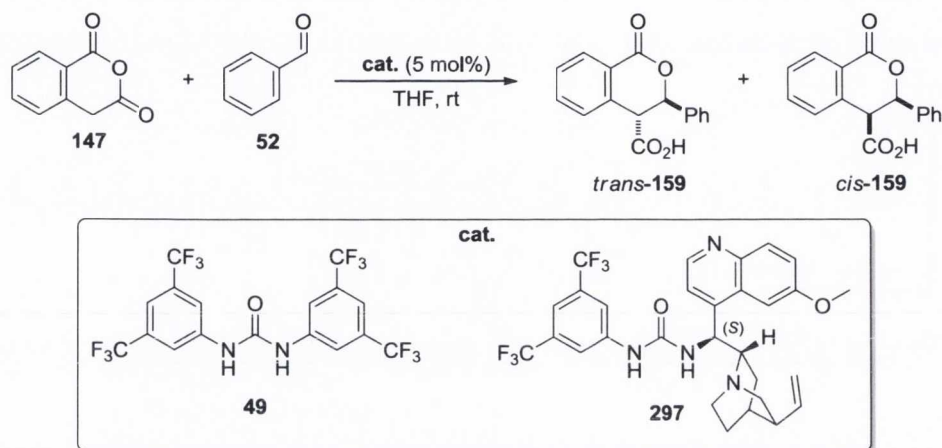
entry	catalyst	conc. (M)	time (h)	yield (%)[a]	dr (*trans:cis*)[b]
1	-	0.4	19	49	71:29
2	-	0.2	1	0	-
3	-	0.2	2	0	-
4	-	0.2	19	20	75:25
5	*i*-Pr$_2$NEt	0.2	0.33	52	75:25
6	*i*-Pr$_2$NEt	0.2	19	95	75:25
7	*i*-Pr$_2$NEt / **49**	0.2	19	93	69:31
8[c]	**49**	0.2	19	32	75:25
9[c]	**297**	0.2	19	97	86:14

[a] Yield of combined diastereomers determined by ^{1}H NMR spectroscopic analysis using *p*-iodoanisole as an internal standard. [b] Diastereomeric ratio determined by ^{1}H NMR spectroscopic analysis. [c] Experiments conducted by Dr. Claudio Cornaggia.

The initial reactions were performed in order to evaluate the extent of the potential background reaction (*i.e.* the uncatalysed reaction). This process takes place in moderate yields, with a preference for the formation of the *trans*-diastereomer of **159** (entry 1, Table 2.1). Decreasing the reaction concentration (entries 2-4) retarded the rate

of the background reaction, with concomitant small increase of diastereoselectivity (entry 4).

Under the same conditions, the reaction promoted by a catalytic amount (*i.e.* 5 mol%) of Hünig's base (entries 5 and 6) led to considerably shorter reaction times with no improvement in diastereoselectivity; however, it was pleasing to observe that sub-stoichiometric catalysis of this reaction by an amine base was possible. The observed catalysis of this reaction by a non-nucleophilic base lends weight to the hypothesis that the enol of anhydride **147** acts as a nucleophilic species in the reaction.

Addition of a H-bond donating species, *i.e.* the *N,N*-diaryl urea **49**, to the base-promoted reaction (entry 7), resulted in comparable yields to those obtained using the base alone (entry 6); however, with lower diastereoselectivity. Fellow researcher Dr. Claudio Cornaggia observed that when the reaction was carried out with *N,N*-diaryl urea **49** as the catalyst (entry 8), it furnished yields only marginally above those obtained in the uncatalysed process (entry 4) and with no improvement in stereocontrol. This result demonstrated the importance of the general base functionality in catalysing the reaction under the conditions evaluated. The same researcher also reported that the use of the bifunctional C-9-urea substituted cinchona alkaloid organocatalyst **297** (previously synthesised by Dr. Aldo Peschiulli), promoted the reaction in high yields furnishing the highest diastereoselectivity observed in these preliminary tests (entry 9). This was attributed to the simultaneous activation of both the nucleophile (*i.e.* anhydride) and electrophile (*i.e.* aldehyde) by both functionalities of the catalyst in the correct relative spatial arrangement. Kinetic studies, conducted by Dr. Claudio Cornaggia, involving monitoring the reaction over time (Table 2.2), revealed that high yields of the lactone-acid product **159** can be obtained in short reaction times (entries 1 and 2). He also observed that diastereocontrol was independent of conversion (entries 1, 2 and 3), demonstrating that no epimerisation of the lactone-acid product **159** by catalyst-mediated enolisation occurred during the reaction (Table 2.2).

Table 2.2   Diastereocontrol in the cycloaddition between homophthalic anhydride (**147**) and benzaldehyde (**52**). All the reactions were executed by Dr. Claudio Cornaggia.
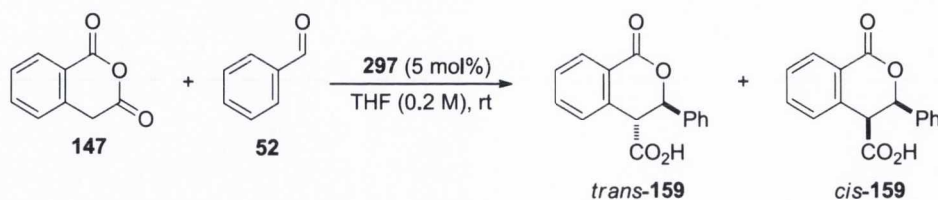
entry	time (h)	yield (%)^a	dr (*trans:cis*)^b
1^c	1	85	86:14
2^c	2	91	86:14
3^c	19	97	86:14

^{a} Yield of combined diastereomers determined by ^{1}H NMR spectroscopic analysis using *p*-iodoanisole as an internal standard. ^{b} Diastereomeric ratio determined by ^{1}H NMR spectroscopic analysis. ^{c} Experiment conducted by Dr. Claudio Cornaggia.

Epimerisation of product **159** on work-up was also avoided by extracting it from the crude reaction mixture following Cushman's procedure. Extraction with sodium bicarbonate solution followed by acidification with hydrochloric acid solution and second extraction with organic solvent allows the isolation of the lactone-acid products without epimerisation of the stereocentres.[144] This was verified by comparison of ^{1}H NMR spectra of the reaction crude with the mixture of diastereomeric product **159** extracted from the reaction following the method above.

Evaluation of the enantioselectivity of the process by analysis by chiral stationary phase high performance liquid chromatography (CSP-HPLC) was then required. In order to achieve this, the two diastereomeric structures of the lactone-acid product **159** needed to be isolated. Conversion of the carboxylic acid substituent of **159** to the methyl ester derivative, followed by purification by flash column chromatography on silica gel seemed the most useful procedure. Dr. Claudio Cornaggia developed a useful methodology using an equimolar amount of Hünig's base (*i*-Pr$_2$NEt) and 2.0 equivalents of methyl iodide (MeI) as the alkylant agent, furnishing a diastereomeric mixture of lactone-ester **170** in moderate yields with only trace amounts of the side-reaction product **171**, which was formed in high yield using other methodologies (Scheme 2.3).

*trans-*159   *cis-*159   *trans-*170   *cis-*170   171 trace
                                                            combined yield 50 %
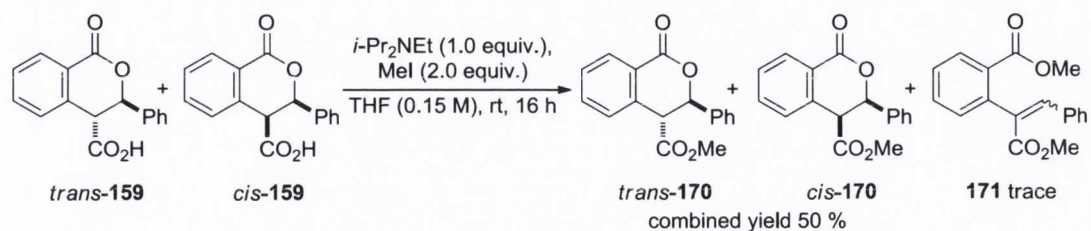
Scheme 2.3   Conversion of the lactone-acid product **159** to lactone-ester **170**
                        (executed by Dr. Claudio Cornaggia).

2.2   Catalyst evaluation and optimisation studies for the formal cycloaddition reaction between homophthalic anhydride and benzaldehyde

Attention now turned to the evaluation of several cinchona-based organocatalysts as reaction promoters. These catalysts were previously made by fellow researchers in our group during successful studies of different types of reactions. For this reason, it was possible, in collaboration with Dr. Claudio Cornaggia, to evaluate a wide number of different structures in the reaction between homophthalic anhydride (**147**) and benzaldehyde (**52**).

The protocol used involved the reaction of equimolar amounts of **147** and **52** promoted by 5 mol% of catalyst at room temperature in THF (0.2 M). After 19 h products yields were determined by ^{1}H NMR analysis of the crude using *p*-iodoanisole as an internal standard. Subsequently, extraction of the diastereomeric mixture of lactone-acids and subsequent ^{1}H NMR spectroscopic analysis allowed the diastereoselectivity of the reactions to be quantified. The mixtures of the lactone-acid were then converted to their methyl ester derivatives by the previously described procedure and purified by flash column chromatography on silica gel. In this phase of the study, the two diastereomers were not separated prior to the CSP-HPLC analysis, as an efficient method for the simultaneous determination of the relative amounts of all four product stereoisomers had been identified.

Table 2.3   Catalyst evaluation in the formal cycloaddition reaction between homophthalic anhydride (**147**) and benzaldehyde (**52**).
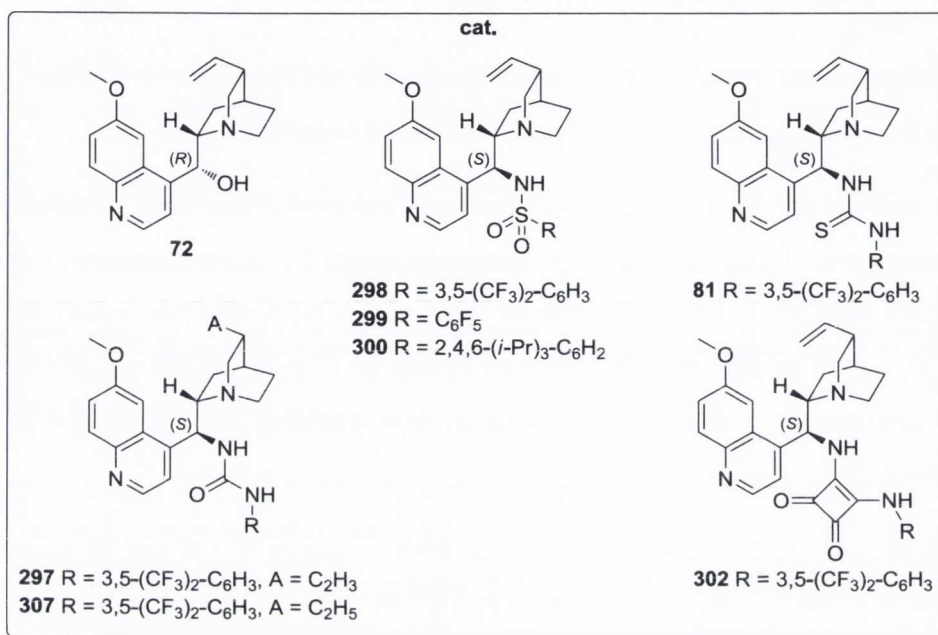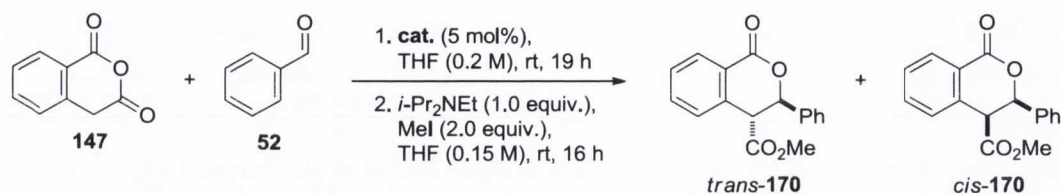
entry	cat.	yield (%)^a	dr (trans:cis)^b	ee$_{trans}$ (%)^c	ee$_{cis}$ (%)^c
1	72	84	81:19	-7	26
2	298	98	90:10	5	30
3	299	97	91:9	-69	35
4	300	98	85:15	-21	24
5^d	81	92	90:10	79	76
6^d	297	97	86:14	66	70
7	301	92	85:15	62	68
8	302	80	84:16	90	67

^{a} Yield of combined diastereomers determined by ^{1}H NMR spectroscopic analysis using *p*-iodoanisole as an internal standard. ^{b} Diastereomeric ratio determined by ^{1}H NMR spectroscopic analysis. ^{c} Determined by CSP-HPLC. ^{d} Reaction executed by Dr. Claudio Cornaggia.

Using this protocol, the abundant natural cinchona alkaloid quinine (**72**) promoted the reaction with marginally higher diastereoselectivity compared to the reaction catalysed by *i*-Pr₂NEt (*i.e.* entry 6, Table 2.1); this demonstrates the superiority of bifunctional catalysts compared to monofunctional analogues that are not capable of directing H-bonding. However, the enantiomeric excess of the product was inadequate (entry 1).

The bifunctional sulfonamide-substituted catalysts **298-300** (catalysts previously synthesised by Dr. Aldo Peschiulli), which have proven to be highly efficacious in the catalysis of asymmetric additions to anhydrides,[103,269,271] promoted the formation of predominantly *trans*-**170** in excellent yield, however with poor to moderate levels of enantioselectivity (entries 2-4). Use of catalysts **81**, **297** (reactions executed by Dr. Claudio Cornaggia) and **301** (catalysts previously synthesised by Dr. Aldo Peschiulli) in which the sulfonamide substituent has been exchanged for a (thio)urea, resulted in the promotion of the reaction with higher enantioselectivity (entries 5-7). In this context it is possible to compare the efficacy of these double H-bonding catalysts (entries 5-7) to single H-bonding moieties (entries 1-4). It is notable that the former catalyst class have a stronger stereocontrolling effect on the reaction; with the thiourea-based catalyst **81** superior to the others.

It is also possible to compare the effect of the quinuclidine ring substituent by analysing the reactions promoted by **297** and **301** (entries 6 and 7). Catalyst **297**, which bears an alkene substituent on the quinuclidine ring, proved to be slightly superior in the reaction (executed by Dr. Claudio Cornaggia, entry 6): it promoted the reaction with higher yield and better stereoselectivity compared to the reaction catalysed by the saturated analogue **301** (entry 7).

At this point of the study cooperative work between the author and Dr. Claudio Cornaggia permitted the evaluation of a small library of 14 different cinchona-based organocatalysts, of which **81** proved to be superior to the others. However, in order to further improve the stereocontrol of the reaction, further modifications to the structure of C-9 (thio)urea-substituted cinchona alkaloids appeared futile. In this regard, it was then decided to evaluate bifunctional catalysts with alternative H-bonding capabilities.

Recently, Rawal[99] successfully introduced a class of squaramide-substituted catalysts as an alternative to (thio)urea-based materials (Section 1.4.1.1.2). We therefore decided

75

that the evaluation of C-9 squaramide-substituted cinchona alkaloids was a logical step. We were pleased to observe that catalyst **302** (synthesised by Dr. Seán Tallon) could catalyse the formation of *trans*-**170** with good diastereoselectivity and 90% *ee* (entry 8); however, although **302** proved to be the most promising of the known materials evaluated, it did not yet represent an optimal catalytic solution.

We speculated that this may be due to the steric requirement around the C-4'–C-9 axis of the catalyst **302** quinoline ring (Figure 2.2). Rotation of the quinoline unit around this single bond will inevitably lead to the asymmetric occupation of the quadrants defining the three-dimensional space around the squaramide moiety. Depending on whether the methoxy-substituted portion of the quinoline ring is orientated either towards the carbonyl moieties (*i.e.* **A**, Figure 2.2) or the N-H bonds (*i.e.* **B**, Figure 2.2), the steric environment of the catalysts 'active site' could be quite different. We therefore proposed that the installation of a phenyl substituent at C-2' of the quinoline ring would be able to more appropriately balance the steric requirement of the quinoline ring (*i.e.* **C**, **D**, Figure 2.2) rendering the performance of catalyst **303** less dependent on the orientation of this heterocyclic substituent.
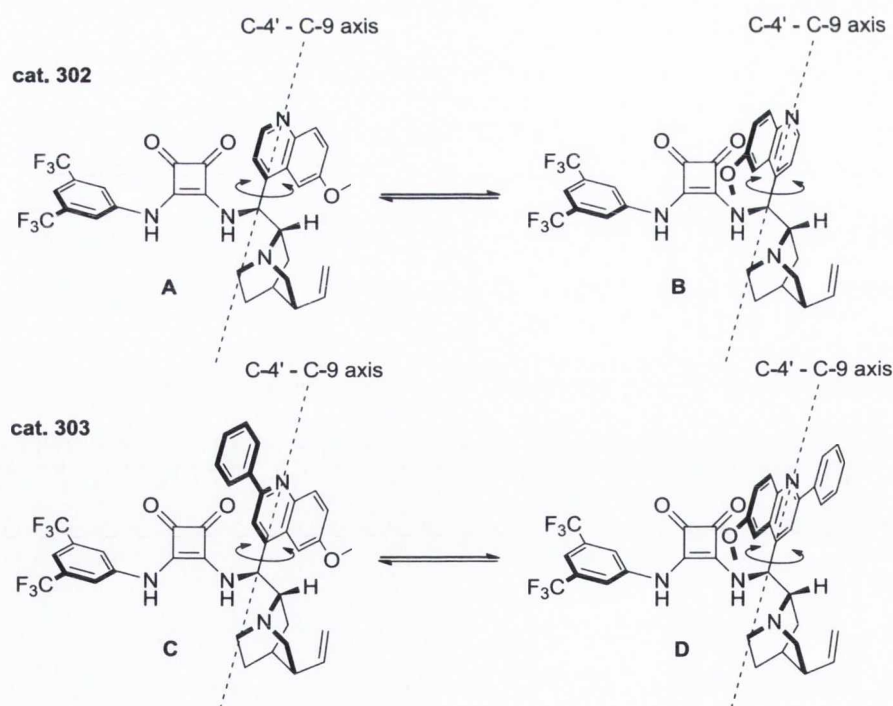
Figure 2.2   Rationale underpinning the design of the C-2' substituted cinchona alkaloid organocatalyst based on squaramide.

Gratifyingly, the use of C-2' substituted catalyst **303** (synthesised by Dr. Seán Tallon and evaluated by Dr. Claudio Cornaggia) as promoter for the reaction gave considerably better results, furnishing the diastereomeric mixture of the lactone-ester **170** in 96% yield and high diastereo- and enantioselectivity (*i.e.* 91:9 *dr* (*trans:cis*), 93% *ee*$_{trans}$, 65% *ee*$_{cis}$).

2.3 Optimisation of the reaction temperature

The next goal became the further optimisation of the reaction conditions in order to improve the stereoselectivity of the process.

Dr. Claudio Cornaggia demonstrated that superior results can be obtained by conducting the reaction at a lower concentration (0.1 M) and by using either methyl *t*-butyl ether (MTBE) or THF as solvents, furnishing **170** as mixture of diastereomers in excellent yield and high stereoselectivity (*i.e.* THF: 23 °C, 18 h, 98% yield, 91:9 *dr* (*trans:cis*), 94% *ee*$_{trans}$, 73% *ee*$_{cis}$; MTBE: 23 °C, 18 h, >99% yield, 92:8 *dr* (*trans:cis*), 95% *ee*$_{trans}$, 61% *ee*$_{cis}$).

The reaction temperature was the next variable to be examined. The two sets of reaction conditions previously mentioned (disclosed by Dr. Claudio Cornaggia) established a good starting point for this optimisation study (Table 2.4). When repeated at a lower temperature (*i.e.* 0 °C) both of the reactions exhibited improvement in the diastereo- and enantiocontrol, furnishing product **170** in high yields, although in longer reaction times (entries 1 and 2). However, reducing the temperature to 0 °C affected the yield of the reaction conducted in THF, reducing it to 87% (entry 1), while the yield of the reaction conducted in MTBE was not affected (entry 2), leading to the decision to use MTBE as reaction solvent. Decreasing the reaction temperature to -15 °C (entry 3) further improved the stereocontrol of the process disclosing the best conditions in which conduct the reaction.

Table 2.4   The cycloaddition reaction between homophthalic anhydride (**147**) and benzaldehyde (**52**): optimisation of the reaction temperature.
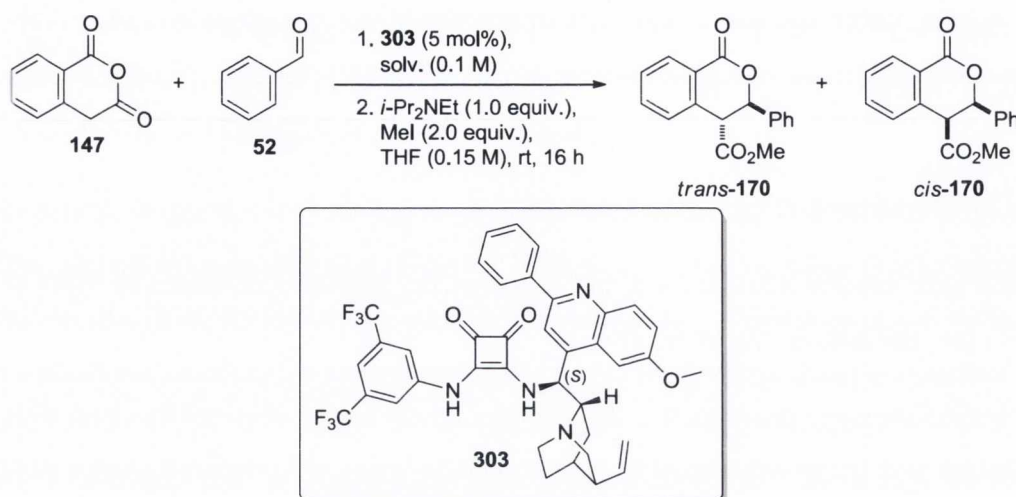
entry	time (h)	solvent	temp. (°C)	yield (%)[a]	dr (*trans:cis*)[b]	ee*trans* (%)[c]	ee*cis* (%)[c]
1	36	THF	0	87	93:7	96	n.d.[d]
2	36	MTBE	0	>99	95:5	96	n.d.[d]
3	22	MTBE	-15	98	96:4	97	n.d.[d]

[a] Yield of combined diastereomers determined by ^{1}H NMR spectroscopic analysis using *p*-iodoanisole as an internal standard. [b] Diastereomeric ratio determined by ^{1}H NMR spectroscopic analysis. [c] Determined by CSP-HPLC. [d] Not determined.

2.4   Evaluation of substrate scope: the aldehyde component

With a synthetically useful protocol now in hand, our attention turned to the important question of substrate scope (Table 2.5). We evaluated several type of aldehydes in the reaction with homophthalic anhydride (**147**) catalysed by 5 mol% of catalyst **303** under the optimised conditions.

However, the low yields furnished by the esterification procedure (previously developed by Dr. Claudio Cornaggia) used as an efficient strategy during the evaluation of the catalysts where isolated yields of products were not fundamental, proved to be inadequate for the study of the substrate scope, where the isolated yields are required. To obviate this major drawback, an alternative esterification procedure, based on the use of trimethylsilyl diazomethane (TMSCHN$_2$, 1.2 equiv.) and methanol *in situ* upon completion of the reaction was utilised.

Table 2.5   Evaluation of substrate scope: the aldehyde component.
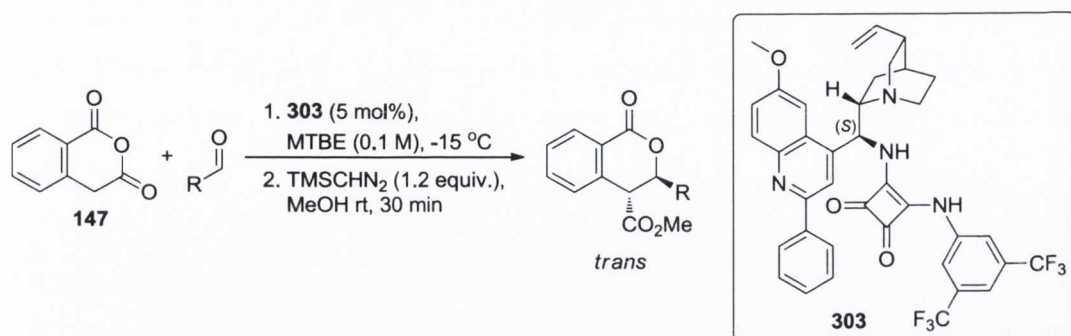
entry	product	temp. (°C)	yield (%)^a	dr (*trans:cis*)^b	ee$_{trans}$ (%)^c
1	*trans*-**304**	40	93	95:5	95
2	*trans*-**305**	48	92	93:7	96
3	*trans*-**306**	115	78	90:10	91
4	*trans*-**307**	48	84	94:6	97
5	*trans*-**308**	22	94^d	75:25	98 (90)^e

^{a} Isolated yield of the *trans*-diastereomer after column chromatography. ^{b} Diastereomeric ratio determined by ^{1}H NMR spectroscopic analysis. ^{c} Determined by CSP-HPLC. ^{d} Diastereomers not separable: combined isolated yield. ^{e} ee of *cis*-isomer in parenthesis.

Under these improved conditions the methodology proved extraordinarily robust: reactions between **147** and electron-deficient (entries 1 and 2), electron-rich (entry 3) and heterocyclic aromatic (entry 4) aldehydes were well tolerated by the catalyst. Yields

and enantiomeric excesses of the isolated *trans*-diastereomers **304-307** were generally excellent (≥92% yield and ≥95% *ee* respectively). The deactivated *p*-anisaldehyde proved a greater challenge than the other electrophiles evaluated in this study, yet product *trans*-**306** could still be obtained in good yield and >90% *ee*, although in a longer reaction time (entry 3). Thiophene carbaldehyde also proved to be a relatively difficult substrate, resulting in an 84% isolated yield (97% *ee*, entry 4) of *trans*-**307**. Aliphatic aldehydes also underwent the formal cycloaddition: the straight-chain hydrocinnamaldehyde could be converted to **308** in a short reaction time and in excellent yield (entry 5). However, while the *dr* is uniformly excellent in the case of aromatic aldehydes, the use of this aliphatic aldehyde lead to acceptable but elevated levels of the *cis*-diastereomer that could not be chromatographically separated from the *trans*-diastereomer. This was somewhat mitigated by the fact that both diastereomers were formed with high enantioselectivity. The *trans*-diastereomer was formed in near optical purity (entry 5).

The absolute stereochemistry of the products was then assigned by X-ray diffraction analysis of a recrystallised sample of *trans*-**307**. This sample was chosen as it incorporates a heavy atom (*i.e.* sulfur) in the structure facilitating the resolution of the diffraction image. The result obtained allowed the unequivocal assignment of the absolute stereochemistry of *trans*-**307** (Figure 2.3) as (3*R*,4*R*).
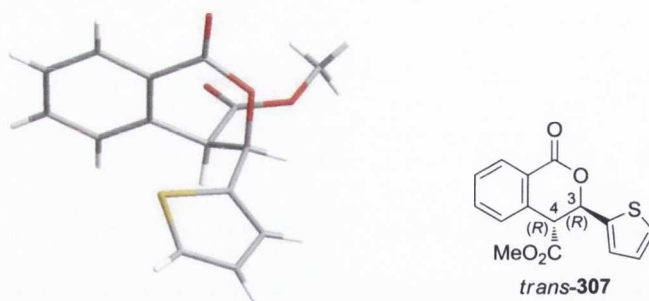
Figure 2.3   Absolute stereochemical assignment of product *trans*-**307**.

As further confirmation, Dr. Claudio Cornaggia also obtained the absolute stereochemistry of *trans*-**309** and *trans*-**170** (Figure 2.4), assigning them as (3*R*,4*R*).

trans-**309**
(obtained by Dr. Claudio Cornaggia)

trans-**170**
(obtained by Dr. Claudio Cornaggia)
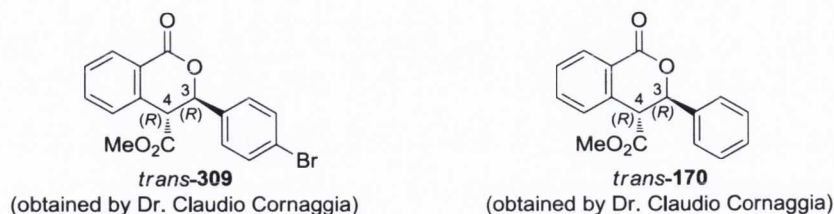
Figure 2.4 Absolute stereochemical assignment of product *trans*-**309** and *trans*-**170**.

2.5 Evaluation of substrate scope: anhydride component

After obtaining good results in the evaluation of the aldehyde substrate scope (which confirmed the general applicability of the asymmetric process developed for the cycloaddition of aldehydes to homophthalic anhydride (**147**)), our attention turned to the anhydride scope.

Substitution at the aromatic ring is a feature of several of the medicinally relevant bicyclic dihydroisocoumarin compounds,[250–261] therefore, to evaluate the effect of the installation of electron-withdrawing and electron-donating functionalities on the performance of the homophthalic anhydride pronucleophile in the reaction, substituted homophthalic anhydrides were synthesised in good yields (Scheme 2.4) and evaluated in the reaction with benzaldehyde (Table 2.6).
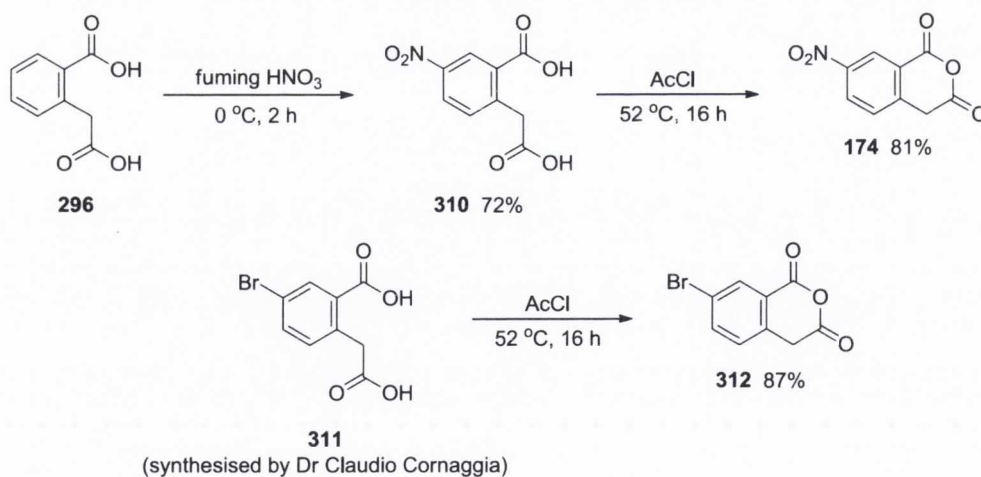
Scheme 2.4 Synthesis of substituted homophthalic anhydrides.

Anhydrides **174** and **312** were synthesised by cyclisation of the substituted homophthalic acids **310** and **311** by reaction with acetyl chloride (Scheme 2.4). The nitro-substituted homophthalic acid **310** was synthesised by reacting homophthalic acid **296** with fuming HNO_3, according to the procedure reported in the literature (Scheme

81

2.4).[274] Bromo-substituted homophthalic acid **311** was synthesised by Dr. Claudio Cornaggia following the reported procedure by Balci and co-workers (Scheme 2.4).[275] A methoxy-substituted homophthalic anhydride (*i.e.* **313**) was also synthesised and evaluated in the reaction by Dr. Claudio Cornaggia.

Table 2.6   Evaluation of the substrate scope: homophthalic anhydride component.

entry	product	time (h)	yield (%)^a	dr (*trans:cis*)^b	ee$_{trans}$ (%)^c
1	*trans*-**314**	96	63 (87)^d	94:6	91
2	*trans*-**315**	64	68 (95)^d	95:5	93
3 ^{e}	*trans*-**316**	164	65 (81)^d	95:5	96

^{a} Isolated yield of the *trans*-diastereomer after column chromatography. ^{b} Diastereomeric ratio determined by ^{1}H NMR spectroscopic analysis. ^{c} Determined by CSP-HPLC. ^{d} Yield (determined by ^{1}H NMR spectroscopic analysis using *p*-iodoanisole as an internal standard prior to esterification and chromatography in parenthesis). ^{e} Reaction performed by Dr. Claudio Cornaggia.

Substrates incorporating nitro- (entry 1) and bromo- (entry 2) functional groups can be used to form **314** and **315** respectively in excellent *dr* and *ee* (Table 2.6). While the yield of the crude acids (determined by ^{1}H NMR spectroscopic analysis using *p*-iodoanisole as an internal standard) was excellent in both cases, in preliminary experiments we found that the isolation of these lactones is more difficult due to ring-opening of the (now more electrophilic) lactones upon both esterification and during careful column chromatography on silica gel to separate the diastereomeric products. For this reason, a new esterification procedure based on the use of equimolar amount

(5.0 equiv.) of TMSCHN$_2$ and *i*-PrOH (less nucleophilic and more hindered than MeOH) on the isolated mixture of diastereomeric acids was developed. Although the deleterious lactone ring-opening reaction could be inhibited using this new protocol, it was not possible to completely suppress it. Nonetheless, synthetically useful yields of pure *trans*-**314** and *trans*-**315** were obtained (entries 2 and 3, Table 2.6). The electron-donating methoxy group was also found to be compatible in the reaction (performed by Dr. Claudio Cornaggia); *trans*-**316** was prepared in good yield and excellent *dr* and *ee* (entry 3, Table 2.6).

2.6   Stereochemical outcome: rationale

The stereochemical outcome of these new processes was then rationalised. Although the models proposed to describe the mechanism of action of the catalytic species (*e.g.* **303**) extensively fit the results obtained, no computational studies or spectroscopic evidence to support these pathways were collected. As such, the models proposed below should be considered speculative.

It has been shown that when catalysed by the squaramide-derived cinchona alkaloid organocatalyst **303** under the optimised conditions described above (entry 3, Table 2.4), the reaction between homophthalic anhydride (**147**) and benzaldehyde (**52**) produced *trans*-**170** in high yield (*i.e.* 98%) with remarkable enantioselectivity (*i.e.* 97% *ee*). This product (as the methyl ester derivative) was later demonstrated (by X-ray diffraction analysis) to possess the absolute stereochemistry (3*R*,4*R*) shown in Figure 2.4.

To explain the stereochemical outcome of the reaction we proposed two plausible binding modes for the catalyst in the pre-transition state of the reaction: one in which the catalyst binds to the enolate and the other to the aldehyde. In the former model (Figure 2.5) the catalyst acts *via* specific acid/base catalysis respectively through double H-bonding by the squaramide moiety (acid) on the enolate species (formed by deprotonation before the C-C bond formation occurs) and through aldehyde activation by the ammonium ion (base) formed upon deprotonation.
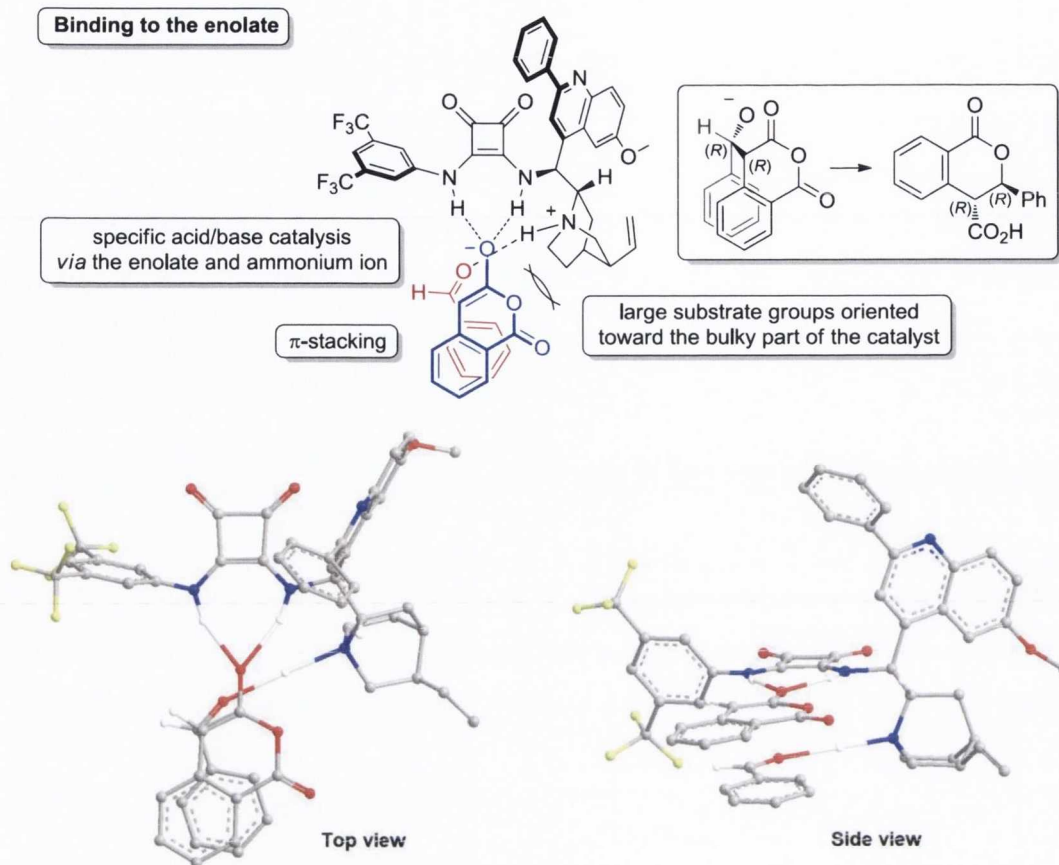
Figure 2.5   Rationale for the stereochemical outcome of the reaction with the catalyst binding the enolate.

In this case, in order to satisfy the stereochemical outcome, both the aldehyde and the anhydride substrates must orient the bulky part of their molecules towards the sterically hindered portion of the catalyst (*i.e.* quinuclidine ring) generating steric clash and thus destabilising the transition state.

A more stable-looking and thus plausible pre-transition state can be obtained in the second possible catalyst binding mode: the binding of the squaramide to the aldehyde (Figure 2.6). In this situation the catalyst acts *via* general acid/base catalysis, activating the aldehyde through double H-bonding, with concomitant deprotonation of the enol tautomer of the anhydride <u>during</u> the transition state. According to this model, in order to obtain the absolute stereochemistry found in the products, both aldehyde and anhydride substrates orient their bulky substituents away from the hindered quinuclidine ring, thus avoiding any destabilising steric clashes.
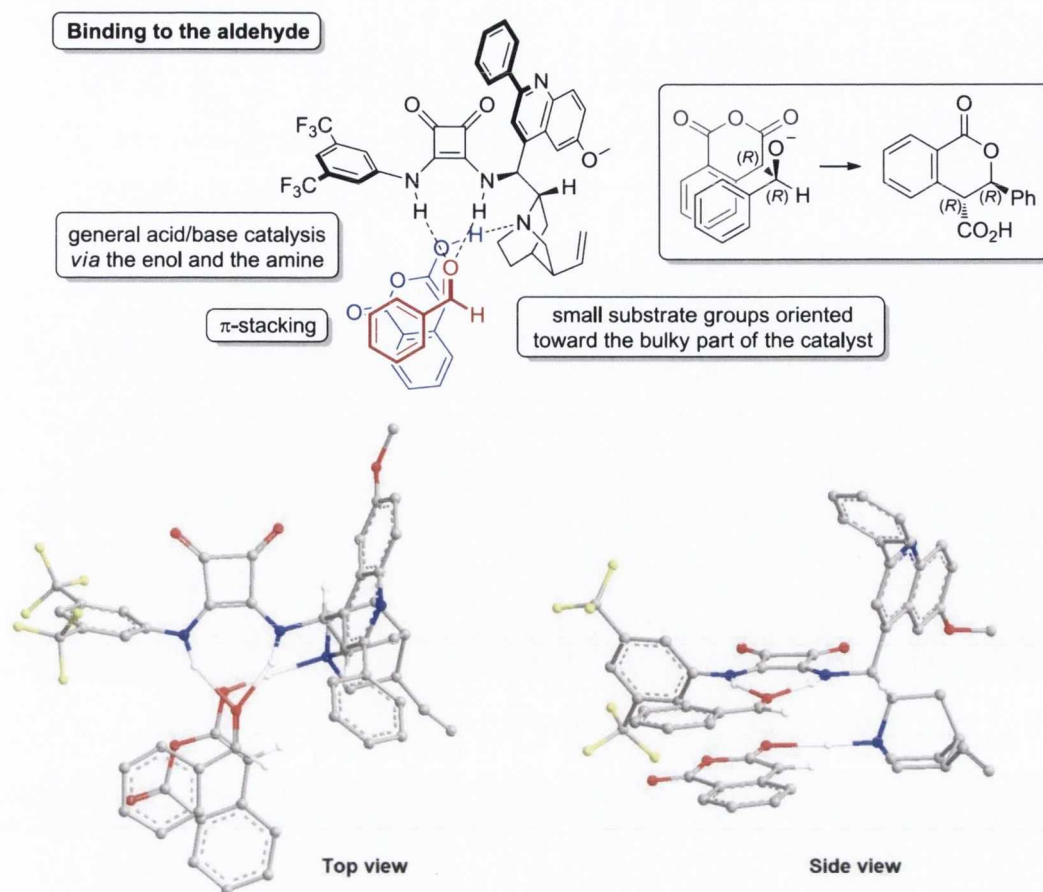
Figure 2.6   Rationale for the stereochemical outcome of the reaction with the squaramide binding the aldehyde.

In both cases, a certain (not proven) level of π-stacking between the aromatic moieties of the anhydride and the aldehyde may aid in organising the pre-transition state assembly. This finds support in the results obtained from the reaction involving aliphatic aldehydes (*e.g.* entry 5, Table 2.5). In this context it has been speculated that the lack of π-stacking between the two substrates is responsible for the lower diastereoselectivity obtained.

2.7   Conclusion

This work demonstrated the possibility of employing cinchona alkaloid-derived bifunctional organocatalysts to promote the enantioselective cycloaddition reaction between homophthalic anhydrides and aldehydes, revealing for the first time that anhydrides can be employed as nucleophiles in asymmetric catalysis.

The reactions catalysed by a novel squaramide-substituted cinchona alkaloid organocatalyst generated densely functionalised dihydroisocoumarins (a core structure in many medicinally relevant natural products) with the formation of two new stereocentres in high yield and excellent stereocontrol under convenient conditions. The scope of the reaction has been proved to be wide as various aldehydes and anhydrides underwent the reaction.

The absolute stereochemistry of the products formed was assigned either by analogy or direct X-ray crystallography of recrystallised samples.

A rationale which predicts the stereochemical outcome of the process has also been formulated, however no computational studies are available in support of the hypothesis made.

3. Asymmetric organocatalytic formal cycloaddition of succinic anhydrides to aldehydes

While the scope of the process with respect to the aldehyde component was quite broad, an obvious limitation in terms of synthetic utility is the requirement for the enol-stabilising benzo-fused anhydride, which restricts the potential scope considerably.

Accordingly, we became interested in exploring the possibility of utilising other anhydrides. As a starting point, we targeted the use of simple succinic anhydrides, which would potentially allow one-pot access to γ-butyrolactones (a highly abundant feature of natural product structures,[239,276,277] and in particular, the carboxylic acid group-bearing paraconic acid class of antitumor, antifungal and antibiotic natural products).[159,278–284]

3.1 Preliminary experiments

In preliminary experiments, we attempted the catalytic formal cycloaddition of succinic anhydride (**129**) with benzaldehyde (**52**) in the presence of catalyst **303** (synthesised by Dr. Seán Tallon) under the same conditions previously optimised for the cycloaddition of homophthalic anhydride (**147**) to benzaldehyde (**52**) and discussed in the previous section (Scheme 3.1).
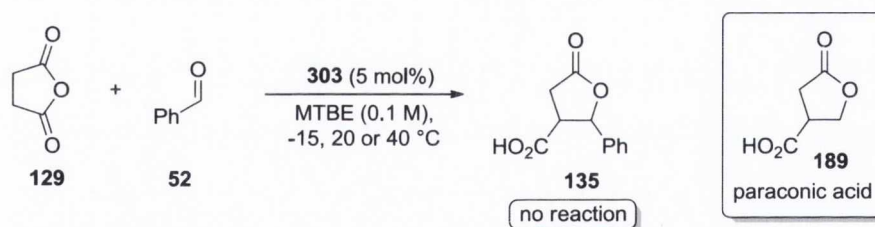
Scheme 3.1   Attempted one-step synthesis of paraconic acid derivatives.

Unfortunately, succinic anhydride (**129**) proved to be entirely unreactive in the reaction. Even elevation of the temperature failed to furnish the paraconic acid (**189**) natural product derivative **135**. We believed that the failure of **129** to serve as an effective substrate was due to ineffective catalysis of the tautomeric equilibrium under these mild conditions, leading to impractically low concentrations of the enol **316** in solution (Figure 3.1). Shaw and co-workers demonstrated that anhydride enolisation is a fundamental requirement in order to allow the reaction involving succinic anhydride

derivatives to occur under mild conditions (Section 1.5.1).[148–150] If this hypothesis was correct, then the installation of an enol-stabilising group (*i.e.* **317**, Figure 3.1) would (if appropriately chosen) circumvent the problem by increasing the concentration of **318** in solution.
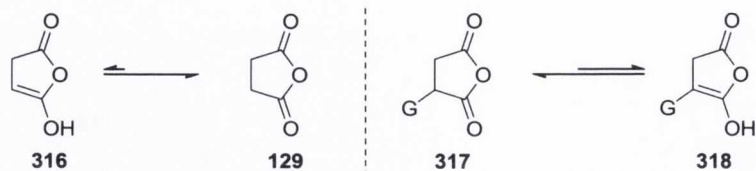
Figure 3.1   Rationale for the enol formation of succinic anhydride derivatives.

We therefore decided to employ arylsuccinic anhydrides, as they could afford us the opportunity to tune the keto-enol equilibrium through the variation of the electronic characteristics of the aromatic substituent. Furthermore, upon reaction with an aldehyde, one of the two new stereocentres formed in the C–C bond forming event would be quaternary. This constitutes a very interesting synthetic methodology, as paraconic acid derivatives with quaternary stereocentres have recently been evaluated as antitumor agents, one of which possessed sub-micromolar activity against multiple cancer cell lines.[285]

3.2   Evaluation of phenylsuccinic anhydride as substrate

The study began with exploratory reactions, conducted by Mr. James Murray, between the readily available phenylsuccinic anhydride (**320**) and benzaldehyde (**52**) catalysed by cinchona alkaloid organocatalysts, which demonstrated the feasibility of the process in principle. The further development of the process, reported below, is the result of studies carried out by the author.

The anhydride **320** was easily synthesised by reaction of the commercially available phenylsuccinic acid (**319**) with acetyl chloride under reflux (Scheme 3.2).
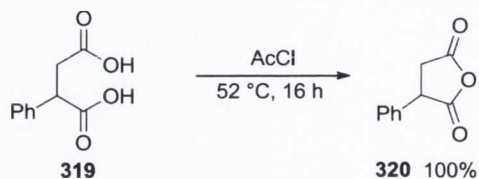
Scheme 3.2   Synthesis of phenylsuccinic anhydride (**320**).

In the previous study concerning homophthalic anhydrides, the thiourea-based cinchona alkaloid (*i.e.* entry 5, Table 2.3) possessed similar activity and selectivity profiles to the marginally superior squaramide analogues. Therefore, in the current study, in addition to the previous benchmark catalyst **303**, the squaramide variant lacking the C–2' phenyl substituent (*i.e.* **302**) and the corresponding thiourea-based catalyst **81** were evaluated (Table 3.1). All catalysts were synthesised by Dr. Seán Tallon.

Table 3.1   Catalyst evaluation in the reaction involving phenylsuccinic anhydride (**320**).
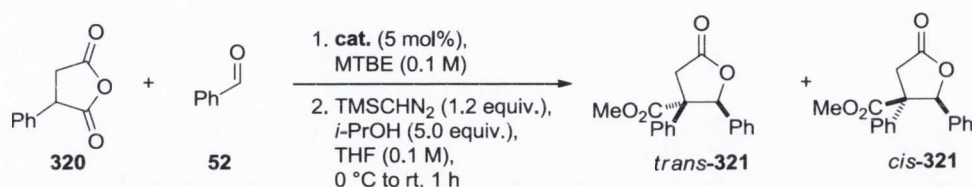
entry	cat.	time (h)	temp. (°C)	yield (%)^a	dr (*trans:cis*)^b	ee_{trans} (%)^c
1	-	24	rt	0	-	-
2	*i*-Pr$_2$NEt	27	rt	46	89:11	-
3	**303**	24	rt	44	90:10	68
4	**303**	168	rt	66	90:10	n.d.^{d}
5	**303**	288	rt	74	90:10	n.d.^{d}
6	**302**	24	rt	21	80:20	35
7	**81**	24	rt	41	88:12	34
8	**303**	110	-15	34	97:3	83
9	**303**	110	-30	17	>99:1	83

^{a} Yield of combined diastereomers determined by ^{1}H NMR spectroscopic analysis using either styrene or *p*-iodoanisole as an internal standard. ^{b} Diastereomeric ratio determined by ^{1}H NMR spectroscopic analysis. ^{c} Determined by CSP-HPLC. ^{d} Not determined.

As in the previous study involving homophthalic anhydrides, the product formed in the reaction is a lactone-acid. In order to facilitate separation of the diastereomers and the analysis of the enantioselectivity by CSP-HPLC, the product was converted to the corresponding lactone-ester by reaction of TMSCHN$_2$ (1.2 equiv.) and *i*-PrOH (5.0 equiv.) with the crude (isolated by the previously described double extraction) mixture of diastereomeric lactone-acids in THF.

When the reaction was performed in the absence of catalyst at room temperature, it failed to form **321** (entry 1). In the presence of 5 mol% of Hünig's base however, product **321** could be formed in moderate yield, with good diastereoselectivity (entry 2), probably due to the highly hindered substituents of the product molecule which favour the formation of the most stable isomer (*i.e. trans*-**321**). In the reaction catalysed by **303**, phenylsuccinic anhydride (**320**) underwent conversion to the corresponding phenyl paraconic acid product **321** at ambient temperature in 44% yield with good diastereocontrol and moderate enantioselectivity (entry 3). Although prolonged reaction increased the product **303** yield (entries 4 and 5), this was considered impractical as only a moderate yield of 74% was obtained after 12 days reaction time (entry 5).

The importance of the presence of a C-2' phenyl substituent regarding the performance of **303** in this reaction is highlighted by the clear inferiority of the unsubstituted variant **302** (entry 6). The thiourea-based catalyst **81** proved comparable to **303** in terms of activity and product diastereoselectivity but not enantioselectivity (entry 7).

The reaction is thought to proceed *via* a similar pre-transition state as proposed for the reaction involving homophthalic anhydride (**147**) described in Section 2.6.

In order to improve the stereoselectivity of the process, the reactions were then performed at lower temperature. Catalyst **303** proved to be able to mediate the formal cycloaddition reaction between **320** and **52** with excellent diastereocontrol and good enantio- and diastereoselectivity (favouring the *trans*-diastereomer); although at the expense of a synthetically useful product yield (entries 8 and 9).

3.3   Synthesis of arylsuccinic anhydrides

In order to further influence the keto-enol tautomeric equilibrium of the anhydride substrate, variation of the electronic characteristics of the aromatic substituent by introduction of electron-withdrawing substituents on the ring was necessary. To this end, we decided to synthesise 3,5-dibromophenylsuccinic anhydride (**328**, Scheme 3.3) and 4-nitrophenylsuccinic anhydride (**329**, Scheme 3.4). The former was produced in 36% overall yield by a seven-step synthetic procedure starting with the commercially available phenylsuccinic acid (**319**, Scheme 3.3). This, after nitration with fuming HNO_3 at 0 °C for 2 h and following recrystallisations from water gave **322** in moderate yield. Reduction of the nitro group by catalytic hydrogenation on palladium furnished

323 in excellent yield which, after high yield esterification of the two carboxylic acid functionalities to **324**, underwent bromination resulting in the production of **325** in 97% yield.
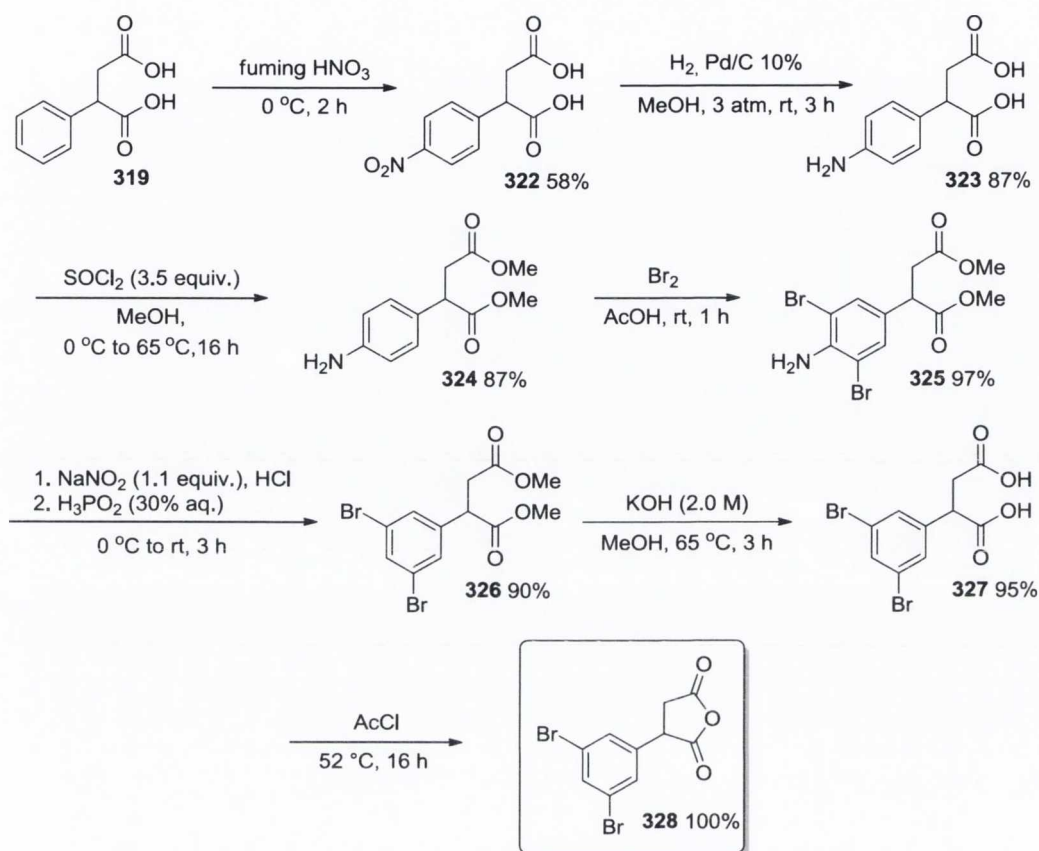
Scheme 3.3   Synthesis of 3,5-dibromophenylsuccinic anhydride (**328**).

Diazotisation and reduction of the diazonium salt by hypophosphorous acid gave the diester **326** in high yield, which was purified by column chromatography on silica gel and subsequently hydrolysed, furnishing **327** in excellent yield. The resulting 3,5-dibromophenylsuccinic acid (**327**) was then transformed to its anhydride by reaction with acetyl chloride under reflux, furnishing **328** in quantitative yield (Scheme 3.3).

The synthesis of 4-nitrophenylsuccinic anhydride (**329**) also began with nitration of phenylsuccinic acid (**319**) and recrystallisation of the products from water, to furnish **322** in 58% yield. The 4-nitrophenylsuccinic acid (**322**) obtained was then reacted with acetyl chloride at reflux to furnish crude anhydride **329**, which was purified by a rapid column chromatography on silica gel, furnishing the 4-nitrophenylsuccinic anhydride (**329**) in 71% yield (Scheme 3.4).

91
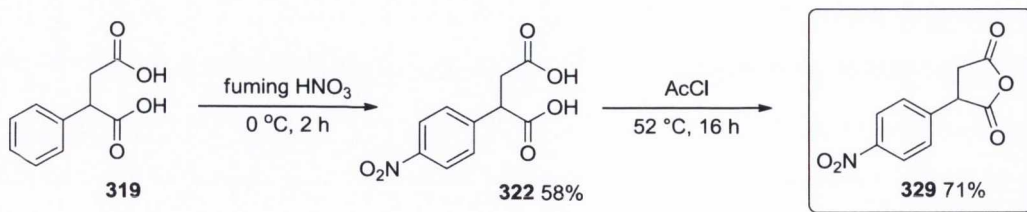
Scheme 3.4 Synthesis of 4-nitrophenylsuccinic anhydride (**329**).

3.4 Evaluation of arylsuccinic anhydrides as substrates

The evaluation of these two more enolisable anhydrides in the cycloaddition reaction with benzaldehyde was then the next step in the study. The reactions involving 3,5-dibromophenylsuccinic anhydride (**328**) and 4-nitrophenylsuccinic anhydride (**329**) were performed in the presence of **303** (Table 3.2). A temperature of -15 °C was chosen, as in the previous reaction involving phenylsuccinic anhydride (**320**, Table 3.1) a lower temperature of -30 °C (*i.e.* entry 9, Table 3.1) did not furnish substantial improvement of stereocontrol but did result in lower product yield when compared to the reaction performed at -15 °C (see entry 8, Table 3.1).

Table 3.2 Evaluation of arylsuccinic anhydrides.
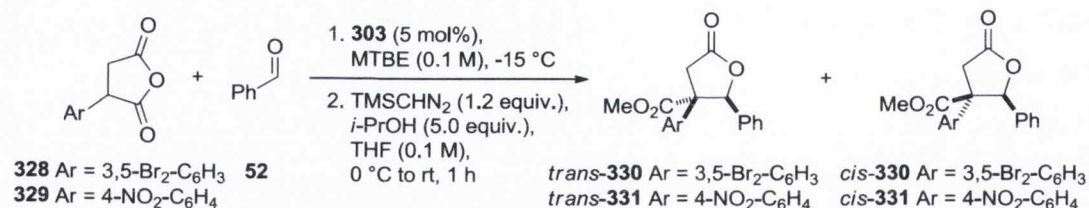
entry	product	time (h)	yield (%)^a	dr (trans:cis)^b	ee$_{trans}$ (%)^c
1	**330**	97	76	94:6	76
2	**331**	99	96	97:3	86

^{a} Yield of combined diastereomers determined by ^{1}H NMR spectroscopic analysis using either styrene or *p*-iodoanisole as an internal standard. ^{b} Diastereomeric ratio determined by ^{1}H NMR spectroscopic analysis. ^{c} Determined by CSP-HPLC.

Replacement of the phenyl unit with a 3,5-bromophenyl analogue (-Br σ_m = 0.37) resulted in faster, more efficient formation of **330**. However, diastereoselectivity and enantioselectivity diminished marginally (entry 1, Table 3.2) compared to the analogous reaction involving phenylsuccinic anhydride (**320**, *i.e.* entry 8, Table 3.1). The reaction involving the powerful enol-stabilising *p*-nitro substituted variant **329** (-NO$_2$ σ_p = 0.81)

furnished **331** in excellent product yield and diastereocontrol with a concomitant increase in product *ee* to 86% (entry 2).

3.5   Evaluation of the substrate scope: aldehyde component

With an optimum catalyst (*i.e.* **303**) and an improved substrate (*i.e.* **329**) in hand, the substrate scope with respect to the aldehyde component was then investigated (Table 3.3). In collaboration with Dr. Claudio Cornaggia, several aldehydes were evaluated in the reaction with **329**, but only those performed by the author are reported here. Upon completion, the reactions were esterified *in situ* by reaction with TMSCHN$_2$ (1.2 equiv.) and *i*-PrOH (5.0 equiv.) as previously described, and the products formed were then purified by column chromatography on silica gel.

The protocol proved quite robust as all the aldehydes underwent formal cycloaddition reaction with **329**. Activated aldehydes (*e.g.* *p*-bromobenzaldehyde) gave the isolated *trans*-butyrolactones such as **332** (entry 1, Table 3.3) with product yields and levels of enantio/diastereocontrol in line with those of our preliminary studies outlined in Table 3.2.

Use of π-excessive heterocyclic aldehydes (entries 2 and 3) resulted in a sharp increase in enantioselectivity, forming *trans*-**333** and *trans*-**334** with excellent product *ee* (>90%) without diastereoselectivity being compromised. However, in the case involving the use of furan-2-carbaldehyde (entry 2), separation of the diastereomers of ester product **333** was not possible. The use of an aliphatic aldehyde in the reaction is also tolerated by the catalyst **303**. Following this protocol hydrocinnamaldehyde can be converted to *trans*-**335** (entry 4) with excellent enantiocontrol (95% *ee*) although with less efficient diastereocontrol. Furthermore, separation of the two diastereomers by column chromatography on silica gel was not possible.

Table 3.3   Investigation of substrate scope: the aldehyde component.
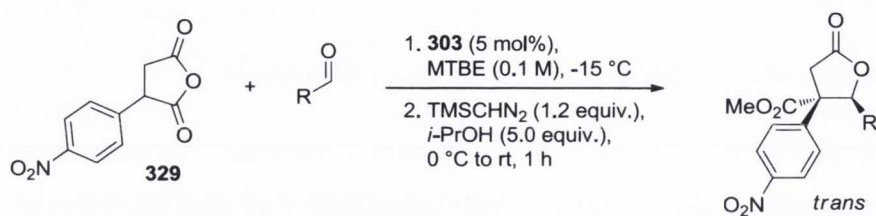
entry	product	time (h)	yield (%)[a]	dr (trans:cis)[b]	ee_trans (%)[c]
1	*trans*-**332**	97	92	94:6	77
2[d]	*trans*-**333**	98	95	99:1	99
3	*trans*-**334**	161	90	98:2	91
4[d]	*trans*-**335**	100	98	72:28	95

[a] Isolated yield of *trans*-diastereomer. [b] Diastereomeric ratio determined by ^{1}H NMR spectroscopic analysis. [c] Determined by CSP-HPLC. [d] Diastereomers inseparable.

The 3,5-dibromophenylsuccinic anhydride (**328**) also proved to be a viable substrate under optimised conditions. The *trans*-lactone **336** (which can either be dehalogenated to the corresponding phenylsuccinic anhydride-derived lactone or elaborated *via* Pd(0)-

mediated coupling chemistry) can be readily prepared in 81% yield with high enantioselectivity by reaction with furan-2-carbaldehyde (Scheme 3.5).
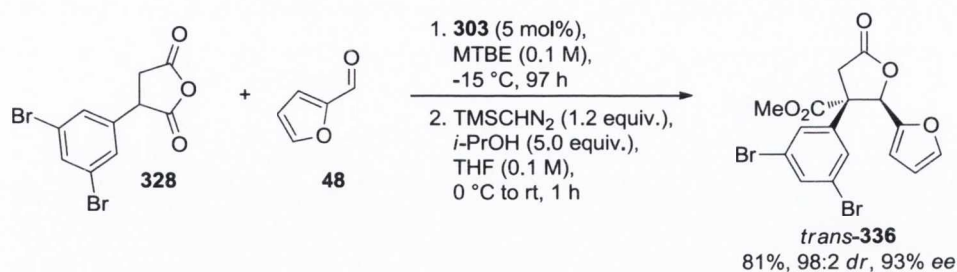
Scheme 3.5   The use of 3,5-dibromphenylsuccinic anhydride (**328**) as a substrate.

Although high diastereoselectivity (*i.e.* 98:2) was exhibited, with a preference for the formation of the *trans*-isomer, separation by column chromatography of the two diastereomeric lactone-ester products could not be achieved. In this case, the esterification of the lactone-acid product was also carried out by reaction with TMSCHN$_2$ (1.2 equiv.) and *i*-PrOH (5.0 equiv.) on the isolated mixture of diastereomeric acids obtained by the double extraction method previously described.

3.6   Absolute stereochemical assignment

The absolute stereochemistry of the products formed was assigned by X-ray crystallography of a recrystallised sample of *trans*-**334**.
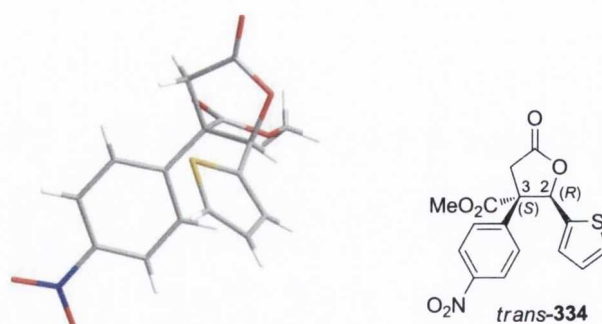
Figure 3.2   Absolute stereochemical assignment of product *trans*-**334**.

This was unequivocally assigned as (2*R*,3*S*) as shown in Figure 3.2. This configuration was subsequently assigned by analogy to all of the major diastereomers obtained *via* this methodology during this study. However, due to the nature of one substituent present on the C-2 stereocentre in *trans*-**334** (*i.e.* thiophenyl), the priority numbers assigned to the substituents of that stereocentre, according to the CIP (Cahn–Ingold–

Prelog) rules, are different to those assigned to the C-2 stereocentre of *trans*-**331** which bear a different substituent (*i.e.* phenyl). This is reflected in the different absolute stereochemistry of the products (Figure 3.3). Those derived from heterocyclic aldehydes (*e.g.* entries 2 and 3) present absolute stereochemistry as (2*R*,3*S*), while all the others have absolute stereochemistry (2*S*,3*S*).
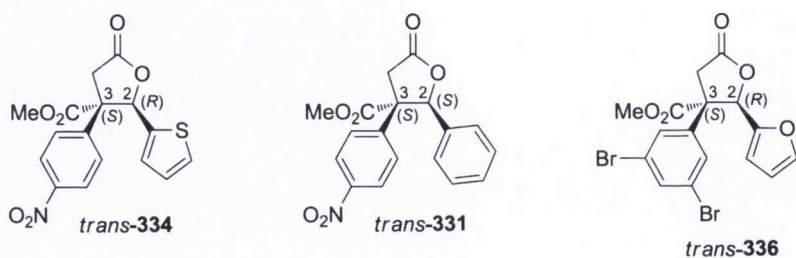
Figure 3.3   Absolute stereochemistry (nomenclature) differs depending on the nature of the substituent.

3.7   Conclusion

The results obtained in this project demonstrated the possibility of expanding the organocatalytic asymmetric formal cycloaddition reaction between cyclic anhydrides and aldehydes to arylsuccinic anhydrides. The process provided high yield one-pot access to functionalised paraconic acid derivatives (a class of natural products of considerable pharmacological activity based on γ-butyrolactones) with the formation of two new stereocentres, one of which is quaternary, under mild conditions with good-excellent stereocontrol.

It was speculated that the inactivity of succinic anhydride in the process was related to poor enolisability in the presence of the catalyst. This hypothesis was supported by the finding that the more enolisable phenylsuccinic anhydride participated in the reaction, albeit with unsatisfactory yield and stereocontrol.

It was demonstrated that the introduction of electron-withdrawing functionalities on the aromatic ring of phenylsuccinic anhydride resulted in a significant increase in reactivity, allowing the optimisation of the protocol and the identification of the optimum substrate (*i.e.* **329**).

The absolute stereochemistry of the products obtained was assigned either by direct or analogy X-ray crystallography of recrystallised sample.

4. The cycloaddition reaction between homophthalic anhydride and different electrophiles

After the development of a catalytic asymmetric reaction between homophthalic- and arylsuccinic anhydrides with aldehydes, we decided to explore the reactivity of different electrophiles in the reaction with homophthalic anhydride.

4.1 Preliminary studies: exploratory reactions

The reaction (both thermal and base-catalysed) between homophthalic anhydride and different electrophiles has already been studied to a large extent by Tamura *et al.* (see Section 1.5.3). It is believed that the reaction proceeds by a concerted Diels-Alder mechanism where the anhydride plays the diene role through its dienol-tautomer (*i.e.* **152**, Scheme 1.51). While this pathway is supported by the successful reaction of various dienophiles (see Section 1.5.3), the step-wise Michael addition, which has also been proposed as plausible mechanism, (*i.e.* Scheme 1.49, Section 1.5.3) could never be fully ruled out.

Based on the results obtained in our studies of the asymmetric cycloaddition between homophthalic anhydride and aldehydes (Chapter 2), where enolisation of the anhydride (presumably by general base catalysis) mediated by the cinchona-based organocatalyst and concomitant electrophile activation by double hydrogen bonding by the (thio)urea (or squaramide) catalyst substituent, promoted the formation of lactone-products in high yield and stereoselectivity, we hypothesised that a similar process, in which the role of electrophile would be played by a Michael acceptor, could be developed.

We believed that under the appropriate conditions the Michael addition of homophthalic anhydride (**147**) to Michael acceptors of general type **337** could be brought about in favour of the Diels-Alder pathway described by Tamura,[146] allowing for the catalytic formation of products such as **338**, generating two new carbon-carbon bonds and up to three new stereocentres (Figure 4.1).
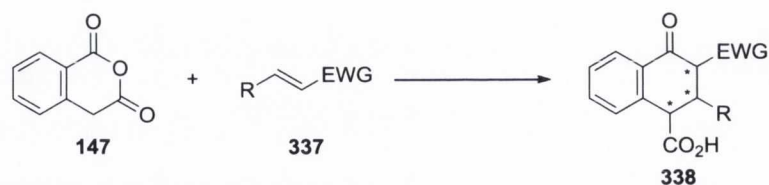
Figure 4.1 Rationale for the cycloaddition reaction involving Michael acceptors.

To test the feasibility of the process, we initially decided to evaluate the reaction between **147** and a number of common Michael acceptors at room temperature in MTBE (0.1 M) promoted by catalyst **303** (*i.e.* the optimum conditions in both of the preceding studies involving anhydrides and aldehydes, Table 4.1).

Table 4.1 Preliminary evaluation of Michael acceptors as substrates.
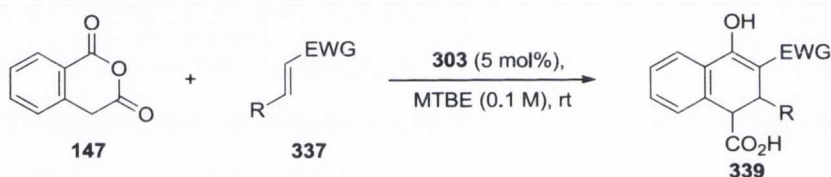
entry	acceptor	time (h)	product	yield (%)[a]
1	**340**	65	-	0
2	**341**	65	-	0
3	**44**	97	**342**	48%
4	**63**	97	**343**	53%

[a] Determined by ^{1}H NMR spectroscopic analysis using *p*-iodoanisole as an internal standard.

The reaction involving both ethyl acrylate (**340**, entry 1) and acrylonitrile (**341**, entry 2) failed to produce the corresponding annulated products. When (*E*)-chalcone (**44**) was

evaluated as the electrophile, the reaction proceeded, forming product **342** in moderate yield (entry 3). Similar results were obtained for the reaction involving (*E*)-nitrostyrene (**63**), which produced **343** in slightly higher yield (entry 4). In both cases however, the products formed were the most stable enol tautomer of the expected product as, aided by the extremely high acidity of the proton in the position 3 of the 1,3-diketone or 1,3-nitroketone portion of the molecules produced, the desired products **344** and **345** spontaneously tautomerised to **342** and **343** respectively (Scheme 4.1).

344 R = COPh
345 R = NO$_2$

342 R = COPh
343 R = NO$_2$

Scheme 4.1   Tautomerisation of the annulated products.

Furthermore, complications arose during the 'standard' esterification procedure based on the use of TMSCHN$_2$ and methanol. When products **342** and **343** underwent the derivatisation reaction, degradation by unidentified side-reactions took place, making the isolation of the desired products impossible, if not in extremely low yields (isolation performed by Dr. Esther Torrente De Haro) for the product **343** derived from (*E*)-nitrostyrene (**63**, entry 4, Table 4.1).

In order to circumvent these major drawbacks and develop a new catalytic asymmetric process capable of creating molecules with three stereocentres, the employment of Michael acceptors bearing trisubstituted double bonds such as the commercially available β-methyl-(*E*)-nitrostyrene (**346**, Scheme 4.2) was attempted. We postulated that the use of this activated alkene in the reaction with anhydride **147** under the same conditions depicted in Table 4.1 would avoid any deleterious complications arising from the tautomerisation, which can no longer occur due to the absence of the acidic proton in position 3, and would produce annulated molecules containing three stereocentres, one of which would be quaternary (Scheme 4.2).
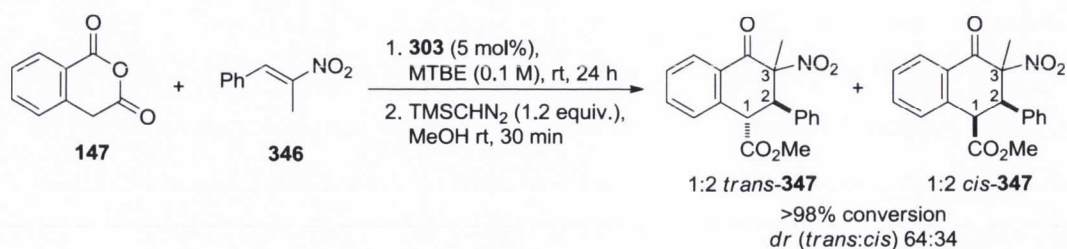
Scheme 4.2   Cycloaddition reaction between homophthalic anhydride (**147**) and a trisubstituted nitroalkene (**346**) as Michael acceptor.

The results of these preliminary experiments were extremely encouraging: after 24 h almost complete conversion of starting materials was achieved, allowing the formation of product **347** as a mixture of two diastereomers. Although the reaction should be able to produce up to four diastereomers, only two of them were formed in sufficient amounts to be detected by ^{1}H NMR spectroscopic analysis of the crude reaction mixture.

The relative stereochemistry of the two isomers was then assigned as depicted in Scheme 4.2 by analysis of the coupling constants (*J*) between H-1 and H-2 in the ^{1}H NMR spectra of the two molecules. The major product was found to possess the *trans* geometry as a value of *J* = 12.3 Hz was measured between the two hydrogen atoms, while for the minor product, a value of *J* = 6.2 Hz allowed the assignment of *cis* geometry to this structure. The relative stereochemistry of the quaternary stereocentre in position 3 in relation to the other substituents was not assigned by NMR spectroscopic analysis as it was decided to analyse compound **347** by X-ray crystallography (Section 4.9). The enantioselectivity of the process was then determined by analysing the enantiomeric excess of both isolated diastereomers by CSP-HPLC, furnishing 61% *ee* for the major *trans*-isomer and 98% *ee* for the minor *cis*-isomer. The excellent results obtained in this preliminary reaction pushed us toward the optimisation of the reaction conditions in order to improve diastereocontrol.

We therefore embarked on a series of experiments to evaluate the effect of reaction temperature on stereoselectivity. However, even with the maximum care taken while performing these reactions, the results obtained were inconclusive. Reactions performed several times under the same conditions furnished different results in terms of *dr* and *ee*, showing that the process was not reproducible.

100

4.2 Standard procedure development

A closer and deeper inspection of the reaction revealed a strong dependency between reaction time, temperature and the diastereoselectivity obtained. It was observed that a slow side-process which converted the minor diastereomer to the major one, and thus changing diastereoselectivity of the reaction, usually took place over time after the reactions had reached full conversion. This process was also being found to occur during the esterification reaction and during the evaporation of the solvent on the rotary evaporator (due to the water bath temperature) after the workup (if executed) or after the esterification reaction when the sample was prepared for the column chromatography.

It was therefore decided to establish a set of standard conditions composed of several actions to be executed in an exact sequence and timing, aiming to achieve higher reproducibility. This would then permit us to compare different reaction conditions, allowing for the development of a useful synthetic protocol.

Subsequently, all the reactions were performed at an equilibrated temperature of 30 °C at 0.1 M concentration in MTBE for 22 h. The temperature of 30 °C was chosen in view of the extremely high dependency of the diastereomer converting side-reaction on temperature. Higher temperatures such as 55 °C, were found, in reactions not reported here, to increase the rate of conversion, while lower temperature such as 0 °C or -15 °C (in general any temperature below room temperature) would potentially not be practical as the *dr* of the reaction would change upon the temperature increase prior to purification. The reaction time of 22 h was chosen as in the initial experiments, (almost) full conversion of starting materials to products was always achieved by this time. Finally, the solvent and the concentration were chosen on the basis of the optimum results obtained in the previous works involving aldehydes (Chapters 2 and 3).

The crude reaction mixtures so obtained were analysed by ^{1}H NMR spectroscopy to measure the *dr* and then cooled to 0 °C. At this point the esterification process using TMSCHN$_2$ (1.2 equiv.) and MeOH (75.0 equiv.) was allowed to proceed for 20 minutes. At this time the mixture was directly loaded onto the silica column and the two diastereomers were chromatographically isolated together. The removal of the solvent *in vacuo* was carried out at temperature below 30 °C. The *dr* of the mixtures of esterified products, in conjunction with the enantiomeric excesses were then determined

by CSP-HPLC. The difference between the *dr* determined by ^{1}H NMR spectroscopic analysis and CSP-HPLC was a quantification of the extent of the conversion of the diastereomers that took place under these conditions. Although this effect of the side-reaction had been drastically minimised by adopting the developed standard procedure, it could never be fully suppressed. However, by adopting this new set of conditions, higher reproducibility of the process was guaranteed, thus making analysis of the process feasible.

4.3 Catalyst evaluation under standard procedure conditions

Now in possession of a reproducible standard procedure, our attention turned to the evaluation of the catalysts (Table 4.2). Catalyst **303** was synthesised according to our previously developed procedure.[286] Catalysts **302** and **297** were synthesised by Dr. Seán Tallon.

Table 4.2 Catalyst evaluation in the cycloaddition of homophthalic anhydride (**147**) to β-methyl-(*E*)-nitrostyrene (**346**).
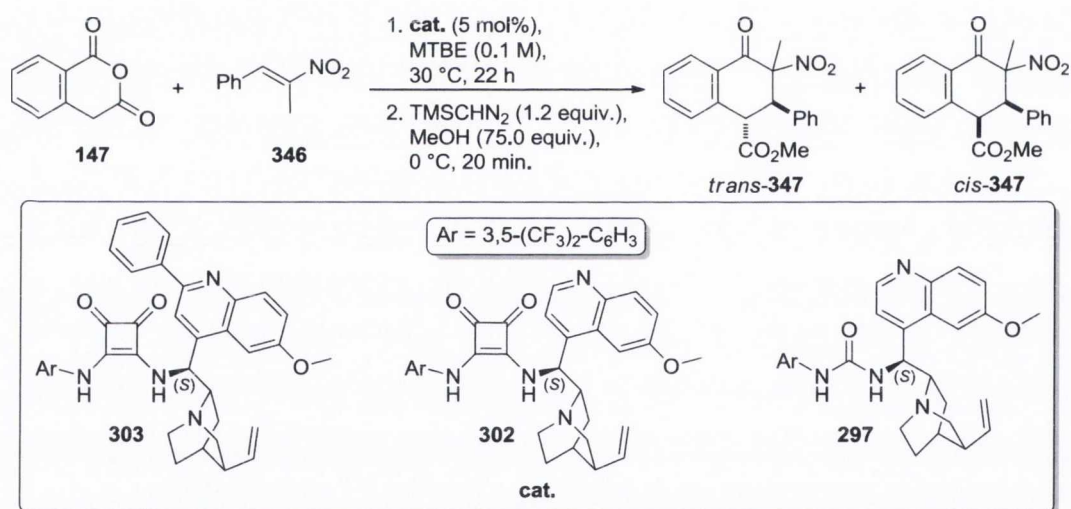
entry	cat.	conversion (%)[a]	dr (*trans:cis*)[b] (acids)	dr (*trans:cis*)[c] (esters)	ee$_{trans}$ (%)[d]	ee$_{cis}$ (%)[d]
1	**303**	>98	68:32	72:28	60	97
2	**302**	>98	64:36	67:33	70	99
3	**297**	>98	56:44	62:38	58	97

[a] Conversion of both reagents determined by ^{1}H NMR spectroscopic analysis. [b] Diastereomeric ratio determined by ^{1}H NMR spectroscopic analysis. [c] Diastereomeric ratio determined by CSP-HPLC. [d] Determined by CSP-HPLC.

All of the catalysts evaluated proved to be efficient promoters for the reaction, as product **347** was formed with nearly quantitative conversion in all cases (entries 1, 2 and 3).

As expected, catalyst **303** furnished results (entry 1, Table 4.2) comparable to those obtained from the reaction depicted in Scheme 4.2. In this situation it is possible to see the effect that small variations in temperature (30 °C compared to rt) and reaction time (22 h compared to 24 h) have on the diastereomer conversion reaction. In general, if a process capable of furnishing a product as a mixture of two diastereomers (*cis* and *trans*) is conducted at lower temperature, the selective formation of one diastereomer (generally the *trans*) over the other is enhanced and a mixture enriched with one diastereomer is obtained, leading to an increased *dr*. The reverse is found when the reaction is conducted at higher temperature. In this situation a mixture containing substantial amounts of both diastereomers is produced, exhibiting no selectivity in their formation thus giving a poor *dr*. Comparing the reaction in entry 1 of Table 4.2 and the reaction in Scheme 4.2, it is noticeable that the *dr* (*trans:cis*) of the former reaction is higher than the latter (68:32 *vs* 64:36), even though the reaction was conducted at higher temperature. It is believed that this is a consequence of the diastereomer conversion reaction (from *cis* to *trans*) which took place after full conversion was achieved.

It is evident that this side-reaction also takes place during the esterification process. The three *drs* determined by CSP-HPLC are higher than those obtained by ^{1}H NMR spectroscopic analysis of the crude reaction mixtures, proving that small amounts of the *cis*-isomers converted to the *trans*-isomers (comparison between column 4 and 5 of entries 1, 2 and 3, Table 4.2) during the derivatisation to methyl esters. Despite this, the three catalysts exhibited only moderate diastereoselectivity, towards the *trans*-isomer, producing the acid mixtures up to 68:32 *dr* (entry 1).

The reactions also furnished moderate to good enantioselectivity in the formation of the *trans*-isomer, with a maximum of 70% *ee* obtained in the reaction catalysed by the squaramide-substituted cinchona alkaloid **302** (entry 2). Conversely, the *cis*-isomer, was always formed in excellent *ee* (entries 1, 2 and 3); approaching optical purity in the reaction promoted by catalyst **302** (entry 2). However, despite intensive studies devoted to the development of conditions leading to the formation of the *cis*-diastereomer exclusively, no useful protocols have been found. This is mostly due to the diastereomer

converting side-reaction which, as explained above, takes place as soon as the reaction temperature - maintained below 0 °C in order to enhance the formation of the *cis*-isomer - rises during the work-up and purification.

4.4   Diastereomer epimerisation: rationale and preliminary studies

The results, in terms of enantioselectivity, obtained in the formation of minor (*cis*) product in the catalyst evaluation reactions, alerted us to the possibility of taking advantage of the diastereomers converting side-reaction.

The assignment of the absolute stereochemistry (that will be further examined in Section 4.9), achieved by X-ray crystallographic analysis, permitted the determination of the three-dimensional structure of the two diastereomers of product **347** as depicted in Figure 4.2.

1:2-*trans*-2:3-*trans*-**347**   1:2-*cis*-2:3-*trans*-**347**
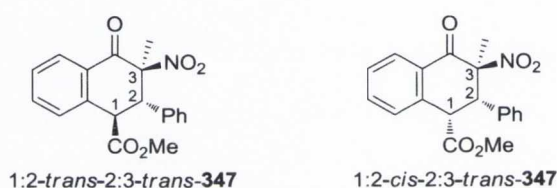
Figure 4.2   Absolute stereochemistry of the diastereomers of product **347**.

It is possible to see that the two isomers differ only in the stereochemistry of the carbon in position 1, making the diastereomer conversion side-reaction a 'simple' epimerisation at the carbon 1. (From now on, the simplified annotation *trans*-**347** and *cis*-**347** will be used as description of 1:2-*trans*-2:3-*trans*-**347** and of 1:2-*cis*-2:3-*trans*-**347** respectively).

We believed that, if the epimerisation of the *cis*-isomer to the *trans*-isomer of product **347** takes place while preserving the enantioselectivity of the other chiral centres (*i.e.* only the configuration of the carbon in position 1 is inverted), this process could be induced on an isolated diastereomeric mixture of product **347**, allowing the increase of the *ee* of the *trans*-product. For example, Table 4.3 shows the (theoretical) maximum enantioselectivity achievable by such transformation if conducted on the diastereomeric mixtures of product **347** obtained during the preliminary catalyst evaluation summarised in Table 4.2.

104

Table 4.3   Theoretical epimerisation of diastereomeric mixtures of product **347**.
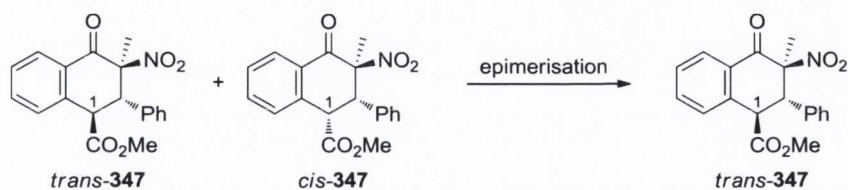
entry	cat.	*dr (trans:cis)*[a] (esters)	ee_{trans} (%)[b]	ee_{cis} (%)[b]	max[c] ee_{trans} (%)
1	**303**	72:28	60	97	70.4
2	**302**	67:33	70	99	79.6
3	**297**	62:38	58	97	72.4

[a] Diastereomeric ratio determined by CSP-HPLC. [b] Determined by CSP-HPLC. [c] Calculated theoretical maximum *ee* (%) achievable by epimerisation.

As further explanation, entry 1 (Table 4.3) is used as an example. It is possible to see that 72% (*i.e.* 0.72) of the product formed is *trans* and possesses 60% *ee*, while 28% (*i.e.* 0.28) of it is *cis* and possesses 97% *ee*. Considering a theoretical full conversion of the *cis* product to the *trans* isomer with preservation of the enantioselectivity, the resulting *trans* product would exhibit an enantiomeric excess value calculated according to the following equation:

$$0.72 \bullet 60\% \ ee + 0.28 \bullet 97\% \ ee = 70.36\% \ ee \ \underline{\text{theoretical maximum } ee \text{ achievable}}$$

It is possible to see that if full epimerisation of the *cis*-isomer to the *trans* could be achieved, the enantiomeric excess of the *trans*-diastereomer could be, in the best case (*i.e.* entry 2), increased from 70% to 79.6%.

We therefore decided to test our hypothesis by evaluating the epimerisation reaction on an isolated sample of *cis*-**347**. It was known that if the reaction mixture, after the *in situ* esterification process, was heated at a temperature above that at which the catalytic transformation was conducted (*i.e.* 30 °C), the epimerisation of *cis*-**347** to *trans*-**347** would take place. For this reason, we decided to evaluate this test reaction under the same conditions utilised during the esterification process; but heating to 55 °C and using **303** as 'standard' catalyst (Scheme 4.3).
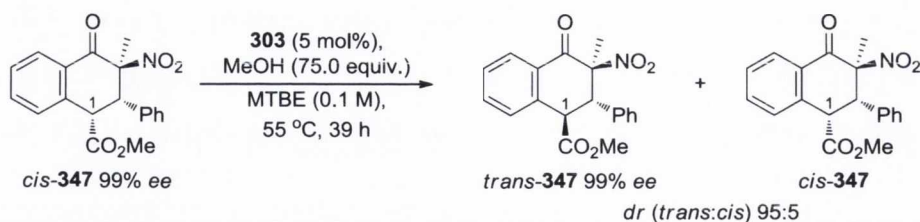
Scheme 4.3   Preliminary epimerisation experiment.

The results obtained were very gratifying. The *cis*-isomer was converted in an almost quantitative yield to the *trans*-isomer with retention of enantioselectivity, proving the feasibility of the process.

4.5 Synthesis and evaluation of novel cinchona alkaloid-based organocatalysts

Although the encouraging results obtained in the preliminary epimerisation experiment (Scheme 4.3) prompted us to further develop the process, we were not fully satisfied with the (theoretical) maximum enantioselectivity achievable in the epimerisation process (*i.e.* 79.6%, entry 2, Table 4.3).

We reasoned that, if better enantiocontrol in the parent reaction that generates the diastereomeric mixture of product **347** can be achieved, higher enantioselectivity values for the *trans*-isomer could be obtained upon the epimerisation reaction. We therefore decided to attempt the synthesis and consequent evaluation of two new substituted cinchona alkaloid organocatalysts.

Analysis of the data depicted in Table 4.3 revealed the superior behaviour of squaramide-substituted cinchona alkaloid organocatalyst **302** (entry 2, Table 4.3) compared to the relative urea-substituted **297** (entry 3, Table 4.3) illustrated in Figure 4.3.

Ar = 3,5-(CF₃)₂-C₆H₃
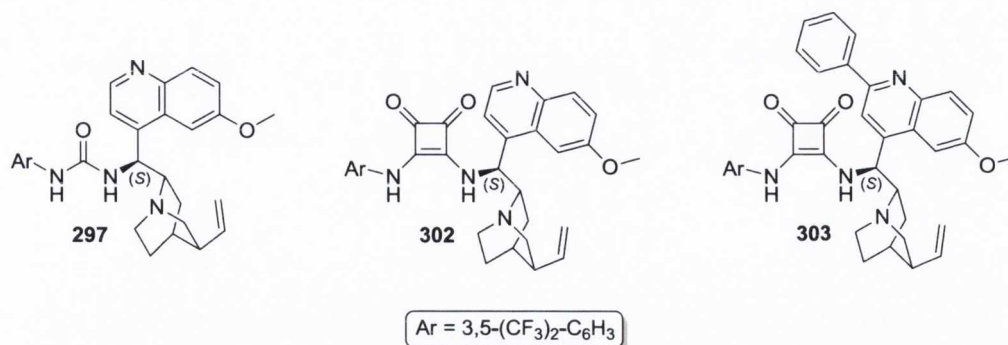
Figure 4.3   Comparison between urea- and squaramide-substituted cinchona alkaloid organocatalysts.

It is also apparent, comparing the results obtained with catalyst **302** (entry 2, Table 4.3) with **303** (entry 1, Table 4.3), that the steric requirement of the three-dimensional structure of the reaction promoter is an important factor that drastically influences the enantiocontrol of the process. In this reaction, in contrast to those involving aldehydes (discussed in Chapters 2 and 3), the introduction of a phenyl substituent in C-2' position of the quinoline ring had a negative effect on the stereocontrol exerted by the catalyst. The reaction promoted by catalyst **303**, which possess the phenyl substituent, would theoretically be able to produce the *trans*-isomer in 70.4% *ee* upon epimerisation, while use of the analogous structure lacking the substituent (*i.e.* **302**) could generate the *trans*-isomer in a potential 79.6% *ee*.

This suggested that altering or further modifying the alkaloid-derived portion of the catalyst would be futile as the best performances in the reaction were obtained by the catalysts bearing unmodified cinchona alkaloid moieties (*i.e.* **297** and **302**). As a result, we decided to evaluate the effect that modification of the aromatic achiral substituent of the squaramide organocatalyst (*i.e.* 3,5-(CF₃)₂-C₆H₃) would generate over the stereocontrol of the reaction.

Considering the bulky substituent of catalyst **302** (Figure 4.4) it is possible to see that the disubstituted aromatic ring cannot provide a 'constant and equal' steric hindrance around the active region of the catalyst, due to its relatively planar character. Depending on the rotameric preferences of this portion of the molecule in relation to the catalytic pocket of the catalyst, different effects on the stereocontrol of the reaction could result. We believed that the introduction of a bulky, non-planar substituent such as *t*-butyl (*i.e.*

catalyst **348**) and trityl (*i.e.* catalyst **349**, Figure 4.4), could guarantee the formation of a catalytic pocket of more consistent steric characteristic during the reaction.
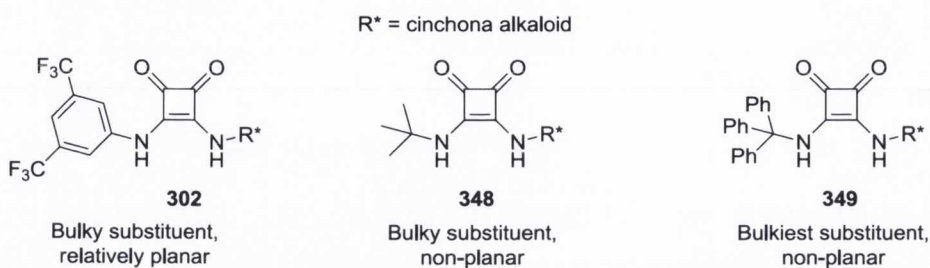
Figure 4.4   Comparison between substituents in potential squaramide-substituted cinchona alkaloid organocatalyst-designs.

We therefore decided to synthesise catalysts **348** and **349** following the general procedure depicted in Scheme 4.4.
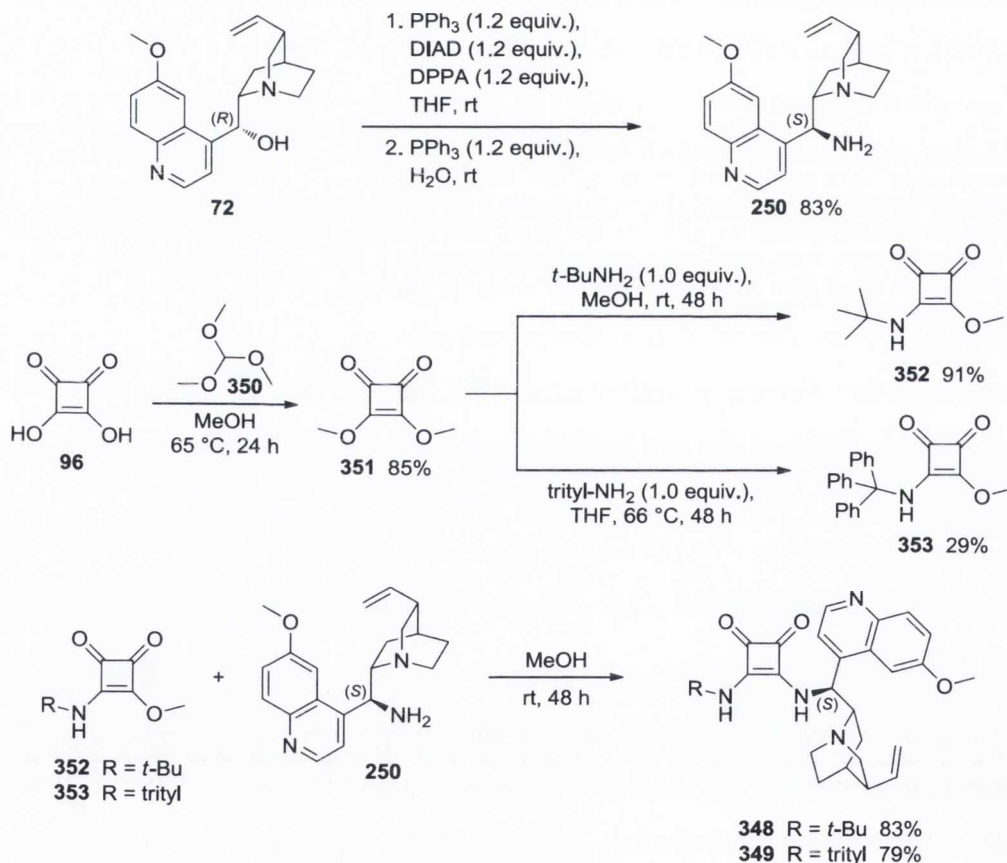
Scheme 4.4   Synthesis of catalyst **348** and **349**.

The syntheses began with the substitution of the C-9 hydroxy group with a free amino functionality by Mitsunobu reaction between the quinine substrate (**72**) and triphenyl

phosphine (PPh$_3$), diisopropyl azodicarboxylate (DIAD) and diphenylphosphoryl azide (DPPA) in THF at room temperature. The C-9 azide-substituted quinine so obtained was then reduced *in situ* to the free amino group by reaction with PPh$_3$ / H$_2$O to furnish product **250** in 83% yield.

Concurrently, squaric acid (**96**) was converted to the corresponding dimethyl ester **351** in 85% yield by reaction with trimethyl orthoformate (**350**) in methanol at reflux. After isolation and purification by column chromatography on silica gel, **351** was treated with the appropriate amine (*t*-butyl amine in the case of **348** and trityl amine in the case of **349**) in methanol at room temperature to furnish **352** in 91% yield and in THF at reflux temperature to furnish **353** in 29% yield after purification by column chromatography on silica gel. In the case involving the use of trityl amine, however, due to its high hindrance, product **349** was obtained in very low yield under forcing conditions (reflux temperature) on only one occasion. Despite repeated, arduous attempts repeating the reaction under the same conditions, the formation of product **353** was not observed on subsequent occasions. However, a sufficient amount of **353** was prepared to allow the synthesis and consequent evaluation of catalyst **349**, albeit only in preliminary studies aimed at verifying the assumptions made in the choice of the substituents depicted in Figure 4.4.

Products **352** and **353** were then reacted at room temperature in methanol with **250** to furnish catalysts **348** and **349** in 83% and 79% yield, respectively. After purification by column chromatography on silica gel, they were evaluated in the reaction between **147** and **346** under the previously developed standard conditions (Table 4.4).

The results obtained in the evaluation of the two novel organocatalysts synthesised (*i.e.* **348** and **349**) proved that the hypotheses for the choice of the substituents were correct. Catalyst **348** (entry 2) easily promoted the reaction, generating the diastereomeric mixture of product **347** with higher enantiocontrol than catalyst **302**. This is reflected in an augmentation of the theoretical *ee* (%) achievable for the *trans*-isomer from 79.6% (with **302**, entry 1) to 83.6% (with **348**, entry 2). Further improved results were obtained in the reaction catalysed by **349** that theoretically would allow, upon epimerisation, the formation of *trans*-**347** in 88.8% *ee*.

Table 4.4   Evaluation of catalyst **348** and **349** in comparison with **302**.
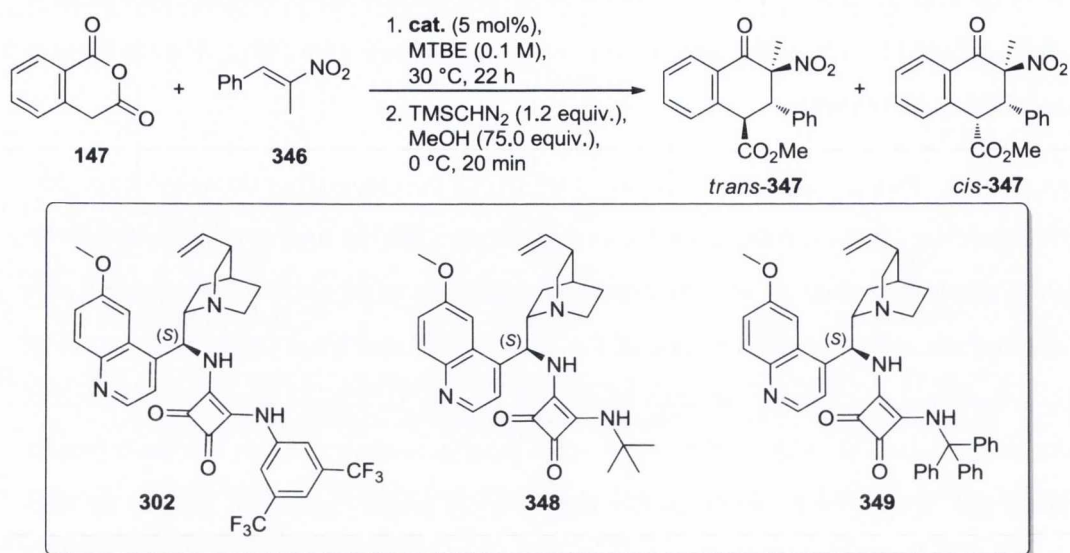
entry	cat.	conv. (%)^a	dr (trans:cis)^b (acids)	dr (trans:cis)^c (esters)	ee$_{trans}$ (%)^d	ee$_{cis}$ (%)^d	max^e ee$_{trans}$ (%)
1	**302**	>98	64:36	67:33	70	99	79.6
2	**348**	>98	53:47	57:43	72	99	83.3
3	**349**	>98	63:37	68:32	84	99	88.8

^{a} Conversion of both reagents determined by ^{1}H NMR spectroscopic analysis. ^{b} Diastereomeric ratio determined by ^{1}H NMR spectroscopic analysis. ^{c} Diastereomeric ratio determined by CSP-HPLC. ^{d} Determined by CSP-HPLC. ^{e} Calculated theoretical maximum ee (%) achievable by epimerisation.

This favourable result is however blighted by the impossibility of using catalyst **349** due lack of reproducibility in the synthesis of its precursor **353**, as explained above. For this reason it was decided to continue the studies on the cycloaddition reaction between **147** and **346** while using the novel organocatalyst **348**, which still proved superior to the others evaluated in Table 4.2, and could be reproducibly synthesised easily.

4.6   Studies of the epimerisation reaction

Encouraged by the preliminary epimerisation test results (Section 4.4) and by the improved enantiocontrol exerted by the novel organocatalyst **348** (Table 4.4), we decided to evaluate different conditions for the epimerisation reaction of a mixture of diastereomers of product **347**.

Table 4.5   Larger scale batch reaction between **147** and **346**.

conv. (%)[a]	dr (*trans:cis*)[b] (acids)	dr (*trans:cis*)[c] (esters)	ee_{trans} (%)[d]	ee_{cis} (%)[d]	max[e] ee_{trans} (%)
>98	56:44	63:37	88	>99	92.1

[a] Conversion of both reagents determined by ^{1}H NMR spectroscopic analysis. [b] Diastereomeric ratio determined by ^{1}H NMR spectroscopic analysis. [c] Diastereomeric ratio determined by CSP-HPLC. [d] Determined by CSP-HPLC. [e] Calculated theoretical maximum *ee* (%) achievable by epimerisation.

In order to avoid any further complications derived from the 'naturally' occurring epimerisation process that would generate small differences in the resulted stereocontrol of distinct reactions, a single large scale reaction between **147** and **346** catalysed by **348** was performed (Table 4.5). The reaction, once worked up and the ester products isolated, was split in four smaller and equal batches, the epimerisation of which, under different conditions, were investigated.

The results obtained were surprising (Table 4.5). It can be seen that, comparing entry 1 of Table 4.5 with entry 2 of Table 4.4, the reactions, conducted under the same conditions, produced the diastereomeric mixture of product **347** in comparable diastereoselectivity but with higher enantioselectivity for the process executed in large scale. It is also possible to notice that this reaction could furnish the highest theoretical *ee* achievable upon epimerisation (*i.e.* 92.1%). This is also higher even than that obtained using the most efficient catalyst previously evaluated (*i.e.* **349**, entry 3, Table 4.4). It has been suggested that the difference may be due to non-uniform heating applied to the mixture on large scale. The large scale reaction required a higher volume of solvent compared to the other transformations executed in this study. As a result, the volume exceeded the height of the aluminium heating mantle, leaving the majority part of it exposed to lower temperature (*i.e.* room temperature) and thus generating gradients of temperatures that may have influenced the stereocontrol of the process. For this reason, the values expressed in Table 4.5 should not be considered as true results of the

reaction studied in this work, but just as an indicative data aimed to disclose of the best condition for the epimerisation reaction reported next.

The diastereomeric mixture of product **347** obtained in Table 4.5 was, upon isolation and purification by column chromatography on silica gel, divided into four equal batches and each batch was evaluated in the epimerisation reaction under different conditions (Table 4.6).

The reaction conducted under identical conditions to those used in the preliminary experiment (*i.e.* Scheme 4.3) proved to be extremely efficient, transforming the *cis*-isomer almost entirely to the *trans*-isomer with a product enantiomeric excess almost equal to the theoretical value (entry 1, Table 4.6).

Surprisingly, the adoption of the same conditions but with the involvement of catalyst **348** instead of **302** promoted the reaction in an unsatisfactory manner, converting only a small portion of the *cis*-isomer to the *trans* equivalent. The two chemical compounds responsible for the epimerisation (*i.e.* methanol and catalyst **302**) were then evaluated separately in the reaction in order to establish the actual promoter of the transformation.

Table 4.6   Evaluation of the conditions for the epimerisation reaction.

trans-**347** 88% ee   cis-**347** >99% ee   trans-**347**   cis-**347**
                   dr (trans:cis) 63:37
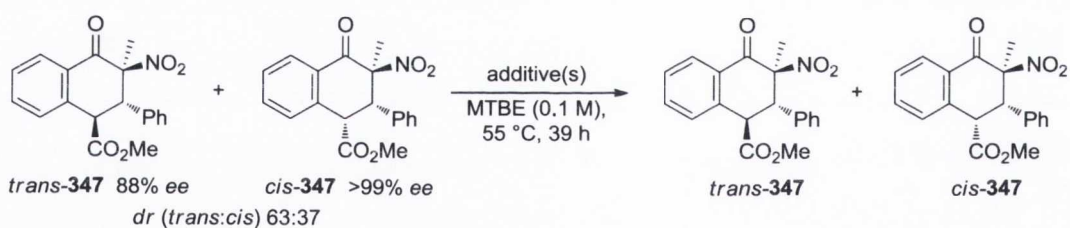
entry	max^a ee$_{trans}$ (%)	additive(s)	products dr (trans:cis)^b	ee$_{trans}$ (%)^c	yield (%)^d
1	92	MeOH (75.0 equiv.) **302** (5 mol%)	94:6	91	90
2	92	MeOH (75.0 equiv.) **348** (5 mol%)	72:28	n.d.^{e}	-
3	92	**302** (5 mol%)	65:35	n.d.^{e}	-
4	92	MeOH (75.0 equiv.)	92:8	92	89

^{a} Calculated theoretical maximum ee (%) achievable by epimerisation. ^{b} Diastereomeric ratio determined by CSP-HPLC. ^{c} Determined by CSP-HPLC. ^{d} Isolated yield of *trans*-diastereomer. ^{e} Not determined.

112

The reaction promoted solely by catalyst **302** (entry 3, Table 4.6) failed to convert the *cis*-isomer, furnishing the diastereomeric mixture of product **347** almost unaltered. Conversely, when methanol was employed as the only additive in reaction, close to 100% conversion of the *cis*-isomer was obtained, achieving the maximum value of enantiomeric excess expected (entry 4, Table 4.6).

Although the use of methanol (entry 4) was slightly less efficient than the combined used of methanol and catalyst **302** (entry 1), the use of the former procedure was chosen as the epimerisation protocol. This decision was made in consideration of the atom economy for the reaction and in view of the marginally enhanced enantioselectivity obtained.

The results suggested that the epimerisation process was not a base-promoted transformation, as the employment of only a base (*i.e.* catalyst **302**) in the reaction failed to promote such a process. We therefore proposed a mechanism (discussed in Section 4.10) based on the nucleophilic attack of methanol to the highly electrophilic ketone as a more plausible pathway.

4.7 Evaluation of substrate scope: the nitroalkene

Now in possession of a reproducible procedure for the synthesis of the diastereomeric mixture of product **347** and of an extremely efficient epimerisation protocol, our attention turned to the expansion of the substrate scope.

In order to achieve this, various trisubstituted nitroalkenes were synthesised. This was accomplished by following a general procedure based on the nitroaldol reaction (Henry reaction) between nitroethane (**354**) and the appropriate aldehyde **16** to furnish the relative β-nitroalcohol **355** (Scheme 4.5). This intermediate was, upon work-up and without further purification, directly dehydrated to the desired trisubstituted nitroalkene product **356** by reaction with trifluoroacetic anhydride (TFAA) and triethylamine (TEA).
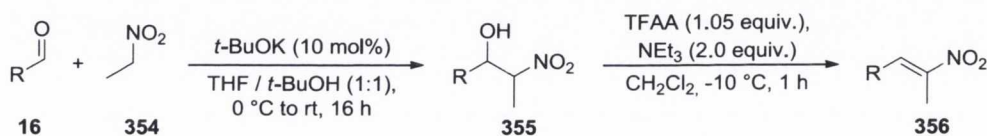
Scheme 4.5   General procedure for the synthesis of trisubstituted nitroalkenes.

Following this procedure, the series of activated electrophiles depicted in Figure 4.5 below, was readily synthesised, furnishing the products in moderate overall yields.
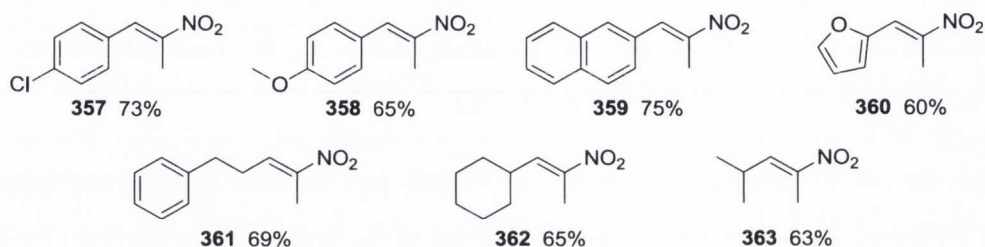
Figure 4.5   Substrates synthesised for the evaluation of the reaction scope.

The evaluation of such substrates in the reaction with **147** catalysed by **348** under standard conditions (described in Section 4.2) was the next step (Table 4.7). To avoid any possible temperature gradient (as in the large scale reaction described in Section 4.6), all the reactions were conducted on such a scale that the reaction mixture was fully exposed to the aluminium heating mantle, guaranteeing a uniform internal temperature.

Electron-neutral (**346** and **359**, entry 1 and 4), electron-poor (**357**, entry 2), electron-rich (**358**, entry 3), heteroaromatic (**360**, entry 5) and aliphatic (**361**, entry 6) trisubstituted nitroalkenes were all efficiently reacted under the depicted conditions to furnish the diastereomeric mixture of products **347, 364-368** in moderate *dr* with preference for the *trans*-isomer. In all these cases, almost complete conversion was achieved in convenient reaction times. As previously described in Section 4.2, variations in the *dr* of the products due to epimerisation, which occurs during the esterification process, favours the formation of the *trans*-isomer (compare column 6 with 7). It is possible to see how the substituent of the activated alkene influences the epimerisation process (Table 4.7). Products bearing aromatic electron-poor **364**, electron-rich **365**, and heteroaromatic **367** substituent (entry 2, 3 and 5, Table 4.7) tend to epimerise more easily than the corresponding products **347** and **366** which bear aromatic electron-neutral substituents (entries 1 and 4, Table 4.7), with variation of up to 16% in the case involving product **364** (entry 2). Product **368** which bears an aliphatic substituent, behaves similarly to **366** with only a slight variation in the *dr* upon esterification.

114

Table 4.7   Substrate evaluation in the reaction with homophthalic anhydride (**147**).
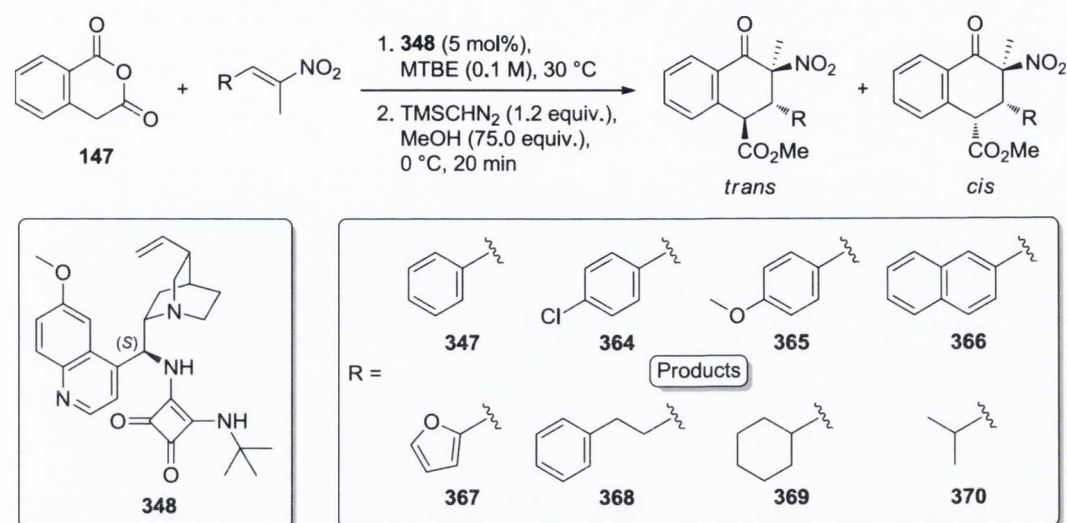
entry	sub.	prod.	time (h)	conv. (%)[a]	dr (*trans:cis*)[b] (acids)	dr (*trans:cis*)[c] (esters)	ee_{trans} (%)[d]	ee_{cis} (%)[d]
1	**346**	**347**	22	>98	53:47	57:43	72	99
2	**357**	**364**	66	>95	63:31	79:21	80	99
3	**358**	**365**	66	>96	57:43	59:41	74	99
4	**359**	**366**	66	>98	54:46	56:44	67	96
5	**360**	**367**	40	>98	77:23	86:14	12	96
6	**361**	**368**	24	>90	88:12	89:11	51	87
7	**362**	**369**	8d	55	n.d.[e]	98:2	49	-
8	**363**	**370**	7d	51	n.d.[e]	>99:1	52	-

[a] Conversion of both reagents determined by ^{1}H NMR spectroscopic analysis. [b] Diastereomeric ratio determined by ^{1}H NMR spectroscopic analysis. [c] Diastereomeric ratio determined by CSP-HPLC. [d] Determined by CSP-HPLC. [e] Not determined.

Products **369** and **370** (entry 7 and 8, Table 4.7), both synthesised using aliphatic-substituted nitroalkenes (*i.e.* **362** and **363**), behaved differently compared to the analogous product **368** (entry 6). Despite lengthy reaction times, the conversion of **362** and **363** to the corresponding ketone products reached only ca. 50%. This was attributed to the greater steric bulk that substrate **362** and **363** possess in the vicinity of the electrophilic centre of the alkene compared to **361**. This steric hindrance is also proposed as an explanation for the extremely high *dr* exhibited by the reactions

involving these two substrates (entry 7 and 8) compared to the others. However, it has not been possible to obtain a reaction *dr* before the esterification process, as the ^{1}H NMR spectra of both product **369** and **370** were characterised by overlapping key resonances. For this reason, the only *dr* measurement of the reactions was obtained by CSP-HPLC on the diastereomeric mixture of products upon esterification. Although it is known that the epimerisation process takes place during the esterification reaction, it was presumed that this side-reaction, in the cases involving **369** and **370**, occurred only to a small extent. This conclusion was made by analogy with product **368** which, similarly to **369** and **370**, bears an aliphatic substituent and exhibited the lowest variation of the *dr* upon esterification (entry 6, Table 4.7).

Analysis of the enantioselectivity of the reaction in the cases involving substrates **357**, **358** and **359** (entries 2, 3 and 4) shows that the *trans*-isomers of products **364**, **365** and **366** were all formed in moderate to good *ee*, while the *cis*-isomers were always formed in high *ee*, and almost optical purity in the case of **365** and **366** (entries 2 and 3). These results are consistent with the preliminary experiment described in Section 4.5 involving **346** as substrate (entry 2, Table 4.4), also reported in Table 4.7 (entry 1).

The reaction involving the use of **360** (entry 5, Table 4.7) however, despite producing the *cis*-isomer in high *ee* (*i.e.* 96%), generated the *trans*-isomer unexpectedly only in 12% *ee*.

The reactions involving aliphatic-substituted nitroalkenes **361**, **362** and **363** also failed to furnish satisfactory results (entries 6, 7 and 8, Table 4.7). Product **368** (entry 6) was formed with moderate *ee* for the *trans*-isomer and good for the *cis*-isomer. The results obtained for products **369** and **370** were similarly disappointing; despite the high *dr* observed, the *trans*-isomer were formed in only moderate *ee* (entries 7 and 8).

The next step in the study was the evaluation of the induced epimerisation reaction (Section 4.6) for the products obtained in the reactions shown in Table 4.7. Exception was made for products **369** and **370** for which, considering the high diastereoselectivity exhibited by the reaction, no epimerisation reaction was required. Following the developed procedure, which involves methanol as an 'additive', products **347, 364-368** were allowed to react in MTBE (0.1 M) at 55 °C for the time indicated in Table 4.8.

Table 4.8 Induced epimerisation of the diastereomeric mixture of products.
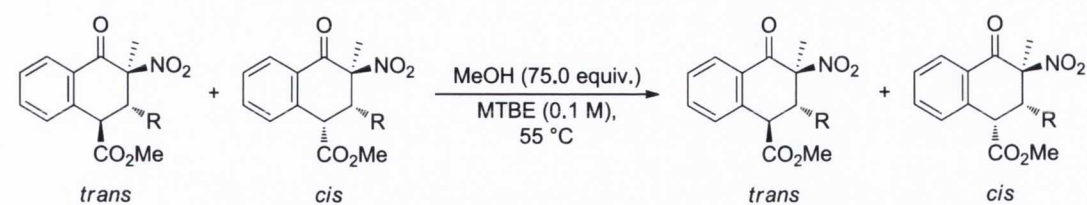
entry	prod.	initial _dr_ (_trans:cis_)[a]	_ee_trans (%)[b]	_ee_cis (%)[b]	max[c] _ee_trans (%)	time (h)	final _dr_ (_trans:cis_)[d]	_ee_trans (%)[b]	yield (%)[e]
1	**347**	57:43	72	99	83.3	44	96:4	80	91
2	**364**	79:21	80	99	83.5	39	>98:2	83	93
3	**365**	59:41	74	99	84.4	39	96:4	82	92
4	**366**	56:44	67	96	79.7	39	>99:1	77	93
5	**367**	86:14	12	96	23.7	64	93:7	28	88
6	**368**	89:11	51	87	55.0	64	89:11	50	82
7[e]	**369**	98:2	49	-	-	-	-	-	50[f]
8	**370**	>99:1	52	-	-	-	-	-	47[f]

[a] Diastereomeric ratio determined by CSP-HPLC. [b] Determined by CSP-HPLC. [c] Calculated theoretical maximum _ee_ (%) achievable by epimerisation. [d] Diastereomeric ratio determined by ^{1}H NMR spectroscopic analysis. [e] Isolated yield of _trans_-diastereomer. [e] Reaction performed with 20 mol% catalyst loading. [f] Calculated yield based on the mass return of the impure samples considering the spectroscopically determined amount of the known impurity present.

The reaction proved to be extremely efficient in almost all cases, transforming the _cis_-isomer of products **347**, **364-367** (entries 1-5) to the relative _trans_-isomer in relatively short reaction times, predominately furnishing _trans_-isomers from 93:7 _dr_ in the case involving **367** (entry 5) to >99:1 _dr_ using **366** (entry 4). The enantioselectivity obtained in all cases reached values close to the calculated maximum, proving the efficiency of the process. The reaction involving the aliphatic-substituted product **368** (entry 6), however, failed to epimerise the _cis_-isomer.

The other two products bearing an aliphatic substituent (_i.e._ **369** and **370**, entries 7 and 8), as previously explained, were not evaluated in the reaction as an already extremely high _dr_ was obtained during the synthesis of the diastereomeric mixture reported in Table 4.7 and are reported in Table 4.8 only for description of the isolated yields of the _trans_-isomers. However, due to the low conversion achieved in these two reactions,

products (*i.e.* **369** and **370**, entries 7 and 8) were isolated with a small amount of impurity (*i.e.* 17% for product **369** and 3% for product **370**), which ^{1}H NMR spectroscopic analysis revealed to be the *bis*-methyl ester **371** of the homophthalic acid. This product was formed by methanolysis and subsequent esterification by TMSCHN$_2$ of the unreacted anhydride **147** during the esterification reaction for the formation of products **369** and **370** (Scheme 4.6).

147   MeOH, TMSCHN$_2$ **371**
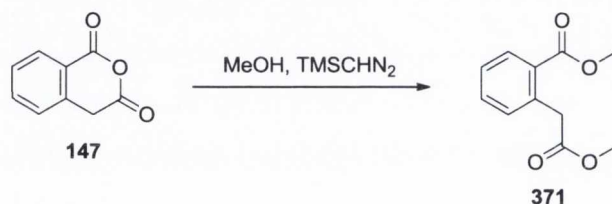
Scheme 4.6   Impurity formation in the reactions involving substrate **369** and **370**.

The *trans*-isomers obtained in the epimerisation reaction were all isolated and purified by column chromatography on silica gel in high yield. The yields of **369** and **370** (entries 7 and 8) were based on the mass return of the impure samples considering the measured (by ^{1}H NMR spectroscopic analysis) amount of the known impurity present (*i.e.* **371**).

4.8   Evaluation of substrate scope: the anhydride

As further expansion of the process and as prove of its general applicability, the use of a different anhydride (*i.e.* **312**) was then evaluated in the reaction with **346** (Table 4.9).

Table 4.9   Evaluation of anhydride **312** in the reaction with **346**.
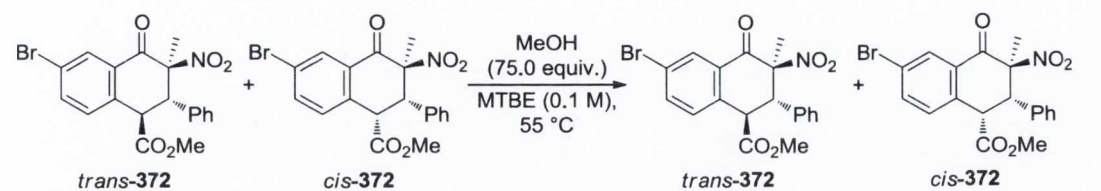
time (h)	conv. (%)^a	dr (trans:cis)^b (acids)	dr (trans:cis)^c (esters)	ee_{trans} (%)^d	ee_{cis} (%)^d	max^e ee_{trans} (%)
24	>97	50:50	58:42	75	>99	85.1

^{a} Conversion of both reagents determined by ^{1}H NMR spectroscopic analysis. ^{b} Diastereomeric ratio determined by ^{1}H NMR spectroscopic analysis. ^{c} Diastereomeric ratio determined by CSP-HPLC. ^{d} Determined by CSP-HPLC. ^{e} Calculated theoretical maximum *ee* (%) achievable by epimerisation.

The reaction efficiently produced the diastereomeric mixture of product **372** with values of *dr* and *ee* in line with those obtained in the reaction between **147** and **346** (entry 1, Table 4.7).

Table 4.10   Epimerisation reaction of product **372**.

initial *dr* (*trans:cis*)[a]	ee_{trans} (%)[b]	ee_{cis} (%)[b]	max[c] ee_{trans} (%)	time (h)	final *dr* (*trans:cis*)[d]	ee_{trans} (%)[b]	yield (%)[e]
58:42	74.6	99	85.1	30	>99:1	86	92

[a] Diastereomeric ratio determined by CSP-HPLC. [b] Determined by CSP-HPLC. [c] Calculated theoretical maximum *ee* (%) achievable by epimerisation. [d] Diastereomeric ratio determined by ^{1}H NMR spectroscopic analysis. [e] Isolated yield of *trans*-diastereomer.

Next, the epimerisation reaction of product **372** was examined (Table 4.10) in methanol under identical conditions to those reported in Table 4.8.

The reaction proved efficient, smoothly promoting the epimerisation of *cis*-**372** to *trans*-**372** in nearly quantitative amounts, while also furnishing the calculated highest *ee* expected for the reaction. The desired product was then isolated and purified by chromatography, to afford *trans*-**372** in high yield (Table 4.10).

4.9   Assignment of the absolute stereochemistry

In order to confirm the stereochemical outcome of the reaction, the assignment of the absolute stereochemistry of both the diastereomers of the products was required. As such, pure samples of *cis*-**372** and of *trans*-**372** were recrystallised and analysed by X-ray crystallography.

The absolute stereochemistry of the *cis*-isomer of **372** was readily assigned as (1*S*,2*S*,3*S*) as depicted in Figure 4.6. By analogy, the same absolute stereochemistry was assigned to the other *cis*-isomers of products **347**, **364-368** described in Table 4.7.
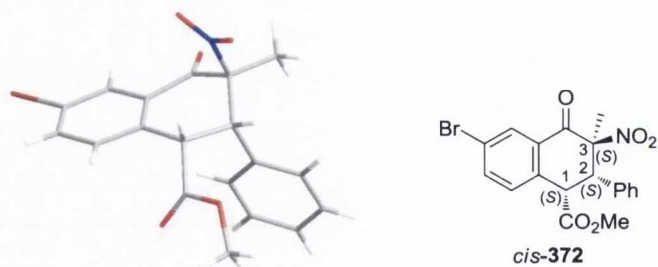
Figure 4.6   Absolute stereochemistry of *cis*-**372**.

The X-ray diffraction analysis of *trans*-**372** however, presented some difficulties. Although the analysis was repeated three times, resolution of the crystal structure data obtained was never achieved. Therefore, it was decided to attempt the reduction of the carbonyl group of a pure sample of *trans*-**347** (previously prepared in a large scale reaction, Section 4.6) by reaction with sodium borohydride (NaBH$_4$) in methanol, in order to obtain a more crystalline material that would hopefully simplify the analysis (Scheme 4.7).
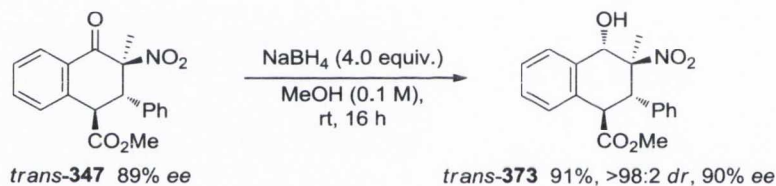
Scheme 4.7   Reduction of the ketone functionality of product **347**.

The reaction proved efficient as the reduction of the ketone took place in high yield and *ee* with almost full diastereocontrol, producing the alcohol **373** as the *trans*-isomer without either racemisation or epimerisation. This new product, that now contains four stereogenic centres, was then isolated and purified by chromatography and, upon recrystallisation, analysed by X-ray crystallography.

The absolute stereochemistry of *trans*-**373** was unequivocally assigned as (1*R*,2*S*,3*S*,4*S*) as shown in Figure 4.7.
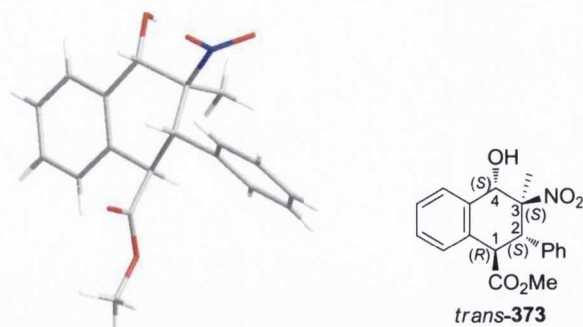
Figure 4.7   Absolute stereochemistry assignment of *trans*-**373**.

By comparison of the ^{1}H NMR spectra of *trans*-**373** and *trans*-**347** it can be observed that the coupling constant (J) between the hydrogen in position 1 and 2 remained almost identical (*i.e.* 11.8 Hz for *trans*-**373** and 12.3 Hz for *trans*-**347**), characteristic of *trans* stereochemistry.
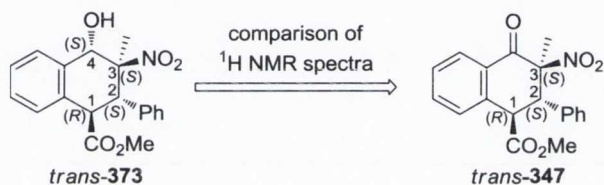
Figure 4.8   Assignment of the absolute stereochemistry of *trans*-**347**.

These results allowed the conclusion that, although a new stereocentre was created, the three initially present in *trans*-**347** did not epimerise during the reduction of the ketone carbonyl functionality. This permitted the disclosure of the absolute stereochemistry of the *trans*-isomers of product **347** as (1*R*,2*S*,3*S*) as shown in Figure 4.7. By analogy, the absolute stereochemistry of the *trans*-isomers of the other products synthesised by the reactions depicted in Table 4.7 was also assigned as (1*R*,2*S*,3*S*).

4.10 The proposed epimerisation mechanism

A mechanism for the epimerisation process promoted by methanol was then proposed. Analysis of the structure of *cis*-**372** obtained by X-ray crystallography revealed that the distance between the oxygen of the nitro group in position 3 and the hydrogen in position 1 in the crystal structure is 2.8 Å (**A**, Figure 4.9). This is too long to permit any kind of interaction between the two atoms. However, it must be considered that in solution at 55 °C, the nitro group would be able to freely rotate around the carbon-nitrogen bond. This will result in the reduction of the distance between the oxygen and

121

the hydrogen to a minimum value of 1.9 Å (**B**, Figure 4.9) and a correct H-bonding angle.
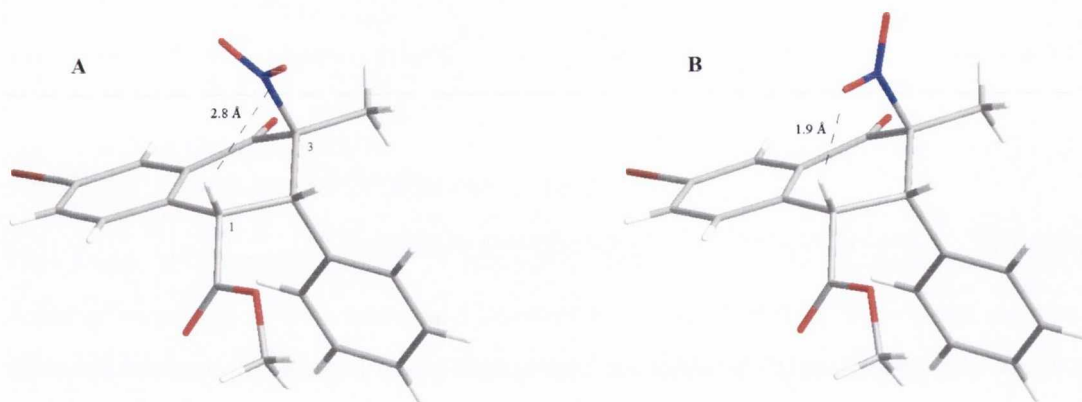
Figure 4.9   Distance between the nitro group and the hydrogen in position 1.

We believed that, in methanol, at this reduced distance the oxygen of the nitro group could act as a 'base' for the epimerisation process, according to the mechanism reported below (Scheme 4.8).
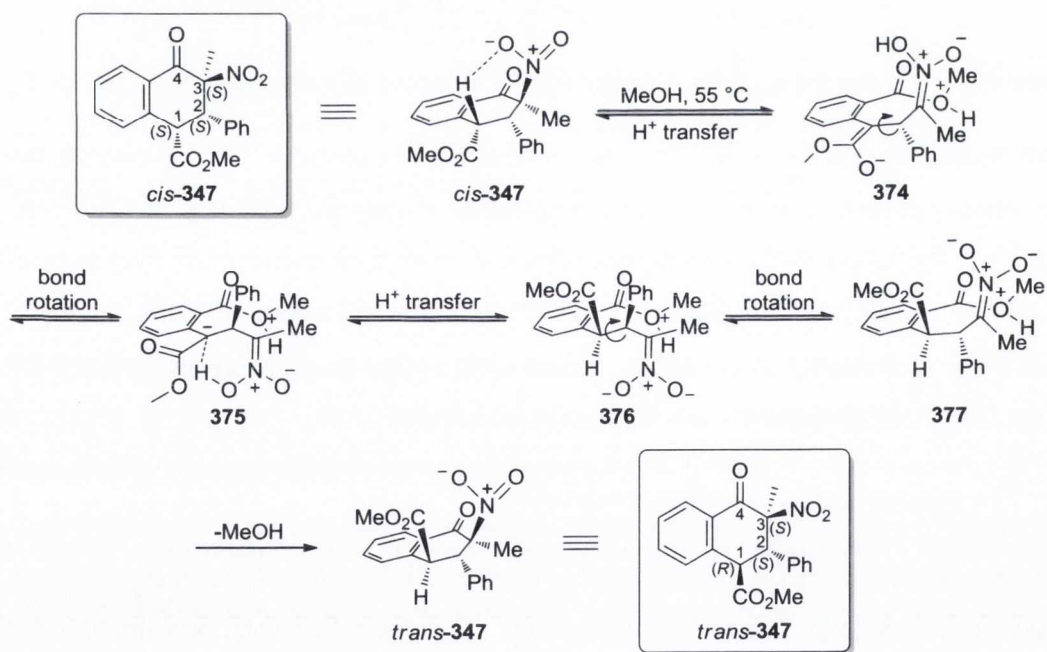
Scheme 4.8   Proposed mechanism for the epimerisation reaction promoted by methanol.

The weak interaction between the oxygen of the nitro group and the hydrogen in C-1 shields the upper face of *cis*-**347**. This is reflected in the attack of methanol to the carbonyl functionality that only takes place from the lower face (as drawn) of the

structure. Next, in a concerted step, the bond between carbon atom 3 and 4 breaks and generates the nitronate ion which deprotonates the carbon atom in position 1 with concomitant formation of the enolate **374**.

At this point, rotation of the bond between carbon atoms 1 and 2 generates **375**, which then reprotonates the enolate previously formed on the *re* face of the molecule through a six-membered ring transition state, generating the nitronate ion **376**. A second rotation of the bond between carbon atoms 1 and 2 to **377** and subsequent intramolecular attack of nitronate on the protonated ester - with loss of methanol - furnishes the epimerised *trans*-**347**. It is noteworthy that this final step appears thermodynamically unfavourable at first glance; however, it should be noted that it is entropically favourable, and we previously observed very strong temperature dependence in the epimerisation process. At higher temperature the more entropically favourable ring closing final step would become more favourable relative to the reverse process.

4.11 Conclusion

The results of this project demonstrate that the reaction involving homophthalic anhydrides as pronucleophile species can be expanded to the use of activated trisubstituted nitroalkenes. The reaction leads to the formation of bicyclic structures bearing three stereogenic centres, one of which quaternary. Although this should lead to the formation of four diastereomers, only two were observed in the reaction. It was also found that, an epimerisation process promoted by methanol could be induced in order to convert the *cis*-isomer to the *trans*-isomer, and a mechanism for this process has been proposed. Despite the difficulties encountered during the development of this study, all of them due to the partially controllable, naturally occurring epimerisation process, the reaction could be applied to a range of trisubstituted nitroalkenes substrates to produce diastereomeric mixture of products, which, upon induced epimerisation process, were generally isolated in good yields, with good *dr* and *ee*. To the best of our knowledge this represents the first asymmetric catalytic cycloaddition of enolisable anhydride with Michael acceptors. Two new squaramide-substituted cinchona alkaloid organocatalysts were also synthesised in order to improve the control over the reaction. However, the most successful of the two has not been further used in the development of the process as difficulties in the reproducibility of its synthesis were encountered, making its use unpractical.

5. The enantioselective cycloaddition reaction between anhydrides and alkylidene-2-oxindoles

Following the disclosure of the cycloaddition reaction between homophthalic anhydride and trisubstituted nitroolefins (described in Chapter 4), we became interested in the development of a similar process that involved the reaction of substituted alkylidene-2-oxindoles, such as **378**, as electrophiles (Scheme 5.1).
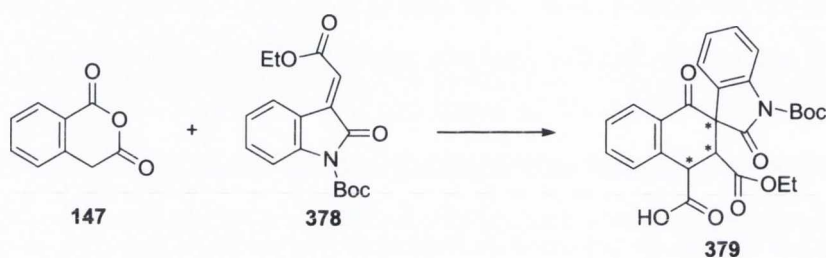
Scheme 5.1   The proposed reaction between homophthalic anhydride (**147**) and **378**.

These substrates were chosen as they would lead to the creation of structures similar to those obtained using trisubstituted nitroalkenes (*i.e.* bearing three stereocentres one of which would be quaternary), however with the presence of a spiro-carbon (**379**, Scheme 5.1). These products belong to a large family of compounds known as spirooxindoles. For almost two decades their synthesis has been the subject of study of many research groups around the world,[287–290] as this core structure is found in many natural compounds that possess biological activity.[291–297] More recently, with the advent of efficient asymmetric organocatalysis, the enantioselective synthesis of such challenging molecules began to expand. Currently, it represents one of the most intensive studied reactions catalysed by organocatalytic processes.[298–301]

5.1   Preliminary experiments

In order to study the feasibility of the process by evaluating the reaction between **147** and **378**, the substituted oxindole **378** had to be synthesised. This was achieved according to the known literature procedure[302] described below (Scheme 5.2).

The synthesis began with the reaction between ethyl bromoacetate (**380**) and triphenylphosphine (**381**) in toluene at 90 °C to give the intermediate phosphonium salt

382 in high yield, which upon deprotonation by sodium hydroxide solution and extraction with dichloromethane gave the ylide **383** in quantitative amount.
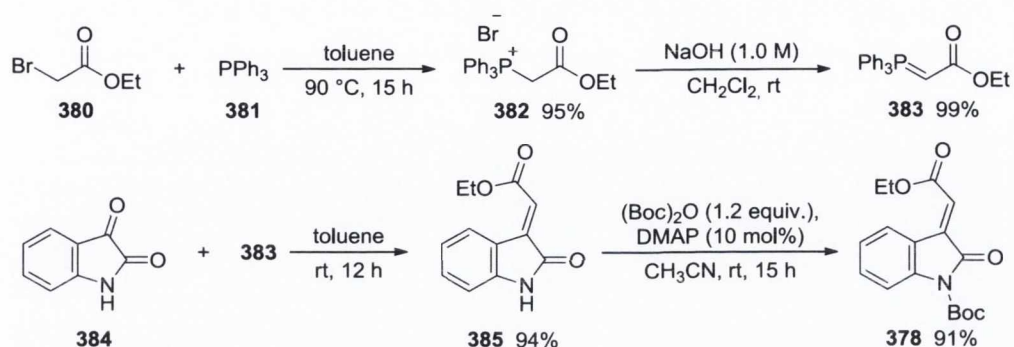
Scheme 5.2   Synthesis of the substituted oxindole **378**.

The Wittig reaction in toluene at room temperature between this compound and isatin (**384**) furnished the oxindole **385** which was then purified and isolated in 94% yield by column chromatography on silica gel. Protection of the nitrogen atom by reaction with di-*t*-butyl dicarbonate ((Boc)₂O) in presence of a catalytic amount of DMAP in acetonitrile at room temperature, led to the final product **378**, which was isolated and purified by column chromatography on silica gel in high yield.

Now in possession of both the pronucleophile (*i.e.* **147**) and electrophile (*i.e.* **378**); the reaction depicted in Table 5.1 was investigated under the optimised conditions developed for the project involving the use of trisubstituted nitroalkenes (Section 4.7) using catalyst **348** as reaction promoter.

The reaction readily produced **386** in almost quantitative yield after a short time under mild conditions. Analysis by ¹H NMR spectroscopy of the crude reaction mixture (prior to esterification) revealed the presence of only one diastereomer which, by measurement of the coupling constant between the proton at C-3' and that at C-4' (*i.e.* 11.8 Hz), was assigned to possess *trans* relative stereochemistry between the substituents in C-3' and C-4'. Unfortunately, during this analysis it was not possible to assign the relative stereochemistry of the carbon at C-2'. When the sample, upon *in situ* esterification by reaction with TMSCHN₂ and methanol under the conditions reported in Table 5.1, was analysed by CSP-HPLC, the chromatogram revealed the presence of two further diastereomers (*i.e.* B and C) in very small amounts (*i.e.* 4% and 1.5 % respectively).

Table 5.1   Preliminary reaction between **147** and **378** catalysed by **348**.
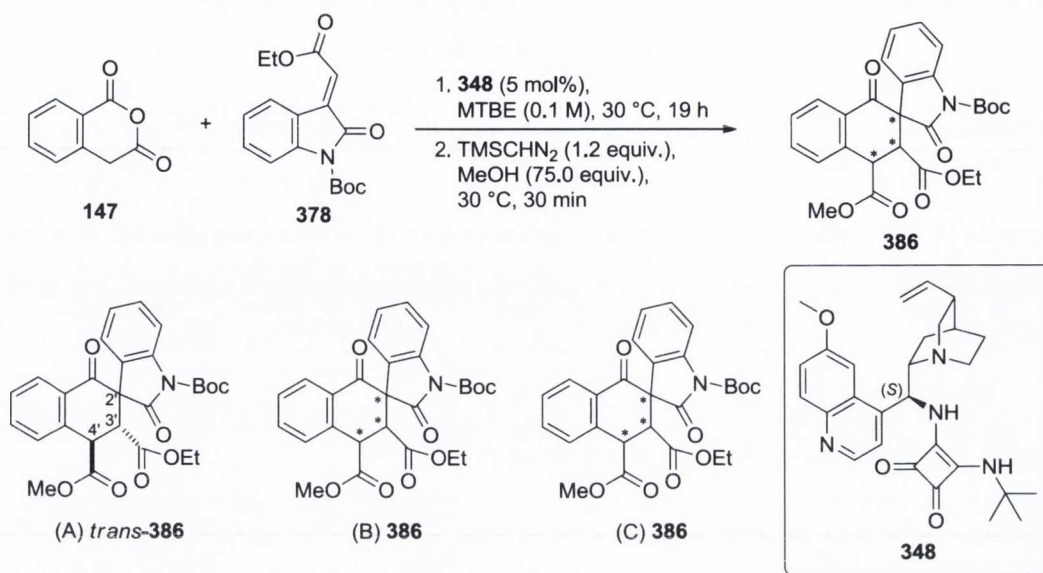
conversion (%)^a	dr (A:B:C)^b	ee$_A$ (%)^c	ee$_B$ (%)^c	ee$_C$ (%)^c
>98	94.5:4:1.5	95	-	-

^{a} Conversion of both reagents determined by ^{1}H NMR spectroscopic analysis. ^{b} Diastereomeric ratio determined by CSP-HPLC. ^{c} Determined by CSP-HPLC.

It was now clear that the ^{1}H NMR resonances associated with the two minor diastereomers could not be observed in the spectrum of the crude reaction mixture due to the overlap with those associated with the major diastereomer (*i.e.* A, *trans*-**386**). It was therefore decided, in order to obtain more accurate results, to determine the *dr* of the reactions by CSP-HPLC analysis only. The diastereomeric mixtures formed in the reactions, upon *in situ* esterification with TMSCHN$_2$ and MeOH at 30 °C, were purified by column chromatography on silica gel and the three diastereomeric products collected and analysed together with an appropriately developed CSP-HPLC method that allowed the separation of all the enantiomeric peaks of the products. The reaction depicted in Table 5.1 proved to be extremely efficient, furnishing product **386** with exceptionally high diastereoselectivity and enantioselectivity, favouring the formation of *trans*-**386**. The *ee* of the other diastereomers (*i.e.* B and C) were not determined however, as the relatively low peak area for these structures resulted in an inaccurate analysis.

5.2 Catalyst evaluation

After the encouraging results obtained in the preliminary reaction, we decided to evaluate the effect that different catalysts could exert in the promotion of the reaction. Using the same conditions employed in the preliminary reaction (Table 5.1), a further five catalysts were evaluated in the reaction between **147** and **378** (Table 5.2). Catalyst **297**, **81** and **302** were synthesised by Dr. Seán Tallon.

Table 5.2   Catalyst evaluation for the reaction between **147** and **378**.
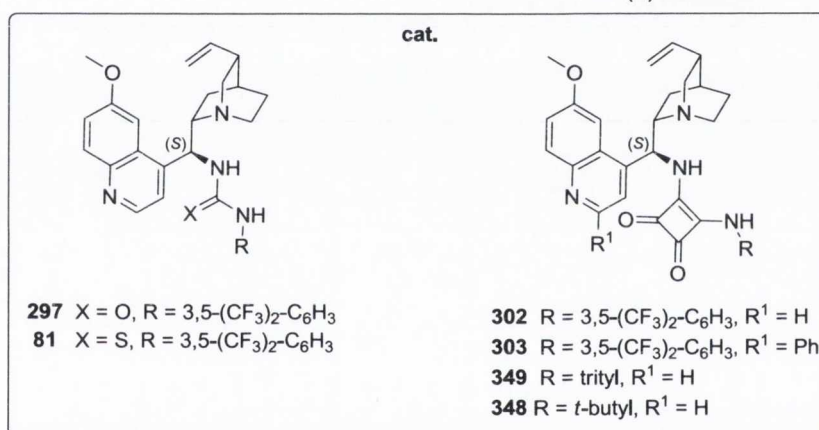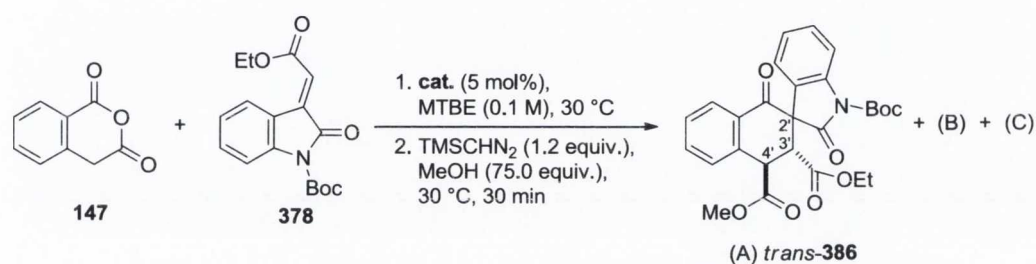
entry	cat.	time (h)	conversion (%)[a]	dr (A:B:C)[b]	ee_A (%)[c]	ee_B (%)[c]	ee_C (%)[c]
1	**297**	13	>97	98:1:1	88	-	-
2	**81**	19	>97	98.5:1:0.5	88	-	-
3	**302**	16	>97	97.5:2:0.5	83	-	-
4	**303**	19	>98	96:3:1	93	-	-
5	**349**	25	>97	97:2:1	90	-	-
6	**348**	19	>98	94.5:4:1.5	95	-	-

[a] Conversion of both reagents determined by ^{1}H NMR spectroscopic analysis. [b] Diastereomeric ratio determined by CSP-HPLC. [c] Determined by CSP-HPLC.

All catalysts evaluated proved to be extremely successful, promoting the reaction with high diastereoselectivity and enantioselectivity in reasonably short reaction times and with almost quantitative conversion. Comparison between (thio)urea-substituted cinchona alkaloids (entries 1 and 2) with the squaramide-substituted analogue (entry 3) revealed superior stereocontrol by the former two structures. However, either the introduction of phenyl substituent at the C-2' position of catalyst **302**, or replacement of the aromatic and relatively planar squaramide *N*-substituent of **302** (*i.e.* 3,5-(CF$_3$)$_2$-C$_6$H$_3$) with a non-planar and bulky substituent (*i.e.* trityl for **348** and *t*-butyl for **349**, see Section 4.5) allowed catalysts **303**, **349** and **348** (entries 4, 5 and 6) respectively, to promote the reaction with enhanced enantiocontrol up to 95% *ee* for the reaction promoted by **348** (entry 6). Despite the reduced diastereocontrol exhibited by **303** and **348** (entries 4 and 6) compared to the other catalysts examined, these two structures proved to be the most efficient, promoting the only two reactions that provided enantioselectivity above 90% (*i.e.* 93% for **303**, entry 4 and 95% for **348**, entry 6, Table 5.2).

5.3 The effect of the temperature on the reaction

After the identification of the two most successful reaction promoters (*i.e.* **303** and **348**), the effect of reaction temperature on the stereocontrol of the process was studied (Table 5.3). In general, the reactions proceeded with almost complete conversion to product **386** in relatively convenient reaction times. As expected, an increase of the reaction temperature to 60 °C (entry 2) drastically diminished the enantiocontrol of the reaction to 37% with a concomitant marginal reduction in the diastereocontrol for the reaction catalysed by **303**. However, when the reaction temperature was reduced incrementally in order to determine the best conditions for the achievement of greatest stereocontrol compared to the 'benchmark' reaction conducted at 30 °C with catalyst **303** (entry 1), the results were quite surprising. As the reaction temperature decreased, we expected to observe an improvement in the *dr* and *ee* of the reaction for the *trans*-isomer (*i.e.* A) from the 'initial condition' (entry 1). Conversely, it was found that an increase in the formation of the second diastereomer (*i.e.* B) with concomitant reduction in the production of *trans*-**386** (*i.e.* A) took place when the reaction was performed at gradually lower temperature (*i.e.* 20 °C, 0 °C and -15 °C, entries 3, 4 and 5 respectively, Table 5.3). Furthermore, while the *ee* of the newly formed diastereomer (*i.e.* B) was

always above 90%, the enantiomeric excess of *trans*-**386** (*i.e.* A) generally decreased with decreasing temperature, from 95% *ee* at 30 °C to 63% *ee* at -15 °C. The reaction time however, in this final case (*i.e.* entry 5) had to be extended in order to achieve full conversion.

Temperature variations in the reactions promoted by catalyst **348** had similar results. When the reaction was conducted at temperatures below 30 °C, formation of the second diastereomer (*i.e.* B) took place in high *ee* with concomitant reduction in the levels of *trans*-**386** (*i.e.* A) detected, and with gradually lower *ee* (entries 7-12). Following this strategy, it was possible to 'switch' the diastereoselectivity of the reaction toward the predominant formation of (B); with the maximum diastereo- and enantioselectivity exhibited at -50 °C (entry 11). However, the low conversion and the extremely long reaction time required in this situation were not satisfactory. This prompted us to repeat this reaction with a higher catalyst loading (*i.e.* 20 mol%, entry 12). In doing so, a shorter reaction time and enhanced conversion were achieved although with no variation in the diastereoselectivity of the process. Under these conditions the diastereomer (B) was formed with almost 100% optical purity. After the evaluation of temperature variation in the reactions catalysed by **303** and **348**, it was clear that both catalysts could be successfully employed as reaction promoters, as similar results were obtained using **303** and **348**. However, the slight superiority of catalyst **348**, with regards to the *ee* for the reaction performed at 30 °C and diastereocontrol in the formation of the diastereomer (B) at lower temperature, prompted us to continue the study employing only catalyst **348**. Also, considering the results reported in Table 5.3, it is clear that the temperature of 30 °C is the most practical at which to conduct the reaction. Thus, it was decided no further optimisation for the reaction was necessary, as the conditions used in the preliminary evaluation (*i.e.* Table 5.1) proved to be the most useful.

Table 5.3   Evaluation of the effect of temperature on the reaction between **147** and **378**.

(A) *trans*-**386**

cat.
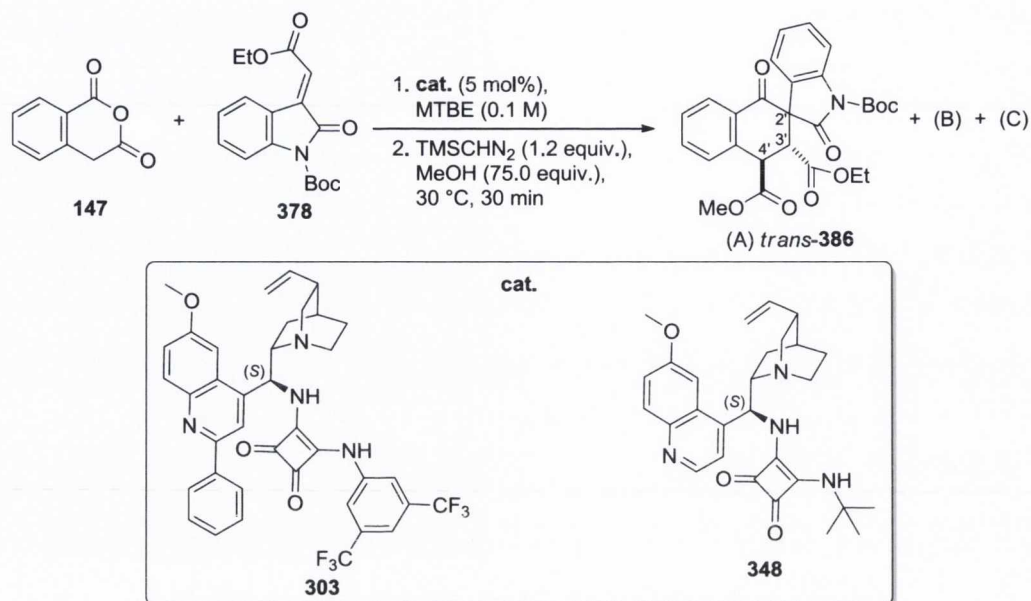
entry	cat.	temp. (°C)	time (h)	conv. (%)[a]	dr (A:B:C)[b]	ee$_A$ (%)[c]	ee$_B$ (%)[c]	ee$_C$ (%)[c]
1	**303**	30	19	>98	96:3:1	93	-	-
2	**303**	60	22	>97	92:2:6	37	-	-
3[e]	**303**	20	19	>97	67:33:1	85	95	-
4[e]	**303**	0	18	>97	65:35:1	83	96	-
5[e]	**303**	-15	90	>95	n.d.	63	97	-
6	**348**	30	19	>98	94.5:4:1.5	95	-	-
7[e]	**348**	20	19	>96	90:9.5:0.5	93	97	-
8[e]	**348**	0	17	>95	40:59:1	85	97	-
9[e]	**348**	-15	44	>98	34:65:1	95	96	-
10[e]	**348**	-30	69	>98	22:77:1	83	98	-
11[e]	**348**	-50	432	ca. 85	16:82:2	43	>99	-
12[de]	**348**	-50	360	ca. 91	17:82:1	94	99	-

[a] Conversion of both reagents determined by ^{1}H NMR spectroscopic analysis. [b] Diastereomeric ratio determined by CSP-HPLC. [c] Determined by CSP-HPLC. [d] Reaction performed with 20 mol% catalyst loading. [e] Esterification process performed at the same temperature of the reaction.

5.4   Assignment of relative stereochemistry

As described before, the ^{1}H NMR spectrum of the diastereomeric mixture of **386** presents overlapping products resonances, making quantification of the level of diastereomer (B) present impossible. Therefore, in order to identify the correct structure and assign the relative stereochemistry of (B), separation of this molecule from the diastereomeric mixture of **386**, produced in the reactions shown in Table 5.3, was necessary.

However, despite the intensive efforts devoted to the separation of the three diastereomers by column chromatography on silica gel, this was never fully achieved. As a solution, the employment of an automated flash chromatographic purification system (*i.e.* Biotage SP4) which uses high performance prepacked silica cartridges, allowed the complete separation of the three diastereomers, eluting the mixture using a developed gradient method.

The two major diastereomers (A) and (B), now separated, were then analysed by ^{1}H NMR spectroscopy in order to determine the relative orientation between the ring substituents (Figure 5.1).

(A) 2',3'-*trans*-3',4'-*trans*-**386**   (B) 2',3'-*cis*-3',4'-*cis*-**386**
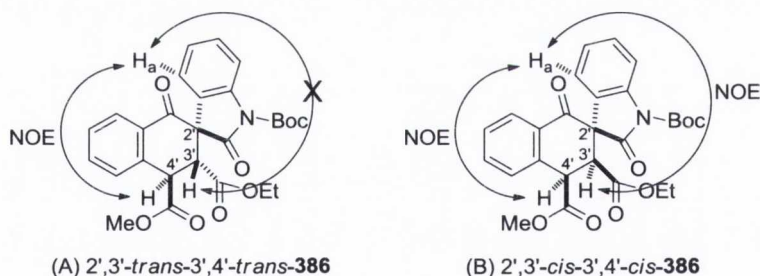
Figure 5.1   Relative stereochemistry of the diastereomers (A) and (B) of product **386** determined by NOE NMR techniques.

As expected, the relative stereochemistry of (A) was confirmed to be 3',4'-*trans*-**386** as a coupling constant value of 11.8 Hz was measured between protons at positions C-4' and C-3'. With regards to the diastereomer (B), a coupling constant of 5.8 Hz was measured between the same relative protons, allowing the assignment of its relative stereochemistry as 3',4'-*cis*-**386**. The relative stereocentre at position C-2' was assigned as depicted in Figure 5.1, by ^{1}H NMR Nuclear Overhauser Effect (NOE) experiments (see the Appendix for details). Analysing the diastereomer (A), a NOE contact was

detected between the proton at C-4' and proton H_a of the oxindole moiety, revealing that the two protons are on the same face of the molecule. Considering the relative *trans* stereochemistry between protons at C-3' and C-4', a NOE contact between the former and proton H_a should not be visible. The experiment proved this supposition correct, as no contact between the two protons was determined, allowing the assignment of the relative stereochemistry of (A) as 2',3'-*trans*-3',4'-*trans*.

Analysis of the diastereomer (B) using the same technique revealed NOE contact between proton H_a and both protons at C-3' and C-4', demonstrating that all the three protons are on the same side of the molecule and also further supporting the assignment of the *cis* stereochemistry between the protons at C-3' and C-4'. This allowed the assignment of the relative stereochemistry of (B) as 2',3'-*cis*-3',4'-*cis* (see the Appendix for details). The minor diastereomer (C) was not analysed, as it was only formed in trace amounts in all the reactions evaluated.

For clarity, from here on in the diastereomer 2',3'-*trans*-3',4'-*trans*-**386** (*i.e.* A) will be referred to as *trans*-**386** while the diastereomer 2',3'-*cis*-3',4'-*cis*-**386** (*i.e.* B) will be referred to as *cis*-**386**.

5.5   Assignment of absolute stereochemistry

The next step in the study was the assignment of the absolute stereochemistry by X-ray crystallographic analysis of a recrystallised sample of the two diastereomers formed in the reaction (*i.e.* *trans*-**386** and *cis*-**386**). In order to facilitate the resolution of the diffraction data, the presence of a large atom in the molecule is beneficial. We therefore decided to employ the bromo-substituted homophthalic anhydride **312** in the reaction with **378** catalysed by **348** at two different temperatures (Table 5.4).

Table 5.4   The employment of bromo-substituted homophthalic anhydride **312** in the reaction with **378** catalysed by **348**.
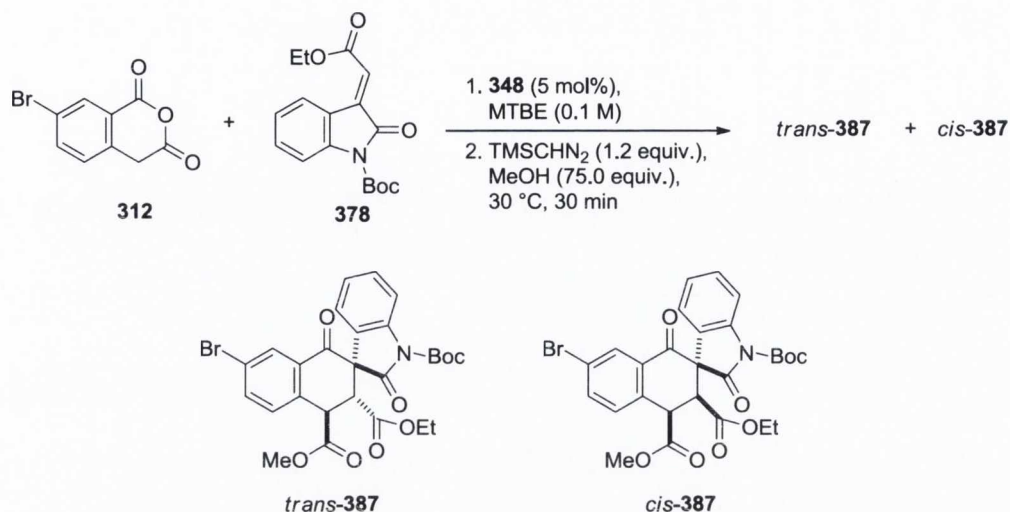
entry	temp. (°C)	time (h)	conv. (%)^a	dr (trans:cis)^b	ee_{trans} (%)^c	ee_{cis} (%)^c
1	30	30	>98	>98:2	92	-
2^d	-30	144	>98	22:78	-	92

^{a} Conversion of both reagents determined by ^{1}H NMR spectroscopic analysis. ^{b} Diastereomeric ratio of the two major diastereomers determined by ^{1}H NMR spectroscopic analysis. ^{c} Determined by CSP-HPLC. ^{d} Esterification process performed at the same temperature of the reaction.

The reactions readily formed the diastereomeric mixture of product **387** in nearly full conversion. When performed at 30 °C, the reaction exhibited high *dr* and *ee* in the formation of *trans*-**387**. As expected, conducting the reaction at lower temperature (*i.e.* -30 °C, entry 2) resulted in the formation of *cis*-**387** predominantly, although with lower enantioselectivity compared to the reaction involving anhydride **147** under the same conditions (*i.e.* entry 10, Table 5.3). The temperature of -30 °C was chosen as the reaction time required for the conversion under these conditions was more practical then that required for conversion to occur at -50 °C.

The major diastereomer formed in each of the two reactions depicted in Table 5.4 were then isolated and purified by automated flash chromatographic purification system (*i.e.* Biotage SP4), and recrystallised. Analysis of the crystals obtained by X-ray crystallography allowed the assignment of the absolute stereochemistry of *trans*-**387** as (2'*R*,3'*R*,4'*R*) as depicted in Figure 5.2.
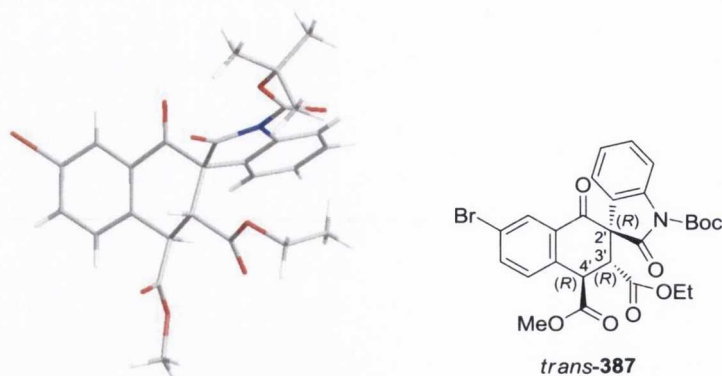
Figure 5.2   Absolute stereochemical assignment for *trans*-**387**.

By analogy, the *trans*-isomer of product **386** was assigned with the same absolute stereochemistry, confirming the relative stereochemistry previously assigned by ^{1}H NMR NOE experiments (Figure 5.1).

Unfortunately, despite intensive efforts, crystallisation of the *cis*-isomer of product **387** could never be achieved, thus preventing the disclosure of the absolute stereochemistry of this isomer by X-ray crystallography. However, in view of the relative stereochemistry of *cis*-**386** obtained in the NOE experiments (Section 5.4) and with the knowledge of the absolute stereochemistry of the *trans*-isomer (Section 5.5), the only two possible structures for major enantiomer of the *cis*-isomer were proposed (Figure 5.3).
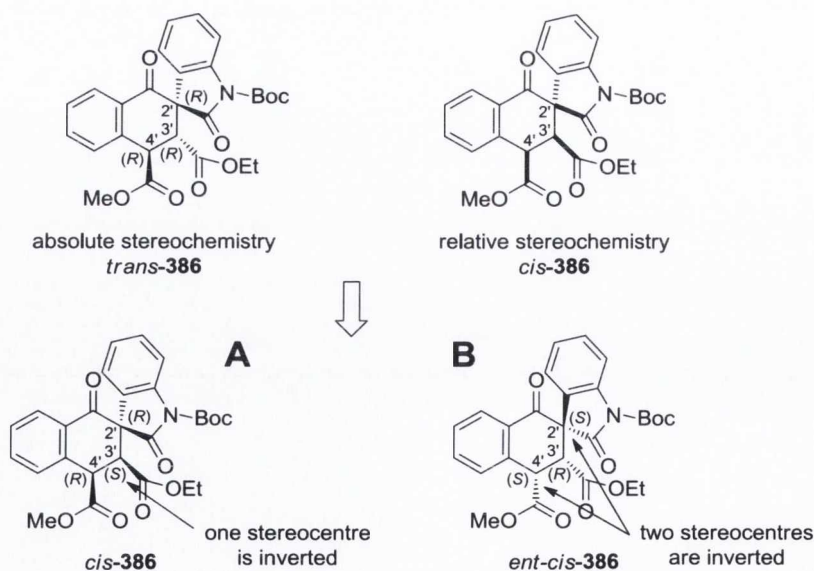
Figure 5.3   Proposed structures for the absolute stereochemical assignment of *cis*-**386**.

134

In the first case (**A**, Figure 5.3) the isomers *trans* and *cis* differ only for the stereochemistry at the C-3' centre, while in the second case (**B**, Figure 5.3) they differ for the stereochemistry at two stereocentres (*i.e.* C-2'and C-3'). We believed that the structure depicted in **A** is the most plausible, as epimerisation of only one centre would take place more easily during the transition state of the reaction due to *E/Z* isomerisation of the double bond of the alkyliden-2-oxindole substrate than a double epimerisation at two centres.

5.6   Substrate scope: the anhydride

The next step in the study was the expansion of the substrate scope, with the evaluation of different anhydrides. In preliminary experiments, not reported here, we observed that the reaction catalysed by **348** between anhydride **329**, which already proved a successful substrate for the cycloaddition reaction with aldehydes (Chapter 3), failed to form the expected product **388** when reacted with oxindole **378** even under forcing conditions (Scheme 5.3). This was probably due to the higher steric clash in the transition state leading to the formation of a product with two all carbon quaternary centres.
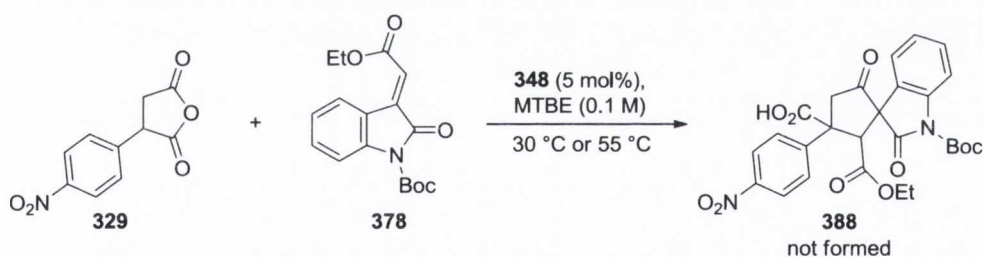
Scheme 5.3   Preliminary evaluation of anhydride **329** as substrate.

Tamura[183–186] and Jung,[189,190] had both demonstrated the successful employment of enolisable anhydrides beyond those derived from homophthalic anhydride (**147**), in the thermal- and strong base- promoted cycloaddition of anhydrides to electrophiles (see Sections 1.5.4 and 1.5.4.1). We were therefore interested in the evaluation of five of these structures in the organocatalytic reaction with **378** under optimum conditions used in the preliminary test (*i.e.* Section 5.1).

5.6.1 Synthesis of anhydrides

The anhydrides that were chosen for the evaluation of the substrate scope are depicted in Figure 5.4.
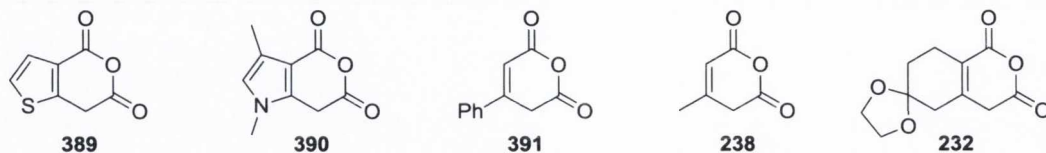
Figure 5.4 Anhydrides synthesised for the evaluation of the substrate scope

Following reported literature procedures with small modifications, each structure was successfully synthesised according to the schemes below.

5.6.1.1 The synthesis of anhydride 389

Anhydride **389** was synthesised according the three step synthetic pathway described in Scheme 5.4. The first step of the synthesis consists of the formation of the *bis*-ester **395** in 86% yield by reaction between 1,4-dithiane-2,5-diol (**393**, dimer of 2-mercaptoacetaldehyde (**392**)) and diethyl 1,3-acetonedicarboxylate (**394**), promoted by lithium bromide at reflux temperature for 16 hours in 1,4-dioxane, according to the known literature procedure.[303]
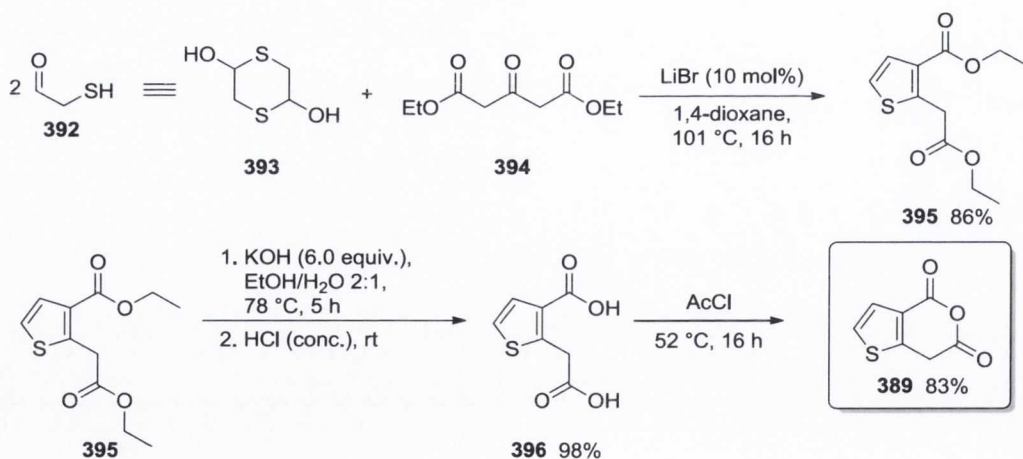
Scheme 5.4 The synthesis of anhydride **395**.

The product **395** was, upon purification on column chromatography on silica gel, hydrolysed with potassium hydroxide in a mixture of EtOH/H$_2$O (2:1) at reflux temperature, followed by protonation with hydrochloric acid to give the relative *bis*-acid

396, which was reacted with acetyl chloride at reflux temperature for 16 hours to furnish the crude anhydride **389** The desired product was then purified by short, rapid column chromatography on silica gel in 83% yield.

5.6.1.2   The synthesis of anhydride 390

Anhydride **390** was produced by reaction between acetyl chloride and the *bis*-acid **399**, which was synthesised according the known literature two step synthetic procedure[304] shown in Scheme 5.5.
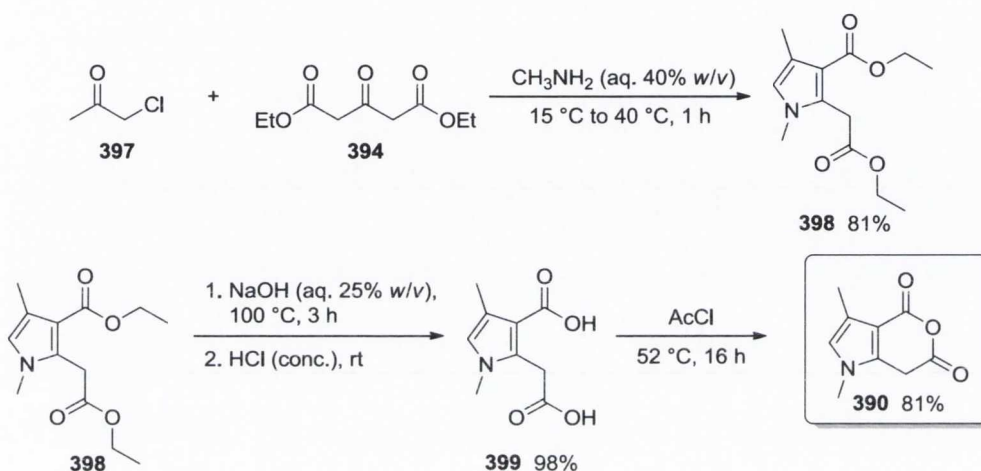
Scheme 5.5   The synthesis of anhydride **390**.

Similar to the pathway for anhydride **389**, the synthesis of **390** began with the formation of the *bis*-ester **398** produced in 81% yield by the reaction between chloroacetone (**397**) and aqueous methylamine at temperature below 40 °C for 1 hour. The *bis*-ester **398** so obtained, upon purification by column chromatography on silica gel, was hydrolysed to the *bis*-acid (**399**) by an aqueous sodium hydroxide solution at reflux temperature for 3 h, with subsequent protonation with hydrochloric acid. The obtained residue was then reacted with acetyl chloride at 52 °C for 16 hours, to furnish **390** which was purified by short, rapid column chromatography on silica gel in 80% yield.

5.6.1.3   The synthesis of anhydride 391

Anhydride **391** was synthesised *via* the three step synthetic pathway described in Scheme 5.6.
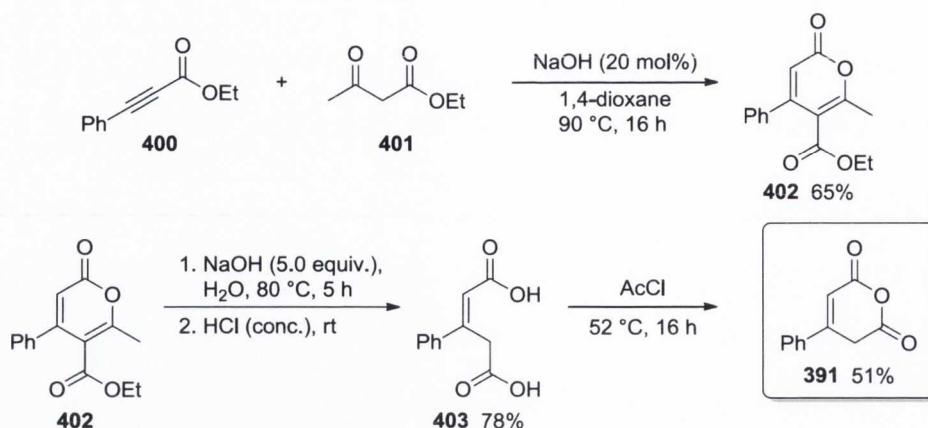
Scheme 5.6   The synthesis of anhydride **391**.

The synthesis of anhydride **391** began with the modified known reaction[305] between ethyl phenylpropiolate (**400**) and ethyl acetoacetate (**401**) promoted by a catalytic amount of sodium hydroxide in 1,4-dioxane at 90 °C for 16 hours to form the lactone **402** intermediate in moderate yield. This molecule, after purification by column chromatography on silica gel, was hydrolysed with sodium hydroxide in water at 80 °C and protonated by hydrochloric acid to the corresponding *bis*-acid **403**. This was then cyclised to form anhydride **391** by reaction at 52 °C with acetyl chloride for 16 hours. Also in this case, the desired product **391** was isolated and purified by short, rapid column chromatography on silica gel, however in moderate yield. The moderate yields obtained in the formation of products **403** and **391** are believed to be a consequence of a decarboxylative side-reaction that takes place at high temperature during the hydrolysis of **402** and during the cyclisation of **403**.

5.6.1.4   The synthesis of anhydride 238

Anhydride **238** was synthesised by reaction of the *bis*-acid **405**, synthesised according the slightly modified known literature two step synthetic procedure,[190] with acetyl chloride (Scheme 5.7).
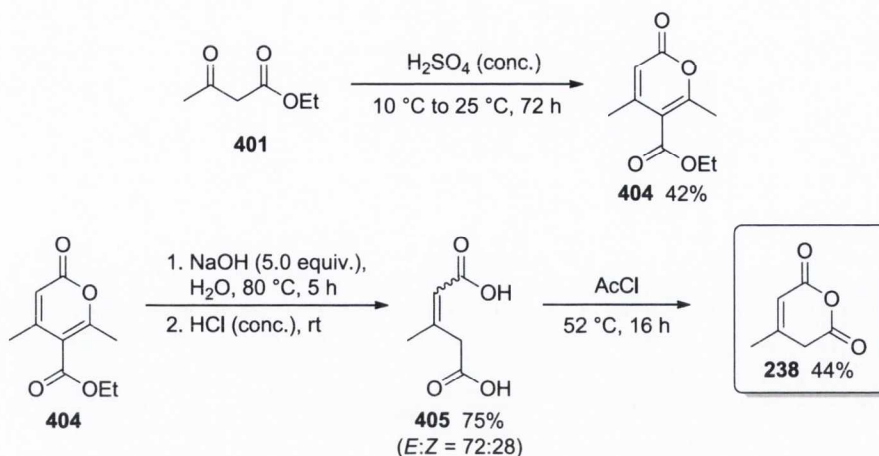
Scheme 5.7   The synthesis of anhydride **238**.

The synthesis of anhydride **238** is similar to that of **391**. It began with the formation of the lactone intermediate **404** by reaction of ethyl acetoacetate with concentrated sulfuric acid for three days, however in low yield. The product **404** so obtained was then purified by chromatography on silica gel and subsequently hydrolysed with sodium hydroxide in water at 80 °C for 5 h and protonated by an hydrochloric acid to form a mixture (*E:Z* = 72:28) of product **405** that was not separated. Reaction of this mixture with acetyl chloride at 52 °C for 16 hours furnished anhydride **238**, which was purified by short, rapid column chromatography on silica gel. Also in this case, it is also believed that a side decarboxylative process is responsible for the low to moderate yields observed in the formation of **405** and **238**.

5.6.1.5   The synthesis of anhydride 232

Anhydride **232** was synthesised according to the seven step synthetic pathway described in Scheme 5.5. The *bis*-acid **414** precursor was synthesised according the known literature procedure.[177]
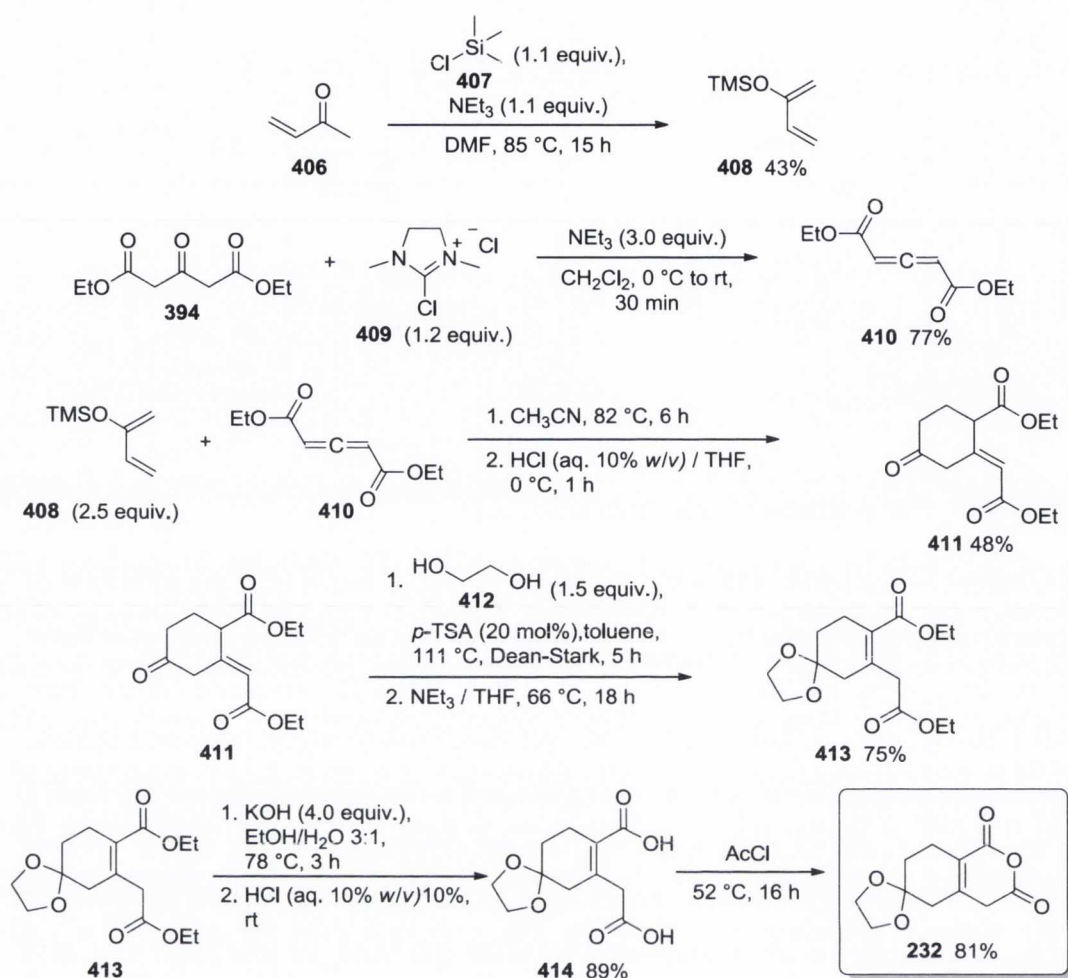
Scheme 5.8   Synthetic pathway for the synthesis of anhydride **232**.

The first step of the synthesis was the formation of products **408** and **410** that would later be coupled together to form the 'skeleton' of anhydride precursor **411**. Product **408** was synthesised according the known literature procedure[306] by trapping the enol tautomer of methyl vinyl ketone (**406**) by reaction with trimethylsilyl chloride (**407**) in presence of triethylamine at 85 °C in dimethylformamide (DMF) for 15 hours according to the reported procedure.[306] The product was then purified by fractional distillation under vacuum in 43% yield. The allene product **410** was synthesised following the known literature procedure[307,308] involving the reaction between diethyl 1,3-acetonedicarboxylate (**394**) and the commercially available 2-chloro-1,3-dimethylimidazolinium chloride (DMC, **409**) in the presence of triethylamine in dichloromethane at 0 °C for 30 minutes, and then purified by chromatography on silica gel in good yield.

At this point compounds **408** and **410** were allowed to react together in a Diels-Alder reaction in acetonitrile at reflux temperature for 6 hours according the known procedure.[177] The residue obtained was separated and directly treated with a 10% hydrochloric acid solution at 0 °C for 1 hour, in order to cleave the silyl protecting group and lead to the formation of **411** that was purified by chromatography on silica gel in 48% yield. The substituted cyclohexanone obtained (*i.e.* **411**) was then reacted in a Dean-Stark apparatus with ethylene glycol (**412**) and a catalytic amount of *p*-toluenesulfonic acid in toluene for 5 hours. Next, the residue was treated with triethylamine in THF at 66 °C for 16 hours in order to isomerise the double bond to the most stable isomer, leading to the formation of **413**, which was purified by chromatography on silica gel in 75%. Hydrolysis with potassium hydroxide in EtOH/H_2O (3:1) at reflux temperature and subsequent protonation with a 10% hydrochloric acid solution gave the *bis*-acid **414** in 89% yield. This was reacted with acetyl chloride at 52 °C for 18 hours to furnished anhydride **232**. The desired product was then purified by short, rapid column chromatography on silica gel in good yield.
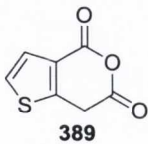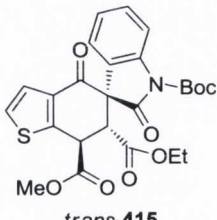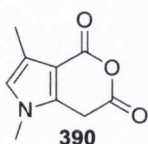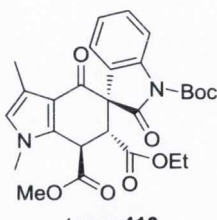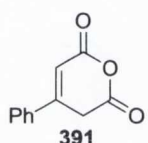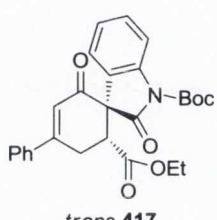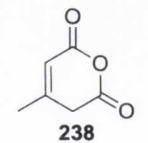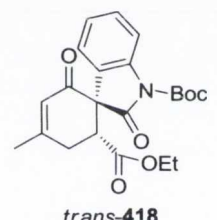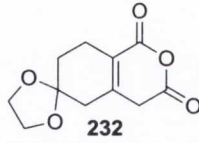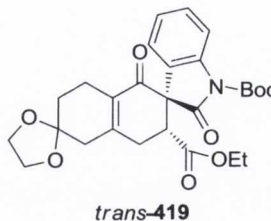
5.7 Evaluation of the substrate scope: the anhydride

Now in possession of a number of different anhydride substrates and of the optimum conditions for the reaction, the evaluation of these new substrates in the reaction with **378** promoted by a catalytic presence of **348** was the next step in the study. In this case we decided to evaluate the reactions at a temperature of 30 °C (Table 5.5). The diastereomeric mixtures of the products formed, after *in situ* esterification and analysis of the *dr* by CSP-HPLC, were separated (in each case) by an automated flash chromatographic purification system (*i.e.* Biotage SP4) to give the isolated yield of the major diastereomer reported in Table 5.5.

The reactions depicted in entries 1-4 have been reported only for descriptive purposes to show the isolated yields, as they have already been reported in Table 5.3 (for entries 1 and 2) and in Table 5.4 (for entries 3 and 4). The *dr* for the products reported in entry 1 and entry 2, have been recalculated considering only two diastereomers (*i.e. trans* and *cis*).

Table 5.5   Evaluation of different anhydrides in the reaction with **378** promoted by **348** (Table continues on the following page).

entry	anhydride	temp (°C)	product (major diastereomer)	time (h)	conv. (%)^a	dr (trans:cis)^b	ee (%)^c	yield (%)^d
1	**147**	30	*trans*-**386**	19	>98	96:4	95	92
2^e	**147**	-30	*cis*-**386**	69	>98	22:78	98	74
3	**312**	30	*trans*-**387**	30	>98	>98:2^f	92	95
4^e	**312**	-30	*cis*-**387**	6d	>98	22:78^f	92	73

5	**389**	30	*trans*-**415**	21	>98	95:5	>99	91
6	**390**	30	*trans*-**416**	22	>98	>99:1	96	95
7	**391**	30	*trans*-**417**	19	>98	>99:1	>99	94
8	**238**	30	*trans*-**418**	21	>98	>99:1	>99	95
9	**232**	30	*trans*-**419**	26	>95	n.d.	99	82

a Conversion of both reagents determined by ¹H NMR spectroscopic analysis. *b* Diastereomeric ratio of the two major diastereomers determined by CSP-HPLC. *c* Enantiomeric excess of the major diastereomer determined by CSP-HPLC. *d* Isolated yield of the major diastereomer. *e* Esterification process performed at the same temperature of the reaction. *f* Diastereomeric ratio of the two major diastereomers determined by ¹H NMR spectroscopic analysis.

The reactions involving the newly synthesised anhydrides all proceeded smoothly in a relatively short reaction time, producing the *trans*-isomers in nearly quantitative conversions and high yields.

143

The use of heteroaromatic fused anhydrides such as **389** and **390** (entries 5 and 6) resulted in the formation of the expected products (*i.e.* **415** and **416**) in almost 100% optical purity for *trans*-**415** and with almost total diastereocontrol in the formation of *trans*-**416**.

When anhydrides **391**, **238** and **232** all with the structural core of glutaconic anhydride (**244**) in common, were evaluated in the reaction (entries 7, 8 and 9), the products formed were not those expected. This was initially suspected when a lack of nitrogen gas formation was noticed during the esterification process with TMSCHN$_2$ suggesting the absence of the carboxylic acid substituent. Further NMR spectroscopic analysis of the structures obtained supported this initial hypothesis confirming that a decarboxylation process takes place after the formation (but prior to the *in situ* esterification) of all the products generated from substrates (*i.e.* **391**, **238** and **232**) derived from glutaconic anhydride (**244**). This process is most likely a consequence of a vinylogous decarboxylation that substrates with a similar structure undergo. For example, it is known that the Hagemann's ester (**420**),[309] which is widely used in natural product synthesis, readily undergoes spontaneous decarboxylation on hydrolysis to give the relative cyclohexenone **421** (Scheme 5.9).[310]
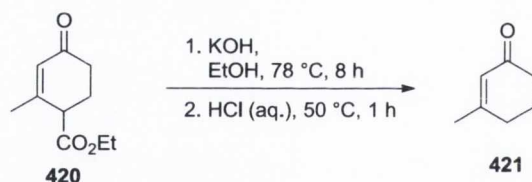
Scheme 5.9   Decarboxylation of Hagemann's ester (**420**).

This decarboxylation process resulted in the formation of products **417-419** with excellent enantio- and diastereocontrol (entries 7-9) and in high yields. However, the reported *dr* are related to different diastereomers compared to the those obtained for the other products (entries 1-6). In the latter situation they refer to the two major diastereomers (*i.e.* A and B, Sections 5.4 and 5.5) which are differentiated only by the relative stereochemistry between the two tertiary stereocentres in position C-3' and C-4', while the third diastereoisomer (*i.e.* C) is not reported as it was formed only in trace amounts.

In the former case (*i.e.* formation of products **417-419**), as a consequence of the decarboxylative process, due to the absence of the substituent at C-4' position, the *dr* reported refer to the decarboxylated products from diastereomers (A) and (B) which differ only in the stereochemistry between the stereocentre at C-3' and the quaternary stereocentre at C-2' position. For example, considering the results obtained in the reaction involving anhydride **391** (entry 7), the expected products of the reaction (in absence of a decarboxylative process) would have been diastereomers (A) and (B) as depicted in Scheme 5.10. The *dr* of this hypothetical reaction would have been the ratio between (A) and (B).
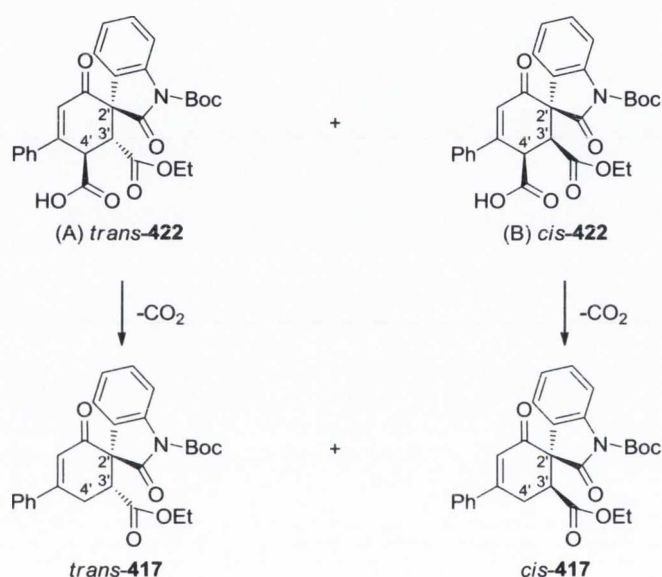
Scheme 5.10 Clarification of the diastereomeric ratio in the products involving substituted glutaconic anhydrides.

However, upon decarboxylation of the diastereomeric mixture (*i.e.* A, B) of product **422**, the two diastereomers formed are *trans*-**417**, generated from the decarboxylation of (A), and *cis*-**417** generated from the decarboxylation of (B). This explanation also applies to the reactions involving anhydrides **238** and **232** (entries 8 and 9) that readily produced *trans*-**418** and *trans*-**419** respectively in high diastereocontrol and high isolated yields. The enantioselectivity is noteworthy for all processes involving substituted glutaconic anhydrides (entries 7-9), as all reached values approaching to optical purity.

5.8   The assignment of the absolute stereochemistry of product 417

In order to confirm the absolute stereochemistry attributed to the structures produced from anhydrides **391**, **238** and **232** (entries 7-9, Table 5.5) and of the occurrence of the decarboxylation process, a recrystallised sample of *trans*-**417** was analysed by X-ray crystallography. The results revealed that all the assumptions made in the explanation of the process involving such anhydrides were correct, and allowed the assignment of the absolute stereochemistry of *trans*-**417** (2'*R*,3'*R*), as depicted in Figure 5.5.
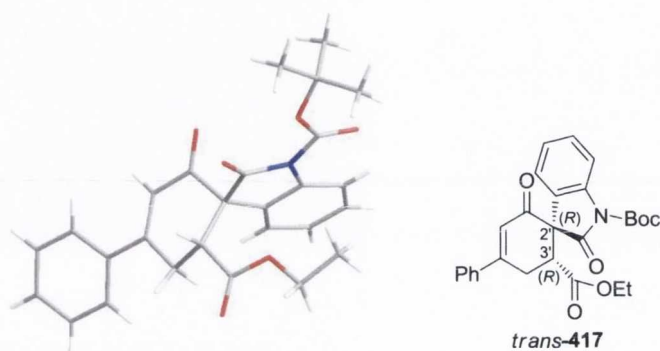
Figure 5.5   Absolute stereochemical assignment of product *trans*-**417**.

By analogy, the two further products (*i.e.* *trans*-**418** and *trans*-**419**) formed using substituted glutaconic anhydrides were assigned with the same absolute configuration, as depicted in Figure 5.6.
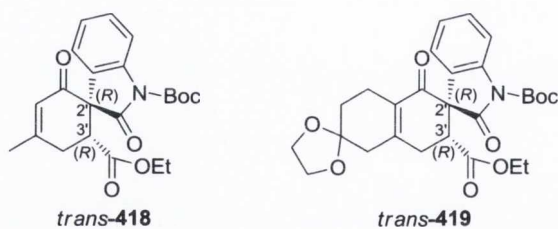
Figure 5.6   Absolute stereochemical assignment of products *trans*-**418** and *trans*-**419**.

The absolute stereochemical configuration of products *trans*-**415** and *trans*-**416,** derived from anhydrides **389** and **390**, respectively, was assigned as shown in Figure 5.7, by analogy with that obtained for *trans*-**387** by X-ray analysis (Section 5.5).
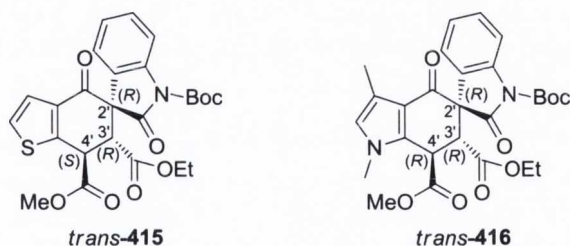
Figure 5.7   Absolute stereochemical assignment of products *trans*-**415** and *trans*-**416**.

It can be seen that the Cahn-Ingold-Prelog assignment of the chiral centre at C-4' of *trans*-**415** has been inverted (compared to the other products formed) without modifying the three-dimensional geometry of the substituents of that carbon. This, as discussed for *trans*-**334** (Section 3.6), is due to the different priorities that the substituents of that carbon are given according to the CIP rules.

5.9   Substrate scope: the alkylidene-2-oxindole

After the evaluation of different anhydrides with expansion of the substrate scope that proved the extreme efficiency and generality of the process, we decided to attempt further scope expansion by evaluating a different alkylidene-2-oxindole in the reaction with selected anhydrides.

We believed that either modification of the substituent on the nitrogen atom of **378** or installation of a substituent on the aromatic ring of **378** would not be of interest in this study, as the modifications introduced would be too far from the reactive centre of the molecule, and thus their influence on the reactivity of the substrate would be minimal. We therefore decided to change the substituent on the terminal double bond of the alkylidene-2-oxindole and evaluate the effect that this modification would have on both the reactivity of the substrate and on the stereochemical outcome of the reaction.

5.9.1   The synthesis of oxindole 423

The structure chosen to expand the substrate scope of the reaction was **423** (Scheme 5.11). The synthesis of the oxindole **423**, similarly to the analogue **378**, began with formation of the phosphonium salt **425** in 93% yield by reaction between benzyl bromide (**424**) and triphenylphosphine (**381**) in toluene at reflux temperature for 15 hours according to the known procedure (slightly modified in our hands).[311]
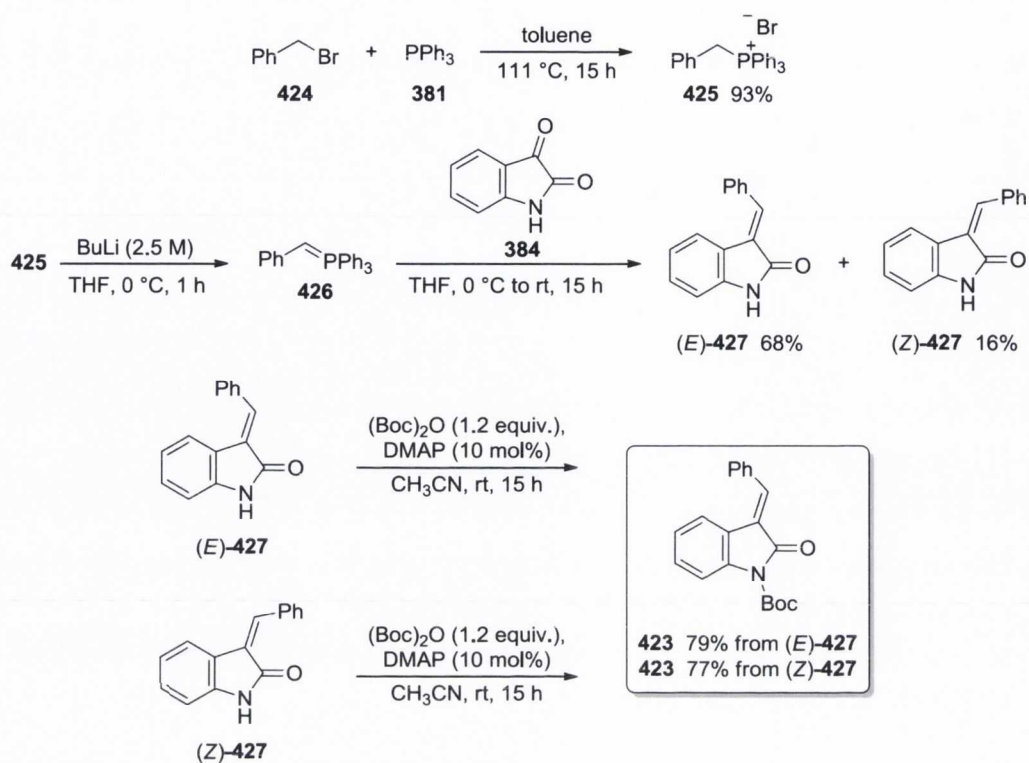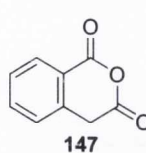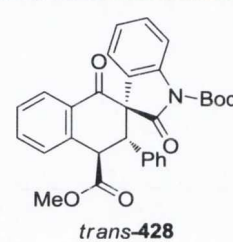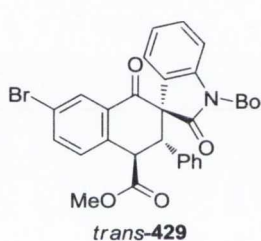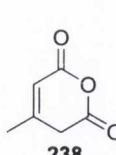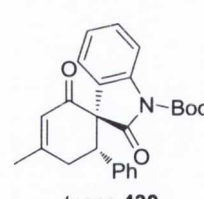
Scheme 5.11 Synthesis of the oxindole **423**.

The salt obtained, once isolated, was allowed to react with a solution of butyl lithium in THF at 0 °C for 1 h to form ylide **426**, which was reacted *in situ* with isatin (**384**) in THF from 0 °C to 15 °C in 15 h.[311] The reaction led to the formation of a mixture of (*E*) and (*Z*) isomers (81:19) of product **427** in 84% combined yield that were separated by column chromatography on silica gel. The two isomers of product **427** were then separately allowed to react with di-*t*-butyl dicarbonate ((Boc)₂O) in presence of a catalytic amount of DMAP in acetonitrile at room temperature for 15 h, both furnishing the desired product **423** which was purified by recrystallisation from ethanol in 79% yield from the (*E*)-isomer and 77% yield from the (*Z*)-isomer. Isomerisation of the double bond of (*Z*)-**427** to (*E*)-**427** was promoted by nucleophilic attack of DMAP at the electrophilic end of the α,β-unsaturated amide, allowing the reaction of both isomers of **427** to converge to form only the most stable isomer of product **423**.

5.10 Evaluation of 423 as substrate

The new oxindole **423** obtained was then allowed to react with anhydride **147**, **312** and **238**, employing the same methodology adopted for the reaction between oxindole **378** with the other anhydrides (Table 5.6).

Table 5.6 Evaluation of the oxindole **423** in the reaction with anhydride **147**, **312** and **238**.

anhydride + [structure **423**]

1. **348** (5 mol%),
MTBE (0.1 M),
30 °C
→
2. TMSCHN$_2$ (1.2 equiv.),
MeOH (75.0 equiv.),
30 °C, 30 min
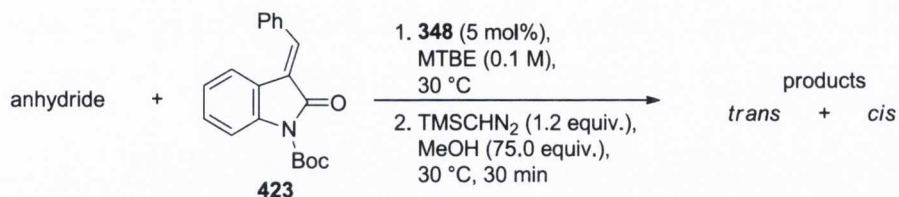
products
trans + *cis*

entry	anhydride	product (major diastereomer)	time (h)	conv. (%)^a	dr (trans:cis)^b	ee (%)^c	yield (%)^d
1	**147**	*trans*-**428**	20	>98	>99:1	89	96
2	**312**	*trans*-**429**	20	>98	>99:1	89	98
3	**238**	*trans*-**430**	20	88	n.d.	>99	65

^{a} Conversion of both reagents determined by ^{1}H NMR spectroscopic analysis. ^{b} Diastereomeric ratio of the two major diastereomers determined by CSP-HPLC. ^{c} Enantiomeric excess of the major diastereomer determined by CSP-HPLC. ^{d} Isolated yield of the major diastereomer.

The reactions shown in Table 5.6 all readily produced the desired products in relatively short reaction times with almost full conversion. The use of homophthalic and bromo-substituted homophthalic anhydride (*i.e.* **147** and **312** respectively) allowed the formation of products **428** and **429** in extremely high diastereoselectivity and with high enantioselectivity (entries 1 and 2). The use of the methyl-substituted glutaconic anhydride **238** (entry 3), however, resulted in a slightly lower conversion compared to the aromatic anhydrides **147** and **312**, producing product **430** in only 88% conversion. This is most likely as a result of the lower electrophilic character of the oxindole **423**

compared to the previously evaluated oxindole **378**. Despite this, product **430**, derived from a decarboxylative process of the expected ester product as in the reactions involving **378** with substituted glutaconic anhydrides described in Table 5.5 (entries 7, 8 and 9), was formed in high diastereoselectivity and with almost optical purity.

5.11 The assignment of the absolute stereochemistry of product 429

A recrystallised sample of product *trans*-**429** was then analysed by X-ray crystallography and assigned (2'*R*,3'*S*,4'*R*) as shown in Figure 5.8.
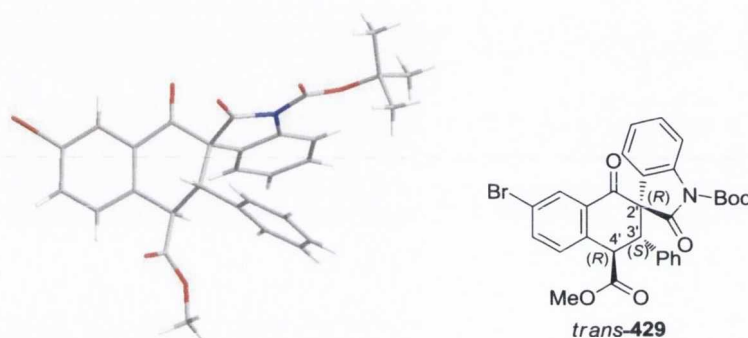
Figure 5.8   Absolute stereochemical assignment of product *trans*-**429**.

By analogy, products *trans*-**428** and *trans*-**430** were assigned with the same stereochemistry as depicted in Figure 5.9
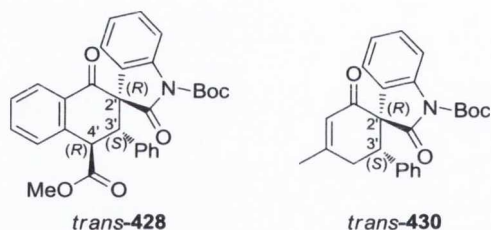
Figure 5.9   Absolute stereochemical assignment of products *trans*-**428** and *trans*-**430**.

Comparison of the absolute stereochemical assignment of products *trans*-**387** and *trans*-**429**, derived from the two oxindoles evaluated in the study (*i.e.* **378** and **423**) and bromo-substituted anhydride **312**, reveals that they present the same three-dimensional geometry of the substituents of the three chiral centres (Figure 5.10).
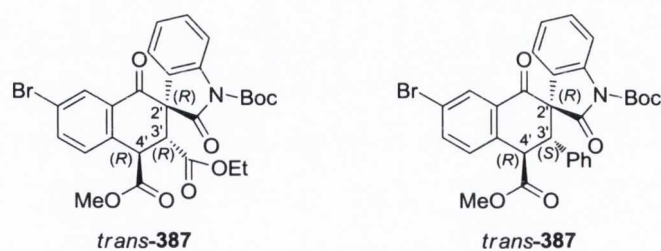
Figure 5.10   Absolute stereochemical comparison between products *trans*-**387** and *trans*-**429**.

However, it can be seen that the stereochemical assignment of the carbon C-3' of the two molecules is inverted. This is again due to the difference in the priority of the carbon substituents according to the CIP rules.

5.12 Rationale for the reaction stereochemical outcome

Based on the rationale proposed for the stereochemical outcome of the reaction involving homophthalic anhydride (**147**) and benzaldehyde (**52**), where the binding of the electrophile species by the squaramide unit stabilised the forming negative charge in the pre-transition state of the reaction (Section 2.6), a similar model was proposed to explain the stereochemical outcome of the reactions involving anhydrides and alkyliden-2-oxindoles. However, in this proposed pre-transition state a certain degree of steric clash between the catalyst and the large ester substituents of the oxindole moieties was always encountered, even when several different binding modes were evaluated. Due to this level of uncertainty of the correct binding mode, the model proposed is not reported here.

5.13 Conclusion

This work has demonstrated the further expansion of the cycloaddition reaction between anhydrides and electrophiles. Both cyclic anhydrides bearing (hetero)aromatic fused rings, and substituted glutaconic anhydrides have been shown to readily react as pronucleophiles with two different electrophilic alkylidene-oxindoles in a reaction catalysed by a novel organocatalyst. The highly functionalised annulated structures generated bear up to three stereocentres, one of which is spiro and are generally formed in extremely high diastereo- and enantioselectivity and in high isolated yields. The absolute stereochemistry of all the structures was assigned either by analogy or direct X-ray crystallography of recrystallised samples with supporting evidence from ^{1}H NMR

spectroscopic analysis. The products synthesised belong to the family of spirooxindoles, a core structure found in many natural compounds with biological activity and are an important area of research in organocatalysis. It was found that when the reaction was performed at temperatures below 0 °C, formation of the *cis* diastereomer (over the more commonly formed *trans*) took place, allowing the selective formation of one of the two major diastereomers of the reaction simply by changing the operative temperature. Furthermore, when the reaction was carried out employing substituted glutaconic anhydrides, the expected acid products went through a decarboxylative process for which an explanation has been given.

6. Intermolecular thiolate-catalysed crossed Tishchenko reaction

6.1   Preamble

As discussed in Section 1.6, the Tishchenko reaction is the catalytic disproportionation of two aldehyde molecules to furnish an ester product. Despite the outstanding number of catalysts available to promote such reaction, the process is generally limited to the homo-coupling of the same aldehyde and no intermolecular aldehyde-ketone process were reported in literature, making the challenge of promoting such a process extremely synthetically interesting.

In 2010, Connon *et al.*, encouraged to attempt the development of an alternative catalyst system for the intermolecular homo-Tishchenko reaction, found that thiols (thiolates) could be employed as efficient reaction promoters.[312] Inspired by the mode of action of the glycolytic enzyme glyceraldehyde-3-phospate dehydrogenase (G3PDHase) the group postulated an artificial process capable of emulating the enzyme's natural mechanism of action.

The G3PDHase promotes aldehyde oxidation *via* a base-catalysed addition of a cysteine residue to the aldehyde substrate to give the corresponding hemithioacetal conjugate base **431** (Scheme 6.1).
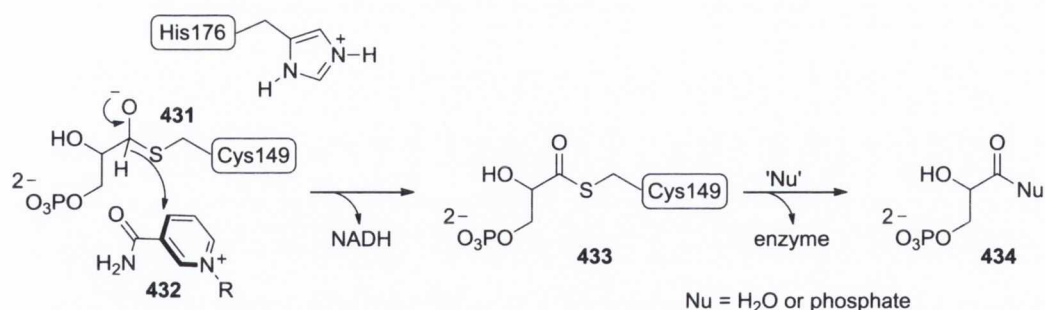
Scheme 6.1   Aldehyde oxidation catalysed by G3PDHase.

This intermediate then participates in an intermolecular hydride-transfer reaction with enzyme-bound NAD$^+$ **432**, generating the electrophilic thioester **433** that then undergoes either hydrolysis or substitution by inorganic phosphate to form **434**, depending on the enzyme variety.[313–315]

Based on the above mechanism, Connon and co-workers postulated that an analogous hemithioacetal anion **436** could be generated by reacting benzaldehyde (**52**) with catalytic amounts of bromomagnesium thiolate (**435**), formed by the *in situ* reaction between a Grignard reagent (*i.e.* phenylmagnesium bromide) and an opportune thiol. This anionic intermediate **436** could then transfer a hydride to another carbonyl moiety to give the magnesium alkoxide **437** and the thioester **438**, which would subsequently couple to form the ester product **439** with regeneration of the thiolate catalyst (Scheme 6.2).[312]
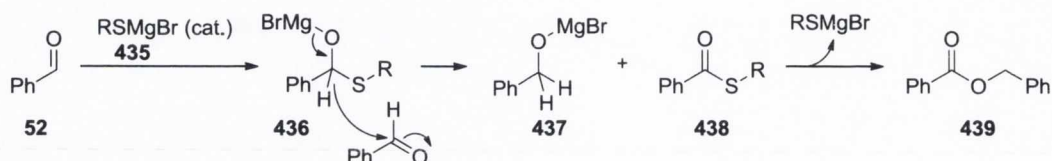
Scheme 6.2   The proposed bio-inspired catalytic Tishchenko reaction by thiolate catalysis.

It was proposed that the hydride transfer step takes place through the six-membered ring pre-transition state assembly **440** depicted in Scheme 6.3.
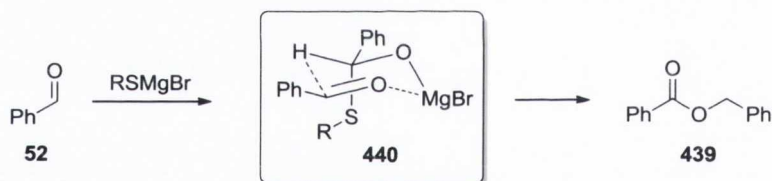
Scheme 6.3   The proposed pre-transition state assembly for the thiolate-catalysed Tishchenko reaction.

Dr. Linda Cronin studied the above mention process, and having discovered the ideal catalyst (*i.e.* **442**) and optimised operative conditions, was able to promote the homo-Tishchenko reaction for a number of aldehydes such as **441**, in high yields and in convenient reaction times (Scheme 6.4).[312]
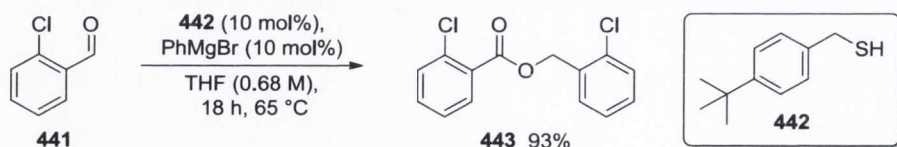
Scheme 6.4   Thiolate-catalysed homo-Tishchenko reaction of aldehyde **441**.

154

In view of the excellent results obtained, the group was next interested in employing this strategy towards the development of an intermolecular aldehyde-ketone Tishchenko coupling process. Such a reaction however, presented two major difficulties associated with the 'nature' of the ketone itself that had to be addressed prior the development of the study.

The first problem arose from the inherent lack of reactivity of ketones relative to aldehydes, meaning that aldehyde dimerisation was likely to be the favoured pathway; the second problem was recognised in studies conducted by the author (prior to the postgraduate studies here reported) on the intramolecular variant of such a process. Due to the basicity of the catalyst used and with the hydride-transfer step likely to be slower in cases involving ketone electrophiles, the employment of enolisable ketones in the reaction was not possible, as the destructive aldol pathway, that such substrates underwent, could never be fully avoided.

It was therefore decided to employ non-enolisable trifluoromethylketone substrates with the expectation that they would be sufficiently activated to react with the hemithioacetal intermediate preferentially over another aldehyde molecule.
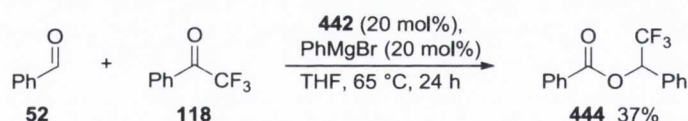
Scheme 6.5 The preliminary Tishchenko reaction between **52** and **118**.

However, the employment of an alternative thiol precatalyst appeared fundamental for the optimisation of the Tishchenko reaction between aldehydes and trifluoromethyl ketones as the use of **442** in the reaction between **52** and **118** (performed by Dr. Linda Cronin) resulted in the formation of **444** in low yields (Scheme 6.5). Deeper analysis of the reaction by ^{1}H NMR spectroscopy revealed the presence of the thioester intermediate **448** (Scheme 6.6), indicating that the coupling process was the rate-limiting step in this reaction as the attack of the alkoxide **447** on **448**, which releases the catalyst and allows turnover, was prohibitively slow resulting in the termination of the catalytic cycle.

For this reason, it was proposed that the use of a more acidic thiol precatalyst would generate a more electrophilic thioester and, if a balance between thiolate nucleophilicity

and thioester electrophilicity could be found, the turnover frequency could be improved without slowing the redox step prohibitively.

Dr. Linda Cronin evaluated several aromatic and aliphatic thiol precatalysts in the reaction between **52** and **118**. The study proved that when the reaction was performed with the use of the aromatic thiol precatalyst **445**, superior reactivity of the corresponding thioester intermediate **446** in the reaction with the nucleophilic intermediate alkoxide **447** (formed by hydride transfer from the aldehyde to the ketone) could be observed. This was rationalised by considering the higher electrophilicity of the thioester **446** (in comparison with **448**), generated when the reaction was performed employing **442** as thiol precatalyst. The substituted thiophenol **445** was found to be the optimum reaction promoter, catalysing the Tishchenko coupling with excellent yield of product **444** under the optimised conditions (Scheme 6.6).
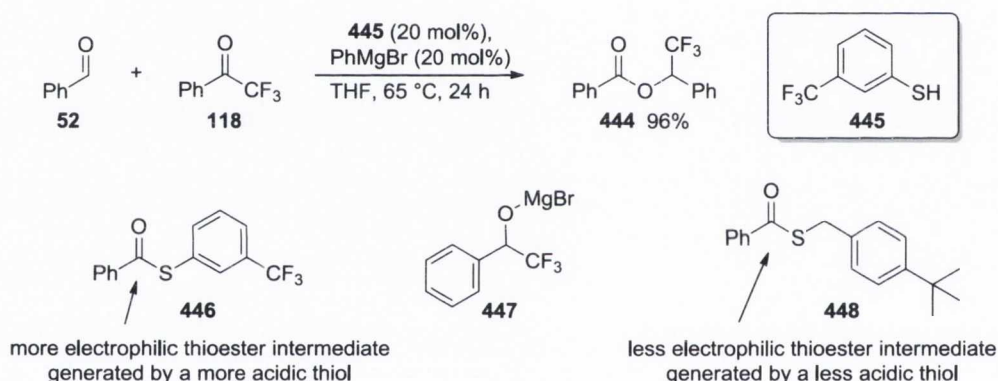
Scheme 6.6   Rationale for the catalyst design for the aldehyde-ketone Tishchenko reaction.

6.2   Evaluation of the substrate scope: the ketone component

Now in possession of the optimum catalyst (*i.e.* **445**) and of the optimised procedure (both developed by Dr. Linda Cronin), the evaluation of the scope of the Tishchenko reaction between benzaldehyde (**52**) and various trifluoromethylketones incorporating various aromatic ring substituents was carried out (Table 6.1). Under the conditions reported, the reactions with benzaldehyde (**52**) and both activated *p*-halo-substituted trifluoromethylketones (*i.e.* 4'-chloro-2,2,2-trifluoroacetophenone (**449**) and 4'-bromo-2,2,2-trifluoroacetophenone (**451**)) readily proceeded to afford the ester products **450** and **452** in high yields; however, with longer reaction times compared to the reaction involving **118** (entries 1 and 2).

156

Table 6.1   Evaluation of the substrate scope for the intermolecular crossed-Tishchenko reaction: the trifluoromethylketone component.
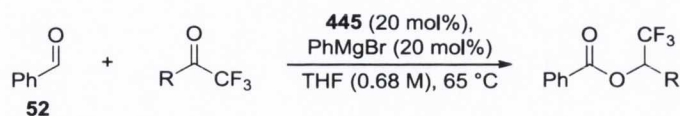
entry	trifluoromethyl ketone	product	time (h)	yield (%)[a]
1	**449**	**450**	30	91
2	**451**	**452**	30	93
3	**453**	**454**	40	94
4	**455**	**456**	40	80
5	**457**	**458**	40	78

[a] Isolated yield after column chromatography on silica gel.

We believed that this was as a consequence of the electron-withdrawing substituent on the aromatic ring of ketones **449** and **451** that reduced the rate of the coupling step between the *p*-halo-benzyl alkoxides and thioester intermediates, due to the relatively lower nucleophilicity of the alkoxides. For the same reason, strongly activated ketones, such as 3'-fluoro-2,2,2-trifluoroacetophenone (**453**) and 3'-trifluoromethyl-2,2,2-trifluoroacetophenone (**455**), required even longer reaction times to produce the ester products **454** and **456** in good yields (entries 3 and 4). The 'deactivated' 2-(trifluoroacetyl)-thiophene (**457**) proved to be a more challenging substrate, undergoing conversion to ester **458** in 78% yield, only after extended reaction times and several reaction condition optimisations (entry 5). This was due to the relatively electron-rich
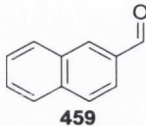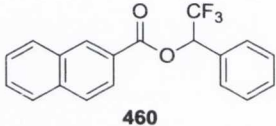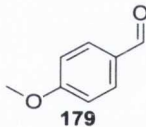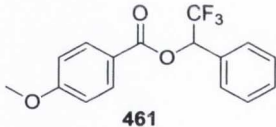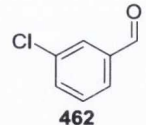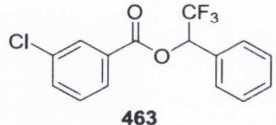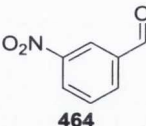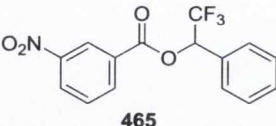
nature of the carbonyl group of ketone **457** which slowed the rate of the hydride transfer process.

6.3 Evaluation of the substrate scope: the aldehyde component

In view of the results obtained in the evaluation of a number of trifluoromethylketones in the reaction with **52**, we decided to extend the scope of this new reaction to include different aldehydes (Table 6.2).

Table 6.2   Evaluation of the substrate scope for the intermolecular crossed-Tishchenko reaction: the aldehyde component.
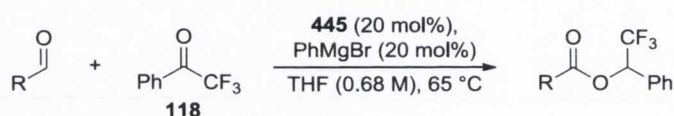
entry	aldehyde	product	time (h)	yield (%)[a]
1	**459**	**460**	24	86
2	**179**	**461**	67	92[b]
3	**462**	**463**	24	87
4	**464**	**465**	24	46[c]

[a] Isolated yield after column chromatography on silica gel. [b] Reaction performed at a concentration of 0.9 M. [c] Average of three experiments, the average yield of the aldehyde-dimerisation product was 22%.

The coupling between **118** and various aromatic substituted aldehydes catalysed by the thiol precatalyst **445** generally proceeded smoothly and with high products yields (Table 6.2). Naphthaldehyde (**459**), *p*-anisaldehyde (**179**) and *m*-chlorobenzaldehyde (**462**) were allowed to react with **118** to furnish the ester products **460**, **461** and **463** in high yields (entries 1-3). However, after optimisation, it was found that an extended reaction

time and higher reaction concentration were both necessary in the reaction involving **179** in order to obtain a satisfactory yield of product **461** (entry 2). This was attributed to the lower electrophilicity of aldehyde **179** due to the electron-donating methoxy substituent present on the ring, which reduced the rate of the initial nucleophilic attack of the thiolate catalyst to the carbonyl functionality of **179**.

The reaction involving the highly electron deficient *m*-nitrobenzaldehyde (**462**) however, was found to deliver generally low yields of product **463**. It was speculated that this was due to competition from the homo-dimerisation pathway of **462**, a process not observed in any of the other reactions, as a result of the extremely high electrophilicity of this aldehyde compared to the others evaluated (entry 4).

During our investigation, we also encountered other problematic substrates which either failed to undergo reaction or were converted in extremely poor yield. These substrates are depicted in Figure 6.1.
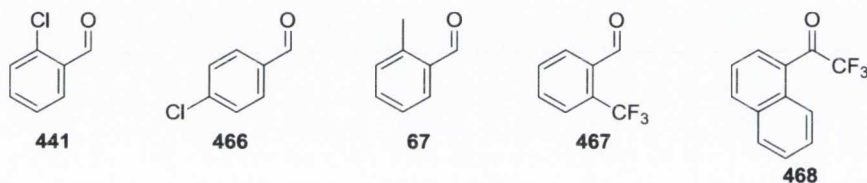
Figure 6.1 Problematic substrates for the thiolate-catalysed crossed Tishchenko reaction.

In the case of substrates **441** and **466** it was speculated that the reaction may have failed due to the competition from a nucleophilic aromatic substitution pathway in presence of the thiolate catalyst. This was confirmed when three different resonance signals for the aldehyde proton in the crude reaction mixture ^{1}H NMR spectra involving these substrates were observed. In the cases involving substrates **67**, **467**, and **468**, it is believed that the reaction did not occur due to prohibitive steric hindrance in proximity to the carbonyl functionality of the substrates involved.

Despite this, the process illustrated above represents (to the best of our knowledge) the first example of an intermolecular thiolate-catalysed aldehyde-ketone Tishchenko reaction in the literature.

6.4   Microwave-assisted intermolecular aldehyde-ketone Tishchenko reaction: preamble

The major drawback associated with the protocol developed for the thiolate-catalysed intermolecular crossed Tishchenko process described in Sections 6.2 and 6.3 was the reaction rate. A number of transformations required prolonged times (up to 4 days for cases involving difficult substrates) at reflux temperature, which marginally reduced the applicability and the utility of the reaction. For that reason, Connon and co-workers embarked on a series of experiments aimed at increasing the reaction rate without resorting to the use of impractical catalyst loadings, by investigating the effect of microwave radiation on the process.[316] Dr. Cornelius O'Connor developed and optimised the process for the homo-coupling reaction of aromatic aldehydes.

6.5   Evaluation of the substrate scope in the microwave-assisted thiolate-catalysed intermolecular aldehyde-ketone Tishchenko reaction

The new protocol obtained was then applied (by the author) to the intermolecular crossed-Tishchenko reaction between aldehydes and trifluoromethyl ketones. Significant rate acceleration was observed on irradiating to a maximum reaction temperature of 110 °C under conditions otherwise identical (except for the concentration) to those described in Sections 6.2 and 6.3. The author, in collaboration with fellow researcher Mr. Simon Curran, expanded the substrate scope of the reaction, evaluating many aldehydes and trifluoromethyl ketones. Only the results obtained by the author (Table 6.3) are reported here.

Treatment of a 1:1 mixture of benzaldehyde (**52**) and ketone **451** in THF at 110 °C under microwave irradiation in the presence of the precatalyst **445** (20 mol%) and phenylmagnesium bromide (20 mol%) resulted in the formation of the coupled product **452** in high yield after only 3 hours (entry 1). The reaction proceeded chemoselectively, as ^{1}H NMR spectroscopic analysis did not detect any homo-Tishchenko product (*i.e.* **439**) in the crude reaction mixture.

Electron-neutral aromatic aldehydes such as **459** also participated in the process with **449** furnishing **469** in good yield in three hours (entry 2). The highly hindered mesitaldehyde (**470**) however, appears to be beyond the scope of this methodology,

failing to produce **471** under the reported conditions, even in presence of 2.0 equivalent of the aldehyde substrate (entry 3).

Table 6.3   Substrate scope for the microwave-assisted intermolecular crossed-Tishchenko reactions.

$$R^1\text{-CHO} + R^2\text{-CO-CF}_3 \xrightarrow[\substack{\text{THF (1.2 M),}\\ \text{MW irradiation, 110 °C}}]{\substack{\textbf{445} \text{ (20 mol\%),}\\ \text{PhMgBr (20 mol\%)}}} R^1\text{-CO-O-CH(CF}_3)\text{-}R^2$$
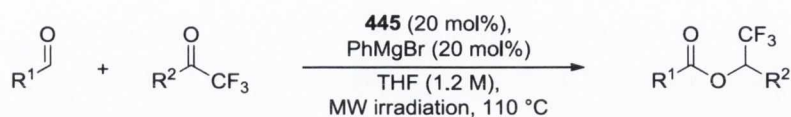
products:
469 R^1 = naphthyl, R^2 = 4-Cl-C$_6$H$_4$
471 R^1 = mesityl, R^2 = 4-Cl-C$_6$H$_4$
472 R^1 = 3-Cl-C$_6$H$_4$, R^2 = 4-Cl-C$_6$H$_4$
474 R^1 = 4-F-C$_6$H$_4$, R^2 = 4-Cl-C$_6$H$_4$
475 R^1 = 3-Cl-C$_6$H$_4$, R^2 = thienyl

476 R^1 = 2-CF$_3$-C$_6$H$_4$, R^2 = 4-Cl-C$_6$H$_4$
478 R^1 = 2-Br-5-MeO-C$_6$H$_3$, R^2 = 4-Cl-C$_6$H$_4$
479 R^1 = 4-MeO-C$_6$H$_4$, R^2 = 4-Cl-C$_6$H$_4$
481 R^1 = 2-pyridinyl, R^2 = 4-Cl-C$_6$H$_4$
267 R^1 = cyclohexyl, R^2 = Ph
482 R^1 = cyclohexyl, R^2 = 4-Cl-C$_6$H$_4$

entry	aldehyde	trifluoromethyl ketone	product	time (h)	yield (%)[a]
1	**52** R^1 = Phenyl	**451** R^2 = 4-Br-C$_6$H$_4$	**452**	3	81
2	**459** R^1 = naphthyl	**449** R^2 = 4-Cl-C$_6$H$_4$	**469**	3	68
3	**470** R^1 = mesityl	**449** R^2 = 4-Cl-C$_6$H$_4$	**471**	3	0[d]
4	**462** R^1 = 3-Cl-C$_6$H$_4$	**118** R^2 = Phenyl	**463**	2	73
5	**462** R^1 = 3-Cl-C$_6$H$_4$	**449** R^2 = 4-Cl-C$_6$H$_4$	**472**	3	83
6	**473** R^1 = 4-F-C$_6$H$_4$	**449** R^2 = 4-Cl-C$_6$H$_4$	**474**	3	76
7	**462** R^1 = 3-Cl-C$_6$H$_4$	**457** R^2 = thienyl	**475**	3	12[b]
8	**467** R^1 = 2-CF$_3$-C$_6$H$_4$	**449** R^2 = 4-Cl-C$_6$H$_4$	**476**	3	3[b]
9	**477** R^1 = 2-Br-5-MeO-C$_6$H$_3$	**449** R^2 = 4-Cl-C$_6$H$_4$	**478**	3	20[b]
10	**179** R^1 = 4-MeO-C$_6$H$_4$	**449** R^2 = 4-Cl-C$_6$H$_4$	**479**	3	34[b]
11	**480** R^1 = 2-pyridinyl	**449** R^2 = 4-Cl-C$_6$H$_4$	**481**	3	0
12	**265** R^1 = cyclohexyl	**118** R^2 = Phenyl	**267**	3	56[c]
13	**265** R^1 = cyclohexyl	**449** R^2 = 4-Cl-C$_6$H$_4$	**482**	3	58[b,d]

[a] Isolated yield after column chromatography on silica gel. [b] Product not isolated, yield determined by ^{1}H NMR spectroscopic analysis using (*E*)-stilbene as an internal standard. [c] Reaction performed using 2.0 equiv. of ketone. [d] Reaction performed using 2.0 equiv. of aldehyde.

Smooth coupling was observed in the cases involving the halo-substituted aldehyde **462** in the reactions with ketones **118** and **449**, and aldehyde **473** in the reaction with **118**, furnishing the ester products **463**, **472** and **474** in less than two or three hour reaction times (entries 4-6).

However, the coupling between **462** and **457** (entry 7) and that of **467** and **449** (entry 8) furnished the ester products **475** and **476** in poor yields as a result of low reactivity of the ketone in the former reaction and to the steric hindrance of the aldehyde in the latter reaction.

Deactivated aldehydes such as **477** and **179** were also evaluated as substrates in this process, however generating the products **478** and **479** in low yields (entries 9 and 10). In the case involving aldehyde **477**, it is believed that the reaction was impeded not only by the deactivating effect of the electron-donating substituent, but also by the steric hindrance caused by the large bromine atom in the α position to the carbonyl.

We were then interested in extending the protocol to heterocyclic aldehydes: and attempt the reaction between aldehyde **480** and **449** under the same conditions previously employed. Unfortunately, this reaction was unsuccessful, as no formation of the ester product **481** was detected (entry 11).

Of particular interest was the coupling between the aliphatic aldehyde **265** with both **118** and **449** to give the ester products **267** and **482** in moderate yields (entries 12 and 13). These reactions were complicated by competing deleterious thiolate-catalysed aldol pathways; however, after intensive investigation we found that in the presence of a modest excess of the ketone **118** (entry 12), and of the aldehyde **265** (entry 13), a substantial yield of the ester products **267** and **482** could be obtained, leading to the first example of such a coupling between these substrate classes.

6.6   Evaluation of imines as electrophiles in the crossed-Tishchenko reaction with aldehydes

After the results obtained in the Tishchenko reaction between aldehydes and trifluoromethyl ketone described above, we were eager to further extend the substrate scope of the process. We therefore decided to investigate if imines could take part as the electrophilic species in the thiolate-catalysed crossed-Tishchenko reaction.

The study began with the synthesis of the imine **483**, derived from benzaldehyde (**52**) and benzylamine by condensation of these two molecules in dichloromethane in presence of magnesium sulfate as a dehydrating agent. The product **483** so obtained, was then allowed to react with **52** in THF in presence of the thiol precatalyst **445** and phenylmagnesium bromide for 24 h, under the same conditions employed for the reaction involving trifluoromethyl ketones (Scheme 6.7).
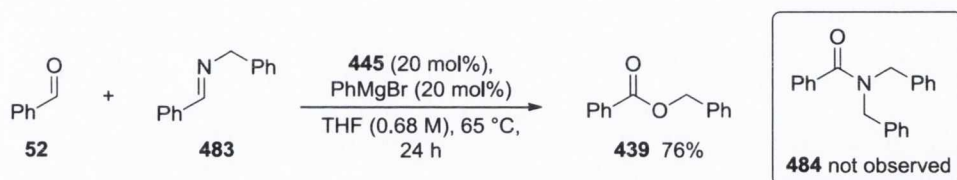
Scheme 6.7   Thiolate-catalysed intermolecular aldehyde-imine Tishchenko reaction.

However, only the formation of the homo-Tishchenko product **439** in 76% yield was observed by ¹H NMR spectroscopic analysis of the reaction mixture, while none of the expected reaction product **484** was formed, and the starting imine **483** was still present in almost quantitative amounts. We suggested two plausible causes for the failure of this reaction. Firstly, the insufficient electrophilicity of the imine would lead to aldehyde self-coupling; secondly, we believed that using imines as electrophiles, the consequent six-membered cyclic pre-transition state assembly (**485**, Figure 6.2), fundamental for the hydride step, may be less energetically favoured than the one involving two aldehydes (*i.e.* **440**). This can be rationalised by considering the higher affinity of the magnesium for the oxygen atom compared to its affinity for a nitrogen atom, leading to a homo-coupling pathway and no coupling between benzaldehyde and imine (Figure 6.2).
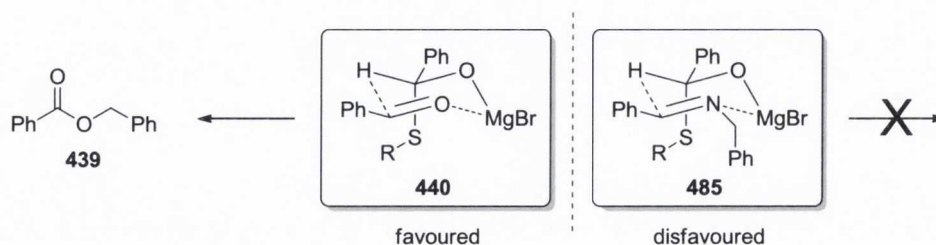
Figure 6.2   The six-membered cyclic pre-transition state assembly for the hydride transfer step.

In order to overcome these problems, we decided to synthesise and employ imines **486-488** which bear strong electron-withdrawing substituents, thus making the imine more electrophilic (Figure 6.3). We also synthesised oxygen-containing imines (*i.e.* **489** and **490**) with the expectation of making them capable of coordinating to the magnesium cation, thereby facilitating the formation of the cyclic transition state necessary for the hydride transfer (Figure 6.3).
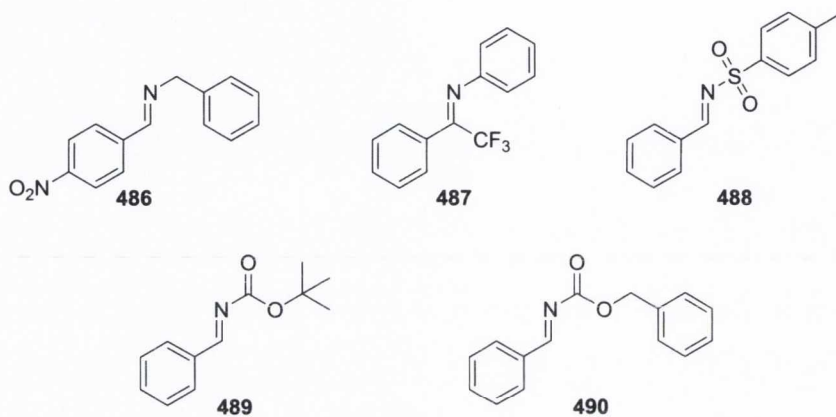
Figure 6.3   Imines evaluated in the crossed-Tishchenko reaction with **52**.

Despite intensive efforts, the use of imines **486-490** in the reaction with **52** under the 'standard' conditions failed to produce the desired products. In each case the reaction generally furnished the aldehyde homo-coupling product (*i.e.* **439**) in variable yields, while use of imines **489** and **490** afforded, in addition to **439**, unidentifiable side-reaction products.

6.7   Conclusion

In conclusion, inspired by the mode of action of enzymes which exploit nucleophilic sulfur to promote oxidation processes, an efficient and reliable thiolate-catalysed intermolecular Tishchenko reaction has been developed. The reaction was then expanded to trifluoromethyl ketone substrates, thereby providing a solution to the limitations of an intermolecular aldehyde-ketone coupling which was never previously achieved. A key advantage associated with the use of this thiolate-mediated system relative to more complex transition metal-catalysed predecessors has been demonstrated to be tunability, allowing the rational selection of specific catalysts to address specific challenges presented by either a particular reaction or substrate. The process was demonstrated to be broad in scope and can be utilised to couple a wide range of

substituted aldehydes and trifluoromethyl ketones leading to the first example in literature of crossed Tishchenko reaction between such molecules.

The synthetic utility of this new reaction was unfortunately potentially limited by poor catalyst turnover frequency, which led to a requirement for long reaction times. As a solution, the effect of microwave radiation on the process was investigated. It was found that the corresponding microwave assisted reactions proceeded with significant rate acceleration. Aldehyde and ketone couplings generally proceeded in good yields in just two or three hour reaction times under the developed conditions.

The possibility of using imines as the substrate for the crossed-Tishchenko reaction was also investigated with the expectation that the electrophilicity exhibited by the carbonyl-derived functionality would prove sufficient for the reaction to take place. It was found, however, that under the conditions employed in the aldehyde-ketone process the reactions between aldehydes and imines did not occur. This was most likely due to the relative inability of the nitrogen atom of the imine to be coordinated by the magnesium atom in preference to a molecule of aldehyde, thus rendering the formation of the cyclic transition state necessary for the hydride transfer step to the imine less energetically favourable then the corresponding transition state involving an aldehyde hydride acceptor.

7. Experimental procedures and data

7.1 General

Proton Nuclear Magnetic Resonance (NMR) spectra were recorded on Bruker DPX 400 MHz and Bruker Avance II 600MHz spectrometers, using as solvent $CDCl_3$, DMSO-d_6 or D_2O and referenced relative to residual $CHCl_3$ (δ = 7.26 ppm) DMSO (δ = 2.50 ppm) or H_2O (δ = 4.79 ppm). Chemical shifts are reported in ppm and coupling constants (J) in Hertz. Carbon NMR spectra were recorded on the same instruments (100.6 MHz and 150.9 MHz respectively) with total proton decoupling. Fluorine NMR spectra were recorded on the Bruker DPX400 machine (376.5 MHz). HSQC, HMBC, TOCSY NOE and ROESY NMR experiments were used to aid assignment of NMR peaks when required. An arbitrary numbering system is employed to aid the assignment of the ^1H NMR signals. All melting points are uncorrected. Infrared spectra were obtained on a Perkin Elmer Spectrum 100 FT-IR spectrometer equipped with a universal ATR sampling accessory. ESI mass spectra were acquired using a Waters Micromass LCT-time of flight mass spectrometer (TOF), interfaced to a Waters 2690 HPLC. The instrument was operated in positive or negative mode as required. EI mass spectra were acquired using a GCT Premier Micromass time of flight mass spectrometer (TOF). The instrument was operated in positive mode. Chemical Ionization (CI) mass spectra were determined using a GCT Premier Micromass mass spectrometer in CI mode utilising methane as the ionisation gas. APCI experiments were carried out on a Bruker microTOF-Q III spectrometer interfaced to a Dionex UltiMate 3000 LC or direct insertion probe. The instrument was operated in positive or negative mode as required. Agilent tuning mix APCI-TOF was used to calibrate the system. Flash chromatography was carried out using silica gel, particle size 0.04-0.063 mm. TLC analysis was performed on precoated $60F_{254}$ slides, and visualized by UV irradiation and $KMnO_4$ staining. Optical rotation measurements are quoted in units of 10^{-1} deg cm^2 g^{-1}. Acetonitrile, toluene and dichloromethane (CH_2Cl_2) were distilled over calcium hydride and stored under argon. Tetrahydrofuran (THF) and diethyl ether were distilled over sodium-benzophenone and stored under argon. Methanol (MeOH) and isopropyl alcohol (*i*-PrOH) were dried over activated 3Å molecular sieves. Commercially available anhydrous *t*-butyl methyl ether (MTBE) was used. Analytical CSP-HPLC was performed on Daicel Chiralpak, AD, AD-H, IA, or Chiralcel OD, OD-H, OJ-H (4.6 mm

x 25 cm) columns. The X-ray crystallography data for crystal samples *trans*-**307**, *trans*-**334** and *cis*-**372** were collected on a Rigaku Saturn 724 CCD diffractometer. A suitable crystal from each compound was selected and mounted on a glass fibre tip and placed on the goniometer head in a 150K N_2 gas stream. The data sets were collected using Crystalclear-SM 1.4.0 software and, for each crystal, 1246 diffraction images, of 0.5° per image, were recorded. Data integration, reduction and correction for absorption and polarisation effects were all performed using Crystalclear-SM 1.4.0 software. Space group determination, structure solution and refinement were obtained using Crystalstructure ver. 3.8 and Bruker Shelxtl Ver. 6.14 software. The data for the crystal structures *trans*-**373**, *trans*-**387**, *trans*-**417** and *trans*-**429** were collected on a Bruker Smart Apex2 CCD Diffractometer. For each dataset, a suitable crystal was selected and mounted using inert oil on a 0.3 mm MiTeGen loop and placed on the goniometer head in a 100K N_2 gas 178 stream. The datasets were collected using Bruker APEX2 v2011.8-0 software. Data integrations, reductions and corrections for absorption and polarization effects were all performed using APEX2 v2011.8-0 software. Space group determination, structure solution and refinement were obtained using Bruker Shelxtl* Ver. 6.14 software. The structures were solved with Direct Methods using the SHELXTL program and refined against IF2I with the program XL from SHELX-97 using all data. Non-hydrogen atoms were refined with anisotropic thermal parameters. Hydrogen atoms were placed into geometrically calculated positions and refined using a riding model. (*Software Reference Manual, version 5.625; Bruker Analytical X-Ray Systems Inc.: Madison, WI, 2001. Sheldrick, G. M. SHELXTL, An Integrated System for Data Collection, Processing, Structure Solution and Refinement; Bruker Analytical X-Ray Systems Inc.: Madison, WI, 2001).

7.2   Experimental procedures and data for Chapter 2

Racemic preparation of dihydroisocoumarin 170

An oven-dried 10 mL reaction vessel containing a magnetic stirring bar under argon atmosphere was charged with homophthalic anhydride (**147**, 39.9 mg, 0.246 mmol). Anhydrous MTBE (2.5 mL, 0.1 M) was added *via* syringe followed by freshly distilled benzaldehyde (**52**, 25 μL, 0.246 mmol). *N*,*N*-Diisopropylethylamine (8.6 μL, 0.0492 mmol - 20 mol%) was added *via* syringe and the resulting mixture was allowed to stir for 20 h at room temperature. The reaction was then diluted with EtOAc (15 mL) and extracted with an aqueous solution of NaHCO$_3$ (10% *w/v*, 3 x 15 mL). The combined aqueous extracts were acidified with aqueous HCl (2.0 N), a white precipitate formed and the mixture was then extracted with EtOAc (3 x 15 mL). The combined organic extracts were dried over anhydrous MgSO$_4$ and the solvent was removed *in vacuo* to yield the diastereomeric mixture of carboxylic acids. The acids were then dissolved in THF (0.15 M) followed by the addition *via* syringe of *i*-Pr$_2$NEt (1.0 equiv.) and MeI (2.0 equiv.) and the mixture was allowed to stir at room temperature for 16 h. The solvent was then removed *in vacuo* and the crude mixture of diastereomeric esters was purified by flash column chromatography, eluting in gradient from 100% hexanes to 5% EtOAc in hexanes to isolate both diastereomers combined.

General procedure I: **Catalyst evaluation and temperature optimisation in the organocatalysed cycloaddition reaction between homophthalic anhydride (147) and benzaldehyde (52) (Table 2.3 and Table 2.4)**

An oven-dried 10 mL reaction vessel containing a magnetic stirring bar under argon atmosphere was charged with homophthalic anhydride (**147**, 39.9 mg, 0.246 mmol) and the relevant catalyst (0.0123 mmol - 5 mol%). Anhydrous MTBE (2.5 mL, 0.1 M) was added *via* syringe and the reaction mixture was brought to the temperature indicated in Table 2.3 and Table 2.4. Freshly distilled benzaldehyde (**52**, 25 μL, 0.246 mmol) was then added *via* syringe and the resulting mixture was allowed to stir for the time indicated in Table 2.3 and Table 2.4. The yield and diastereomeric ratio of the products were determined by ^{1}H NMR spectroscopic analysis using *p*-iodoanisole (28.8 mg, 0.123 mmol) as an internal standard. The reaction was then diluted with EtOAc (15 mL)

and extracted with an aqueous solution of NaHCO₃ (10% *w/v*, 3 x 15 mL). The combined aqueous extracts were acidified with aqueous HCl (2.0 N), a white precipitate formed and the mixture was then extracted with EtOAc (3 x 15 mL). The combined organic extracts were dried over anhydrous MgSO₄ and the solvent was removed *in vacuo* to yield the diastereomeric mixture of carboxylic acids. The acids were then dissolved in THF (0.15 M) followed by the addition *via* syringe of *i*-Pr₂NEt (1.0 equiv.) and MeI (2.0 equiv.) and the mixture was allowed to stir at room temperature for 16 h. The solvent was then removed *in vacuo* and the crude mixture of diastereomeric esters was purified by flash column chromatography, eluting in gradient from 100% hexanes to 5% EtOAc in hexanes to isolate both diastereomers combined. The enantiomeric excess of the products was determined by CSP-HPLC using the conditions indicated.

CSP-HPLC analysis. Chiralcel OD-H (4.6 mm x 25 cm), hexane/IPA: 83/17, 0.5 mL min⁻¹, RT, UV detection at 254 nm, retention times: *trans*-**170** 96.5 min (minor enantiomer) and 133.0 min (major enantiomer); *cis*-**170** 104.0 min (minor enantiomer) and 108.5 min (major enantiomer).

General procedure II: Racemic preparation of dihydroisocoumarins 304-308

An oven-dried 10 mL reaction vessel containing a magnetic stirring bar under argon atmosphere was charged with homophthalic anhydride (**147**, 39.9 mg, 0.246 mmol). Anhydrous MTBE (2.5 mL, 0.1 M) was added *via* syringe followed by the relevant aldehyde (0.246 mmol). *N,N*-Diisopropylethylamine (8.6 μL, 0.0492 mmol - 20 mol%) was added *via* syringe and the resulting mixture was allowed to stir for 20 h at room temperature. To the reaction mixture containing the corresponding carboxylic acids, anhydrous MeOH (750 μL, 18.5 mmol), followed by trimethylsilyldiazomethane (2.0 M solution in diethyl ether, 150 μL, 0.300 mmol) were added *via* syringe and the reaction was allowed to stir for 30 min at room temperature. The solvent was then removed *in vacuo* and the crude mixture of diastereomeric esters was purified by flash column chromatography, eluting in gradient from 100% hexanes to 5% EtOAc in hexanes to isolate the major diastereomer. In the case of dihydroisocoumarin **308** synthesised with an aliphatic aldehyde, both diastereomers were recovered combined after purification by flash column chromatography.

General procedure III: **Enantioselective preparation of dihydroisocoumarins 304-308 (Table 2.5)**

An oven-dried 10 mL reaction vessel containing a magnetic stirring bar under argon atmosphere was charged with homophthalic anhydride (**147**, 39.9 mg, 0.246 mmol) and catalyst **303** (8.7 mg, 0.0123 mmol - 5 mol%). Anhydrous MTBE (2.5 mL, 0.1 M) was added *via* syringe and the reaction mixture was then cooled to -15 °C. The relevant aldehyde (0.246 mmol) was added *via* syringe and the resulting mixture was allowed to stir for the time indicated in Table 2.5. The yield and diastereomeric ratio of the products were determined by ^{1}H NMR spectroscopic analysis using *p*-iodoanisole (28.8 mg, 0.123 mmol) as an internal standard. To the reaction mixture containing the corresponding carboxylic acids, anhydrous MeOH (750 µL, 18.5 mmol), followed by trimethylsilyldiazomethane (2.0 M solution in diethyl ether, 150 µL, 0.300 mmol) were added *via* syringe and the reaction was allowed to stir for 30 min at room temperature. The solvent was then removed *in vacuo* and the crude mixture of diastereomeric esters was purified by flash column chromatography, eluting in gradient from 100% hexanes to 5% EtOAc in hexanes to isolate the major diastereomer. The enantiomeric excess of the products was determined by CSP-HPLC using the conditions indicated for each case.

General procedure IV: **Racemic preparation of dihydroisocoumarins 314 and 315**

An oven-dried 10 mL reaction vessel containing a magnetic stirring bar under argon atmosphere was charged with the relevant homophthalic anhydride (0.246 mmol). Anhydrous MTBE (2.5 mL, 0.1 M) was added *via* syringe followed by freshly distilled benzaldehyde (**52**, 25 µL, 0.246 mmol). The reaction was cooled to 0 °C and *N,N*-diisopropylethylamine (2.2 µL, 0.0123 mmol - 5 mol%) was added *via* syringe. The reaction was allowed to stir for 20 h at room temperature then it was diluted with EtOAc (15 mL) and extracted with an aqueous solution of NaHCO$_3$ (10% *w/v*, 3 x 15 mL). The combined aqueous extracts were acidified with aqueous HCl (2.0 N), a white precipitate formed and the mixture was then extracted with EtOAc (3 x 15 mL). The organic extracts were dried over anhydrous MgSO$_4$ and the solvent was removed *in vacuo* to yield the diastereomeric mixture of carboxylic acids as an off-white solid. The

acids were then dissolved in THF (0.15 M) and the solution was cooled to 0 °C. Anhydrous isopropyl alcohol (94 μL 1.23 mmol) immediately followed by trimethylsilyldiazomethane (2.0 M solution in diethyl ether, 615 μL, 1.23 mmol) were added *via* syringe and the reaction was allowed to stir for 1 h at room temperature. The solvent was then removed *in vacuo* at room temperature and the crude mixture of diastereomeric esters was purified by flash column chromatography, eluting in gradient from 100% hexanes to 5% EtOAc in hexanes to isolate the major diastereomer.

General procedure V: Enantioselective preparation of dihydroisocoumarins 314 and 315 (Table 2.6)

An oven-dried 10 mL reaction vessel containing a magnetic stirring bar under argon atmosphere was charged with the relevant homophthalic anhydride (0.246 mmol). Anhydrous MTBE (2.5 mL, 0.1 M) was added *via* syringe and the reaction mixture was then cooled to -15 °C. Freshly distilled benzaldehyde (**52**, 25 μL, 0.246 mmol) was added *via* syringe followed by catalyst **303** (8.7 mg, 0.0123 mmol - 5 mol%) and the resulting mixture was allowed to stir for the time indicated in Table 2.6. The yield and diastereomeric ratio of the products were determined by ^{1}H NMR spectroscopic analysis using *p*-iodoanisole (28.8 mg, 0.123 mmol) as an internal standard. The reaction was then diluted with EtOAc (15 mL) and extracted with an aqueous solution of NaHCO$_3$ (10% *w/v*, 3 x 15 mL). The combined aqueous extracts were acidified with aqueous HCl (2.0 N), a white precipitate formed and the mixture was then extracted with EtOAc (3 x 15 mL). The combined organic extracts were dried over anhydrous MgSO$_4$ and the solvent was removed *in vacuo* to yield the diastereomeric mixture of carboxylic acids. The acids were then dissolved in THF (0.15 M) and the solution was cooled to 0 °C. Anhydrous isopropyl alcohol (94 μL 1.23 mmol) immediately followed by trimethylsilyldiazomethane (2.0 M solution in diethyl ether, 615 μL, 1.23 mmol) were added *via* syringe and the reaction was allowed to stir for 1 h at room temperature. The solvent was then removed *in vacuo* at room temperature and the crude mixture of diastereomeric esters was purified by flash column chromatography, eluting in gradient from 100% hexanes to 5% EtOAc in hexanes to isolate the major diastereomer. The

enantiomeric excess of the products was determined by CSP-HPLC using the conditions indicated for each case.

Homophthalic anhydride (147)
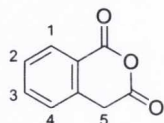
A 100 mL round-bottomed flask containing a magnetic stirring bar was charged with homophthalic acid (**296**, 2.00 g, 11.1 mmol). Acetic anhydride (25 mL) was added, the flask was fitted with a condenser and the reaction mixture was heated at 80 °C for 2 h. The excess acetic anhydride was removed *in vacuo* and the solid obtained was triturated with diethyl ether (10 mL), filtered and dried to obtain homophthalic anhydride (**147**) as an off white solid (1.53 g, 85%). M.p. 141-142 °C (lit.[317] m.p. 143-144 °C).

Spectral data for this compound were consistent with those in the literature.[317]

δ_H (400 MHz, DMSO-d_6):   8.05 (1 H, d, J 7.9, H-1), 7.75 (1 H, app. t, H-3), 7.52 (1 H, app. t, H-2), 7.44 (1 H, d, J 7.8, H-4), 4.28 (2 H, s, H-5).

HRMS (*m/z* - ESI):   Found: 161.0232 (M-H)⁻ $C_9H_5O_3$ Requires: 161.0239.

2-(Carboxymethyl)-5-nitrobenzoic acid (310)
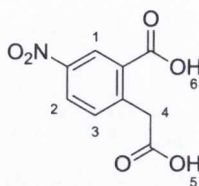
A 100 mL three-necked round-bottomed flask containing a magnetic stirring bar and fitted with a thermometer was charged with fuming nitric acid (15 mL) and cooled to 0 °C. Homophthalic acid (**296**, 5.00 g, 27.8 mmol) was then added portionwise over 30 min maintaining the temperature below 20 °C. The reaction mixture was then allowed to stir at 0 °C for 2 h, and then poured onto ice and allowed to stir vigorously until the ice was dissolved. The precipitate formed was filtered, washed with water and

recrystallised from water to yield **310** as an off-white solid (4.50 g, 72%). M.p. 230-233 °C (lit.[274] 235 °C).

Spectral data for this compound were consistent with those in the literature.[274]

δ_H (400 MHz, DMSO-d_6): 12.78 (2 H, bs, H-5 and H-6), 8.63 (1 H, d, *J* 2.1, H-1), 8.38 (1 H, dd, *J* 2.1, 8.4, H-2), 7.69 (1 H, d, *J* 8.4, H-3), 4.18 (2 H, s, H-4).

7-Nitroisochroman-1,3-dione (174)
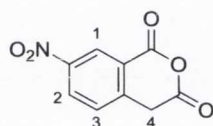
An oven-dried 10 mL round-bottomed flask containing a magnetic stirring bar was charged with **310** (500.0 mg, 2.22 mmol). Freshly distilled acetyl chloride (5.0 mL) was added, the flask was fitted with a condenser and the reaction mixture was heated at reflux temperature under an argon atmosphere for 16 h. The reaction was then cooled to room temperature and the excess acetyl chloride was removed *in vacuo*. The solid obtained was triturated with diethyl ether (5 mL), filtered and dried to give **174** as an off white solid (372.5 mg, 81%). M.p. 154-156 °C (lit.[318] m.p. 154-155 °C).

Spectral data for this compound were consistent with those in the literature.[319]

δ_H (400 MHz, DMSO-d_6): 8.67 (1 H, s, H-1), 8.54 (1 H, d, *J* 7.5, H-2), 7.72 (1 H, d, *J* 7.5, H-3), 4.41 (2 H, s, H-4).

δ_C (100 MHz, DMSO-d_6): 164.7 (C=O), 160.6 (C=O), 146.9 (q), 143.5 (q), 129.6, 128.8, 123.8, 123.2 (q), 34.6.

ν_{max} (neat)/cm^{-1}: 3105, 3074, 2962, 2890, 1798, 1746, 1608, 1523, 1434, 1344, 1270, 1165, 1084, 1035, 942, 836, 738.

7-Bromoisochroman-1,3-dione (312)
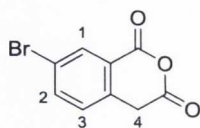
An oven-dried 10 mL round-bottomed flask containing a magnetic stirring bar was charged with 5-bromo-2-(carboxymethyl)benzoic acid (**311**, 500.0 mg, 1.93 mmol). Freshly distilled acetyl chloride (5.0 mL) was added, the flask was fitted with a condenser and the reaction mixture was heated at reflux temperature under an argon atmosphere for 16 h. The reaction was then cooled to room temperature and the excess acetyl chloride was removed *in vacuo*. The solid obtained was triturated with diethyl ether (5 mL), filtered and dried to give **312** as an off white solid (404.7 mg, 87%). M.p. 176-177 °C (lit.[320] M.p. 171-173 °C).

Spectral data for this compound were consistent with those in the literature.[320]

δ_H (400 MHz, DMSO-d_6):   8.13 (1 H, d, *J* 2.0, H-1), 7.94 (1 H, dd, *J* 2.0, 8.3, H-2), 7.41 (1 H, d, *J* 8.3, H-3), 4.23 (2 H, s, H-4).

HRMS (*m/z* - ESI):   Found: 238.9335 (M-H)⁻ $C_9H_4BrO_3$ Requires: 238.9344.

(3*R*,4*R*)-Methyl 1-oxo-3-phenylisochroman-4-carboxylate (*trans*-170, Table 2.4, entry 3)
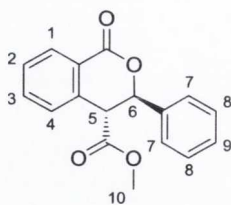
Prepared according to general procedure III, using freshly distilled benzaldehyde (**52**, 25 µL, 0.246 mmol). The reaction was allowed to stir for 22 h to give a diastereomeric mixture of carboxylic acids in a 96:4 (*trans:cis*) ratio. After esterification, the major diastereomer (*trans*-**170**) was isolated and purified by flash column chromatography to give a white solid (63.8 mg, 92%). M.p. 118-120 °C (lit.[152] m.p. 129-132 °C); TLC (hexanes:EtOAc, 8:2 *v/v*): R_f = 0.34; $[\alpha]_D^{20}$ = +26.0 (*c* = 0.20, CHCl₃).

CSP-HPLC analysis. Chiralcel OD-H (4.6 mm x 25 cm), hexane/IPA: 83/17, 0.5 mL min^{-1}, RT, UV detection at 254 nm, retention times: 96.5 min (minor enantiomer) and 133.0 min (major enantiomer).

Spectral data for this compound were consistent with those in the literature.[152]

δ_H (400 MHz, CDCl$_3$):	8.19 (1 H, d, J 8.0, H-1), 7.60 (1 H, app. t, H-3), 7.49 (1 H, app. t, H-2), 7.44-7.30 (5 H, m, H-7, H-8 and H-9), 7.20 (1 H, d, J 7.7, H-4), 5.86 (1 H, d, J 8.3, H-6), 4.35 (1 H, d, J 8.3, H-5), 3.69 (3 H, s, H-10).
δ_C (100 MHz, CDCl$_3$):	170.3 (C=O), 164.1 (C=O), 136.8 (q), 136.3 (q), 134.5, 130.8, 129.2, 129.0, 128.9, 126.92, 126.90, 124.8 (q), 80.8, 52.8, 50.9.
v_{max} (neat)/cm^{-1}:	2957, 1722, 1601, 1456, 1441, 1244, 1080, 997, 782, 701.
HRMS (m/z - ESI):	Found: 305.0805 (M+Na)$^+$ C$_{17}$H$_{14}$O$_4$Na Requires: 305.0790.

(3R,4R)-Methyl 3-(4-chlorophenyl)-1-oxoisochroman-4-carboxylate (*trans*-304, Table 2.5, entry 1)
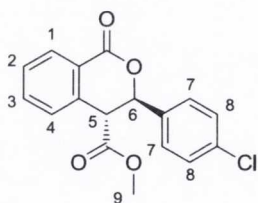
Prepared according to general procedure III, using recrystallised 4-chlorobenzaldehyde (**466**, 34.6 mg, 0.246 mmol). The reaction was allowed to stir for 40 h to give a diastereomeric mixture of carboxylic acids in a 95:5 (*trans:cis*) ratio. After esterification, the major diastereomer (*trans*-**304**) was isolated and purified by flash column chromatography to give a white solid (72.7 mg, 93%). M.p. 95-97 °C; TLC (hexanes:EtOAc, 8:2 *v/v*): R$_f$ = 0.28; $[\alpha]_D^{20}$ = +16.0 (c = 0.20, CHCl$_3$).

CSP-HPLC analysis. Chiralcel OD-H (4.6 mm x 25 cm), hexane/IPA: 99/1, 1.0 mL min^{-1}, RT, UV detection at 254 nm, retention times: 77.7 min (major enantiomer) and 94.2 min (minor enantiomer).

δ_H (400 MHz, CDCl$_3$):	8.18 (1 H, d, J 7.7, H-1), 7.61 (1 H, app. t, H-3), 7.50 (1 H, app. t, H-2), 7.39-7.29 (4 H, m, H-7 and H-8), 7.19 (1 H, d, J 7.7, H-4), 5.82 (1 H, d, J 8.7, H-6), 4.30 (1 H, d, J 8.7, H-5), 3.71 (3 H, s, H-9).
δ_C (100 MHz, CDCl$_3$):	170.0 (C=O), 163.9 (C=O), 136.1 (q), 135.3 (q), 135.2 (q), 134.7, 130.9, 129.12, 129.11, 128.4, 126.7, 124.5 (q), 80.1, 52.9, 50.8.
ν_{max} (neat)/cm^{-1}:	2955, 2926, 2862, 1736, 1709, 1602, 1459, 1261, 1001, 826, 740.
HRMS (*m/z* - ESI):	Found: 317.0572 (M+H)$^+$ C$_{17}$H$_{14}$O$_4$Cl Requires: 317.0581.

(3*R*,4*R*)-Methyl 3-(4-nitrophenyl)-1-oxoisochroman-4-carboxylate (*trans*-305, Table 2.5, entry 2)
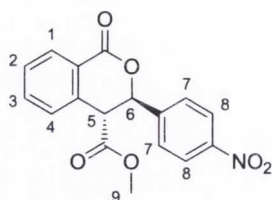
Prepared according to general procedure III, using recrystallised 4-nitrobenzaldehyde (37.2 mg, 0.246 mmol). The reaction was allowed to stir for 48 h to give a diastereomeric mixture of carboxylic acids in a 93:7 (*trans:cis*) ratio. After esterification, the major diastereomer (*trans*-305) was isolated and purified by flash column chromatography in gradient from 100% hexanes to 15% EtOAc in hexanes in 92% yield as a white solid (74.2 mg, 92%). M.p. 131-133 °C; TLC (hexanes:EtOAc, 8:2 *v/v*): R$_f$ = 0.14; [α]$_D^{20}$ = +22.0 (*c* = 0.20, CHCl$_3$).

176

CSP-HPLC analysis. Chiralcel OD-H (4.6 mm x 25 cm), hexane/IPA: 90/10, 0.7 mL min^{-1}, RT, UV detection at 254 nm, retention times: 97.6 min (major enantiomer) and 133.0 min (minor enantiomer).

δ_H (400 MHz, CDCl$_3$):	8.24 (2 H, d, J 8.6, H-8), 8.19 (1 H, d, J 7.8, H-1), 7.68-7.57 (3 H, m, H-3 and H-7), 7.52 (1 H, app. t, H-2), 7.21 (1 H, d, J 7.8, H-4), 5.97 (1 H, d, J 8.3, H-6), 4.32 (1 H, d, J 8.3, H-5), 3.73 (3 H, s, H-9).
δ_C (100 MHz, CDCl$_3$):	169.7 (C=O), 163.4 (C=O), 148.4 (q), 143.7 (q), 135.5 (q), 134.9, 131.0, 129.4, 127.9, 126.8, 124.3 (q), 124.1, 79.5, 53.1, 50.7.
ν_{max} (neat)/cm^{-1}:	3080, 2956, 2925, 2849, 1730, 1600, 1524, 1458, 1438, 1352, 1247, 1079, 1012, 859, 750, 693.
HRMS (*m/z* - ESI):	Found: 326.0674 (M-H)$^-$ C$_{17}$H$_{12}$NO$_6$ Requires: 326.0665.

(3*R*,4*R*)-Methyl 3-(4-methoxyphenyl)-1-oxoisochroman-4-carboxylate (*trans*-306, Table 2.5, entry 3)
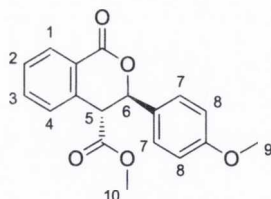
Prepared according to general procedure III, using freshly distilled 4-methoxybenzaldehyde (**179**, 30 μL, 0.246 mmol). The reaction was allowed to stir for 115 h to give a diastereomeric mixture of carboxylic acids in a 90:10 (*trans:cis*) ratio. After esterification, the major diastereomer (*trans*-**306**) was isolated and purified by flash column chromatography in gradient from 100% hexanes to 10% EtOAc in hexanes to give a white solid (60.1 mg, 78%). M.p. 82-84 °C; TLC (hexanes:EtOAc, 8:2 *v/v*): R$_f$ = 0.20; $[\alpha]_D^{20}$ = +13.5 (*c* = 0.20, CHCl$_3$).

CSP-HPLC analysis. Chiralpak AD-H (4.6 mm x 25 cm), hexane/IPA: 97/3, 1.0 mL min^{-1}, RT, UV detection at 254 nm, retention times: 81.3 min (minor enantiomer) and 89.5 min (major enantiomer).

δ_H (400 MHz, CDCl$_3$):   8.18 (1 H, d, J 7.8, H-1), 7.60 (1 H, app. t, H-3), 7.49 (1 H, app. t, H-2), 7.31 (2 H, d, J 8.6, H-7), 7.19 (1 H, d, J 7.8, H-4), 6.88 (2 H, d, J 8.6, H-8), 5.77 (1 H, d, J 9.0, H-6), 4.34 (1 H, d, J 9.0, H-5), 3.80 (3 H, s, H-9), 3.69 (3 H, s, H-10).

δ_C (100 MHz, CDCl$_3$):   170.3 (C=O), 164.4 (C=O), 160.2 (q), 136.6 (q), 134.5, 130.8, 128.9, 128.7 (q), 128.5, 126.7, 124.7 (q), 114.2, 80.7, 55.4, 52.8, 50.9.

ν_{max} (neat)/cm^{-1}:   3012, 2962, 2932, 2844, 1713, 1604, 1516, 1249, 990, 734.

HRMS (*m/z* - ESI):   Found: 335.0905 (M+Na)$^+$ C$_{18}$H$_{16}$O$_5$Na Requires: 335.0895.

(3*R*,4*R*)-Methyl 1-oxo-3-(thiophen-2-yl)isochroman-4-carboxylate (*trans*-307, Table 2.5, entry 4)
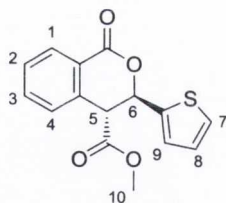
Prepared according to general procedure III, using freshly distilled 2-thiophenecarboxaldehyde (23 µL, 0.246 mmol). The reaction was allowed to stir for 48 h to give a diastereomeric mixture of carboxylic acids in a 94:6 (*trans*:*cis*) ratio. After esterification, the major diastereomer (*trans*-**307**) was isolated and purified by flash column chromatography to give a white solid (59.5 mg, 84%). M.p. 110-112 °C (lit.[153] m.p. 126-128 °C); TLC (hexanes:EtOAc, 8:2 *v/v*): R$_f$ = 0.25; [α]$_D^{20}$ = -68.0 (*c* = 0.20, CHCl$_3$).

CSP-HPLC analysis. Chiralcel OD-H (4.6 mm x 25 cm), hexane/IPA: 90/10, 1.0 mL min^{-1}, RT, UV detection at 254 nm, retention times: 32.7 min (minor enantiomer) and 35.6 min (major enantiomer).

Spectral data for this compound were consistent with those in the literature.[153]

δ_H (400 MHz, CDCl$_3$): 8.16 (1 H, d, *J* 7.9, H-1), 7.63 (1 H, app. t, H-3), 7.51 (1 H, app. t, H-2), 7.33-7.21 (2 H, m, H-4 and H-7), 7.09-7.01 (1 H, m, H-9), 6.96-6.89 (1 H, m, H-8), 6.19 (1 H, d, *J* 6.1, H-6), 4.35 (1 H, d, *J* 6.1, H-5), 3.75 (3 H, s, H-10).

δ_C (100 MHz, CDCl$_3$): 169.8 (C=O), 163.4 (C=O), 139.6 (q), 135.5 (q), 134.4, 130.7, 129.2, 127.8, 127.3, 126.9, 126.8, 124.8 (q), 76.4, 53.1, 50.5.

ν_{max} (neat)/cm^{-1}: 3104, 3011, 2951, 2925, 1727, 1703, 1605, 1459, 1431, 1359, 1332, 1226, 1081, 943, 714.

HRMS (*m/z* - ESI): Found: 289.0527 (M+H)$^+$ C$_{15}$H$_{13}$O$_4$S Requires: 289.0535.

Methyl 1-oxo-3-phenethylisochroman-4-carboxylate (*trans*-308 - *cis*-308, Table 2.5, entry 5)
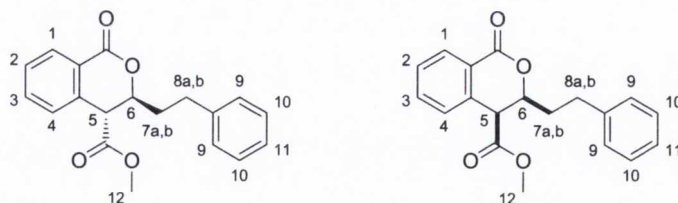
Prepared according to general procedure III, using freshly distilled hydrocinnamaldehyde (32 µL, 0.246 mmol). The reaction was allowed to stir for 22 h to give a diastereomeric mixture of carboxylic acids in a 75:25 (*trans:cis*) ratio. After esterification, both diastereomers (*trans*-308 and *cis*-308) were purified by flash column chromatography to give a pale yellow oil (71.7 mg, 94%, combined yield for both diastereomers). The diastereomeric ratio of the esters was found to be 79:21 (*trans*-308:*cis*-308) by ^{1}H NMR spectroscopic analysis. TLC (hexanes:EtOAc, 8:2 *v/v*): R$_f$ = 0.35.

179

CSP-HPLC analysis. Chiralcel OJ-H (4.6 mm x 25 cm), hexane/IPA: 80/20, 0.5 mL min^{-1}, RT, UV detection at 254 nm, retention times: *trans*-**308** 52.6 min (major enantiomer) and 76.2 min (minor enantiomer); *cis*-**308** 66.5 min (major enantiomer) and 106.6 min (minor enantiomer).

***trans*-308**:

δ_H (600 MHz, CDCl$_3$):	8.15 (1 H, d, *J* 7.8, H-1), 7.59 (1 H, app. t, H-3), 7.47 (1 H, app. t, H-2), 7.35-7.25 (3 H, m, H-9 and H-11), 7.25-7.15 (3 H, m, H-4 and H-10), 4.91-4.84 (1 H, m, H-6), 3.92 (1 H, d, *J* 6.8, H-5), 3.76 (3 H, s, H-12), 2.92-3.02 (1 H, m, H-8a), 2.83-2.75 (1 H, m, H-8b), 2.13-2.03 (1 H, m, H-7a), 1.97-1.87 (1 H, m, H-7b).
δ_C (151 MHz, CDCl$_3$):	170.6 (C=O), 164.0 (C=O), 140.6 (q), 136.0 (q), 134.3, 130.7, 128.9, 128.7, 128.6, 127.3, 126.40, 124.7 (q), 78.3, 52.9, 48.7, 35.7, 31.3.

***cis*-308**:

δ_H (600 MHz, CDCl$_3$):	8.15 (1 H, d, *J* 7.9, H-1), 7.56 (1 H, app. t, H-3), 7.48 (1 H, app. t, H-2), 7.35-7.25 (2 H, m, H-9), 7.25-7.15 (4 H, m, H-4, H-10 and H-11), 4.60-4.53 (1 H, m, H-6), 3.83 (1 H, d, *J* 3.2, H-5), 3.68 (3 H, s, H-12), 3.02-2.92 (1 H, m, H-8a), 2.90-2.83 (1 H, m, H-8b), 2.30-2.21 (1 H, m, H-7a), 2.14-2.02 (1 H, m, H-7b).
δ_C (151 MHz, CDCl$_3$):	169.4 (C=O), 164.8 (C=O), 140.5 (q), 136.8 (q), 133.9, 130.9, 129.2, 128.8, 128.7, 127.4, 126.42, 125.5 (q), 77.3, 52.8, 48.1, 34.5, 31.4.
ν_{max} (neat)/cm^{-1}:	3062, 3027, 2952, 2927, 2860, 1723, 1603, 1457, 1244, 1159, 1120, 1086, 700.

180

HRMS (*m/z* - ESI):   Found: 333.1103   (M+Na)$^+$ C$_{19}$H$_{18}$O$_4$Na   Requires: 333.1103.

(3*R*,4*R*)-Methyl 7-nitro-1-oxo-3-phenylisochroman-4-carboxylate (*trans*-314, Table 2.6, entry 1)
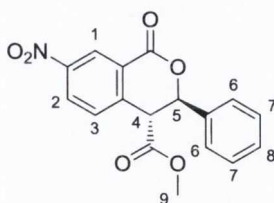
Prepared according to general procedure V, using 7-nitroisochroman-1,3-dione (**174**, 51.0 mg, 0.246 mmol). The reaction was allowed to stir for 96 h to give a diastereomeric mixture of carboxylic acids in a 92:8 (*trans*:*cis*) ratio. After esterification, the major diastereomer (*trans*-**314**) was isolated and purified by a rapid flash column chromatography, eluting in gradient from 20% EtOAc in hexanes to 30% EtOAc in hexanes to give a white solid (51.1 mg, 63%). M.p. 148-150 °C; TLC (hexanes:EtOAc, 8:2 *v/v*): R$_f$ = 0.17; $[\alpha]_D^{20}$ = +31.0 (*c* = 0.20, CHCl$_3$).

CSP-HPLC analysis. Chiralcel OD-H (4.6 mm x 25 cm), hexane/IPA: 90/10, 1.0 mL min^{-1}, RT, UV detection at 254 nm, retention times: 110.6 min (minor enantiomer) and 122.8 min (major enantiomer).

δ$_H$ (600 MHz, CDCl$_3$):   8.98 (1 H, d, *J* 2.1, H-1), 8.42 (1 H, dd, *J* 2.1, 8.5, H-2), 7.45 (1 H, d, *J* 8.5, H-3), 7.41-7.29 (5 H, m, H-6, H-7 and H-8), 5.98 (1 H, d, *J* 6.9, H-5), 4.43 (1 H, d, *J* 6.9, H-4), 3.73 (3 H, s, H-9).

δ$_C$ (151 MHz, CDCl$_3$):   169.1 (C=O), 162.0 (C=O), 148.4 (q), 142.0 (q), 136.0 (q), 129.5, 129.14, 129.12, 128.6, 126.53, 126.50 (q), 125.8, 80.5, 53.3, 50.4.

ν$_{max}$ (neat)/cm^{-1}:   2956, 2923, 2853, 1745, 1718, 1614, 1530, 1439, 1349, 1259, 1160, 1125, 999, 911, 802, 740.

HRMS (*m/z* - ESI):   Found: 326.0665 (M-H)⁻ C₁₇H₁₂NO₆ Requires: 326.0665.

(3*R*,4*R*)-Methyl 7-bromo-1-oxo-3-phenylisochroman-4-carboxylate (*trans*-315, Table 2.6, entry 2)
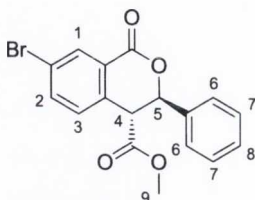
Prepared according to general procedure V using 7-bromoisochroman-1,3-dione (**312**, 59.3 mg, 0.246 mmol). The reaction was allowed to stir for 64 h to give a diastereomeric mixture of carboxylic acids in a 95:5 (*trans:cis*) ratio. After esterification, the major diastereomer (*trans*-315) was isolated and purified by flash column chromatography to give a white solid (60.6 mg, 68%). M.p. 132-134 °C; TLC (hexanes:EtOAc, 8:2 *v/v*): R_f = 0.33; $[\alpha]_D^{20}$ = +29.0 (*c* = 0.20, CHCl₃).

CSP-HPLC analysis. Chiralcel OD-H (4.6 mm x 25 cm), hexane/IPA: 90/10, 1.0 mL min⁻¹, RT, UV detection at 254 nm, retention times: 26.9 min (minor enantiomer) and 43.9 min (major enantiomer).

δ_H (400 MHz, CDCl₃):   8.30 (1 H, s, H-1), 7.71 (1 H, d, *J* 8.1, H-2), 7.43-7.29 (5 H, m, H-6, H-7 and H-8), 7.10 (1 H, d, *J* 8.3, H-3), 5.89 (1 H, d, *J* 7.6, H-5), 4.28 (1 H, d, *J* 7.6, H-4), 3.70 (3 H, s, H-9).

δ_C (100 MHz, CDCl₃):   169.8 (C=O), 162.8 (C=O), 137.4, 136.4 (q), 134.8 (q), 133.5, 129.3, 129.0, 128.9, 126.7, 126.4 (q), 122.9 (q), 80.6, 53.0, 50.2.

ν_{max} (neat)/cm⁻¹: 2954, 2924, 2854, 1723, 1592, 1406, 1255, 1132, 1080, 997, 765.

HRMS (*m/z* - ESI):   Found: 361.0063 (M+H)⁺ C₁₇H₁₄O₄Br Requires: 361.0075.

7.3   Experimental procedures and data for Chapter 3

<u>General procedure VI:</u> **Racemic preparation of γ-butyrolactones 321, 332-336**

An oven-dried 10 mL reaction vessel containing a magnetic stirring bar under argon atmosphere was charged with the relevant anhydride (1.0 equiv.). Anhydrous MTBE (0.1 M) was added *via* syringe and the reaction mixture was then cooled to 0 °C. The relevant aldehyde (1.0 equiv.) was added to the reaction mixture followed by *N,N*-diisopropylethylamine (5 mol%) and the resulting mixture was allowed to warm to room temperature and allowed to stir for 20 h. To the reaction mixture containing the corresponding carboxylic acids, anhydrous isopropyl alcohol (5.0 equiv.), followed by trimethylsilyldiazomethane (2.0 M solution in diethyl ether, 1.2 equiv.) were added *via* syringe at 0 °C and the reaction was allowed to stir for 1 h at room temperature. The solvent was then removed *in vacuo* and the crude mixture of diastereomeric esters was purified by flash column chromatography to isolate the major diastereomer.

<u>General procedure VII:</u> **Catalyst evaluation and temperature optimisation in the organocatalysed cycloaddition reaction between arylsuccinic anhydrides and benzaldehyde (52) (Table 3.1 and Table 3.2)**

An oven-dried 10 mL reaction vessel containing a magnetic stirring bar under argon atmosphere was charged with the relevant anhydride (1.0 equiv.). Anhydrous MTBE (0.1 M) was added *via* syringe and the reaction mixture was then cooled to the temperature reported in Table 3.1 and Table 3.2. Benzaldehyde (**52**, 1.0 equiv.) was added to the reaction mixture followed by the relevant catalyst (5 mol%) and the resulting mixture was allowed to stir for the time indicated in Table 3.1 and Table 3.2. The yield and diastereomeric ratio of the products were determined by ^{1}H NMR spectroscopic analysis using either *p*-iodoanisole or styrene (0.5 equiv.) as an internal standard. The reaction was then diluted with EtOAc (15 mL) and extracted with an aqueous solution of NaHCO$_3$ (10% *w/v*, 3 x 15 mL). The combined aqueous extracts were acidified with aqueous HCl (2.0 N), a white precipitate formed and the mixture was then extracted with EtOAc (3 x 15 mL). The combined organic extracts were dried over anhydrous MgSO$_4$ and the solvent was removed *in vacuo* to yield the diastereomeric mixture of carboxylic acids. The acids were then dissolved in dry THF

(0.1 M) and the solution was cooled to 0 °C, anhydrous isopropyl alcohol (5.0 equiv.), followed by trimethylsilyldiazomethane (2.0 M solution in diethyl ether, 1.2 equiv.) were added *via* syringe at 0 °C and the reaction was allowed to stir for 1 h at room temperature. The solvent was then removed *in vacuo* and the crude mixture of diastereomeric esters was purified by flash column chromatography to isolate the major diastereomer. The enantiomeric excess of the products was determined by CSP-HPLC using the conditions indicated for each case.

General procedure VIII: Enantioselective preparation of γ-butyrolactones 332-336 (Table 3.3 and Scheme 3.5)

An oven-dried 10 mL reaction vessel containing a magnetic stirring bar under argon atmosphere was charged with 3-(4-nitrophenyl)dihydrofuran-2,5-dione (**329**, 1.0 equiv.) Anhydrous MTBE (0.1 M) was added *via* syringe and the reaction mixture was then cooled to -15 °C. The relevant aldehyde (1.0 equiv.) was added to the reaction mixture followed by catalyst **303** (5 mol%) and the resulting mixture was allowed to stir at -15 °C for the time indicated in Table 3.3. The yield and diastereomeric ratio of the products were determined by ^{1}H NMR spectroscopic analysis using either *p*-iodoanisole or styrene (0.5 equiv.) as an internal standard. To the reaction mixture containing the corresponding carboxylic acids, anhydrous isopropyl alcohol (5.0 equiv.), followed by trimethylsilyldiazomethane (2.0 M solution in diethyl ether, 1.2 equiv.) were added *via* syringe at 0 °C and the reaction was allowed to stir for 1 h at room temperature. The solvent was then removed *in vacuo* and the crude mixture of diastereomeric esters was purified by flash column chromatography to isolate the major diastereomer. The enantiomeric excess of the products was determined by CSP-HPLC using the conditions indicated for each case.

Dihydrofuran-2,5-dione (Succinic anhydride, 129)
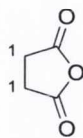
A 50 mL round-bottomed flask containing a magnetic stirring bar was charged with succinic acid (2.00 g, 16.9 mmol). Acetic anhydride (25 mL) was added, the flask was fitted with a condenser and the reaction mixture was heated at 80 °C for 2 h. The excess acetic anhydride was removed *in vacuo* to obtain **129** as a white solid (1.69 g, 100%). M.p. 118-120 °C (lit.[321] m.p. 117-119 °C).

Spectral data for this compound were consistent with those in the literature.[322]

δ_H (400 MHz, DMSO-d_6):   2.89 (4 H, s, H-1).

3-Phenyldihydrofuran-2,5-dione (Phenylsuccinic anhydride, 320)
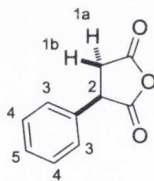
A 50 mL round-bottomed flask containing a magnetic stirring bar was charged with phenylsuccinic acid (**319**, 2.00 g, 10.3 mmol). Freshly distilled acetyl chloride (15 mL) was added, the flask was fitted with a condenser and the reaction mixture was heated at reflux temperature under an argon atmosphere for 16 h. The acetyl chloride was then removed *in vacuo* to obtain **320** as a white solid (1.81 g, 100%). M.p. 50-52 °C (lit.[323] m.p. 51-53 °C).

Spectral data for this compound were consistent with those in the literature.[324]

δ_H (400 MHz, CDCl$_3$):   7.48-7.33 (3 H, m, H-4 and H-5), 7.31-7.22 (2 H, m, H-3), 4.35 (1 H, dd, *J* 6.5, 10.3, H-2), 3.47 (1 H, dd, *J* 10.3, 19.1, H-1b), 3.13 (1 H, dd, *J* 6.5, 19.1, H-1a).

2-(4-Nitrophenyl)succinic acid (*p*-Nitrophenyl succinic acid, 322)
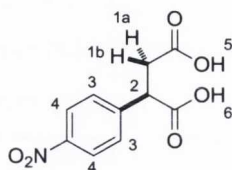
A three-necked oven-dried 100 mL round-bottomed flask fitted with a thermometer and containing a magnetic stirring bar was charged with fuming HNO_3 (30 mL) and cooled to 0 °C. Phenylsuccinic acid (**319**, 10.0 g, 51.5 mmol) was added portionwise while keeping the temperature below 20 °C. The solution was allowed to stir at 0 °C for 2 h, then crushed ice (30 g) and water (20 mL) were added to the reaction mixture. The white precipitate formed was filtered, washed with water, dried, and then recrystallised from water to obtain **322** as a white solid (7.2 g, 58%). M.p. 233-235 °C.

δ_H (400 MHz, DMSO-d_6): 12.6 (2 H, bs, H-5 and H-6), 8.19 (2 H, d, *J* 8.8, H-4), 7.60 (2 H, d, *J* 8.8, H-3), 4.10 (1 H, dd, *J* 5.5, 9.7, H-2), 3.00 (1 H, dd, *J* 9.7, 17.0, H-1b), 2.64 (1 H, dd, *J* 5.5, 17.0, H-1a).

δ_C (100 MHz, DMSO-d_6): 173.1 (C=O), 172.4 (C=O), 146.7 (q), 146.4 (q), 129.4, 123.7, 46.7, 36.9.

ν_{max} (neat)/cm^{-1}: 2862, 2576, 1703, 1596, 1520, 1435, 1347, 1255, 926, 732.

HRMS (*m/z* - ESI): Found: 238.0353 (M-H)⁻ $C_{10}H_8NO_6$ Requires: 238.0352.

2-(4-Aminophenyl)succinic acid (323)
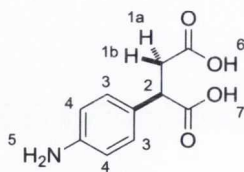
In an oven-dried 500 mL reaction vessel, **322** (4.50 g, 18.8 mmol) was dissolved in MeOH (25 mL). 10% Pd/C (2 mol%) was added, the flask was evacuated, placed under an atmosphere of hydrogen gas at a pressure of 3 atm and allowed to stir for 3 h at room temperature. The flask was then evacuated and filled with an inert atmosphere. Water

(30 mL) was added, the reaction mixture was heated under reflux for 10 minutes and then filtered hot through a pad of Celite and washed with hot water (5 mL). The filtrate was cooled to room temperature and the precipitate formed was collected by suction filtration and dried *in vacuo* to obtain **323** as a pale yellow solid (2.91 g, 74%). A second batch of product was obtained after removal of MeOH from the mother liquor under reduced pressure followed by extraction with EtOAc (3 x 50 mL). The combined organic extracts were dried over anhydrous $MgSO_4$ and the solvent was removed *in vacuo* to afford a yellow solid (520 mg, 13%). M.p. 202-204 °C.

δ_H (400 MHz, DMSO-d_6):* 6.91 (2 H, d, *J* 8.3, H-3), 6.49 (2 H, d, *J* 8.3, H-4), 3.66 (1 H, dd, *J* 5.0, 10.5, H-2), 2.86 (1 H, dd, *J* 10.5, 16.9, H-1b), 2.42 (1 H, dd, *J* 5.0, 16.9, H-1a).

δ_C (100 MHz, DMSO-d_6): 174.8 (C=O), 173.0 (C=O), 147.8 (q), 128.2, 125.5 (q), 114.0, 46.0, 37.7.

v_{max} (neat)/cm^{-1}: 3230, 2836, 2602, 1706, 1624, 1572, 1511, 1401, 1262, 1164, 632.

HRMS (*m/z* - ESI): Found: 208.0612 (M-H)$^-$ $C_{10}H_{10}NO_4$ Requires: 208.0610.

* The protic signals (H-5, H-6 and H-7) are not visible in DMSO-d_6.

Dimethyl 2-(4-aminophenyl)succinate (324)
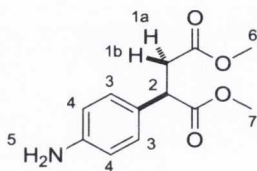
An oven-dried 100 mL round-bottomed flask containing a magnetic stirring bar was charged with **323** (2.60 g, 12.4 mmol) and anhydrous MeOH (20 mL) under an argon atmosphere. The reaction mixture was cooled to 0 °C then freshly distilled thionyl chloride (3.2 mL, 43.5 mmol) was added dropwise *via* syringe. The flask was fitted with a condenser and the reaction mixture was heated under reflux under an argon atmosphere for 16 h. The reaction was then cooled to room temperature and the excess

thionyl chloride was quenched by addition of a saturated aqueous solution of $NaHCO_3$. MeOH was then removed *in vacuo*, and the mixture obtained was extracted with EtOAc (3 x 50 mL). The combined organic extracts were dried over anhydrous $MgSO_4$ and the solvent was removed under reduced pressure to afford **324** as a peach coloured solid (2.57 g, 87%). M.p. 110-112 °C.

δ_H (400 MHz, $CDCl_3$):*   7.05 (2 H, d, *J* 8.3, H-3), 6.62 (2 H, d, *J* 8.3, H-4), 3.96 (1 H, dd *J* 5.3, 10.2, H-2), 3.65 (6 H, app. s, H-6 and H-7), 3.15 (1 H, dd, *J* 10.2, 17.0, H-1b), 2.61 (1 H, dd, *J* 5.3, 17.0, H-1a).

δ_C (100 MHz, $CDCl_3$):   174.0 (C=O), 172.3 (C=O), 146.0 (q), 128.7, 127.5 (q), 115.5, 52.4, 51.9, 46.3, 37.8.

ν_{max} (neat)/cm^{-1}:   3385, 3217, 2952, 1718, 1611, 1515, 1437, 1308, 1149, 1003, 730.

HRMS (*m/z* - ESI):   Found: 236.0933 (M-H)$^-$ $C_{12}H_{14}NO_4$ Requires: 236.0923.

* The protic signal (H-5) is not visible in $CDCl_3$.

Dimethyl 2-(4-amino-3,5-dibromophenyl)succinate (325)

In an oven-dried 50 mL round-bottomed flask containing a magnetic stirring bar **324** (1.00 g, 4.21 mmol) was dissolved in acetic acid (10 mL), then Br_2 (540 μL, 10.5 mmol) was added slowly at room temperature and the reaction mixture was allowed to stir for 1 h. The excess Br_2 was then quenched by addition of a saturated aqueous solution of $Na_2S_2O_3$ and the resulting solution was adjusted to pH = 8 by addition of a saturated aqueous solution of $NaHCO_3$. The reaction mixture was extracted with dichloromethane (3 x 50 mL), the combined organic extracts were dried over anhydrous $MgSO_4$ and the solvent was removed *in vacuo* to obtain **325** as a yellow oil (1.61 g, 97%).

δ_H (400 MHz, CDCl$_3$):   7.30 (2 H, s, H-3), 4.55 (2 H, bs, H-4), 3.90 (1 H, dd, J 5.5, 9.8, H-2), 3.69 (3 H, s, H-6), 3.67 (3 H, s, H-5), 3.12 (1 H, dd, J 9.8, 17.1, H-1b), 2.61 (1 H, dd, J 5.5, 17.1, H-1a).

δ_C (100 MHz, CDCl$_3$):   173.2 (C=O), 171.8 (C=O), 141.7 (q), 131.1, 128.8 (q), 108.9 (q x 2), 52.7, 52.1, 45.6, 37.6.

ν_{max} (neat)/cm^{-1}:   3474, 3376, 2952, 1735, 1616, 1479, 1473, 1197, 1165, 735.

HRMS (*m/z* - ESI):   Found: 415.9126 (M+Na)$^+$ C$_{12}$H$_{13}$Br$_2$NO$_4$Na Requires: 415.9109.

Dimethyl 2-(3,5-dibromophenyl)succinate (326)
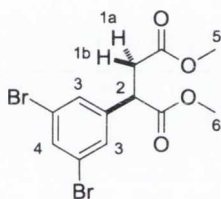
A three-necked oven-dried 100 mL round-bottomed flask fitted with a thermometer and containing a magnetic stirring bar was charged with **325** (1.50 g, 3.80 mmol) and concentrated HCl (15 mL) and it was cooled to 0 °C. A solution of NaNO$_2$ (288.2 mg, 4.28 mmol) in 10 mL of water was added slowly while keeping the temperature of the reaction mixture below 5 °C. The reaction was allowed to stir at 0 °C for 20 minutes after which time it was added to a solution of H$_3$PO$_2$ (45 mL, 30% *w/v* in water) at 0 °C. The reaction was allowed to warm to room temperature and allowed to stir for 2 h. Water (20 mL) was added and the reaction mixture was extracted with dichloromethane (3 x 50 mL). The combined organic extracts were dried over anhydrous MgSO$_4$ and the solvent was removed *in vacuo* to obtain a yellow oil which was purified by flash column chromatography (hexanes:EtOAc 9:1 *v/v*) to afford **326** as a white solid (1.30 g, 90%). M.p. 89-91 °C; TLC (hexanes:EtOAc, 8:2 *v/v*): R$_f$ = 0.26.

δ_H (400 MHz, CDCl$_3$):   7.59-7.56 (1 H, m, H-4), 7.38-7.34 (2 H, m, H-3), 4.01 (1 H, dd, J 5.6, 9.7, H-2), 3.70 (3 H, s, H-6), 3.68 (3 H, s, H-5),

3.15 (1 H, dd, *J* 9.7, 17.0, H-1b) 2.64 (1 H, dd, *J* 5.6, 17.0, H-1a).

δ_C (100 MHz, CDCl$_3$): 172.4 (C=O), 171.5 (C=O), 141.3 (q), 133.6, 129.9, 123.4 (q), 52.9, 52.2, 46.5, 37.3.

v_{max} (neat)/cm^{-1}: 3070, 2953, 1725, 1584, 1556, 1435, 1338, 1170, 864, 740, 674.

HRMS (*m/z* - ESI): Found: 376.9024 (M-H)$^-$ C$_{12}$H$_{11}$O$_4$Br$_2$ Requires: 376.9026.

2-(3,5-Dibromophenyl)succinic acid (327)

In a 100 mL round-bottomed flask containing a magnetic stirring bar, **326** (1.15 g, 3.03 mmol) was dissolved in MeOH (15 mL). A 2.0 M aqueous solution of KOH (15 mL) was added and the reaction was heated under reflux for 3 h. The reaction mixture was cooled to room temperature, MeOH was removed under reduced pressure and the solution was adjusted to pH = 2 by addition of a 2.0 M aqueous solution of HCl. The white precipitate formed was collected by suction filtration and dried *in vacuo* to yield **327** as a white solid (1.01 g, 95%). M.p. 227-229 °C.

δ_H (400 MHz, DMSO-d$_6$): 12.5 (2 H, bs, H-5 and H-6), 7.76 (1 H, app. s, H-4), 7.54 (2 H, app. s, H-3), 3.94 (1 H, dd, *J* 5.6, 9.6, H-2), 2.96 (1 H, dd, *J* 9.6, 17.0, H-1b), 2.63 (1 H, dd, *J* 5.6, 17.0, H-1a).

δ_C (100 MHz, DMSO-d$_6$): 173.2 (C=O), 172.4 (C=O), 143.3 (q), 132.3, 130.1, 122.5 (q), 46.1, 36.8.

v_{max} (neat)/cm^{-1}: 2868, 2541, 1693, 1582, 1558, 1417, 1292, 1182, 945, 841, 746, 673.

HRMS (*m/z* - ESI): Found: 348.8720 (M-H)$^-$ C$_{10}$H$_7$Br$_2$O$_4$ Requires: 348.8711.

3-(3,5-Dibromophenyl)dihydrofuran-2,5-dione (328)

A 10 mL round-bottomed flask containing a magnetic stirring bar was charged with **327** (400.0 mg, 1.14 mmol). Freshly distilled acetyl chloride (4.0 mL) was added, the flask was fitted with a condenser and the reaction mixture was heated at reflux temperature under an argon atmosphere for 16 h. The acetyl chloride was then removed *in vacuo* to obtain **328** as a white solid (380.4 mg, 100%). M.p. 112-115 °C.

δ_H (400 MHz, CDCl$_3$): 7.69 (1 H, app. s, H-4), 7.38 (2 H, app. s, H-3), 4.31 (1 H, dd, *J* 7.2, 10.3, H-2), 3.48 (1 H, dd, *J* 10.3, 18.9, H-1b), 3.11 (1 H, dd, *J* 7.2, 18.9, H-1a).

δ_C (100 MHz, CDCl$_3$): 170.4 (C=O), 168.4 (C=O), 137.8 (q), 134.7, 129.5, 124.1 (q), 45.6, 36.2.

v_{max} (neat)/cm^{-1}: 3072, 3004, 1846, 1778, 1557, 1429, 1220, 1044, 858, 813, 741, 679.

HRMS (*m/z* - ESI): Found: 330.8614 (M-H)$^-$ C$_{10}$H$_5$Br$_2$O$_3$ Requires: 330.8605.

3-(4-Nitrophenyl)dihydrofuran-2,5-dione (329)
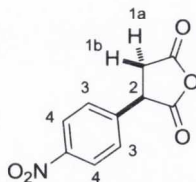
A 50 mL round-bottomed flask containing a magnetic stirring bar was charged with **322** (2.00 g, 8.36 mmol). Freshly distilled acetyl chloride (15 mL) was added, the flask was fitted with a condenser and the reaction mixture was heated at reflux temperature under an argon atmosphere for 16 h. The acetyl chloride was then removed *in vacuo* to obtain

a dark yellow oil that was purified by passing it through a plug of silica eluting with hexanes:EtOAc 1:1 *v/v* to obtain **329** as a viscous yellow oil (1.31 g, 71%).

Spectral data for this compound were consistent with those in the literature.[325]

δ_H (400 MHz, CDCl$_3$):   8.29 (2 H, d, *J* 8.8, H-4), 7.51 (2 H, d, *J* 8.8, H-3), 4.51 (1 H, dd, *J* 7.2, 10.4, H-2), 3.56 (1 H, dd, *J* 10.4, 18.8, H-1b), 3.18 (1 H, *J* 7.2, dd, 18.8, H-1a).

HRMS (*m/z* - ESI):   Found: 220.0243 (M-H)⁻ C$_{10}$H$_6$NO$_5$ Requires: 220.0246.

(2*S*,3*S*)-Methyl 5-oxo-2,3-diphenyltetrahydrofuran-3-carboxylate (*trans*-321, Table 3.1, entry 3)
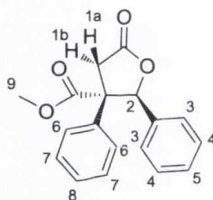
Prepared according to general procedure VII using 3-phenyldihydrofuran-2,5-dione (**320**, 43.3 mg, 0.492 mmol), anhydrous MTBE (4.9 mL, 0.1 M), freshly distilled benzaldehyde (50 µL, 0.492 mmol) and catalyst **303** (17.4 mg, 0.0246 mmol - 5 mol%). The reaction was allowed to stir for 24 h at room temperature to give a diastereomeric mixture of carboxylic acids in a 90:10 (*trans:cis*) ratio. After esterification, the major diastereomer (*trans*-**321**) was isolated and purified by flash column chromatography, eluting in gradient from 100% hexanes to 20% EtOAc in hexanes to give a colourless viscous oil (56.4 mg, 39%). TLC (hexanes:EtOAc, 8:2 *v/v*): R$_f$ = 0.35; $[\alpha]_D^{20}$ = -94.2 (*c* = 0.50, CHCl$_3$).

CSP-HPLC analysis. Chiralcel OD-H (4.6 mm x 25 cm), hexane/IPA: 90/10, 1.0 mL min⁻¹, RT, UV detection at 254 nm, retention times: 18.2 min (minor enantiomer) and 31.0 min (major enantiomer).

δ_H (400 MHz, CDCl$_3$):   7.21-7.02 (6 H, m, H-4, H-5, H-7 and H-8), 6.97 (2 H, d, *J* 7.3, H-3), 6.81 (2 H, d, *J* 7.3, H-6), 6.30 (1 H, s, H-2), 3.78

(3 H, s, H-9), 3.42 (1 H, d, *J* 17.6, H-1b); 3.33 (1 H, d, *J* 17.6, H-1a).

δ_C (100 MHz, CDCl$_3$):   174.1 (C=O), 172.9 (C=O), 134.9 (q), 134.5 (q), 128.5, 128.4, 128.1, 127.8, 127.0, 126.8, 85.6, 59.7 (q), 53.3, 38.3.

ν_{max} (neat)/cm^{-1}:   3039, 2954, 1782, 1731, 1499, 1435, 1235, 1178, 1008, 898, 753, 695.

HRMS (*m/z* - ESI):   Found: 319.0941 (M+Na)$^+$ C$_{18}$H$_{16}$O$_4$Na Requires: 319.0946.

(2*S*,3*S*)-Methyl 3-(3,5-dibromophenyl)-5-oxo-2-phenyltetrahydrofuran-3-carboxylate (*trans*-330, Table 3.2, entry 1)

Prepared according to general procedure VII using 3-(3,5-dibromophenyl)dihydrofuran-2,5-dione (**328**, 77.4 mg, 0.232 mmol), anhydrous MTBE (2.3 mL, 0.1 M), freshly distilled benzaldehyde (23.5 µL, 0.232 mmol) and catalyst **303** (8.2 mg, 0.0116 mmol - 5 mol%). The reaction was allowed to stir for 97 h to give a diastereomeric mixture of carboxylic acids in a 94:6 (*trans:cis*) ratio. After esterification, the major diastereomer (*trans*-**330**) was isolated and purified by flash column chromatography, eluting in gradient from 100% hexanes to 10% EtOAc in hexanes to give a white solid (68.5 mg, 65%). M.p. 51-53 °C; TLC (hexanes:EtOAc, 9:1 *v/v*): R$_f$ = 0.10; [α]$_D^{20}$ = -78.0 (*c* = 0.20, CHCl$_3$).

CSP-HPLC analysis. Chiralcel OD-H (4.6 mm x 25 cm), hexane/IPA: 85/15, 0.6 mL min^{-1}, RT, UV detection at 254 nm, retention times: 23.9 min (minor enantiomer) and 28.2 min (major enantiomer).

δ_H (400 MHz, CDCl$_3$):   7.46 (1 H, s, H-7), 7.25-7.14 (3 H, m, H-4 and H-5), 7.99 (2 H, d, *J* 6.8, H-3), 6.89-6.78 (2 H, m, H-6), 6.27 (1 H, s, H-2), 3.81 (3 H, s, H-8), 3.33 (2 H, app. s, H-1).

δ_C (100 MHz, CDCl$_3$):   173.0 (C=O), 171.8 (C=O), 138.6 (q), 133.9, 133.8 (q), 129.1, 129.0, 128.2, 126.8, 123.0 (q), 85.4, 59.4 (q), 53.8, 37.7.

ν_{max} (neat)/cm^{-1}:   3074, 2954, 1785, 1732, 1584, 1556, 1434, 1411, 1238, 1174, 1012, 901, 855, 743, 698, 680.

HRMS (*m/z* - APCI):   Found: 452.9332 (M+H)$^+$ C$_{18}$H$_{15}$Br$_2$O$_4$ Requires: 452.9330.

(2*S*,3*S*)-Methyl 3-(4-nitrophenyl)-5-oxo-2-phenyltetrahydrofuran-3-carboxylate (*trans*-331, Table 3.2, entry 2)
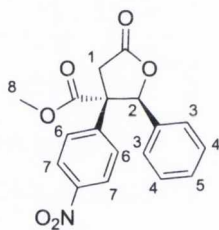
Prepared according to general procedure VIII using 3-(4-nitrophenyl)dihydrofuran-2,5-dione (**329**, 55.1 mg, 0.249 mmol), anhydrous MTBE (2.5 mL, 0.1 M), freshly distilled benzaldehyde (25 µL, 0.249 mmol) and catalyst **303** (8.8 mg, 0.0125 mmol, 5 mol%). The reaction was allowed to stir for 99 h to give a diastereomeric mixture of carboxylic acids in a 97:3 (*trans*:*cis*) ratio. After esterification, the major diastereomer (*trans*-**331**) was isolated and purified by flash column chromatography, eluting in gradient from 100% hexanes to 20% EtOAc in hexanes to give an off-white solid (78.2 mg, 92%). M.p. 59-61 °C; TLC (hexanes:EtOAc, 8:2 *v/v*): R$_f$ = 0.17; $[\alpha]_D^{20}$ = -94.0 (*c* = 0.20, CHCl$_3$).

CSP-HPLC analysis. Chiralcel OD-H (4.6 mm x 25 cm), hexane/IPA: 80/20, 1.0 mL min^{-1}, RT, UV detection at 254 nm, retention times: 36.2 min (minor enantiomer) and 41.7 min (major enantiomer).

δ_H (400 MHz, CDCl$_3$):   7.97 (2 H, d, *J* 8.8, H-7), 7.22-7.06 (3 H, m, H-4 and H-5), 7.03-6.98 (4 H, m, H-3 and H-6), 6.35 (1 H, s, H-2), 3.82 (3 H, s, H-8), 3.42 (2 H, app. s, H-1).

δ_C (100 MHz, CDCl$_3$):   173.0 (C=O), 171.9 (C=O), 147.4 (q), 142.3 (q), 133.8 (q), 129.1, 128.3, 128.2, 126.7, 123.5, 85.3, 59.9 (q), 53.8, 38.4.

ν_{max} (neat)/cm^{-1}:   3091, 2955, 2927, 1778, 1729, 1608, 1518, 1434, 1349, 1236, 1178, 1088, 999, 850, 731, 701.

HRMS (*m/z* - APCI-DIP):   Found: 342.0978 (M+H)$^+$ C$_{18}$H$_{16}$NO$_6$ Requires: 342.0975.

(2*S*,3*S*)-Methyl 2-(4-bromophenyl)-3-(4-nitrophenyl)-5-oxotetrahydrofuran-3-carboxylate (*trans*-332, Table 3.3, entry 1)

Prepared according to general procedure VIII using 3-(4-nitrophenyl)dihydrofuran-2,5-dione (**329**, 312.3 mg, 1.41 mmol), anhydrous MTBE (14.1 mL, 0.1 M), recrystallised 4-bromobenzaldehyde (260.9 mg, 1.41 mmol) and catalyst **303** (49.8 mg, 0.0705 mmol - 5 mol%). The reaction was allowed to stir for 97 h to give a diastereomeric mixture of carboxylic acids in a 94:6 (*trans:cis*) ratio. After esterification, the major diastereomer (*trans*-**332**) was isolated and purified by flash column chromatography, eluting in gradient from 100% hexanes to 20% EtOAc in hexanes to give an off-white solid (547.4 mg, 92%). M.p. 68-70 °C; TLC (hexanes:EtOAc, 8:2 *v/v*): R$_f$ = 0.13; $[\alpha]_D^{20}$ = -49.0 (*c* = 0.20, CHCl$_3$).

CSP-HPLC analysis. Chiralcel OD-H (4.6 mm x 25 cm), hexane/IPA: 85/15, 1.0 mL min^{-1}, RT, UV detection at 254 nm, retention times: 86.5 min (minor enantiomer) and 100.0 min (major enantiomer).

δ_H (400 MHz, CDCl$_3$):   8.02 (2 H, d, *J* 8.6, H-6), 7.25 (2 H, d, *J* 8.3, H-4), 6.98 (2 H, d, *J* 8.6, H-5), 6.89 (2 H, d, *J* 8.3, H-3), 6.26 (1 H, s, H-2), 3.81 (3 H, s, H-7), 3.40 (2 H, app. s, H-1).

δ_C (100 MHz, CDCl$_3$):   172.7 (C=O), 171.7 (C=O), 147.5 (q), 142.0 (q), 132.8 (q), 131.5, 128.4, 128.1, 123.7, 123.2 (q), 84.5, 59.6 (q), 53.8, 38.7.

v_{max} (neat)/cm^{-1}:   2955, 2928, 2853, 1787, 1734, 1603, 1520, 1490, 1348, 1251, 1173, 1006, 853, 823, 736, 710.

HRMS (*m/z* - ESI):   Found: 417.9916 (M-H)$^-$ C$_{18}$H$_{13}$NO$_6$Br Requires: 417.9926.

Methyl 2-(furan-2-yl)-3-(4-nitrophenyl)-5-oxotetrahydrofuran-3-carboxylate (*trans*-333 - *cis*-333, Table 3.3, entry 2)
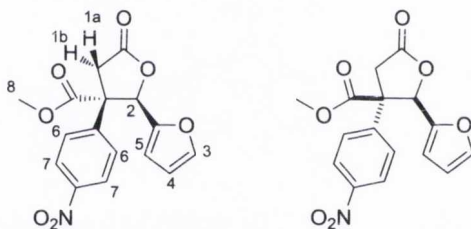
Prepared according to general procedure VII using 3-(4-nitrophenyl)dihydrofuran-2,5-dione (**329**, 51.3 mg, 0.232 mmol), anhydrous MTBE (2.3 mL, 0.1 M), freshly distilled furan-2-carboxaldehyde (**48**, 19 μL, 0.232 mmol) and catalyst **303** (8.2 mg, 0.0116 mmol - 5 mol%). The reaction was allowed to stir for 98 h to give a diastereomeric mixture of carboxylic acids in a 99:1 (*trans*:*cis*) ratio. After esterification and purification by flash column chromatography, eluting in gradient from 100% hexanes to 20% EtOAc in hexanes, *trans*-**333** and *cis*-**333** were isolated together as a pale yellow solid (73.1 mg, 95%, combined yield for both diastereomers). M.p. 56-58 °C; TLC (hexanes:EtOAc, 8:2 *v/v*): R$_f$ = 0.18; $[\alpha]_D^{20}$ = -135.5 (*c* = 0.20, CHCl$_3$)*.

CSP-HPLC analysis. Chiralcel OD (4.6 mm x 25 cm), hexane/IPA: 75/25, 0.3 mL min^{-1}, RT, UV detection at 254 nm, retention times: *trans*-**333** 60.9 min (minor enantiomer) and 64.2 min (major enantiomer); *cis*-**333** 158.1 min (both enantiomers).

δ_H (400 MHz, CDCl$_3$):   8.09 (2 H, d, *J* 8.8, H-7), 7.34 (2 H, d, *J* 8.8, H-6), 7.10 (1 H, app. s, H-3), 6.44 (1 H, s, H-2), 6.41 (1 H, d, H-5), 6.19-6.13 (1 H, m, H-4), 3.77 (3 H, s, H-8), 3.69 (1 H, d, *J* 16.9, H-1b), 3.60 (1 H, d, *J* 16.9, H-1a).

δ_C (151 MHz, CDCl$_3$):   173.0 (C=O), 171.4 (C=O), 147.61 (q), 147.59 (q), 144.0, 142.2 (q), 128.2, 123.7, 112.9, 110.6, 78.9, 59.4 (q), 54.3, 35.5.

ν_{max} (neat)/cm^{-1}:   3131, 3010, 2953, 2925, 1780, 1739, 1599, 1525, 1410, 1350, 1238, 1210, 1163, 978, 929, 877, 759, 736.

HRMS (*m/z* - ESI):   Found: 330.0600 (M-H)$^-$ C$_{16}$H$_{12}$NO$_7$ Requires: 330.0614.

* $[\alpha]_D^{20}$ refers to a mixture of *trans*-**333**:*cis*-**333** - 99:1

(2*R*,3*S*)-Methyl 3-(4-nitrophenyl)-5-oxo-2-(thiophen-2-yl)tetrahydrofuran-3-carboxylate (*trans*-334, Table 3.3, entry 3)
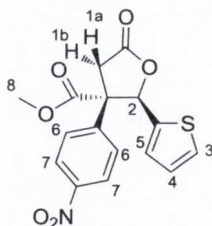
Prepared according to general procedure VII using 3-(4-nitrophenyl)dihydrofuran-2,5-dione (**329**, 50.0 mg, 0.226 mmol), anhydrous MTBE (2.3 mL, 0.1 M), freshly distilled 2-thiophenecarboxaldehyde (21 μL, 0.226 mmol) and catalyst **303** (8.0 mg, 0.0113 mmol - 5 mol%,). The reaction was allowed to stir for 161 h to give a diastereomeric mixture of carboxylic acids in a 98:2 (*trans*:*cis*) ratio. After esterification, the major diastereomer (*trans*-**334**) was isolated and purified by flash column chromatography, eluting in gradient from 100% hexanes to 20% EtOAc in hexanes to give a pale yellow solid (70.6 mg, 90%). M.p. 101-103 °C; TLC (hexanes:EtOAc, 8:2 *v/v*): R$_f$ = 0.15; $[\alpha]_D^{20}$ = -112.0 (*c* = 0.20, CHCl$_3$).

CSP-HPLC analysis. Chiralcel OD-H (4.6 mm x 25 cm), hexane/IPA: 85/15, 1.0 mL min^{-1}, RT, UV detection at 254 nm, retention times: 50.0 min (minor enantiomer) and 67.1 min (major enantiomer).

δ_H (400 MHz, CDCl$_3$): 8.07 (2 H, d, *J* 8.8, H-7), 7.22 (2 H, d, *J* 8.8, H-6), 7.13 (1 H, d, *J* 5.0, H-3), 6.94 (1 H, d, *J* 3.5, H-5), 6.82 (1 H, dd, *J* 3.5, 5.0, H-4), 6.63 (1 H, s, H-2), 3.82 (3 H, s, H-8), 3.51 (1 H, d, *J* 17.5, H-1b), 3.45 (1 H, d, *J* 17.5, H-1a).

δ_C (100 MHz, CDCl$_3$): 172.4 (C=O), 171.5 (C=O), 147.7 (q), 142.2 (q), 136.4 (q), 128.3, 128.2, 127.2, 126.8, 123.7, 82.3, 59.9 (q), 54.1, 36.7.

ν_{max} (neat)/cm^{-1}: 3115, 3086, 2956, 2931, 1789, 1731, 1603, 1519, 1437, 1349, 1244, 1160, 1009, 851, 704.

HRMS (*m/z* - ESI): Found: 346.0388 (M-H)$^-$ C$_{16}$H$_{12}$NO$_6$S Requires: 346.0385.

Methyl 3-(4-nitrophenyl)-5-oxo-2-phenethyltetrahydrofuran-3-carboxylate (*trans*-335 - *cis*-335, Table 3.3, entry 4)
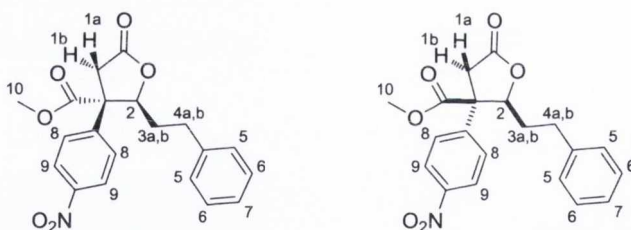
Prepared according to general procedure VII using 3-(4-nitrophenyl)dihydrofuran-2,5-dione (**329**, 57.7 mg, 0.261 mmol), anhydrous MTBE (2.6 mL, 0.1 M), freshly distilled hydrocinnamaldehyde (34 μL, 0.261 mmol) and catalyst **303** (9.3 mg, 0.0131 mmol - 5 mol%). The reaction was allowed to stir for 100 h to give a diastereomeric mixture of carboxylic acids in a 72:28 (*trans:cis*) ratio. After esterification and purification by flash column chromatography, eluting in gradient from 100% hexanes to 20% EtOAc in hexanes, *trans*-335 and *cis*-335 were isolated together as an off-white solid (94.5 mg, 98%, combined yield for both diastereomers). M.p. 57-60 °C TLC (hexanes:EtOAc, 8:2 *v/v*): R$_f$ = 0.19.

198

CSP-HPLC analysis. Chiralcel OD-H (4.6 mm x 25 cm), hexane/IPA: 85/15, 1.0 mL min^{-1}, RT, UV detection at 254 nm, retention times: *trans*-**335** 41.9 min (minor enantiomer) and 47.4 min (major enantiomer); *cis*-**335** 91.4 min (minor enantiomer) and 133.6 min (major enantiomer).

trans-335:

δ_H (600 MHz, CDCl$_3$):	8.23 (2 H, d, *J* 8.5, H-9), 7.35 (2 H, d, *J* 8.5, H-8), 7.31-7.22 (2 H, m, H-6), 7.22-7.15 (1 H, m, H-7), 7.10 (2 H, d, *J* 7.4, H-5), 5.14 (1 H, d, *J* 10.9, H-2), 3.76 (3 H, s, H-10), 3.37 (1 H, d, *J* 17.4, H-1b), 3.14 (1 H, d, *J* 17.4, H-1a), 2.90-2.78 (1 H, m, H-4a), 2.72-2.63 (1 H, m, H-4b), 1.80-1.65 (1 H, m, H-3a), 1.37-1.20 (1 H, m, H-3b).
δ_C (151 MHz, CDCl$_3$):	173.1 (C=O), 171.7 (C=O), 147.9 (q), 142.8 (q), 140.2 (q), 128.7, 128.6, 128.2, 126.5, 124.3, 83.4, 58.2 (q), 53.8, 37.6, 33.3, 32.2.

cis-335:

δ_H (600 MHz, CDCl$_3$):	8.15 (2 H, d, *J* 8.4, H-9), 7.39-7.31 (2 H, m, H-8), 7.31-7.22 (3 H, m, H-6 and H-7), 7.22-7.15 (2 H, m, H-5), 4.88 (1 H, d, *J* 10.6, H-2), 3.75 (3 H, s, H-10), 3.52 (1 H, d, *J* 17.1, H-1a), 3.10-3.00 (1 H, m, H-4a), 2.90-2.78 (1 H, m, H-4b), 2.75 (1 H, d, *J* 17.1, H-1b), 2.22-2.11 (1 H, m, H-3a), 2.02-1.90 (1 H, m, H-3b).
δ_C (151 MHz, CDCl$_3$):	172.6 (C=O), 170.9 (C=O), 147.6 (q), 145.8 (q), 140.0 (q), 129.0, 128.9, 127.4, 126.8, 124.3, 82.2, 58.0 (q), 53.4, 40.5, 33.8, 32.3.
ν_{max} (neat)/cm^{-1}:	2957, 2933, 2872, 1785, 1732, 1603, 1521, 1436, 1349, 1240, 1170, 1034, 952, 853, 751, 700.
HRMS (*m/z* - ESI):	Found: 368.1136 (M-H)$^-$ C$_{20}$H$_{18}$NO$_6$ Requires: 368.1134.

Methyl 3-(3,5-dibromophenyl)-2-(furan-2-yl)-5-oxotetrahydrofuran-3-carboxylate (*trans*-336 - *cis*-336, Scheme 3.5)
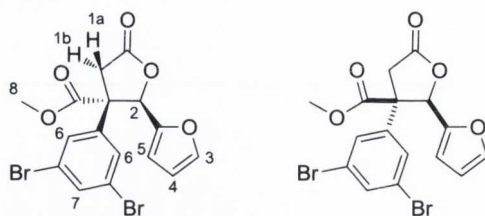
Prepared according to general procedure VIII using 3-(3,5-dibromophenyl)dihydrofuran-2,5-dione (**328**, 75.7 mg, 0.227 mmol), anhydrous MTBE (2.3 mL, 0.1 M), freshly distilled furan-2-carboxaldehyde (19 μL, 0.227 mmol) and catalyst **303** (8.1 mg, 0.0114 mmol - 5 mol%,). The reaction was allowed to stir for 97 h to give a diastereomeric mixture of carboxylic acids in a 98:2 (*trans:cis*) ratio. After esterification and purification by flash column chromatography, eluting in gradient from 100% hexanes to 10% EtOAc in hexanes, *trans*-336 and *cis*-336 were isolated together as a white solid (81.5 mg, 81%, combined yield for both diastereomers). M.p. 96-98 °C; TLC (hexanes:EtOAc, 8:2 *v/v*): R_f = 0.14; $[\alpha]_D^{20}$ = -102.0 (*c* = 0.20, CHCl$_3$).*

CSP-HPLC analysis. Chiralcel OD-H (4.6 mm x 25 cm), hexane/IPA: 85/15, 0.6 mL min^{-1}, RT, UV detection at 254 nm, retention times: *trans*-336 29.0 min (minor enantiomer) and 32.2 min (major enantiomer); *cis*-336 48.4 min (both enantiomers).

δ_H (400 MHz, CDCl$_3$):	7.51 (1 H, app. s, H-7), 7.22 (2 H, app. s, H-6), 7.18 (1 H, d, *J* 1.5, H-3), 6.42 (1 H, d, *J* 3.2, H-5), 6.35 (1 H, s, H-2), 6.23-6.23 (1 H, dd, *J* 1.5, 3.2. H-4), 3.79 (3 H, s, H-8), 3.58 (1 H, d, *J* 16.9, H-1b), 3.50 (1 H, d, *J* 16.9, H-1a).
δ_C (100 MHz, CDCl$_3$):	173.0 (C=O), 171.5 (C=O), 147.5 (q), 144.0, 138.9 (q), 134.1, 129.0, 123.0 (q), 112.9, 110.6, 78.9, 58.8 (q), 54.4, 35.3.
ν_{max} (neat)/cm^{-1}:	2955, 2922, 2853, 1789, 1731, 1584, 1555, 1434, 1412, 1248, 1154, 1044, 1013, 988, 923, 743, 681.
HRMS (*m/z* - APCI-DIP):	Found: 442.9124 (M+H)$^+$ C$_{16}$H$_{13}$Br$_2$O$_5$ Requires: 442.9120.

* $[\alpha]_D^{20}$ refers to a mixture of *trans*-336:*cis*-336 - 98:2

7.4   Experimental procedures and data for Chapter 4

3,4-Dimethoxycyclobut-3-ene-1,2-dione (351)
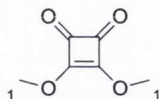
A 50 mL round-bottomed flask containing a magnetic stirring bar under argon atmosphere was charged with squaric acid (**96**, 2.00 g, 17.5 mmol). Dry MeOH (20 mL), followed by trimethyl orthoformate (**350**, 5.75 mL, 52.6 mmol) and TFA (269 μL, 3.51 mmol - 20 mol%), were then added *via* syringe. The flask was fitted with a condenser and the reaction mixture was heated at reflux temperature for 48 h and then cooled to room temperature. The volatiles were removed *in vacuo* and the residue obtained was purified by flash column chromatography (hexanes:EtOAc, 2:1 *v/v*) to give **351** as a white solid (2.12 g, 85%). M.p. 51-53 °C (lit.[326] m.p. 52-54 °C); TLC (hexanes:EtOAc, 2:1 *v/v*): R_f = 0.22.

Spectral data for this compound were consistent with those in the literature.[326]

δ_H (400 MHz, CDCl$_3$):   4.38 (6 H, s, H-1).

3-((3,5-*bis*(Trifluoromethyl)phenyl)amino)-4-methoxycyclobut-3-ene-1,2-dione (303a)
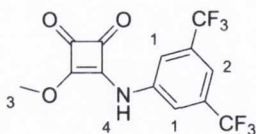
A 50 mL round-bottomed flask containing a magnetic stirring bar under argon atmosphere was charged with **351** (500.0 mg, 3.52 mmol). Dry MeOH (10 mL), followed by 3,5-*bis*-(trifluoromethyl)aniline (550 μL, 3.52 mmol), were then added *via* syringe. The reaction mixture was allowed to stir at room temperature for 3 days and then the solvent was removed *in vacuo*. Purification by flash column chromatography (hexanes:EtOAc, 2:1 *v/v*) of the residue obtained furnished **303a** as a white solid (776.2 mg, 65%). M.p. 192-194 °C (lit.[327] m.p. 179-181 °C); TLC (hexanes:EtOAc, 2:1 *v/v*): R_f = 0.28.

Spectral data for this compound were consistent with those in the literature.[327]

δ_H (400 MHz, DMSO-d$_6$):   11.21 (1 H, s, H-4), 8.04 (2 H, s, H-1), 7.79 (1 H, s, H-2), 4.41 (3 H, s, H-3).

(R)-(6-Methoxy-2-phenylquinolin-4-yl)((1S,2S,4S,5R)-5-vinylquinuclidin-2-yl)methanol (303b)
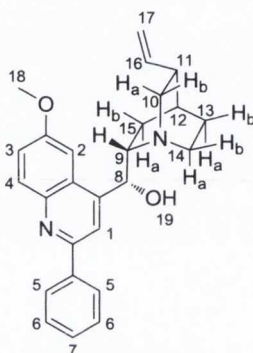
An oven dried 500 mL round-bottomed flask containing a magnetic stirring bar was charged with quinine (**72**, 6.48 g, 20.0 mmol) fitted with a septum and placed under an argon atmosphere. Anhydrous MTBE (120 mL) was added *via* syringe and the suspension was cooled to -10 °C. A solution of phenyl lithium (1.8 M in THF, 33.3 mL, 59.9 mmol) was added *via* syringe in two equal portions to the vigorously stirred suspension and the reaction mixture was allowed to stir at -10 °C for 30 min then warmed to room temperature and allowed to stir for 2 h. Acetic acid (15 mL) was added dropwise *via* syringe to the reaction at 0 °C, followed by water (50 mL) and EtOAc (50 mL). The reaction was then allowed to warm to room temperature and iodine was added in several portions to the stirred mixture until the appearance of a persistent deep brown colouration. A solution of sodium thiosulfate (Na$_2$S$_2$O$_3$, 3.00 g) in water (50 mL), followed by a concentrated solution of aqueous ammonia (35%, 30 mL) were added and the mixture was allowed to stir for 10 min. The organic phase was then washed with brine and the aqueous phase extracted with dichloromethane (3 x 40 mL), the combined organic extracts were dried over anhydrous MgSO$_4$, filtered and the solvent removed *in vacuo*. The crude oily residue was purified by flash column chromatography, eluting in gradient from 100% EtOAc to 5% MeOH in EtOAc to 5% MeOH, 5% triethylamine in

EtOAc to obtain **303b** (3.12 g, 39%) as a white solid. M.p. 160-162 °C (lit.[328] m.p. 151 °C); $[\alpha]_D^{20}$ = -168.2 (*c* = 1.0, CHCl₃); TLC (EtOAc:MeOH, 9:1 *v/v*): R_f = 0.14.

Spectral data for this compound were consistent with those in the literature.[329]

δ_H (400 MHz, CDCl₃):*   8.11-8.01 (3 H, m, H-4 and H-5), 7.90 (1 H, s, H-1), 7.51-7.37 (3 H, m, H-6 and H-7), 7.34 (1 H, dd, *J* 2.6, 9.2, H-3), 7.15 (1 H, d, *J* 2.5, H-2), 5.73 (1 H, ddd, *J* 7.7, 10.3, 17.3, H-16), 5.50 (1 H, d, *J* 3.7, H-8), 5.01-4.85 (2 H, m, H-17), 3.89 (3 H, s, H-18), 3.52-3.37 (1 H, m, H-10b), 3.18-3.03 (2 H, m, H-9 and H-14a), 2.73-2.59 (2 H, m, H-14b and H-10a), 2.32-2.19 (1 H, m, H-11), 1.84-1.65 (3 H, m, H-13b, H-15b and H-12), 1.61-1.41 (2 H, m, H-13a and H-15a).

* The protic signal (H-19) is not visible in CDCl₃.

(*S*)-(6-Methoxy-2-phenylquinolin-4-yl)((1*S*,2*S*,4*S*,5*R*)-5-vinylquinuclidin-2-yl)methanamine (303c)
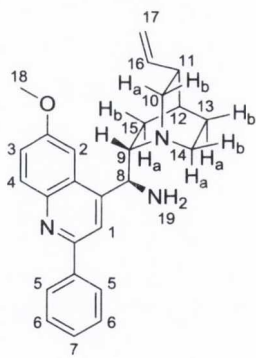
Diisopropyl azodicarboxylate (DIAD, 1.7 mL, 8.4 mmol) was added to a stirred solution of **303b** (2.80 g, 7.0 mmol) and triphenylphosphine (2.20 g, 8.4 mmol) in dry THF (50 mL) at 0 °C *via* syringe under argon atmosphere in a 100 mL round-bottomed flask. After 30 min diphenylphosphoryl azide (DPPA, 1.8 mL, 8.4 mmol) was added dropwise *via* syringe and the reaction mixture was allowed to stir at 0 °C to rt for 16 h, then heated at 50 °C for 2 h. Triphenylphosphine (**381**, 2.20 g, 8.4 mmol) was added portionwise and heating was maintained for 2 h. After cooling the reaction mixture to room temperature, water (10 mL) was added and the mixture allowed to stir for 4 h. The

THF was removed *in vacuo* and the residue was dissolved in aqueous HCl (2 N, 20 mL) and washed with dichloromethane (3 x 20 mL). The aqueous layer was basified with aqueous NaOH (2 N) and extracted with dichloromethane (4 x 10 mL), the combined organic extracts were dried over anhydrous $MgSO_4$ and the solvent removed *in vacuo* to yield **303c** as a viscous pale yellow oil (2.46 g, 88%). $[\alpha]_D^{20} = +28.6$ ($c = 0.5$, $CHCl_3$).

Spectral data for this compound were consistent with those in the literature.[286]

δ_H (400 MHz, $CDCl_3$):	8.15 (2 H, d, *J* 7.3, H-5), 8.11 (1 H, d, *J* 9.2, H-4), 7.99 (1 H, bs, H-1), 7.80-7.61 (1 H, m, H-2), 7.52 (2 H, app. t, H-6), 7.48-7.36 (2 H, m, H-3 and H-7), 5.79 (1 H, ddd, *J* 7.8, 10.1, 17.5, H-16), 5.05-4.91 (2 H, m, H-17), 4.78-4.57 (1 H, m, H-8), 3.98 (3 H, s, H-18), 3.36-3.05 (3 H, m, H-9, H-10b and H-14a), 2.90-2.75 (2 H, m, H-10a and H-14b), 2.35-2.23 (1 H, m, H-11), 2.13-1.77 (2 H, m, H-19), 1.67-1.51 (3 H, m, H-12, H-13a and H-13b), 1.50-1.36 (1 H, m, H-15b), 0.92-0.78 (1 H, m, H-15a).
HRMS (*m/z* - ESI):	Found: 400.2382 (M+H)$^+$ $C_{26}H_{30}N_3O$ Requires: 400.2389.

3-((3,5-*bis*(Trifluoromethyl)phenyl)amino)-4-((((*S*)-(6-methoxy-2-phenylquinolin-4-yl)((1*S*,2*S*,4*S*,5*R*)-5-vinylquinuclidin-2-yl)methyl)amino)cyclobut-3-ene-1,2-dione (303)
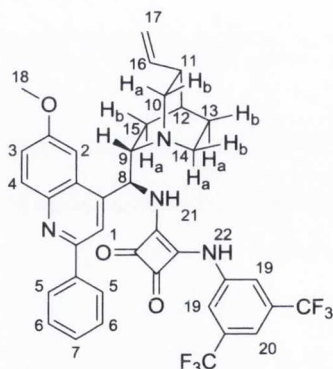
To a stirred solution of amine **303c** (1.80 g, 4.51 mmol) in MeOH (15 mL) under argon atmosphere in a 100 mL round-bottomed flask, was added a solution of **303a** (1.39 g,

4.09 mmol) in MeOH (10 mL) *via* syringe. The resultant mixture was allowed to stir at room temperature for 48 h. The solvent was removed *in vacuo* and the residue purified by flash column chromatography, eluting in gradient from 100% EtOAc to 5% MeOH in EtOAc to yield **303** as a white solid (2.55 g, 88%). M.p. 198 °C, decomposition (lit.[286] m.p. 192 °C, decomposition); $[\alpha]_D^{20} = +112.3$ (*c* = 0.50, MeOH); TLC (EtOAc:MeOH, 9.5:0.5 *v/v*): $R_f = 0.48$.

Spectral data for this compound were consistent with those in the literature.[286]

δ_H (400 MHz, DMSO-d$_6$):* 8.25 (2 H, d, *J* 7.6, H-5), 8.18 (1 H, bs, H-20), 8.05 (1 H, d, *J* 9.2, H-4), 7.97 (2 H, bs, H-19), 7.78 (1 H, bs, H-1), 7.64 (1 H, bs, H-2), 7.58 (2 H, app. t, H-6), 7.54-7.44 (2 H, m, H-3 and H-7), 6.28-5.81 (2 H, m, H-8 and H-16), 5.12-4.87 (2 H, m, H-17), 3.98 (3 H, s, H-18), 3.76-3.59 (1 H, m, H-9), 3.38-3.12 (2 H, m, H-10b and H-14a), 2.87-2.59 (2 H, m, H-10a, H-14b), 2.39-2.22 (1 H, m, H-11), 1.70-1.36 (4 H, m, H-12, H-13a, H-13b and H-15b), 0.84-0.56 (1 H, m, H-15a).

* The protic signals (H-21 and H-22) are not visible in DMSO-d$_6$.

(*S*)-(6-Methoxyquinolin-4-yl)((1*S*,2*S*,4*S*,5*R*)-5-vinylquinuclidin-2-yl)methanamine·3HCl (250a)
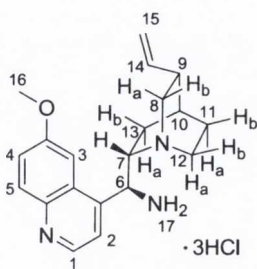
To a stirred solution of **72** (10.0 g, 30.8 mmol) and triphenylphosphine (9.70 g, 37.0 mmol) in dry THF (140 mL) at 0 °C under argon atmosphere in a 100 mL round-bottomed flask, was added diisopropyl azodicarboxylate (DIAD) (7.3 mL, 37.0 mmol) *via* syringe. After 30 min a solution of diphenylphosphoryl azide (DPPA, 8.0 mL, 37.0

mmol) in dry THF (64 mL) was added dropwise. The reaction mixture was allowed to warm to room temperature, allowed to stir for 12 h and then heated at 50 °C for 2 h. The reaction was then cooled to room temperature and triphenylphosphine (**381**, 10.5 g, 40.1 mmol) was added portionwise. The reaction was then heated at 50 °C until the gas evolution had ceased (2 h). After cooling the reaction mixture to room temperature, water (10 mL) was added and the mixture was allowed to stir for an additional 4 h. The THF was removed *in vacuo* and the residue was dissolved in aqueous HCl (2 N, 80 mL). The aqueous layer washed with dichloromethane (3 x 40 mL) and concentrated under reduced pressure to yield **250a** as a yellow solid (11.07 g, 83%). M.p. 218-222 °C, decomposition (lit.[330] m.p. 220-222 °C); $[\alpha]_D^{20} = +22.1$ ($c = 0.75$, MeOH).

Spectral data for this compound were consistent with those in the literature.[330]

δ_H (400 MHz, D$_2$O):*   9.04 (1 H, d, J 5.8, H-1), 8.29 (1 H, d, J 9.4, H-5), 8.15 (1 H, d, J 5.8, H-2), 7.94 (1 H, dd, J 2.4, 9.4 H-4), 7.84 (1 H, bs, H-3), 5.90 (1 H, ddd, J 6.8, 10.5, 17.2, H-14), 5.56 (1 H, d, J 10.6, H-6), 5.32-5.18 (2 H, m, H-15), 4.35-4.23 (1 H, m, H-7), 4.13 (3 H, s, H-16), 4.04-3.92 (1 H, m, H-12a), 3.85 (1 H, dd, J 10.6, 13.3, H-8b), 3.59-3.45 (2 H, m, H-8a, H-12b), 3.00-2.90 (1 H, m, H-9), 2.17-2.00 (3 H, m, H-10, H-11a and H-11b), 1.96-1.84 (1 H, m, H-13b), 1.18 (1 H, dd, J 7.2, 14.2, H-13a).

* The protic signal (H-17) is not visible in D$_2$O.

3-(*tert*-Butylamino)-4-methoxycyclobut-3-ene-1,2-dione (352)
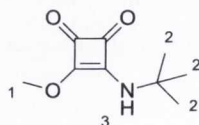
To a stirred solution of **351** (570.0 mg, 4.01 mmol) in MeOH (15 mL) under argon atmosphere was added *t*-butylamine (423 μL 4.01 mmol) *via* syringe and the resultant mixture was allowed to stir at room temperature for 48 h. The solvent was then removed *in vacuo* and the residue was purified by flash column chromatography

(hexanes:EtOAc, 2:1 *v/v*) furnishing **352** as a white solid (670.3 mg, 91%). M.p. 99-100 °C; TLC (hexanes:EtOAc, 2:1 *v/v*): R_f = 0.17.

δ_H (400 MHz, CDCl$_3$):	6.09 (1 H, bs, H-3), 4.44 (3 H, s, H-1), 1.39 (9 H, s, H-2).
δ_C (100 MHz, CDCl$_3$):	190.1 (C=O), 183.5 (C=O), 176.2 (q), 170.8 (q), 60.3, 53.3 (q), 30.0.
ν_{max} (neat)/cm^{-1}:	3276, 3040, 2979, 2928, 2869, 1802, 1693, 1621, 1526, 1440, 1360, 1214, 1107, 1049, 1033, 933, 838, 672.
HRMS (*m/z* - ESI):	Found: 206.0784 (M+Na)$^+$ C$_9$H$_{13}$NO$_3$Na Requires: 206.0793.

3-Methoxy-4-(tritylamino)cyclobut-3-ene-1,2-dione (353)
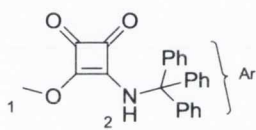
The synthesis of this compound was complicated by the lack of reproducibility of the reaction, and it was achieved in low yield in only one case.

To a stirred solution of **351** (207.0 mg, 1.46 mmol) in dry THF (8.0 mL) under argon atmosphere in a 25 mL round-bottomed flask was added tritylamine (377.8 mg 1.46 mmol). The flask was fitted with a condenser and the mixture was heated at reflux temperature for 48 h. The solvent was removed *in vacuo* and the residue was purified by flash column chromatography (hexanes:EtOAc, 2:1 *v/v*) furnishing **353** as a white solid (155.8 mg, 29 %).

Full characterisation and assignment of this compound cannot be obtained as the only batch produced by the reaction was used entirely in the following reaction step of the synthesis of catalyst **349**. As evidence for the formation, the ^{1}H NMR spectrum of product **349** is attached in the Appendix.

δ_H (400 MHz, CDCl$_3$):	7.37-7.30 (9 H, m, H-Ar), 7.14-7.06 (6 H, m, H-Ar), 6.78 (1 H, bs, H-2), 3.78 (3 H, bs, H-1).

3-(*tert*-Butylamino)-4-((((*S*)-(6-methoxyquinolin-4-yl)((1*S*,2*S*,4*S*,5*R*)-5-vinylquinuclidin-2-yl)methyl)amino)cyclobut-3-ene-1,2-dione (348)
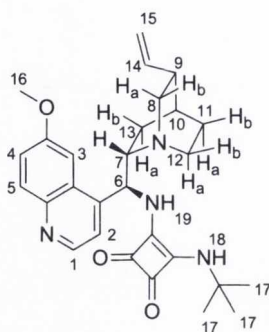
To a stirred solution of amine **250** (1.26 g, 3.90 mmol) in MeOH (10 mL) under argon atmosphere in a 50 mL round-bottomed flask, was added a solution of **351** (650.0 mg, 3.55 mmol) in MeOH (10 mL) *via* syringe. The resultant mixture was allowed to stir at room temperature for 48 h. The solvent was removed *in vacuo* and the residue was purified by flash column chromatography (EtOAc:MeOH, 9:1 *v/v*) furnishing **348** as a white solid (1.40 g, 83%). M.p. 250 °C decomposition; TLC (EtOAc:MeOH, 9:1 *v/v*): $R_f = 0.10$; $[\alpha]_D^{20} = +233.0$ ($c = 0.20$, CHCl$_3$).

δ_H (400 MHz, CDCl$_3$):	8.70 (1 H, d, *J* 4.0, H-1), 8.02 (1 H, d, *J* 9.2, H-5), 7.78 (1 H bs, H-3), 7.56 (1 H, d, *J* 4.0, H-2), 7.40 (1 H, d, *J* 9.2, H-4), 6.29-5.84 (1 H, m, H-6), 5.82-5.65 (1 H, m, H-14), 5.05-4.88 (2 H, m, H-15), 3.96 (3 H, s, H-16), 3.67-3.27 (2 H, m, H-7 and H-12a), 3.15 (1 H, app. t, H-8b), 2.82-2.62 (2 H, m, H-8a and H-12b), 2.36-2.19 (1 H, m, H-9), 1.75-1.52 (3 H, m, H-10, H-11a and H-11b), 1.51-1.38 (1 H, m, H-13b), 1.17 (9 H, s, H-17), 0.91-0.72 (1 H, m, H-13a).
δ_C (100 MHz, CDCl$_3$):*	182.6 (C=O), 181.5 (C=O), 168.3 (q), 168.1 (q), 158.9 (q), 147.9, 145.0 (q), 144.1 (q), 141.1, 132.0, 128.0 (q), 122.5, 120.0, 115.1, 101.5, 60.8, 56.2, 56.0, 53.4 (q), 41.0, 39.5, 30.5, 27.7, 27.6, 26.0.
ν_{max} (neat)/cm^{-1}:	3307, 3224, 2974, 2943, 2861, 1792, 1654, 1562, 1522, 1468, 1432, 1369, 1196, 1028, 914, 848, 710.
HRMS (*m/z* - ESI):	Found: 475.2712 (M+H)$^+$ C$_{28}$H$_{35}$N$_4$O$_3$ Requires: 475.2709.

* The protic signals (H-18 and H-19) are not visible in CDCl₃.

* The resonance of one carbon could not be identified in the spectrum.

3-((((S)-(6-Methoxyquinolin-4-yl)((1S,2S,4S,5R)-5-vinylquinuclidin-2-yl)methyl)amino)-4-(tritylamino)cyclobut-3-ene-1,2-dione (349)
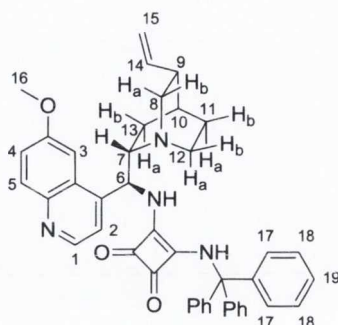
To a stirred solution of amine **250** (150.2 mg, 0.465 mmol) in MeOH (5.0 mL) under argon atmosphere in a 25 mL round-bottomed flask, was added a solution of **351** (156.0 mg, 0.422 mmol) in MeOH (5.0 mL) *via* syringe. The resultant mixture was allowed to stir at room temperature for 48 h. The solvent was removed *in vacuo* and the residue was purified by flash column chromatography (EtOAc:MeOH, 9:1 *v/v*) furnishing **349** as a white solid (220.5 mg, 79%). M.p. 160-162 °C; $[\alpha]_D^{20}$ = +41.8 (*c* = 0.10, CHCl₃).

δ_H (400 MHz, CDCl₃):   8.63 (1 H, d, *J* 4.5, H-1), 8.02 (1 H, d, *J* 9.2, H-5), 7.59-7.46 (1 H, bs, H-3), 7.40 (1 H, dd, *J* 2.5, 9.2, H-4), 7.23-7.10 (9 H, m, H-18 and H-19), 7.07-6.94 (6 H, m, H-17), 6.55 (1 H, bs, H-2), 6.50 (1 H, bs, N-H), 5.93-5.72 (2 H, m, H-6 and H-14), 5.11-4.93 (2 H, m, H-15), 3.93 (3 H, s, H-16), 3.73 (1 H, bs, N-H), 3.37-3.11 (2 H, m, H-8b and H-12a), 2.76-2.43 (3 H, m, H-7, H-8a and H-12b), 2.28 (1 H, m, H-9), 1.72-1.61 (1 H, m, H-10), 1.54-1.40 (3 H, m, H-11a, H-11b and H-13b), 0.74-0.59 (1 H, m, H-13a).

δ_C (151 MHz, CDCl₃):*   183.7 (C=O), 183.3 (C=O), 167.0 (q), 158.8 (q), 147.0 145.1 (q), 144.3 (q), 142.9 (q), 142.1, 131.7, 128.7, 128.6,

128.4, 123.0, 118.0, 114.5, 101.3, 72.3 (q), 60.3, 56.7, 56.3, 52.7, 41.0, 39.9, 28.0, 27.7, 26.8.

v_{max} (neat)/cm^{-1}:   3281, 3090, 3021, 2953, 1798, 1764, 1671, 1578, 1507, 1436, 1221, 1024, 915, 843, 701.

HRMS (*m/z* - APCI):   Found: 661.3173 (M+H)$^+$ C$_{43}$H$_{41}$N$_4$O$_3$ Requires: 661.3143.

* The resonance of two quaternary carbons belonging to the quinoline unit could not be identified in the spectrum.

General procedure IX: Preparation of nitroalkenes 357-363

An oven-dried 25 mL round-bottomed flask containing a magnetic stirring bar under argon atmosphere was charged with dry THF (2.5 mL), *t*-butanol (2.5 mL) and nitroethane (**354**, 1.1 mL, 15.0 mmol). The mixture was then cooled at 0 °C and the relevant aldehyde (10.0 mmol), followed by potassium *t*-butoxide (*t*-BuOK, 112.2 mg, 1.00 mmol - 10 mol%), were added. The reaction was allowed to warm to room temperature and was allowed to stir for 12 h. The mixture was then poured into water (10 mL) and extracted with EtOAc (3 x 10 mL), the combined organic phases were dried over anhydrous MgSO$_4$, filtered and concentrated under reduced pressure to give the relative crude β-nitroalcohol that was used in the next step without any further purification.

The relative β-nitroalcohol obtained was dissolved in dichloromethane (10 mL) and added *via* syringe to a 50 mL oven-dried reaction vessel containing a magnetic stirring bar under argon atmosphere and cooled to -10 °C. To this solution was then added *via* syringe trifluoroacetic anhydride (TFAA, 1.5 mL, 10.5 mmol) and the reaction was allowed to stir for 30 min at -10 °C. Triethylamine (2.8 mL, 20.0 mmol) was then added dropwise and the reaction was allowed to stir for additional 30 min at -10 °C. The resulting mixture was quenched with the addition of saturated aqueous NH$_4$Cl solution (15 mL) and extracted with EtOAc (3 x 10 mL). The combined organic phases were then dried over anhydrous MgSO$_4$, filtered and concentrated *in vacuo* to give a residue

that was purified by flash column chromatography, eluting from 100% hexanes to 5% EtOAc in hexanes to furnish the relative nitroalkene.

(*E*)-1-Chloro-4-(2-nitroprop-1-en-1-yl)benzene (357)
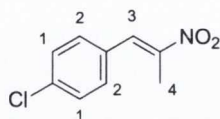
Prepared according to general procedure IX, using recrystallised 4-chlorobenzaldehyde (**466**, 1.41 g, 10 mmol). After purification, product **357** was obtained as a yellow solid (1.44 g, 73%). M.p. 81-82 °C (lit.[331] m.p. 84-85 °C); TLC (hexanes:EtOAc, 9:1 *v/v*): R_f = 0.46.

Spectral data for this compound were consistent with those in the literature.[331]

δ_H (400 MHz, CDCl$_3$):   8.03 (1 H, s, H-3), 7.44 (2 H, d, *J* 8.8, H-1), 7.37 (2 H, d, *J* 8.8, H-2), 2.44 (3 H, s, H-4).

δ_C (100 MHz, CDCl$_3$):   148.2 (q), 136.2 (q), 132.4, 131.3, 130.9 (q), 129.4, 14.1.

(*E*)-1-Methoxy-4-(2-nitroprop-1-en-1-yl)benzene (358)
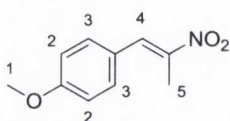
Prepared according to general procedure IX, using freshly distilled 4-methoxybenzaldehyde (**179**, 1.2 mL, 10.0 mmol). After purification, product **358** was obtained as a yellow solid (1.26 g, 65%). M.p. 41-42 °C (lit.[331] m.p. 46-47 °C); TLC (hexanes:EtOAc, 9:1 *v/v*): R_f = 0.26.

Spectral data for this compound were consistent with those in the literature.[331]

δ_H (400 MHz, CDCl$_3$):   8.07 (1 H, s, H-4), 7.43 (2 H, d, *J* 8.7, H-3), 6.98 (2 H, d, *J* 8.7, H-2), 3.86 (3 H, s, H-1), 2.47 (3 H, s, H-5).

HRMS (*m/z* - APCI):   Found: 194.0812 (M+H)$^+$ $C_{10}H_{12}NO_3$ Requires: 194.0817.

(*E*)-2-(2-Nitroprop-1-en-1-yl)naphthalene (359)
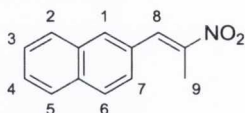
Prepared according to general procedure IX, using recrystallised 2-naphthaldehyde (**459**, 1.56 g, 10.0 mmol). After purification, product **359** was obtained as a yellow solid (1.60 g, 75%). M.p. 86-87 °C (lit.[332] m.p. 81-83.5 °C); TLC (hexanes:EtOAc, 9:1 *v/v*): $R_f = 0.43$.

Spectral data for this compound were consistent with those in the literature.[332]

δ_H (400 MHz, CDCl$_3$):   8.26 (1 H, s, H-8), 7.95-7.84 (4 H, m, H-1, H-2, H-5 and H-6), 7.61-7.50 (3 H, m, H-3, H-4 and H-7), 2.55 (3 H, s, H-9).

δ_C (100 MHz, CDCl$_3$):   147.9 (q), 133.9, 133.7 (q), 133.1 (q), 130.7, 129.9 (q), 128.8, 128.6, 127.9, 127.8, 127.1, 126.5, 14.3.

ν_{max} (neat)/cm^{-1}:   3066, 2979, 2928, 1623, 1510, 1440, 1386, 1313, 1159, 1028, 991, 954, 930, 826, 759, 725.

HRMS (*m/z* - APCI):   Found: 214.0863 (M+H)$^+$ $C_{13}H_{12}NO_2$ Requires: 214.0865.

(*E*)-2-(2-Nitroprop-1-en-1-yl)furan (360)
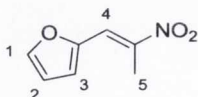
Prepared according to general procedure IX, using freshly distilled furan-2-carbaldehyde (**48**, 828 μL, 10.0 mmol). After purification, product **360** was obtained as a yellow solid (918.8 mg, 60%). M.p. 46-48 °C (lit.[333] m.p. 46-47 °C); TLC (hexanes:EtOAc, 9:1 *v/v*): $R_f = 0.35$.

Spectral data for this compound were consistent with those in the literature.[333]

δ_H (400 MHz, CDCl$_3$):   7.86 (1 H, s, H-4), 7.64 (1 H, d, *J* 1.7, H-1), 6.82 (1 H, d, *J* 3.5, H-3), 6.58 (1 H, dd, *J* 1.7, 3.5, H-2), 2.60 (3 H, s, H-5).

HRMS (*m/z* - APCI-DIP):   Found: 154.0499 (M+H)$^+$ C$_7$H$_8$NO$_3$ Requires: 154.0494.

(*E*)-(4-Nitropent-3-en-1-yl)benzene (361)
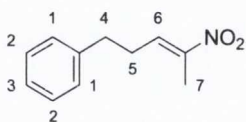
Prepared according to general procedure IX, using freshly distilled hydrocinnamaldehyde (1.3 mL, 10.0 mmol). After purification, product **361** was obtained as yellow oil (1.31 g, 69%). TLC (hexanes:EtOAc, 9:1 *v/v*): R$_f$ = 0.36.

Spectral data for this compound were consistent with those in the literature.[334]

δ_H (400 MHz, CDCl$_3$):   7.31 (2 H, app. t, H-2), 7.23-7.18 (1 H, t, *J* 7.4, H-3), 7.18-7.09 (3 H, m, H-1 and H-6), 2.80 (2 H, t, *J* 7.5, H-4), 2.53 (2 H, app. q, H-5), 2.03 (3 H, s, H-7).

δ_C (100 MHz, CDCl$_3$):   148.3 (q), 140.1 (q), 135.0, 128.7, 128.5, 126.6, 34.4, 30.1, 12.5.

HRMS (*m/z* - APCI-DIP):   Found: 190.0868 (M-H)$^-$ C$_{11}$H$_{12}$NO$_2$ Requires: 190.0863.

(*E*)-(2-Nitroprop-1-en-1-yl)cyclohexane (362)
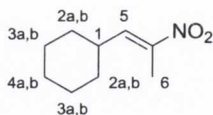
Prepared according to general procedure IX, using freshly distilled cyclohexanecarboxaldehyde (**265**, 1.21 mL, 10.0 mmol). After purification, product **362** was obtained as yellow oil (1.08 g, 65%). TLC (hexanes:EtOAc, 9:1 *v/v*): R$_f$ = 0.61.

Spectral data for this compound were consistent with those in the literature.[331]

δ_H (400 MHz, CDCl$_3$):   6.97 (1 H, d, *J* 10.0, H-5), 2.34-2.20 (1 H, m, H-1), 2.17 (3
                             H, s, H-6), 1.84-1.63 (5 H, m, H-2a, H-3a and H-4a), 1.40-
                             1.16 (5 H, m, H-2b, H-3b and H-4b).

δ_C (100 MHz, CDCl$_3$):   146.4 (q), 141.0, 37.7, 31.8, 25.7, 25.4, 12.7.

HRMS (*m/z* - APCI):   Found: 170.1176 (M+H)$^+$ C$_9$H$_{16}$NO$_2$ Requires: 170.1168.

(*E*)-4-Methyl-2-nitropent-2-ene (363)
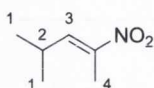
Prepared according to general procedure IX, using freshly distilled isobutyraldehyde
(**11**, 913 µL, 10.0 mmol). After purification, product **363** was obtained as yellow oil
(813.2 mg, 63%). TLC (hexanes:EtOAc, 9:1 *v/v*): R$_f$ = 0.54.

Spectral data for this compound were consistent with those in the literature.[331]

δ_H (400 MHz, CDCl$_3$):   6.95 (1 H, d, *J* 10.3, H-3), 2.66-2.50 (1 H, m, H-2), 2.17 (3
                             H, s, H-4), 1.11 (6 H, d, *J* 6.7, H-1).

HRMS: Analysis of product **363** by high resolution mass spectrometry was not
successful despite intensive efforts. ESI, EI, APCI and APCI-DIP techniques were all
performed. Due to technical issues on the instrument, the CI technique could not be
performed. As proof for the formation of **363**, the ^{1}H NMR spectrum is attached in the
Appendix.

5-Bromo-2-(carboxymethyl)benzoic acid (311)

In a three-necked 250 mL round-bottomed flask containing a magnetic stirring bar, homophthalic acid (**296**, 5.00 g, 27.8 mmol) and potassium bromate (6.58 g, 39.4 mmol) were mixed in water (30 mL). The flask was then fitted with a condenser and the reaction mixture was heated at 90 °C. A mixture of sulfuric acid (24 mL, 95%) and water (40 mL) was added dropwise to the resulting mixture at 90 °C over a period of 30 min. After completion of addition, the mixture was allowed to stir for 2 h and was cooled to the room temperature. The solid formed was isolated by suction filtration, washed with water and recrystallised from EtOAc/hexanes (4:1) to furnish **311** as a white solid (4.23 g, 58%). M.p. 214-216 °C (lit.[275] m.p. 216-217 °C).

Spectral data for this compound were consistent with those in the literature.[275]

δ_H (400 MHz, DMSO-d_6):* 7.98 (1 H, d, *J* 2.0, H-1), 7.71 (1 H, dd, *J* 2.0, 8.1, H-2), 7.31 (1 H, d, *J* 8.1, H-3), 3.91 (2 H, s, H-4).

* The protic signals (H-5 and H-6) are not visible in DMSO-d_6.

General procedure X: Racemic preparation of products 347, 364-370

An oven-dried 10 mL reaction vessel containing a magnetic stirring bar under argon atmosphere was charged with the relevant β-methyl-(*E*)-nitroalkene (0.246 mmol) and with the relevant homophthalic anhydride (0.246 mmol). Anhydrous MTBE (2.5 mL, 0.1 M), followed by *N*,*N*-diisopropylethylamine (8.6 μL, 0.0492 mmol - 20 mol%), were then added *via* syringe and the reaction mixture was allowed to stir at room temperature for 22 h. The reaction mixture containing the corresponding carboxylic acid was then cooled to 0 °C and anhydrous MeOH (750 μL, 18.5 mmol), followed by trimethylsilyldiazomethane (2.0 M solution in diethyl ether, 150 μL, 0.300 mmol) were added *via* syringe and the reaction was allowed to stir for 20 min. The crude reaction

mixture containing the diastereomeric esters was directly loaded onto the silica column and the two major diastereomers were chromatographically isolated together. Temperature was maintained below 30 °C during the removal of the solvent under reduced pressure.

General procedure XI: Catalyst evaluation in the organocatalysed cycloaddition reaction between homophthalic anhydride (147) and β-methyl-(*E*)-nitrostyrene (316) (Table 4.2 and Table 4.4)

An oven-dried 10 mL reaction vessel containing a magnetic stirring bar under argon atmosphere was charged with the β-methyl-(*E*)-nitrostyrene (**346**, 40.1 mg, 0.246 mmol) and with the relevant catalyst (0.0123 mmol - 5 mol%). Anhydrous MTBE (2.5 mL, 0.1 M) was then added *via* syringe and the reaction mixture was warmed at the equilibrated temperature of 30 °C while stirring. Homophthalic anhydride (**147**, 39.9 mg, 0.246 mmol) was added to the mixture and the reaction was allowed to stir for 22 h. The diastereomeric ratio of the acid product **347** was then determined by ^{1}H NMR spectroscopic analysis. The reaction was cooled to 0 °C and anhydrous MeOH (750 μL, 18.5 mmol), followed by trimethylsilyldiazomethane (2.0 M solution in diethyl ether, 150 μL, 0.300 mmol), were added *via* syringe to the reaction that was allowed to stir for 20 min. The crude reaction mixture containing the diastereomeric esters was directly loaded onto the silica column and the two diastereomers were chromatographically isolated together. Temperature was maintained below 30 °C during the removal of the solvent under reduced pressure. The diastereomeric ratio and the enantiomeric excess of product **347**, after esterification, were determined by CSP-HPLC using the conditions indicated.

CSP-HPLC analysis. Chiralpak AD-H (4.6 mm x 25 cm), hexane/IPA: 95/5, 1.0 mL min^{-1}, RT, UV detection at 254 nm, retention times: *trans*-**347** 14.0 min (minor enantiomer) and 25.0 min (major enantiomer); *cis*-**347** 7.9 min (major enantiomer) and 8.9 min (minor enantiomer).

General procedure XII: **Enantioselective preparation of products 347, 364-370, 372 (Table 4.7 and Table 4.9)**

An oven-dried 10 mL reaction vessel containing a magnetic stirring bar under argon atmosphere was charged with the relevant β-methyl-(*E*)-nitroalkene (0.246 mmol) and with catalyst **348** (5.8 mg, 0.0123 mmol - 5 mol%). Anhydrous MTBE (2.5 mL, 0.1 M) was then added *via* syringe and the reaction mixture was warmed at the equilibrated temperature of 30 °C while stirring. The relevant anhydride (0.246 mmol) was then added to the mixture and the reaction was allowed to stir for the time indicated in Table 4.7 and Table 4.9. The diastereomeric ratio of the acid product formed was then determined by ^{1}H NMR spectroscopic analysis. The reaction was cooled to 0 °C and anhydrous MeOH (750 μL, 18.5 mmol), followed by trimethylsilyldiazomethane (2.0 M solution in diethyl ether, 150 μL, 0.300 mmol), were added *via* syringe to the reaction that was allowed to stir for 20 min. The crude reaction mixture containing the diastereomeric esters was directly loaded onto the silica column and the two diastereomers were chromatographically isolated together. Temperature was maintained below 30 °C during the removal of the solvent under reduced pressure. The diastereomeric ratio and the enantiomeric excess of the product formed, upon esterification, were then determined by CSP-HPLC using the conditions indicated in each case.

General procedure XIII: **Optimised epimerisation reaction (Table 4.8 and Table 4.10)**

The two isolated diastereomers of the product formed with the general procedures XI and XII were then dissolved in a mixture of MTBE (2.5 mL) and MeOH (750 μL) and transferred *via* syringe to an oven-dried 10 mL round-bottomed flask containing a magnetic stirring bar. The flask was fitted with a condenser and the mixture was heated at reflux temperature for the time indicated in Table 4.8 and Table 4.10. Solvent was removed *in vacuo* and the residue obtained was analysed by ^{1}H NMR spectroscopy to determine the diastereomeric ratio of product formed upon epimerisation reaction. The major diastereomer (*trans*) was then isolated by flash column chromatography, eluting

from 100% hexanes to 20% EtOAc in hexanes and the enantiomeric excess was determined by CSP-HPLC analysis using the conditions indicated in each case.

(1*R*,2*S*,3*S*)-Methyl 3-methyl-3-nitro-4-oxo-2-phenyl-1,2,3,4-tetrahydronaphthalene-1-carboxylate (*trans*-347, Table 4.8, entry 1)
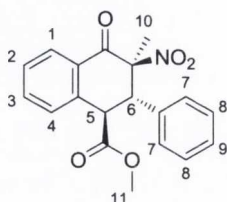
Prepared according to the consecutive use of general procedures XI and XIII using catalyst **348** (5.8 mg, 0.0123 mmol - 5 mol%). Upon epimerisation, the reaction gave a diastereomeric mixture of esters in a 96:4 (*trans*:*cis*) ratio. The major diastereomer (*trans*-**347**) was purified by flash column chromatography, eluting in gradient from 100% hexanes to 20% EtOAc in hexanes, to give a white solid (75.8 mg, 91%). M.p. 180-181 °C; TLC (hexanes:EtOAc, 8:2 *v/v*): $R_f = 0.24$; $[\alpha]_D^{20} = +90.8$ ($c = 0.20$, CHCl$_3$).

CSP-HPLC analysis. Chiralpak AD-H (4.6 mm x 25 cm), hexane/IPA: 95/5, 1.0 mL min^{-1}, RT, UV detection at 254 nm, retention times: *trans*-**347** 14.0 min (minor enantiomer) and 25.0 min (major enantiomer); *cis*-**347** 7.9 min (major enantiomer) and 8.9 min (minor enantiomer).

δ_H (400 MHz, CDCl$_3$):	8.22 (1 H, d, *J* 8.0, H-1), 7.67 (1 H, app. t, H-3), 7.53 (1 H, app. t, H-2), 7.38-7.31 (4 H, m, H-4, H-7 and H-9), 7.29-7.22 (2 H, m, H-8), 4.82 (1 H, d, *J* 12.3, H-6), 4.58 (1 H, d, *J* 12.3, H-5), 3.57 (3 H, s, H-11), 1.72 (3 H, s, H-10).
δ_C (100 MHz, CDCl$_3$):	189.9 (C=O), 171.0 (C=O), 138.9 (q), 135.4, 133.3 (q), 129.6, 129.2, 129.1, 129.07, 129.0, 128.8 (q), 127.3, 97.0 (q), 52.8, 50.3, 48.9, 16.2.
ν_{max} (neat)/cm^{-1}:	3008, 2955, 1732, 1692, 1598, 1550, 1453, 1345, 1211, 1166, 970, 794, 733, 700.

HRMS (*m/z* - ESI):   Found: 338.1027 (M-H)⁻ C₁₉H₁₆NO₅ Requires: 338.1028.

(1*S*,2*S*,3*S*)-Methyl 3-methyl-3-nitro-4-oxo-2-phenyl-1,2,3,4-tetrahydronaphthalene-1-carboxylate (*cis*-347, Table 4.2, entry 2)
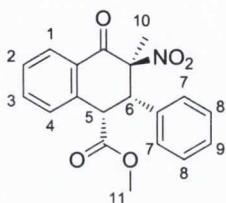
Prepared according to general procedure XI using catalyst **302** (7.8 mg, 0.0123 mmol - 5 mol%). Upon esterification, the reaction gave a diastereomeric mixture of esters in a 67:33 (*trans*:*cis*) ratio. The minor diastereomer (*cis*-**347**) was purified by flash column chromatography, eluting in gradient from 100% hexanes to 20% EtOAc in hexanes, to give a white solid (22.6 mg, 27%). M.p. 76-78 °C; TLC (hexanes:EtOAc, 8:2 *v/v*): R_f = 0.39; $[\alpha]_D^{20}$ = -76.4 (*c* = 0.10, CHCl₃).

CSP-HPLC analysis. Chiralpak AD-H (4.6 mm x 25 cm), hexane/IPA: 95/5, 1.0 mL min⁻¹, RT, UV detection at 254 nm, retention times: *cis*-**347** 7.6 min (major enantiomer) and 8.6 min (minor enantiomer).

δ_H (400 MHz, CDCl₃):   8.18 (1 H, d, *J* 7.8, H-1), 7.65 (1 H, app. t, H-3), 7.52 (1 H, app. t, H-2), 7.42 (1 H, d, *J* 7.9, H-4), 7.22-7.26 (1 H, m, H-9), 7.18 (2 H, app. t, H-8), 6.97 (2 H, d, *J* 7.4, H-7), 4.66 (1 H, d, *J* 6.2, H-6), 4.58 (1 H, d, *J* 6.2, H-5), 3.45 (3 H, s, H-11), 1.64 (3 H, s, H-10).

δ_C (100 MHz, CDCl₃):   187.5 (C=O), 170.8 (C=O), 136.9 (q), 134.6, 133.7 (q), 132.2 (q), 130.8, 129.6, 129.1, 128.9, 128.5, 128.2, 93.3 (q), 53.1, 52.3, 46.1, 21.7.

ν_{max} (neat)/cm⁻¹: 3004, 2952, 1743, 1701, 1599, 1542, 1457, 1298, 1200, 1179, 1003, 941, 816, 765, 705.

HRMS (*m/z* - ESI):   Found: 338.1026 (M-H)⁻ C₁₉H₁₆NO₅ Requires: 338.1028.

(1*R*,2*S*,3*S*)-Methyl 2-(4-chlorophenyl)-3-methyl-3-nitro-4-oxo-1,2,3,4-tetrahydronaphthalene-1-carboxylate (*trans*-364, Table 4.8, entry 2)
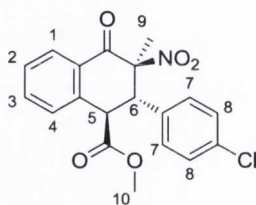
Prepared according to the consecutive use of general procedures XII and XIII, using β-methyl-(*E*)-nitroalkene **357** (48.6 mg, 0.246 mmol) and anhydride **147** (39.9 mg, 0.246 mmol). Upon epimerisation, the reaction gave a diastereomeric mixture of esters in a >98:2 (*trans*:*cis*) ratio. The major diastereomer (*trans*-**364**) was purified by flash column chromatography, eluting in gradient from 100% hexanes to 20% EtOAc in hexanes, to give a white solid (85.6 mg, 93%). M.p. 200-202 °C; TLC (hexanes:EtOAc, 8:2 *v/v*): R_f = 0.24; $[\alpha]_D^{20}$ = +88.5 (*c* = 0.20, CHCl$_3$).

CSP-HPLC analysis. Chiralpak AD-H (4.6 mm x 25 cm), hexane/IPA: 95/5, 1.0 mL min^{-1}, RT, UV detection at 254 nm, retention times: *trans*-**364** 19.9 min (minor enantiomer) and 38.8 min (major enantiomer); *cis*-**364** 8.7 min (major enantiomer) and 9.7 min (minor enantiomer).

δ$_H$ (400 MHz, CDCl$_3$):	8.22 (1 H, d, *J* 7.2, H-1), 7.68 (1 H, app. t, H-3), 7.54 (1 H, app. t, H-2), 7.38-7.29 (3 H, m, H-4 and H-8), 7.21 (2 H, d, *J* 6.8, H-7), 4.81 (1 H, d, *J* 12.3, H-6), 4.52 (1 H, d, *J* 12.3, H-5), 3.60 (3 H, s, H-10), 1.70 (3 H, s, H-9).
δ$_C$ (100 MHz, CDCl$_3$):	189.5 (C=O), 170.8 (C=O), 138.5 (q), 135.8, 135.2 (q), 131.8 (q), 130.5, 129.7, 129.4, 129.2, 128.7 (q), 127.3, 96.8 (q), 52.9, 49.7, 48.8, 16.1.
ν_{max} (neat)/cm^{-1}:	3001, 2956, 2924, 2851, 1741, 1698, 1596, 1550, 1491, 1438, 1290, 1255, 1166, 1091, 1004, 844, 795, 740.
HRMS (*m/z* - ESI):	Found: 372.0639 (M-H)$^-$ C$_{19}$H$_{15}$NO$_5$Cl Requires: 372.0639.

(1*R*,2*S*,3*S*)-Methyl 2-(4-methoxyphenyl)-3-methyl-3-nitro-4-oxo-1,2,3,4-tetrahydronaphthalene-1-carboxylate (*trans*-365, Table 4.8, entry 3)
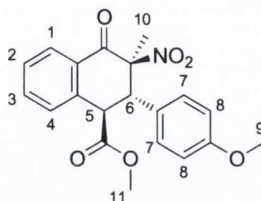
Prepared according to the consecutive use of general procedures XII and XIII, using β-methyl-(*E*)-nitroalkene **358** (47.5 mg, 0.246 mmol) and anhydride **147** (39.9 mg, 0.246 mmol). Upon epimerisation, the reaction gave a diastereomeric mixture of esters in a 96:4 (*trans:cis*) ratio. The major diastereomer (*trans*-365) was purified by flash column chromatography, eluting in gradient from 100% hexanes to 20% EtOAc in hexanes, to give a white solid (83.2 mg, 92%). M.p. 193-195 °C; TLC (hexanes:EtOAc, 8:2 *v/v*): R_f = 0.17; $[\alpha]_D^{20}$ = +81.0 (*c* = 0.10, CHCl$_3$).

CSP-HPLC analysis. Chiralpak AD-H (4.6 mm x 25 cm), hexane/IPA: 95/5, 1.0 mL min^{-1}, RT, UV detection at 254 nm, retention times: *trans*-365 22.7 min (minor enantiomer) and 41.0 min (major enantiomer); *cis*-365 10.9 min (major enantiomer) and 12.2 min (minor enantiomer).

δ_H (400 MHz, CDCl$_3$):	8.21 (1 H, d, *J* 7.9, H-1), 7.66 (1 H, app. t, H-3), 7.52 (1 H, app. t, H-2), 7.32 (1 H, d, *J* 7.8, H-4), 7.18 (2 H, d, *J* 8.2, H-7), 6.86 (2 H, d, *J* 8.2, H-8), 4.76 (1 H, d, *J* 12.4, H-6), 4.52 (1 H, d, *J* 12.4, H-5), 3.79 (3 H, s, H-9), 3.58 (3 H, s, H-11), 1.70 (3 H, s, H-10).
δ_C (100 MHz, CDCl$_3$):	190.1 (C=O), 171.1 (C=O), 159.9 (q), 139.0 (q), 135.6, 130.3, 129.6, 129.0, 128.9 (q), 127.3, 125.1 (q), 114.4, 97.2 (q), 55.3, 52.8, 49.7, 49.1, 16.1.
ν_{max} (neat)/cm^{-1}:	3000, 2960, 2927, 2849, 1739, 1693, 1595, 1550, 1513, 1438, 1385, 1344, 1294, 1250, 1182, 1107, 1027, 837, 796, 737.
HRMS (*m/z* - ESI):	Found: 368.1147 (M-H)$^-$ C$_{20}$H$_{18}$NO$_6$ Requires: 368.1134.

(1*R*,2*S*,3*S*)-Methyl 3-methyl-3-nitro-4-oxo-1,2,3,4-tetrahydro-[2,2'-binaphthalene]-1-carboxylate (*trans*-366, Table 4.8, entry 4)
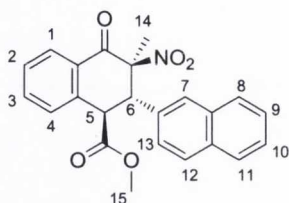
Prepared according to the consecutive use of general procedures XII and XIII, using β-methyl-(*E*)-nitroalkene **359** (52.5 mg, 0.246 mmol) and anhydride **147** (39.9 mg, 0.246 mmol). Upon epimerisation, the reaction gave a diastereomeric mixture of esters in a >99:1 (*trans*:*cis*) ratio. The major diastereomer (*trans*-**366**) was purified by flash column chromatography, eluting in gradient from 100% hexanes to 20% EtOAc in hexanes, to give a white solid (88.7 mg, 93%). M.p. 205-207 °C; TLC (hexanes:EtOAc, 8:2 *v/v*): R_f = 0.21; $[\alpha]_D^{20}$ = +116.3 (*c* = 0.10, CHCl$_3$).

CSP-HPLC analysis. Chiralcel OD-H (4.6 mm x 25 cm), hexane/IPA: 95/5, 1.0 mL min^{-1}, RT, UV detection at 254 nm, retention times: *trans*-**366** 19.8 min (minor enantiomer) and 22.6 min (major enantiomer); *cis*-**366** 10.5 min (major enantiomer) and 11.5 min (minor enantiomer).

δ_H (400 MHz, CDCl$_3$):	8.25 (1 H, d, *J* 7.9, H-1), 7.87-7.79 (3 H, m, H-8, H-11 and H-12), 7.74 (1 H, s, H-7), 7.69 (1 H, app. t, H-3), 7.59-7.47 (3 H, m, H-2, H-9 and H-10), 7.37 (2 H, app. d, H-4 and H-13), 5.0 (1 H, d, *J* 12.2, H-6), 4.72 (1 H, d, *J* 12.2, H-5), 3.52 (3 H, s, H-15), 1.78 (3 H, s, H-14).
δ_C (100 MHz, CDCl$_3$):	189.9 (C=O), 171.0 (C=O), 138.9 (q), 135.7, 133.4 (q), 133.3 (q), 130.8 (q), 129.7, 129.1, 128.9 (2 x C), 128.8 (q), 128.4, 127.8, 127.3, 126.9, 126.7, 126.3, 97.1 (q), 52.9, 50.4, 49.0, 16.4.
ν_{max} (neat)/cm^{-1}:	3063, 3029, 3009, 2955, 2924, 2850, 1729, 1691, 1599, 1548, 1392, 1346, 1289, 1201, 1159, 968, 820, 733.
HRMS (*m/z* - ESI):	Found: 388.1194 (M-H)$^-$ C$_{23}$H$_{18}$NO$_5$ Requires: 388.1185.

(1*R*,2*R*,3*S*)-Methyl 2-(furan-2-yl)-3-methyl-3-nitro-4-oxo-1,2,3,4-tetrahydronaphthalene-1-carboxylate (*trans*-367, Table 4.8, entry 5)
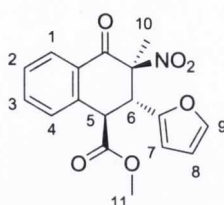
Prepared according to the consecutive use of general procedures XII and XIII, using β-methyl-(*E*)-nitroalkene **360** (37.7 mg, 0.246 mmol) and anhydride **147** (39.9 mg, 0.246 mmol). Upon epimerisation, the reaction gave a diastereomeric mixture of esters in a 93:7 (*trans*:*cis*) ratio. The major diastereomer (*trans*-367) was purified by flash column chromatography, eluting in gradient from 100% hexanes to 20% EtOAc in hexanes, to give a white solid (71.1 mg, 88%). M.p. 136-138 °C; TLC (hexanes:EtOAc, 8:2 *v/v*): R_f = 0.22; $[\alpha]_D^{20}$ = +20.3 (*c* = 0.20, CHCl$_3$).

CSP-HPLC analysis. Chiralpak AD-H (4.6 mm x 25 cm), hexane/IPA: 95/5, 1.0 mL min^{-1}, RT, UV detection at 254 nm, retention times: *trans*-367 11.7 min (minor enantiomer) and 15.7 min (major enantiomer); *cis*-367 8.7 min (major enantiomer) and 9.7 min (minor enantiomer).

δ_H (400 MHz, CDCl$_3$):	8.18 (1 H, d, *J* 7.9, H-1), 7.67 (1 H, app. t, H-3), 7.51 (1 H, app. t, H-2), 7.40 (1 H, app. s, H-9), 7.36 (1 H, d, *J* 7.8, H-4), 6.37-6.30 (1 H, m, H-8), 6.29-6.23 (1 H, m, H-7), 4.99 (1 H, d, *J* 12.0, H-6), 4.57 (1 H, d, *J* 12.0, H-5), 3.70 (3 H, s, H-11), 1.72 (3 H, s, H-10).
δ_C (100 MHz, CDCl$_3$):	189.2 (C=O), 171.0 (C=O), 148.1 (q), 143.6, 138.1 (q), 135.7, 129.6, 129.1, 128.8 (q), 127.4, 110.8, 110.5, 96.2 (q), 53.1, 47.5, 44.6, 16.8.
ν_{max} (neat)/cm^{-1}:	2954, 2923, 2852, 1732, 1694, 1598, 1549, 1436, 1347, 1293, 1206, 1160, 974, 920, 731.
HRMS (*m/z* - ESI):	Found: 328.0838 (M-H)$^-$ C$_{17}$H$_{14}$NO$_6$ Requires: 328.0821.

(1*R*,2*R*,3*S*)-Methyl 3-methyl-3-nitro-4-oxo-2-phenethyl-1,2,3,4-tetrahydronaphthalene-1-carboxylate (*trans*-368, Table 4.8, entry 6)
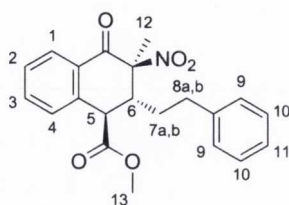
Prepared according to the consecutive use of general procedures XII and XIII, using β-methyl-(*E*)-nitroalkene **361** (47.0 mg, 0.246 mmol) and anhydride **147** (39.9 mg, 0.246 mmol). Upon epimerisation, the reaction gave a diastereomeric mixture of esters in a 89:11 (*trans:cis*) ratio. The major diastereomer (*trans*-**368**) was purified by flash column chromatography, eluting in gradient from 100% hexanes to 20% EtOAc in hexanes, to give a white solid (74.0 mg, 82%). M.p. 138-140 °C; TLC (hexanes:EtOAc, 8:2 *v/v*): R_f = 0.29; $[\alpha]_D^{20}$ = -38.8 (*c* = 0.20, CHCl$_3$).

CSP-HPLC analysis. Chiralpak IA (4.6 mm x 25 cm), hexane/IPA: 95/5, 1.0 mL min^{-1}, RT, UV detection at 254 nm, retention times: *trans*-**368** 11.8 min (major enantiomer) and 13.5 min (minor enantiomer); *cis*-**368** 9.8 min (minor enantiomer) and 13.9 min (major enantiomer).

δ_H (400 MHz, CDCl$_3$):	8.12 (1 H, d, *J* 7.9, H-1), 7.64 (1 H, app. t, H-3), 7.48 (1 H, app. t, H-2), 7.32-7.24 (3 H, m, H-4 and H-10), 7.20 (1 H, t, *J* 7.3, H-11), 7.11 (1 H, d, *J* 7.4, H-9), 3.94 (1 H, d, *J* 10.5, H-5), 3.82 (3 H, s, H-13), 3.75-3.66 (1 H, m, H-6), 2.57 (2 H, app. t, H-8a and H-8b), 1.82-1.64 (5 H, m, H-7a, H-7b and H-12).
δ_C (100 MHz, CDCl$_3$):	189.8 (C=O), 172.4 (C=O), 140.8 (q), 138.4 (q), 135.5, 129.2, 129.0 (q), 128.9, 128.7, 128.4, 127.8, 126.5, 96.4 (q), 53.0, 50.8, 43.4, 34.2, 32.8, 16.1.
ν_{max} (neat)/cm^{-1}:	3063, 3004, 2958, 2924, 2878, 1732, 1689, 1597, 1549, 1451, 1342, 1293, 1210, 1165, 999, 969, 752, 729.cm^{-1}.

HRMS (*m/z* - ESI):   Found: 390.1335 (M+Na)$^+$ C$_{21}$H$_{21}$NO$_5$Na Requires: 390.1317.

(1*R*,2*R*,3*S*)-Methyl 2-cyclohexyl-3-methyl-3-nitro-4-oxo-1,2,3,4-tetrahydronaphthalene-1-carboxylate (*trans*-369, Table 4.8, entry 7)
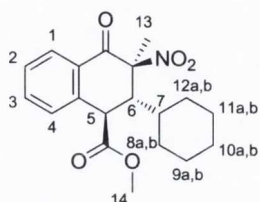
Prepared according to general procedure XII, using β-methyl-(*E*)-nitroalkene **362** (41.6 mg, 0.246 mmol), catalyst **348** (23.3 mg, 0.0492 mmol – 20 mol%) and anhydride **147** (39.9 mg, 0.246 mmol). Upon esterification, the reaction gave a diastereomeric mixture of esters in a 98:2 (*trans*:*cis*) ratio. The major diastereomer (*trans*-**369**) was isolated by flash column chromatography, eluting in gradient from 100% hexanes to 20% EtOAc in hexanes, to give a pale yellow oil which contained 17% of dimethyl homophthalate (**371**) as impurity that was not possible to separate. The given yield is calculated based on the mass return of the impure sample considering the spectroscopically determined amount of the known impurity (42.2 mg, 50%). TLC (hexanes:EtOAc, 8:2 *v/v*): R$_f$ = 0.38.

CSP-HPLC analysis. Chiralpak AD (4.6 mm x 25 cm), hexane/IPA: 90/10, 1.0 mL min^{-1}, RT, UV detection at 254 nm, retention times: *trans*-**369** 6.6 min (major enantiomer) and 7.4 min (minor enantiomer).

δ$_H$ (400 MHz, CDCl$_3$):   8.07 (1 H, d, *J* 7.7, H-1), 7.60 (1 H, app. t, H-3), 7.44 (1 H, app. t, H-2), 7.31 (1 H, d, *J* 7.8 H-4), 4.11 (1 H, d, *J* 8.8, H-5), 3.77 (3 H, s, H-14), 3.62-3.55 (1 H, m, H-6), 1.79-1.49 (8 H, m, H-8a, H-9a, H-10a, H-11a, H-12a and H-13), 1.48-1.36 (1 H, m, H-7), 1.35-0.95 (5 H, m, H-8b, H-9b, H-10b, H-11b, H-12b).

δ_C (100 MHz, CDCl$_3$):   189.8 (C=O), 172.9 (C=O), 138.9 (q), 135.2, 129.7 (q), 128.7, 128.6, 128.3, 96.7 (q), 52.9, 48.2, 45.5, 39.3, 33.9, 30.0, 27.2, 26.8, 26.1, 18.2.

ν_{max} (neat)/cm^{-1}:   2929, 2854, 1735, 1704, 1596, 1549, 1449, 1432, 1289, 1199, 1161, 1081, 967, 740.

HRMS (*m/z* - ESI):   Found: 344.1488 (M-H)$^-$ C$_{19}$H$_{22}$NO$_5$ Requires: 344.1498.

(1*R*,2*R*,3*S*)-Methyl 2-isopropyl-3-methyl-3-nitro-4-oxo-1,2,3,4-tetrahydronaphthalene-1-carboxylate (*trans*-370, Table 4.8, entry 8)
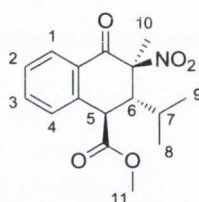
Prepared according to general procedure XII, using β-methyl-(*E*)-nitroalkene **363** (39.8 mg, 0.246 mmol) and anhydride **147** (39.9 mg, 0.246 mmol). Upon esterification, the reaction gave a diastereomeric mixture of esters in a >99:1 (*trans*:*cis*) ratio. The major diastereomer (*trans*-**370**) was isolated by flash column chromatography, eluting in gradient from 100% hexanes to 20% EtOAc in hexanes, to give a pale yellow oil which contained 3% of dimethyl homophthalate (**371**) as impurity that was not possible to separate. The given yield is calculated based on the mass return of the impure sample considering the spectroscopically determined amount of the known impurity (35.2 mg, 47%). TLC (hexanes:EtOAc, 8:2 *v/v*): R$_f$ = 0.37 [α]$_D^{20}$ = -53.4 (*c* = 0.20, CHCl$_3$).*

CSP-HPLC analysis. Chiralpak AD (4.6 mm x 25 cm), hexane/IPA: 90/10, 0.5 mL min^{-1}, RT, UV detection at 254 nm, retention times: *trans*-**370** 16.8 min (major enantiomer) and 17.7 min (minor enantiomer).

δ_H (400 MHz, CDCl$_3$):   8.08 (1 H, d, *J* 7.9, H-1), 7.61 (1 H, app. t, H-3), 7.45 (1 H, app. t, H-2), 7.30 (1 H, d, *J* 7.8, H-4), 4.08 (1 H, d, *J* 8.8, H-5), 3.77 (3 H, s, H-11), 3.71-3.63 (1 H, m, H-6), 1.87 (1 H,

m, H-7), 1.74 (3 H, s, H-10), 1.05 (3 H, d, *J* 7.0, H-8), 0.94 (3 H, d, *J* 7.0, H-9).

δ_C (100 MHz, CDCl$_3$):   189.8 (C=O), 172.8 (C=O), 138.9 (q), 135.2, 129.6 (q), 128.7, 128.6, 128.3, 96.7 (q), 52.9, 47.9, 45.2, 28.5, 23.6, 18.8, 17.9.

ν_{max} (neat)/cm^{-1}:   2970, 2894, 1737, 1697, 1599, 1550, 1453, 1386, 1288, 1158, 969, 792, 733, 659.

HRMS (*m/z* - ESI):   Found 304.1190 (M-H)$^-$ C$_{16}$H$_{18}$NO$_5$ Requires: 304.1185.

* $[\alpha]_D^{20}$ refers to *trans*-**370** containing 3% of **371** as impurity.

(1*R*,2*S*,3*S*)-Methyl 6-bromo-3-methyl-3-nitro-4-oxo-2-phenyl-1,2,3,4-tetrahydronaphthalene-1-carboxylate (*trans*-372, Table 4.10)
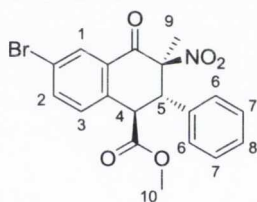
Prepared according to the consecutive use of general procedures XII and XIII, using β-methyl-(*E*)-nitrostyrene (**346**, 40.1 mg, 0.246 mmol) and anhydride **312** (59.3 mg, 0.246 mmol). Upon epimerisation, the reaction gave a diastereomeric mixture of esters in a >99:1 (*trans*:*cis*) ratio. The major diastereomer (*trans*-**372**) was purified by flash column chromatography, eluting in gradient from 100% hexanes to 20% EtOAc in hexanes, to give a white solid (94.9 mg, 92%). M.p. 68-70 °C; TLC (hexanes:EtOAc, 8:2 *v/v*): R$_f$ = 0.36; $[\alpha]_D^{20}$ = +72.2 (*c* = 0.20, CHCl$_3$).

CSP-HPLC analysis. Chiralpak IA (4.6 mm x 25 cm), hexane/IPA: 95/5, 1.0 mL min^{-1}, RT, UV detection at 254 nm, retention times: *trans*-**372** 14.7 min (minor enantiomer) and 18.8 min (major enantiomer); *cis*-**372** 8.0 min (minor enantiomer) and 8.6 min (major enantiomer).

δ_H (400 MHz, CDCl$_3$):	8.33 (1 H, d, J 2.1, H-1), 7.77 (1 H, dd, J 2.1, 8.3, H-2), 7.37-7.31 (3 H, m, H-6 and H-8), 7.26-7.20 (3 H, m, H-3 and H-7), 4.78 (1 H, d, J 12.0, H-5), 4.49 (1 H, d, J 12.0, H-4), 3.57 (3 H, s, H-10), 1.71 (3 H, s, H-9).
δ_C (100 MHz, CDCl$_3$):	188.8 (C=O), 170.6 (C=O), 138.4, 137.4 (q), 133.0 (q), 132.2, 130.4 (q), 129.3, 129.2 (2 C), 129.1, 123.4 (q), 96.6 (q), 53.0, 50.2, 48.6, 16.3.
ν_{max} (neat)/cm^{-1}:	3080, 3038, 2958, 1741, 1698, 1589, 1547, 1433, 1341, 1293, 1251, 1169, 990, 907, 756, 705.
HRMS (m/z - ESI):	Found: 416.0125 (M-H)$^-$ C$_{19}$H$_{15}$NO$_5$Br Requires: 416.0134.

(1S,2S,3S)-Methyl 6-bromo-3-methyl-3-nitro-4-oxo-2-phenyl-1,2,3,4-tetrahydronaphthalene-1-carboxylate (*cis*-372, Table 4.9)
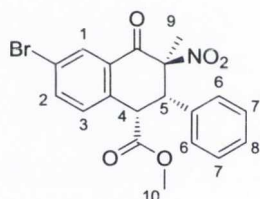
Prepared according to general procedure XII, using β-methyl-(*E*)-nitrostyrene (**346**, 40.1 mg, 0.246 mmol) and anhydride **312** (59.3 mg, 0.246 mmol). Upon esterification, the reaction gave a diastereomeric mixture of esters in a 58:42 (*trans*:*cis*) ratio. The minor diastereomer (*cis*-**372**) was purified by flash column chromatography, eluting in gradient from 100% hexanes to 20% EtOAc in hexanes, to give a white solid (36.1 mg, 35%). M.p. 185-186 °C; TLC (hexanes:EtOAc, 8:2 *v/v*): R$_f$ = 0.24; $[\alpha]_D^{20}$ = -69.7 (*c* = 0.20, CHCl$_3$).

CSP-HPLC analysis. Chiralpak IA (4.6 mm x 25 cm), hexane/IPA: 95/5, 1.0 mL min^{-1}, RT, UV detection at 254 nm, retention times: *cis*-**372** 8.0 min (minor enantiomer) and 8.6 min (major enantiomer).

δ_H (400 MHz, CDCl$_3$):	8.30 (1 H, d, *J* 1.5, H-1), 7.75 (1 H, dd, *J* 1.5, 8.5, H-2), 7.34 (1 H, d, *J* 8.5, H-3), 7.30-7.23 (1H, m, H-8), 7.20 (2 H, app. t, H-7), 6.93 (2 H, d, *J* 7.6, H-6), 4.64 (1 H, d, *J* 6.1, H-5), 4.47 (1 H, d, *J* 6.1, H-4), 3.45 (3 H, s, H-10), 1.62 (3 H, s, H-9).
δ_C (151 MHz, CDCl$_3$):	186.3 (C=O), 170.3 (C=O), 137.4, 135.6 (q), 133.7 (q), 133.3 (q), 132.8, 130.8, 129.5, 129.2, 129.1, 122.9 (q), 93.1 (q), 53.1, 52.4, 45.7, 21.6.
ν_{max} (neat)/cm^{-1}:	3088, 3000, 2948, 1745, 1705, 1593, 1543, 1433, 1196, 1176, 1003, 903, 836, 702.
HRMS (*m/z* - ESI):	Found: 416.0123 (M-H)$^-$ C$_{19}$H$_{15}$NO$_5$Br Requires: 416.0134.

(1*R*,2*S*,3*S*,4*S*)-Methyl 4-hydroxy-3-methyl-3-nitro-2-phenyl-1,2,3,4-tetrahydronaphthalene-1-carboxylate (*trans*-373, Scheme 4.7)
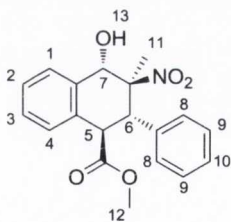
An oven-dried 10 mL round-bottomed flask containing a magnetic stirring bar was charged with *trans*-347 (83.5 mg, 0.246 mmol) and anhydrous MeOH (2.5 mL, 0.1 M) under argon atmosphere. To the mixture was added NaBH$_4$ (37.2 mg, 0.984 mmol) and the reaction was allowed to stir at room temperature for 16 h. The excess NaBH$_4$ was then quenched by addition of a saturated aqueous NH$_4$Cl solution (5 mL) followed by removal of MeOH under reduced pressure. The resulting aqueous mixture was then extracted with EtOAc (3 x 10 mL). The combined organic extracts were dried over anhydrous MgSO$_4$, filtered and the solvent was removed under reduced pressure to afford a crude diastereomeric mixture of product 373 in a >98:2 (*trans:cis*) ratio. The major diastereomer (*trans*-373) was purified by flash column chromatography, eluting in gradient from 100% hexanes to 20% EtOAc in hexanes, to give a white solid (76.6

mg, 91%). M.p. 197-195 °C; TLC (hexanes:EtOAc, 8:2 *v/v*): R_f = 0.27; $[\alpha]_D^{20}$ = +122.1 (*c* = 0.20, CHCl$_3$).

CSP-HPLC analysis. Chiralcel ODH (4.6 mm x 25 cm), hexane/IPA: 90/10, 1.0 mL min^{-1}, RT, UV detection at 254 nm, retention times: 9.2 min (major enantiomer) and 11.7 min (minor enantiomer).

δ_H (400 MHz, CDCl$_3$):*   7.68 (1 H, d, *J* 7.5, H-1), 7.44-7.37 (1 H, m, H-3), 7.36-7.29 (5 H, m, H-2, H-4, H-9 and H-10), 7.29-7.22 (2 H, m, H-8), 5.91 (1 H, s, H-7), 4.42 (1 H, d, *J* 11.8, H-5), 4.28 (1 H, d, *J* 11.8, H-6), 3.57 (3 H, s, H-12), 1.49 (3 H, s, H-11).

δ_C (100 MHz, CDCl$_3$):   172.3 (C=O), 136.4 (q), 134.4 (q), 130.9 (q), 129.1, 128.9, 128.8, 128.6, 128.5, 127.0, 126.5, 95.9 (q), 74.9, 52.7, 50.6, 50.0, 10.8.

ν_{max} (neat)/cm^{-1}:   3472, 3214, 1722, 1544, 1445, 1352, 1301, 1193, 1054, 989, 750, 702.

HRMS (*m/z* - APCI):   Found: 342.1336 (M+H)$^+$ C$_{19}$H$_{20}$NO$_5$ Requires: 342.1338.

* The protic signal (H-13) is not visible in CDCl$_3$.

7.5   Experimental procedures and data for Chapter 5

(2-Ethoxy-2-oxoethyl)triphenylphosphonium bromide (382)
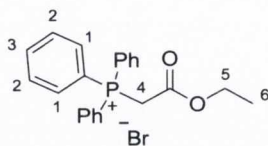
A 250 mL round-bottomed flask containing a magnetic stirring bar was charged with triphenylphosphine (**381**, 13.1 g, 50.0 mmol) and toluene (125 mL). To the mixture was then added *via* syringe ethyl bromoacetate (**380**, 5.5 mL, 50.0 mmol), the flask was fitted with a condenser and the reaction was heated at 90 °C for 15 h. The mixture was then cooled to room temperature and the solid formed was isolated by suction filtration, washed with diethyl ether (3 x 20 mL) and dried *in vacuo* to give product **382** as a white solid (20.3 g, 95%). M.p. 151-154 °C (lit.[335] m.p. 155-156 °C).

Spectral data for this compound were consistent with those in the literature.[336]

δ_H (400 MHz, CDCl$_3$):   7.88 (6 H, dd, *J* 7.8, 13.4, H-1), 7.78 (3 H, t, *J* 7.8, H-3), 7.71-7.61 (6 H, m, H-2), 5.53 (2 H, d, *J* 13.7, H-4), 4.02 (2 H, q, *J* 7.1, H-5), 1.05 (3 H, t, *J* 7.1, H-6).

(*E*)-Ethyl 2-(2-oxindolin-3-ylidene)acetate (385)
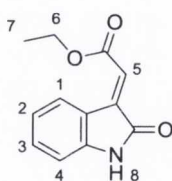
A 500 mL round-bottomed flask containing a magnetic stirring bar was charged with **382** (12.0 g, 28.0 mmol) and dichloromethane (100 mL). To the mixture was then added an aqueous solution of NaOH (1.0 M, 100 mL) and the reaction was allowed to stir vigorously at room temperature for 15 min. The organic layer was separated and the aqueous phase was extracted with dichloromethane (3 x 30 mL). The combined organic layers were dried over anhydrous MgSO$_4$, filtered and concentrated *in vacuo* to afford a residue containing the relative crude ylide (**383**, 9.6 g, 99%) which was dissolved in

toluene and transferred *via* syringe to a 250 mL round-bottomed flask containing a magnetic stirring bar. To the mixture was added isatin (**384**, 3.74 g, 25.4 mmol) and the reaction was allowed to stir at room temperature for 12 h. Volatiles were then removed under reduced pressure and the residue obtained was purified by flash column chromatography, eluting from 100% hexanes to 20% EtOAc in hexanes, to give **385** as an orange solid (5.18 g, 94%). M.p. 163-165 °C (lit.[337] m.p. 164-165 °C); TLC (hexanes:EtOAc, 8:2 *v/v*): R_f = 0.21.

Spectral data for this compound were consistent with those in the literature.[337]

δ_H (400 MHz, CDCl$_3$):   8.54 (1 H, d, *J* 7.8, H-1), 8.22 (1 H, bs, H-8), 7.32 (1 H, app. t, H-3), 7.05 (1 H, app. t, H-2), 6.88 (1 H, s, H-5), 6.85 (1 H, d, *J* 7.8, H-4), 4.33 (2 H, q, *J* 7.1, H-6), 1.37 (3 H, t, *J* 7.1, H-7).

(*E*)-*tert*-Butyl 3-(2-ethoxy-2-oxoethylidene)-2-oxindoline-1-carboxylate (378)
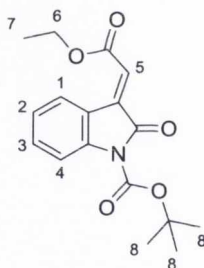
A 100 mL round-bottomed flask containing a magnetic stirring bar was charged with **385** (1.50 g, 6.91 mmol), DMAP (84.4 mg, 0.691 mmol – 10 mol%) and acetonitrile (30 mL) was added *via* syringe. To the mixture was then added a solution of (Boc)$_2$O (1.81 g, 8.29 mmol) in acetonitrile (10 mL) dropwise *via* syringe over 30 min, and the reaction was allowed to stir at room temperature for 15 h. The solvent was then removed *in vacuo* and the residue obtained was purified by flash column chromatography, eluting from 100% hexanes to 20% EtOAc in hexanes, to give **378** as a yellow solid (1.99 g, 91%). M.p. 64-65 °C (lit.[337] m.p. 65-67 °C); TLC (hexanes:EtOAc, 9:1 *v/v*): R_f = 0.49.

Spectral data for this compound were consistent with those in the literature.[337]

δ_H (400 MHz, CDCl$_3$):   8.68 (1 H, d, J 7.7, H-1), 7.91 (1 H, d, J 8.2, H-4), 7.43 (1 H, app. t, H-3), 7.19 (1 H, app. t, H-2), 6.92 (1 H, s, H-5), 4.33 (2 H, q, J 7.1, H-6), 1.65 (9 H, s, H-8), 1.37 (3 H, t, J 7.1, H-7).

Benzyltriphenylphosphonium bromide (425)
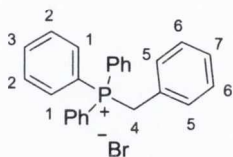
A 250 mL round-bottomed flask containing a magnetic stirring bar was charged with triphenylphosphine (**381**, 13.1 g, 50.0 mmol) and toluene (125 mL). To the mixture was then added benzyl bromide (**424**, 6.0 mL, 50.0 mmol) *via* syringe, the flask was fitted with a condenser and the reaction was heated at 90 °C for 15 h. The mixture was then cooled to room temperature and the solid formed was isolated by suction filtration, washed with diethyl ether (3 x 20 mL) and dried *in vacuo* to give **425** as a white solid (20.2 g, 93%). M.p. 239-242 °C (lit.[338] m.p. 241 °C).

Spectral data for this compound were consistent with those in the literature.[338]

δ_H (400 MHz, CDCl$_3$):   7.81-7.68 (9 H, m, H-1 and H-3), 7.66-7.57 (6 H, m, H-2), 7.24-7.17 (1 H, m, H-7), 7.15-7.04 (4 H, m, H-5 and H-6), 5.39 (2 H, d, J 14.4, H-4).

3-Benzylideneindolin-2-one (427)
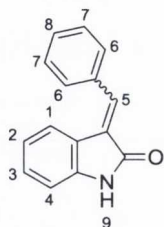
An oven-dried 250 mL round-bottomed flask containing a magnetic stirring bar under argon atmosphere was charged with **425** (4.42 g, 10.2 mmol). Anhydrous THF (70 mL) was then added *via* syringe and the solution was cooled to 0 °C. A solution of butyl lithium (2.5 M in hexanes, 4.1 mL, 10.2 mmol) was added dropwise *via* syringe and the reaction was allowed to stir for 1 h to allow for the formation of **426**. A solution of isatin (**384**, 1.50 g, 10.2 mmol) in dry THF (70 mL) was added dropwise *via* syringe over 30 min at 0 °C and the resulting solution was allowed to stir at room temperature for 15 h. The reaction mixture was then poured into a saturated solution of NH_4Cl (70 mL) at 0 °C and extracted with dichloromethane (3 x 50 mL). The combined organic layers were dried over anhydrous $MgSO_4$, filtered and concentrated *in vacuo* to afford a residue containing a *E/Z* mixture (ca. 4:1) of product **427** that was separated by flash column chromatography, eluting from 100% hexanes to 30% EtOAc in hexanes, to give (*E*)-**427** (1.54 g, 68%) and (*Z*)-**427** (358.6 mg, 68%) as yellow solids.

Spectral data for these compounds were consistent with those in the literature.[339]

(*E*)-427:

M.p 175-177 °C (lit[339] m.p. 178-179 °C); TLC (hexanes:EtOAc, 8:2 *v/v*): R_f = 0.14.

δ_H (400 MHz, CDCl$_3$):   8.85 (1 H, bs, H-9), 7.85 (1 H, s, H-5), 7.67 (2 H, d, *J* 7.9, H-6), 7.64 (1 H, d, *J* 7.8, H-1), 7.51-7.39 (3 H, m, H-7 and H-8), 7.22 (1 H, app. t, H-3), 6.93 (1 H, d, *J* 7.8, H-4), 6.87 (1 H, app. t, H-2).

(*Z*)-427:

M.p 173-175 °C (lit[339] m.p. 172-173 °C); TLC (hexanes:EtOAc, 8:2 *v/v*): R_f = 0.25.

δ_H (400 MHz, CDCl$_3$):   8.27 (2 H, m, H-6), 7.56 (1 H, s, H-5), 7.54 (1 H, d, *J* 7.7, H-1), 7.50-7.38 (4 H, m, H-7, H-8 and H-9), 7.23 (1 H, app. t, H-3), 7.05 (1 H, app. t, H-2), 6.83 (1 H, d, *J* 7.8, H-4).

(*E*)-*tert*-Butyl 3-benzylidene-2-oxindoline-1-carboxylate (423)
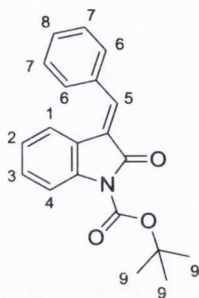
This product can be synthesised according to the following procedure by the reaction of either (*E*) or (*Z*) isomers of **427** with (Boc)$_2$O under the same conditions. Reported here is the reaction involving the use of (*E*)-**427**.

A 100 mL round-bottomed flask containing a magnetic stirring bar was charged with (*E*)-**427** (1.22 g, 5.50 mmol), DMAP (67.2 mg, 0.550 mmol - 10 mol%) and acetonitrile (30 mL) was added *via* syringe. To the mixture was then added a solution of (Boc)$_2$O (1.44 g, 6.60 mmol) in acetonitrile (10 mL) dropwise *via* syringe over 30 min, and the reaction was allowed to stir at room temperature for 15 h. The solvent was removed *in vacuo* and the residue obtained was purified by recrystallisation from EtOH to furnish **423** as a yellow solid (1.44 g, 79%). M.p. 107-108 °C (lit.[340] m.p. 96-98 °C). The yield for the reaction involving (*Z*)-**427** was (77%).

Spectral data for this compound were consistent with those in the literature.[340]

δ_H (400 MHz, CDCl$_3$):   7.91 (1 H, d, *J* 8.3, H-4), 7.88 (1 H, s, H-5), 7.66 (1 H, d, *J* 7.7, H-1), 7.62 (2 H, d, *J* 6.9, H-6), 7.51-7.40 (3 H, m, H-7 and H-8), 7.30 (1 H, app. t, H-3), 6.98 (1 H, app. t, H-2), 1.67 (9 H, s, H-9).

HRMS (*m/z* - ESI):   Found: 344.1266 (M+Na)$^+$ C$_{20}$H$_{19}$NO$_3$Na Requires: 344.1263.

Ethyl 2-(2-ethoxy-2-oxoethyl)thiophene-3-carboxylate (395)
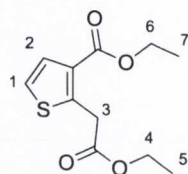
A 250 mL round-bottomed flask containing a magnetic stirring bar was charged with 1,4-dithiane-2,5-diol (**393**, 2.00 g, 13.1 mmol), diethyl 3-oxopentanedioate (**394**, 7.2 mL, 39.4 mmol), LiBr (342.5 mg, 1.31 mmol) and 1,4-dioxane (60 mL). The flask was fitted with a condenser and the mixture was heated at reflux temperature for 16 h. The reaction was then cooled to room temperature and the solvent removed under reduced pressure to give a residue that was purified by flash column chromatography, eluting from 100% hexanes to 20% EtOAc in hexanes, to give **395** as a pale yellow oil (2.73 g, 86%). TLC (hexanes:EtOAc, 8:2 *v/v*): $R_f = 0.59$.

δ_H (400 MHz, CDCl$_3$):   7.45 (1 H, d, *J* 5.4, H-1), 7.14 (1 H, d, *J* 5.4, H-2), 4.30 (2 H, q, *J* 7.1, H-6), 4.23-4.15 (4 H, m, H-3 and H-4), 1.35 (3 H, t, *J* 7.1, H-7), 1.27 (3 H, t, *J* 7.1, H-5).

δ_C (100 MHz, CDCl$_3$):   170.0 (C=O), 163.3 (C=O), 143.7 (q), 129.9 (q), 129.2, 123.1, 61.2, 60.5, 34.7, 14.3, 14.2.

ν_{max} (neat)/cm^{-1}:   2982, 2937, 2903, 1737, 1706, 1537, 1447, 1372, 1333, 1259, 1180, 1135, 1025, 843, 712.

HRMS (*m/z* - ESI):   Found: 265.0502 (M+Na)$^+$ C$_{11}$H$_{14}$O$_4$NaS Requires: 265.0511.

2-(Carboxymethyl)thiophene-3-carboxylic acid (396)
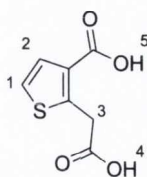
A 100 mL round-bottomed flask containing a magnetic stirring bar was charged with **395** (2.70 g, 11.1 mmol) and EtOH (10 mL). A solution of KOH (3.75g, 66.9 mmol) in EtOH:H$_2$O 1:1 (20 mL) was then added to the mixture. The flask was fitted with a condenser and the reaction was heated at reflux temperature for 5 h and then cooled to room temperature. EtOH was removed *in vacuo* and the aqueous solution obtained was adjusted to pH = 2 by addition of concentrated HCl. The solid obtained was isolated by suction filtration, washed with small amount of cold water (10 mL) and dried *in vacuo* to give **396** as a white solid (2.03 g, 98%). M.p. 201-203 °C (lit.[303] m.p. 207-209 °C).

Spectral data for this compound were consistent with those in the literature.[303]

δ_H (400 MHz, DMSO-d$_6$):   12.58 (2 H, bs, H-4 and H-5), 7.40 (1 H, d, *J* 5.4, H-1), 7.33
(1 H, d, *J* 5.4, H-2), 4.14 (2 H, s, H-3).

δ_C (100 MHz, DMSO-d$_6$):   171.1 (C=O), 164.2 (C=O), 144.4 (q), 130.2 (q), 128.8,
123.9, 34.0.

HRMS (*m/z* - ESI):   Found: 184.9901 (M-H)$^-$ C$_7$H$_5$O$_4$S Requires: 184.9909.

Ethyl 2-(2-ethoxy-2-oxoethyl)-1,4-dimethyl-1*H*-pyrrole-3-carboxylate (398)
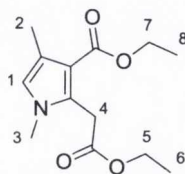
To a 250 mL round-bottomed flask containing a magnetic stirring bar and 40% aqueous CH$_3$NH$_2$ (15.0 mL), diethyl 3-oxopentanedioate (**394**, 3.6 mL, 20.0 mmol) was rapidly added *via* syringe at 15 °C with formation of a white precipitate. To the mixture was then slowly added chloroacetone (**397**, 3.3 mL, 40.0 mmol) at a rate to maintain the

reaction temperature below 40 °C. The mixture was allowed to stir at room temperature for 1 h and poured into ice-HCl (30 mL). The precipitate formed was collected by suction filtration, washed with cold water (2 x 10 mL) and dried *in vacuo* to furnish a residue that was purified by flash column chromatography, eluting from 100% hexanes to 20% EtOAc in hexanes, to give **398** as white solid (4.11 g, 81%). M.p. 64-66 °C (lit.[304] m.p. 71-73 °C); TLC (hexanes:EtOAc, 8:2 *v/v*): R_f = 0.35.

δ_H (400 MHz, CDCl$_3$):　　　6.33 (1 H, s, H-1), 4.25 (2 H, q, *J* 7.1, H-7), 4.16 (2 H, q, *J* 7.1, H-5), 4.03 (2 H, s, H-4), 3.50 (3 H, s, H-3), 2.21 (3 H, s, H-2), 1.32 (3 H, t, *J* 7.1, H-8), 1.26 (3 H, t, *J* 7.1, H-6).

δ_C (100 MHz, CDCl$_3$):　　　170.3 (C=O), 165.9 (C=O), 131.7 (q), 121.3, 120.8 (q), 112.7 (q), 61.2, 59.3, 33.9, 31.6, 14.6, 14.4, 12.6.

v_{max} (neat)/cm^{-1}:　　　2986, 2976, 2914, 1724, 1671, 1519, 1477, 1422, 1341, 1269, 1189, 1151, 1087, 1037, 769.

HRMS (*m/z* - ESI):　　　Found: 276.1200 (M+Na)$^+$ C$_{13}$H$_{19}$NO$_4$Na Requires: 276.1212.

2-(Carboxymethyl)-1,4-dimethyl-1*H*-pyrrole-3-carboxylic acid (399)
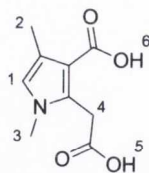
In a 25 mL round-bottomed flask containing a magnetic stirring bar, a 25% (*w/v*) aqueous solution of NaOH (8.5 mL) was mixed with **398** (850.0 mg, 3.36 mmol). The flask was fitted with a condenser and the reaction was heated at reflux temperature for 3 h and then cooled to room temperature. The solution obtained was adjusted to pH = 2 by addition of concentrated HCl and the solid formed was isolated by suction filtration, washed with a small amount of cold water (5 mL) and dried *in vacuo* to give **399** as an off white solid (647.7 mg, 98%). M.p. 223-225 °C (lit.[304] m.p. 220-222 °C).

δ_H (400 MHz, DMSO-d$_6$):   11.97 (2 H, bs, H-5 and H-6), 6.49 (1 H, s, H-1), 3.97 (2 H, s, H-4), 3.44 (3 H, s, H-3), 2.09 (3 H, s, H-2).

δ_C (100 MHz, DMSO-d$_6$):   171.3 (C=O), 166.6 (C=O), 132.6 (q), 121.0, 118.9 (q), 111.8 (q), 33.2, 30.9, 12.4.

ν_{max} (neat)/cm^{-1}:   3067, 2966, 2718, 2609, 2545, 1680, 1629, 1516, 1432, 1335, 1275, 1235, 1160, 1084, 963, 844, 767, 667.

HRMS (*m/z* - ESI):   Found: 196.0606 (M-H)$^-$ C$_9$H$_{10}$NO$_4$ Requires: 196.0610.

Ethyl 6-methyl-2-oxo-4-phenyl-2*H*-pyran-5-carboxylate (402)
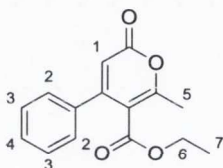
In a 100 mL round-bottomed flask containing a magnetic stirring bar ethyl 3-phenylpropiolate (**400**, 3.0 g, 17.2 mmol) and ethyl 3-oxobutanoate (**401**, 2.2 mL, 17.2 mmol) were dissolved in 1,4-dioxane (33 mL). After the addition of NaOH (137.6. mg, 1.72 mmol – 20 mol%), the flask was fitted with a condenser and the reaction mixture was heated at 90 °C for 16 h. The mixture was then cooled to room temperature, diluted with water (60 mL) and extracted with EtOAc (3 x 30 mL). The combined organic phases were dried over anhydrous MgSO$_4$ and the solvent was evaporated under reduced pressure to give a residue that was purified by flash column chromatography in gradient from 100% hexanes to 20% EtOAc in hexanes furnishing **402** as a white solid (2.9 g, 65%). M.p. 86-88 °C (lit.[305] m.p. 95-96 °C); TLC (hexanes:EtOAc, 8:2 *v/v*): R$_f$ = 0.41.

Spectral data for this compound were consistent with those in the literature.[305]

δ_H (400 MHz, CDCl$_3$):   7.45-7.37 (3 H, m, H-2 and H-4), 7.32-7.24 (2 H, m, H-3), 6.16 (1 H, s, H-1), 3.97 (2 H, q, *J* 7.1, H-6), 2.46 (3 H, s, H-5), 0.87 (3 H, t, *J* 7.1, H-7).

δ_C (100 MHz, CDCl$_3$):   165.9 (C=O), 164.7 (C=O), 160.9 (q), 156.2 (q), 137.3 (q), 129.6, 128.8, 126.8, 113.0 (q), 111.9, 61.7, 19.1, 13.5.

(*E*)-3-Phenylpent-2-enedioic acid (403)

In a 100 mL round-bottomed flask containing a magnetic stirring bar **402** (2.10 g, 8.13 mmol) was added to water (30 mL). After the addition of NaOH (1.63 g, 40.7 mmol) the flask was fitted with a condenser and the reaction mixture was heated at 80 °C for 5 h. The mixture was then cooled to room temperature and the resulting aqueous solution was washed with diethyl ether (2 x 15 mL). The aqueous layer was adjusted to pH = 2 by addition of concentrated HCl and extracted with diethyl ether (3 x 20 mL). The combined organic extracts were dried over anhydrous MgSO$_4$, filtered and concentrated *in vacuo* to give a residue that was triturated with a small amount of diethyl ether (5 mL) to furnish **403** as an off white solid (1.31 g, 78%). M.p. 134-136 °C.

δ_H (400 MHz, DMSO-d$_6$):   12.36 (2 H, bs, H-6 and H-7), 7.54-7.48 (2 H, m, H-3), 7.45-7.35 (3 H, m, H-2 and H-4), 6.22 (1 H, s, H-1), 4.11 (2 H, s, H-5).

δ_C (100 MHz, DMSO-d$_6$):   171.3 (C=O), 167.2 (C=O), 150.4 (q), 140.2 (q), 129.2, 128.7, 126.4, 119.8, 35.8.

ν_{max} (neat)/cm^{-1}:   3114, 2911, 2617, 2542, 1677, 1608, 1402, 1289, 1213, 876, 769, 682.

HRMS (*m/z* - ESI):   Found: 161.0603 (M-COOH)$^-$ C$_{10}$H$_9$O$_2$ Requires: 161.0603.

Ethyl 4,6-dimethyl-2-oxo-2*H*-pyran-5-carboxylate (404)
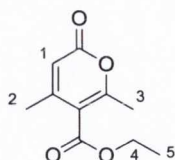
In a 100 mL round-bottomed flask containing a magnetic stirring bar was added concentrated H_2SO_4 (10 mL) *via* syringe and the reaction was cooled to 10 °C. Ethyl 3-oxobutanoate (**401**, 13.3 g, 102 mmol) was added dropwise *via* syringe at a rate to maintain the reaction temperature below 15 °C and the mixture was allowed to stir at room temperature for 72 h. The reaction was poured into ice (30 g) and extracted with diethyl ether (3 x 50 mL). The combined organic phases were washed with 10% aqueous Na_2CO_3 (1 x 50 mL), dried over anhydrous $MgSO_4$, filtered and the solvent was evaporated *in vacuo* to give a residue that was purified by flash column chromatography in gradient from 100% hexanes to 20% EtOAc in hexanes furnishing **404** as a pale yellow oil (4.24 g, 42%). TLC (hexanes:EtOAc, 8:2 *v/v*): $R_f = 0.31$.

Spectral data for this compound were consistent with those in the literature.[190]

δ_H (400 MHz, CDCl$_3$):   6.01 (1 H, s, H-1), 4.34 (2 H, q, *J* 7.1, H-4), 2.40 (3 H, s, H-3), 2.22 (2 H, s, H-2), 1.37 (3 H, t, *J* 7.1, H-5).

HRMS (*m/z* -ESI):   Found: 195.0653 (M-H)$^-$ C$_{10}$H$_{11}$O$_4$ Requires: 195.0657.

3-Methylpent-2-enedioic acid (405)
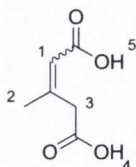
In a 100 mL round-bottomed flask containing a magnetic stirring bar **404** (4.0 g, 20.4 mmol) was added to water (50 mL). After the addition of NaOH (4.08 g, 102 mmol) the flask was fitted with a condenser and the reaction mixture was heated at 80 °C for 5 h. The mixture was then cooled to room temperature and the resulting aqueous solution was washed with diethyl ether (2 x 25 mL). The aqueous layer was adjusted to pH = 2

by addition of concentrated HCl and extracted with diethyl ether (3 x 30 mL). The combined organic extracts were dried over anhydrous $MgSO_4$, filtered and concentrated *in vacuo* to give a residue that was triturated with a small amount of diethyl ether (5 mL) to furnish **405** as mixture of (*E*) and (*Z*) isomers (72:28) as an off white solid (2.20 g, 75%). M.p.* 103-105 °C (lit.[190] m.p. 101-105 °C).

Spectral data for these compounds were consistent with those in the literature.[190]

(*E*)-405:

δ_H (400 MHz, DMSO-d_6):   12.23 (2 H, bs, H-4 and H-5), 5.70 (1 H, s, H-1), 3.12 (2 H, s, H-3), 2.10 (3 H, s, H-2).

δ_C (100 MHz, DMSO-d_6):   171.4 (C=O), 167.2 (C=O), 151.3 (q), 119.5, 45.1, 18.5.

(*Z*)-405:

δ_H (400 MHz, DMSO-d_6):   12.23 (2 H, bs, H-4 and H-5), 5.75 (1 H, s, H-1), 3.63 (2 H, s, H-3), 1.89 (3 H, s, H-2).

δ_C (100 MHz, DMSO-d_6):   171.3 (C=O), 167.0 (C=O), 151.3 (q), 119.0, 37.8, 25.2.

* Refers to a mixture of (*E*) and (*Z*) isomers (72:28).

(Buta-1,3-dien-2-yloxy)trimethylsilane (408)
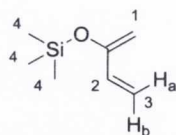
An oven-dried 500 mL three-necked round-bottomed flask containing a magnetic stirring bar under argon atmosphere was charged with of *N,N*-dimethylformamide (DMF, 120 mL) and triethylamine (33 mL, 235 mmol). The flask was fitted with a condenser and the mixture was heated at 90 °C. At this temperature a solution of methyl vinyl ketone (**406**, 18 mL, 214 mmol) in DMF (15 mL) and a solution of trimethylsilyl chloride (**407**, 30 mL, 235 mmol) in DMF (15 mL) were simultaneously added dropwise to the reaction over 30 min and the mixture was allowed to stir for 15 h. The

reaction was then cooled to room temperature and directly filtered into a separation funnel containing hexanes (200 mL), and a cold 5% aqueous solution of $NaHCO_3$ (600 mL). The organic layer was separated and the aqueous phase was extracted with hexanes (2 x 200 mL). The combined organic layers were dried over anhydrous $MgSO_4$, filtered and the volatiles were removed by fractional distillation at atmospheric pressure at 70 °C (oil bath). Vacuum was then applied (68 mbar) and product **408** was distilled as a colourless oil (13.1 g, 43%). B.p. 40-45 °C at 68 mbar (lit.[341] b.p. 42-44 °C at 70 mbar).

Spectral data for this compound were consistent with those in the literature.[341]

δ_H (400 MHz, $CDCl_3$):   6.20 (1 H, dd, *J* 10.5, 16.9, H-2), 5.47 (1 H, dd, *J* 1.7, 16.9, H-3a), 5.12-5.05 (1 H, app. d, H-3b), 5.39-5.32 (2 H, m, H-1), 0.23 (9 H, s, H-4).

Diethyl penta-2,3-dienedioate (410)
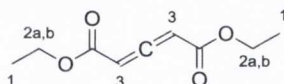
An oven-dried 100 mL round-bottomed flask containing a magnetic stirring bar under argon atmosphere was charged with 2-chloro-1,3-dimethylimidazolinium chloride (DMC, **409**, 2.68 g, 15.9 mmol). Dry dichloromethane (50 mL) and ethyl 3-oxobutanoate (**394**, 2.4 mL, 13.2 mmol) were then added *via* syringe and the solution was cooled to 0 °C. To the mixture was then added triethylamine (5.5 mL, 39.6 mmol) dropwise *via* syringe and the reaction was allowed to stir for 30 min at room temperature. The mixture was then concentrated under reduced pressure, and the residue obtained was purified by flash column chromatography, eluting from 100% hexanes to 20% EtOAc in hexanes furnishing **410** as a pale yellow oil (1.87 g, 77%). TLC (hexanes:EtOAc, 8:2 *v/v*): R_f = 0.50.

Spectral data for this compound were consistent with those in the literature.[307]

δ_H (400 MHz, $CDCl_3$):   6.03 (2 H, s, H-3), 4.24 (4 H, dq, *J* 2.6, 7.1, H-2a and H-2b), 1.30 (6 H, t, *J* 7.1, H-1).

δ_C (100 MHz, CDCl$_3$):   219.6 (C=O), 163.6 (q), 92.6, 61.8, 14.3.

HRMS (*m/z* - ESI):   Found: 207.0632 (M+Na)$^+$ C$_9$H$_{12}$O$_4$Na Requires: 207.0633.

(*E*)-Ethyl 2-(2-ethoxy-2-oxoethylidene)-4-oxocyclohexanecarboxylate (411)
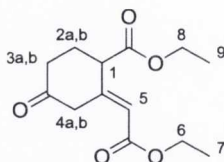
An oven-dried 50 mL round-bottomed flask containing a magnetic stirring bar under argon atmosphere was charged with **408** (1.70 g, 9.23 mmol) and **410** (3.28 g, 23.1 mmol). Acetonitrile (17 mL) was then added *via* syringe and the mixture was heated at reflux temperature for 6 h. The reaction was cooled to room temperature and concentrated under reduced pressure. The residue obtained was dissolved in THF (160 mL), transferred *via* syringe to a 500 mL round-bottomed flask and cooled to 0 °C. A 10% aqueous solution of HCl (32 mL) was then added dropwise *via* syringe and allowed to stir at the same temperature for 1 h. The excess of acid was neutralised with a 10% aqueous solution of NaOH and the mixture was extracted with EtOAc (3 x 50 mL). The combined organic phases were dried over anhydrous MgSO$_4$, filtered and the solvent was evaporated *in vacuo* to give a residue that was purified by flash column chromatography, eluting in gradient from 100% hexanes to 20% EtOAc in hexanes furnishing **411** as a pale yellow oil (1.13 g, 48%). TLC (hexanes:EtOAc, 8:2 v/v): R$_f$ = 0.24.

Spectral data for this compound were consistent with those in the literature.[177]

δ_H (400 MHz, CDCl$_3$):   6.02 (1 H, s, H-5), 4.24-4.12 (4 H, m, H-6 and H-8), 3.60-3.52 (1 H, m, H-1), 3.45 (1 H, d, *J* 16.1, H-4a), 3.29 (1 H, d, *J* 16.1, H-4b), 2.66-2.50 (1 H, m, H-2a), 2.47-2.34 (2 H, m, H-2b and H-3b), 2.31-2.18 (1 H, m, H-3b), 1.33-1.23 (6 H, m, H-7 and H-9).

δ_C (100 MHz, CDCl$_3$):   198.3 (C=O), 171.2 (C=O), 169.5 (C=O), 152.5 (q), 130.7, 61.7, 61.5, 44.2, 42.2, 34.5, 26.2, 14.3, 14.2.

HRMS (*m/z* - ESI):   Found: 277.1065   (M+Na)$^+$ $C_{13}H_{18}O_5Na$ Requires: 277.1052.

Ethyl 7-(2-ethoxy-2-oxoethyl)-1,4-dioxaspiro[4.5]dec-7-ene-8-carboxylate (413)
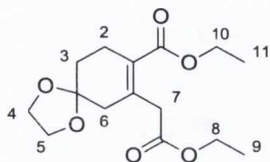
In a 100 mL round-bottomed flask containing a magnetic stirring bar, **411** (1.06 g, 4.17 mmol), ethylene glycol (**412**, 349 µL, 6.25 mmol) and *p*-TSA (158.6 mg, 0.834 mmol) were mixed together in toluene (30 mL). The flask was then fitted with a Dean-Stark apparatus for azeotropic removal of water and the reaction was heated at reflux temperature for 5 h. The mixture was then cooled to room temperature, diluted with toluene (30 mL) and washed with 5% aqueous solution of NaHCO$_3$ (30 mL). The organic phase was separated, dried over anhydrous MgSO$_4$, filtered and concentrated under reduced pressure to afford a residue that was dissolved in THF (50 mL) and transferred *via* syringe to a 250 mL round-bottomed flask containing a magnetic stirring bar. To the solution was then added triethylamine (50 mL) *via* syringe and the reaction was heated at reflux temperature for 18 h. The mixture was then cooled to room temperature, concentrated *in vacuo* and partitioned between toluene (100 mL) and water (20 mL). The organic layer was separated, dried over anhydrous MgSO$_4$, filtered and the solvent was removed under reduced pressure to give a residue that was purified by flash column chromatography, eluting in gradient from 100% hexanes to 20% EtOAc in hexanes furnishing **413** as a colourless oil (937.9 mg, 75%). TLC (hexanes:EtOAc, 8:2 *v/v*): R$_f$ = 0.24.

Spectral data for this compound were consistent with those in the literature.[177]

δ$_H$ (400 MHz, CDCl$_3$):   4.17 (2 H, q, *J* 7.1, H-10), 4.15 (2 H, q, *J* 7.1, H-8), 3.99 (4 H, app. s, H-4 and H-5), 3.47 (2 H, s, H-7), 2.59 (2 H, t, *J* 6.5, H-2), 2.48 (2 H, s, H-6), 1.79 (2 H, t, *J* 6.5, H-3), 1.27 (3 H, t, *J* 7.1, H-11), 1.26 (3 H, t, *J* 7.1, H-9).

δ_C (100 MHz, CDCl$_3$): 170.8 (C=O), 167.6 (C=O), 139.7 (q), 127.2 (q), 107.2 (q), 64.6 (2 x C), 60.8, 60.5, 42.6, 40.5, 30.7, 25.8, 14.4, 14.3.

HRMS (*m/z* - ESI): Found: 299.1505 (M+H)$^+$ C$_{15}$H$_{23}$O$_6$ Requires: 299.1495.

7-(Carboxymethyl)-1,4-dioxaspiro[4.5]dec-7-ene-8-carboxylic acid (414)
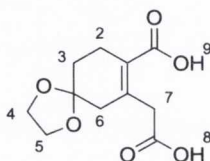
In a 100 mL round-bottomed flask containing a magnetic stirring bar, **413** (800.0 mg, 2.68 mmol) was dissolved in a mixture (3:1) of EtOH (24 mL) and water (8.0 mL). KOH (601.9 mg, 10.7 mmol) was then added to the mixture and the reaction mixture was heated at reflux temperature for 3 h. The mixture was then cooled to room temperature, concentrated under reduced pressure and the resulting aqueous solution was adjusted to pH = 3 by addition of a 10% aqueous solution of HCl and extracted with diethyl ether (3 x 30 mL). The combined organic extracts were dried over anhydrous MgSO$_4$, filtered and concentrated *in vacuo* to give a residue that was triturated with a small amount of diethyl ether (5 mL) to furnish **413** as an off white solid (578.9 mg, 89%). M.p. 132-134 °C (lit.[177] m.p. 137.5-138.5 °C).

Spectral data for this compound were consistent with those in the literature.[177]

δ_H (600 MHz, DMSO-d$_6$):* 3.99 (4 H, app. s, H-4 and H-5), 3.46 (2 H, s, H-7), 2.61 (2 H, t, *J* 6.5, H-2), 2.52 (2 H, s, H-6), 1.79 (2 H, t, *J* 6.5, H-3).

δ_C (151 MHz, DMSO-d$_6$): 175.5 (C=O), 172.4 (C=O), 143.6 (q), 126.7 (q), 106.9 (q), 64.7 (2 x C), 44.0, 41.3, 30.6, 25.3.

HRMS (*m/z* - ESI): Found: 265.0681 (M+Na)$^+$ C$_{11}$H$_{14}$O$_6$Na Requires: 265.0688.

* The protic signals (H-8 and H-9) are not visible in DMSO-d$_6$.

General procedure XIV: Synthesis of anhydride 389-391, 238 and 232

In an oven-dried 25 mL round-bottomed flask containing a magnetic stirring bar under argon atmosphere was added the relevant *bis*-acid precursor (300.0 mg) of the desired anhydride. Freshly distilled acetyl chloride (10 mL) was then added *via* syringe. The flask was fitted with a condenser and the reaction was heated at reflux temperature for 16 h. The mixture was then cooled to room temperature and the volatiles were removed under reduced pressure to afford the crude anhydride that was purified by rapid flash column chromatography (hexanes:EtOAc, 2:1 *v/v*) to furnish the desired compound.

4*H*-Thieno[3,2-*c*]pyran-4,6(7*H*)-dione (389)
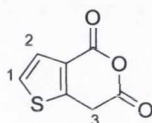
Synthesised according to general procedure XIV, using **396** as *bis*-acid precursor (300.0 mg, 1.61 mmol). After purification, **389** was obtained as a pale brown solid (224.1 mg, 83%). M.p. 152-154 °C.

δ_H (400 MHz, DMSO-d_6):   7.66 (1 H, d, *J* 5.3, H-1), 7.45 (1 H, d, *J* 5.3, H-2), 4.42 (2 H, s, H-3).

δ_C (100 MHz, DMSO-d_6):   165.5 (C=O), 156.6 (C=O), 149.0 (q), 127.3, 125.0, 124.5 (q), 32.6.

ν_{max} (neat)/cm^{-1}:   3110, 3092, 2949, 2904, 1780, 1735, 1548, 1409, 1386, 1326, 1265, 1162, 1034, 961, 872, 714.

HRMS (*m/z* - ESI):   Found: 166.9805 (M-H)$^-$ $C_7H_3O_3S$ Requires: 166.9803.

1,3-Dimethylpyrano[4,3-*b*]pyrrole-4,6(1*H*,7*H*)-dione (390)
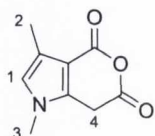
Synthesised according to general procedure XIV, using **400** as *bis*-acid precursor (300.0 mg, 1.52 mmol). After purification, **390** was obtained as an off white solid (221.7 mg, 81%). M.p. 174-176°C (lit.[342] m.p. 162-165 °C).

Spectral data for this compound were consistent with those in the literature.[342]

δ_H (400 MHz, DMSO-d_6):   6.71 (1 H, s, H-1), 4.17 (2 H, s, H-4), 3.50 (3 H, s, H-3), 2.15 (3 H, s, H-2).

δ_C (100 MHz, DMSO-d_6):   166.3 (C=O), 157.4 (C=O), 136.9 (q), 123.4, 118.4 (q), 104.2 (q), 33.2, 29.7, 10.4.

HRMS (*m/z* - ESI):   Found: 180.0662 (M+H)$^+$ $C_9H_{10}NO_3$ Requires: 180.0661.

4-Phenyl-2*H*-pyran-2,6(3*H*)-dione (391)
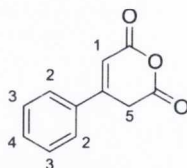
Synthesised according to general procedure XIV, using **404** as *bis*-acid precursor (300.0 mg, 1.45 mmol). After purification, **391** was obtained as a white solid (140.3 mg, 51%). M.p. 198-201°C (lit.[343] m.p. 193-195 °C).

Spectral data for this compound were consistent with those in the literature.[343]

δ_H (400 MHz, DMSO-d_6):   7.81 (2 H, d, *J* 7.2, H-2), 7.58-7.45 (3 H, m, H-3 and H-4), 6.80 (1 H, s, H-1), 4.16 (2 H, s, H-5).

δ_C (100 MHz, DMSO-d_6):   166.2 (C=O), 161.4 (C=O), 154.1 (q), 134.0 (q), 131.5, 129.0, 126.7, 110.8, 33.4.

HRMS (*m/z* - ESI):   Found: 189.0553 (M+H)$^+$ $C_{11}H_9O_3$ Requires: 189.0552.

4-Methyl-2*H*-pyran-2,6(3*H*)-dione (238)
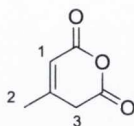
Synthesised according to general procedure XIV, using **406** as *bis*-acid precursor (300.0 mg, 2.08 mmol). After purification, **238** was obtained as a white solid (116.1 mg, 44%). M.p. 78-82 °C (lit.[190] m.p. 79-83 °C).

Spectral data for this compound were consistent with those in the literature.[190]

δ_H (400 MHz, DMSO-d$_6$):   6.09 (1 H, s, H-1), 3.64 (2 H, s, H-3), 1.97 (3 H, s, H-2).

δ_C (100 MHz, DMSO-d$_6$):   166.3 (C=O), 160.8 (C=O), 159.2 (q), 112.6, 36.4, 21.5.

7',8'-Dihydrospiro[[1,3]dioxolane-2,6'-isochromene]-1',3'(4'*H*,5'*H*)-dione (232)
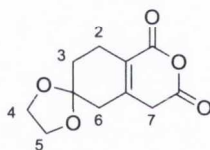
Synthesised according to general procedure XIV, using **414** as *bis*-acid precursor (300.0 mg, 1.24 mmol). After purification, **232** was obtained as a white solid (225.8 mg, 81%). M.p. 178-180 °C (lit.[177] m.p. 181-184 °C).

Spectral data for this compound were consistent with those in the literature.[177]

δ_H (400 MHz, CDCl$_3$):   4.00 (4 H, app. s, H-4 and H-5), 3.40 (2 H, s, H-7), 2.66-2.57 (2 H, m, H-2), 2.44 (2 H, s, H-6), 1.85 (2 H, t, *J* 6.5, H-3).

δ_C (100 MHz, CDCl$_3$):   164.6 (C=O), 160.7 (C=O), 146.7 (q), 122.1 (q), 106.5 (q), 64.9 (2 x C), 39.9, 36.3, 30.7, 22.9.

HRMS (*m/z* - ESI):   Found: 225.0771 (M+H)$^{+}$ $C_{11}H_{13}O_5$ Requires: 225.0763.

General procedure XV: Racemic preparation of products 386, 387, 415-419, 428-430

An oven-dried 10 mL reaction vessel containing a magnetic stirring bar under argon atmosphere was charged with the relevant anhydride (0.246 mmol). Anhydrous MTBE (2.5 mL, 0.1 M) was added *via* syringe followed by the appropriate oxindole (0.246 mmol). *N,N*-Diisopropylethylamine (8.6 µL, 0.0492 mmol - 20 mol%) was added *via* syringe and the resulting mixture was allowed to stir for 18 h at room temperature. To the reaction mixture containing the corresponding carboxylic acids, anhydrous MeOH (750 µL, 18.5 mmol), followed by trimethylsilyldiazomethane (2.0 M solution in diethyl ether, 150 µL, 0.300 mmol) were added *via* syringe and the reaction was allowed to stir for 30 min at room temperature. The crude mixture was then directly loaded onto a flash chromatographic column and two diastereomers were chromatographically isolated together eluting in gradient of EtOAc from 100% hexanes.

General procedure XVI: Catalyst evaluation in the organocatalysed cycloaddition of homophthalic anhydride (147) to oxindole 378 and effect of variation of the temperature on the reaction (Table 5.2 and Table 5.3)

An oven-dried 10 mL reaction vessel containing a magnetic stirring bar under argon atmosphere was charged with the oxindole **378** (78.1 mg, 0.246 mmol). Anhydrous MTBE (2.5 mL, 0.1 M) was added *via* syringe followed by the relevant catalyst (0.0123 mmol - 5 mol%) and the mixture was brought to the equilibrated temperature reported in Table 5.2 and Table 5.3, while stirring. Homophthalic anhydride (**147**, 39.9 mg, 0.246 mmol) was then added to the mixture and the reaction was allowed to stir for the time indicated in Table 5.2 and Table 5.3. Anhydrous MeOH (750 µL, 18.5 mmol), followed by trimethylsilyldiazomethane (2.0 M solution in diethyl ether, 150 µL, 0.300 mmol), were then added *via* syringe (at the same temperature at which the reaction was conducted) to the mixture that was allowed to stir for 30 min. The crude reaction mixture containing the diastereomeric esters was then directly loaded onto the silica

column and the two diastereomers were chromatographically isolated together eluting in gradient from 100% hexanes to 20% EtOAc in hexanes. The diastereomeric ratio and the enantiomeric excess of the product formed were then determined by CSP-HPLC using the conditions indicated.

CSP-HPLC analysis. Chiralpak AD-H (4.6 mm x 25 cm), hexane/IPA: 95/5, 1.0 mL min^{-1}, RT, UV detection at 254 nm, retention times: *trans*-**386** 16.8 min (minor enantiomer) and 28.0 min (major enantiomer); *cis*-**386** 23.4 min (minor enantiomer) and 31.5 min (major enantiomer); diastereomer (C) 18.3 min (minor enantiomer) and 23.3 min (major enantiomer).

General procedure XVII: **Substrate evaluation in the organocatalysed cycloaddition of aromatic anhydrides to oxindoles 378 and 423 (Table 5.4, Table 5.5 and Table 5.6)**

An oven-dried 10 mL reaction vessel containing a magnetic stirring bar under argon atmosphere was charged with the relevant oxindole (0.246 mmol). Anhydrous MTBE (2.5 mL, 0.1 M) was added *via* syringe followed by catalyst **348** (5.8 mg, 0.0123 mmol - 5 mol%) and the mixture was brought to the equilibrated temperature reported in Table 5.4, Table 5.5 and Table 5.6, while stirring. The relevant anhydride (0.246 mmol) was added to the mixture and the reaction was allowed to stir for the time indicated in Table 5.4, Table 5.5 and Table 5.6. Anhydrous MeOH (750 μL, 18.5 mmol), followed by trimethylsilyldiazomethane (2.0 M solution in diethyl ether, 150 μL, 0.300 mmol), were added *via* syringe (at the same temperature at which the reaction was conducted) to the mixture that was allowed to stir for 30 min. The crude reaction mixture containing the diastereomeric esters was then directly loaded onto the silica column and the two diastereomers were chromatographically isolated together eluting in gradient of EtOAc from 100% hexanes to the ratio indicated by the TLC solvent system reported in each case. The diastereomeric ratio and the enantiomeric excess of the product formed were determined by CSP-HPLC using the conditions indicated in each case. The major diastereomer produced in the reaction was then purified by the employment of an automated flash chromatographic purification system (Biotage SP4) using two high performance prepacked silica cartridges (Biotage SNAP 10 g) connected in series,

eluting the mixture in gradient of EtOAc from 100% hexanes according the following developed method.

Flow: 15 mL/min; Unit: CV = column volume = 15 mL = 1 min.

Gradient: 100% hexanes for 2 CV; 5% EtOAc in hexanes for 2 CV; from 5% EtOAc in hexanes to 30% EtOAc in hexanes in 10 CV; 30% EtOAc in hexanes for 5 CV; from 30% EtOAc in hexanes to 40% EtOAc in hexanes in 5 CV; 40% EtOAc in hexanes for 5 CV.

General procedure XVIII: Substrate evaluation in the organocatalysed cycloaddition of substituted glutaconic anhydrides to oxindoles 378 and 423 (Table 5.5 and Table 5.6)

An oven-dried 10 mL reaction vessel containing a magnetic stirring bar under argon atmosphere was charged with the relevant oxindole (0.246 mmol). Anhydrous MTBE (2.5 mL, 0.1 M) was added *via* syringe followed by catalyst **348** (5.8 mg, 0.0123 mmol - 5 mol%) and warmed at the equilibrated temperature of 30 °C, while stirring. The relevant anhydride (0.246 mmol) was added to the mixture and the reaction was allowed to stir for the time indicated in Table 5.5 and Table 5.6. The crude reaction mixture containing the diastereomeric product was directly loaded onto the silica column and the two diastereomers were chromatographically isolated together eluting in gradient of EtOAc from 100% hexanes to the ratio indicated by the TLC solvent system reported in each case. The diastereomeric ratio and the enantiomeric excess of the product formed were determined by CSP-HPLC using the conditions indicated in each case. The major diastereomer produced in the reaction was then purified by the employment of an automated flash chromatographic purification system (Biotage SP4) using two high performance prepacked silica cartridges (Biotage SNAP 10 g) connected in series, eluting the mixture in gradient of EtOAc from 100% hexanes according the following developed method.

Flow: 15 mL/min; Unit: CV = column volume = 15 mL = 1 min.

Gradient: 100% hexanes for 2 CV; 5% EtOAc in hexanes for 2 CV; from 5% EtOAc in hexanes to 30% EtOAc in hexanes in 10 CV; 30% EtOAc in hexanes for 5 CV; from

30% EtOAc in hexanes to 40% EtOAc in hexanes in 5 CV; 40% EtOAc in hexanes for 5 CV.

(2'*R*,3'*R*,4'*R*)-1-*tert*-Butyl 3'-ethyl 4'-methyl 1',2-dioxo-3',4'-dihydro-1'*H*-spiro[indoline-3,2'-naphthalene]-1,3',4'-tricarboxylate (*trans*-386, Table 5.5, entry 1)
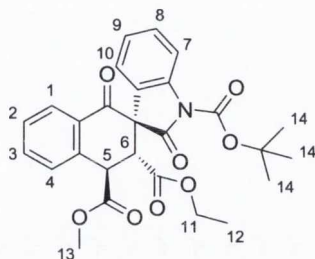
Synthesised according to general procedure XVII by reaction of oxindole **378** (78.1 mg, 0.246 mmol) with anhydride **147** (39.9 mg, 0.246 mmol) at 30 °C. After purification (Biotage SP4), *trans*-**386** was isolated as a white solid (111.8 mg, 92%). M.p. 66-68 °C; TLC (hexanes:EtOAc, 8:2 *v/v*): R_f = 0.26; $[\alpha]_D^{20}$ = +251.8 (*c* = 0.20, CHCl$_3$).

CSP-HPLC analysis. Chiralpak IA (4.6 mm x 25 cm), hexane/IPA: 95/5, 1.0 mL min^{-1}, RT, UV detection at 254 nm, retention times: 12.7 min (minor enantiomer) and 22.5 min (major enantiomer).

δ_H (400 MHz, CDCl$_3$):   8.04 (1 H, d, *J* 7.9, H-1), 7.97 (1 H, d, *J* 8.2, H-7), 7.68 (1 H, app. t, H-3), 7.59 (1 H, d, *J* 7.9, H-4), 7.46 (1 H, app. t, H-2), 7.31 (1 H, app. t, H-8), 6.98 (1 H, app. t, H-9), 6.86 (1 H, d, *J* 7.6, H-10), 4.76 (1 H, d, *J* 11.8, H-5), 4.64 (1 H, d, *J* 11.8, H-6), 4.00-3.82 (5 H, m, H-11 and H-13), 1.67 (9 H, s, H-14), 0.97 (3 H, t, *J* 7.1, H-12).

δ_C (100 MHz, CDCl$_3$):   190.7 (C=O), 173.2 (C=O), 172.0 (C=O), 169.5 (C=O), 149.2 (C=O), 141.4 (q), 137.5 (q), 135.6, 129.9, 129.5 (q), 129.4, 128.9, 127.1, 125.2 (q), 124.5, 123.0, 116.2, 84.7 (q), 62.1, 61.4 (q), 53.0, 47.6, 44.3, 28.2, 13.4.

v_{max} (neat)/cm^{-1}: 2983, 1775, 1731, 1681, 1598, 1478, 1345, 1284, 1241, 1147, 1097, 1014, 845, 751.

HRMS (*m/z* - ESI): Found: 516.1635 (M+Na)$^+$ C$_{27}$H$_{27}$NO$_8$Na Requires: 516.1634.

(2'*R*,3'*S*,4'*R*)-1-*tert*-Butyl 3'-ethyl 4'-methyl 1',2-dioxo-3',4'-dihydro-1'*H*-spiro[indoline-3,2'-naphthalene]-1,3',4'-tricarboxylate (*cis*-386, Table 5.5, entry 2)
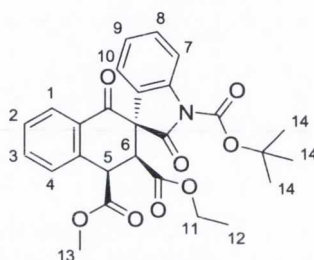
Synthesised according to general procedure XVII by reaction of oxindole **378** (78.1 mg, 0.246 mmol) with anhydride **147** (39.9 mg, 0.246 mmol) at -30 °C. After purification (Biotage SP4), *cis*-**386** was isolated as a white solid (90.3 mg, 74%). M.p. 68-70 °C; TLC (hexanes:EtOAc, 8:2 *v/v*): R$_f$ = 0.16; [α]$_D^{20}$ = -55.0 (*c* = 0.20, CHCl$_3$).

CSP-HPLC analysis. Chiralpak IA (4.6 mm x 25 cm), hexane/IPA: 95/5, 1.0 mL min^{-1}, RT, UV detection at 254 nm, retention times: 21.8 min (minor enantiomer) and 24.8 min (major enantiomer).

δ$_H$ (400 MHz, CDCl$_3$): 8.01 (1 H, d, *J* 7.6, H-1), 7.93 (1 H, d, *J* 8.2, H-7), 7.67 (1 H, app. t, H-3), 7.51-7.43 (2 H, m, H-2 and H-4), 7.35 (1 H, app. t, H-8), 7.09 (1 H, app. t, H-9), 6.88 (1 H, d, *J* 7.5, H-10), 4.68 (1 H, d, *J* 5.8, H-5), 4.10 (2 H, q, *J* 7.2, H-11), 3.96 (1 H, d, *J* 5.8, H-6), 3.74 (3 H, s, H-13), 1.60 (9 H, s, H-14), 1.14 (3 H, t, *J* 7.2, H-12).

δ$_C$ (151 MHz, CDCl$_3$): 190.7 (C=O), 171.3 (C=O), 170.0 (C=O), 168.9 (C=O), 149.1 (C=O), 141.7 (q), 138.5 (q), 134.5, 130.8, 130.7 (q), 129.5, 129.0 (q), 128.9, 128.8, 124.6, 121.8, 115.6, 84.4 (q), 61.8, 60.8 (q), 52.9, 49.6, 45.2, 28.2, 13.8.

ν_{max} (neat)/cm^{-1}:	2983, 2953, 1731, 1680, 1601, 1481, 1347, 1245, 1147, 1095, 840, 751.
HRMS (*m/z* - ESI):	Found: 516.1628 (M+Na)$^+$ $C_{27}H_{27}NO_8Na$ Requires: 516.1634.

(2′*R*,3′*R*,4′*R*)-1-*tert*-Butyl 3′-ethyl 4′-methyl 7′-bromo-1′,2-dioxo-3′,4′-dihydro-1′*H*-spiro[indoline-3,2′-naphthalene]-1,3′,4′-tricarboxylate (*trans*-387, Table 5.5, entry 3)
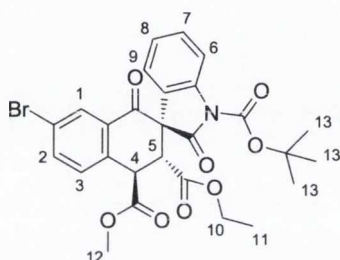
Synthesised according to general procedure XVII by reaction of oxindole **378** (78.1 mg, 0.246 mmol) with anhydride **312** (59.3 mg, 0.246 mmol) at 30 °C. After purification (Biotage SP4), *trans*-**387** was isolated as a white solid (133.6 mg, 95%). M.p. 80-82 °C; TLC (hexanes:EtOAc, 8:2 *v/v*): R_f = 0.30; $[\alpha]_D^{20}$ = +141.0 (*c* = 0.20, CHCl$_3$).

CSP-HPLC analysis. Chiralpak AD-H (4.6 mm x 25 cm), hexane/IPA: 95/5, 1.0 mL min^{-1}, RT, UV detection at 254 nm, retention times: 13.6 min (minor enantiomer) and 33.1 min (major enantiomer).

δ_H (400 MHz, CDCl$_3$):	8.14 (1 H, d, *J* 2.1, H-1), 7.98 (1 H, d, *J* 8.3, H-6), 7.88 (1 H, dd, *J* 2.1, 8.5, H-2), 7.49 (1 H, d, *J* 8.5, H-3), 7.33 (1 H, app. t, H-7), 6.99 (1 H, app. t, H-8), 6.83 (1 H, d, *J* 7.5, H-9), 4.67 (1 H, d, *J* 11.7, H-4), 4.60 (1 H, d, *J* 11.7, H-5), 4.00-3.82 (5 H, m, H-10 and H-12), 1.68 (9 H, s, H-13), 0.97 (3 H, t, *J* 7.2, H-11).
δ_C (100 MHz, CDCl$_3$):	189.5 (C=O), 172.8 (C=O), 171.5 (C=O), 169.3 (C=O), 149.1 (C=O), 141.3 (q), 138.4, 136.2 (q), 132.0, 131.1 (q),

130.1, 129.0, 124.7 (q), 124.6, 123.4 (q), 123.0, 116.3, 84.9 (q), 62.3, 61.2 (q), 53.2, 47.4, 44.0, 28.3, 13.5.

ν_{max} (neat)/cm^{-1}:   2983, 2953, 1775, 1732, 1685, 1588, 1478, 1345, 1291, 1222, 1147, 1015, 837, 755.

HRMS (*m/z* - ESI):   Found: 594.0735 (M+Na)$^+$ C$_{27}$H$_{26}$NO$_8$BrNa Requires: 594.0739.

(2'R,3'S,4'R)-1-*tert*-Butyl 3'-ethyl 4'-methyl 7'-bromo-1',2-dioxo-3',4'-dihydro-1'H-spiro[indoline-3,2'-naphthalene]-1,3',4'-tricarboxylate (*cis*-387, Table 5.5, entry 4)
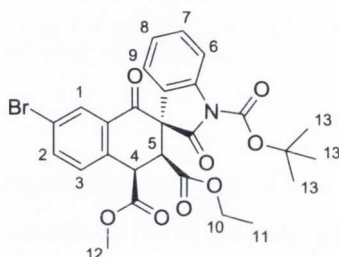
Synthesised according to general procedure XVII by reaction of oxindole **378** (78.1 mg, 0.246 mmol) with anhydride **312** (53.9 mg, 0.246 mmol) at -30 °C. After purification (Biotage SP4), *cis*-**387** was isolated as a white solid (102.7 mg, 73%). M.p. 84-86 °C; TLC (hexanes:EtOAc, 8:2 *v/v*): R$_f$ = 0.20; [α]$_D^{20}$ = -29.5 (*c* = 0.20, CHCl$_3$).

CSP-HPLC analysis. Chiralpak AD-H (4.6 mm x 25 cm), hexane/IPA: 95/5, 1.0 mL min^{-1}, RT, UV detection at 254 nm, retention times: 26.9 min (minor enantiomer) and 35.4 min (major enantiomer).

δ_H (400 MHz, CDCl$_3$):   8.12 (1 H, d, *J* 2.1, H-1), 7.93 (1 H, d, *J* 8.2, H-6), 7.77 (1 H, dd, *J* 2.1, 8.3, H-2), 7.39-7.33 (2 H, m, H-3 and H-7), 7.10 (1 H, app. t, H-8), 6.86 (1 H, d, *J* 7.4, H-9), 4.63 (1 H, d, *J* 5.8, H-4), 4.10 (2 H, q, *J* 7.2, H-10), 3.92 (1 H, d, *J* 5.8, H-5), 3.74 (3 H, s, H-12), 1.60 (9 H, s, H-13), 1.14 (3 H, t, *J* 7.2, H-11).

δ_C (151 MHz, CDCl$_3$):   189.5 (C=O), 170.9 (C=O), 169.5 (C=O), 168.7 (C=O), 148.9 (C=O), 141.6 (q), 137.3, 137.2 (q), 132.5, 132.1 (q), 131.5, 129.7, 128.3 (q), 124.7, 123.0 (q), 121.9, 115.7, 84.6 (q), 62.0, 60.6 (q), 53.0, 49.3, 44.7, 28.2, 13.8.

ν_{max} (neat)/cm^{-1}:   2983, 2949, 1733, 1683, 1590, 1480, 1345, 1243, 1146, 1008, 833, 751.

HRMS (*m/z* - ESI):   Found: 594.0738 (M+Na)$^+$ C$_{27}$H$_{26}$NO$_8$BrNa Requires: 594.0739.

(3'*R*,6*R*,7*S*)-1'-*tert*-Butyl 6-ethyl 7-methyl 2',4-dioxo-6,7-dihydro-4*H*-spiro[benzo[*b*]thiophene-5,3'-indoline]-1',6,7-tricarboxylate (*trans*-415, Table 5.5, entry 5)
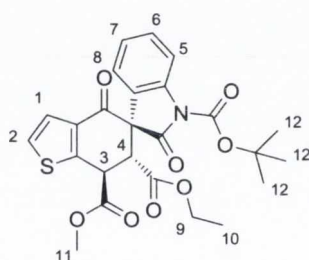
Synthesised according to general procedure XVII by reaction of oxindole **378** (78.1 mg, 0.246 mmol) with anhydride **389** (41.4 mg, 0.246 mmol) at 30 °C. After purification (Biotage SP4), *trans*-**415** was isolated as a white solid (111.6 mg, 91%). M.p. 144-147 °C; TLC (hexanes:EtOAc, 8:2 *v/v*): R$_f$ = 0.25; [α]$_D^{20}$ = +284.5 (*c* = 0.20, CHCl$_3$).

CSP-HPLC analysis. Chiralpak AD-H (4.6 mm x 25 cm), hexane/IPA: 95/5, 1.0 mL min^{-1}, RT, UV detection at 254 nm, retention times: 15.7 min (minor enantiomer) and 24.1 min (major enantiomer).

δ_H (400 MHz, CDCl$_3$):   7.96 (1 H, d, *J* 8.2, H-5), 7.40 (1 H, d, *J* 5.4, H-2), 7.33 (1 H, app. t, H-6), 7.28 (1 H, d, *J* 5.4, H-1), 7.02 (1 H, app. t, H-7), 6.91 (1 H, d, *J* 7.5, H-8), 4.86 (1 H, d, *J* 11.2, H-3), 4.66 (1 H, d, *J* 11.2, H-4), 3.97-3.81 (5 H, m, H-9 and H-11), 1.68 (9 H, s, H-12), 0.96 (3 H, t, *J* 7.1, H-10).

257

δ_C (100 MHz, CDCl$_3$): 185.0 (C=O), 173.1 (C=O), 170.3 (C=O), 169.1 (C=O), 149.6 (q), 149.2 (C=O), 141.2 (q), 134.9 (q), 130.1, 126.6, 126.4, 125.1 (q), 124.6, 122.9, 116.2, 84.8 (q), 62.2, 61.9 (q), 53.4, 48.7, 42.3, 28.3, 13.5.

ν_{max} (neat)/cm^{-1}: 3088, 2993, 2960, 1769, 1728, 1673, 1603, 1526, 1479, 1346, 1264, 1171, 1145, 1095, 1019, 888, 836, 770, 744, 717.

HRMS (*m/z* - ESI): Found: 522.1107 (M+Na)$^+$ C$_{25}$H$_{25}$NO$_8$NaS Requires: 522.1199.

(3'R,6R,7R)-1'-*tert*-Butyl 6-ethyl 7-methyl 1,3-dimethyl-2',4-dioxo-1,4,6,7-tetrahydrospiro[indole-5,3'-indoline]-1',6,7-tricarboxylate (*trans*-416, Table 5.5, entry 6)
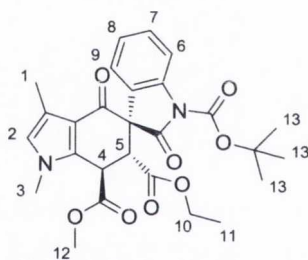
Synthesised according to general procedure XVII by reaction of oxindole **378** (78.1 mg, 0.246 mmol) with anhydride **390** (44.1 mg, 0.246 mmol) at 30 °C. After purification (Biotage SP4), *trans*-**416** was isolated as a white solid (119.5 mg, 95%). M.p. 82-84 °C; TLC (hexanes:EtOAc, 7:3 *v/v*): R$_f$ = 0.14; [α]$_D^{20}$ = +314.0 (*c* = 0.20, CHCl$_3$).

CSP-HPLC analysis. Chiralpak AD-H (4.6 mm x 25 cm), hexane/IPA: 95/5, 1.0 mL min^{-1}, RT, UV detection at 254 nm, retention times: 27.1 min (major enantiomer) and 33.8 min (minor enantiomer).

δ_H (400 MHz, CDCl$_3$): 7.95 (1 H, d, *J* 8.2, H-6), 7.31-7.25 (1 H, m, H-7), 6.99 (1 H, app. t, H-8), 6.82 (1 H, dd, *J* 1.0, 7.5, H-9), 6.41 (1 H, s,

H-2), 4.61 (1 H, d, *J* 10.7, H-4), 4.53 (1 H, d, *J* 10.7, H-5), 3.94-3.80 (5 H, m, H-10 and H-12), 3.60 (3 H, s, H-3), 2.16 (3 H, s, H-1), 1.65 (9 H, s, H-13), 0.96 (3 H, t, *J* 7.2, H-11).

δ_C (100 MHz, CDCl$_3$):	186.3 (C=O), 174.0 (C=O), 171.3 (C=O), 169.3 (C=O), 149.3 (C=O), 141.4 (q), 135.5 (q), 129.5, 126.3 (q), 125.1, 124.2, 122.8, 120.8 (q), 118.0 (q), 115.9, 84.4 (q), 62.3 (q), 62.1, 53.2, 50.2, 40.9, 34.9, 28.2, 13.4, 11.2.
ν_{max} (neat)/cm^{-1}:	2983, 2932, 1773, 1730, 1658, 1478, 1345, 1292, 1250, 1146, 1009, 840, 757.
HRMS (*m/z* - ESI):	Found: 509.1918 (M-H)$^-$ C$_{27}$H$_{29}$N$_2$O$_8$ Requires: 509.1924.

(2*R*,3*R*)-1'-*tert*-Butyl 3-ethyl 1,2'-dioxo-5-phenylspiro[cyclohex[5]ene-2,3'-indoline]-1',3-dicarboxylate (*trans*-417, Table 5.5, entry 7)
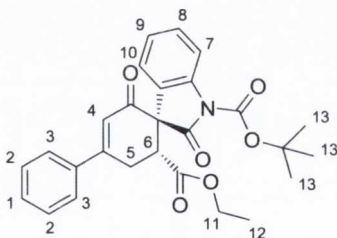
Synthesised according to general procedure XVIII by reaction of oxindole **378** (78.1 mg, 0.246 mmol) with anhydride **391** (46.3 mg, 0.246 mmol). After purification (Biotage SP4), *trans*-**417** was isolated as a white solid (106.5 mg, 94%). M.p. 121-123 °C; TLC (hexanes:EtOAc, 8:2 *v/v*): R$_f$ = 0.33; [α]$_D^{20}$ = +228.0 (*c* = 0.20, CHCl$_3$).

CSP-HPLC analysis. Chiralpak AD-H (4.6 mm x 25 cm), hexane/IPA: 90/10, 1.0 mL min^{-1}, RT, UV detection at 254 nm, retention times: 21.4 min (major enantiomer) and 36.8 min (minor enantiomer).

δ_H (400 MHz, CDCl$_3$):	7.96 (1 H, d, *J* 8.2, H-7), 7.75-7.66 (2 H, m, H-2), 7.55-7.46 (3 H, m, H-1 and H-3), 7.33 (1 H, app. t, H-8), 7.12-7.02 (2 H, m, H-9 and H-10), 6.60 (1 H, s, H-4), 4.07 (1 H,

dd, *J* 7.8, 9.9, H-6), 4.02-3.86 (2 H, m, H-11), 3.48-3.41 (2 H, m, H-5), 1.67 (9 H, s, H-13), 1.00 (3 H, t, *J* 7.2, H-12).

δ_C (100 MHz, CDCl$_3$):   192.4 (C=O), 174.1 (C=O), 170.0 (C=O), 157.4 (q), 149.2 (C=O), 141.3 (q), 137.3 (q), 131.3, 129.6, 129.3, 126.5, 125.7 (q), 124.5, 123.6, 122.9, 116.1, 84.6 (q), 61.7, 60.9 (q), 45.1, 28.3, 27.2, 13.6.

ν_{max} (neat)/cm^{-1}:   2983, 2932, 1777, 1737, 1722, 1652, 1606, 1477, 1350, 1247, 1152, 1093, 1006, 895, 845, 759, 706.

HRMS (*m/z* - ESI):   Found: 460.1754 (M-H)$^-$ C$_{27}$H$_{26}$NO$_6$ Requires: 460.1760.

(1*R*,6*R*)-1'-*tert*-Butyl 6-ethyl 4-methyl-2,2'-dioxospiro[cyclohex[3]ene-1,3'-indoline]-1',6-dicarboxylate (*trans*-418, Table 5.5, entry 8)
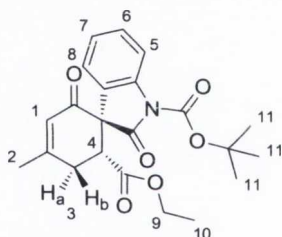
Synthesised according to general procedure XVIII by reaction of oxindole **378** (78.1 mg, 0.246 mmol) with anhydride **238** (31.0 mg, 0.246 mmol). After purification (Biotage SP4), *trans*-**418** was isolated as a white solid (93.6 mg, 95%). M.p. 45-47 °C; TLC (hexanes:EtOAc, 8:2 *v/v*): R$_f$ = 0.19; [α]$_D^{20}$ = +181.5 (*c* = 0.20, CHCl$_3$).

CSP-HPLC analysis. Chiralpak IA (4.6 mm x 25 cm), hexane/IPA: 95/5, 1.0 mL min^{-1}, RT, UV detection at 254 nm, retention times: 18.8 min (major enantiomer) and 24.7 min (minor enantiomer).

δ_H (400 MHz, CDCl$_3$):   7.94 (1 H, d, *J* 8.2, H-5), 7.31 (1 H, app. t, H-6), 7.10-6.98 (2 H, m H-7 and H-8,), 6.04 (1 H, s, H-1), 3.98-3.81 (3 H, m, H-3b and H-9), 3.04 (1 H, dd, *J* 11.6, 19.8, H-3a), 2.87 (1 H, dd, *J* 6.4, 19.8, H-3b), 2.16 (3 H, s, H-2), 1.65 (9 H, s, H-11), 0.96 (3 H, t, *J* 7.2, H-10).

δ_C (100 MHz, CDCl$_3$): 191.9 (C=O), 174.2 (C=O), 169.9 (C=O), 161.0 (q), 149.2 (C=O), 141.2 (q), 129.5, 125.8 (q), 125.3, 124.4, 122.8, 116.0, 84.5 (q), 61.6, 60.8 (q), 44.9, 30.2, 28.3, 24.6, 13.6.

ν_{max} (neat)/cm^{-1}: 2983, 2932, 1773, 1727, 1665, 1478, 1464, 1346, 1287, 1237, 1147, 1093, 1008, 891, 841, 751.

HRMS (*m/z* - ESI): Found: 398.1616 (M-H)$^-$ C$_{22}$H$_{24}$NO$_6$ Requires: 398.1604.

1''-*tert*-Butyl 7'-ethyl (6'*R*,7'*R*)-2'',5'-dioxo-1',1'',2'',3',4',5',7',8'-octahydrodispiro[1,3-dioxolane-2,2'-naphthalene-6',3''-indole]-1'',7'-dicarboxylate (*trans*-419, Table 5.5, entry 9)
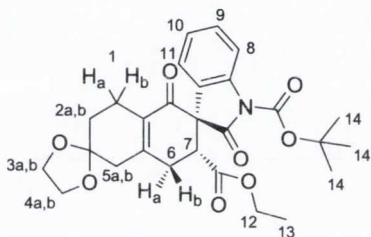
Synthesised according to general procedure XVIII by reaction of oxindole **378** (78.1 mg, 0.246 mmol) with anhydride **232** (55.2 mg, 0.246 mmol). After purification (Biotage SP4), *trans*-**419** was isolated as a white solid (100.5 mg, 82%). M.p. 140-143 °C; TLC (hexanes:EtOAc, 7:3 *v/v*): R$_f$ = 0.14; [α]$_D^{20}$ = +154.0 (*c* = 0.20, CHCl$_3$).

CSP-HPLC analysis. Chiralpak AD-H (4.6 mm x 25 cm), hexane/IPA: 95/5, 1.0 mL min^{-1}, RT, UV detection at 254 nm, retention times: 44.4 min (major enantiomer) and 68.5 min (minor enantiomer).

δ_H (400 MHz, CDCl$_3$): 7.93 (1 H, d, *J* 8.1, H-8), 7.30 (1 H, app. t, H-9), 7.10-6.99 (2 H, m, H-10 and H-11), 4.07-3.98 (4 H, m, H-3a, H-3b, H-4a and H-4b), 3.97-3.78 (3 H, m, H-7 and H-12), 2.99 (1 H, dd, *J* 12.2, 19.5, H-6a), 2.75 (1 H, dd, *J* 6.1, 19.5, H-6b), 2.69-2.48 (3 H, m, H-1a, H-5a and H-5b), 2.37-2.24 (1 H, m, H-1b), 1.90-1.69 (2 H, m, H-2a and H-2b), 1.65 (9 H, s, H-14), 0.95 (3 H, t, *J* 7.2, H-13).

δ_C (100 MHz, CDCl$_3$):   191.2 (C=O), 174.3 (C=O), 170.0 (C=O), 152.4 (q), 149.2
(C=O), 141.2 (q), 130.8 (q), 129.5, 125.7 (q), 124.4, 122.9,
115.9, 107.1 (q), 84.5 (q), 64.8, 64.7, 61.5 (q), 61.2, 44.3,
42.0, 30.7, 29.7, 28.2, 22.0, 13.5.

ν_{max} (neat)/cm^{-1}:   2958, 2932, 1772, 1728, 1665, 1641, 1478, 1347, 1247,
1147, 1095, 1059, 946, 841, 750.

HRMS (*m/z* - ESI):   Found: 496.1979 (M-H)⁻ C$_{27}$H$_{30}$NO$_8$ Requires: 496.1971.

(2'*R*,3'*S*,4'*R*)-1-*tert*-Butyl 4'-methyl 1',2-dioxo-3'-phenyl-3',4'-dihydro-1'*H*-spiro[indoline-3,2'-naphthalene]-1,4'-dicarboxylate (*trans*-428, Table 5.6, entry 1)
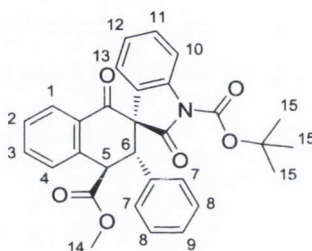
Synthesised according to general procedure XVII by reaction of oxindole **423** (79.1 mg, 0.246 mmol) with anhydride **147** (39.9 mg, 0.246 mmol) at 30 °C. After purification (Biotage SP4), *trans*-**428** was isolated as a white solid (117.9 mg, 96%). M.p. 169-172 °C; TLC (hexanes:EtOAc, 8:2 *v/v*): R$_f$ = 0.34; [α]$_D^{20}$ = +297.0 (*c* = 0.20, CHCl$_3$).

CSP-HPLC analysis. Chiralpak AD-H (4.6 mm x 25 cm), hexane/IPA: 95/5, 1.0 mL min^{-1}, RT, UV detection at 254 nm, retention times: 11.9 min (minor enantiomer) and 33.8 min (major enantiomer).

δ_H (400 MHz, CDCl$_3$):   8.19 (1 H, d, *J* 7.9, H-1), 7.72-7.65 (2 H, m, H-3 and H-10),
7.52 (1 H, app. t, H-2), 7.43 (1 H, d, *J* 8.1, H-4), 7.31 (1 H,
app. t, H-11), 7.14 (1 H, t, *J* 7.3, H-9), 7.11-7.03 (3 H, m,
H-8 and H-12), 6.97 (1 H, d, *J* 7.2, H-13), 6.83 (2 H, d, *J*
7.4, H-7), 4.86 (1 H, d, *J* 12.4, H-5), 4.53 (1 H, d, *J* 12.4, H-
6), 3.55 (3 H, s, H-14), 1.49 (9 H, s, H-15).

δ_C (100 MHz, CDCl$_3$):   191.2 (C=O), 172.0 (C=O), 171.8 (C=O), 148.4 (C=O), 141.1 (q), 139.5 (q), 135.2, 134.4 (q), 130.6 (q), 129.8, 129.4, 128.8, 128.7, 128.3, 128.2, 127.5, 124.4 (q), 124.3, 123.6, 116.1, 84.3 (q), 65.3 (q), 52.6, 49.8, 48.5, 28.1.

ν_{max} (neat)/cm^{-1}:   2983, 2932, 2857, 1775, 1733, 1686, 1597, 1459, 1289, 1244, 1146, 1093, 1025, 836, 751, 700.

HRMS (*m/z* - ESI):   Found: 496.1770 (M-H)$^-$ C$_{30}$H$_{26}$NO$_6$ Requires: 496.1760.

(2'*R*,3'*S*,4'*R*)-1-*tert*-Butyl 4'-methyl 7'-bromo-1',2-dioxo-3'-phenyl-3',4'-dihydro-1'*H*-spiro[indoline-3,2'-naphthalene]-1,4'-dicarboxylate (*trans*-429, Table 5.6, entry 2)
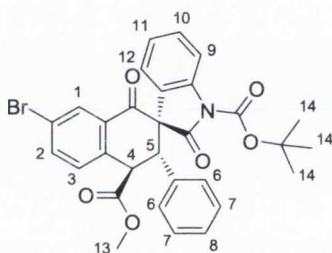
Synthesised according to general procedure XVII by reaction of oxindole **423** (79.1 mg, 0.246 mmol) with anhydride **312** (59.3 mg, 0.246 mmol) at 30 °C. After purification (Biotage SP4), *trans*-**429** was isolated as a white solid (138.8 mg, 98%). M.p. 172-174 °C; TLC (hexanes:EtOAc, 8:2 *v/v*): R$_f$ = 0.45; $[\alpha]_D^{20}$ = +244.0 (*c* = 0.20, CHCl$_3$).

CSP-HPLC analysis. Chiralpak AD-H (4.6 mm x 25 cm), hexane/IPA: 85/15, 1.0 mL min^{-1}, RT, UV detection at 254 nm, retention times: 5.9 min (minor enantiomer) and 20.8 min (major enantiomer).

δ_H (400 MHz, CDCl$_3$):   8.29 (1 H, d, *J* 2.1, H-1), 7.79 (1 H, dd, *J* 2.1, 8.2, H-2), 7.69 (1 H, d, *J* 8.2, H-9), 7.36-7.29 (2 H, m, H-3 and H-10), 7.15 (1 H, t, *J* 7.3, H-8), 7.12-7.03 (3 H, m, H-7 and H-11), 6.93 (1 H, d, *J* 7.4, H-12), 6.81 (2 H, d, *J* 7.5, H-6), 4.76 (1 H, d, *J* 12.4, H-4), 4.48 (1 H, d, *J* 12.4, H-5), 3.54 (3 H, s, H-13), 1.49 (9 H, s, H-14).

δ_C (100 MHz, CDCl$_3$):   190.0 (C=O), 171.6 (C=O), 171.3 (C=O), 148.3 (C=O), 141.1 (q), 138.2 (q), 138.0 134.0 (q), 132.1 (q), 132.0, 130.0, 129.4, 128.7, 128.5, 128.3, 124.4, 123.9 (q), 123.5, 123.2 (q), 116.2, 84.4 (q), 65.1 (q), 52.8, 49.6, 48.2, 28.0.

ν_{max} (neat)/cm^{-1}:   2983, 2953, 2907, 1764, 1738, 1675, 1588, 1479, 1344, 1289, 1244, 1151, 1093, 911, 765, 699, 660.

HRMS (*m/z* - ESI):   Found: 574.0855 (M-H)⁻ C$_{30}$H$_{25}$NO$_6$Br Requires: 574.0865.

(1*S*,2*R*)-*tert*-Butyl 5-methyl-2',3-dioxo-1-phenylspiro[cyclohex[4]ene-2,3'-indoline]-1'-carboxylate (*trans*-430, Table 5.6, entry 3)
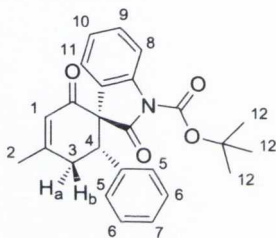
Synthesised according to general procedure XVIII by reaction of oxindole **423** (79.1 mg, 0.246 mmol) with anhydride **238** (31.0 mg, 0.246 mmol). After purification (Biotage SP4), *trans*-**430** was isolated as a white solid (64.9 mg, 65%). M.p. 155-157 °C; TLC (hexanes:EtOAc, 8:2 *v/v*): R$_f$ = 0.33; $[\alpha]_D^{20}$ = +233.0 (*c* = 0.20, CHCl$_3$).

CSP-HPLC analysis. Chiralpak AD-H (4.6 mm x 25 cm), hexane/IPA: 95/5, 1.0 mL min^{-1}, RT, UV detection at 254 nm, retention times: 10.5 min (minor enantiomer) and 16.3 min (major enantiomer).

δ_H (400 MHz, CDCl$_3$):   7.64 (1 H, d, *J* 8.2, H-8), 7.32-7.23 (1 H, m, H-9), 7.21 (1 H, d, *J* 6.6, H-11), 7.18-7.09 (2 H, m, H-7 and H-10), 7.05 (2 H, app. t, H-6), 6.81 (2 H, d, *J* 7.3, H-5), 6.20 (1 H, s, H-1), 4.05 (1 H, dd, *J* 4.9, 12.3, H-4), 3.11 (1 H, dd, *J* 12.3, 19.3, H-3a), 2.61 (1 H, dd, *J* 4.9, 19.3, H-3b), 2.19 (3 H, s, H-2), 1.49 (9 H, s, H-12).

δ_C (100 MHz, CDCl$_3$):   192.9 (C=O), 173.1 (C=O), 162.7 (q), 148.5 (C=O), 140.8 (q), 136.7 (q), 129.4, 128.3, 128.1, 127.9, 126.2, 124.9 (q), 124.1, 123.6, 115.9, 84.1 (q), 65.0 (q), 47.7, 34.4, 28.1, 24.7.

v_{max} (neat)/cm^{-1}:   2974, 2924, 2853, 1759, 1729, 1656, 1627, 1511, 1370, 1222, 1145, 1075, 837, 762, 694.

HRMS (*m/z* - ESI):   Found: 402.1720 (M-H)$^-$ C$_{25}$H$_{24}$NO$_4$ Requires: 402.1705.

7.6 Experimental procedures and data for Chapter 6

<u>**General procedure XIX:**</u> **Substrate evaluation in the thiolate-catalysed intermolecular aldehyde-ketone Tishchenko reaction (Table 6.1 and Table 6.2)**

To an oven-dried 10 mL reaction vessel charged with a magnetic stirring bar under argon atmosphere were added *via* syringe anhydrous THF (0.68 M) and 3-trifluorothiophenol (**445**, 49 µL, 0.408 mmol - 20 mol%). The flask was cooled to 0 °C and phenylmagnesium bromide (3.0 M solution in diethyl ether, 136 µL, 0.408 mmol - 20 mol%) was added dropwise *via* syringe while stirring. The reaction mixture was allowed to warm to room temperature and the relevant trifluoromethyl ketone (2.04 mmol) followed by the relevant aldehyde (2.04 mmol) were added. The resulting solution was heated at reflux temperature for time indicated in Table 6.1 and Table 6.2. Volatiles were removed under reduced pressure and the residue obtained was purified by flash column chromatography to give the desired product.

1-(4-Chlorophenyl)-2,2,2-trifluoroethyl benzoate (450, Table 6.1, entry 1)
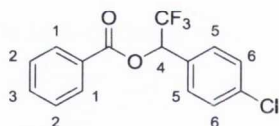
Synthesised according to general procedure XIX using THF (2.4 mL), 4'-chloro-2,2,2-trifluoroacetophenone (**449**, 308 µL, 2.04 mmol) and benzaldehyde (**52**, 207 µL, 2.04 mmol). After purification, eluting in gradient from 100% hexanes to 10% dichloromethane in hexanes, product **450** was isolated as a white solid (583.5 mg, 91%). M.p. 62-64 °C; TLC (hexanes:CH$_2$Cl$_2$, 9:1 *v/v*): R$_f$ = 0.38.

δ_H (400 MHz, CDCl$_3$): 8.12 (2 H, d, *J* 7.3, H-1), 7.64 (1 H, t, *J* 7.5, H-3), 7.54-7.46 (4 H, m, H-2 and H-6), 7.04 (2 H, d, *J* 8.5, H-5), 6.33 (1 H, q, *J* 6.8, H-4).

δ_C (100 MHz, CDCl$_3$): 164.6 (C=O), 136.5 (q), 134.4, 130.4, 130.2 (q), 129.7, 129.4, 129.0, 128.8 (q), 123.4 (q, ^1J 280.6) (q), 72.2 (q, ^2J 33.7).

δ_F (376.5 MHz, CDCl$_3$):   -76.4.

ν_{max} (neat)/cm^{-1}:   2962, 1729, 1356, 1250, 1186, 1135, 1090, 916, 705.

HRMS (m/z - CI):   Found: 314.0332 (M)$^+$ C$_{15}$H$_{10}$O$_2$ClF$_3$ Requires: 314.0321.

1-(4-Bromophenyl)-2,2,2-trifluoroethyl benzoate (452, Table 6.1, entry 2)
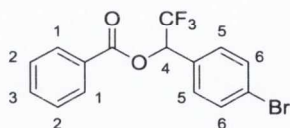
Synthesised according to general procedure XIX using THF (2.4 mL), 4'-bromo-2,2,2-trifluoroacetophenone (**451**, 317 μL, 2.04 mmol) and benzaldehyde (**52**, 207 μL, 2.04 mmol). After purification, eluting in gradient from 100% hexanes to 10% dichloromethane in hexanes, product **452** was isolated as a white solid (683.6 mg, 93%). M.p. 72-74 °C; TLC (hexanes:CH$_2$Cl$_2$, 8:2 v/v): R$_f$ = 0.41.

δ_H (400 MHz, CDCl$_3$):   8.12 (2 H, d, J 7.0, H-1), 7.64 (1 H, t, J 7.5, H-3), 7.57 (2 H, d, J 8.5, H-6), 7.50 (2 H, app. t, H-2), 7.43 (2 H, d, J 8.5, H-6), 6.32 (1 H, q, J 6.7, H-4).

δ_C (100 MHz, CDCl$_3$):   164.6 (C=O), 134.4, 132.4, 130.7 (q), 130.4, 130.0, 129.0, 128.8 (q), 124.7 (q), 123.4 (q, ^1J 280.6) (q), 72.3 (q, ^2J 33.7).

ν_{max} (neat)/cm^{-1}:   3059, 2965, 1727, 1355, 1250, 1185, 1135, 1097, 1010, 803, 711.

HRMS (m/z - CI):   Found: 357.9822 (M)$^+$ C$_{15}$H$_{10}$O$_2$F$_3$^{79}Br Requires: 357.9816.

2,2,2-Trifluoro-1-(3-fluorophenyl)ethyl benzoate (454, Table 6.1, entry 3)
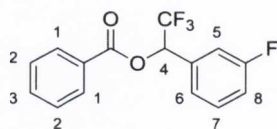
Synthesised according to general procedure XIX using THF (2.5 mL), 2,2,2,3'-tetrafluoroacetophenone (**453**, 286 µL, 2.04 mmol) and benzaldehyde (**52**, 207 µL, 2.04 mmol). After purification, eluting in gradient from 100% hexanes to 10% dichloromethane in hexanes, product **454** was isolated as a pale yellow oil (572.1 mg, 94%). TLC (hexanes:CH$_2$Cl$_2$, 9:1 *v/v*): R$_f$ = 0.25.

δ_H (400 MHz, CDCl$_3$):   8.13 (2 H, d, *J* 7.0, H-1), 7.64 (1 H, t, *J* 7.5, H-3), 7.51 (2 H, app. t, H-2), 7.44-7.37 (1 H, m, H-8), 7.34 (1 H, d, *J* 7.5, H-5), 7.28 (1 H, d, *J* 9.5, H-6), 7.20-7.09 (1 H, m, H-7), 6.36 (1 H, q, *J* 6.7, H-4).

δ_C (100 MHz, CDCl$_3$):   164.6 (C=O), 163.1 (d, ^1J 247.8) (q), 134.4, 133.9 (d, ^3J 7.8) (q), 130.8 (d, ^3J 7.8), 130.4, 129.1, 128.7 (q), 124.2 (d, ^4J 2.9), 123.4 (q, ^1J 280.9) (q), 117.4 (d, ^2J 20.4), 115.4 (d, ^2J 23.3), 72.1 (q, ^2J 34.0).

δ_F (376.5 MHz, CDCl$_3$):   -112.2, -76.3.

ν_{max} (neat)/cm^{-1}:   3066, 2971, 1737, 1596, 1452, 1255, 1242, 1178, 1149, 1130, 1091, 872, 771.

HRMS (*m/z* - CI):   Found: 299.0698 (M+H)$^+$ C$_{15}$H$_{11}$O$_2$F$_4$ Requires: 299.0695.

2,2,2-Trifluoro-1-(3-(trifluoromethyl)phenyl)ethyl benzoate (456, Table 6.1, entry 4)
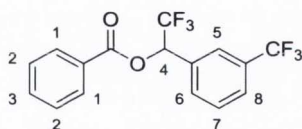
Synthesised according to general procedure XIX using THF (2.4 mL), 2,2,2-trifluoro-3'-(trifluoromethyl)acetophenone (**455**, 349 μL, 2.04 mmol) and benzaldehyde (**52**, 207 μL, 2.04 mmol). After purification, eluting in gradient from 100% hexanes to 10% dichloromethane in hexanes, product **456** was isolated as a white solid (569.3 mg, 80% yield). M.p. 39-41 °C; TLC (hexanes:CH_2Cl_2, 9:1 *v/v*): R_f = 0.28.

δ_H (400 MHz, $CDCl_3$):   8.14 (2 H, d, *J* 7.0, H-1), 7.82 (1 H, s, H-5), 7.76 (1 H, d, *J* 8.0, H-8), 7.71 (1 H, d, *J* 7.5, H-6), 7.65 (1 H, t, *J* 7.5, H-3), 7.57 (1 H, app. t, H-7), 7.52 (2 H, app. t, H-2), 6.44 (1 H, q, *J* 6.7, H-4).

δ_C (100 MHz, $CDCl_3$):   164.6 (C=O), 134.5, 132.7 (q), 131.7, 131.7 (q, ^2J 33.0) (q), 130.4, 129.8, 129.1, 128.6 (q), 127.2 (q, ^3J 3.6), 125.2 (q, ^3J 3.9), 124.0 (q, ^1J 272.5) (q), 123.3 (q, ^1J 280.9) (q), 72.2 (q, ^2J 33.7).

δ_F (376.5 MHz, $CDCl_3$):   -76.3, -63.2.

ν_{max} (neat)/cm^{-1}:   3063, 2966, 1727, 1356, 1250, 1182, 1134, 1097, 1070, 803, 711.

HRMS (*m/z* - CI):   Found: 349.0674 (M+H)$^+$ $C_{16}H_{11}O_2F_6$ Requires: 349.0663.

2,2,2-Trifluoro-1-(thiophen-2-yl)ethyl benzoate (458, Table 6.1, entry 5)
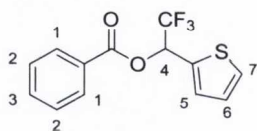
Synthesised according to general procedure XIX using THF (2.5 mL), 2-(trifluoroacetyl)thiophene (**457**, 262 μL, 2.04 mmol) and benzaldehyde (**52**, 207 μL, 2.04 mmol). After purification, eluting in gradient from 100% hexanes to 10% dichloromethane in hexanes, product **458** was isolated as a pale yellow oil (454.7 mg, 78%). TLC (hexanes:CH_2Cl_2, 9:1 *v/v*): R_f = 0.32.

δ_H (400 MHz, CDCl$_3$):   8.11 (2 H, d, *J* 7.0, H-1), 7.62 (1 H, t, *J* 7.5, H-3), 7.48 (2 H, app. t, H-2), 7.42 (1 H, d, *J* 5.0, H-7), 7.34 (1 H, d, *J* 3.5, H-5), 7.06 (1 H, dd, *J* 3.5, 5.0, H-6), 6.71 (1 H, q, *J* 6.5, H-4).

δ_C (100 MHz, CDCl$_3$):   164.6 (C=O), 134.3, 132.8 (q), 130.5, 129.7, 129.0, 128.8 (q), 128.2, 127.3, 123.2 (q, ^1J 280.6) (q), 68.8 (q, ^2J 34.7).

δ_F (376.5 MHz, CDCl$_3$):   -76.6.

ν_{max} (neat)/cm^{-1}:   3070, 2959, 1743, 1254, 1242, 1177, 1131, 1086, 1067, 1026, 908, 703.

HRMS (*m/z* - EI):   Found: 286.0273 (M)$^+$ C$_{13}$H$_9$O$_2$F$_3$S Requires: 286.0275.

2,2,2-Trifluoro-1-phenylethyl 2-naphthoate (460, Table 6.2, entry 1)
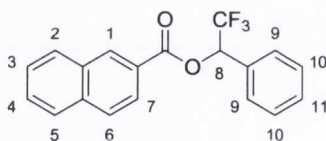
Synthesised according to general procedure XIX using THF (1.7 mL), 2,2,2-trifluoroacetophenone (**118**, 278 μL, 2.04 mmol) and a solution in THF (1.0 mL) of 2-naphthaldehyde (**459**, 318.9 mg, 2.04 mmol). After purification, eluting in gradient from

100% hexanes to 10% dichloromethane in hexanes, product **460** was isolated as an off white solid (579.2 mg, 86%). M.p. 93-95 °C; TLC (hexanes:CH_2Cl_2, 9:1 v/v): R_f = 0.20.

δ_H (400 MHz, CDCl$_3$):	8.71 (1 H, s, H-1), 8.12 (1 H, d, J 8.5, H-7), 8.01 (1 H, d, J 8.0, H-2), 7.92 (2 H, app. t, H-5 and H-6), 7.67-7.55 (4 H, m, H-3, H-4 and H-10), 7.48-7.41 (3 H, m, H-9 and H-11), 6.45 (1 H, q, J 6.9, H-8).

δ_C (100 MHz, CDCl$_3$): 164.9 (C=O), 136.2 (q), 132.7 (q), 132.2, 131.7 (q), 130.3, 129.9, 129.2, 129.1, 128.9, 128.4, 128.2, 127.3, 126.2 (q), 125.5, 123.2 (q, ^1J 280.9) (q), 72.9 (q, ^2J 33.4).

δ_F (376.5 MHz, CDCl$_3$): -76.2.

ν_{max} (neat)/cm^{-1}: 3069, 2956, 1730, 1351, 1259, 1172, 1129, 1090, 908, 761.

HRMS (m/z - EI): Found: 330.0855 (M)$^+$ C$_{19}$H$_{13}$O$_2$F$_3$ Requires: 330.0868.

2,2,2-Trifluoro-1-phenylethyl 4-methoxybenzoate (461, Table 6.2, entry 2)
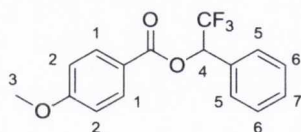
Synthesised according to general procedure XIX using THF (1.7 mL, 0.9 M), 2,2,2-trifluoroacetophenone (**118**, 278 µL, 2.04 mmol) and 4-methoxybenzaldehyde (**179**, 254 µL, 2.04 mmol). After purification, eluting in gradient from 100% hexanes to 10% dichloromethane in hexanes, product **461** was isolated as a pale yellow oil (583.3 mg, 92%). TLC (hexanes:CH_2Cl_2, 9:1 v/v): R_f = 0.29.

δ_H (400 MHz, CDCl$_3$): 8.10 (2 H, d, J 9.0, H-1), 7.59-7.52 (2 H, m, H-6), 7.45-7.39 (3 H, m, H-5 and H-7), 6.96 (2 H, d, J 9.0, H-2), 6.36 (1 H, q, J 7.0, H-4), 3.88 (3 H, s, H-3).

δ_C (100 MHz, CDCl$_3$): 164.4 (C=O), 164.4 (q), 132.5, 131.9 (q), 130.2, 129.0, 128.3, 123.7 (q, ^1J 280.6) (q), 121.3 (q), 114.2, 72.5 (q, ^2J 33.0), 55.9.

δ_F (376.5 MHz, CDCl$_3$):   -76.3.

ν_{max} (neat)/cm^{-1}:   2964, 2843, 1726, 1606, 1511, 1250, 1166, 1130, 1089, 1027, 845, 756, 699.

HRMS (*m/z* - ESI):   Found: 333.0715 (M+Na)$^+$ C$_{16}$H$_{13}$O$_3$NaF$_3$ Requires: 333.0714.

2,2,2-Trifluoro-1-phenylethyl 3-chlorobenzoate (463, Table 6.2, entry 3)
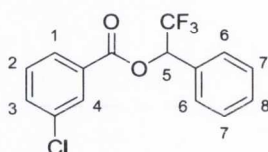
Synthesised according to general procedure XIX using THF (2.4 mL), 2,2,2-trifluoroacetophenone (**118**, 278 μL, 2.04 mmol) and 3-chlorobenzaldehyde (**462**, 240 μL, 2.04 mmol). After purification, eluting in gradient from 100% hexanes to 10% dichloromethane in hexanes, product **463** was isolated as a pale yellow oil (559.8 mg, 87%). TLC (hexanes:CH$_2$Cl$_2$, 9:1 *v/v*): R$_f$ = 0.22.

δ_H (400 MHz, CDCl$_3$):   8.11-8.07 (1 H, m, H-4), 8.01 (1 H, d, *J* 7.8, H-1), 7.62-7.58 (1 H, m, H-3), 7.57-7.52 (2 H, m, H-7), 7.48-7.40 (4 H, m, H-2, H-6 and H-8), 6.36 (1 H, q, *J* 6.8, H-5).

δ_C (100 MHz, CDCl$_3$):   163.6 (C=O), 135.2 (q), 134.3, 131.3 (q), 130.7 (q), 130.4, 130.3, 129.2, 128.5, 128.4, 128.3, 123.5 (q, ^1J 280.4) (q), 73.1 (q, ^2J 34.0).

δ_F (376.5 MHz, CDCl$_3$):   -76.3.

ν_{max} (neat)/cm^{-1}:   3071, 2964, 1738, 1243, 1178, 1131, 1071, 907, 741, 698.

HRMS (*m/z* - EI):   Found: 314.0331 (M)$^+$ C$_{15}$H$_{10}$O$_2$F$_3$Cl Requires: 314.0321.

2,2,2-Trifluoro-1-phenylethyl 3-nitrobenzoate (465, Table 6.2, entry 4)
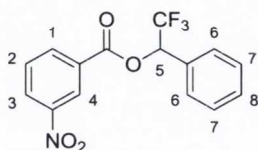
Synthesised according to general procedure XIX using THF (1.7 mL), and *i*-propylmagnesium bromide (1.0 M solution in THF, 408 μL, 0.408 mmol), 2,2,2-trifluoroacetophenone (**118**, 278 μL, 2.04 mmol) and a solution of 3-nitrobenzaldehyde (**464**, 308.6 mg, 2.04 mmol) in THF (1.0 mL). After purification, eluting in gradient from 100% hexanes to 10% EtOAc in hexanes, product **465** was isolated as a pale yellow oil (298.2 mg, 45%). TLC (hexanes:EtOAc, 9:1 *v/v*): R_f = 0.34.

δ_H (400 MHz, CDCl$_3$): 8.93 (1 H, s, H-4), 8.53-8.40 (2 H, m, H-1 and H-3), 7.72 (1 H, app. t, H-2), 7.62-7.52 (2 H, m, H-7), 7.50-7.40 (3 H, m, H-6 and H-8), 6.40 (1 H, q, *J* 6.7, H-5).

δ_C (100 MHz, CDCl$_3$): 162.8 (C=O), 148.7 (q), 135.9, 130.9 (q), 130.8 (q), 130.6, 130.3, 129.3, 128.6, 128.4, 125.3, 123.4 (q, ^1J 280.6) (q), 73.6 (q, ^2J 33.7).

δ_F (376.5 MHz, CDCl$_3$): -76.2.

v_{max} (neat)/cm^{-1}: 3091, 2967, 1742, 1533, 1249, 1250, 1179, 1124, 918, 715, 698.

HRMS (*m/z* - EI): Found: 325.0560 (M)$^+$ C$_{15}$H$_{10}$NO$_4$F$_3$ Requires: 325.0562.

General procedure XX: Substrate evaluation in the microwave-assisted thiolate-catalysed intermolecular aldehyde-ketone Tishchenko reaction (Table 6.3)

An oven-dried microwave-transparent reaction vessel containing a magnetic stirring bar under argon atmosphere was charged with 3-trifluorothiophenol (**445**, 57 μL, 0.424 mmol - 20 mol%). THF (1.2 M) was added *via* syringe followed by a solution of phenylmagnesium bromide (3.0 M solution in diethyl ether, 140 μL, 0.424 mmol - 20 mol%) added dropwise *via* syringe. The reaction was allowed to stir at ambient

temperature for 5 min and the relevant trifluoromethyl ketone (2.12 mmol) was added. After a further 2 min of stirring, the relevant aldehyde (2.12 mmol) was added. The reaction vessel was then fitted with a microwave reaction vessel cap and the mixture was irradiated at 110 °C for the time indicated in Table 6.3. Volatiles were removed *in vacuo* and the residue obtained was purified by flash column chromatography to give the desired product.

1-(4-Chlorophenyl)-2,2,2-trifluoroethyl 2-naphthoate (469, Table 6.3, entry 2)
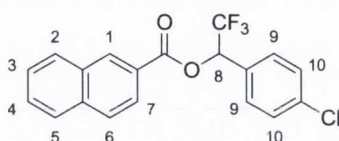
Synthesised according to general procedure XX using THF (1.4 mL), 1-(4-chlorophenyl)-2,2,2-trifluoroacetophenone (**449**, 316 μL, 2.12 mmol) and 2-naphthaldehyde (**459**, 331.1 mg, 2.12 mmol). After purification, eluting in gradient from 100% hexanes to 10% dichloromethane in hexanes, product **469** was isolated as a white solid (525.3 mg, 68%). M.p. 129-131 °C; TLC (hexanes:CH_2Cl_2, 9:1 *v/v*): R_f = 0.13.

δ_H (400 MHz, $CDCl_3$):	8.70 (1 H, s, H-1), 8.10 (1 H, d, *J* 8.5, H-7), 8.01 (1 H, d, *J* 8.0, H-2), 7.92 (2 H, app. t, H-5 and H-6), 7.69-7.56 (2 H, m, H-3 and H-4), 7.55 (2 H, d, *J* 8.6, H-10), 7.42 (2 H, d, *J* 8.6, H-9), 6.40 (1 H, q, *J* 6.7, H-8).
δ_C (100 MHz, $CDCl_3$):	164.8 (C=O), 136.5 (q), 136.3 (q), 132.7 (q), 132.3, 130.2 (q), 129.9, 129.7, 129.4, 129.2, 128.9, 128.2, 127.3, 125.9 (q), 125.4, 125.5 (q, ^1J 280.9) (q), 72.3 (q, ^2J 33.4).
ν_{max} (neat)/cm^{-1}:	1732, 1628, 1598, 1494, 1347, 1260, 1198, 1132, 1091, 1013, 823, 780, 762, 730, 677.
HRMS (*m/z* - EI):	Found: 364.0480 (M)$^+$ $C_{19}H_{12}O_2F_3Cl$ Requires: 364.0478.

1-(4-Chlorophenyl)-2,2,2-trifluoroethyl 3-chlorobenzoate (472, Table 6.3, entry 5)
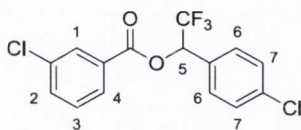
Synthesised according to general procedure XX using THF (1.2 mL), 1-(4-chlorophenyl)-2,2,2-trifluoroacetophenone (**449**, 316 µL, 2.12 mmol) and 3-chlorobenzaldehyde (**462**, 240 µL, 2.12 mmol). After purification, eluting in gradient from 100% hexanes to 10% dichloromethane in hexanes, product **472** was isolated as a pale yellow oil (614.6 mg, 83%). TLC (hexanes:CH_2Cl_2, 9:1 v/v): R_f = 0.32.

δ_H (400 MHz, CDCl$_3$):	8.07 (1 H, m, H-1), 8.00 (1 H, d, J 7.5, H-4), 7.61 (1 H, m, H-2), 7.54-7.37 (5 H, m, H-3, H-6 and H-7), 6.32 (1 H, q, J 6.7, H-5).
δ_C (100 MHz, CDCl$_3$):	163.5 (C=O), 136.7 (q), 135.3 (q), 134.4, 130.5 (q), 130.4, 130.3, 129.8 (q), 129.7, 129.5, 128.5, 123.3 (q, ^1J 280.6) (q), 72.5 (q, ^2J 33.7).
ν_{max} (neat)/cm^{-1}:	1739, 1600, 1577, 1494, 1427, 1352, 1244, 1183, 1134, 1091, 1072, 1015, 915, 847, 813, 743, 672.
HRMS (m/z - EI):	Found: 347.9945 (M)$^+$ C$_{15}$H$_9$O$_2$F$_3$Cl$_2$ Requires: 347.9932.

1-(4-Chlorophenyl)-2,2,2-trifluoroethyl 4-fluorobenzoate (474, Table 6.3, entry 6)
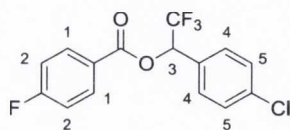
Synthesised according to general procedure XX using THF (1.2 mL), 1-(4-chlorophenyl)-2,2,2-trifluoroacetophenone (**449**, 316 µL, 2.12 mmol) and 4-fluorobenzaldehyde (**473**, 227 µL, 2.12 mmol). After purification, eluting in gradient from 100% hexanes to 10% dichloromethane in hexanes, product **474** was isolated as a pale yellow oil (525.4 mg, 75%). TLC (hexanes:CH_2Cl_2, 9:1 v/v): R_f = 0.30.

δ_H (400 MHz, CDCl$_3$): 8.19-8.09 (2 H, m, H-1), 7.49 (2 H, d, *J* 8.5, H-5), 7.41 (2 H, d, *J* 8.5, H-4), 7.17 (2 H, app. t, H-2), 6.31 (1 H, q, *J* 6.7, H-3).

δ_C (100 MHz, CDCl$_3$): 166.7 (d, ^1J 255.6) (q), 163.6 (C=O), 136.6 (q), 133.1 (d, ^3J 8.8), 130.0 (q), 129.7, 129.5, 125.0 (d, ^4J 2.9) (q), 123.4 (q, ^1J 280.6) (q), 116.3 (d, ^2J 21.4), 72.3 (q, ^2J 33.4).

ν_{max} (neat)/cm^{-1}: 1737, 1602, 1508, 1494, 1415, 1352, 1255, 1182, 1133, 1086, 1015, 910, 853, 817, 763, 730, 687.

HRMS (*m/z* - EI): Found: 332.0227 (M)$^+$ C$_{15}$H$_9$O$_2$F$_4$Cl Requires: 332.0227.

2,2,2-Trifluoro-1-phenylethyl cyclohexanecarboxylate (267, Table 6.3, entry 12)
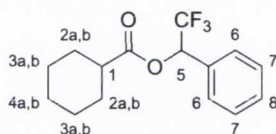
Synthesised according to general procedure XX using THF (875 µL), 2,2,2-trifluoroacetophenone (**118**, 593 µL, 2.12 mmol) and cyclohexanecarboxy aldehyde (**265**, 257 µL, 2.12 mmol). After purification, eluting in gradient from 100% hexanes to 10% dichloromethane in hexanes, product **267** was isolated as a colourless oil (339.9 mg, 56%). TLC (hexanes:CH$_2$Cl$_2$, 9:1 *v/v*): R$_f$ = 0.26.

δ_H (400 MHz, CDCl$_3$): 7.50-7.43 (2 H, m, H-7), 7.43-7.37 (3 H, m, H-6 and H-8), 6.14 (1 H, q, *J* 6.9, H-5), 2.46 (1 H, tt, *J* 11.0, 3.5, H-1), 2.06-1.87 (2 H, m, H-2a), 1.85-1.71 (2 H, m, H-3a), 1.70-1.62 (1 H, m, H-4a), 1.58-1.41 (2 H, m, H-2b), 1.40-1.18 (3 H, m, H-3b and H-4b).

δ_C (100 MHz, CDCl$_3$): 174.0 (C=O), 131.8 (q), 130.1, 129.0, 128.3, 123.6 (q, ^1J 280.7) (q), 71.8 (q, ^2J 32.9), 43.1, 29.1, 29.0, 26.0, 25.6.

ν_{max} (neat)/cm^{-1}: 2935, 2859, 1749, 1498, 1453, 1348, 1268, 1176, 1130, 1044, 1028, 939, 879, 759, 699.

HRMS (*m/z* - EI):   Found: 286.1175 (M)$^+$ $C_{15}H_{17}O_2F_3$ Requires: 286.1181.

(*E*)-*N*-Benzylidene-1-phenylmethanamine (483)
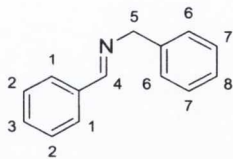
In an oven-dried 50 mL round-bottomed flask containing a magnetic stirring bar under argon atmosphere were added *via* syringe dichloromethane (15 mL), freshly distilled benzaldehyde (**52**, 1.0 mL, 10.0 mmol) and freshly distilled benzylamine (1.1 mL, 10.0 mmol). To the mixture was then added anhydrous $MgSO_4$ (2.50 g) and the reaction was allowed to stir for 12 h at room temperature. The reaction was then filtered and concentrated *in vacuo* to furnish **483** as a colourless oil (1.95 g, 100%).

Spectral data for this compound were consistent with those in the literature.[344]

δ_H (400 MHz, $CDCl_3$):   8.43 (1 H, s, H-4), 7.88-7.77 (2 H, m, H-1), 7.50-7.42 (3 H, m, H-2 and H-3), 7.42-7.35 (4 H, m, H-6 and H-7), 7.35-7.27 (1 H, m, H-8), 4.87 (2 H, s, H-5).

HRMS (*m/z* - EI):   Found: 195.1051 (M)$^+$ $C_{14}H_{13}N$ Requires: 195.1048.

(*E*)-*N*-(4-Nitrobenzylidene)-1-phenylmethanamine (486)
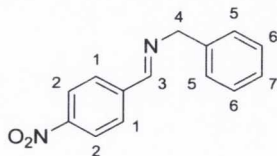
In an oven-dried 50 mL round-bottomed flask containing a magnetic stirring bar under argon atmosphere were added *via* syringe dichloromethane (15 mL), recrystallised 4-nitrobenzaldehyde (1.51 g, 10.0 mmol) and freshly distilled benzylamine (1.1 mL, 10.0 mmol). To the mixture was added anhydrous $MgSO_4$ (2.50 g) and the reaction was

allowed to stir for 12 h at room temperature. The reaction was then filtered and concentrated *in vacuo* to furnish **486** as a yellow oil (2.40 g, 100%).

Spectral data for this compound were consistent with those in the literature.[344]

δ_H (400 MHz, CDCl$_3$):   8.47 (1 H, s, H-3), 8.27 (2 H, d, *J* 8.8, H-2), 7.95 (2 H, d, *J* 8.8, H-1), 7.42-7.27 (5 H, m, H-5, H-6 and H-7), 4.89 (2 H, s, H-4).

(*Z*)-*N*-(2,2,2-Trifluoro-1-phenylethylidene)aniline (487)
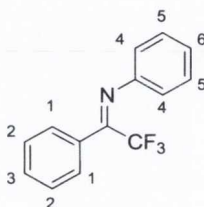
In an oven-dried 50 mL round-bottomed flask containing a magnetic stirring bar under argon atmosphere, toluene (10 mL), followed by freshly distilled aniline (911 μL, 10.0 mmol) and 2,2,2-trifluoroacetophenone (1.4 mL, 10.0 mmol), were added *via* syringe. To the mixture was then added *p*-TSA (95.1 mg, 0.500 mmol - 5 mol%), the flask was then fitted with a Dean-Stark apparatus for azeotropic removal of water and the reaction was heated at reflux temperature for 12 h. The reaction was cooled to room temperature and volatiles were removed under reduced pressure to afford the crude imine **487** which was purified by vacuum distillation to furnish a pale yellow oil (2.09 g, 84%).

Spectral data for this compound were consistent with those in the literature.[345]

δ_H (400 MHz, CDCl$_3$):   7.34 (1 H, t, *J* 7.2, H-3), 7.30 (2 H, app. t, H-2), 7.24-7.16 (4 H, m, H-1 and H-5), 7.04 (1 H, t, *J* 7.4, H-6), 6.74 (2 H, d, *J* 8.1, H-4).

(*E*)-*N*-Benzylidene-4-methylbenzenesulfonamide (488)
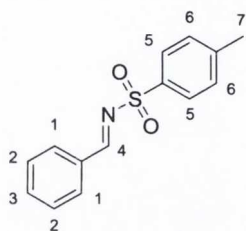
An oven-dried 50 mL round-bottomed flask containing a magnetic stirring bar under argon atmosphere was charged *via* syringe with anhydrous dichloromethane (15 mL), benzaldehyde (**52**, 1.0 mL, 10.0 mmol) and triethylamine (4.2 mL, 30.0 mmol). *p*-Toluenesulfonamide was then added to the mixture and the reaction was cooled to 0 °C. A solution of titanium tetrachloride (551 μL, 5.00 mmol) in dry dichloromethane (10 mL) was then added dropwise *via* syringe to the stirring solution and the reaction was allowed to stir for 1 h at room temperature. The solid formed was then removed by suction filtration through celite, washed with dichloromethane (20 mL) and the solution was concentrated under reduced pressure to afford a white solid. Diethyl ether (30 mL) was then added and the mixture was heated at reflux temperature for 15 min to dissolve the solid product formed. The reaction mixture was cooled to room temperature, the remaining white solid (Et₃N·HCl) was removed by suction filtration and the mother liquor concentrated *in vacuo* to give the crude imine **488** that was purified by recrystallisation (hexanes:dichloromethane) to furnish **488** as a white solid (1.64 g, 63%). M.p. 108-110 °C (lit.[346] m.p. 110-111 °C).

Spectral data for this compound were consistent with those in the literature.[346]

δ_H (400 MHz, CDCl₃):   9.03 (1 H, s, H-4), 7.93 (2 H, d, *J* 7.4, H-1), 7.89 (2 H, d, *J* 8.2, H-5), 7.62 (1 H, t, *J* 7.4, H-3), 7.49 (2 H, app. t, H-2), 7.35 (2 H, d, *J* 8.2, H-6), 2.44 (3 H, s, H-7).

(*E*)-*tert*-Butyl benzylidenecarbamate (489)
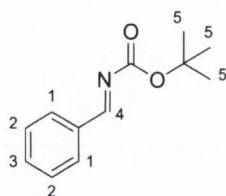
A 100 mL round-bottomed flask containing a magnetic stirring bar was charged with *t*-butyl carbamate (1.17 g, 10.0 mmol), benzenesulfinic acid sodium salt (3.28 g, 20.0 mmol) and a mixture (1:2) of MeOH:H_2O (30 mL). Benzaldehyde (2.0 mL, 20.0 mmol) followed by formic acid (760 µL, 20.0 mmol) were added *via* syringe and the mixture was allowed to stir at room temperature for 3 days. The white solid formed was isolated by suction filtration, washed with water and diethyl ether, dissolved in dichloromethane, dried over anhydrous $MgSO_4$, filtered and concentrated *in vacuo* to furnish the α-amido benzenesulphone intermediate as a white solid (2.45 g) which was used in the next step without purification.

An oven-dried 250 mL round-bottomed flask containing a magnetic stirring bar under argon atmosphere was charged with anhydrous potassium carbonate (6.00 g) and dry THF (71 mL, 10 mL/mmol). The respective α-amido benzenesulphone (2.45 g, 7.05 mmol) was added and the mixture was heated to reflux for 17 h. The reaction was then cooled to room temperature, filtered through a short pad of celite and concentrated under reduced pressure. The residue obtained was dissolved in dichloromethane, dried over anhydrous $MgSO_4$, filtered and concentrated *in vacuo* to afford the imine **489** as a colourless oil which (1.34 g, 65%).

Spectral data for this compound were consistent with those in the literature.[75]

δ_H (400 MHz, $CDCl_3$):   8.87 (1 H, s, H-4), 7.91 (2 H, d, *J* 7.6, H-1), 7.42 (1 H, t, *J* 7.4, H-3), 7.46 (2 H, app. t, H-2), 1.59 (9 H, s, H-5).

(*E*)-Benzyl benzylidenecarbamate (490)
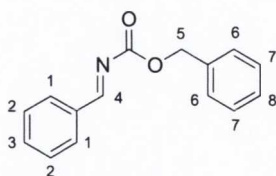
A 100 mL round-bottomed flask containing a magnetic stirring bar was charged with benzyl carbamate (1.51 g, 10.0 mmol), benzenesulfinic acid sodium salt (3.28 g, 20.0 mmol) and a mixture (1:2) of MeOH:H$_2$O (30 mL). Benzaldehyde (1.5 mL, 15.0 mmol) followed by formic acid (760 μL, 20.0 mmol) were then added *via* syringe and the mixture was allowed to stir at room temperature for 3 days. The white solid formed was isolated by suction filtration, washed with water and diethyl ether, dissolved in dichloromethane, dried over anhydrous MgSO$_4$, filtered and concentrated *in vacuo* to furnish the α-amido benzenesulphone intermediate as a white solid (2.28 g) which was used in the next step without purification.

An oven-dried 250 mL round-bottomed flask containing a magnetic stirring bar under argon atmosphere was charged with anhydrous potassium carbonate (5.00 g) and dry THF (60 mL, 10 mL/mmol). The respective α-amido benzenesulphone (2.28 g, 5.98 mmol) was added and the mixture was heated to reflux for 17 h. The reaction was then cooled to room temperature, filtered through a short pad of celite and concentrated under reduced pressure. The residue obtained was dissolved in dichloromethane, dried over anhydrous MgSO$_4$, filtered and concentrated *in vacuo* to afford imine **490** as colourless oil (1.32 g, 55%).

Spectral data for this compound were consistent with those in the literature.[346]

δ$_H$ (400 MHz, CDCl$_3$):   8.95 (1 H, s, H-4), 7.93 (2 H, d, *J* 7.6, H-1), 7.59 (1 H, t, *J* 7.4), 7.52-7.43 (4 H, m, H-2 and H-6), 7.42-7.32 (3 H, m, H-7 and H-8), 5.32 (2 H, s, H-5)

References

1. A. D. McNaught and A. Wilkinson, *IUPAC. Compendium of Chemical Terminology, 2nd Ed. (the "Gold Book")*, Blackwell Scientific Publications, Oxford (1997). XML on-line corrected version: http://goldbook.iupac.org (2006-) created by M. Nic, J. Jirat, B. Kosata; updates compiled by A. Jenkins.

2. H.-J. Federsel, *Stereoselective Synthesis of Drugs – An Industrial Perspective, in Chirality in Drug Research, Volume 33*, (eds E. Francotte and W. Lindner), Wiley-VCH Verlag GmbH & Co. KGaA, Weinheim, FRG, 2006.

3. V. Farina, J. T. Reeves, C. H. Senanayake, and J. J. Song, *Chem. Rev.*, 2006, **106**, 2734.

4. D. J. Triggle, *Drug. Discov. Ther.*, 1997, **2**, 138.

5. J. Gal, *Chirality*, 2012, **24**, 959.

6. FDA's Policy Statement, *Chirality*, 1992, **4**, 338.

7. L. Pasteur, *Cr. Hebd. Acad. Sci.*, 1848, **26**, 535.

8. E. Pálovics, F. Faigl, and E. Fogassy, *Separation of the Mixtures of Chiral Compounds by Crystallization, Advances in Crystallization Processes*, Dr. Yitzhak Mastai (Ed.), InTech, 2012.

9. H.-U. Blaser, *Chem. Rev.*, 1992, **92**, 935.

10. G. Stork and S. Raucher, *J. Am. Chem. Soc.*, 1976, **98**, 1583.

11. G. Stork, T. Takahashi, I. Kawamoto, and T. Suzuki, *J. Am. Chem. Soc.*, 1978, **100**, 8272.

12. E. J. Corey and H. E. Ensley, *J. Am. Chem. Soc.*, 1975, **97**, 6908.

13. Y. Gnas and F. Glorius, *Synthesis*, 2006, **12**, 1899.

14. D. A. Evans, G. Helmchen, and M. Rüping, *Chiral Auxiliaries in Asymmetric Synthesis, Asymmetric Synthesis – The Essentials*, WILEY-VCH Verlag GmbH & Co. KGaA, Weinheim, 2007.

15. E. N. Jacobsen, A. Pfaltz, and H. Yamamoto, *Comprehensive Asymmetric Catalysis*, Springer, Berlin, 1999.

16. I. Ojima, *Catalytic Asymmetric Synthesis, 3rd Ed.*, Wiley, New York, 2010.

17. M. Heitbaum, F. Glorius, and I. Escher, *Angew. Chem. Int. Ed.*, 2006, **45**, 4732.

18. H.-U. Blaser and E. Schmidt, *Asymmetric Catalysis on Industrial Scale: Challenges, Approaches and Solutions*, Wiley, New York, 2004.

19. B. J. A. Osborn, F. H. Jardine, J. F. Young, and G. Wilkinson, *J. Chem. Soc. (A)*, 1966, 1711.

20. W. S. Knowles, *Acc. Chem. Res.*, 1983, **16**, 106.

21.   U. T. Bornscheuer, G. W. Huisman, R. J. Kazlauskas, S. Lutz, J. C. Moore, and K. Robins, *Nature*, 2012, **485**, 185.

22.   A. Schmid, J. S. Dordick, B. Hauer, A. Kiener, M. Wubbolts, and B. Witholt, *Nature*, 2001, **409**, 258.

23.   C. Wandrey, A. Liese, and D. Kihumbu, *Org. Proc. Res. Dev.*, 2000, **4**, 286.

24.   T. Johannes, M. R. Simurdiak, and H. Zhao, *Biocatalysis, Encyclopedia of Chemical Processing*, Taylor & Francis, 2006.

25.   B. List, *Chem. Rev.*, 2007, **107**, 5413.

26.   J. Von Liebig, *Justus Liebigs Ann. Chem.*, 1860, **113**, 246.

27.   P. I. Dalko and L. Moisan, *Angew. Chem. Int. Ed.*, 2001, **40**, 3726.

28.   P. I. Dalko and L. Moisan, *Angew. Chem. Int. Ed.*, 2004, **43**, 5138.

29.   D. W. C. MacMillan, *Nature*, 2008, **455**, 304.

30.   U. Eder, G. Sauer, and R. Wiechert, *Angew. Chem. Int. Ed.*, 1971, **10**, 496.

31.   Z. G. Hajos and D. R. Parrish, *J. Org. Chem.*, 1974, **39**, 1615.

32.   Z. G. Hajos, D. R. Parrish, and E. P. Oliveto, *Tetrahedron*, 1968, **24**, 2039.

33.   Z. G. Hajos and D. R. Parrish, *J. Org. Chem.*, 1973, **38**, 3244.

34.   D. Yang, Y.-C. Yip, M.-W. Tang, M.-K. Wong, J.-H. Zheng, and K.-K. Cheung, *J. Am. Chem. Soc.*, 1996, **118**, 491.

35.   Y. Tu, Z.-X. Wang, and Y. Shi, *J. Am. Chem. Soc.*, 1996, **118**, 9806.

36.   S. E. Denmark, Z. Wu, C. M. Crudden, and H. Matsuhashi, *J. Org. Chem.*, 1997, **62**, 8288.

37.   S. J. Miller, G. T. Copeland, N. Papaioannou, T. E. Horstmann, and E. M. Ruel, *J. Am. Chem. Soc.*, 1998, **120**, 1629.

38.   M. S. Sigman and E. N. Jacobsen, *J. Am. Chem. Soc.*, 1998, **120**, 4901.

39.   E. J. Corey and M. J. Grogan, *Org. Lett.*, 1999, **1**, 157.

40.   B. List, R. A. Lerner, and C. F. Barbas III, *J. Am. Chem. Soc.*, 2000, **122**, 2395.

41.   K. A. Ahrendt, C. J. Borths, and D. W. C. MacMillan, *J. Am. Chem. Soc.*, 2000, **122**, 4243.

42.   C. Y. Lai, N. Nakai, and D. Chang, *Science*, 1974, **183**, 1204.

43.   A. J. Morris and D. R. Tolan, *Biochemistry*, 1994, **33**, 12291.

44.   P. Melchiorre, M. Marigo, A. Carlone, and G. Bartoli, *Angew. Chem. Int. Ed.*, 2008, **47**, 6138.

45.   B. List, *Synlett*, 2001, 1675.

46.   B. List, *Chem. Commun.*, 2006, 819.

47.   S. J. Connon, *Chem. Eur. J.*, 2006, **12**, 5418.

48.   H. Yamamoto, *Lewis Acids In Organic Synthesis*, Wiley-VCH, Weinheim, 2000.

49.   H. Yamamoto, *Lewis Acids Reagents*, Oxford University Press, New York, 1999.

50.   M. S. Taylor and E. N. Jacobsen, *Angew. Chem. Int. Ed.*, 2006, **45**, 1520.

51.   H. Hiemstra and H. Wynberg, *J. Am. Chem. Soc.*, 1981, **103**, 417.

52.   J.-I. Oku and S. Inoue, *J. Chem. Soc. Chem. Commun.*, 1981, 229.

53.   U.-H. Dolling, P. Davis, and E. J. J. Grabowski, *J. Am. Chem. Soc.*, 1984, **106**, 446.

54.   J. Hine, S.-M. Linden, and V. M. Kanagasabapathy, *J. Am. Chem. Soc.*, 1985, **107**, 1082.

55.   J. Hine, S.-M. Linden, and V. M. Kanagasabapathy, *J. Org. Chem.*, 1985, **50**, 5096.

56.   J. Hine, K. Ahn, J. C. Gallucci, and S.-M. Linden, *J. Am. Chem. Soc.*, 1984, **106**, 7980.

57.   T. R. Kelly, P. Meghani, and V. S. Ekkundi, *Tetrahedron Lett.*, 1990, **31**, 3381.

58.   J. F. Blake and W. L. Jorgensen, *J. Am. Chem. Soc.*, 1991, **113**, 7430.

59.   D. L. Severance and W. L. Jorgensen, *J. Am. Chem. Soc.*, 1992, **114**, 10966.

60.   M. C. Etter and T. W. Panunto, *J. Am. Chem. Soc.*, 1988, **110**, 5896.

61.   M. C. Etter, Z. Urbakzyk-Lipkowska, M. Zia-Ebrahimi, and T. W. Panunto, *J. Am. Chem. Soc.*, 1990, **112**, 8415.

62.   D. P. Curran and L. H. Kuo, *J. Org. Chem.*, 1994, **59**, 3259.

63.   D. P. Curran and L. H. Kuo, *Tetrahedron Lett.*, 1995, **36**, 6647.

64.   P. R. Schreiner and A. Wittkopp, *Org. Lett.*, 2002, **4**, 217.

65.   A. Wittkopp and P. R. Schreiner, *Chem. Eur. J.*, 2003, **9**, 407.

66.   T. Okino, Y. Hoashi, and Y. Takemoto, *Tetrahedron Lett.*, 2003, **44**, 2817.

67.   D. J. Maher and S. J. Connon, *Tetrahedron Lett.*, 2004, **45**, 1301.

68.   G. Dessole, R. P. Herrera, and A. Ricci, *Synlett*, 2004, 2374.

69.   Z. Zhang and P. R. Schreiner, *Synlett*, 2007, 1455.

70.   S. A. Kavanagh, A. Piccinini, E. M. Fleming, and S. J. Connon, *Org. Biomol. Chem.*, 2008, **6**, 1339.

71.   S. Tallon, A. C. Lawlor, and S. J. Connon, *ARKIVOC*, 2011, **iv**, 115.

72.   P. Vachal and E. N. Jacobsen, *J. Am. Chem. Soc.*, 2002, **124**, 10012.

73.   M. S. Sigman, P. Vachal, and E. N. Jacobsen, *Angew. Chem. Int. Ed.*, 2000, **39**, 1279.

74.   P. Vachal and E. N. Jacobsen, *Org. Lett.*, 2000, **2**, 867.

75.   A. G. Wenzel and E. N. Jacobsen, *J. Am. Chem. Soc.*, 2002, **124**, 12964.

76.   G. D. Joly and E. N. Jacobsen, *J. Am. Chem. Soc.*, 2004, **126**, 4102.

77.   M. S. Taylor and E. N. Jacobsen, *J. Am. Chem. Soc.*, 2004, **126**, 10558.

78.   T. P. Yoon and E. N. Jacobsen, *Angew. Chem. Int. Ed.*, 2005, **44**, 466.

79.   T. Okino, Y. Hoashi, and Y. Takemoto, *J. Am. Chem. Soc.*, 2003, **125**, 12672.

80.   T. Okino, Y. Hoashi, T. Furukawa, X. Xu, and Y. Takemoto, *J. Am. Chem. Soc.*, 2005, **127**, 119.

81.   Y. Hoashi, T. Okino, and Y. Takemoto, *Angew. Chem. Int. Ed.*, 2005, **44**, 4032.

82.   T. Okino, S. Nakamura, T. Furukawa, and Y. Takemoto, *Org. Lett.*, 2004, **6**, 625.

83.   X. Xu, T. Furukawa, T. Okino, H. Miyabe, and Y. Takemoto, *Chem. Eur. J.*, 2006, **12**, 466.

84.   D. E. Fuerst and E. N. Jacobsen, *J. Am. Chem. Soc.*, 2005, **127**, 8964.

85.   C. E. Song, *Cinchona Alkaloids in Synthesis ans Catalysis, Ligands, Immobilisation and Organocatalysis*, WILEY-VCH Verlag GmbH & Co. KGaA, Weinheim, 2009.

86.   T. Marcelli and H. Hiemstra, *Synthesis*, 2010, 1229.

87.   H. M. R. Hoffmann and J. Frackenpohl, *Eur. J. Org. Chem.*, 2004, 4293.

88.   L. Pasteur, *Cr. Hebd. Acad. Sci.*, 1853, **37**, 162.

89.   G. Bredig and P. S. Fiske, *Biochem. Z.*, 1912, **46**, 7.

90.   H. Pracejus and H. Mätje, *J. Prakt. Chem.*, 1964, **24**, 195.

91.   S. J. Connon, *Chem. Commun.*, 2008, 2499.

92.   A. G. Doyle and E. N. Jacobsen, *Chem. Rev.*, 2007, **107**, 5713.

93.   T. P. Yoon and E. N. Jacobsen, *Science*, 2003, **299**, 1691.

94.   H. C. Kolb, M. S. VanNieuwenhze, and K. B. Sharpless, *Chem. Rev.*, 1994, **94**, 2483.

95.   B.-J. Li, L. Jiang, M. Liu, Y.-C. Chen, L.-S. Ding, and Y. Wu, *Synlett*, 2005, 603.

96.   B. Vakulya, S. Varga, A. Csámpai, and T. Soós, *Org. Lett.*, 2005, **7**, 1967.

97.   S. H. McCooey and S. J. Connon, *Angew. Chem. Int. Ed.*, 2005, **44**, 6367.

98.   J. Ye, D. J. Dixon, and P. S. Hynes, *Chem. Commun.*, 2005, 4481.

99. J. P. Malerich, K. Hagihara, and V. H. Rawal, *J. Am. Chem. Soc.*, 2008, **130**, 14416.

100. J. Alemán, A. Parra, H. Jiang, and K. A. Jørgensen, *Chem. Eur. J.*, 2011, **17**, 6890.

101. R. I. Storer, C. Aciro, and L. H. Jones, *Chem. Soc. Rev.*, 2011, **40**, 2330.

102. M. Bandini, R. Sinisi, and A. Umani-Ronchi, *Chem. Commun.*, 2008, 4360.

103. A. Peschiulli, B. Procuranti, C. J. O' Connor, and S. J. Connon, *Nature Chem.*, 2010, **2**, 380.

104. C. Quigley, Z. Rodríguez-Docampo, and S. J. Connon, *Chem. Commun.*, 2012, **48**, 1443.

105. Z. Rodríguez-Docampo, C. Quigley, S. Tallon, and S. J. Connon, *J. Org. Chem.*, 2012, **77**, 2407.

106. Y.-C. Chen, *Synlett*, 2008, 1919.

107. G. Bartoli and P. Melchiorre, *Synlett*, 2008, 1759.

108. Y. Iwabuchi, M. Nakatani, N. Yokoyama, and S. Hatakeyama, *J. Am. Chem. Soc.*, 1999, **121**, 10219.

109. H. Li, Y. Wang, L. Tang, and L. Deng, *J. Am. Chem. Soc.*, 2004, **126**, 9906.

110. T. Marcelli, R. N. S. van der Haas, J. H. van Maarseveen, and H. Hiemstra, *Angew. Chem. Int. Ed.*, 2006, **45**, 929.

111. N. Abermil, G. Masson, and J. Zhu, *J. Am. Chem. Soc.*, 2008, **130**, 12596.

112. H. Waldmann, V. Khedkar, H. Dückert, M. Schürmann, I. M. Oppel, and K. Kumar, *Angew. Chem. Int. Ed.*, 2008, **47**, 6869.

113. Y. Liu, B. Sun, B. Wang, M. Wakem, and L. Deng, *J. Am. Chem. Soc.*, 2009, **131**, 418.

114. C. C. C. Johansson, N. Bremeyer, S. V. Ley, D. R. Owen, S. C. Smith, and M. J. Gaunt, *Angew. Chem. Int. Ed.*, 2006, **45**, 6024.

115. Y. Wu and L. Deng, *J. Am. Chem. Soc.*, 2012, **134**, 14334.

116. A. Lee, A. Michrowska, S. Sulzer-Mosse, and B. List, *Angew. Chem. Int. Ed.*, 2011, **50**, 1707.

117. W. Zhang, J. Hu, D. J. Young, and T. S. A. Hor, *Organometallics*, 2011, **30**, 2137.

118. S. Brandes, B. Niess, M. Bella, A. Prieto, J. Overgaard, and K. A. Jørgensen, *Chem. Eur. J.*, 2006, **12**, 6039.

119. X. Liu, B. Sun, and L. Deng, *Synlett*, 2009, 1685.

120. C. Palacio and S. J. Connon, *Org. Lett.*, 2011, **13**, 1298.

121. C. Palacio and S. J. Connon, *Chem. Commun.*, 2012, **48**, 2849.

122. O. Gleeson, G.-L. Davies, A. Peschiulli, R. Tekoriute, Y. K. Gun'ko, and S. J. Connon, *Org. Biomol. Chem.*, 2011, **9**, 7929.

123. M. Benaglia, A. Puglisi, and F. Cozzi, *Chem. Rev.*, 2003, **103**, 3401.

124. S. Shylesh, V. Schünemann, and W. R. Thiel, *Angew. Chem. Int. Ed.*, 2010, **49**, 3428.

125. F. Cozzi, *Adv. Synth. Catal.*, 2006, **348**, 1367.

126. T. Ooi and K. Maruoka, *Angew. Chem. Int. Ed.*, 2007, **46**, 4222.

127. S. Shirakawa and K. Maruoka, *Angew. Chem. Int. Ed.*, 2013, **52**, 4312.

128. J. March, *Advanced Organic Chemistry, 4th Ed.*, Wiley, New York, 1992.

129. A. Verley and F. Bölsing, *Ber. Dtsch. Chem. Ges.*, 1901, **34**, 3354.

130. M. González-López and J. T. Shaw, *Chem. Rev.*, 2009, **109**, 164.

131. W. Perkin, *J. Chem. Soc.*, 1868, **21**, 53.

132. W. H. Perkin, *J. Chem. Soc.*, 1868, **21**, 181.

133. W. H. Perkin, *J. Chem. Soc.*, 1877, **31**, 388.

134. R. Adams, *Organic Reactions vol. I*, John Wiley & Sons, New York, 1942.

135. R. Fittig and H. W. Jayne, *Justus Liebigs Ann. Chem*, 1883, **216**, 97.

136. E. Müller, *Justus Liebigs Ann. Chem.*, 1931, **491**, 251.

137. J. B. Jones and A. R. Pinder, *J. Chem. Soc.*, 1958, 2612.

138. N. Castagnoli, *J. Org. Chem.*, 1969, **34**, 3187.

139. M. Cushman and N. Castagnoli, *J. Org. Chem.*, 1973, **38**, 440.

140. M. Cushman and N. Castagnoli, *J. Org. Chem.*, 1974, **39**, 1546.

141. R. L. Hively, W. A. Mosher, and F. W. Hoffmann, *J. Am. Chem. Soc.*, 1966, **88**, 1832.

142. M. A. Haimova, N. M. Mollov, S. C. Ivanova, A. I. Dimitrova, and V. I. Ognyanov, *Tetrahedron*, 1977, **33**, 331.

143. M. Cushman, J. Gentry, and F. W. Dekow, *J. Org. Chem.*, 1977, **42**, 1111.

144. M. Cushman and E. J. Madaj, *J. Org. Chem.*, 1987, **52**, 907.

145. Y. Tamura, A. Wada, M. Sasho, and Y. Kita, *Tetrahedron Lett.*, 1981, **22**, 4283.

146. Y. Tamura, A. Wada, M. Sasho, and Y. Kita, *Chem. Pharm. Bull.*, 1983, **31**, 2691.

147. M. Cushman and N. Castagnoli, *J. Org. Chem.*, 1971, **36**, 3404.

148. C. E. Masse, P. Y. Ng, Y. Fukase, M. Sanchez-Roselló, and J. T. Shaw, *J. Comb. Chem.*, 2006, **8**, 293.

149. P. Y. Ng, C. E. Masse, and J. T. Shaw, *Org. Lett.*, 2006, **8**, 3999.

150. J. Wei and J. T. Shaw, *Org. Lett.*, 2007, **9**, 4077.

151. K. Nozawa, M. Yamada, Y. Tsuda, K.-I. Kawai, and S. Nakajima, *Chem. Pharm. Bull.*, 1981, **29**, 3486.

152. R. Okunaka, T. Honda, M. Kondo, Y. Tamura, and Y. Kita, *Chem. Pharm. Bull.*, 1991, **39**, 1298.

153. M. G. Bogdanov and M. D. Palamareva, *Tetrahedron*, 2004, **60**, 2525.

154. M. G. Bogdanov, M. Kandinska, B. Yliev, and M. D. Palamareva, *Pharmacia*, 2005, **52**, 7.

155. N. Yu, R. Poulain, A. Tartar, and J.-C. Gesquiere, *Tetrahedron*, 1999, **55**, 13735.

156. N. N. Girotra and N. L. Wendler, *J. Org. Chem.*, 1969, **34**, 3192.

157. Y. Tamura, M. Sasho, K. Nakagawa, T. Tsugoshi, and Y. Kita, *J. Org. Chem.*, 1984, **49**, 473.

158. J. M. Lawlor and M. B. McNamee, *Tetrahedron Lett.*, 1983, **24**, 2211.

159. R. Bandichhor, B. Nosse, and O. Reiser, *Top. Curr. Chem.*, 2005, **243**, 43.

160. D. R. Stevens, C. P. Till, and D. A. Whiting, *J. Chem. Soc., Perkin Trans. 1*, 1992, 185.

161. L. A. Bonner, B. R. Chemel, V. J. Watts, and D. E. Nichols, *Bioorg. Med. Chem.*, 2010, **18**, 6763.

162. R. C. Fuson, *J. Am. Chem. Soc.*, 1924, **46**, 2779.

163. J. B. Shoesmith and A. Guthrie, *J. Chem. Soc.*, 1928, 2332.

164. J. A. Tran, C. W. Chen, F. C. Tucci, W. Jiang, B. A. Fleck, and C. Chen, *Bioorg. Med. Chem. Lett.*, 2008, **18**, 1124.

165. S. Yoshida, T. Ogiku, H. Ohmizu, and T. Iwasaki, *Tetrahedron Lett.*, 1995, **36**, 1455.

166. S. Yoshida, H. Ohmizu, and T. Iwaski, *Tetrahedron Lett.*, 1995, **36**, 8225.

167. S. Yoshida, T. Ogiku, H. Ohmizu, and T. Iwasaki, *J. Org. Chem.*, 1997, **62**, 1310.

168. N. Minami and I. Kuwajima, *Tetrahedron Lett.*, 1977, **18**, 1423.

169. R. J. Spangler and J. H. Kim, *Tetrahedron Lett.*, 1972, **13**, 1249.

170. K. Rathwell and M. A. Brimble, *Synthesis*, 2007, 643.

171. M. Karthikeyan, R. Kamakshi, V. Sridar, and B. S. R. Reddy, *Synth. Comm.*, 2003, **33**, 4199.

172. M. G. Constantino, V. Lacerda Júnior, and G. V. J. da Silva, *Molecules*, 2002, **7**, 456.

173. X. Li and S. J. Danishefsky, *J. Am. Chem. Soc.*, 2010, **132**, 11004.

174. M. D. Rozeboom, I.-M. Tegmo-Larsson, and K. N. Houk, *J. Org. Chem.*, 1981, **46**, 2338.

175. G. Roberge and P. Brassard, *J. Org. Chem.*, 1981, **46**, 4161.

176. Y. Tamura, F. Fukata, M. Sasho, T. Tsugoshi, and Y. Kita, *J. Org. Chem.*, 1985, **50**, 2273.

177. Y. Tamura, M. Sasho, S. Akai, A. Wada, and Y. Kita, *Tetrahedron*, 1984, **40**, 4539.

178. Y. Tamura, A. Wada, M. Sasho, K. Fukunaga, H. Maeda, and Y. Kita, *J. Org. Chem.*, 1982, **47**, 4376.

179. C. D. Cox, T. Siu, and S. J. Danishefsky, *Angew. Chem. Int. Ed.*, 2003, **42**, 5625.

180. A. Georgieva, E. Stanoeva, S. Spassov, M. Haimova, N. De Kimpe, M. Boelens, M. Keppens, A. Kemme, and A. Mishnev, *Tetrahedron*, 1995, **51**, 6099.

181. A. Georgieva, S. Spassov, E. Stanoeva, I. Topalova, and C. Tchanev, *J. Chem. Research (S)*, 1997, 148.

182. P. G. Jagtap, E. Baloglu, G. Southan, W. Williams, A. Roy, A. Nivorozhkin, N. Landrau, K. Desisto, A. L. Salzman, and C. Szabó, *Org. Lett.*, 2005, **7**, 1753.

183. Y. Tamura, S. Mohri, H. Maeda, T. Tsugoshi, M. Sasho, and Y. Kita, *Tetrahedron Lett.*, 1984, **25**, 309.

184. Y. Kita, S.-I. Mohri, T. Tsugoshi, H. Maeda, and Y. Tamura, *Chem. Pharm. Bull.*, 1985, **33**, 4723.

185. Y. Tamura, S. Akai, M. Sasho, and Y. Kita, *Tetrahedron Lett.*, 1984, **25**, 1167.

186. Y. Tamura, M. Sasho, H. Ohe, S. Akai, and Y. Kita, *Tetrahedron Lett.*, 1985, **26**, 1549.

187. Y. Kita, R. Okunaka, M. Sasho, M. Taniguchi, T. Honda, and Y. Tamura, *Tetrahedron Lett.*, 1988, **29**, 5943.

188. Y. Kita, R. Okunaka, T. Honda, M. Shindo, M. Taniguchi, M. Kondo, and M. Sasho, *J. Org. Chem.*, 1991, **56**, 119.

189. M. E. Jung and J. A. Lowe, *J. Chem. Soc. Chem. Commun.*, 1978, 95.

190. M. E. Jung, J. A. Lowe III, M. A. Lyster, and M. Node, *Tetrahedron*, 1984, **40**, 4751.

191. K. Afarinkia, V. Vinader, T. D. Nelson, and G. H. Posner, *Tetrahedron*, 1992, **48**, 9111.

192. Y. Wang, H. Li, Y.-Q. Wang, Y. Liu, B. M. Foxman, and L. Deng, *J. Am. Chem. Soc.*, 2007, **129**, 6364.

193. R. P. Singh, K. Bartelson, Y. Wang, H. Su, X. Lu, and L. Deng, *J. Am. Chem. Soc.*, 2008, **130**, 2422.

194. O. P. Törmäkangas and A. M. P. Koskinen, *Recent Res. Devel. Organic Chem.*, 2001, **5**, 225.

195. T. Seki, T. Nakajo, and M. Onaka, *Chem. Lett.*, 2006, **35**, 824.

196. L. Claisen, *Ber. Dtsch. Chem. Ges.*, 1887, **20**, 646.

197. W. E. Tischtschenko, *J. Russ. Phys. Chem. Soc.*, 1906, **38**, 355.

198. W. E. Tischtschenko, *Chem. Zentralbl.*, 1906, **77**, 1309.

199. D. Ulrich and H. Jankowsky, *Chem. Tech.*, 1988, **40**, 393.

200. K. Weissermel and H. J. Arpe, *Industrial Organic Chemistry, 4th Ed.*, Wiley-VCH, Weinheim, 2003.

201. R. E. Kirk and D. F. Othmer, *Encyclopedia of Chemical Technology, 3rd Ed.*, John Wiley & Sons, New York, 2007.

202. A. S. Hester and K. Himmler, *Ind. Eng. Chem.*, 1959, **51**, 1424.

203. I. Lin and A. R. Day, *J. Am. Chem. Soc.*, 1952, **75**, 5133.

204. Y. Ogata and A. Kawasaki, *Tetrahedron*, 1969, **25**, 929.

205. W. F. Luder and S. Zuffanti, *Chem. Rev.*, 1944, **34**, 345.

206. Y. Ogata, A. Kawasaki, and I. Kishi, *Tetrahedron*, 1967, **23**, 825.

207. W. C. Child and H. Adkins, *J. Am. Chem. Soc.*, 1925, **47**, 798.

208. F. J. Villani and F. F. Nord, *J. Am. Chem. Soc.*, 1947, **69**, 2605.

209. T. Saegusa and T. Ueshima, *J. Org. Chem.*, 1968, **33**, 3310.

210. T. Ooi, T. Miura, K. Takaya, and K. Maruoka, *Tetrahedron Lett.*, 1999, **40**, 7695.

211. T. Ooi, K. Ohmatsu, K. Sasaki, T. Miura, and K. Maruoka, *Tetrahedron Lett.*, 2003, **44**, 3191.

212. Y.-S. Hon, C.-P. Chang, and Y.-C. Wong, *Tetrahedron Lett.*, 2004, **45**, 3313.

213. M. Yamashita, Y. Watanabe, T.-A. Mitsudo, and Y. Takegami, *Bull. Chem. Soc. Jpn.*, 1976, **49**, 3597.

214. M. Yamashita and T. Ohishi, *App. organomet. chem.*, 1993, **7**, 357.

215. H. Horino, T. Ito, and A. Yamamoto, *Chem. Lett.*, 1978, **7**, 17–20.

216. T. Ito, H. Horino, Y. Yoshitaka, and A. Yamamoto, *Bull. Chem. Soc. Jpn.*, 1982, **55**, 504.

217. S. H. Bergens, D. P. Fairlie, and B. Bosnich, *Organometallics*, 1990, **9**, 566.

218. K.-I. Morita, Y. Nishiyama, and Y. Ishii, *Organometallics*, 1993, **12**, 3748.

219. P. Barrio, M. A. Esteruelas, and E. Oñate, *Organometallics*, 2004, **23**, 1340.

220. T. Suzuki, T. Yamada, T. Matsuo, K. Watanabe, and T. Katoh, *Synlett*, 2005, 1450.

221. S. Ogoshi, Y. Hoshimoto, and M. Ohashi, *Chem. Commun.*, 2010, **46**, 3354.

222. Y. Hoshimoto, M. Ohashi, and S. Ogoshi, *J. Am. Chem. Soc.*, 2011, **133**, 4668.

223. P. R. Stapp, *J. Org. Chem.*, 1973, **38**, 1433.

224. S.-Y. Onozawa, T. Sakakura, M. Tanaka, and M. Shiro, *Tetrahedron*, 1996, **52**, 4291.

225. H. Berberich and P. W. Roesky, *Angew. Chem. Int. Ed.*, 1998, **37**, 1569.

226. M. R. Bürgstein, H. Berberich, and P. W. Roesky, *Chem. Eur. J.*, 2001, **7**, 3078.

227. T. Andrea, E. Barnea, and M. S. Eisen, *J. Am. Chem. Soc.*, 2008, **130**, 2454.

228. M. Sharma, T. Andrea, N. J. Brookes, B. F. Yates, and M. S. Eisen, *J. Am. Chem. Soc.*, 2011, **133**, 1341.

229. M. M. Mojtahedi, E. Akbarzadeh, R. Sharifi, and M. S. Abaee, *Org. Lett.*, 2007, **9**, 2791.

230. D. C. Waddell and J. Mack, *Green Chem.*, 2009, **11**, 79.

231. T. Werner and J. Koch, *Eur. J. Org. Chem.*, 2010, 6904.

232. M. R. Crimmin, A. G. M. Barrett, M. S. Hill, and P. A. Procopiou, *Org. Lett.*, 2007, **9**, 331.

233. B. M. Day, N. E. Mansfield, M. P. Coles, and P. B. Hitchcock, *Chem. Commun.*, 2011, **47**, 4995.

234. T. Seki, H. Kabashima, K. Akutsu, H. Tachikawa, and H. Hattori, *J. Catal.*, 2001, **204**, 393.

235. T. Seki and H. Hattori, *Cat. Surv. Asia*, 2003, **7**, 145.

236. Y. Chen, Z. Zhu, J. Zhang, J. Shen, and X. Zhou, *J. Organomet. Chem.*, 2005, **690**, 3783.

237. W. H. Urry, A. Nishihara, and J. H. Y. Niu, *J. Org. Chem.*, 1967, **32**, 347.

238. A. Chan and K. A. Scheidt, *J. Am. Chem. Soc.*, 2006, **128**, 4558.

239. S. S. Canan Koch and A. R. Chamberlin, in *Enantiomerically pure γ-butyrolactones in natural products synthesis in Studies in Natural Products Chemistry*, Ed. Atta-ur-Rahman, Elsevier Science B. V., 1995, vol. 16, p. 687.

240. Y. Waché, M. Aguedo, J.-M. Nicaud, and J.-M. Belin, *Appl. Microbiol. Biotechnol.*, 2003, **61**, 393.

241. M. I. Konaklieva and B. J. Plotkin, *Mini-Rev. Med. Chem.*, 2005, **5**, 73.

242. J. Uenishi, S. Masuda, and A. Wakabayashi, *Tetrahedron Lett.*, 1991, **32**, 5097.

243. T. H. Chuang, J. M. Fang, W.-T. Jiaang, and Y.-M. Tsai, *J. Org. Chem.*, 1996, **61**, 1794.

244. Z. Shen, H. A. Khan, and V. M. Dong, *J. Am. Chem. Soc.*, 2008, **130**, 2916.

245. D. H. T. Phan, B. Kim, and V. M. Dong, *J. Am. Chem. Soc.*, 2009, **131**, 15608.

246. S. Omura, T. Fukuyama, Y. Murakami, H. Okamoto, and I. Ryu, *Chem. Commun.*, 2009, 6741.

247. D. C. Gerbino, D. Augner, N. Slavov, and H. G. Schmalz, *Org. Lett.*, 2012, **14**, 2338.

248. J.-L. Hsu, C.-T. Chen, and J.-M. Fang, *Org. Lett.*, 1999, **1**, 1989.

249. J.-L. Hsu and J.-M. Fang, *J. Org. Chem.*, 2001, **66**, 8573.

250. R. H. Cichewicz, F. A. Valeriote, and P. Crews, *Org. Lett.*, 2004, **6**, 1951.

251. Y. F. Huang, L. H. Li, L. Tian, L. Qiao, H.-M. Hua, and Y.-H. Pei, *J. Antibiot.*, 2006, **59**, 355.

252. S. Wan, F. Wu, J. C. Rech, M. E. Green, R. Balachandran, W. S. Horne, B. W. Day, and P. E. Floreancig, *J. Am. Chem. Soc.*, 2011, **133**, 16668.

253. M. Enomoto and S. Kuwahara, *Angew. Chem. Int. Ed.*, 2009, **48**, 1144.

254. M. G. Bogdanov, M. I. Kandinska, D. B. Dimitrova, B. T. Gocheva, and M. D. Palamareva, *Z. Naturforsch*, 2007, **62**, 477.

255. T. K. Tabopda, G. W. Fotso, J. Ngoupayo, A.-C. Mitaine-Offer, B. T. Ngadjui, and M.-A. Lacaille-Dubois, *Planta Med.*, 2009, **75**, 1258.

256. H. Hussain, N. Akhtar, S. Draeger, B. Schulz, G. Pescitelli, P. Salvadori, S. Antus, T. Kurtán, and K. Krohn, *Eur. J. Org. Chem.*, 2009, 749.

257. Y. Shimojima, T. Shirai, T. Baba, and H. Hayashi, *J. Med. Chem.*, 1985, **28**, 3.

258. B. V. McInerney, W. C. Taylor, M. J. Lacey, R. K. Akhurst, and R. P. Gregson, *J. Nat. Prod.*, 1991, **54**, 785.

259. P. Kongsaeree, S. Prabpai, N. Sriubolmas, C. Vongvein, and S. Wiyakrutta, *J. Nat. Prod.*, 2003, **66**, 709.

260. N. Nazir, S. Koul, M. A. Qurishi, M. H. Najar, and M. I. Zargar, *Eur. J. Med. Chem.*, 2011, **46**, 2415.

261. M. Yoshikawa, E. Uchida, N. Chatani, H. Kobayashi, Y. Naitoh, Y. Okuno, H. Matsuda, J. Yamahara, and N. Murakami, *Chem. Pharm. Bull.*, 1992, **40**, 3352.

262. C. Bolm, A. Gerlach, and C. L. Dinter, *Synlett*, 1999, 195.

263. C. Bolm, I. Schiffers, C. L. Dinter, and A. Gerlach, *J. Org. Chem.*, 2000, **65**, 6984.

264. Y. Chen, S.-K. Tian, and L. Deng, *J. Am. Chem. Soc.*, 2000, **122**, 9542.

265. Y. Chen, P. McDaid, and L. Deng, *Chem. Rev.*, 2003, **103**, 2965.

266. T. Honjo, S. Sano, M. Shiro, and Y. Nagao, *Angew. Chem. Int. Ed.*, 2005, **44**, 5838.

267. I. Atodiresei, I. Schiffers, and C. Bolm, *Chem. Rev.*, 2007, **107**, 5683.

268. H. S. Rho, S. H. Oh, J. W. Lee, J. Y. Lee, J. Chin, and C. E. Song, *Chem. Commun.*, 2008, 1208.

269. S. H. Oh, H. S. Rho, J. W. Lee, J. E. Lee, S. H. Youk, J. Chin, and C. E. Song, *Angew. Chem. Int. Ed.*, 2008, **47**, 7872.

270. H. Li, X. Liu, F. Wu, L. Tang, and L. Deng, *Proc. Natl. Acad. Sci. USA*, 2010, **107**, 20625.

271. Z. Rodríguez-Docampo and S. J. Connon, *ChemCatChem*, 2012, **4**, 151.

272. A. Peschiulli, Y. K. Gun'ko, and S. J. Connon, *J. Org. Chem.*, 2008, **73**, 2454.

273. A. Peschiulli, C. Quigley, S. Tallon, Y. K. Gun'ko, and S. J. Connon, *J. Org. Chem.*, 2008, **73**, 6409.

274. M. Billamboz, F. Bailly, M. L. Barreca, L. De Luca, J.-F. Mouscadet, C. Calmels, M.-L. Andréola, M. Witvrouw, F. Christ, Z. Debyser, and P. Cotelle, *J. Med. Chem.*, 2008, **51**, 7717.

275. M. K. Deliömeroğlu, S. Özcan, and M. Balci, *ARKIVOC*, 2010, **ii**, 148.

276. H. M. R. Hoffmann and J. Rabe, *Angew. Chem. Int. Ed.*, 1985, **24**, 94.

277. M. Seitz and O. Reiser, *Curr. Opin. Chem. Biol.*, 2005, **9**, 285.

278. J. M. Crawforth and B. J. Rawlings, *Tetrahedron Lett.*, 1995, **36**, 6345.

279. T. Martín, C. M. Rodríguez, and V. S. Martín, *J. Org. Chem.*, 1996, **61**, 6450.

280. Y. Masaki, H. Arasaki, and A. Itoh, *Tetrahedron Lett.*, 1999, **40**, 4829.

281. C. Böhm and O. Reiser, *Org. Lett.*, 2001, **3**, 1315.

282. R. B. Chhor, B. Nosse, S. Sörgel, C. Böhm, M. Seitz, and O. Reiser, *Chem. Eur. J.*, 2003, **9**, 260.

283. M. T. Barros, C. D. Maycock, and M. R. Ventura, *Org. Lett.*, 2003, **5**, 4097.

284. S. Braukmüller and R. Brückner, *Eur. J. Org. Chem.*, 2006, 2110.

285. C. Le Floch, E. Le Gall, E. Léonel, T. Martens, and T. Cresteil, *Bioorg. Med. Chem. Lett.*, 2011, **21**, 7054.

286. C. Cornaggia, F. Manoni, E. Torrente, S. Tallon, and S. J. Connon, *Org. Lett.*, 2012, **14**, 1850.

287. C. Marti and E. M. Carreira, *Eur. J. Org. Chem.*, 2003, 2209.

288. C. V. Galliford and K. A. Scheidt, *Angew. Chem. Int. Ed.*, 2007, **46**, 8748.

289. B. Trost and M. Brennan, *Synthesis*, 2009, 3003.

290. G. S. Singh and Z. Y. Desta, *Chem. Rev.*, 2012, **112**, 6104.

291. S. Edmondson, S. J. Danishefsky, L. Sepp-Lorenzino, and N. Rosen, *J. Am. Chem. Soc.*, 1999, **121**, 2147.

292. P. R. Sebahar and R. M. Williams, *J. Am. Chem. Soc.*, 2000, **122**, 5666.

293. T. D. Bagul, G. Lakshmaiah, T. Kawabata, and K. Fuji, *Org. Lett.*, 2002, **4**, 249.

294. T. Onishi, P. R. Sebahar, and R. M. Williams, *Org. Lett.*, 2003, **5**, 3135.

295. B. M. Trost, N. Cramer, and H. Bernsmann, *J. Am. Chem. Soc.*, 2007, **129**, 3086.

296. J. Yang, X. Z. Wearing, P. W. Le Quesne, J. R. Deschamps, and J. M. Cook, *J. Nat. Prod.*, 2008, **71**, 1431.

297. K. A. Miller, S. Tsukamoto, and R. M. Williams, *Nature Chem.*, 2009, **1**, 63.

298. F. Zhou, Y.-L. Liu, and J. Zhou, *Adv. Synth. Catal.*, 2010, **352**, 1381.

299. N. R. Ball-Jones, J. J. Badillo, and A. K. Franz, *Org. Biomol. Chem.*, 2012, **10**, 5165.

300. R. Dalpozzo, G. Bartoli, and G. Bencivenni, *Chem. Soc. Rev.*, 2012, **41**, 7247.

301. L.-T. Shen, W.-Q. Jia, and S. Ye, *Angew. Chem. Int. Ed.*, 2013, **52**, 585.

302. S.-H. Cao, X.-C. Zhang, Y. Wei, and M. Shi, *Eur. J. Org. Chem.*, 2011, 2668.

303. G. Koza and M. Balci, *Tetrahedron*, 2011, **67**, 8679.

304. J. R. Carson and S. Wong, *J. Med. Chem.*, 1973, **16**, 172.

305. W.-B. Liu, H.-F. Jiang, and C.-L. Qiao, *Tetrahedron*, 2009, **65**, 2110.

306. M. E. Jung and C. A. Mccombs, *Org. Synth.*, 1978, **58**, 163.

307. T. Katoh, C. Noguchi, H. Kimura, T. Fujiwara, S. Ichihashi, K. Nishide, T. Kajimoto, and M. Node, *Tetrahedron-Asymmetr*, 2006, **17**, 2943.

308. M. Node, T. Fujiwara, S. Ichihashi, and K. Nishide, *Tetrahedron Lett.*, 1998, **39**, 6331.

309. G. P. Pollini, S. Benetti, C. De Risi, and V. Zanirato, *Tetrahedron*, 2010, **66**, 2775.

310. A. J. B. Edgar, S. H. Harper, and M. A. Kazi, *J. Chem. Soc.*, 1957, 1083.

311. P. Galzerano, G. Bencivenni, F. Pesciaioli, A. Mazzanti, B. Giannichi, L. Sambri, G. Bartoli, and P. Melchiorre, *Chem. Eur. J.*, 2009, **15**, 7846.

312. L. Cronin, F. Manoni, C. J. O'Connor, and S. J. Connon, *Angew. Chem. Int. Ed.*, 2010, **49**, 3045.

313. A. Soukri, A. Mougin, C. Corbier, A. Wonacott, C. Branlant, and G. Branlant, *Biochemistry*, 1989, **28**, 2586.

314. J. M. Berg, J. L. Tymoczko, and L. Strayer, *Biochemistry, 5th Ed.*, Freeman, New York, 2002.

315. K. D'Ambrosio, A. Pailot, F. Talfournier, C. Didierjean, E. Benedetti, A. Aubry, G. Branlant, and C. Corbier, *Biochemistry*, 2006, **45**.

316. C. J. O' Connor, F. Manoni, S. P. Curran, and S. J. Connon, *New J. Chem.*, 2011, **35**, 551.

317. S. Özcan and M. Balci, *Tetrahedron*, 2008, **64**, 5531.

318. W. F. Whitmore and R. C. Cooney, *J. Am. Chem. Soc.*, 1944, **66**, 1237.

319. D. Bardiot, E. Blanche, P. Chaltin, M. Koukni, P. Leyssen, J. Neyts, A. Marchand, and I. Vliegen, *WO 2010/055163 A2*, 2010.

320. S. Ozcan, C. Dengiz, M. K. Deliömeroglu, E. Sahin, and M. Balci, *Tetrahedron Lett.*, 2011, **52**, 1495.

321. F. Chang, H. Kim, B. Lee, S. Park, and J. Park, *Tetrahedron Lett.*, 2010, **51**, 4250.

322. D. W. Manley, R. T. McBurney, P. Miller, R. F. Howe, S. Rhydderch, and J. C. Walton, *J. Am. Chem. Soc.*, 2012, **134**, 13580.

323. H. E. Zimmerman, H. G. Dürr, R. S. Givens, and R. G. Lewis, *J. Am. Chem. Soc.*, 1967, **89**, 1863.

324. J. K. Crandall and T. Schuster, *J. Org. Chem.*, 1990, **55**, 1973.

325. C. Li, G. Yuan, and H. Jiang, *Chin. J. Chem*, 2010, **28**, 1685.

326. M. Mohamed, T. P. Gonçalves, R. J. Whitby, H. F. Sneddon, and D. C. Harrowven, *Chem. Eur. J.*, 2011, **17**, 13698.

327. W. Yang and D.-M. Du, *Org. Lett.*, 2010, **12**, 5450.

328. J. P. Yardley, R. E. Bright, L. Rane, R. W. A. Rees, P. B. Russell, and H. Smith, *J. Med. Chem.*, 1971, **14**, 62.

329. L. Hintermann, M. Schmitz, and U. Englert, *Angew. Chem. Int. Ed.*, 2007, **46**, 5164.

330. S. Tallon, Ph. D. Thesis, Trinity College Dublin, 2013.

331. Y. Kawai, Y. Inaba, and N. Tokitoh, *Tetrahedron: Asymmetry*, 2001, **12**, 309.

332. M. Vilches-Herrera, J. Miranda-Sepúlveda, M. Rebolledo-Fuentes, A. Fierro, S. Lühr, P. Iturriaga-Vasquez, B. K. Cassels, and M. Reyes-Parada, *Bioorg. Med. Chem.*, 2009, **17**, 2452.

333. M.-Y. Chang, C.-H. Lin, and H.-Y. Tai, *Tetrahedron Lett.*, 2013, **54**, 3194.

334. R. Ballini, M. Noè, A. Perosa, and M. Selva, *J. Org. Chem.*, 2008, **73**, 8520.

335. F. Castaneda, C. Aliaga, C. Acuña, P. Silva, and C. A. Bunton, *Phosphorus Sulfur*, 2008, **183**, 1188.

336. Y. Mao and F. Mathey, *Org. Lett.*, 2012, **14**, 1162.

337. K. S. Halskov, T. K. Johansen, R. L. Davis, M. Steurer, F. Jensen, and K. A. Jørgensen, *J. Am. Chem. Soc.*, 2012, **134**, 12943.

338. M. Müller, M. Albrecht, J. Sackmann, A. Hoffmann, F. Dierkes, A. Valkonen, and K. Rissanen, *Dalton Trans.*, 2010, **39**, 11329.

339. S. Ueda, T. Okada, and H. Nagasawa, *Chem. Commun.*, 2010, **46**, 2462.

340. G. Wang, X. Liu, T. Huang, Y. Kuang, L. Lin, and X. Feng, *Org. Lett.*, 2012, **15**, 76.

341. M. Avi, R. M. Wiedner, H. Griengl, and H. Schwab, *Chem. Eur. J.*, 2008, **14**, 11415.

342. Y. Kita, S. Akai, N. Ajimura, M. Yoshigi, T. Tsugoshi, H. Yasuda, and Y. Tamura, *J. Org. Chem.*, 1986, **51**, 4150.

343. D. C. England and C. G. Krespan, *J. Org. Chem.*, 1970, **35**, 3308.

344. H. Tian, X. Yu, Q. Li, J. Wang, and Q. Xu, *Adv. Synth. Catal.*, 2012, **354**, 2671.

345. C.-L. Li, M.-W. Chen, and X.-G. Zhang, *J. Fluorine Chem.*, 2010, **131**, 856.

346. C. Palomo, M. Oiarbide, R. Halder, A. Laso, and R. López, *Angew. Chem. Int. Ed.*, 2005, **45**, 117.

Appendix

^{1}H NMR spectrum of product 353
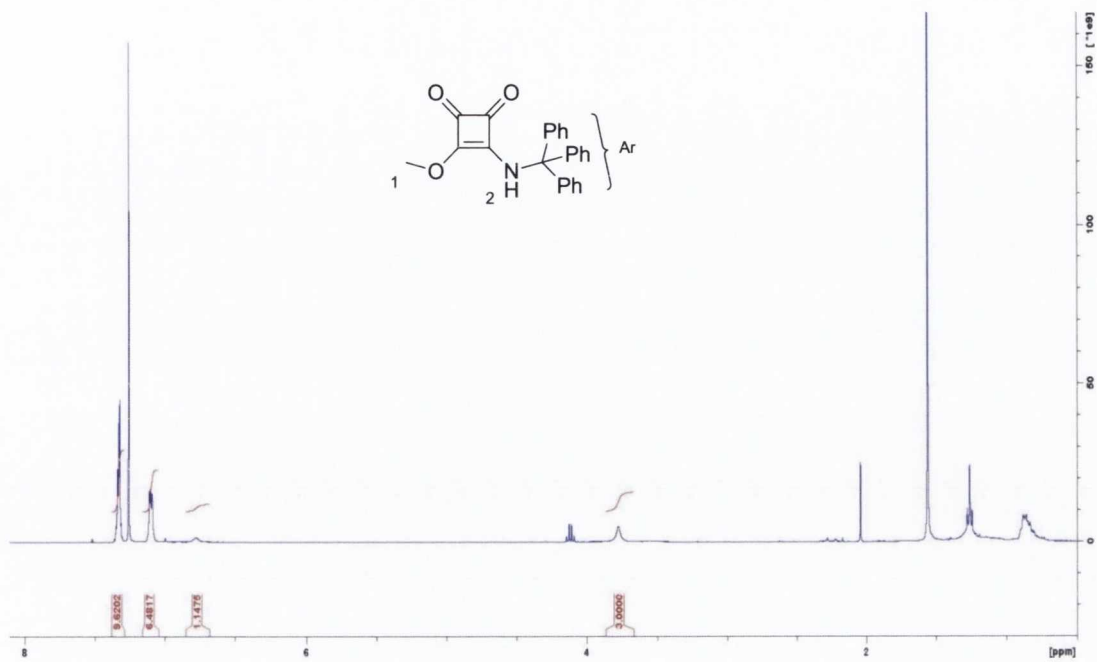
^{1}H NMR spectrum of product 363
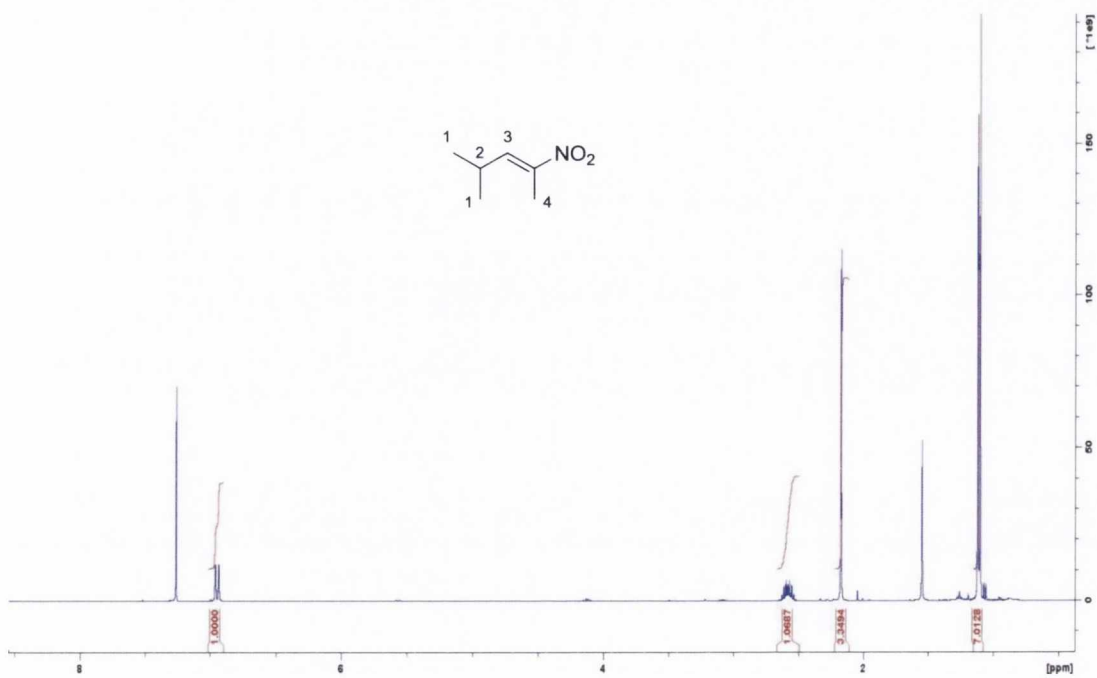
NOESY experiment for *trans*-386
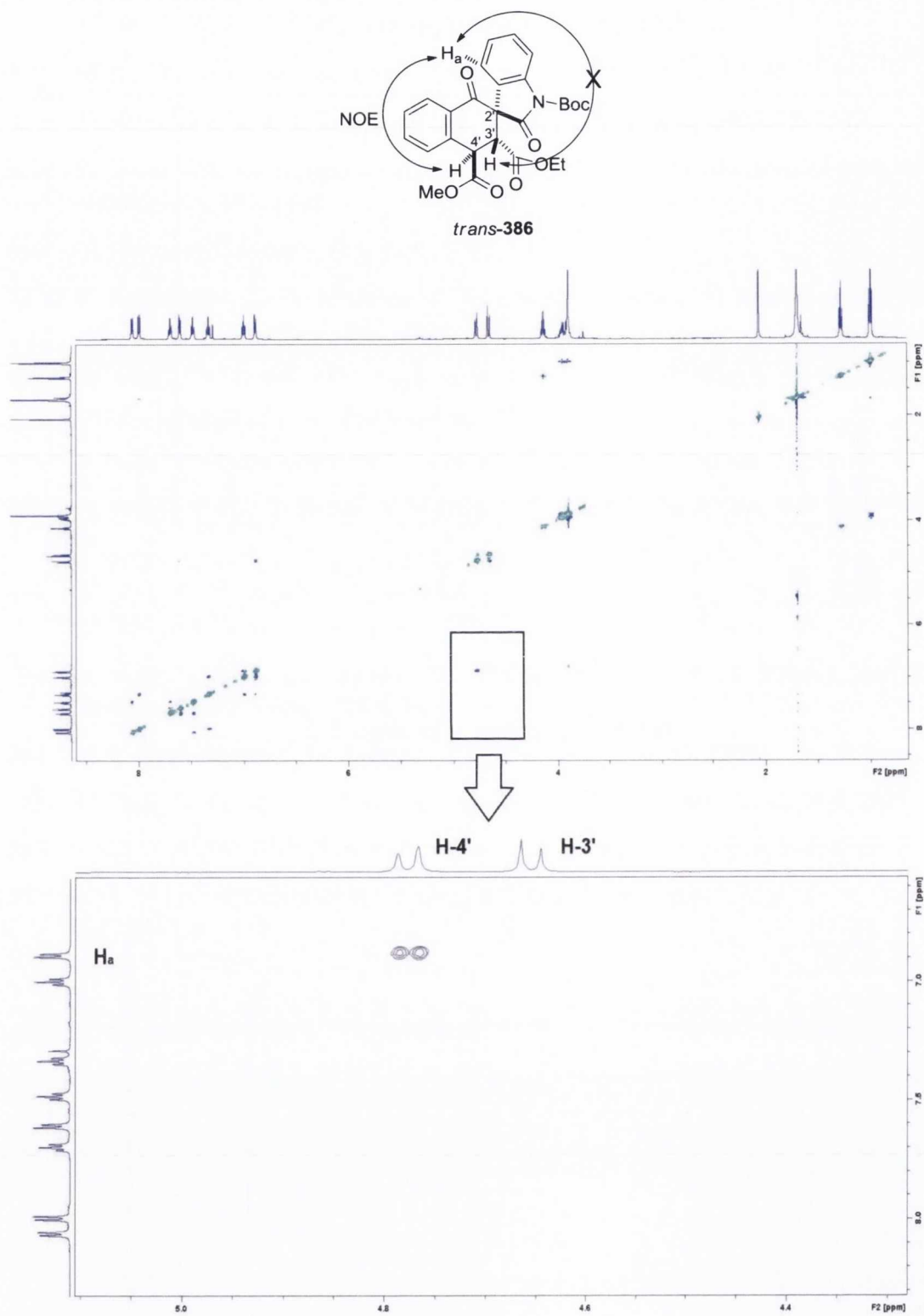
trans-**386**

Figure A.1   NOE contact between protons H-4' and H$_a$.

NOESY experiment for *cis*-386

cis-386
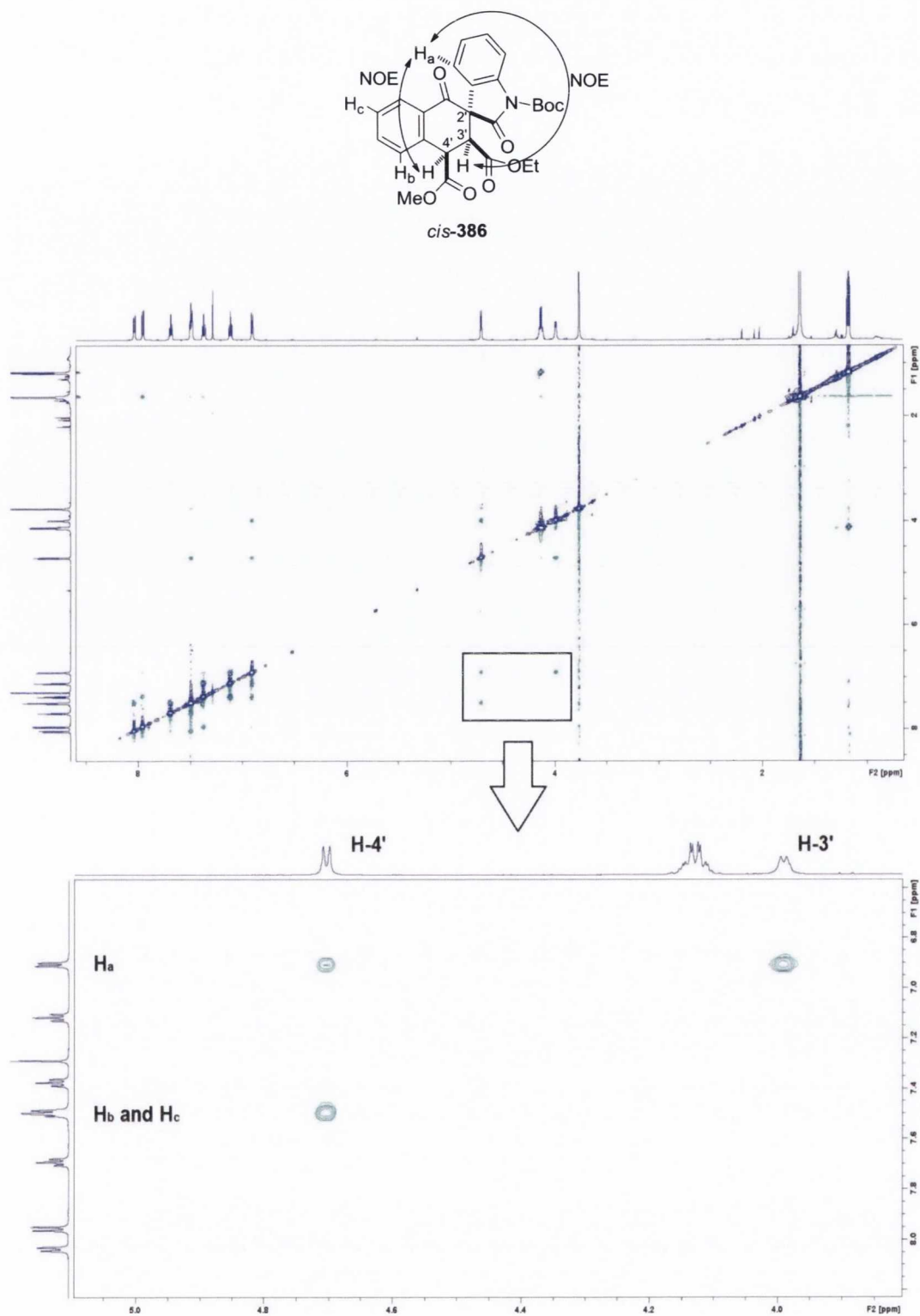
Figure A.2   NOE contacts between protons H-3' and H-4' with Hₐ.

X-ray crystallography data for lactone *trans*-307.

Table 1. Crystal data and structure refinement for *trans*-307.

Identification code	shelxl
Empirical formula	$C_{60} H_{48} O_{16} S_4$
Formula weight	1153.22
Temperature	293(2) K
Wavelength	0.71073 Å
Crystal system	Orthorhombic
Space group	P2(1)2(1)2(1)
Unit cell dimensions	a = 7.3800(15) Å $\quad$ α= 90°.
	b = 9.5110(19) Å $\quad$ β= 90°.
	c = 18.800(4) Å $\quad$ γ = 90°.
Volume	1319.6(5) Å^3
Z	1
Density (calculated)	1.451 Mg/m^3
Absorption coefficient	0.255 mm^{-1}
F(000)	600
Crystal size	0.20 x 0.10 x 0.04 mm^3
Theta range for data collection	2.17 to 25.00°.
Index ranges	-8<=h<=7, -11<=k<=9, -14<=l<=22
Reflections collected	5329
Independent reflections	2304 [R(int) = 0.0655]
Completeness to theta = 25.00°	99.5 %
Absorption correction	Semi-empirical from equivalents
Max. and min. transmission	1.0000 and 0.5531
Refinement method	Full-matrix least-squares on F^2
Data / restraints / parameters	2304 / 0 / 182
Goodness-of-fit on F^2	1.186
Final R indices [I>2sigma(I)]	R1 = 0.0740, wR2 = 0.2123
R indices (all data)	R1 = 0.1019, wR2 = 0.2826
Absolute structure parameter	-0.1(3)
Largest diff. peak and hole	1.363 and -1.325 e.Å^{-3}

Table 2. Atomic coordinates (x 10^4) and equivalent isotropic displacement parameters (Å^{2}x 10^3) for *trans*-307.

U(eq) is defined as one third of the trace of the orthogonalised U^{ij} tensor.

	x	y	z	U(eq)
S(1)	3448(3)	3493(2)	33(1)	26(1)
O(2)	1716(7)	7986(5)	1918(3)	29(1)
O(3)	5303(6)	6628(5)	492(2)	20(1)
O(4)	7562(6)	5887(5)	1164(3)	22(1)
O(10)	2753(8)	8941(5)	907(3)	31(1)
C(1)	4018(9)	3213(7)	2326(3)	18(1)
C(2)	5272(9)	4021(6)	1943(3)	18(1)
C(3)	4621(9)	5073(7)	1471(3)	19(1)
C(4)	2766(10)	5310(6)	1409(3)	18(1)
C(5)	1536(9)	4526(7)	1805(3)	20(1)
C(6)	2182(9)	3464(8)	2252(3)	21(1)
C(7)	5966(8)	5873(7)	1053(3)	19(1)

300

C(8)	2181(8)	6467(7)	912(3)	17(1)
C(9)	3445(8)	6476(7)	258(3)	19(1)
C(10)	3267(8)	5241(7)	-231(3)	16(1)
C(11)	2921(10)	5316(8)	-946(4)	24(2)
C(12)	2842(9)	3984(8)	-1282(4)	25(2)
C(13)	3127(9)	2912(7)	-823(4)	22(2)
C(14)	2180(9)	7890(7)	1311(4)	22(2)
C(30)	2793(12)	10333(7)	1248(4)	35(2)

Table 3.   Bond lengths [Å] and angles [°] for *trans*-307.

S(1)-C(13)	1.718(7)
S(1)-C(10)	1.740(7)
O(2)-C(14)	1.195(9)
O(3)-C(7)	1.365(8)
O(3)-C(9)	1.448(8)
O(4)-C(7)	1.197(7)
O(10)-C(14)	1.324(8)
O(10)-C(30)	1.472(8)
C(1)-C(6)	1.383(10)
C(1)-C(2)	1.403(9)
C(1)-H(1)	0.9300
C(2)-C(3)	1.420(9)
C(2)-H(2)	0.9300
C(3)-C(4)	1.392(10)
C(3)-C(7)	1.478(10)
C(4)-C(5)	1.391(9)
C(4)-C(8)	1.508(9)
C(5)-C(6)	1.398(10)
C(5)-H(5)	0.9300
C(6)-H(6)	0.9300
C(8)-C(9)	1.543(9)
C(8)-C(14)	1.547(9)
C(8)-H(8)	0.9800
C(9)-C(10)	1.497(9)
C(9)-H(9)	0.9800
C(10)-C(11)	1.369(10)
C(11)-C(12)	1.417(10)
C(11)-H(11)	0.9300
C(12)-C(13)	1.353(10)
C(12)-H(12)	0.9300
C(13)-H(13)	0.9300
C(30)-H(30A)	0.9600
C(30)-H(30B)	0.9600
C(30)-H(30C)	0.9600
C(13)-S(1)-C(10)	91.7(3)
C(7)-O(3)-C(9)	121.5(5)
C(14)-O(10)-C(30)	115.8(6)
C(6)-C(1)-C(2)	120.0(6)
C(6)-C(1)-H(1)	120.0
C(2)-C(1)-H(1)	120.0
C(1)-C(2)-C(3)	118.9(6)
C(1)-C(2)-H(2)	120.5
C(3)-C(2)-H(2)	120.5
C(4)-C(3)-C(2)	119.9(6)

C(4)-C(3)-C(7)	122.1(6)
C(2)-C(3)-C(7)	117.9(6)
C(5)-C(4)-C(3)	120.7(6)
C(5)-C(4)-C(8)	122.4(6)
C(3)-C(4)-C(8)	116.9(6)
C(4)-C(5)-C(6)	119.1(6)
C(4)-C(5)-H(5)	120.5
C(6)-C(5)-H(5)	120.5
C(1)-C(6)-C(5)	121.3(6)
C(1)-C(6)-H(6)	119.3
C(5)-C(6)-H(6)	119.3
O(4)-C(7)-O(3)	118.8(6)
O(4)-C(7)-C(3)	125.0(6)
O(3)-C(7)-C(3)	116.2(5)
C(4)-C(8)-C(9)	109.0(5)
C(4)-C(8)-C(14)	109.7(5)
C(9)-C(8)-C(14)	112.4(5)
C(4)-C(8)-H(8)	108.5
C(9)-C(8)-H(8)	108.5
C(14)-C(8)-H(8)	108.5
O(3)-C(9)-C(10)	110.4(5)
O(3)-C(9)-C(8)	109.3(5)
C(10)-C(9)-C(8)	115.6(5)
O(3)-C(9)-H(9)	107.1
C(10)-C(9)-H(9)	107.1
C(8)-C(9)-H(9)	107.1
C(11)-C(10)-C(9)	125.3(6)
C(11)-C(10)-S(1)	110.1(5)
C(9)-C(10)-S(1)	124.6(5)
C(10)-C(11)-C(12)	113.5(6)
C(10)-C(11)-H(11)	123.2
C(12)-C(11)-H(11)	123.2
C(13)-C(12)-C(11)	112.5(6)
C(13)-C(12)-H(12)	123.8
C(11)-C(12)-H(12)	123.8
C(12)-C(13)-S(1)	112.1(5)
C(12)-C(13)-H(13)	123.9
S(1)-C(13)-H(13)	123.9
O(2)-C(14)-O(10)	125.5(6)
O(2)-C(14)-C(8)	122.0(6)
O(10)-C(14)-C(8)	112.4(6)
O(10)-C(30)-H(30A)	109.5
O(10)-C(30)-H(30B)	109.5
H(30A)-C(30)-H(30B)	109.5
O(10)-C(30)-H(30C)	109.5
H(30A)-C(30)-H(30C)	109.5
H(30B)-C(30)-H(30C)	109.5

Symmetry transformations used to generate equivalent atoms:

Table 4.   Anisotropic displacement parameters ($\text{Å}^2 \times 10^3$) for *trans*-307.

The anisotropic displacement factor exponent takes the form: $-2\pi^2[\,h^2\,a^{*2}U^{11} + ... + 2\,h\,k\,a^*\,b^*\,U^{12}\,]$

	U^{11}	U^{22}	U^{33}	U^{23}	U^{13}	U^{12}
S(1)	44(1)	16(1)	19(1)	0(1)	-4(1)	-2(1)
O(2)	32(3)	28(3)	26(3)	-5(2)	8(2)	-2(2)
O(3)	28(2)	15(2)	18(2)	-3(2)	-2(2)	-2(2)
O(4)	12(2)	25(2)	28(2)	3(2)	-1(2)	1(2)
O(10)	50(3)	15(2)	29(3)	-2(2)	-2(2)	3(2)
C(1)	28(3)	9(3)	16(3)	2(2)	-2(3)	3(2)
C(2)	29(3)	12(3)	13(3)	-4(2)	2(3)	1(3)
C(3)	31(3)	10(3)	16(3)	-1(3)	-2(3)	7(3)
C(4)	31(3)	13(3)	11(3)	-3(2)	-4(3)	-4(3)
C(5)	21(3)	17(3)	21(3)	-4(2)	5(3)	-1(3)
C(6)	26(3)	23(3)	14(3)	0(3)	-1(3)	-14(3)
C(7)	19(3)	17(3)	20(3)	-3(3)	-8(3)	5(2)
C(8)	16(3)	17(3)	19(3)	1(3)	-5(3)	4(3)
C(9)	19(3)	18(3)	20(3)	1(3)	-4(3)	-2(3)
C(10)	7(3)	21(3)	21(3)	1(3)	2(2)	-1(2)
C(11)	26(3)	29(4)	18(3)	5(3)	6(3)	-1(3)
C(12)	25(3)	30(4)	19(3)	-8(3)	0(3)	-3(3)
C(13)	22(3)	22(3)	21(3)	-2(3)	-6(3)	-2(3)
C(14)	19(3)	22(3)	25(4)	0(3)	-4(3)	-4(3)
C(30)	53(5)	15(3)	37(4)	-3(3)	-14(4)	1(3)

Table 5.   Hydrogen coordinates (x 10^4) and isotropic displacement parameters ($\text{Å}^2 \times 10^3$) for *trans*-307.

	x	y	z	U(eq)
H(1)	4421	2509	2631	21
H(2)	6510	3870	1996	22
H(5)	300	4705	1772	24
H(6)	1361	2915	2504	25
H(8)	944	6268	751	21
H(9)	3147	7317	-20	23
H(11)	2753	6159	-1187	29
H(12)	2620	3861	-1765	29
H(13)	3146	1969	-955	26
H(30A)	2757	10221	1756	52
H(30B)	1763	10870	1096	52
H(30C)	3885	10815	1116	52

Table 6. Torsion angles [°] for *trans*-307.

C(6)-C(1)-C(2)-C(3)	-1.1(9)
C(1)-C(2)-C(3)-C(4)	1.5(9)
C(1)-C(2)-C(3)-C(7)	-177.7(6)
C(2)-C(3)-C(4)-C(5)	0.0(9)
C(7)-C(3)-C(4)-C(5)	179.2(6)
C(2)-C(3)-C(4)-C(8)	178.6(5)
C(7)-C(3)-C(4)-C(8)	-2.3(9)
C(3)-C(4)-C(5)-C(6)	-1.9(9)
C(8)-C(4)-C(5)-C(6)	179.6(6)
C(2)-C(1)-C(6)-C(5)	-0.8(10)

C(4)-C(5)-C(6)-C(1)	2.3(9)
C(9)-O(3)-C(7)-O(4)	169.7(6)
C(9)-O(3)-C(7)-C(3)	-9.3(8)
C(4)-C(3)-C(7)-O(4)	167.0(7)
C(2)-C(3)-C(7)-O(4)	-13.9(10)
C(4)-C(3)-C(7)-O(3)	-14.1(9)
C(2)-C(3)-C(7)-O(3)	165.1(5)
C(5)-C(4)-C(8)-C(9)	-144.4(6)
C(3)-C(4)-C(8)-C(9)	37.0(7)
C(5)-C(4)-C(8)-C(14)	92.0(7)
C(3)-C(4)-C(8)-C(14)	-86.5(7)
C(7)-O(3)-C(9)-C(10)	-83.6(6)
C(7)-O(3)-C(9)-C(8)	44.6(7)
C(4)-C(8)-C(9)-O(3)	-56.3(7)
C(14)-C(8)-C(9)-O(3)	65.6(6)
C(4)-C(8)-C(9)-C(10)	68.9(7)
C(14)-C(8)-C(9)-C(10)	-169.2(5)
O(3)-C(9)-C(10)-C(11)	-110.6(7)
C(8)-C(9)-C(10)-C(11)	124.7(7)
O(3)-C(9)-C(10)-S(1)	70.1(6)
C(8)-C(9)-C(10)-S(1)	-54.5(7)
C(13)-S(1)-C(10)-C(11)	1.8(5)
C(13)-S(1)-C(10)-C(9)	-178.9(5)
C(9)-C(10)-C(11)-C(12)	179.3(6)
S(1)-C(10)-C(11)-C(12)	-1.4(7)
C(10)-C(11)-C(12)-C(13)	0.1(8)
C(11)-C(12)-C(13)-S(1)	1.3(7)
C(10)-S(1)-C(13)-C(12)	-1.8(6)
C(30)-O(10)-C(14)-O(2)	-0.5(11)
C(30)-O(10)-C(14)-C(8)	-180.0(6)
C(4)-C(8)-C(14)-O(2)	-37.4(9)
C(9)-C(8)-C(14)-O(2)	-158.9(6)
C(4)-C(8)-C(14)-O(10)	142.1(6)
C(9)-C(8)-C(14)-O(10)	20.6(8)

Symmetry transformations used to generate equivalent atoms:

Table 7. Hydrogen bonds for *trans*-307 [Å and °].

D-H...A	d(D-H)	d(H...A)	d(D...A)	<(DHA)

X-ray crystallography data for lactone *trans*-334.

A specimen of $C_{16}H_{13}NO_6S$ was used for the X-ray crystallographic analysis. The X-ray intensity data were measured. The integration of the data using a monoclinic unit cell yielded a total of 11607 reflections to a maximum θ angle of 66.39° (0.84 Å resolution), of which 4629 were independent (average redundancy 2.507, completeness = 96.5%, R_{int} = 3.76%, R_{sig} = 5.56%) and 4622 (99.85%) were greater than $2\sigma(F^2)$. The final cell constants of $\underline{a}$ = 12.4236(4) Å, $\underline{b}$ = 8.6723(3) Å, $\underline{c}$ = 15.4909(4) Å, β = 111.6880(10)°, volume = 1550.86(8) Å³, are based upon the refinement of the XYZ-centroids of reflections above 20 $\sigma(I)$. The structure was solved and refined using the Bruker SHELXTL Software Package, using the space group P 1 21 1, with Z = 4 for the

304

formula unit, $C_{16}H_{13}NO_6S$. The final anisotropic full-matrix least-squares refinement on F^2 with 435 variables converged at R1 = 3.28%, for the observed data and wR2 =7.87% for all data. The goodness-of-fit was 1.073. The largest peak in the final difference electron density synthesis was 0.357 e⁻/Å³ and the largest hole was -0.538 e⁻/Å³ with an RMS deviation of 0.078 e⁻/Å³. On the basis of the final model, the calculated density was 1.488 g/cm³ and F(000), 720 e⁻.

Table 1. Sample and crystal data for *trans*-334.

Identification code	fm1
Chemical formula	$C_{16}H_{13}NO_6S$
Formula weight	347.33
Temperature	123(2) K
Wavelength	1.54178 Å
Crystal system	monoclinic
Space group	P 1 21 1
Unit cell dimensions	a = 12.4236(4) Å α = 90°
	b = 8.6723(3) Å β = 111.6880(10)°
	c = 15.4909(4) Å γ = 90°
Volume	1550.86(8) Å³
Z	4
Density (calculated)	1.488 g/cm³
Absorption coefficient	2.170 mm⁻¹
F(000)	720

Table 2. Data collection and structure refinement for *trans*-334.

Theta range for data collection	3.83 to 66.39°
Index ranges	-14<=h<=14, -9<=k<=9, -18<=l<=18
Reflections collected	11607
Independent reflections	4629 [R(int) = 0.0376]
Structure solution technique	direct methods
Structure solution program	SHELXS-97 (Sheldrick, 2008)
Refinement method	Full-matrix least-squares on F^2
Refinement program	SHELXL-97 (Sheldrick, 2008)
Function minimized	$\Sigma \, w(F_o^2 - F_c^2)^2$
Data / restraints / parameters	4629 / 1 / 435
Goodness-of-fit on F^2	1.073
Δ/σ_{max}	0.011
Final R indices	4622 data; I>2σ(I) R1 = 0.0328, wR2 = 0.0785
	all data R1 = 0.0328, wR2 = 0.0787
Weighting scheme	w=1/[σ²(F_o^2)+(0.0326P)²+0.5712P] where P=(F_o^2+2F_c^2)/3
Absolute structure parameter	0.1(0)
Largest diff. peak and hole	0.357 and -0.538 eÅ⁻³
R.M.S. deviation from mean	0.078 eÅ⁻³

Table 3. Atomic coordinates and equivalent isotropic atomic displacement parameters (Å^2) for *trans*-334.

U(eq) is defined as one third of the trace of the orthogonalised U$_{ij}$ tensor.

	x/a	y/b	z/c	U(eq)
S1	0.65937(5)	0.45510(8)	0.64566(4)	0.02679(15)
O3	0.67826(15)	0.3036(2)	0.85646(13)	0.0315(4)
O4	0.81041(13)	0.1452(2)	0.93853(10)	0.0227(4)
O9	0.30635(14)	0.6705(2)	0.81958(11)	0.0246(4)
O10	0.45350(13)	0.5027(2)	0.86021(10)	0.0239(4)
O11	0.17248(12)	0.4731(2)	0.55984(10)	0.0222(4)
O12	0.36182(12)	0.43001(19)	0.63353(9)	0.0164(3)
N2	0.71501(15)	0.1729(2)	0.87907(12)	0.0177(4)
C7	0.64072(18)	0.0407(3)	0.83433(14)	0.0159(4)
C8	0.52903(18)	0.0703(3)	0.77211(14)	0.0189(5)
C9	0.68304(18)	0.8930(3)	0.85761(14)	0.0173(4)
C10	0.61094(18)	0.7705(3)	0.81722(14)	0.0159(4)
C11	0.49688(17)	0.7949(3)	0.75558(13)	0.0141(4)
C12	0.45759(17)	0.9451(3)	0.73336(14)	0.0179(4)
C13	0.53279(17)	0.5530(3)	0.62401(13)	0.0152(4)
C14	0.50140(15)	0.6468(3)	0.54036(13)	0.0153(5)
C15	0.58793(19)	0.6231(3)	0.50172(15)	0.0214(5)
C16	0.67541(19)	0.5279(3)	0.54926(15)	0.0226(5)
C21	0.41606(16)	0.6584(3)	0.72157(13)	0.0138(4)
C25	0.39509(17)	0.5990(3)	0.80853(13)	0.0149(4)
C26	0.2841(2)	0.6273(4)	0.90203(16)	0.0291(6)
C27	0.26635(17)	0.5237(3)	0.60544(13)	0.0159(4)
C28	0.46578(16)	0.5198(3)	0.68522(13)	0.0142(4)
C32	0.29997(16)	0.6845(3)	0.64153(13)	0.0152(4)
S2	0.72955(4)	0.71412(7)	0.20194(3)	0.02095(14)
O1	0.02863(15)	0.31432(19)	0.12523(11)	0.0246(4)
O2	0.09106(13)	0.1611(2)	0.04399(10)	0.0207(3)
O5	0.88883(12)	0.49114(19)	0.46924(10)	0.0199(3)
O6	0.90801(12)	0.44475(19)	0.33421(9)	0.0160(3)
O7	0.16319(12)	0.4780(2)	0.32692(10)	0.0200(3)
O8	0.21685(11)	0.68316(19)	0.42127(10)	0.0172(3)
N1	0.05360(14)	0.1855(2)	0.10605(11)	0.0151(4)
C1	0.04355(17)	0.9070(3)	0.12632(13)	0.0140(4)
C2	0.04023(16)	0.0529(3)	0.16023(13)	0.0131(4)
C3	0.03275(17)	0.7814(3)	0.17775(14)	0.0149(4)
C4	0.01952(15)	0.8036(2)	0.26336(12)	0.0106(4)
C5	0.01664(16)	0.9529(3)	0.29549(13)	0.0130(4)
C6	0.02656(17)	0.0794(3)	0.24386(13)	0.0148(4)
C17	0.63596(19)	0.6897(3)	0.08874(16)	0.0263(5)

	x/a	y/b	z/c	U(eq)
C18	0.6770(2)	0.5863(3)	0.04352(15)	0.0272(5)
C19	0.78607(19)	0.5248(3)	0.09977(14)	0.0204(5)
C20	0.82485(17)	0.5807(3)	0.18828(14)	0.0152(4)
C22	0.01641(16)	0.6625(2)	0.32040(12)	0.0113(4)
C23	0.14347(16)	0.6089(3)	0.36296(12)	0.0120(4)
C24	0.28160(19)	0.4237(3)	0.36506(15)	0.0256(5)
C29	0.97214(16)	0.6885(3)	0.40000(13)	0.0138(4)
C30	0.92019(17)	0.5355(3)	0.40922(13)	0.0144(4)
C31	0.93509(17)	0.5324(3)	0.26410(13)	0.0136(4)

Table 4. Bond lengths (Å) for *trans*-334.

S1-C16	1.699(2)	S1-C13	1.708(2)
O3-N2	1.223(3)	O4-N2	1.227(2)
O9-C25	1.330(3)	O9-C26	1.453(3)
O10-C25	1.198(3)	O11-C27	1.201(3)
O12-C27	1.369(3)	O12-C28	1.467(2)
N2-C7	1.474(3)	C7-C9	1.381(3)
C7-C8	1.390(3)	C8-C12	1.390(3)
C8-H8	0.95	C9-C10	1.382(3)
C9-H9	0.95	C10-C11	1.402(3)
C10-H10	0.95	C11-C12	1.389(4)
C11-C21	1.516(3)	C12-H12	0.95
C13-C14	1.456(3)	C13-C28	1.503(3)
C14-C15	1.425(3)	C14-H14	0.95
C15-C16	1.347(4)	C15-H15	0.95
C16-H16	0.95	C21-C32	1.532(3)
C21-C28	1.549(3)	C21-C25	1.551(3)
C26-H26A	0.98	C26-H26B	0.98
C26-H26C	0.98	C27-C32	1.504(3)
C28-H28	1.0	C32-H32A	0.99
C32-H32B	0.99	S2-C17	1.722(2)
S2-C20	1.724(2)	O1-N1	1.225(3)
O2-N1	1.231(2)	O5-C30	1.197(3)
O6-C30	1.364(3)	O6-C31	1.463(2)
O7-C23	1.327(3)	O7-C24	1.446(3)
O8-C23	1.206(3)	N1-C2	1.469(3)
C1-C2	1.377(3)	C1-C3	1.385(3)
C1-H1A	0.95	C2-C6	1.387(3)
C3-C4	1.409(3)	C3-H3	0.95
C4-C5	1.393(3)	C4-C22	1.518(3)
C5-C6	1.390(3)	C5-H5	0.95
C6-H6	0.95	C17-C18	1.348(4)

307

C17-H17	0.95	C18-C19	1.417(3)
C18-H18	0.95	C19-C20	1.363(3)
C19-H19	0.95	C20-C31	1.497(3)
C22-C23	1.541(3)	C22-C29	1.541(2)
C22-C31	1.551(3)	C24-H24A	0.98
C24-H24B	0.98	C24-H24C	0.98
C29-C30	1.505(3)	C29-H29A	0.99
C29-H29B	0.99	C31-H31	1.0

Table 5. Bond angles (°) for *trans*-334.

C16-S1-C13	92.36(11)	C25-O9-C26	115.41(19)
C27-O12-C28	110.07(17)	O3-N2-O4	123.48(19)
O3-N2-C7	118.88(18)	O4-N2-C7	117.6(2)
C9-C7-C8	122.6(2)	C9-C7-N2	119.13(18)
C8-C7-N2	118.3(2)	C12-C8-C7	118.1(2)
C12-C8-H8	121.0	C7-C8-H8	121.0
C7-C9-C10	118.34(19)	C7-C9-H9	120.8
C10-C9-H9	120.8	C9-C10-C11	121.0(2)
C9-C10-H10	119.5	C11-C10-H10	119.5
C12-C11-C10	119.0(2)	C12-C11-C21	121.31(18)
C10-C11-C21	119.4(2)	C11-C12-C8	121.02(19)
C11-C12-H12	119.5	C8-C12-H12	119.5
C14-C13-C28	129.80(18)	C14-C13-S1	112.14(15)
C28-C13-S1	117.73(16)	C15-C14-C13	107.32(19)
C15-C14-H14	126.3	C13-C14-H14	126.3
C16-C15-C14	116.1(2)	C16-C15-H15	121.9
C14-C15-H15	121.9	C15-C16-S1	112.04(16)
C15-C16-H16	124.0	S1-C16-H16	124.0
C11-C21-C32	118.04(19)	C11-C21-C28	115.50(16)
C32-C21-C28	101.73(16)	C11-C21-C25	105.05(16)
C32-C21-C25	110.00(15)	C28-C21-C25	106.01(18)
O10-C25-O9	124.42(18)	O10-C25-C21	123.83(18)
O9-C25-C21	111.73(18)	O9-C26-H26A	109.5
O9-C26-H26B	109.5	H26A-C26-H26B	109.5
O9-C26-H26C	109.5	H26A-C26-H26C	109.5
H26B-C26-H26C	109.5	O11-C27-O12	120.6(2)
O11-C27-C32	129.3(2)	O12-C27-C32	110.08(16)
O12-C28-C13	109.80(15)	O12-C28-C21	102.78(15)
C13-C28-C21	117.96(18)	O12-C28-H28	108.6
C13-C28-H28	108.6	C21-C28-H28	108.6
C27-C32-C21	102.27(17)	C27-C32-H32A	111.3
C21-C32-H32A	111.3	C27-C32-H32B	111.3
C21-C32-H32B	111.3	H32A-C32-H32B	109.2

C17-S2-C20	91.63(11)	C30-O6-C31	110.44(16)
C23-O7-C24	115.11(17)	O1-N1-O2	123.32(18)
O1-N1-C2	118.88(16)	O2-N1-C2	117.79(18)
C2-C1-C3	118.72(17)	C2-C1-H1A	120.6
C3-C1-H1A	120.6	C1-C2-C6	122.68(19)
C1-C2-N1	118.42(17)	C6-C2-N1	118.88(19)
C1-C3-C4	120.3(2)	C1-C3-H3	119.9
C4-C3-H3	119.9	C5-C4-C3	119.39(19)
C5-C4-C22	122.14(16)	C3-C4-C22	118.37(19)
C6-C5-C4	120.60(17)	C6-C5-H5	119.7
C4-C5-H5	119.7	C2-C6-C5	118.3(2)
C2-C6-H6	120.8	C5-C6-H6	120.8
C18-C17-S2	111.60(17)	C18-C17-H17	124.2
S2-C17-H17	124.2	C17-C18-C19	113.0(2)
C17-C18-H18	123.5	C19-C18-H18	123.5
C20-C19-C18	112.8(2)	C20-C19-H19	123.6
C18-C19-H19	123.6	C19-C20-C31	124.8(2)
C19-C20-S2	111.02(17)	C31-C20-S2	124.22(16)
C4-C22-C23	104.48(15)	C4-C22-C29	116.20(17)
C23-C22-C29	108.29(14)	C4-C22-C31	114.25(15)
C23-C22-C31	111.87(17)	C29-C22-C31	101.84(15)
O8-C23-O7	124.48(18)	O8-C23-C22	122.06(19)
O7-C23-C22	113.42(17)	O7-C24-H24A	109.5
O7-C24-H24B	109.5	H24A-C24-H24B	109.5
O7-C24-H24C	109.5	H24A-C24-H24C	109.5
H24B-C24-H24C	109.5	C30-C29-C22	103.86(17)
C30-C29-H29A	111.0	C22-C29-H29A	111.0
C30-C29-H29B	111.0	C22-C29-H29B	111.0
H29A-C29-H29B	109.0	O5-C30-O6	120.7(2)
O5-C30-C29	129.1(2)	O6-C30-C29	110.12(16)
O6-C31-C20	109.46(16)	O6-C31-C22	103.96(14)
C20-C31-C22	117.02(18)	O6-C31-H31	108.7
C20-C31-H31	108.7	C22-C31-H31	108.7

Table 6. Torsion angles (°) for *trans*-334.

O3-N2-C7-C9	178.1(2)	O4-N2-C7-C9	-3.0(3)
O3-N2-C7-C8	-3.8(3)	O4-N2-C7-C8	175.11(18)
C9-C7-C8-C12	0.9(3)	N2-C7-C8-C12	-177.12(17)
C8-C7-C9-C10	-0.1(3)	N2-C7-C9-C10	177.97(18)
C7-C9-C10-C11	-1.3(3)	C9-C10-C11-C12	1.7(3)
C9-C10-C11-C21	-172.80(18)	C10-C11-C12-C8	-0.8(3)
C21-C11-C12-C8	173.60(18)	C7-C8-C12-C11	-0.5(3)
C16-S1-C13-C14	-0.64(17)	C16-S1-C13-C28	173.44(17)

C28-C13-C14-C15	-172.0(2)	S1-C13-C14-C15	1.2(2)
C13-C14-C15-C16	-1.3(3)	C14-C15-C16-S1	0.9(3)
C13-S1-C16-C15	-0.1(2)	C12-C11-C21-C32	16.4(3)
C10-C11-C21-C32	-169.20(17)	C12-C11-C21-C28	137.0(2)
C10-C11-C21-C28	-48.6(2)	C12-C11-C21-C25	-106.6(2)
C10-C11-C21-C25	67.8(2)	C26-O9-C25-O10	1.5(3)
C26-O9-C25-C21	-177.1(2)	C11-C21-C25-O10	-90.6(2)
C32-C21-C25-O10	141.4(2)	C28-C21-C25-O10	32.2(3)
C11-C21-C25-O9	88.0(2)	C32-C21-C25-O9	-40.0(3)
C28-C21-C25-O9	-149.24(17)	C28-O12-C27-O11	178.09(17)
C28-O12-C27-C32	-3.0(2)	C27-O12-C28-C13	-102.16(19)
C27-O12-C28-C21	24.19(19)	C14-C13-C28-O12	65.6(3)
S1-C13-C28-O12	-107.23(17)	C14-C13-C28-C21	-51.6(3)
S1-C13-C28-C21	135.55(16)	C11-C21-C28-O12	-163.95(16)
C32-C21-C28-O12	-34.83(19)	C25-C21-C28-O12	80.19(17)
C11-C21-C28-C13	-43.0(2)	C32-C21-C28-C13	86.1(2)
C25-C21-C28-C13	-158.90(17)	O11-C27-C32-C21	159.1(2)
O12-C27-C32-C21	-19.7(2)	C11-C21-C32-C27	160.23(16)
C28-C21-C32-C27	32.73(18)	C25-C21-C32-C27	-79.3(2)
C3-C1-C2-C6	0.0(3)	C3-C1-C2-N1	179.04(17)
O1-N1-C2-C1	165.93(18)	O2-N1-C2-C1	-15.0(3)
O1-N1-C2-C6	-15.0(3)	O2-N1-C2-C6	164.06(18)
C2-C1-C3-C4	-0.5(3)	C1-C3-C4-C5	0.4(3)
C1-C3-C4-C22	-175.81(17)	C3-C4-C5-C6	0.1(3)
C22-C4-C5-C6	176.15(18)	C1-C2-C6-C5	0.4(3)
N1-C2-C6-C5	-178.56(17)	C4-C5-C6-C2	-0.5(3)
C20-S2-C17-C18	-0.7(2)	S2-C17-C18-C19	-0.3(3)
C17-C18-C19-C20	1.5(3)	C18-C19-C20-C31	177.7(2)
C18-C19-C20-S2	-1.9(3)	C17-S2-C20-C19	1.50(18)
C17-S2-C20-C31	-178.12(19)	C5-C4-C22-C23	-100.7(2)
C3-C4-C22-C23	75.4(2)	C5-C4-C22-C29	18.5(3)
C3-C4-C22-C29	-165.36(17)	C5-C4-C22-C31	136.72(19)
C3-C4-C22-C31	-47.2(2)	C24-O7-C23-O8	2.1(3)
C24-O7-C23-C22	179.97(17)	C4-C22-C23-O8	68.4(2)
C29-C22-C23-O8	-56.1(2)	C31-C22-C23-O8	-167.49(17)
C4-C22-C23-O7	-109.51(18)	C29-C22-C23-O7	126.04(17)
C31-C22-C23-O7	14.6(2)	C4-C22-C29-C30	151.28(16)
C23-C22-C29-C30	-91.58(18)	C31-C22-C29-C30	26.46(18)
C31-O6-C30-O5	170.99(18)	C31-O6-C30-C29	-7.3(2)
C22-C29-C30-O5	168.7(2)	C22-C29-C30-O6	-13.12(19)
C30-O6-C31-C20	-101.20(19)	C30-O6-C31-C22	24.6(2)
C19-C20-C31-O6	-111.1(2)	C30-O6-C31-C22 ...	
C19-C20-C31-O6	-111.1(2)	S2-C20-C31-O6	68.4(2)
C19-C20-C31-C22	131.0(2)	S2-C20-C31-C22	-49.4(2)

C4-C22-C31-O6	-156.91(15)	C23-C22-C31-O6	84.64(17)
C29-C22-C31-O6	-30.80(19)	C4-C22-C31-C20	-36.1(2)
C23-C22-C31-C20	-154.55(16)	C29-C22-C31-C20	90.00(19)

Table 7. Anisotropic atomic displacement parameters (Å^2) for *trans*-334.

The anisotropic atomic displacement factor exponent takes the form: $-2\pi^2[\, h^2\, a^{*2}\, U_{11} + ... + 2\, h\, k\, a^*\, b^*\, U_{12}\,]$

	U_{11}	U_{22}	U_{33}	U_{23}	U_{13}	U_{12}
S1	0.0214(3)	0.0330(4)	0.0311(3)	0.0051(2)	0.0157(2)	0.0088(2)
O3	0.0270(9)	0.0188(10)	0.0429(10)	-0.0027(8)	0.0061(7)	-0.0003(7)
O4	0.0163(7)	0.0290(10)	0.0214(7)	-0.0016(7)	0.0053(6)	-0.0051(7)
O9	0.0278(8)	0.0290(10)	0.0258(7)	0.0029(7)	0.0200(6)	0.0071(7)
O10	0.0148(7)	0.0360(11)	0.0209(7)	0.0098(7)	0.0066(6)	0.0026(7)
O11	0.0141(7)	0.0256(10)	0.0246(7)	0.0027(7)	0.0047(6)	-0.0074(7)
O12	0.0126(7)	0.0159(8)	0.0223(7)	-0.0019(6)	0.0083(5)	-0.0044(6)
N2	0.0166(9)	0.0204(11)	0.0185(8)	-0.0021(8)	0.0094(7)	-0.0026(8)
C7	0.0156(10)	0.0179(12)	0.0162(9)	-0.0026(8)	0.0083(8)	-0.0028(9)
C8	0.0151(10)	0.0171(12)	0.0231(10)	0.0000(9)	0.0054(8)	0.0037(9)
C9	0.0122(9)	0.0214(13)	0.0177(9)	0.0000(8)	0.0049(7)	-0.0005(8)
C10	0.0131(9)	0.0160(12)	0.0189(9)	0.0007(8)	0.0060(8)	0.0015(8)
C11	0.0115(9)	0.0184(12)	0.0149(9)	-0.0012(8)	0.0078(7)	0.0002(8)
C12	0.0136(10)	0.0178(12)	0.0215(9)	0.0008(9)	0.0055(8)	0.0022(9)
C13	0.0135(9)	0.0150(12)	0.0173(9)	-0.0008(8)	0.0061(7)	-0.0014(8)
C14	-0.0004(8)	0.0309(13)	0.0176(9)	-0.0145(9)	0.0059(7)	-0.0062(8)
C15	0.0221(11)	0.0237(13)	0.0206(10)	-0.0032(9)	0.0105(8)	-0.0029(9)
C16	0.0198(11)	0.0279(14)	0.0269(11)	-0.0047(10)	0.0165(9)	0.0007(10)
C21	0.0101(9)	0.0170(12)	0.0150(8)	-0.0007(8)	0.0055(7)	-0.0006(8)
C25	0.0092(9)	0.0197(12)	0.0165(9)	-0.0043(8)	0.0056(7)	-0.0037(8)
C26	0.0322(12)	0.0396(16)	0.0258(11)	-0.0005(11)	0.0228(10)	0.0010(11)
C27	0.0134(10)	0.0225(12)	0.0137(9)	0.0026(8)	0.0074(8)	-0.0024(9)
C28	0.0097(9)	0.0149(11)	0.0180(9)	-0.0018(8)	0.0051(7)	-0.0040(8)
C32	0.0103(9)	0.0199(12)	0.0157(9)	-0.0008(8)	0.0051(7)	0.0007(8)
S2	0.0111(2)	0.0265(3)	0.0231(2)	-0.0028(2)	0.00370(19)	0.0020(2)
O1	0.0386(9)	0.0129(10)	0.0297(8)	0.0024(7)	0.0214(7)	0.0051(7)
O2	0.0266(8)	0.0213(9)	0.0218(7)	0.0028(6)	0.0177(6)	0.0016(7)
O5	0.0161(7)	0.0262(10)	0.0215(7)	0.0067(6)	0.0116(6)	0.0005(6)
O6	0.0166(7)	0.0151(8)	0.0176(6)	0.0023(6)	0.0080(5)	-0.0042(6)
O7	0.0143(7)	0.0243(10)	0.0200(7)	-0.0038(6)	0.0047(5)	0.0077(6)
O8	0.0104(6)	0.0193(9)	0.0205(7)	-0.0013(6)	0.0042(5)	-0.0016(6)
N1	0.0147(8)	0.0150(10)	0.0165(8)	0.0021(7)	0.0070(6)	0.0002(7)
C1	0.0139(9)	0.0167(12)	0.0134(8)	-0.0008(8)	0.0074(7)	-0.0010(8)
C2	0.0087(9)	0.0152(11)	0.0162(9)	0.0042(8)	0.0054(7)	-0.0005(8)
C3	0.0149(9)	0.0153(11)	0.0180(9)	-0.0032(8)	0.0102(8)	-0.0021(8)

	U_{11}	U_{22}	U_{33}	U_{23}	U_{13}	U_{12}
C4	0.0071(8)	0.0134(11)	0.0121(8)	0.0005(8)	0.0044(7)	-0.0005(8)
C5	0.0135(9)	0.0133(11)	0.0140(8)	-0.0001(8)	0.0070(7)	0.0011(8)
C6	0.0167(10)	0.0124(11)	0.0162(9)	-0.0014(8)	0.0072(7)	0.0029(8)
C17	0.0147(10)	0.0316(15)	0.0268(10)	0.0028(10)	0.0011(8)	-0.0028(10)
C18	0.0228(11)	0.0337(15)	0.0184(9)	0.0005(10)	0.0000(9)	-0.0042(10)
C19	0.0189(10)	0.0242(13)	0.0173(9)	-0.0006(9)	0.0059(8)	-0.0021(9)
C20	0.0122(9)	0.0172(12)	0.0177(9)	0.0012(8)	0.0074(8)	-0.0042(8)
C22	0.0082(9)	0.0132(11)	0.0135(8)	0.0000(8)	0.0053(7)	0.0002(8)
C23	0.0123(9)	0.0139(11)	0.0128(8)	0.0039(8)	0.0083(7)	0.0008(8)
C24	0.0176(10)	0.0341(15)	0.0253(10)	0.0004(10)	0.0084(9)	0.0149(10)
C29	0.0113(8)	0.0181(12)	0.0140(8)	0.0012(8)	0.0070(7)	0.0017(8)
C30	0.0090(9)	0.0188(12)	0.0161(9)	0.0039(8)	0.0053(7)	0.0035(8)
C31	0.0140(9)	0.0149(11)	0.0139(8)	0.0004(8)	0.0076(8)	-0.0018(8)

Table 8. Hydrogen atomic coordinates and isotropic atomic displacement parameters ($Å^2$) for *trans*-334.

	x/a	y/b	z/c	U(eq)
H8	0.5023	1.1730	0.7565	0.023
H9	0.7598	0.8761	0.9003	0.021
H10	0.6391	0.6681	0.8314	0.019
H12	0.3807	0.9626	0.6910	0.021
H14	0.4355	0.7118	0.5160	0.018
H15	0.5841	0.6717	0.4457	0.026
H16	0.7386	0.5042	0.5311	0.027
H26A	0.3525	0.6502	0.9575	0.044
H26B	0.2671	0.5167	0.9000	0.044
H26C	0.2176	0.6857	0.9042	0.044
H28	0.5157	0.4575	0.7396	0.017
H32A	0.2421	0.7302	0.6640	0.018
H32B	0.3090	0.7523	0.5932	0.018
H1A	1.0531	0.8928	0.0688	0.017
H3	1.0343	0.6799	0.1552	0.018
H5	1.0078	0.9684	0.3532	0.016
H6	1.0240	1.1815	0.2653	0.018
H17	0.5643	0.7426	0.0615	0.032
H18	0.6369	0.5577	-0.0195	0.033
H19	0.8277	0.4524	0.0781	0.024
H24A	1.3044	0.4070	0.4320	0.038
H24B	1.3327	0.5009	0.3540	0.038
H24C	1.2879	0.3265	0.3350	0.038
H29A	1.0366	0.7162	0.4583	0.017
H29B	0.9131	0.7712	0.3842	0.017

	x/a	y/b	z/c	U(eq)
H31	0.9794	0.4644	0.2369	0.016

X-ray crystallography data for lactone *cis*-372.

Table 1. Crystal data and structure refinement for *cis*-372.

Identification code	shelxl
Empirical formula	$C_{3.45} H_{2.91} Br_{0.18} N_{0.18} O_{0.91}$
Formula weight	76.04
Temperature	150(2) K
Wavelength	0.71073 Å
Crystal system	Orthorhombic
Space group	P2(1)2(1)2(1)
Unit cell dimensions	a = 10.415(2) Å $\alpha = 90°$.
	b = 11.469(2) Å $\beta = 90°$.
	c = 15.047(3) Å $\gamma = 90°$.
Volume	1797.4(6) $Å^3$
Z	22
Density (calculated)	1.546 Mg/m^3
Absorption coefficient	2.317 mm^{-1}
F(000)	848
Crystal size	1.50 x 0.80 x 0.4 mm^3
Theta range for data collection	2.23 to 25.00°.
Index ranges	-12<=h<=12, -8<=k<=13, -17<=l<=13
Reflections collected	7478
Independent reflections	3106 [R(int) = 0.0693]
Completeness to theta = 25.00°	98.0 %
Absorption correction	Semi-empirical from equivalents
Max. and min. transmission	1.0000 and 0.5272
Refinement method	Full-matrix least-squares on F^2
Data / restraints / parameters	3106 / 0 / 237
Goodness-of-fit on F^2	0.885
Final R indices [I>2sigma(I)]	R1 = 0.0422, wR2 = 0.1096
R indices (all data)	R1 = 0.0448, wR2 = 0.1249
Absolute structure parameter	0.035(14)
Largest diff. peak and hole	0.490 and -0.687 e.$Å^{-3}$

Table 2. Atomic coordinates (x 10^4) and equivalent isotropic displacement parameters ($Å^2$x 10^3) for *cis*-372.

U(eq) is defined as one third of the trace of the orthogonalised U^{ij} tensor.

	x	y	z	U(eq)
Br(1)	-231(1)	6534(1)	1121(1)	34(1)
O(4)	2819(3)	9945(3)	-210(2)	22(1)
N(1)	2150(4)	12040(3)	1189(3)	21(1)
O(5)	4822(3)	10918(3)	3584(2)	24(1)
C(19)	4054(5)	11995(4)	236(3)	24(1)
C(15)	2787(4)	10164(4)	577(3)	17(1)
C(18)	2225(4)	9358(4)	1245(3)	16(1)

313

O(6)	4319(3)	9025(3)	3442(2)	25(1)
O(2)	1094(3)	11712(3)	940(3)	32(1)
C(6)	3275(4)	10493(4)	2504(3)	15(1)
C(5)	1467(4)	8443(4)	930(3)	21(1)
C(13)	5434(4)	9255(4)	1437(3)	19(1)
C(1)	815(4)	7763(4)	1543(3)	24(1)
C(4)	2381(4)	9558(4)	2152(3)	17(1)
C(7)	4126(4)	11099(4)	1789(3)	17(1)
C(3)	1688(4)	8865(4)	2746(3)	21(1)
C(9)	6508(5)	11090(4)	1571(4)	29(1)
C(17)	4171(4)	10037(4)	3229(3)	16(1)
C(2)	890(5)	7985(4)	2443(3)	24(1)
C(12)	6607(5)	8717(4)	1288(3)	25(1)
C(8)	5382(4)	10454(4)	1589(3)	17(1)
O(1)	2337(4)	12937(3)	1605(3)	39(1)
C(14)	3328(4)	11307(4)	936(3)	18(1)
C(16)	5826(6)	10597(5)	4200(4)	38(1)
C(10)	7680(5)	10544(5)	1425(5)	41(2)
C(11)	7733(5)	9350(5)	1289(4)	28(1)

Table 3.   Bond lengths [Å] and angles [°] for *cis*-372.

Br(1)-C(1)	1.891(5)
O(4)-C(15)	1.210(6)
N(1)-O(2)	1.220(5)
N(1)-O(1)	1.219(5)
N(1)-C(14)	1.536(5)
O(5)-C(17)	1.329(6)
O(5)-C(16)	1.445(6)
C(19)-C(14)	1.517(6)
C(15)-C(18)	1.486(6)
C(15)-C(14)	1.526(6)
C(18)-C(4)	1.394(7)
C(18)-C(5)	1.396(6)
O(6)-C(17)	1.214(6)
C(6)-C(4)	1.516(6)
C(6)-C(17)	1.527(6)
C(6)-C(7)	1.558(6)
C(5)-C(1)	1.385(7)
C(13)-C(12)	1.387(6)
C(13)-C(8)	1.395(6)
C(1)-C(2)	1.381(7)
C(4)-C(3)	1.397(7)
C(7)-C(8)	1.532(6)
C(7)-C(14)	1.548(6)
C(3)-C(2)	1.385(7)
C(9)-C(10)	1.390(7)
C(9)-C(8)	1.381(7)
C(12)-C(11)	1.380(7)
C(10)-C(11)	1.386(7)
O(2)-N(1)-O(1)	124.2(4)
O(2)-N(1)-C(14)	118.3(3)
O(1)-N(1)-C(14)	117.5(4)
C(17)-O(5)-C(16)	115.7(4)

314

O(4)-C(15)-C(18)	122.9(4)
O(4)-C(15)-C(14)	121.0(4)
C(18)-C(15)-C(14)	116.1(4)
C(4)-C(18)-C(5)	121.4(4)
C(4)-C(18)-C(15)	121.0(4)
C(5)-C(18)-C(15)	117.4(4)
C(4)-C(6)-C(17)	112.5(4)
C(4)-C(6)-C(7)	115.1(4)
C(17)-C(6)-C(7)	107.4(4)
C(1)-C(5)-C(18)	118.4(4)
C(12)-C(13)-C(8)	120.0(4)
C(2)-C(1)-C(5)	121.4(5)
C(2)-C(1)-Br(1)	119.9(4)
C(5)-C(1)-Br(1)	118.6(4)
C(18)-C(4)-C(3)	118.2(4)
C(18)-C(4)-C(6)	122.0(4)
C(3)-C(4)-C(6)	119.8(4)
C(8)-C(7)-C(14)	111.8(4)
C(8)-C(7)-C(6)	113.9(4)
C(14)-C(7)-C(6)	109.6(3)
C(4)-C(3)-C(2)	121.0(4)
C(10)-C(9)-C(8)	120.7(4)
O(6)-C(17)-O(5)	123.7(4)
O(6)-C(17)-C(6)	126.4(4)
O(5)-C(17)-C(6)	109.8(4)
C(1)-C(2)-C(3)	119.4(4)
C(13)-C(12)-C(11)	121.0(4)
C(13)-C(8)-C(9)	119.0(4)
C(13)-C(8)-C(7)	122.8(4)
C(9)-C(8)-C(7)	118.2(4)
C(15)-C(14)-C(19)	112.6(4)
C(15)-C(14)-N(1)	105.3(3)
C(19)-C(14)-N(1)	106.5(4)
C(15)-C(14)-C(7)	111.1(4)
C(19)-C(14)-C(7)	112.8(4)
N(1)-C(14)-C(7)	108.0(4)
C(9)-C(10)-C(11)	120.3(5)
C(10)-C(11)-C(12)	119.1(5)

Symmetry transformations used to generate equivalent atoms:

Table 4. Anisotropic displacement parameters (Å^2x 10^3) for *cis*-372.

The anisotropic displacement factor exponent takes the form: $-2\pi^2[\, h^2 \, a^{*2} U^{11} + \ldots + 2\, h\, k\, a^* \, b^* \, U^{12}\,]$

	U^{11}	U^{22}	U^{33}	U^{23}	U^{13}	U^{12}
Br(1)	35(1)	23(1)	44(1)	-7(1)	3(1)	-16(1)
O(4)	28(2)	19(2)	18(2)	-3(1)	0(1)	0(1)
N(1)	28(2)	17(2)	20(2)	2(2)	-5(2)	8(2)
O(5)	27(2)	20(2)	25(2)	-2(1)	-11(1)	-1(1)
C(19)	33(3)	16(2)	22(2)	4(2)	1(2)	-6(2)
C(15)	16(2)	14(2)	21(2)	2(2)	0(2)	4(2)
C(18)	15(2)	9(2)	22(2)	2(2)	1(2)	2(2)
O(6)	31(2)	17(2)	26(2)	6(1)	-2(1)	4(1)

O(2)	27(2)	29(2)	40(2)	-5(2)	-5(2)	9(2)
C(6)	18(2)	11(2)	17(2)	-2(2)	-3(2)	2(2)
C(5)	20(2)	18(2)	23(2)	-2(2)	-2(2)	0(2)
C(13)	18(2)	12(2)	27(2)	-2(2)	-1(2)	-2(2)
C(1)	16(2)	19(2)	36(3)	3(2)	-1(2)	-6(2)
C(4)	16(2)	13(2)	20(2)	1(2)	1(2)	3(2)
C(7)	21(2)	8(2)	21(2)	-1(2)	3(2)	-3(2)
C(3)	22(2)	23(2)	17(2)	1(2)	-4(2)	4(2)
C(9)	27(2)	14(2)	48(3)	-2(2)	9(2)	-3(2)
C(17)	20(2)	18(2)	11(2)	2(2)	0(2)	3(2)
C(2)	23(2)	19(2)	28(3)	10(2)	3(2)	-1(2)
C(12)	30(2)	17(2)	28(3)	-1(2)	3(2)	3(2)
C(8)	17(2)	13(2)	21(2)	2(2)	-3(2)	0(2)
O(1)	44(2)	20(2)	54(2)	-18(2)	-6(2)	11(2)
C(14)	18(2)	11(2)	25(2)	1(2)	1(2)	2(2)
C(16)	40(3)	34(3)	41(3)	-5(2)	-25(3)	2(3)
C(10)	18(2)	24(3)	81(5)	-1(3)	10(3)	-3(2)
C(11)	21(2)	26(2)	37(3)	-1(2)	6(2)	11(2)

Table 5. Hydrogen coordinates (x 10^4) and isotropic displacement parameters (Å^2x 10^3) for *cis*-372.

	x	y	z	U(eq)
H(19A)	4751	11533	12	36
H(19B)	4386	12697	496	36
H(19C)	3483	12190	-242	36
H(6)	2738	11098	2774	18
H(5)	1401	8294	325	25
H(13)	4683	8817	1434	23
H(7)	4360	11867	2023	20
H(3)	1763	8997	3353	25
H(9)	6481	11893	1657	35
H(2A)	408	7547	2843	28
H(12)	6634	7917	1186	30
H(16A)	5469	10130	4669	57
H(16B)	6202	11288	4448	57
H(16C)	6473	10158	3893	57
H(10)	8432	10981	1419	49
H(11)	8518	8980	1200	34

Table 6. Torsion angles [°] for *cis*-372.

O(4)-C(15)-C(18)-C(4)	170.1(4)
C(14)-C(15)-C(18)-C(4)	-10.2(6)
O(4)-C(15)-C(18)-C(5)	-14.1(6)
C(14)-C(15)-C(18)-C(5)	165.7(4)
C(4)-C(18)-C(5)-C(1)	3.1(7)
C(15)-C(18)-C(5)-C(1)	-172.7(4)
C(18)-C(5)-C(1)-C(2)	0.9(7)
C(18)-C(5)-C(1)-Br(1)	179.2(3)
C(5)-C(18)-C(4)-C(3)	-4.3(6)
C(15)-C(18)-C(4)-C(3)	171.4(4)
C(5)-C(18)-C(4)-C(6)	175.5(4)
C(15)-C(18)-C(4)-C(6)	-8.8(6)

C(17)-C(6)-C(4)-C(18)	-130.8(4)
C(7)-C(6)-C(4)-C(18)	-7.4(6)
C(17)-C(6)-C(4)-C(3)	49.1(5)
C(7)-C(6)-C(4)-C(3)	172.4(4)
C(4)-C(6)-C(7)-C(8)	-86.0(5)
C(17)-C(6)-C(7)-C(8)	40.1(5)
C(4)-C(6)-C(7)-C(14)	40.0(5)
C(17)-C(6)-C(7)-C(14)	166.1(4)
C(18)-C(4)-C(3)-C(2)	1.5(7)
C(6)-C(4)-C(3)-C(2)	-178.3(4)
C(16)-O(5)-C(17)-O(6)	5.4(7)
C(16)-O(5)-C(17)-C(6)	-172.4(4)
C(4)-C(6)-C(17)-O(6)	9.7(6)
C(7)-C(6)-C(17)-O(6)	-117.9(5)
C(4)-C(6)-C(17)-O(5)	-172.7(4)
C(7)-C(6)-C(17)-O(5)	59.7(4)
C(5)-C(1)-C(2)-C(3)	-3.6(7)
Br(1)-C(1)-C(2)-C(3)	178.2(4)
C(4)-C(3)-C(2)-C(1)	2.3(7)
C(8)-C(13)-C(12)-C(11)	0.1(7)
C(12)-C(13)-C(8)-C(9)	1.4(7)
C(12)-C(13)-C(8)-C(7)	-177.9(4)
C(10)-C(9)-C(8)-C(13)	-1.6(8)
C(10)-C(9)-C(8)-C(7)	177.7(5)
C(14)-C(7)-C(8)-C(13)	-77.8(5)
C(6)-C(7)-C(8)-C(13)	47.1(6)
C(14)-C(7)-C(8)-C(9)	102.9(5)
C(6)-C(7)-C(8)-C(9)	-132.2(5)
O(4)-C(15)-C(14)-C(19)	-8.7(6)
C(18)-C(15)-C(14)-C(19)	171.6(4)
O(4)-C(15)-C(14)-N(1)	107.0(5)
C(18)-C(15)-C(14)-N(1)	-72.7(4)
O(4)-C(15)-C(14)-C(7)	-136.3(4)
C(18)-C(15)-C(14)-C(7)	43.9(5)
O(2)-N(1)-C(14)-C(15)	-11.8(5)
O(1)-N(1)-C(14)-C(15)	170.4(4)
O(2)-N(1)-C(14)-C(19)	108.0(5)
O(1)-N(1)-C(14)-C(19)	-69.8(5)
O(2)-N(1)-C(14)-C(7)	-130.5(4)
O(1)-N(1)-C(14)-C(7)	51.6(5)
C(8)-C(7)-C(14)-C(15)	69.6(4)
C(6)-C(7)-C(14)-C(15)	-57.7(5)
C(8)-C(7)-C(14)-C(19)	-58.0(5)
C(6)-C(7)-C(14)-C(19)	174.7(4)
C(8)-C(7)-C(14)-N(1)	-175.5(3)
C(6)-C(7)-C(14)-N(1)	57.2(4)
C(8)-C(9)-C(10)-C(11)	0.5(10)
C(9)-C(10)-C(11)-C(12)	0.9(9)
C(13)-C(12)-C(11)-C(10)	-1.2(8)

Symmetry transformations used to generate equivalent atoms:

Table 7. Hydrogen bonds for *cis*-372 [Å and °].

D-H...A	d(D-H)	d(H...A)	d(D...A)	<(DHA)

317

X-ray crystallography data for lactone *trans*-373.

A specimen of $C_{19}H_{19}NO_5$ was used for the X-ray crystallographic analysis. The X-ray intensity data were measured. The integration of the data using a triclinic unit cell yielded a total of 2542 reflections to a maximum θ angle of 66.61° (0.84 Å resolution), of which 1652 were independent (average redundancy 1.539, completeness = 93.1%, R_{int} = 1.93%, R_{sig} = 3.33%) and 1645 (99.58%) were greater than $2\sigma(F^2)$. The final cell constants of $\underline{a}$ = 7.4043(3) Å, $\underline{b}$ = 7.6194(4) Å, $\underline{c}$ = 7.7708(3) Å, α = 92.263(2)°, β = 95.397(2)°, γ = 92.804(2)°, volume = 435.51(3) Å^3, are based upon the refinement of the XYZ-centroids of reflections above 20 $\sigma(I)$. The structure was solved and refined using the Bruker SHELXTL Software Package, using the space group P 1, with Z = 1 for the formula unit, $C_{19}H_{19}NO_5$. The final anisotropic full-matrix least-squares refinement on F^2 with 231 variables converged at R1 = 3.04%, for the observed data and wR2 = 9.14% for all data. The goodness-of-fit was 0.914. The largest peak in the final difference electron density synthesis was 0.215 e⁻/Å^3 and the largest hole was -0.271 e⁻ /Å^3 with an RMS deviation of 0.044 e⁻/Å^3. On the basis of the final model, the calculated density was 1.302 g/cm^3 and F(000), 180 e⁻.

Table 1. Sample and crystal data for *trans*-373.

Identification code	fmm1207	
Chemical formula	$C_{19}H_{19}NO_5$	
Formula weight	341.35	
Temperature	105(2) K	
Wavelength	1.54178 Å	
Crystal system	triclinic	
Space group	P 1	
Unit cell dimensions	a = 7.4043(3) Å	α = 92.263(2)°
	b = 7.6194(4) Å	β = 95.397(2)°
	c = 7.7708(3) Å	γ = 92.804(2)°
Volume	435.51(3) Å^3	
Z	1	
Density (calculated)	1.302 g/cm^3	
Absorption coefficient	0.784 mm^{-1}	
F(000)	180	

Table 2. Data collection and structure refinement for *trans*-373.

Theta range for data collection	5.72 to 66.61°
Index ranges	-8<=h<=7, -8<=k<=8, -9<=l<=8
Reflections collected	2542
Independent reflections	1652 [R(int) = 0.0193]
Structure solution technique	direct methods
Structure solution program	SHELXS-97 (Sheldrick, 2008)
Refinement method	Full-matrix least-squares on F^2
Refinement program	SHELXL-97 (Sheldrick, 2008)

Function minimized	$\Sigma \, w(F_o^2 - F_c^2)^2$
Data / restraints / parameters	1652 / 3 / 231
Goodness-of-fit on F^2	0.914
Δ/σ_{max}	0.003
Final R indices	1645 data; I>2σ(I) R1 = 0.0304, wR2 = 0.0910
	all data R1 = 0.0305, wR2 = 0.0914
Weighting scheme	w=1/[σ²(F_o²)+(0.1000P)²+0.0000P] where P=(F_o²+2F_c²)/3
Absolute structure parameter	0.1(1)
Extinction coefficient	0.0150(40)
Largest diff. peak and hole	0.215 and -0.271 eÅ⁻³
R.M.S. deviation from mean	0.044 eÅ⁻³

Table 3. Atomic coordinates and equivalent isotropic atomic displacement parameters ($Å^2$) for *trans*-373.

U(eq) is defined as one third of the trace of the orthogonalised U_{ij} tensor.

	x/a	y/b	z/c	U(eq)
C7	0.8134(2)	0.4366(2)	0.3222(2)	0.0176(4)
C3	0.9987(2)	0.4809(2)	0.4159(2)	0.0191(4)
C10	0.0657(2)	0.7162(2)	0.2032(2)	0.0181(4)
C9	0.8617(2)	0.6926(2)	0.1400(2)	0.0175(4)
C11	0.1112(2)	0.9111(2)	0.2402(2)	0.0197(4)
C4	0.1162(2)	0.6148(2)	0.3647(2)	0.0184(4)
C5	0.2846(3)	0.6509(3)	0.4610(3)	0.0247(4)
C2	0.0532(2)	0.3874(2)	0.5622(2)	0.0221(4)
C6	0.3357(3)	0.5572(3)	0.6046(3)	0.0285(4)
C1	0.2186(3)	0.4249(3)	0.6552(2)	0.0270(4)
C14	0.6518(3)	0.8745(2)	0.9566(2)	0.0230(4)
C15	0.6016(3)	0.9623(2)	0.8073(3)	0.0309(5)
C13	0.8113(2)	0.7842(2)	0.9723(2)	0.0195(4)
C12	0.3356(3)	0.1423(3)	0.2330(4)	0.0424(6)
C18	0.9202(3)	0.7854(3)	0.8362(3)	0.0275(4)
C17	0.8704(3)	0.8746(3)	0.6873(3)	0.0358(5)
C16	0.7114(3)	0.9623(3)	0.6724(3)	0.0339(5)
O2	0.49591(17)	0.54959(18)	0.14585(19)	0.0285(3)
O3	0.5617(2)	0.38290(19)	0.93235(19)	0.0335(4)
C19	0.8062(2)	0.4931(2)	0.1337(2)	0.0173(4)
N1	0.6048(2)	0.4739(2)	0.0640(2)	0.0213(4)
O5	0.27485(18)	0.95904(17)	0.1943(2)	0.0286(3)
O4	0.01304(17)	0.01063(16)	0.30479(18)	0.0254(3)
C20	0.9123(3)	0.3797(2)	0.0195(2)	0.0212(4)
O1	0.75488(16)	0.25747(15)	0.33036(16)	0.0212(3)

Table 4. Bond lengths (Å) for *trans*-373.

C7-O1	1.417(2)	C7-C3	1.509(3)
C7-C19	1.539(2)	C3-C4	1.402(3)
C3-C2	1.403(2)	C10-C11	1.517(2)
C10-C4	1.526(2)	C10-C9	1.543(2)
C9-C13	1.526(2)	C9-C19	1.553(2)
C11-O4	1.203(2)	C11-O5	1.333(2)
C4-C5	1.401(3)	C5-C6	1.382(3)
C2-C1	1.373(3)	C6-C1	1.390(3)
C14-C15	1.392(3)	C14-C13	1.394(3)
C15-C16	1.386(3)	C13-C18	1.389(3)
C12-O5	1.457(2)	C18-C17	1.394(3)
C17-C16	1.379(4)	O2-N1	1.225(2)
O3-N1	1.221(2)	C19-C20	1.513(2)
C19-N1	1.536(2)		

Table 5. Bond angles (°) for *trans*-373.

O1-C7-C3	113.44(14)	O1-C7-C19	111.26(14)
C3-C7-C19	110.73(14)	C4-C3-C2	118.97(16)
C4-C3-C7	122.41(15)	C2-C3-C7	118.60(16)
C11-C10-C4	109.94(13)	C11-C10-C9	107.86(13)
C4-C10-C9	112.67(13)	C13-C9-C10	113.21(13)
C13-C9-C19	114.63(14)	C10-C9-C19	108.13(13)
O4-C11-O5	123.84(15)	O4-C11-C10	124.38(15)
O5-C11-C10	111.78(14)	C5-C4-C3	119.01(16)
C5-C4-C10	120.04(16)	C3-C4-C10	120.91(15)
C6-C5-C4	121.10(18)	C1-C2-C3	121.21(17)
C5-C6-C1	119.70(17)	C2-C1-C6	120.01(17)
C15-C14-C13	120.78(18)	C16-C15-C14	120.12(19)
C18-C13-C14	118.51(17)	C18-C13-C9	122.77(17)
C14-C13-C9	118.70(16)	C13-C18-C17	120.60(19)
C16-C17-C18	120.47(19)	C17-C16-C15	119.52(18)
C20-C19-N1	108.31(14)	C20-C19-C7	113.73(14)
N1-C19-C7	105.54(13)	C20-C19-C9	114.87(13)
N1-C19-C9	106.72(12)	C7-C19-C9	107.06(14)
O3-N1-O2	123.68(15)	O3-N1-C19	118.62(15)
O2-N1-C19	117.70(14)	C11-O5-C12	116.04(14)

Table 6. Anisotropic atomic displacement parameters (Å^2) for *trans*-373.
The anisotropic atomic displacement factor exponent takes the form: $-2\pi^2[\,h^2\,a^{*2}\,U_{11} + ... + 2\,h\,k\,a^*\,b^*\,U_{12}\,]$

	U_{11}	U_{22}	U_{33}	U_{23}	U_{13}	U_{12}
C7	0.0184(8)	0.0145(8)	0.0198(8)	0.0032(6)	0.0012(6)	-0.0008(6)

	U$_{11}$	U$_{22}$	U$_{33}$	U$_{23}$	U$_{13}$	U$_{12}$
C3	0.0205(9)	0.0168(9)	0.0198(9)	-0.0019(7)	0.0017(7)	0.0022(7)
C10	0.0163(9)	0.0174(9)	0.0204(9)	0.0007(7)	0.0026(6)	-0.0016(7)
C9	0.0162(8)	0.0171(9)	0.0190(8)	0.0000(7)	0.0020(6)	0.0001(6)
C11	0.0194(8)	0.0187(9)	0.0205(8)	0.0040(7)	-0.0001(7)	-0.0025(7)
C4	0.0164(8)	0.0182(9)	0.0204(9)	-0.0003(7)	0.0009(7)	0.0023(7)
C5	0.0214(9)	0.0213(9)	0.0301(9)	0.0001(7)	-0.0015(7)	-0.0040(7)
C2	0.0249(10)	0.0208(9)	0.0206(9)	0.0028(7)	0.0020(7)	-0.0003(7)
C6	0.0236(9)	0.0289(10)	0.0306(10)	0.0013(8)	-0.0084(8)	-0.0005(7)
C1	0.0316(11)	0.0264(10)	0.0213(9)	0.0013(7)	-0.0065(7)	0.0013(7)
C14	0.0257(9)	0.0173(9)	0.0247(10)	0.0033(7)	-0.0040(7)	-0.0021(7)
C15	0.0366(11)	0.0193(9)	0.0344(11)	0.0025(8)	-0.0094(9)	0.0002(8)
C13	0.0242(9)	0.0120(8)	0.0213(9)	-0.0005(6)	-0.0009(7)	-0.0037(6)
C12	0.0242(10)	0.0187(11)	0.0832(18)	0.0011(10)	0.0051(10)	-0.0095(8)
C18	0.0371(10)	0.0230(9)	0.0237(9)	0.0055(8)	0.0068(8)	0.0026(8)
C17	0.0548(13)	0.0282(10)	0.0250(10)	0.0046(8)	0.0081(9)	-0.0016(9)
C16	0.0526(12)	0.0229(10)	0.0242(10)	0.0083(7)	-0.0073(9)	-0.0050(9)
O2	0.0183(7)	0.0285(7)	0.0386(8)	0.0037(6)	0.0026(5)	-0.0010(5)
O3	0.0336(8)	0.0297(7)	0.0330(8)	-0.0035(6)	-0.0144(6)	-0.0030(6)
C19	0.0172(9)	0.0161(8)	0.0180(8)	0.0035(6)	-0.0015(7)	-0.0013(6)
N1	0.0212(8)	0.0180(7)	0.0231(8)	0.0052(6)	-0.0053(6)	-0.0035(6)
O5	0.0186(6)	0.0195(7)	0.0474(9)	0.0030(6)	0.0047(5)	-0.0049(5)
O4	0.0251(7)	0.0178(7)	0.0331(7)	-0.0021(5)	0.0039(5)	-0.0014(5)
C20	0.0271(9)	0.0168(8)	0.0192(8)	-0.0006(7)	0.0016(6)	-0.0002(7)
O1	0.0207(6)	0.0153(6)	0.0272(7)	0.0052(5)	0.0004(5)	-0.0029(5)

Table 7. Hydrogen atomic coordinates and isotropic atomic displacement parameters (Å^2) for *trans*-373.

	x/a	y/b	z/c	U(eq)
H7	0.7252	0.5077	0.3810	0.021
H10	1.1377	0.6738	0.1087	0.022
H9	0.7943	0.7495	0.2309	0.021
H5	1.3649	0.7413	0.4269	0.03
H2	0.9743	0.2966	0.5976	0.027
H6	1.4503	0.5830	0.6686	0.034
H1	1.2530	0.3604	0.7541	0.032
H14	0.5763	0.8761	0.0490	0.028
H15	0.4919	1.0224	-0.2022	0.037
H12A	1.2694	1.2172	0.1519	0.064
H12B	1.4661	1.1570	0.2217	0.064
H12C	1.3120	1.1760	0.3516	0.064
H18	1.0297	0.7249	-0.1553	0.033
H17	0.9464	0.8749	-0.4046	0.043

	x/a	y/b	z/c	U(eq)
H16	0.6775	1.0223	-0.4296	0.041
H2A	0.5405	0.6495	0.1811	0.043
H20A	0.8669	0.2569	0.0210	0.032
H20B	1.0413	0.3895	0.0627	0.032
H20C	0.8976	0.4194	-0.0992	0.032
H1A	0.8365	0.1932	0.3002	0.032

X-ray crystallography data for lactone *trans*-387.

A specimen of $C_{108}H_{104}Br_4N_4O_{32}$ was used for the X-ray crystallographic analysis. The X-ray intensity data were measured. The integration of the data using an orthorhombic unit cell yielded a total of 8894 reflections to a maximum θ angle of 66.85° (0.84 Å resolution), of which 4130 were independent (average redundancy 2.154, completeness = 96.9%, R_{int} = 2.50%, R_{sig} = 4.72%) and 4121 (99.78%) were greater than $2\sigma(F^2)$. The final cell constants of $\underline{a}$ = 10.4309(4) Å, $\underline{b}$ = 14.2240(5) Å, $\underline{c}$ = 17.1308(6) Å, volume = 2541.68(16) $Å^3$, are based upon the refinement of the XYZ-centroids of reflections above 20 $\sigma(I)$. The structure was solved and refined using the Bruker SHELXTL Software Package, using the space group P 21 21 21, with Z = 1 for the formula unit, $C_{108}H_{104}Br_4N_4O_{32}$. The final anisotropic full-matrix least-squares refinement on F^2 with 339 variables converged at R1 = 2.42%, for the observed data and wR2 = 5.94% for all data. The goodness-of-fit was 1.080. The largest peak in the final difference electron density synthesis was 0.297 $e^-/Å^3$ and the largest hole was -0.379 $e^-/Å^3$ with an RMS deviation of 0.074 $e^-/Å^3$. On the basis of the final model, the calculated density was 1.496 g/cm^3 and F(000), 1176 e^-.

Table 1. Sample and crystal data for *trans*-387.

Identification code	fmm1138	
Chemical formula	$C_{108}H_{104}Br_4N_4O_{32}$	
Formula weight	2289.59	
Temperature	100(2) K	
Wavelength	1.54178 Å	
Crystal system	orthorhombic	
Space group	P 21 21 21	
Unit cell dimensions	a = 10.4309(4) Å	$\alpha = 90°$
	b = 14.2240(5) Å	$\beta = 90°$
	c = 17.1308(6) Å	$\gamma = 90°$
Volume	2541.68(16) $Å^3$	
Z	1	
Density (calculated)	1.496 g/cm^3	
Absorption coefficient	2.652 mm^{-1}	
F(000)	1176	

Table 2. Data collection and structure refinement for *trans*-387.

Theta range for data collection	4.04 to 66.85°
Index ranges	-12<=h<=11, -16<=k<=15, -20<=l<=16
Reflections collected	8894
Independent reflections	4130 [R(int) = 0.0250]
Structure solution technique	direct methods
Structure solution program	SHELXS-97 (Sheldrick, 2008)
Refinement method	Full-matrix least-squares on F^2
Refinement program	SHELXL-97 (Sheldrick, 2008)
Function minimized	$\Sigma\ w(F_o^2 - F_c^2)^2$
Data / restraints / parameters	4130 / 0 / 339
Goodness-of-fit on F^2	1.080
Δ/σ_{max}	0.001
Final R indices	4121 data; I>2σ(I) R1 = 0.0242, wR2 = 0.0594
	all data R1 = 0.0243, wR2 = 0.0594
Weighting scheme	$w=1/[\sigma^2(F_o^2)+(0.0167P)^2+0.8161P]$ where $P=(F_o^2+2F_c^2)/3$
Absolute structure parameter	0.0(0)
Largest diff. peak and hole	0.297 and -0.379 eÅ^{-3}
R.M.S. deviation from mean	0.074 eÅ^{-3}

Table 3. Atomic coordinates and equivalent isotropic atomic displacement parameters (Å^2) for *trans*-387.

U(eq) is defined as one third of the trace of the orthogonalised U_{ij} tensor.

	x/a	y/b	z/c	U(eq)
Br1	0.18911(2)	0.412612(13)	0.08962(13)	0.02119(8)
C7	0.17810(19)	0.78269(13)	0.06791(10)	0.0109(4)
C1	0.27239(19)	0.53166(14)	0.09076(13)	0.0164(4)
C4	0.38976(18)	0.70699(13)	0.10202(11)	0.0111(4)
C2	0.3993(2)	0.53711(14)	0.11300(13)	0.0168(4)
C17	0.02837(17)	0.09544(14)	0.07517(12)	0.0140(4)
C10	0.25887(17)	0.92606(13)	0.99788(11)	0.0105(4)
C11	0.18365(19)	0.00688(13)	0.99230(11)	0.0099(4)
C13	0.2660(2)	0.03628(15)	0.86519(12)	0.0173(4)
C6	0.20269(19)	0.61043(14)	0.07292(11)	0.0139(4)
C15	0.33540(18)	0.89878(14)	0.93584(11)	0.0130(4)
C12	0.18648(19)	0.06395(13)	0.92664(11)	0.0143(4)
C5	0.26101(18)	0.69915(13)	0.07999(11)	0.0109(4)
C8	0.45315(17)	0.80284(13)	0.10593(11)	0.0108(4)
C20	0.4005(2)	0.13526(15)	0.16493(15)	0.0218(5)
C3	0.45831(19)	0.62436(14)	0.11716(12)	0.0151(4)
C16	0.42411(19)	0.97380(13)	0.13137(12)	0.0114(4)
C19	0.23787(17)	0.88096(13)	0.07668(11)	0.0097(4)

	x/a	y/b	z/c	U(eq)
C18	0.13386(17)	0.94380(13)	0.11403(11)	0.0107(4)
C9	0.35709(17)	0.87899(13)	0.13006(12)	0.0100(4)
C14	0.33888(19)	0.95518(15)	0.86895(12)	0.0164(4)
O5	0.34713(13)	0.04032(10)	0.16029(9)	0.0159(3)
O2	0.67680(13)	0.79732(10)	0.12701(9)	0.0184(3)
O4	0.53242(13)	0.98660(10)	0.11003(10)	0.0203(3)
O1	0.06508(13)	0.77601(10)	0.05245(9)	0.0149(3)
O3	0.55168(15)	0.81644(11)	0.23303(9)	0.0213(3)
N1	0.10612(15)	0.01594(11)	0.06038(10)	0.0105(3)
O6	0.08982(13)	0.93246(9)	0.17804(8)	0.0147(3)
C21	0.56405(19)	0.80630(14)	0.16346(13)	0.0135(4)
O8	0.94122(13)	0.07386(9)	0.12811(8)	0.0146(3)
O7	0.04447(16)	0.16948(10)	0.04248(10)	0.0249(4)
C23	0.3966(2)	0.18396(15)	0.08744(17)	0.0280(5)
C22	0.7890(2)	0.81225(17)	0.17541(16)	0.0259(5)
C25	0.7862(2)	0.09128(16)	0.22408(12)	0.0203(4)
C24	0.86159(19)	0.14815(14)	0.16540(12)	0.0141(4)
C26	0.7733(2)	0.19295(17)	0.10627(14)	0.0240(5)
C27	0.9493(2)	0.21829(17)	0.20589(16)	0.0291(5)

Table 4. Bond lengths (Å) for *trans*-387.

Br1-C1	1.903(2)	C7-O1	1.212(3)
C7-C5	1.484(3)	C7-C19	1.538(3)
C1-C6	1.370(3)	C1-C2	1.380(3)
C4-C3	1.400(3)	C4-C5	1.399(3)
C4-C8	1.517(3)	C2-C3	1.387(3)
C17-O7	1.204(3)	C17-O8	1.320(2)
C17-N1	1.414(2)	C10-C15	1.385(3)
C10-C11	1.395(3)	C10-C19	1.511(3)
C11-C12	1.387(3)	C11-N1	1.425(3)
C13-C14	1.383(3)	C13-C12	1.397(3)
C6-C5	1.406(3)	C15-C14	1.399(3)
C8-C21	1.520(3)	C8-C9	1.532(3)
C20-O5	1.463(2)	C20-C23	1.498(4)
C16-O4	1.201(3)	C16-O5	1.336(2)
C16-C9	1.519(3)	C19-C9	1.544(3)
C19-C18	1.545(3)	C18-O6	1.200(3)
C18-N1	1.408(3)	O2-C21	1.338(3)
O2-C22	1.450(3)	O3-C21	1.207(3)
O8-C24	1.488(2)	C25-C24	1.511(3)
C24-C26	1.510(3)	C24-C27	1.521(3)

Table 5. Bond angles (°) for *trans*-387.

O1-C7-C5	122.31(17)	O1-C7-C19	119.14(17)
C5-C7-C19	118.54(16)	C6-C1-C2	121.65(18)
C6-C1-Br1	118.89(15)	C2-C1-Br1	119.39(15)
C3-C4-C5	118.25(18)	C3-C4-C8	121.59(16)
C5-C4-C8	120.12(16)	C1-C2-C3	119.34(18)
O7-C17-O8	128.22(18)	O7-C17-N1	122.40(17)
O8-C17-N1	109.38(16)	C15-C10-C11	120.17(18)
C15-C10-C19	130.57(17)	C11-C10-C19	109.25(16)
C12-C11-C10	121.72(18)	C12-C11-N1	128.50(17)
C10-C11-N1	109.73(16)	C14-C13-C12	121.76(19)
C1-C6-C5	119.03(18)	C10-C15-C14	118.86(17)
C11-C12-C13	117.30(18)	C4-C5-C6	120.65(18)
C4-C5-C7	122.21(17)	C6-C5-C7	117.03(17)
C4-C8-C21	112.92(16)	C4-C8-C9	111.24(15)
C21-C8-C9	107.44(16)	O5-C20-C23	111.62(18)
C2-C3-C4	121.01(18)	O4-C16-O5	124.80(18)
O4-C16-C9	124.25(17)	O5-C16-C9	110.95(16)
C10-C19-C7	110.95(15)	C10-C19-C9	114.85(15)
C7-C19-C9	111.59(15)	C10-C19-C18	103.07(14)
C7-C19-C18	106.36(15)	C9-C19-C18	109.32(15)
O6-C18-N1	128.03(18)	O6-C18-C19	124.73(17)
N1-C18-C19	107.21(16)	C16-C9-C8	109.30(15)
C16-C9-C19	111.31(15)	C8-C9-C19	112.31(15)
C13-C14-C15	120.15(19)	C16-O5-C20	116.43(16)
C21-O2-C22	115.40(17)	C18-N1-C17	125.71(17)
C18-N1-C11	110.59(15)	C17-N1-C11	122.98(16)
O3-C21-O2	124.48(19)	O3-C21-C8	124.22(18)
O2-C21-C8	111.29(17)	C17-O8-C24	120.93(15)
O8-C24-C25	101.30(15)	O8-C24-C26	110.61(17)
C25-C24-C26	110.76(18)	O8-C24-C27	109.03(16)
C25-C24-C27	111.16(19)	C26-C24-C27	113.32(19)

Table 6. Torsion angles (°) for *trans*-387.

C6-C1-C2-C3	-0.3(3)	Br1-C1-C2-C3	-177.15(17)
C15-C10-C11-C12	-2.5(3)	C19-C10-C11-C12	178.26(17)
C15-C10-C11-N1	175.25(16)	C19-C10-C11-N1	-4.0(2)
C2-C1-C6-C5	-2.1(3)	Br1-C1-C6-C5	174.78(15)
C11-C10-C15-C14	2.1(3)	C19-C10-C15-C14	-178.90(18)
C10-C11-C12-C13	1.3(3)	N1-C11-C12-C13	-176.01(19)
C14-C13-C12-C11	0.3(3)	C3-C4-C5-C6	-0.3(3)
C8-C4-C5-C6	177.28(18)	C3-C4-C5-C7	175.80(18)
C8-C4-C5-C7	-6.6(3)	C1-C6-C5-C4	2.4(3)

C1-C6-C5-C7	-173.91(18)	O1-C7-C5-C4	-176.42(19)
C19-C7-C5-C4	2.6(3)	O1-C7-C5-C6	-0.2(3)
C19-C7-C5-C6	178.86(17)	C3-C4-C8-C21	-29.1(3)
C5-C4-C8-C21	153.35(18)	C3-C4-C8-C9	-150.01(18)
C5-C4-C8-C9	32.5(2)	C1-C2-C3-C4	2.4(3)
C5-C4-C3-C2	-2.1(3)	C8-C4-C3-C2	-179.67(19)
C15-C10-C19-C7	-62.4(2)	C11-C10-C19-C7	116.71(17)
C15-C10-C19-C9	65.3(3)	C11-C10-C19-C9	-115.59(17)
C15-C10-C19-C18	-175.90(18)	C11-C10-C19-C18	3.23(19)
O1-C7-C19-C10	-76.2(2)	C5-C7-C19-C10	104.78(18)
O1-C7-C19-C9	154.38(17)	C5-C7-C19-C9	-24.7(2)
O1-C7-C19-C18	35.2(2)	C5-C7-C19-C18	-143.82(17)
C10-C19-C18-O6	-179.45(18)	C7-C19-C18-O6	63.8(2)
C9-C19-C18-O6	-56.9(2)	C10-C19-C18-N1	-1.34(18)
C7-C19-C18-N1	-118.13(16)	C9-C19-C18-N1	121.25(16)
O4-C16-C9-C8	5.9(3)	O5-C16-C9-C8	-173.26(16)
O4-C16-C9-C19	-118.7(2)	O5-C16-C9-C19	62.1(2)
C4-C8-C9-C16	-178.73(15)	C21-C8-C9-C16	57.2(2)
C4-C8-C9-C19	-54.7(2)	C21-C8-C9-C19	-178.73(15)
C10-C19-C9-C16	46.4(2)	C7-C19-C9-C16	173.75(16)
C18-C19-C9-C16	-68.9(2)	C10-C19-C9-C8	-76.6(2)
C7-C19-C9-C8	50.8(2)	C18-C19-C9-C8	168.20(15)
C12-C13-C14-C15	-0.7(3)	C10-C15-C14-C13	-0.5(3)
O4-C16-O5-C20	0.7(3)	C9-C16-O5-C20	179.85(17)
C23-C20-O5-C16	79.7(2)	O6-C18-N1-C17	6.6(3)
C19-C18-N1-C17	-171.44(17)	O6-C18-N1-C11	177.07(19)
C19-C18-N1-C11	-1.0(2)	O7-C17-N1-C18	150.98(19)
O8-C17-N1-C18	-29.0(3)	O7-C17-N1-C11	-18.4(3)
O8-C17-N1-C11	161.68(17)	C12-C11-N1-C18	-179.31(19)
C10-C11-N1-C18	3.1(2)	C12-C11-N1-C17	-8.5(3)
C10-C11-N1-C17	173.93(17)	C22-O2-C21-O3	-7.5(3)
C22-O2-C21-C8	172.12(18)	C4-C8-C21-O3	-81.3(2)
C9-C8-C21-O3	41.7(3)	C4-C8-C21-O2	99.07(19)
C9-C8-C21-O2	-137.90(16)	O7-C17-O8-C24	-11.0(3)
N1-C17-O8-C24	168.89(16)	C17-O8-C24-C25	-176.01(17)
C17-O8-C24-C26	66.5(2)	C17-O8-C24-C27	-58.7(2)

Table 7. Anisotropic atomic displacement parameters (Å^2) for *trans*-387.

The anisotropic atomic displacement factor exponent takes the form: $-2\pi^2[\, h^2 a^{*2} U_{11} + ... + 2\, h\, k\, a^* b^* U_{12}\,]$

	U_{11}	U_{22}	U_{33}	U_{23}	U_{13}	U_{12}
Br1	0.02858(12)	0.00894(10)	0.02604(13)	-0.00073(9)	0.00133(9)	-0.00270(8)
C7	0.0136(9)	0.0128(9)	0.0062(9)	0.0027(7)	0.0014(7)	-0.0016(7)

	U_{11}	U_{22}	U_{33}	U_{23}	U_{13}	U_{12}
C1	0.0236(10)	0.0125(9)	0.0132(10)	-0.0016(8)	0.0059(8)	0.0006(7)
C4	0.0145(8)	0.0113(9)	0.0074(9)	0.0009(8)	0.0030(7)	0.0012(7)
C2	0.0202(10)	0.0118(9)	0.0185(11)	0.0032(8)	0.0050(8)	0.0059(8)
C17	0.0123(8)	0.0129(9)	0.0170(10)	0.0001(9)	0.0015(7)	0.0047(7)
C10	0.0102(8)	0.0096(9)	0.0118(9)	0.0018(8)	-0.0028(7)	-0.0025(7)
C11	0.0112(8)	0.0107(8)	0.0077(9)	0.0001(7)	0.0017(8)	-0.0014(8)
C13	0.0218(10)	0.0192(10)	0.0108(10)	0.0070(8)	0.0005(8)	-0.0035(8)
C6	0.0156(8)	0.0167(9)	0.0096(9)	-0.0008(7)	0.0000(7)	-0.0011(7)
C15	0.0126(8)	0.0145(9)	0.0120(9)	-0.0010(8)	-0.0005(7)	0.0017(7)
C12	0.0148(8)	0.0125(9)	0.0154(10)	0.0039(7)	-0.0011(8)	-0.0018(7)
C5	0.0153(8)	0.0107(9)	0.0065(9)	-0.0011(8)	0.0017(7)	-0.0008(7)
C8	0.0109(8)	0.0105(8)	0.0111(10)	0.0026(8)	0.0000(7)	0.0011(7)
C20	0.0223(11)	0.0106(9)	0.0324(13)	-0.0066(10)	-0.0033(10)	-0.0024(8)
C3	0.0139(9)	0.0149(9)	0.0166(11)	0.0024(8)	0.0027(8)	0.0031(7)
C16	0.0148(9)	0.0101(9)	0.0092(9)	-0.0004(8)	-0.0052(8)	0.0023(7)
C19	0.0108(8)	0.0091(8)	0.0093(10)	0.0005(7)	-0.0002(7)	0.0010(7)
C18	0.0102(8)	0.0086(8)	0.0133(10)	0.0009(8)	-0.0010(7)	-0.0011(7)
C9	0.0099(8)	0.0105(9)	0.0097(9)	0.0002(7)	-0.0010(7)	0.0015(7)
C14	0.0154(9)	0.0221(10)	0.0117(10)	-0.0010(8)	0.0036(8)	-0.0004(8)
O5	0.0177(7)	0.0099(6)	0.0201(7)	-0.0042(6)	0.0010(6)	-0.0001(5)
O2	0.0091(6)	0.0189(7)	0.0272(8)	-0.0022(6)	-0.0035(6)	0.0018(6)
O4	0.0125(7)	0.0146(7)	0.0338(9)	0.0008(7)	0.0008(6)	-0.0026(5)
O1	0.0127(6)	0.0135(6)	0.0185(7)	0.0010(6)	-0.0033(6)	-0.0015(5)
O3	0.0212(7)	0.0258(8)	0.0168(8)	0.0029(6)	-0.0062(6)	0.0031(6)
N1	0.0115(7)	0.0079(7)	0.0123(8)	0.0041(6)	0.0028(6)	0.0026(6)
O6	0.0168(6)	0.0145(7)	0.0130(7)	0.0031(6)	0.0043(5)	0.0026(5)
C21	0.0120(9)	0.0100(9)	0.0187(12)	0.0004(8)	-0.0023(8)	0.0013(7)
O8	0.0150(6)	0.0098(6)	0.0190(7)	0.0014(6)	0.0062(6)	0.0041(5)
O7	0.0264(8)	0.0149(7)	0.0333(10)	0.0124(7)	0.0129(7)	0.0077(6)
C23	0.0291(11)	0.0122(9)	0.0428(15)	0.0074(11)	-0.0042(12)	-0.0010(8)
C22	0.0125(10)	0.0260(11)	0.0393(14)	-0.0048(10)	-0.0089(10)	0.0011(9)
C25	0.0234(10)	0.0214(10)	0.0161(10)	0.0015(9)	0.0046(8)	0.0051(9)
C24	0.0150(9)	0.0116(9)	0.0158(10)	-0.0024(8)	0.0020(8)	0.0053(8)
C26	0.0229(10)	0.0303(11)	0.0187(11)	0.0036(10)	0.0017(9)	0.0161(9)
C27	0.0265(12)	0.0220(11)	0.0387(15)	-0.0095(11)	-0.0041(11)	-0.0007(9)

Table 8. Hydrogen atomic coordinates and isotropic atomic displacement parameters ($Å^2$) for *trans*-387.

	x/a	y/b	z/c	U(eq)
H2	0.4459	0.4817	0.1253	0.02
H13	0.2702	1.0742	-0.1804	0.021
H6	0.1162	0.6052	0.0560	0.017

	x/a	y/b	z/c	U(eq)
H15	0.3847	0.8427	-0.0614	0.016
H12	0.1363	1.1196	-0.0764	0.017
H8	0.4868	0.8187	0.0529	0.013
H20A	0.4904	1.1317	0.1832	0.026
H20B	0.3511	1.1724	0.2035	0.026
H3	0.5466	0.6281	0.1305	0.018
H9	0.3277	0.8647	0.1843	0.012
H14	0.3914	0.9377	-0.1740	0.02
H23A	0.4502	1.1497	0.0501	0.042
H23B	0.4289	1.2483	0.0932	0.042
H23C	0.3080	1.1858	0.0684	0.042
H22A	0.7809	0.8723	0.2029	0.039
H22B	0.8659	0.8134	0.1425	0.039
H22C	0.7962	0.7611	0.2135	0.039
H25A	-0.2657	1.0443	0.1966	0.03
H25B	-0.2701	1.1331	0.2539	0.03
H25C	-0.1546	1.0595	0.2598	0.03
H26A	-0.1765	1.2323	0.0706	0.036
H26B	-0.2902	1.2319	0.1333	0.036
H26C	-0.2707	1.1437	0.0765	0.036
H27A	0.0106	1.1844	0.2389	0.044
H27B	-0.1022	1.2607	0.2383	0.044
H27C	-0.0041	1.2549	0.1666	0.044

X-ray crystallography data for lactone *trans*-417.

A specimen of $C_{27}H_{27}NO_6$ was used for the X-ray crystallographic analysis. The X-ray intensity data were measured.

Table 1: Data collection details for *trans*-417.

Axis	dx/mm	2θ/°	ω/°	φ/°	χ/°	Width/°	Frames	Time/s	Wavelength/Å	Voltage/kV	Current/mA	Temperature/K
Phi	37.692	-54.00	248.79	-305.79	22.49	0.50	553	10.00	1.54184	45	0.7	100.24
Omega	37.692	-40.00	-25.50	-200.82	-78.01	0.50	75	10.00	1.54184	45	0.7	100.24
Phi	37.692	-36.00	326.69	-220.42	53.17	0.50	509	10.00	1.54184	45	0.7	100.24
Phi	37.692	80.00	59.26	-240.55	37.41	0.50	511	10.00	1.54184	45	0.7	100.24
Omega	37.692	92.00	-184.03	-205.16	-96.16	0.50	112	5.00	1.54184	45	0.7	100.24
Omega	37.692	94.00	90.97	-27.31	-46.83	0.50	143	5.00	1.54184	45	0.7	100.24
Omega	37.692	94.00	83.55	-12.61	-20.22	0.50	202	5.00	1.54184	45	0.7	100.24
Phi	37.692	96.00	46.39	-290.12	96.43	0.50	739	5.00	1.54184	45	0.7	100.24
Omega	37.692	96.00	-196.14	-192.81	-68.46	0.50	97	5.00	1.54184	45	0.7	100.24
Phi	37.692	96.00	177.08	-13.34	-30.75	0.50	739	5.00	1.54184	45	0.7	100.24

A total of 3680 frames were collected. The total exposure time was 7.40 hours. The frames were integrated with the Bruker SAINT software package using a narrow-frame algorithm. The integration of the data using an orthorhombic unit cell yielded a total

of 18299 reflections to a maximum θ angle of 66.89° (0.84 Å resolution), of which 4143 were independent (average redundancy 4.417, completeness = 98.0%, R_{int} = 3.05%, R_{sig} = 2.31%) and 4124 (99.54%) were greater than $2\sigma(F^2)$. The final cell constants of $\underline{a}$ = 9.9567(3) Å, $\underline{b}$ = 14.4143(5) Å, $\underline{c}$ = 16.9131(6) Å, volume = 2427.35(14) Å^3, are based upon the refinement of the XYZ-centroids of 9880 reflections above 20 σ(I) with 8.059° < 2θ < 133.6°. Data were corrected for absorption effects using the multi-scan method (SADABS). The ratio of minimum to maximum apparent transmission was 0.857. The structure was solved and refined using the Bruker SHELXTL Software Package, using the space group P 21 21 21, with Z = 4 for the formula unit, $C_{27}H_{27}NO_6$. The final anisotropic full-matrix least-squares refinement on F^2 with 312 variables converged at R1 = 2.52%, for the observed data and wR2 =6.66% for all data. The goodness-of-fit was 1.028. The largest peak in the final difference electron density synthesis was 0.192 e$^-$/Å^3 and the largest hole was -0.125 e$^-$/Å^3 with an RMS deviation of 0.029 e$^-$/Å^3. On the basis of the final model, the calculated density was 1.263 g/cm^3 and F(000), 976 e$^-$.

Table 2. Sample and crystal data for *trans*-417.

Identification code	fmm1088	
Chemical formula	$C_{27}H_{27}NO_6$	
Formula weight	461.50	
Temperature	100(2) K	
Wavelength	1.54178 Å	
Crystal system	orthorhombic	
Space group	P 21 21 21	
Unit cell dimensions	a = 9.9567(3) Å	α = 90°
	b = 14.4143(5) Å	β = 90°
	c = 16.9131(6) Å	γ = 90°
Volume	2427.35(14) Å^3	
Z	4	
Density (calculated)	1.263 g/cm^3	
Absorption coefficient	0.732 mm^{-1}	
F(000)	976	

Table 3. Data collection and structure refinement for *trans*-417.

Theta range for data collection	4.03 to 66.89°
Index ranges	-10<=h<=11, -16<=k<=17, -19<=l<=20
Reflections collected	18299
Independent reflections	4143 [R(int) = 0.0305]
Coverage of independent reflections	98.0%
Absorption correction	multi-scan
Structure solution technique	direct methods
Structure solution program	SHELXS-97 (Sheldrick, 2008)
Refinement method	Full-matrix least-squares on F^2
Refinement program	SHELXL-97 (Sheldrick, 2008)
Function minimized	$\Sigma\ w(F_o^2 - F_c^2)^2$

Data / restraints / parameters	4143 / 0 / 312	
Goodness-of-fit on F^2	1.028	
Δ/σ_{max}	0.028	
Final R indices	4124 data; I>2σ(I)	R1 = 0.0252, wR2 = 0.0664
	all data	R1 = 0.0253, wR2 = 0.0666
Weighting scheme	w=1/[σ²(F_o^2)+(0.0399P)²+0.3594P] where P=(F_o^2+2F_c^2)/3	
Absolute structure parameter	0.0(1)	
Extinction coefficient	0.0038(2)	
Largest diff. peak and hole	0.192 and -0.125 eÅ^{-3}	
R.M.S. deviation from mean	0.029 eÅ^{-3}	

Table 4. Atomic coordinates and equivalent isotropic atomic displacement parameters (Å^2) for *trans*-417.

U(eq) is defined as one third of the trace of the orthogonalised U_{ij} tensor.

	x/a	y/b	z/c	U(eq)
C10	0.33598(12)	0.81876(8)	0.91124(7)	0.0230(3)
C15	0.45821(11)	0.62504(8)	0.82689(7)	0.0204(2)
C8	0.46977(12)	0.89140(7)	0.01857(7)	0.0216(2)
C16	0.47754(11)	0.67998(8)	0.89375(7)	0.0196(2)
C21	0.46393(12)	0.78112(8)	0.87168(7)	0.0201(2)
C4	0.47676(13)	0.94096(8)	0.09515(7)	0.0228(2)
C12	0.71624(13)	0.81672(9)	0.85504(7)	0.0252(3)
C22	0.43710(11)	0.77715(8)	0.78268(7)	0.0212(2)
C23	0.39298(12)	0.64776(8)	0.68601(7)	0.0222(2)
C11	0.58302(12)	0.84638(8)	0.89032(7)	0.0212(2)
C17	0.49756(12)	0.63953(8)	0.96703(7)	0.0228(3)
C9	0.35082(12)	0.86900(8)	0.98543(7)	0.0244(3)
C5	0.59427(13)	0.94083(9)	0.14029(7)	0.0273(3)
C18	0.50310(13)	0.54293(8)	0.97175(7)	0.0268(3)
C20	0.46672(13)	0.52914(8)	0.83037(7)	0.0245(3)
C19	0.48937(13)	0.48949(8)	0.90420(8)	0.0273(3)
C7	0.59956(12)	0.86490(8)	0.97886(7)	0.0216(2)
C3	0.36638(13)	0.99013(8)	0.12434(7)	0.0272(3)
C2	0.37242(14)	0.03713(9)	0.19569(8)	0.0327(3)
C13	0.82038(14)	0.72690(10)	0.75367(8)	0.0334(3)
C6	0.59991(14)	0.98774(9)	0.21219(8)	0.0324(3)
C24	0.28736(14)	0.69468(8)	0.56311(7)	0.0276(3)
C1	0.48930(15)	0.03582(9)	0.23992(8)	0.0322(3)
C27	0.2593(2)	0.79040(10)	0.53124(9)	0.0470(4)
C14	0.77254(17)	0.66254(12)	0.68975(9)	0.0464(4)
C25	0.15880(17)	0.64538(14)	0.58406(9)	0.0536(4)
C26	0.3732(2)	0.64058(13)	0.50661(9)	0.0556(5)

	x/a	y/b	z/c	U(eq)
O5	0.22607(9)	0.80214(6)	0.88241(5)	0.0303(2)
O6	0.42454(9)	0.84359(5)	0.74046(5)	0.0276(2)
O3	0.70096(9)	0.75841(6)	0.79466(5)	0.0298(2)
O1	0.38965(11)	0.56593(6)	0.67219(5)	0.0348(2)
O2	0.36174(9)	0.71542(5)	0.63671(5)	0.0279(2)
O4	0.82277(10)	0.84508(9)	0.87721(6)	0.0473(3)
N1	0.42996(10)	0.68264(6)	0.76027(6)	0.0210(2)

Table 5. Bond lengths (Å) for *trans*-417.

C10-O5	1.2218(15)	C10-C9	1.4562(17)
C10-C21	1.5380(16)	C15-C20	1.3862(16)
C15-C16	1.3938(16)	C15-N1	1.4275(14)
C8-C9	1.3495(18)	C8-C4	1.4808(16)
C8-C7	1.5056(17)	C16-C17	1.3840(16)
C16-C21	1.5110(15)	C21-C22	1.5298(16)
C21-C11	1.5460(16)	C4-C5	1.3971(18)
C4-C3	1.3978(18)	C12-O4	1.1970(16)
C12-O3	1.3314(15)	C12-C11	1.5160(17)
C22-O6	1.2011(14)	C22-N1	1.4158(15)
C23-O1	1.2029(15)	C23-O2	1.3202(14)
C23-N1	1.4021(15)	C11-C7	1.5299(16)
C17-C18	1.3959(17)	C5-C6	1.3925(19)
C18-C19	1.3846(18)	C20-C19	1.3917(17)
C3-C2	1.3852(18)	C2-C1	1.384(2)
C13-O3	1.4493(16)	C13-C14	1.502(2)
C6-C1	1.383(2)	C24-O2	1.4789(15)
C24-C26	1.501(2)	C24-C25	1.506(2)
C24-C27	1.5074(18)		

Table 6. Bond angles (°) for *trans*-417.

O5-C10-C9	122.16(11)	O5-C10-C21	119.94(11)
C9-C10-C21	117.80(10)	C20-C15-C16	121.58(11)
C20-C15-N1	128.72(11)	C16-C15-N1	109.71(9)
C9-C8-C4	121.33(11)	C9-C8-C7	120.49(10)
C4-C8-C7	118.18(10)	C17-C16-C15	120.47(10)
C17-C16-C21	129.84(11)	C15-C16-C21	109.58(10)
C16-C21-C22	102.87(9)	C16-C21-C10	107.89(9)
C22-C21-C10	107.26(9)	C16-C21-C11	117.89(10)
C22-C21-C11	110.94(9)	C10-C21-C11	109.38(9)
C5-C4-C3	117.78(11)	C5-C4-C8	121.11(11)
C3-C4-C8	121.11(11)	O4-C12-O3	123.85(12)
O4-C12-C11	123.76(11)	O3-C12-C11	112.33(10)

O6-C22-N1	127.07(11)	O6-C22-C21	124.99(11)
N1-C22-C21	107.94(9)	O1-C23-O2	126.51(11)
O1-C23-N1	122.20(11)	O2-C23-N1	111.27(9)
C12-C11-C7	109.90(10)	C12-C11-C21	114.78(9)
C7-C11-C21	112.85(9)	C16-C17-C18	118.50(11)
C8-C9-C10	124.46(11)	C6-C5-C4	120.68(12)
C19-C18-C17	120.25(11)	C15-C20-C19	117.23(11)
C18-C19-C20	121.86(11)	C8-C7-C11	112.86(10)
C2-C3-C4	121.44(12)	C1-C2-C3	120.05(12)
O3-C13-C14	106.12(11)	C1-C6-C5	120.48(12)
O2-C24-C26	110.83(12)	O2-C24-C25	108.84(10)
C26-C24-C25	112.88(13)	O2-C24-C27	102.05(9)
C26-C24-C27	110.69(13)	C25-C24-C27	111.02(14)
C2-C1-C6	119.56(12)	C12-O3-C13	118.10(10)
C23-O2-C24	120.02(9)	C23-N1-C22	126.72(9)
C23-N1-C15	123.39(9)	C22-N1-C15	109.78(9)

Table 7. Torsion angles (°) for *trans*-417.

C20-C15-C16-C17	-4.12(17)	N1-C15-C16-C17	175.69(10)
C20-C15-C16-C21	179.28(11)	N1-C15-C16-C21	-0.91(13)
C17-C16-C21-C22	-177.33(12)	C15-C16-C21-C22	-1.15(12)
C17-C16-C21-C10	-64.16(15)	C15-C16-C21-C10	112.02(10)
C17-C16-C21-C11	60.27(17)	C15-C16-C21-C11	-123.55(11)
O5-C10-C21-C16	-78.56(13)	C9-C10-C21-C16	97.82(11)
O5-C10-C21-C22	31.65(14)	C9-C10-C21-C22	-151.98(10)
O5-C10-C21-C11	152.05(11)	C9-C10-C21-C11	-31.58(14)
C9-C8-C4-C5	161.36(11)	C7-C8-C4-C5	-17.60(16)
C9-C8-C4-C3	-19.22(17)	C7-C8-C4-C3	161.82(11)
C16-C21-C22-O6	-177.25(11)	C10-C21-C22-O6	69.12(14)
C11-C21-C22-O6	-50.29(15)	C16-C21-C22-N1	2.81(12)
C10-C21-C22-N1	-110.82(10)	C11-C21-C22-N1	129.77(10)
O4-C12-C11-C7	-33.66(16)	O3-C12-C11-C7	148.79(10)
O4-C12-C11-C21	-162.12(12)	O3-C12-C11-C21	20.32(14)
C16-C21-C11-C12	55.95(13)	C22-C21-C11-C12	-62.25(13)
C10-C21-C11-C12	179.63(9)	C16-C21-C11-C7	-71.02(13)
C22-C21-C11-C7	170.79(10)	C10-C21-C11-C7	52.67(13)
C15-C16-C17-C18	2.45(18)	C21-C16-C17-C18	178.27(11)
C4-C8-C9-C10	-178.70(10)	C7-C8-C9-C10	0.24(18)
O5-C10-C9-C8	-178.02(12)	C21-C10-C9-C8	5.69(17)
C3-C4-C5-C6	0.49(18)	C8-C4-C5-C6	179.93(11)
C16-C17-C18-C19	0.29(19)	C16-C15-C20-C19	2.85(18)
N1-C15-C20-C19	-176.92(12)	C17-C18-C19-C20	-1.5(2)
C15-C20-C19-C18	-0.05(19)	C9-C8-C7-C11	21.31(15)

332

C4-C8-C7-C11	-159.71(9)	C12-C11-C7-C8	-177.92(9)
C21-C11-C7-C8	-48.40(13)	C5-C4-C3-C2	-0.16(18)
C8-C4-C3-C2	-179.60(12)	C4-C3-C2-C1	-0.2(2)
C4-C5-C6-C1	-0.41(19)	C3-C2-C1-C6	0.3(2)
C5-C6-C1-C2	0.0(2)	O4-C12-O3-C13	0.43(19)
C11-C12-O3-C13	177.98(10)	C14-C13-O3-C12	179.71(11)
O1-C23-O2-C24	14.66(19)	N1-C23-O2-C24	-164.21(10)
C26-C24-O2-C23	-68.72(15)	C25-C24-O2-C23	55.99(16)
C27-C24-O2-C23	173.40(12)	O1-C23-N1-C22	-179.97(12)
O2-C23-N1-C22	-1.04(16)	O1-C23-N1-C15	-4.17(18)
O2-C23-N1-C15	174.76(10)	O6-C22-N1-C23	-7.19(19)
C21-C22-N1-C23	172.75(10)	O6-C22-N1-C15	176.54(12)
C21-C22-N1-C15	-3.52(12)	C20-C15-N1-C23	6.20(19)
C16-C15-N1-C23	-173.60(10)	C20-C15-N1-C22	-177.38(12)
C16-C15-N1-C22	2.83(12)		

Table 8. Anisotropic atomic displacement parameters (Å^2) for *trans*-417.

The anisotropic atomic displacement factor exponent takes the form: $-2\pi^2[\,h^2\,a^{*2}\,U_{11} + ... + 2\,h\,k\,a^*\,b^*\,U_{12}\,]$

	U_{11}	U_{22}	U_{33}	U_{23}	U_{13}	U_{12}
C10	0.0189(6)	0.0195(5)	0.0305(6)	0.0011(5)	-0.0017(5)	-0.0002(5)
C15	0.0150(5)	0.0215(5)	0.0246(6)	0.0040(4)	0.0010(4)	-0.0002(4)
C8	0.0211(6)	0.0177(5)	0.0261(6)	0.0037(4)	-0.0009(5)	0.0005(5)
C16	0.0140(5)	0.0193(5)	0.0256(6)	0.0019(4)	0.0012(5)	-0.0005(4)
C21	0.0178(5)	0.0187(5)	0.0239(5)	0.0018(4)	-0.0007(5)	-0.0009(4)
C4	0.0226(6)	0.0200(5)	0.0259(6)	0.0027(5)	-0.0006(5)	-0.0018(5)
C12	0.0224(6)	0.0309(6)	0.0223(6)	0.0055(5)	-0.0009(5)	-0.0036(5)
C22	0.0178(6)	0.0181(5)	0.0277(6)	0.0005(5)	-0.0021(5)	-0.0010(4)
C23	0.0213(6)	0.0208(5)	0.0244(6)	0.0007(4)	0.0010(5)	-0.0004(5)
C11	0.0199(6)	0.0191(5)	0.0247(6)	0.0029(4)	-0.0017(5)	-0.0025(4)
C17	0.0186(6)	0.0240(6)	0.0259(6)	0.0030(5)	0.0011(5)	-0.0026(5)
C9	0.0181(6)	0.0241(6)	0.0311(6)	-0.0024(5)	0.0004(5)	0.0015(5)
C5	0.0232(6)	0.0304(6)	0.0285(6)	0.0005(5)	-0.0007(5)	0.0009(5)
C18	0.0250(7)	0.0257(6)	0.0296(6)	0.0087(5)	0.0000(5)	-0.0022(5)
C20	0.0228(6)	0.0190(5)	0.0318(6)	0.0006(5)	0.0004(5)	0.0011(5)
C19	0.0270(7)	0.0192(5)	0.0357(7)	0.0064(5)	-0.0012(5)	0.0000(5)
C7	0.0167(6)	0.0223(5)	0.0258(6)	0.0005(4)	-0.0021(5)	-0.0020(5)
C3	0.0245(6)	0.0271(6)	0.0299(6)	-0.0012(5)	-0.0027(5)	0.0027(5)
C2	0.0330(7)	0.0323(6)	0.0328(7)	-0.0046(5)	0.0027(6)	0.0045(5)
C13	0.0261(7)	0.0400(7)	0.0340(7)	0.0030(6)	0.0093(6)	0.0038(6)
C6	0.0294(7)	0.0390(7)	0.0288(6)	-0.0010(5)	-0.0065(6)	-0.0030(6)
C24	0.0358(7)	0.0258(6)	0.0213(6)	-0.0026(5)	-0.0061(5)	-0.0039(5)
C1	0.0374(7)	0.0341(6)	0.0252(6)	-0.0029(5)	0.0003(6)	-0.0019(6)

	U_{11}	U_{22}	U_{33}	U_{23}	U_{13}	U_{12}
C27	0.0765(12)	0.0325(7)	0.0319(7)	0.0011(6)	-0.0236(8)	0.0034(7)
C14	0.0420(8)	0.0612(10)	0.0359(8)	-0.0087(7)	0.0057(7)	0.0135(8)
C25	0.0421(9)	0.0780(12)	0.0407(8)	0.0116(8)	-0.0157(7)	-0.0242(9)
C26	0.0805(13)	0.0558(10)	0.0304(7)	-0.0024(7)	0.0107(8)	0.0165(9)
O5	0.0175(4)	0.0345(5)	0.0389(5)	-0.0083(4)	-0.0037(4)	-0.0010(4)
O6	0.0345(5)	0.0186(4)	0.0296(4)	0.0041(3)	-0.0077(4)	-0.0014(3)
O3	0.0222(4)	0.0315(4)	0.0357(5)	-0.0047(4)	0.0061(4)	-0.0019(4)
O1	0.0539(6)	0.0195(4)	0.0309(4)	-0.0045(4)	-0.0039(4)	0.0047(4)
O2	0.0377(5)	0.0206(4)	0.0254(4)	0.0016(3)	-0.0102(4)	-0.0041(4)
O4	0.0205(5)	0.0892(8)	0.0321(5)	-0.0141(5)	0.0007(4)	-0.0093(5)
N1	0.0220(5)	0.0171(4)	0.0240(5)	0.0015(4)	-0.0023(4)	-0.0004(4)

Table 9. Hydrogen atomic coordinates and isotropic atomic displacement parameters (Å^2) for *trans*-417.

	x/a	y/b	z/c	U(eq)
H11	0.5606	0.9075	0.8656	0.025
H17	0.5073	0.6767	1.0131	0.027
H9	0.2713	0.8872	1.0123	0.029
H5	0.6711	0.9084	1.1217	0.033
H18	0.5163	0.5137	1.0215	0.032
H20	0.4575	0.4920	0.7843	0.029
H19	0.4956	0.4239	0.9084	0.033
H7A	0.6359	0.8085	1.0046	0.026
H7B	0.6656	0.9155	0.9864	0.026
H3	0.2855	0.9913	1.0946	0.033
H2	0.2962	1.0703	1.2143	0.039
H13A	0.8811	0.6939	0.7905	0.04
H13B	0.8694	0.7801	0.7305	0.04
H6	0.6803	0.9867	1.2424	0.039
H1	0.4936	1.0677	1.2890	0.039
H27A	0.2071	0.8257	0.5701	0.071
H27B	0.2082	0.7854	0.4819	0.071
H27C	0.3445	0.8223	0.5210	0.071
H14A	0.7270	0.6092	0.7137	0.07
H14B	0.8496	0.6409	0.6588	0.07
H14C	0.7098	0.6955	0.6551	0.07
H25A	0.1790	0.5815	0.5999	0.08
H25B	0.0991	0.6447	0.5380	0.08
H25C	0.1147	0.6778	0.6279	0.08
H26A	0.4563	0.6749	0.4962	0.083
H26B	0.3244	0.6314	0.4569	0.083
H26C	0.3951	0.5801	0.5298	0.083

X-ray crystallography data for lactone *trans*-429.

A specimen of $C_{31}HBBrCl_3NO_6$ was used for the X-ray crystallographic analysis. The X-ray intensity data were measured. The integration of the data using an orthorhombic unit cell yielded a total of 12002 reflections to a maximum θ angle of 66.83° (0.84 Å resolution), of which 5027 were independent (average redundancy 2.388, completeness = 97.1%, R_{int} = 3.03%, R_{sig} = 3.97%) and 4992 (99.30%) were greater than $2\sigma(F^2)$. The final cell constants of $\underline{a}$ = 10.3658(4) Å, $\underline{b}$ = 18.2888(7) Å, $\underline{c}$ = 33.3036(13) Å, volume = 6313.6(4) Å^3, are based upon the refinement of the XYZ-centroids of reflections above 20 $\sigma(I)$. The structure was solved and refined using the Bruker SHELXTL Software Package, using the space group C 2 2 21, with Z = 8 for the formula unit, $C_{31}HBBrCl_3NO_6$. The final anisotropic full-matrix least-squares refinement on F^2 with 384 variables converged at R1 = 3.08%, for the observed data and wR2 =7.70% for all data. The goodness-of-fit was 1.057. The largest peak in the final difference electron density synthesis was 0.735 e$^-$/Å^3 and the largest hole was -0.629 e$^-$/Å^3 with an RMS deviation of 0.061 e$^-$/Å^3. On the basis of the final model, the calculated density was 1.432 g/cm^3 and F(000), 2664 e$^-$.

Table 1. Sample and crystal data for *trans*-429.

Identification code	fmm1117	
Chemical formula	$C_{31}HBBrCl_3NO_6$	
Formula weight	680.40	
Temperature	123(2) K	
Wavelength	1.54178 Å	
Crystal system	orthorhombic	
Space group	C 2 2 21	
Unit cell dimensions	a = 10.3658(4) Å	$\alpha = 90°$
	b = 18.2888(7) Å	$\beta = 90°$
	c = 33.3036(13) Å	$\gamma = 90°$
Volume	6313.6(4) Å^3	
Z	8	
Density (calculated)	1.432 g/cm^3	
Absorption coefficient	4.479 mm^{-1}	
F(000)	2664	

Table 2. Data collection and structure refinement for *trans*-429.

Theta range for data collection	2.65 to 66.83°
Index ranges	-12<=h<=11, -21<=k<=19, -25<=l<=39
Reflections collected	12002
Independent reflections	5027 [R(int) = 0.0303]
Structure solution technique	direct methods
Structure solution program	SHELXS-97 (Sheldrick, 2008)
Refinement method	Full-matrix least-squares on F^2
Refinement program	SHELXL-97 (Sheldrick, 2008)

Function minimized	$\Sigma \, w(F_o{}^2 - F_c{}^2)^2$
Data / restraints / parameters	5027 / 0 / 384
Goodness-of-fit on F^2	1.057
Δ/σ_{max}	0.001
Final R indices	4992 data; $I>2\sigma(I)$ R1 = 0.0308, wR2 = 0.0769
	all data R1 = 0.0310, wR2 = 0.0770
Weighting scheme	w=1/[$\sigma^2(F_o{}^2)$+(0.0280P)^2+12.2772P] where P=($F_o{}^2$+2$F_c{}^2$)/3
Absolute structure parameter	0.0(0)
Extinction coefficient	0.0001(0)
Largest diff. peak and hole	0.735 and -0.629 eÅ^{-3}
R.M.S. deviation from mean	0.061 eÅ^{-3}

Table 3. Atomic coordinates and equivalent isotropic atomic displacement parameters (Å^2) for *trans*-429.

U(eq) is defined as one third of the trace of the orthogonalised U_{ij} tensor.

	x/a	y/b	z/c	U(eq)
Br15	0.52987(3)	0.498296(17)	0.412595(8)	0.02004(10)
O1	0.66434(19)	0.30618(11)	0.52692(7)	0.0198(5)
O2	0.13583(19)	0.40922(10)	0.57765(6)	0.0185(4)
O3	0.04843(19)	0.29966(11)	0.56244(6)	0.0182(4)
O4	0.63256(19)	0.32235(10)	0.61820(6)	0.0168(4)
O5	0.68443(19)	0.10584(10)	0.65199(6)	0.0159(4)
O6	0.6972(2)	0.22212(12)	0.67545(7)	0.0268(5)
N1	0.5974(2)	0.19602(12)	0.61575(7)	0.0116(5)
C15	0.4469(3)	0.44062(15)	0.45280(8)	0.0148(6)
C16	0.5219(3)	0.39756(14)	0.47709(8)	0.0135(5)
C17	0.4640(3)	0.35725(13)	0.50774(8)	0.0101(5)
C18	0.3292(3)	0.35961(14)	0.51361(8)	0.0096(6)
C19	0.3141(3)	0.44330(15)	0.45718(9)	0.0145(6)
C20	0.2579(3)	0.40267(14)	0.48749(8)	0.0141(6)
C21	0.2683(3)	0.31556(14)	0.54723(8)	0.0101(5)
C22	0.3615(2)	0.30787(13)	0.58291(8)	0.0101(5)
C23	0.4889(2)	0.27101(14)	0.56822(8)	0.0092(5)
C24	0.4727(3)	0.19094(14)	0.55860(8)	0.0098(5)
C25	0.5301(2)	0.14886(13)	0.58833(8)	0.0102(5)
C27	0.6645(3)	0.17783(15)	0.65111(9)	0.0147(6)
C29	0.3062(3)	0.26901(14)	0.61937(9)	0.0120(6)
C30	0.2345(3)	0.20436(15)	0.61618(9)	0.0167(6)
C31	0.1906(3)	0.16900(17)	0.65044(10)	0.0260(7)
C32	0.3317(3)	0.29625(16)	0.65747(9)	0.0200(7)
C33	0.5494(3)	0.31205(14)	0.53337(8)	0.0117(6)
C34	0.1447(3)	0.34898(15)	0.56365(8)	0.0117(6)

336

	x/a	y/b	z/c	U(eq)
C35	0.4066(3)	0.15899(14)	0.52734(8)	0.0117(5)
C36	0.3925(3)	0.08350(15)	0.52671(9)	0.0147(6)
C37	0.4458(3)	0.04208(14)	0.55765(9)	0.0158(6)
C38	0.5168(3)	0.07335(14)	0.58858(9)	0.0143(5)
C39	0.9335(3)	0.31856(18)	0.58414(11)	0.0259(7)
C40	0.5827(3)	0.26957(14)	0.60348(8)	0.0099(5)
C41	0.2164(4)	0.1970(2)	0.68767(11)	0.0352(9)
C42	0.2877(4)	0.2605(2)	0.69173(11)	0.0358(9)
C43	0.7374(3)	0.07004(15)	0.68869(9)	0.0172(6)
C44	0.7393(4)	0.98972(18)	0.67605(9)	0.0280(8)
C45	0.8727(3)	0.0977(2)	0.69682(11)	0.0314(8)
C46	0.6450(4)	0.0819(2)	0.72317(10)	0.0315(8)
Cl1	0.61035(12)	0.42400(10)	0.71192(5)	0.0913(6)
Cl2	0.86892(12)	0.37662(8)	0.72433(4)	0.0675(4)
Cl3	0.81076(13)	0.46815(6)	0.65742(4)	0.0551(3)
C60	0.7540(3)	0.39737(19)	0.68816(10)	0.0288(8)

Table 4. Bond lengths (Å) for *trans*-429.

Br15-C15	1.909(3)	O1-C33	1.215(3)
O2-C34	1.200(3)	O3-C34	1.346(3)
O3-C39	1.436(4)	O4-C40	1.200(3)
O5-C27	1.333(3)	O5-C43	1.491(3)
O6-C27	1.195(4)	N1-C27	1.408(4)
N1-C40	1.414(3)	N1-C25	1.437(3)
C15-C16	1.370(4)	C15-C19	1.386(4)
C16-C17	1.395(4)	C16-H16	0.95
C17-C18	1.411(4)	C17-C33	1.482(4)
C18-C20	1.387(4)	C18-C21	1.517(4)
C19-C20	1.382(4)	C19-H19	0.95
C20-H20	0.95	C21-C34	1.522(4)
C21-C22	1.537(4)	C21-H21	1.0
C22-C29	1.519(4)	C22-C23	1.561(3)
C22-H22	1.0	C23-C24	1.508(3)
C23-C33	1.518(4)	C23-C40	1.525(4)
C24-C35	1.376(4)	C24-C25	1.388(4)
C25-C38	1.388(4)	C29-C32	1.388(4)
C29-C30	1.401(4)	C30-C31	1.388(4)
C30-H30	0.95	C31-C41	1.368(5)
C31-H31	0.95	C32-C42	1.392(5)
C32-H32	0.95	C35-C36	1.388(4)
C35-H35	0.95	C36-C37	1.393(4)
C36-H36	0.95	C37-C38	1.389(4)

337

C37-H37	0.95	C38-H38	0.95
C39-H39A	0.98	C39-H39B	0.98
C39-H39C	0.98	C41-C42	1.384(5)
C41-H41	0.95	C42-H42	0.95
C43-C46	1.511(5)	C43-C45	1.515(5)
C43-C44	1.528(4)	C44-H44A	0.98
C44-H44B	0.98	C44-H44C	0.98
C45-H45A	0.98	C45-H45B	0.98
C45-H45C	0.98	C46-H46A	0.98
C46-H46B	0.98	C46-H46C	0.98
Cl1-C60	1.755(4)	Cl2-C60	1.736(3)
Cl3-C60	1.752(4)	C60-H60	1.0

Table 5. Bond angles (°) for *trans*-429.

C34-O3-C39	116.0(2)	C27-O5-C43	120.6(2)
C27-N1-C40	121.3(2)	C27-N1-C25	129.0(2)
C40-N1-C25	109.6(2)	C16-C15-C19	121.4(3)
C16-C15-Br15	118.4(2)	C19-C15-Br15	120.1(2)
C15-C16-C17	119.5(3)	C15-C16-H16	120.3
C17-C16-H16	120.3	C16-C17-C18	120.8(2)
C16-C17-C33	117.3(2)	C18-C17-C33	121.9(2)
C20-C18-C17	117.2(2)	C20-C18-C21	122.9(2)
C17-C18-C21	119.9(2)	C20-C19-C15	118.5(3)
C20-C19-H19	120.8	C15-C19-H19	120.8
C19-C20-C18	122.6(3)	C19-C20-H20	118.7
C18-C20-H20	118.7	C18-C21-C34	113.7(2)
C18-C21-C22	111.0(2)	C34-C21-C22	106.7(2)
C18-C21-H21	108.4	C34-C21-H21	108.4
C22-C21-H21	108.4	C29-C22-C21	115.1(2)
C29-C22-C23	111.5(2)	C21-C22-C23	109.2(2)
C29-C22-H22	106.9	C21-C22-H22	106.9
C23-C22-H22	106.9	C24-C23-C33	111.3(2)
C24-C23-C40	102.6(2)	C33-C23-C40	109.5(2)
C24-C23-C22	113.1(2)	C33-C23-C22	112.1(2)
C40-C23-C22	107.8(2)	C35-C24-C25	121.1(2)
C35-C24-C23	128.9(2)	C25-C24-C23	109.8(2)
C24-C25-C38	120.9(3)	C24-C25-N1	109.2(2)
C38-C25-N1	129.9(3)	O6-C27-O5	127.7(3)
O6-C27-N1	123.2(3)	O5-C27-N1	109.2(2)
C32-C29-C30	118.2(3)	C32-C29-C22	119.4(2)
C30-C29-C22	122.3(3)	C31-C30-C29	120.3(3)
C31-C30-H30	119.8	C29-C30-H30	119.8
C41-C31-C30	120.4(3)	C41-C31-H31	119.8

C30-C31-H31	119.8	C29-C32-C42	121.2(3)
C29-C32-H32	119.4	C42-C32-H32	119.4
O1-C33-C17	122.2(3)	O1-C33-C23	119.8(2)
C17-C33-C23	118.0(2)	O2-C34-O3	124.8(3)
O2-C34-C21	124.9(2)	O3-C34-C21	110.1(2)
C24-C35-C36	119.1(3)	C24-C35-H35	120.5
C36-C35-H35	120.5	C35-C36-C37	119.2(3)
C35-C36-H36	120.4	C37-C36-H36	120.4
C38-C37-C36	122.3(2)	C38-C37-H37	118.8
C36-C37-H37	118.8	C25-C38-C37	117.2(3)
C25-C38-H38	121.4	C37-C38-H38	121.4
O3-C39-H39A	109.5	O3-C39-H39B	109.5
H39A-C39-H39B	109.5	O3-C39-H39C	109.5
H39A-C39-H39C	109.5	H39B-C39-H39C	109.5
O4-C40-N1	126.9(2)	O4-C40-C23	125.1(2)
N1-C40-C23	107.9(2)	C31-C41-C42	120.5(3)
C31-C41-H41	119.8	C42-C41-H41	119.8
C41-C42-C32	119.3(3)	C41-C42-H42	120.3
C32-C42-H42	120.3	O5-C43-C46	109.0(2)
O5-C43-C45	109.9(2)	C46-C43-C45	113.8(3)
O5-C43-C44	101.6(2)	C46-C43-C44	110.9(3)
C45-C43-C44	110.9(3)	C43-C44-H44A	109.5
C43-C44-H44B	109.5	H44A-C44-H44B	109.5
C43-C44-H44C	109.5	H44A-C44-H44C	109.5
H44B-C44-H44C	109.5	C43-C45-H45A	109.5
C43-C45-H45B	109.5	H45A-C45-H45B	109.5
C43-C45-H45C	109.5	H45A-C45-H45C	109.5
H45B-C45-H45C	109.5	C43-C46-H46A	109.5
C43-C46-H46B	109.5	H46A-C46-H46B	109.5
C43-C46-H46C	109.5	H46A-C46-H46C	109.5
H46B-C46-H46C	109.5	Cl2-C60-Cl3	109.7(2)
Cl2-C60-Cl1	109.3(2)	Cl3-C60-Cl1	110.1(2)
Cl2-C60-H60	109.3	Cl3-C60-H60	109.3
Cl1-C60-H60	109.3		

Table 6. Torsion angles (°) for *trans*-429.

C19-C15-C16-C17	-2.0(4)	Br15-C15-C16-C17	177.39(19)
C15-C16-C17-C18	0.9(4)	C15-C16-C17-C33	-179.5(2)
C16-C17-C18-C20	0.8(4)	C33-C17-C18-C20	-178.9(2)
C16-C17-C18-C21	-179.8(2)	C33-C17-C18-C21	0.6(4)
C16-C15-C19-C20	1.6(4)	Br15-C15-C19-C20	-177.9(2)
C15-C19-C20-C18	0.1(4)	C17-C18-C20-C19	-1.3(4)
C21-C18-C20-C19	179.3(3)	C20-C18-C21-C34	-29.4(4)

339

C17-C18-C21-C34	151.2(2)	C20-C18-C21-C22	-149.7(2)
C17-C18-C21-C22	30.8(3)	C18-C21-C22-C29	176.0(2)
C34-C21-C22-C29	51.6(3)	C18-C21-C22-C23	-57.7(3)
C34-C21-C22-C23	177.9(2)	C29-C22-C23-C24	56.7(3)
C21-C22-C23-C24	-71.6(3)	C29-C22-C23-C33	-176.5(2)
C21-C22-C23-C33	55.2(3)	C29-C22-C23-C40	-56.0(3)
C21-C22-C23-C40	175.7(2)	C33-C23-C24-C35	-57.3(4)
C40-C23-C24-C35	-174.3(3)	C22-C23-C24-C35	69.9(4)
C33-C23-C24-C25	126.3(2)	C40-C23-C24-C25	9.3(3)
C22-C23-C24-C25	-106.5(3)	C35-C24-C25-C38	-3.4(4)
C23-C24-C25-C38	173.2(2)	C35-C24-C25-N1	177.1(2)
C23-C24-C25-N1	-6.3(3)	C27-N1-C25-C24	177.1(3)
C40-N1-C25-C24	0.2(3)	C27-N1-C25-C38	-2.4(5)
C40-N1-C25-C38	-179.3(3)	C43-O5-C27-O6	9.0(5)
C43-O5-C27-N1	-171.5(2)	C40-N1-C27-O6	10.6(4)
C25-N1-C27-O6	-166.0(3)	C40-N1-C27-O5	-169.0(2)
C25-N1-C27-O5	14.4(4)	C21-C22-C29-C32	-137.8(3)
C23-C22-C29-C32	97.1(3)	C21-C22-C29-C30	45.0(3)
C23-C22-C29-C30	-80.1(3)	C32-C29-C30-C31	0.0(4)
C22-C29-C30-C31	177.2(3)	C29-C30-C31-C41	0.2(5)
C30-C29-C32-C42	0.1(5)	C22-C29-C32-C42	-177.2(3)
C16-C17-C33-O1	-4.3(4)	C18-C17-C33-O1	175.3(3)
C16-C17-C33-C23	176.8(2)	C18-C17-C33-C23	-3.5(4)
C24-C23-C33-O1	-76.1(3)	C40-C23-C33-O1	36.6(3)
C22-C23-C33-O1	156.2(2)	C24-C23-C33-C17	102.8(3)
C40-C23-C33-C17	-144.5(2)	C22-C23-C33-C17	-24.9(3)
C39-O3-C34-O2	-8.2(4)	C39-O3-C34-C21	168.1(2)
C18-C21-C34-O2	-57.8(4)	C22-C21-C34-O2	64.9(3)
C18-C21-C34-O3	125.9(2)	C22-C21-C34-O3	-111.4(2)
C25-C24-C35-C36	3.0(4)	C23-C24-C35-C36	-173.0(3)
C24-C35-C36-C37	-0.2(4)	C35-C36-C37-C38	-2.2(4)
C24-C25-C38-C37	1.0(4)	N1-C25-C38-C37	-179.6(3)
C36-C37-C38-C25	1.8(4)	C27-N1-C40-O4	7.5(4)
C25-N1-C40-O4	-175.2(3)	C27-N1-C40-C23	-171.3(2)
C25-N1-C40-C23	5.9(3)	C24-C23-C40-O4	172.1(3)
C33-C23-C40-O4	53.8(4)	C22-C23-C40-O4	-68.4(3)
C24-C23-C40-N1	-9.0(3)	C33-C23-C40-N1	-127.3(2)
C22-C23-C40-N1	110.5(2)	C30-C31-C41-C42	-0.6(6)
C31-C41-C42-C32	0.7(6)	C29-C32-C42-C41	-0.5(5)
C27-O5-C43-C46	61.4(3)	C27-O5-C43-C45	-63.9(3)
C27-O5-C43-C44	178.5(3)		

Table 7. Anisotropic atomic displacement parameters (Å^2) for *trans*-429.

The anisotropic atomic displacement factor exponent takes the form: $-2\pi^2[\,h^2\,a^{*2}\,U_{11} + \ldots + 2\,h\,k\,a^*\,b^*\,U_{12}\,]$

	U$_{11}$	U$_{22}$	U$_{33}$	U$_{23}$	U$_{13}$	U$_{12}$
Br15	0.02255(15)	0.02149(15)	0.01607(16)	0.00922(13)	0.00640(12)	0.00326(14)
O1	0.0096(10)	0.0281(11)	0.0218(12)	0.0094(9)	0.0032(9)	0.0036(8)
O2	0.0184(10)	0.0117(10)	0.0255(12)	0.0004(8)	0.0064(9)	0.0054(8)
O3	0.0094(10)	0.0214(10)	0.0238(12)	0.0013(8)	0.0028(9)	-0.0019(8)
O4	0.0185(10)	0.0138(10)	0.0182(11)	-0.0012(8)	-0.0063(9)	-0.0036(8)
O5	0.0215(10)	0.0132(9)	0.0129(10)	0.0042(8)	-0.0043(9)	0.0052(8)
O6	0.0415(14)	0.0207(11)	0.0180(12)	-0.0027(9)	-0.0147(10)	0.0011(11)
N1	0.0130(11)	0.0107(11)	0.0113(12)	0.0010(9)	-0.0041(10)	0.0016(9)
C15	0.0203(15)	0.0154(13)	0.0086(13)	0.0010(10)	-0.0005(12)	-0.0012(12)
C16	0.0098(12)	0.0171(13)	0.0136(14)	-0.0010(11)	0.0004(12)	0.0012(11)
C17	0.0104(11)	0.0122(12)	0.0078(14)	-0.0015(10)	0.0008(11)	0.0009(10)
C18	0.0105(12)	0.0090(12)	0.0092(14)	-0.0036(9)	0.0007(10)	-0.0005(10)
C19	0.0186(14)	0.0139(13)	0.0109(14)	0.0030(11)	-0.0043(12)	0.0032(11)
C20	0.0122(13)	0.0127(13)	0.0175(16)	-0.0011(10)	-0.0006(11)	0.0028(10)
C21	0.0096(12)	0.0110(12)	0.0098(14)	0.0017(10)	0.0011(11)	0.0032(10)
C22	0.0094(12)	0.0081(11)	0.0127(14)	-0.0025(10)	0.0012(11)	0.0010(10)
C23	0.0082(12)	0.0087(12)	0.0106(14)	0.0002(10)	-0.0002(11)	0.0009(10)
C24	0.0085(11)	0.0096(12)	0.0112(14)	-0.0013(10)	0.0013(12)	0.0006(11)
C25	0.0081(11)	0.0120(12)	0.0106(14)	-0.0010(10)	-0.0005(12)	0.0012(10)
C27	0.0148(13)	0.0176(14)	0.0117(15)	0.0004(12)	-0.0037(12)	0.0023(11)
C29	0.0107(13)	0.0121(12)	0.0131(15)	0.0012(11)	0.0013(11)	0.0036(11)
C30	0.0164(14)	0.0177(14)	0.0160(16)	0.0019(11)	0.0011(12)	-0.0020(12)
C31	0.0264(17)	0.0234(16)	0.0281(19)	0.0102(14)	0.0011(15)	-0.0033(14)
C32	0.0244(16)	0.0184(14)	0.0172(16)	-0.0028(12)	0.0014(14)	-0.0004(13)
C33	0.0108(14)	0.0120(13)	0.0122(14)	-0.0025(10)	-0.0017(11)	-0.0001(10)
C34	0.0062(12)	0.0185(14)	0.0104(14)	0.0053(11)	0.0011(11)	0.0000(10)
C35	0.0101(12)	0.0125(13)	0.0127(14)	-0.0014(10)	-0.0019(11)	0.0049(10)
C36	0.0127(13)	0.0149(13)	0.0166(15)	-0.0051(11)	-0.0012(12)	0.0024(11)
C37	0.0164(14)	0.0084(13)	0.0225(16)	-0.0013(11)	-0.0025(12)	0.0004(11)
C38	0.0169(13)	0.0114(12)	0.0147(14)	0.0008(11)	0.0007(12)	0.0039(10)
C39	0.0100(13)	0.0332(17)	0.035(2)	0.0030(15)	0.0086(14)	0.0000(12)
C40	0.0102(12)	0.0104(13)	0.0091(14)	0.0013(10)	0.0002(11)	0.0016(10)
C41	0.040(2)	0.044(2)	0.0217(19)	0.0158(16)	0.0089(17)	-0.0069(18)
C42	0.047(2)	0.050(2)	0.0107(18)	-0.0007(15)	0.0000(16)	-0.0005(19)
C43	0.0221(15)	0.0188(15)	0.0107(15)	0.0088(11)	-0.0039(13)	0.0060(12)
C44	0.0420(19)	0.0220(17)	0.0199(16)	0.0099(13)	-0.0024(14)	0.0126(16)
C45	0.0240(17)	0.039(2)	0.0311(19)	0.0091(15)	-0.0100(15)	0.0070(15)
C46	0.039(2)	0.0348(18)	0.0211(17)	0.0102(14)	0.0032(16)	0.0066(16)
Cl1	0.0369(6)	0.1382(14)	0.0989(11)	-0.0823(11)	0.0160(7)	-0.0080(7)

	U_{11}	U_{22}	U_{33}	U_{23}	U_{13}	U_{12}
Cl2	0.0584(7)	0.0913(9)	0.0527(7)	0.0161(6)	-0.0380(6)	-0.0087(7)
Cl3	0.0763(8)	0.0358(5)	0.0534(7)	0.0081(5)	-0.0162(6)	-0.0139(5)
C60	0.0279(17)	0.0364(19)	0.0222(18)	-0.0094(15)	-0.0079(15)	0.0007(15)

Table 8. Hydrogen atomic coordinates and isotropic atomic displacement parameters ($\mathring{A}^2$) for *trans*-429.

	x/a	y/b	z/c	U(eq)
H16	0.6125	0.3952	0.4731	0.016
H19	0.2628	0.4724	0.4398	0.017
H20	0.1668	0.4043	0.4905	0.017
H21	0.2482	0.2656	0.5368	0.012
H22	0.3844	0.3585	0.5917	0.012
H30	0.2158	0.1846	0.5904	0.02
H31	0.1423	0.1251	0.6480	0.031
H32	0.3800	0.3401	0.6602	0.024
H35	0.3712	0.1882	0.5065	0.014
H36	0.3470	0.0604	0.5055	0.018
H37	0.4333	-0.0094	0.5576	0.019
H38	0.5547	0.0443	0.6091	0.017
H39A	-0.0445	0.3291	0.6122	0.039
H39B	-0.1274	0.2776	0.5831	0.039
H39C	-0.1061	0.3618	0.5719	0.039
H41	0.1852	0.1726	0.7109	0.042
H42	0.3064	0.2795	0.7176	0.043
H44A	0.7751	-0.0400	0.6979	0.042
H44B	0.7929	-0.0159	0.6520	0.042
H44C	0.6512	-0.0265	0.6702	0.042
H45A	0.8693	0.1496	0.7040	0.047
H45B	0.9256	0.0914	0.6727	0.047
H45C	0.9106	0.0698	0.7190	0.047
H46A	0.6459	0.1336	0.7309	0.047
H46B	0.6715	0.0519	0.7461	0.047
H46C	0.5577	0.0680	0.7149	0.047
H60	0.7373	0.3531	0.6714	0.035